



University
of Glasgow

Sardella, Thomas Christian Peter (2010) *Promoting bridging axonal regeneration after spinal cord injury*. PhD thesis.

<http://theses.gla.ac.uk/1420/>

Copyright and moral rights for this thesis are retained by the author

A copy can be downloaded for personal non-commercial research or study, without prior permission or charge

This thesis cannot be reproduced or quoted extensively from without first obtaining permission in writing from the Author

The content must not be changed in any way or sold commercially in any format or medium without the formal permission of the Author

When referring to this work, full bibliographic details including the author, title, awarding institution and date of the thesis must be given

**PROMOTING BRIDGING AXONAL REGENERATION
AFTER SPINAL CORD INJURY**

Thomas Christian Peter Sardella

**Promoting bridging axonal regeneration
after spinal cord injury**

by

Thomas Christian Peter Sardella

A thesis presented for the degree of Doctor of Philosophy in the
Faculty of Biomedical and Life Sciences, Division of Neuroscience &
Biomedical Systems, University of Glasgow

October 2009

FBLs, Spinal Cord Group

University of Glasgow

The Lord bless you and keep you!

The Lord let his face shine upon you, and be gracious to you!

The Lord look upon you kindly and give you peace!

Numbers (6:24-26)

SUMMARY

Olfactory ensheathing cells (OECs) are amongst the best candidates for cell transplantation into lesions of the central nervous system. These specialised glial cells are found in the olfactory system and are associated with the physiological restoration of neuronal circuitry in the first cranial nerve of the adult. There is conflicting evidence on the extent to which OECs promote long distance axonal regeneration when transplanted into spinal cord lesions. In the first chapter of Results (chapter 3) we aimed to determine the potential of OEC transplantation in promoting axonal regeneration beyond the injury. This was investigated by producing a transection of the dorsal columns at the lumbar 3-lumbar 4 (L3-L4) border using a wire knife device that cut ascending primary sensory afferents and immediately after, transplanting olfactory bulb derived OECs into the lesion. Regeneration was assessed in these fibres by injecting the neurotracer biotin dextran amine (BDA) into the left L4 and L5 spinal roots and sacrificing the animals 6 weeks after the lesion. We detected axonal labelling in the lumbar and thoracic cord rostral to the dorsal column lesion; but the labelled axons included spared fibres. For this reason it was necessary to develop a quantification method that included only convincing regeneration and excluded sparing or potential sprouting. With care it was possible to detect convincing axonal regeneration of dorsal root ganglia (DRG) neurons across the lesion in animals transplanted with OECs. Although there have been several claims of axonal regeneration following OEC transplantation in spinal cord pathways information is still lacking on the spatial relationship between regenerating axons and transplanted OECs. To understand this, OECs were transduced before transplantation with a lentiviral vector to express green fluorescent protein (GFP). With this technique it was possible to detect the OECs in the transplanted spinal cord and determine that tract traced axons preferentially regenerated through continuous tracts of GFP labelled OECs in continuity with the transplanted lesion, while they did not normally regenerate through the host spinal cord in areas devoid of OECs.

Regeneration beyond the lesion in OEC transplanted animals was very limited in terms of both distance and numbers of axons. The conditioning lesion of the

sciatic nerve is a procedure which appears to prime DRG neurons for growth. We next asked whether the regeneration observed after an OEC transplant alone could be maximised by a combined treatment paradigm that included OEC transplantation and conditioning lesions. Conditioning lesions were performed by transecting the left sciatic nerve at mid thigh level and the spinal cord was lesioned at the L3-L4 level. Long distance bridging axonal regeneration was strongly potentiated (58 fold). As seen in OEC transplanted animals, axons in the distal spinal cord were located preferentially in areas where OECs were also present. Regeneration was also studied at earlier and later time points. The number of regenerating axons was significantly greater if survival time was of 2 weeks from the lesion/transplantation compared to the 6 week survival, while it did not vary significantly between 6 weeks and 17 weeks survival.

Direct comparison of the growth promoting effects exerted by OECs and Schwann cells have not so far been performed on transection type lesions, but only on other lesion models where sparing cannot be ruled out. To understand if these two cell types share similar properties with reference to promoting long distance axonal regeneration, in the second chapter of Results (chapter 4) we consider sciatic nerve derived Schwann cell transplantation alone or in combination with conditioning lesions following the same lesion paradigm in which OECs were transplanted. Interestingly, no significant difference was found between the growth promoting properties of the two glial cells. Furthermore, with Schwann cells as with OECs, regenerating axons in the distal spinal cord were associated mostly with the transplanted cells. To understand whether the long distance axonal regeneration observed was occurring irrespective of the cell type injected, we transplanted sciatic nerve derived fibroblasts in combination with conditioning lesions. With this lesion paradigm significantly less regeneration was detected indicating that fibroblasts are less effective than OECs and Schwann cells in terms of their regeneration promoting properties. On the other hand we determined that OECs, Schwann cells and fibroblasts all preserved the lesion integrity by preventing the lesion from dilating. Importantly, rats are now being used as a model of study for syringomyelia, a pathology that leads to progressive central canal cavitation. We have found that dilation of the central canal normally develops also in the wire knife dorsal column lesion model; however transplantation of OECs or Schwann cells

significantly reduced the central canal dilation compared to non-transplanted animals.

Any clinical use of cell transplantation will likely involve a delay between injury and treatment, and since a glial scar will develop and the regenerative response of the axotomised fibres may subside, it is not clear to what extent regeneration will occur. In the third chapter of results (chapter 5) we have therefore investigated whether delayed OEC transplantation might promote a significant level of regeneration. Surprisingly, the distribution of OECs following delayed transplantation was similar to that after an acute transplant and OECs formed tracts that were in continuity with the lesion transplant. The presence of these OEC tracts allowed regenerating axons to bridge the lesion and grow for relatively long distances on the other side. Delayed conditioning lesions were combined with delayed OEC transplantation and boosted axonal growth 9 times compared to delayed OEC transplanted animals.

ACKNOWLEDGEMENTS

I thank my supervisors Dr. John S. Riddell and Prof. Susan C. Barnett for appointing me to this Ph.D. studentship and giving me the great opportunity to carry out research with the excellent facilities present in the Spinal Cord Group and the Beatson Institute. Thanks to the ISRT for funding my scholarship and Timea Konia for her friendship. I thank Prof. Oswald Steward, Dr. Aileen Anderson, Dr. Leif Havton and Prof. Jacqueline Bresnahan at the Spinal Cord Techniques Course in UCI-California for having influenced my ideas of what a good scientist should be. Thanks to my friends and colleagues in the Beatson, in particular to Dr. Edina Silajdzic, Dr. Mercedes Tome, Dr. Alessandra Santos-Silva, Dr. Susan Lindsay, Bezma Nash, Kalliopi Ioannidou and of course Margaret O'Prey and Thomas Gilbey for their necessary technical assistance. I am very thankful to all my friends and colleagues in the Spinal cord Group for their support and help, including Prof. David Maxwell, my fellow Ph.D. student Tao Meng, Andrew Toft, Dr. Anne Bannantyne, Dr. Erika Polgar, Dr. David Hughes, Robert Kerr, Christine Watt, Sheena Tiong, Dr. Khuloud Al-Khater, Dr Kholood Al Ghamdi, Ting Ting Liu, Sony Shakya Shrestha and Prof. Andrew Todd with whom I am looking forward to starting my postdoc very soon. Thank you to Antonio Napolitano and Elisa Placidi for their assistance in statistical matters and to Dr. Blanka Herrera and her husband Pedro for their important suggestions. Thank you to Father John, Sister Karen and to the whole of Turnball Hall Chaplaincy for their moral guidance and for their prayer. Thank you to my parents for their love and also to my parents in law for their support.

I dedicate this work to my wife Eleonora who has sustained me throughout these 4 years with great love and especially to our son Emanuele, light to our eyes. I thank our Lord through whom all things come!

Declaration

I declare that the work presented in this thesis is my own (except where otherwise stated) and it has not been submitted previously for any higher degree.

TABLE OF CONTENTS

| | | |
|----------|---|----|
| 1 | Introduction..... | 1 |
| 1.1 | Spinal cord injury..... | 1 |
| 1.2 | Spinal cord injury models | 2 |
| 1.2.1 | Contusion and compression..... | 3 |
| 1.2.2 | Transection and the wire knife lesion..... | 4 |
| 1.3 | Treatment strategies..... | 5 |
| 1.3.1 | Neuroprotection | 5 |
| 1.3.2 | Reinforcement of pre-existing pathways | 6 |
| 1.3.3 | Axonal regeneration | 7 |
| 1.4 | Factors preventing long distance axonal regeneration..... | 8 |
| 1.5 | OEC transplantation..... | 9 |
| 1.5.1 | Olfactory system | 9 |
| 1.5.2 | Properties of OECs in the olfactory system | 10 |
| 1.5.3 | Properties of OECs in vitro..... | 11 |
| 1.5.4 | Myelination..... | 11 |
| 1.5.5 | Interaction with astrocyte/CNS | 12 |
| 1.5.6 | Growth factors expressed by OECs | 13 |
| 1.5.7 | Human derived OECs..... | 13 |
| 1.5.8 | Neuroprotective effect on the lesion | 14 |
| 1.5.9 | Association of OECs with fibres in the lesion..... | 14 |
| 1.5.10 | Interaction of OECs and spinal cord astrocytes..... | 15 |
| 1.5.11 | OEC effects on long distance regeneration (anatomy) | 16 |
| 1.5.11.1 | Dorsal root injuries. | 17 |
| 1.5.11.2 | Spinal cord injuries..... | 18 |
| 1.5.12 | Effects of OECs on functional recovery | 24 |
| 1.6 | Sensory neuron anatomy - lumbar 4-5 DRG neurons and primary afferent fibres | 24 |
| 1.7 | Conditioning lesion | 27 |
| 1.7.1 | Modus operandi..... | 29 |
| 1.8 | Aims of the study | 32 |
| 1.8.1 | Aims of Chapter 3 | 32 |
| 1.8.2 | Aims of Chapter 4 | 34 |
| 1.8.3 | Aims of Chapter 5 | 34 |
| 2 | Materials and Methods..... | 36 |
| 2.1 | Cell culture..... | 36 |
| 2.1.1 | Preparation of the olfactory ensheathing cells from the olfactory bulb | 36 |
| 2.1.1.1 | Dissection | 37 |
| 2.1.1.2 | Dissociation | 38 |
| 2.1.1.3 | Cell purification step..... | 38 |
| 2.1.1.4 | GFP lentiviral transduction..... | 39 |
| 2.1.1.5 | OEC propagation | 40 |
| 2.1.2 | Preparation of Schwann cells and fibroblasts from the sciatic nerve | 43 |
| 2.1.2.1 | Dissection | 43 |
| 2.1.2.2 | Dissociation | 43 |

| | | |
|----------|---|-----|
| 2.1.2.3 | Purification and culture of Schwann cells and fibroblasts..... | 44 |
| 2.1.3 | Long-term freezing of OECs, Schwann cells and fibroblast in liquid nitrogen | 53 |
| 2.1.3.1 | Cell freezing..... | 53 |
| 2.1.3.2 | Cell thawing..... | 54 |
| 2.1.4 | Cell preparation for transplantation..... | 54 |
| 2.1.5 | Cell purity and GFP labelling..... | 55 |
| 2.1.6 | Cell culture materials..... | 57 |
| 2.1.6.1 | OECs Media..... | 57 |
| 2.1.6.2 | Bottenstein-Sato's Media (DMEM-BS)..... | 57 |
| 2.1.6.3 | SATO mix..... | 57 |
| 2.1.6.4 | DMEM-10% FBS..... | 58 |
| 2.1.6.5 | Sorting Media..... | 58 |
| 2.1.6.6 | DMEM..... | 58 |
| 2.1.6.7 | Leibovitz's L-15 Medium (L15)..... | 58 |
| 2.1.6.8 | Collagenase..... | 58 |
| 2.1.6.9 | Soya bean trypsin inhibitor and DNase (SD)..... | 59 |
| 2.1.6.10 | Poly-L-lysine (PLL) coated flasks and coverslips..... | 59 |
| 2.1.6.11 | Freezing media..... | 59 |
| 2.1.6.12 | O4, GalC and p75 hybridoma cell lines..... | 59 |
| 2.1.6.13 | Antibody production..... | 60 |
| 2.1.6.14 | Optimem-50% FBS..... | 60 |
| 2.1.6.15 | Optimem-10% FBS..... | 61 |
| 2.1.6.16 | Hybridoma freezing medium..... | 61 |
| 2.2 | Operations on animals..... | 61 |
| 2.2.1 | Perioperative care..... | 61 |
| 2.2.2 | Wire knife dorsal column lesion..... | 62 |
| 2.2.3 | Extended wire knife dorsal column lesion..... | 66 |
| 2.2.4 | Acute cell transplantation..... | 66 |
| 2.2.5 | Delayed cell transplantation..... | 66 |
| 2.2.6 | Tract tracer injection..... | 67 |
| 2.2.7 | Conditioning lesions..... | 70 |
| 2.2.8 | Perfusion and manipulation of spinal cord tissue..... | 70 |
| 2.3 | Post-processing analysis..... | 72 |
| 2.3.1 | Quantification of lesion cavity size..... | 72 |
| 2.3.2 | Quantification of lesion size..... | 72 |
| 2.3.3 | Quantification of central canal cavitation..... | 75 |
| 2.3.4 | Preliminary analysis on all sections..... | 77 |
| 2.3.5 | Distribution of transplanted cells..... | 77 |
| 2.3.6 | Quantification of fibre numbers in the distal spinal cord..... | 77 |
| 2.3.6.1 | Inclusion criteria for quantification..... | 78 |
| 2.3.7 | Determination of section order..... | 81 |
| 2.3.8 | Method of recording data on the distribution and axon numbers.. | 81 |
| 2.3.9 | Quantification of fibres in OEC tracts caudal to the lesion..... | 84 |
| 2.3.10 | Quantification of fibre density in the injury..... | 86 |
| 2.3.11 | Quantification of fibre number in non-lesioned animals..... | 87 |
| 2.3.12 | Statistical analysis..... | 88 |
| 2.3.13 | Confocal microscopy imaging..... | 88 |
| 3 | Transplantation of OECs and conditioning lesions..... | 90 |
| 3.1 | Introduction..... | 90 |
| 3.2 | Results..... | 90 |
| 3.2.1 | Biotinylated dextran amine tract tracing in non-lesioned rats..... | 90 |
| 3.2.2 | Dorsal column wire knife lesion..... | 101 |

| | | |
|-----------|---|-----|
| 3.2.2.1 | Dorsal column wire knife lesion size and morphological characterization | 101 |
| 3.2.2.2 | Characterization of central canal cavitation | 102 |
| 3.2.2.3 | Tract traced fibres caudal to the lesion..... | 107 |
| 3.2.2.4 | Tract traced fibres rostral to the lesion..... | 107 |
| 3.2.2.4.1 | Tract traced axons passing the lesion level..... | 115 |
| 3.2.2.4.2 | Extended wire knife injury of dorsal columns | 121 |
| 3.2.3 | OEC transplantation | 128 |
| 3.2.3.1 | Characterization of the lesion after transplanting OECs..... | 128 |
| 3.2.3.2 | Characterization of the central canal cavitation after an OECs transplant | 132 |
| 3.2.3.3 | Distribution of OECs in the spinal cord | 135 |
| 3.2.3.4 | Density of BDA labelled fibres in areas containing OECs compared to those devoid of OECs caudal to the lesion | 139 |
| 3.2.3.5 | Regeneration within the lesion transplant..... | 143 |
| 3.2.3.6 | BDA labelled fibres rostral to the lesion | 150 |
| 3.2.3.7 | BDA labelling in the lateral spinal cord..... | 155 |
| 3.2.3.8 | BDA labelled fibres in the medial spinal cord | 158 |
| 3.2.3.9 | Genuine regenerating BDA labelled fibres rostral to the lesion level | 167 |
| 3.2.4 | Conditioning lesions coupled with OECs transplant | 176 |
| 3.2.4.1 | OEC distribution in the spinal cord..... | 176 |
| 3.2.4.2 | BDA labelled fibres sprouting within caudally distributed OECs | 177 |
| 3.2.4.3 | Regeneration within the transplant..... | 181 |
| 3.2.4.4 | BDA labelled fibres rostral to the lesion | 181 |
| 3.2.4.5 | Genuine regenerating BDA labelled fibres rostral to the lesion level | 186 |
| 3.2.5 | Conditioning lesions..... | 193 |
| 3.2.5.1 | Lesion and central canal cavity size | 193 |
| 3.2.5.2 | BDA labelling in the medial cord | 196 |
| 3.2.5.3 | BDA labelling in the lateral cord | 196 |
| 3.2.6 | Combined OEC transplant and sciatic nerve transection in rats receiving an extended wire knife dorsal column lesion. | 201 |
| 3.2.7 | Transplantation of OECs into a dorsal column lesion combined with sciatic nerve transection with a 2 week survival..... | 211 |
| 3.2.7.1 | OEC distribution..... | 211 |
| 3.2.7.2 | Axonal labelling rostral to the lesion | 212 |
| 3.2.8 | OECs transplant and conditioning lesion with 17 week survival... | 219 |
| 3.2.8.1 | OEC distribution..... | 219 |
| 3.2.8.2 | Axonal labelling rostral to the lesion | 220 |
| 3.2.9 | OECs transplant with 2 days survival | 227 |
| 3.3 | Discussion | 230 |
| 3.3.1 | Characterization of the BDA labelling..... | 230 |
| 3.3.2 | OEC transplantation | 231 |
| 3.3.2.1 | OEC distribution in the lesion..... | 232 |
| 3.3.2.2 | OEC protective effect on the lesion | 232 |
| 3.3.2.3 | OEC neuroprotective effect on the grey matter surrounding the central canal | 234 |
| 3.3.3 | OEC distribution beyond the transplant site | 236 |
| 3.3.4 | Neurofilament labelling in the lesion | 237 |
| 3.3.5 | Regeneration of BDA labelled fibres in the lesion..... | 238 |
| 3.3.6 | BDA labelling rostral to the injury | 240 |

| | | |
|-----------|--|-----|
| 3.3.6.1 | Two different groups of tract traced fibres rostral to the injury | 240 |
| 3.3.6.2 | Spared fibres in the lateral cord | 241 |
| 3.3.6.3 | Axonal labelling rostral to the lesion in the medial cord after OEC transplantation..... | 242 |
| 3.3.6.3.1 | Regeneration/sprouting/sparing in the medial cord..... | 243 |
| 3.3.6.3.2 | Convincing regeneration | 243 |
| 3.3.6.4 | Conditioning lesions enhance regeneration/sprouting when combined with OEC transplants | 246 |
| 3.3.6.5 | Conditioning lesions did not promote regeneration | 247 |
| 3.3.6.6 | Significance of the level of regeneration observed for future studies | 248 |
| 3.3.6.7 | Regeneration at 2 weeks..... | 249 |
| 3.3.6.8 | Regeneration at later time points..... | 249 |
| 4 | Transplantation of Schwann cells and fibroblasts..... | 251 |
| 4.1 | Introduction | 251 |
| 4.1.1 | Direct comparison of the reparative capacity of OECs and Schwann cells after transplantation..... | 252 |
| 4.1.2 | Direct comparison of regeneration/sparing/sprouting beyond the site of injury after OECs and Schwann cells | 254 |
| 4.2 | Results..... | 256 |
| 4.2.1 | Schwann cell transplantation..... | 256 |
| 4.2.1.1 | Characterization of the lesion after a Schwann cell transplant | 256 |
| 4.2.1.2 | Characterization of central canal cavitation | 257 |
| 4.2.1.3 | Distribution of Schwann cells in the spinal cord after transplantation | 262 |
| 4.2.1.4 | Regeneration of BDA labelled fibres within the Schwann cell transplant | 265 |
| 4.2.1.5 | BDA labelled axons rostral to the spinal cord lesion..... | 265 |
| 4.2.1.6 | Genuine regenerating BDA labelled fibres rostral to the lesion level | 270 |
| 4.2.2 | Transplantation of Schwann cells combined with conditioning lesions | 274 |
| 4.2.2.1 | BDA labelled axons rostral to the spinal cord lesion..... | 274 |
| 4.2.2.2 | Genuine regenerating BDA labelled fibres rostral to the lesion level | 278 |
| 4.2.3 | Sciatic nerve (SN) fibroblast transplantation combined with conditioning lesions..... | 282 |
| 4.2.3.1 | Characterization of the lesion after a SN fibroblast transplant | 283 |
| 4.2.3.2 | Characterization of central canal cavitation | 283 |
| 4.2.3.3 | Distribution of SN fibroblasts in the spinal cord..... | 291 |
| 4.2.3.4 | Regeneration of BDA labelled fibres within the transplant... | 291 |
| 4.2.3.5 | BDA labelled axons rostral to the spinal cord lesion..... | 294 |
| 4.2.3.6 | Genuine long distance regeneration in SN fibroblast transplanted animals | 298 |
| 4.3 | Discussion | 303 |
| 4.3.1 | Integration of Schwann cells in the transplant site and protective effects on the lesion..... | 303 |
| 4.3.2 | Labelling of primary sensory afferents in and beyond the lesion following Schwann cell transplantation..... | 304 |

| | | |
|---------|--|-----|
| 4.3.3 | Conditioning lesions potentiated the Schwann cell growth promoting effect on axons rostral to the lesion | 305 |
| 4.3.4 | Contamination of Schwann cells in OEC cultures | 307 |
| 4.3.5 | Transplantation of fibroblasts | 308 |
| 5 | Delayed OECs transplants and conditioning lesions | 311 |
| 5.1 | Introduction | 311 |
| 5.1.1 | Delayed transplantation | 311 |
| 5.1.1.1 | Timing of transplantation | 311 |
| 5.1.1.2 | Delayed transplantation of OECs | 313 |
| 5.1.1.3 | Delayed conditioning lesions | 315 |
| 5.2 | Results | 316 |
| 5.2.1 | Dorsal column wire knife lesion, 10 week survival | 316 |
| 5.2.2 | Delayed transplantation of OECs | 321 |
| 5.2.2.1 | Characterization of the lesion after a delayed OECs transplant 321 | |
| 5.2.2.2 | Characterization of central canal cavitation | 322 |
| 5.2.2.3 | OEC distribution in the spinal cord | 329 |
| 5.2.2.4 | Regeneration of neurofilament positive fibres into the lesion 332 | |
| 5.2.2.5 | Regeneration of BDA labelled fibres in the lesion | 332 |
| 5.2.2.6 | BDA labelled fibres in distal spinal cord | 337 |
| 5.2.2.7 | Genuine regenerating BDA labelled fibres above the lesion level 340 | |
| 5.2.3 | Combined delayed transplant and delayed conditioning lesion paradigm | 344 |
| 5.2.3.1 | OEC distribution in the spinal cord | 344 |
| 5.2.3.2 | BDA labelled fibres within and rostral to the lesion | 344 |
| 5.2.3.3 | Genuine regenerating BDA labelled fibres above the lesion level 349 | |
| 5.3 | Discussion | 354 |
| 5.3.1 | OEC protective effect on the lesion | 354 |
| 5.3.2 | Syringomyelia | 355 |
| 5.3.3 | Regeneration in the lesion | 356 |
| 5.3.4 | OEC distribution beyond the lesion site | 356 |
| 5.3.5 | BDA labelling beyond the lesion site | 357 |
| 5.3.6 | Long distance axonal regeneration | 358 |
| 5.3.7 | Combined delayed OEC transplant and delayed conditioning lesions 359 | |
| 6 | Conclusions | 361 |
| | References | 369 |

LIST OF TABLES

| | |
|---|-----|
| Table 1. Summary of studies performed on OEC transplantation focusing on OEC distribution, myelination and promotion of long distance axonal regeneration. | 23 |
| Table 2. Quantification of BDA labelled axonal numbers in non-lesioned animals. | 100 |
| Table 3. Number of fibres at increasing distances from the lesion in seven rats six weeks after the dorsal column lesion. | 120 |
| Table 4. Number of spared fibres at increasing distances from the lesion in the lateral spinal cord of OEC transplanted animals. | 156 |
| Table 5. Number of tract traced fibres associated with OECs at increasing distance from the lesion in the medial spinal cord. | 164 |
| Table 6. Number of tract traced fibres, that were not associated with OECs, at increasing distance from the lesion in the medial spinal cord. | 165 |
| Table 7. Number of regenerating fibres at increasing distance from the lesion in the medial spinal cord associated with OECs. | 173 |
| Table 8. Number of fibres associated with OECs at increasing distance from the dorsal column lesion in the medial spinal cord in OEC transplanted and conditioning lesioned animals. | 182 |
| Table 9. Number of fibres not associated with OECs at increasing distance from the dorsal column lesion in the medial spinal cord of OEC transplanted and conditioning lesioned animals. | 183 |
| Table 10. Number of regenerating fibres at increasing distance from the lesion in the medial spinal cord of OEC transplanted and conditioned animals. | 189 |
| Table 11. Number of fibres at increasing distances from the lesion in the medial spinal cord of conditioning lesioned animals that did not receive a transplant. | 198 |
| Table 12. Number of fibres at increasing distances from the lesion in the lateral spinal cord of conditioning lesioned animals that did not receive a transplant. | 199 |
| Table 13. Number of fibres at increasing distances from the lesion in the medial dorsal columns after OEC transplantation into an extended lesion of the dorsal columns of conditioning lesioned animals. | 210 |
| Table 14. Number of regenerating/sprouting fibres at increasing distances from the lesion following OEC transplantation and conditioning lesions in the 2 week survival animals. | 213 |
| Table 15. Number of convincing regenerating fibres at increasing distances from the lesion following OEC transplantation and conditioning lesions in the 2 week survival animals. | 217 |
| Table 16. Number of regenerating/sprouting fibres at increasing distances from the lesion 17 week survival after OEC transplantation. | 221 |
| Table 17. Number of regenerating fibres at increasing distances from the lesion 17 weeks after OEC transplantation. | 225 |
| Table 18. Summary of studies directly comparing OEC and Schwann cell transplantation focusing on distribution, myelination and promotion of long distance axonal regeneration. | 255 |
| Table 19. Number of tract traced fibres associated with Schwann cells rostral to the lesion in the medial spinal cord. | 268 |
| Table 20. Number of tract traced fibres that were not associated with Schwann cells rostral to the lesion in the medial spinal cord. | 269 |
| Table 21. Number of genuine regenerating fibres rostral to the lesion in the medial spinal cord after Schwann cell transplantation. | 273 |

| | |
|---|-----|
| Table 22. Number of fibres associated with Schwann cells rostral to the dorsal column lesion in the medial spinal cord in animals that received conditioning lesions. | 276 |
| Table 23. Number of fibres not associated with Schwann cells rostral to the dorsal column lesion in the medial spinal cord in animals that received conditioning lesions. | 277 |
| Table 24. Number of regenerating fibres rostral to the dorsal column lesion in the medial spinal cord associated with Schwann cells in animals treated with conditioning lesions. | 281 |
| Table 25. Number of tract traced fibres associated with fibroblasts rostral to the lesion in the medial spinal cord. | 295 |
| Table 26. Number of tract traced fibres not associated with fibroblasts rostral to the lesion in the medial spinal cord. | 296 |
| Table 27. Number of genuine regenerating fibres rostral to the lesion in the medial spinal cord associated with fibroblasts. | 301 |
| Table 28. Number of BDA labelled fibres associated with OECs at increasing distance from the lesion in the medial spinal cord following delayed OEC transplantation. | 338 |
| Table 29. Number of BDA labelled fibres not associated with OECs at increasing distance from the dorsal column lesion in the medial spinal cord following delayed OEC transplantation. | 339 |
| Table 30. Number of BDA labelled regenerating axons at increasing distance from the lesion in the medial spinal cord following delayed OEC transplantation. ... | 343 |
| Table 31. Number of BDA labelled fibres associated with OECs at increasing distance from the dorsal column lesion in the medial spinal cord following combined delayed OEC transplantation and conditioning lesions. | 346 |
| Table 32. Number of BDA labelled fibres not associated with OECs at increasing distance from the dorsal column lesion in the medial spinal cord following combined delayed OEC transplantation and conditioning lesions. | 347 |
| Table 33. Number of BDA labelled regenerating axons at increasing distance from the lesion in the medial spinal cord following combined delayed OEC transplantation and conditioning lesions. | 352 |

LIST OF FIGURES

| | |
|---|-----|
| Figure 1-1. The anatomy of primary sensory afferents. | 26 |
| Figure 2-1. Cell culture of rat olfactory bulb FACS purified OECs. | 41 |
| Figure 2-2 Antigenic profile of cultured OECs derived from rat olfactory bulb. . | 41 |
| Figure 2-3 Culture of cells from the sciatic nerve one day after dissociation.... | 47 |
| Figure 2-4. Purification of Schwann cells and fibroblasts by partial trypsinization. | 49 |
| Figure 2-5 Antigenic profile of cultured Schwann cells and fibroblasts derived from rat sciatic nerve..... | 51 |
| Figure 2-6 Diagram to illustrate the phases of the wire knife lesion operation.. | 64 |
| Figure 2-7 Injection of BDA tract tracer into the L4/5 spinal nerves..... | 68 |
| Figure 2-8. Designing the contour of the lesion cavity and of the lesion. | 74 |
| Figure 2-9. Quantification of central canal cavitation..... | 76 |
| Figure 2-10. Schematic representation of the quantification of the number of fibres labelled with BDA rostral to the lesion. | 80 |
| Figure 2-11 Simplified example of spreadsheet used to record observations made when examining individual spinal cord sections. | 82 |
| Figure 2-12 Method to determine which stacked images to project..... | 85 |
| Figure 3-1. Time course of operations performed on the animals used to characterise tract tracer labelling. | 91 |
| Figure 3-2. Labelling at the L3-L4 spinal cord level in a non-lesioned animal following injection of BDA tracer in the left L4-5 spinal nerves..... | 92 |
| Figure 3-3. BDA labelling at the thoracic level in a non-lesioned animal. | 94 |
| Figure 3-4. BDA labelling at the cervical level in a non-lesioned animal. | 96 |
| Figure 3-5. Labelling of BDA at the brain stem level in a non-lesioned animal. . | 98 |
| Figure 3-6. Time course of operations performed on spinal cord lesioned untreated animals. | 101 |
| Figure 3-7. Dorsal column wire knife lesion morphology in non-transplanted animals with a survival time of 6 weeks. | 104 |
| Figure 3-8. Central canal cavitation rostral to and caudal to the lesion..... | 104 |
| Figure 3-9. Lesion and central canal size 6 weeks after a dorsal column injury. | 106 |
| Figure 3-10. BDA labelling caudal to the lesion in a transverse section of the caudal block..... | 109 |
| Figure 3-11. BDA labelling was interrupted at the lesion level in medial dorsal columns. | 111 |
| Figure 3-12. Tract tracing in transverse sections rostral to the dorsal column lesion. | 113 |
| Figure 3-13. Tract traced axons at and rostral to the lesion level on lateral sections from animals receiving a dorsal column lesion. | 116 |
| Figure 3-14. Branching of axons in the most lateral dorsal columns in a rat 6 weeks after a dorsal column lesion. | 118 |
| Figure 3-15. BDA labelling caudal to a laterally extended wire knife dorsal column lesion. | 122 |
| Figure 3-16. Tract tracing rostral to a laterally extended dorsal column lesion in transverse sections. | 124 |
| Figure 3-17. Ablation of all axons in the lateral dorsal columns in a rat receiving a laterally extended dorsal column lesion in parasagittal sections. | 126 |
| Figure 3-18. Time course of procedures performed on spinal cord lesioned animals transplanted with OECs..... | 128 |
| Figure 3-19. Examples of lesion morphology and size after an OEC transplant. | 130 |

| | |
|---|-----|
| Figure 3-20. Lesion and central canal characterization 6 weeks after a dorsal column injury and OEC transplantation. | 133 |
| Figure 3-21. Comparison of lesion, lesion cavity and central canal cavity size between OEC transplanted and non-transplanted rats. | 134 |
| Figure 3-22. Distribution of OECs after transplantation into spinal cord lesions. | 137 |
| Figure 3-23. Examples of tract traced fibres among tracts of OECs caudal to the lesion site compared to tract traced fibres in immediately adjacent tissue. ... | 140 |
| Figure 3-24. Quantification of BDA labelled fibres in sections containing OECs compared to adjacent sections devoid of OECs. | 142 |
| Figure 3-25. Axonal regeneration in a lesion transplanted with OECs. | 144 |
| Figure 3-26. OEC association with tract traced fibres in the lesion. | 146 |
| Figure 3-27. Neurofilament labelling in a lesion transplanted with OECs. | 148 |
| Figure 3-28. Location of tract traced fibres rostral to a dorsal column lesion in an OEC transplanted animal. | 151 |
| Figure 3-29. Definition of the border between medial spinal cord and lateral spinal cord. | 153 |
| Figure 3-30. Comparison of the average number of BDA labelled fibres in the lateral cord between OEC transplanted and non-transplanted rats. | 157 |
| Figure 3-31. Sprouting/regenerating axons rostral to the lesion in the medial spinal cord following OEC transplantation. | 160 |
| Figure 3-32. BDA labelling of sprouting/regenerating axons in the central canal following OEC transplantation. | 162 |
| Figure 3-33. Comparison of the average number of BDA labelled fibres associated and not associated with OECs in the medial spinal cord. | 166 |
| Figure 3-34. OEC tracts in continuity with the lesion were not sufficient to promote regeneration rostral to the lesion in some animals. | 169 |
| Figure 3-35. Regeneration of BDA labelled axons in OEC tracts rostral to the lesion. | 171 |
| Figure 3-36. Axons did not regenerate for the full length of the OEC tract. | 174 |
| Figure 3-37. Time course of procedures performed on lesioned animals receiving an OEC transplant and conditioning lesions. | 176 |
| Figure 3-38. Examples of tract traced fibres among tracts of OECs caudal to the lesion site compared to tract traced fibres in immediately adjacent tissue in conditioning lesioned animals. | 178 |
| Figure 3-39. Axonal density in caudal tracts of OECs transplanted into a dorsal column lesion in animals receiving conditioning lesions. | 180 |
| Figure 3-40. Comparison of the average number of BDA labelled fibres associated and not associated with OECs in the medial spinal cord of conditioned animals. | 184 |
| Figure 3-41. Comparison of sprouting/regeneration rostral to the lesion associated with OECs in the medial spinal cord of conditioned and non-conditioned animals. | 185 |
| Figure 3-42. Regenerating axons in a tract of OECs rostral to the dorsal column lesion following conditioning lesions. | 187 |
| Figure 3-43. Regeneration in OEC transplanted animals with and without conditioning lesion. | 190 |
| Figure 3-44. Following conditioning lesions, axons regenerated the full length of the OEC tract rostral to the dorsal column lesion, with profuse regeneration of sensory afferent axons. | 191 |
| Figure 3-45. Time course of procedures performed on spinal cord injured animals receiving conditioning lesions but not transplantation. | 193 |

| | |
|--|-----|
| Figure 3-46. Comparison of the lesion size, lesion cavity size and central canal cavity size between all OEC transplanted and all non-transplanted animals (including conditioning lesioned animals). | 195 |
| Figure 3-47. The effect of OEC transplantation and conditioning lesions on the number of fibres rostral to the lesion after lesion. | 200 |
| Figure 3-48. Absence of sparing in the lateral spinal cord and regeneration after OEC transplantation into an extended dorsal column lesion of conditioning lesioned animals. | 202 |
| Figure 3-49. No sparing at the thoracic level following OEC transplantation into an extended lesion of the dorsal columns of conditioning lesioned rats. | 204 |
| Figure 3-50. Tract traced axons at and rostral to the lesion level in the lateral cord following OEC transplantation into an extended lesion of the dorsal columns of conditioning lesioned animals. | 206 |
| Figure 3-51. Long distance axonal regeneration occurred after an extended dorsal column lesion transplanted with OECs after conditioning lesions..... | 208 |
| Figure 3-52. Time course of procedures performed on short survival animals transplanted with OEC and subjected to conditioning lesions..... | 211 |
| Figure 3-53. Comparison of sprouting/regeneration rostral to the lesion associated with OECs in the medial spinal cord in the 2 weeks and the 6 week survival animals after OEC transplantation and conditioning lesions. | 214 |
| Figure 3-54. Regeneration occurred as early as 2 weeks after a dorsal column lesion. | 215 |
| Figure 3-55. Comparison of axonal regeneration rostral to the lesion in the medial spinal cord in the 2 weeks and 6 week survival animals after OEC transplantation and conditioning lesions. | 218 |
| Figure 3-56. Time course of procedures performed on animals with 17 week survival subjected to OEC transplantation and conditioning lesions..... | 219 |
| Figure 3-57. Comparison of sprouting/regeneration rostral to the lesion associated with OECs in the medial spinal cord 6 and 17 weeks after OEC transplantation. | 222 |
| Figure 3-58. Long distance regeneration was detected 17 weeks after a dorsal column wire knife lesion. | 223 |
| Figure 3-59. Comparison of regeneration 6 and 17 weeks after the dorsal column lesion. | 226 |
| Figure 3-60. Time course of procedures performed on animals with 2 days survival..... | 227 |
| Figure 3-61. OEC distribution in the spinal cord two days after transplantation. | 228 |
| Figure 4-1. Time course of procedures performed on animals transplanted with Schwann cells. | 256 |
| Figure 4-2. Schwann cell distribution in the lesion and lesion morphology 6 weeks after transplantation..... | 259 |
| Figure 4-3. Lesion and central canal characterization 6 weeks after a dorsal column injury and Schwann cells transplantation. | 261 |
| Figure 4-4. Distribution of Schwann cells in the spinal cord. | 263 |
| Figure 4-5. Axonal regeneration into a lesion transplanted with Schwann cells. | 266 |
| Figure 4-6. Schwann cell tracts in continuity with the lesion were sufficient to promote regeneration rostral to the lesion..... | 271 |
| Figure 4-7. Time course of procedures in animals with combined Schwann cell transplantation and conditioning lesions. | 274 |
| Figure 4-8. Axons regenerating in a tract of Schwann cells rostral to the lesion following conditioning lesions. | 279 |

| | |
|---|-----|
| Figure 4-9. Time course of procedures performed on animals transplanted with SN fibroblasts. | 282 |
| Figure 4-10. Lesion morphology and size after a SN fibroblast transplant..... | 284 |
| Figure 4-11. Effects of fibroblasts on morphology of the spinal cord tissue surrounding the lesion compared to that of OECs and Schwann cells 6 weeks after the dorsal column lesion/transplantation..... | 286 |
| Figure 4-12. Lesion and central canal characterization 6 weeks after a dorsal column injury and fibroblast transplantation. | 288 |
| Figure 4-13. Comparison between lesion size and lesion cavity size of animals with a six week survival transplanted with Schwann cells, SN fibroblasts, OECs or of non-transplanted animals. | 289 |
| Figure 4-14. Comparison of syringomyelia formed in animals with a six week survival transplanted with Schwann cells, fibroblasts or OECs and non-transplanted animals..... | 290 |
| Figure 4-15. Axonal regeneration in a lesion transplanted with SN fibroblasts. | 292 |
| Figure 4-16. Comparison of the number of BDA labelled axons in medial cord rostral to the lesion in Schwann cell, OEC, SN fibroblast transplanted and non-transplanted animals..... | 297 |
| Figure 4-17. Regenerating axons in a tract of fibroblasts rostral to the lesion following conditioning lesions. | 299 |
| Figure 4-18. Comparison of the number of regenerating axons labelled with BDA in the medial spinal cord rostral to lesion in Schwann cell, OEC, SN fibroblast transplanted and non-transplanted animals. | 302 |
| Figure 5-1. Time course of procedures performed on non-transplanted animals 10 weeks after the spinal cord lesion. | 317 |
| Figure 5-2. Lesion morphology in non-transplanted animals with a 10 week survival..... | 318 |
| Figure 5-3. Lesion and central canal size 10 weeks after a dorsal column injury in non-transplanted animals. | 320 |
| Figure 5-4. Time course of procedures performed on delayed OECs transplanted animals. | 321 |
| Figure 5-5. The lesion was filled by OECs and astrocytes after delayed OEC transplantation. | 324 |
| Figure 5-6. Lesion size, lesion cavity size and central canal diameter in all delayed transplanted and delayed conditioning lesioned rats pooled together. | 326 |
| Figure 5-7. Lesion size and lesion cavity size in delayed OEC transplanted animals compared with non-transplanted animals. | 327 |
| Figure 5-8. Comparison between the lesion size, lesion cavity size and central canal size following OEC transplantation into a fresh or a chronic lesion. | 328 |
| Figure 5-9. Images of OEC distribution in the spinal cord after delayed transplantation. | 330 |
| Figure 5-10. Regeneration of neurofilament labelled axons in a lesion 6 weeks after a delayed transplant of OECs. | 333 |
| Figure 5-11. Regeneration of tract traced sensory axons in the lesion of a delayed transplanted animal. | 335 |
| Figure 5-12. Long distance axonal regeneration following a delayed OEC transplant..... | 341 |
| Figure 5-13. Time course of procedures performed on animals receiving delayed OEC transplant and conditioning lesion. | 344 |
| Figure 5-14. Summary of results for sprouting/regeneration of fibres rostral to the lesion in the medial cord. | 348 |
| Figure 5-15. Long distance axonal regeneration following delayed OEC transplantation combined with a delayed conditioning lesion..... | 350 |

Figure 5-16. Summary of regeneration of fibres rostral to the lesion in the medial cord after applying criteria to exclude non regenerating fibres.353

LIST OF ABBREVIATIONS

To ease the reading I have avoided using too many abbreviations which rather than being helpful can often be confusing. The following abbreviations were however necessary:

BDA: biotin dextran amine

C: cervical

CGRP: calcitonin gene-related peptide

CL: conditioning lesion (also termed priming or sciatic nerve transection)

CNS: central nervous system

CSPG: chondroitin sulphate proteoglycans

CST: corticospinal tract

DAPI: 4',6-diamidino-2-phenylindole

DMSO: Dimethyl sulfoxide

DREZ: dorsal root entry zone

DRG: dorsal root ganglia

FACS: fluorescent activated cell sorting

GFAP: glial fibrillary acidic protein

GFP: green fluorescent protein

L: lumbar

MAG: myelin associated glycoprotein

OEC: olfactory ensheathing cell

OMgp: oligodendrocyte myelin glycoprotein

ORN: olfactory receptor neuron

PLL: poly-L-lysine

PNS: peripheral nervous system

RST: rubrospinal tract

SN: sciatic nerve

StErr: standard error of the average value

T: thoracic

1 Introduction

1.1 Spinal cord injury

Spinal cord injury results in the partial or complete interruption of communication between neurons located on either side of the injury. This loss of communication often causes deficits in the sensory and motor systems, autonomic dysreflexia, bladder, bowel and sexual dysfunction and chronic pain (Hagg and Oudega, 2004). Spinal cord injury affects more than 250000 people in the USA with more than 10000 new cases each year (Anderson, 2004, Willerth et al., 2008). These deficits may be transient or even permanent because the central nervous system has very little reparative capacity. In fact, while the peripheral nervous system is able to re-establish functional connections after a lesion, the central nervous system, instead, undergoes a process of abortive restoration which ends with the irreversible degeneration of the lesioned area and surrounding tissue. In more detail, in an injured peripheral nerve, the axons and Schwann cells undergo Wallerian degeneration. The resulting debris is removed by macrophages which subsequently abandon the site of injury while Schwann cells line up longitudinally to form the bands of Bungner which selectively guide the regeneration of axons back to their target organ (Guth, 2007). The same sequence of events does not occur in the injured spinal cord. In the spinal cord following injury nerve fibres undergo Wallerian degeneration of the distal end and partial or total dieback of the proximal end. The products of the degeneration are not removed as efficiently as in the peripheral nervous system (Alexander and Popovich, 2009). Furthermore, the site of injury undergoes an immediate process of necrosis of the cells that receive the direct mechanical impact including neurons and endothelial cells (Hagg and Oudega, 2006) transforming the lesioned area into a structure composed of cysts surrounded by a scar (Guth, 2007). While the scar in other organs is eventually repaired by wound healing, in the central nervous system the lesion expands and aggravates the original pathology conditions (Guth, 2007). Death of endothelial cells leads to haemorrhage and consequent reduction of blood supply with a loss of glucose and oxygen supply in the vicinity of the lesion thus incrementing the

amount of tissue that undergoes degeneration (Hagg and Oudega, 2006). The increase in the extracellular levels of free radicals and the release of glutamate by dying neurons and oligodendrocytes contributes to further apoptotic cell death and expansion of the fluid filled cysts (Park et al., 2006). Furthermore, the immune response, which is important in clearing away debris and generating a suitable environment for axonal growth, also causes the death of glial cells in the lesion vicinity by releasing proteases and oxidative metabolites (Alexander and Popovich, 2009). These events together with the demyelination of fibres in the lesion vicinity leads to the loss of communication between the CNS neurons on either side of the injury causing loss of function.

Tissue disruption is not limited to the original site of injury and to the neighbouring areas, but may extend for considerable distances along the spinal cord leading to loss of neurons located in the grey matter surrounding the central canal by a process of cavitation termed syringomyelia. Central canal cavitation, develops in 20% of injured people (Wirth et al., 2001). Syringomyelia, a pathology also common to many other types of diseases, consists of the progressive enlargement of the central canal above and below the injury level leading to disruption of the ependymal epithelium and loss of grey matter for long distances of the spinal cord (Klekamp, 2002; Radojicic et al., 2007). The enlargement of the central canal can progress for months, years or even decades and is often the cause of pathological conditions that develop in later stages in spinal cord injured people. Common consequences of this pathology are deficits of the sensory and motor pathways, neuropathic pain, and autonomic dysfunction (Seki et al., 2008).

1.2 Spinal cord injury models

Animal models have been developed to understand the mechanisms that underlie the degeneration of the spinal cord at the injury site and the factors that limit the restoration of function in human spinal cord following a traumatic injury. Experimental injury-induced degeneration of the spinal cord resembles closely that observed in humans (Diez and Curt, 2006). Furthermore most of the

information available today is the fruit of research carried out on animal spinal cord injury models. Many different animal models have been devised to examine different aspects of spinal cord injury and these will be discussed in the following sections.

1.2.1 Contusion and compression

Spinal cord injuries in humans are commonly caused by contusive and compressive type impacts, less frequently by transections (Rosenszweig and McDonald, 2004).

Most of the therapies that have reached clinical trial on humans are based on research carried out on contusion injury animal models (Young, 2002). Contusions are generated by hitting the exposed cord with an impactor such as the New York University impactor or the Ohio State University impactor (Rosenszweig and McDonald, 2004). Our group has recently started a pilot study involving contusion injuries with a new generation device termed the Infinite Horizon impactor. This device amongst its many advantages allows the experimenter to select the force to be applied to the spinal cord allowing for studies of varying injury severity and high precision (Cao et al., 2005).

Compression injuries can be a simple and inexpensive procedure most commonly induced by inserting the two tips of a pair of forceps onto either side of the exposed spinal cord and squeezing them together for a determined amount of time. Normally the forceps are modified to allow closure only up to a determined angle in order to control the severity of the lesion.

Contusion and compression injury techniques generally cause the destruction of most of the grey matter in the vicinity of the lesion while the white matter tracts undergo only partial degeneration (Cao et al., 2005). These types of injury are in fact used to produce incomplete lesions of varying severity, thus allowing the study of degenerative and restorative events in the remaining damaged yet intact connections between the two ends of the injured cord. These studies include remyelination of demyelinated spared tracts, potentiation of spared

networks and treatments to optimise the use of these residual pathways (Aoki et al., 1986; Dobkin and Havton, 2004). By means of electrophysiological (i.e. velocity of impulse transmission) and behavioural studies (i.e. Basso, Beattie and Bresnahan score) it is possible for example to register recovery that is likely due to remyelination of demyelinated spared tracts (McDonald and Howard, 2002). These spared fibres that are only transiently dormant at early postinjury intervals underlie many claims of false long distance axonal regeneration and functional recoveries (Steward et al., 2003).

1.2.2 Transection and the wire knife lesion

Unlike compression or contusion models, a transection injury of the spinal cord is necessary to prove true long distance regeneration on the distal side of the lesion (Kwon et al., 2002). In treatments that are aimed at promoting long distance axonal regeneration it is important to distinguish this from sprouting; the former implying growth of a transected fibre through or around the lesion and beyond it for a significant distance while the latter meaning growth of a spared fibre present on the distal spinal cord (Steward et al., 2003). The advantage of a clean complete transection of the spinal cord is that no neuronal tracts survive the injury. While in the mouse model complete transection leads to the formation of a fibrous scar, in rat it causes the separation of the two cord stumps which retract apart leaving a fluid-filled space of many millimetres in length which is a further barrier to axonal regeneration across the lesion (Steward et al., 2003). In the rat model, partial transections have the advantage of maintaining tissue continuity and preventing the separation of the cord stump as seen in complete transections. Partial transections interrupt only certain pathways; for example by making dorsal hemisections to study regeneration of the corticospinal tract axons (Steward et al., 2003).

Partial transections are performed usually with handheld blades thus generating a degree of variability in the extent to which tracts are cut. The wire knife (David Kopf Instruments), instead, is an instrument used more commonly in recent years, including the present study, to generate partial, precise and reproducible transections of the dorsal columns in the spinal cord. Mounted on a

stereotactic device, the wire knife creates minimal destruction of the tissue when extruded and raised through the dorsal columns. The wire knife is made of a tungsten wire, which is extremely thin when compared to the blades used in other transection paradigms, thus in principle reducing laceration and compression and consequently degeneration of the cord. It has been used in studies involving destruction of the corticospinal tracts in the dorsal columns (Weidner et al. 2002; Jones et al., 2003), of rubrospinal tract axons (RST) in the lateral funiculus (Jones et al., 2003), of ascending sensory dorsal root ganglia (DRG) neurons in the dorsal columns (Lu et al., 2006; Toft et al., 2007) and in MRI studies of a dorsal column lesion (Kozlowski et al., 2008).

1.3 Treatment strategies

Three main strategies have been investigated so far to overcome the limited functional restorative capacity of the spinal cord. These are: minimizing the damage by promoting neuroprotection; compensating for the loss in communication by promoting sprouting/remyelination; and repairing injured connections by promoting regeneration and reconnection.

1.3.1 Neuroprotection

Neuroprotection is a rather broad term that includes all those processes that prevent the spinal cord from degenerating after the injury. Regulation of the immune response is a prime target to protect the lesion environment. Following a lesion, granulocytes and monocyte-derived macrophages enter the lesion and clear away the necrotic and apoptotic cells (Alexander and Popovich, 2009). The removal of myelin derivatives and of degenerating tissue by macrophages is thought to promote regeneration, but, importantly, this clearance activity is also accompanied by a non-specific microbicidal activity mediated by the secretion of proteases and oxidant species that leads to the death of resident cells and to the progression of the lesion degeneration (Alexander and Popovich, 2009). For this reason enhancement of the immune response by delivery of

bacterial or fungal derivatives induces axonal regeneration on one hand (Clemente and Windle, 1954; Gensel et al., 2009) but exacerbates the lesion degeneration on the other. On the contrary, suppression of the immune system promotes at least in the short term tissue sparing (Zeman et al., 2009). In fact, the only drug presently administered specifically to spinal cord injured people in the USA is the anti-inflammatory methylprednisolone. Another important approach to support neuroprotection consists of cell replacement therapies that aim to reduce tissue loss preserving the spinal cord tissue near the lesion. These consist of the transplantation of cells including OECs, Schwann cells, fibroblasts or bone marrow stromal cells (Barnett and Riddell, 2007; Willerth and Sakiyama-Elbert, 2008; Vaquero and Zurita, 2009). Transplanted cells provide the lesion with a scaffold that allows revascularization (Li et al., 1998; Toft et al., 2007), cavity stabilization (Plant et al., 2003; Bretzner et al., 2008), preservation of local circuitry and reduction of neuronal loss in descending pathways (Sasaki et al., 2006). Other approaches to the promotion of neuroprotection include neurotrophin delivery (Novikova et al., 2002), dietary starvation (Plunet et al., 2008), and progesterone administration (Stein et al., 2008).

1.3.2 Reinforcement of pre-existing pathways

A second possible approach to treatment of the spinal cord following injury is to reinforce and potentiate the recovery processes that spontaneously take place after injury. These spontaneous processes underlie the recovery in function seen in human and animal studies. For example patients who have only 10% of spared white matter in spinal tracts can recover antigravity strength in antigravity muscles after an initial phase of complete paralysis (Little et al., 1999). In cats, an even lower level of sparing is sufficient for walking without external support (Windle et al., 1958). These functional improvements might occur by a number of modifications; these include two main phenomena: sprouting and remyelination. 1) Sprouting in the central nervous system was demonstrated originally in an ingenious experiment using the Nauta and Gygax silver staining on residual primary sensory afferents in the spinal cord following dorsal root rizotomy in adult rat (Liu and Chambers, 1958). Since then further studies have

confirmed sprouting in the spinal cord by means of tract tracing techniques (Fouad et al., 2001) and in other central nervous areas (Raineteau and Schwab, 2001). Potentiation of sprouting has been reported by delivering to the spinal cord a specific antibody targeting Nogo protein which is an inhibitor to axonal growth (Thallmair et al., 1998), by delivering neurotrophic factors such as BDNF (Jakeman et al., 1998), by delivering the chondroitinase enzyme to digest the chondroitin sulphate proteoglycans in the lesion scar (Barrit et al., 2006) and by cell transplantation (Li et al., 1994). 2) Upon injury to the spinal cord demyelination of axons occurs close to the site of injury (Frei et al., 2000). Spontaneous remyelination mediated by endogenous newly differentiated oligodendrocytes (Gensert and Goldman, 1997) or by infiltration of endogenous Schwann cells occurs (Black et al., 2006). This may underlie functional improvements observed in many reports in the literature after behavioural testing (Steward et al, 2003). Strategies of cellular replacement by cell transplantation have widely shown in animal models that transplanted cells can remyelinate demyelinated axons in the injury and in the spinal cord tissue surrounding the injury (Barnett and Riddell, 2004; Oudega and Xu, 2006).

1.3.3 Axonal regeneration

The experiment designed by David and Aguayo in 1981 showed unequivocally in adult rat by means of tract tracing that when a peripheral nerve is placed in a brain or spinal cord lesion the CNS neurons regenerate into the nerve stump within the bands of Bungner as seen with regeneration of peripheral neurons. However, in the absence of any treatment paradigm, injury results in short distance transient abortive regeneration (Ramon y Cajal, 1928). Regeneration in the spinal cord occurs as early as 6 hours after injury (Kerschensteiner et al., 2005). It is at a later stage, though, 10-14 days, that the restoration process is halted before any connections are made and diverted to a process of definitive atrophy of the nerve sprouts that makes functional damage irreparable (Ramon y Cajal, 1928).

1.4 Factors preventing long distance axonal regeneration

Factors that are thought to be involved in limiting the restorative attempts of neurons in the central nervous system are discussed below. These include 1) the presence of myelin-associated inhibitory molecules in the lesion environment, 2) cavitation and 3) the glial scar.

1) Degenerating oligodendrocytes release myelin-associated molecules that have been shown to inhibit axonal regeneration *in vivo* and *in vitro* (Ma et al., 2009). Myelin associated glycoprotein (MAG), a sialic acid binding protein, is released by degenerating myelin and is inhibitory to regeneration. MAG knockout mice have been shown to extend neurites across a lesion; furthermore the inhibitory effect of MAG was significantly reduced *in vitro* after MAG denaturation (Li et al., 1996). Similarly, neonatal DRG neurons grew longer axons on substrates formed with MAG knockout animals compared to wild type animals (Shen et al., 1998). Also Nogo, a protein present in myelin has been shown to inhibit axonal growth. By using an antibody to Nogo it was possible to promote sprouting in adult rodents (Schnell and Schwab, 1990) and even in adult primates (Freund et al., 2006). Finally, oligodendrocyte myelin glycoprotein, OMgp, a glycosylated protein present in myelin, is also associated with inhibition of axonal growth (Wang et al., 2002) and axons regenerated more in OMgp adult knockout mice compared to wild type (Ji et al., 2008).

2) Fluid filled cavities develop in place of the insulted tissue after necrotic and apoptotic events following the injury (Willerth et al., 2008). Also the migration of astrocytes away from the lesion site might encourage further cell death and consequently cavity formation (Fitch et al., 1999). Although tissue bridges are found within the cavities (Radojicic et al., 2005), these are probably not sufficient to provide a suitable scaffold for axons to regenerate through. Indeed, introducing into the cavity a substrate for the axons to grow on enhances regeneration into the lesion environment as seen in transplantation of tissue explants (Oudega et al., 1994) and of cultured cells including OECs (see section 1.5), Schwann cells (see section 4.1), fibroblasts (Tuszynski et al., 1994; Keyvan-Fouladi et al., 2005), bone marrow stromal cells (Zurita et al., 2008; Chiba et al., 2009).

3) A glial scar forms around the lesion soon after injury to seal off the lesion and reduce the diffusion of cytotoxic molecules out of the impacted area (Rolls and Schwartz, 2006). The scar is formed after meningeal cells enter the lesion and induce the astrocytic hypertrophism and the formation of a glia limitans (Fawcett and Asher, 1999). The astrocytes, closely apposed to one another, release in the extracellular space molecules such as chondroitin sulphate proteoglycans, composed of repeated disaccharide glycosaminoglycan chains (Rolls and Schwartz, 2006), that create a barrier to axonal regeneration (Dou and Levine, 1994; Asher et al., 2002). This inhibitory effect is confirmed by the fact that enzymatic degradation of the components of the scar promote the regeneration of axons through the scar (Bradbury et al., 2002; Grimpe and Silver, 2004).

1.5 OEC transplantation

Cell transplantation into the lesion is thought to provide a permissive environment for axons to regenerate through and moreover to promote neuroprotection and foster myelination and sprouting. OECs are amongst the most promising cell candidates for transplantation in the central nervous system. Therefore, in this experimental work, to overcome the impediments to long distance regeneration described in the previous section OECs have been transplanted. What follows is an overview describing the properties of OECs when residing in the olfactory system, when cultured and when transplanted into the central nervous system.

1.5.1 Olfactory system

The olfactory system can regenerate throughout life (Farbman 1990). It is the most ancient sensory system in the lineage of vertebrates to have evolved. The cell body of olfactory receptor neurons (ORNs) is located in the olfactory epithelium of the olfactory mucosa. ORNs are bipolar neurons with a dendrite that projects to the surface of the olfactory epithelium where sensory

transduction of odours occurs and with an axon which projects to the outer layer of the olfactory bulb and synapses with second order neurons called mitral cells. Non-myelinated axons of ORNs, upon exiting the epithelium and crossing the olfactory lamina propria, form fascicles which comprise the olfactory nerve or first cranial nerve (Graziadei and Monti Graziadei, 1985).

As a consequence of chemical or mechanical insult, ORNs normally die and are replaced throughout life thanks to a physiological turnover by newly differentiated ORNs originating from stem cells located in the basal layers (Lindsay et al., 2009). It is thought that during normal ORN turnover ORNs differentiate from globose basal cells located in the basal lamina, while after more severe damage it is thought that horizontal basal cells also located in the basal epithelium participate in the proliferative and restorative events that repair the olfactory epithelium including the formation of new ORNs (Duggen and Ngai, 2007; Leung et al., 2007). The axon of a newly differentiated ORN must traverse the length of the olfactory nerve and enter the central nervous system to make new connections with the mitral cells. It is important to emphasize that in mammals the turnover of CNS neuronal circuitry by newly differentiated neurons, originating from undifferentiated precursors, is a unique property found only in the olfactory system, the dentate gyrus and the subventricular zone (Raisman, 1985; Kaneko et al., 2009). Because such process may take place in the olfactory system two very unusual events are necessary: first, that the newly generated axons must traverse the olfactory bulb entry zone, a PNS-CNS boundary region; and second, that the newly generated axons must possess the ability to grow within the CNS and form new connections with CNS neurons. These special properties are thought to be mediated by OECs (Farbman, 1990; Barnett and Chang, 2004; Graziadei and Monti Graziadei, 1985).

1.5.2 Properties of OECs in the olfactory system

OECs, a unique glial population present only in the olfactory system, do not share their developmental origin with other known glial cell types and derive from precursors originating from the ectoderm in the olfactory placode (Chuah et al., 1991, Ramon-Cueto et al., 1998). Conversely Schwann cells and CNS glia

derive from the neural crest and the neuroectoderm respectively (Doucette, 1990). OECs are found to exist as two distinct cell sub-types *in vivo*: a spindle-like cell that ensheaths the axons of ORNs and traverses from the mucosa to within the olfactory bulbs and resembles non-myelinating Schwann cells and a cell that does not ensheath ORN axons. This cell is thought to share properties akin to astrocytes (Doucette, 1984) as it possesses similar morphological and histochemical features common to astrocytes (Barber and Lindsay, 1982). OECs *in vivo* have been shown to express several markers including the p75 neurotrophin receptor (p75 throughout the thesis), GFAP, the O4 antigen, S100 and neuropeptide Y (Chuah and West, 2002; Barnett and Chang, 2004).

1.5.3 Properties of OECs *in vitro*

OECs taken from the newborn and adult olfactory nerve, from the olfactory bulb and from the lamina propria give rise *in vitro* to a heterogeneous population of cells comprising of two main morphologies: the first termed, Schwann cell-like OEC has a spindle-like morphology typical of Schwann cells, expresses the low affinity neurotrophin receptor p75 and shows diffuse expression of glial fibrillary acidic protein (GFAP); the second termed astrocyte-like OEC has a flatter morphology, filamentous expression of GFAP, expresses embryonic N-CAM and lacks expression of p75 (Franceschini and Barnett, 1996; Raisman, 2001). Later studies demonstrated the plasticity of these cell types and suggested that each OEC cell subtype may switch between morphologies (van den Pol and Santarelli, 2003). Further evidence for this has been provided recently by time-lapse imaging of single isolated cells (Huang et al., 2008).

1.5.4 Myelination

An OEC in the olfactory nerve ensheaths without myelinating hundreds of thin (~0.2µm diameter) ORN axons. Nonetheless, OECs have the potential to myelinate axons that are above the threshold diameter for myelination. For example *in vitro* studies have shown that when rodent or canine OECs were

cocultured with large diameter axons they could myelinate these axons (Devon and Douchette 1992). However more conclusive evidence has come from transplantation studies using an *in vivo* model of persistently demyelinated CNS lesions. One of the first studies used a clonal OEC line and demonstrated myelination with peripheral type myelin (Franklin et al., 1996). Further studies have confirmed these original findings in rat (Imaizumi et al., 1998) and monkey (Radtke et al., 2004). Furthermore, OECs transplanted in rat spinal cord myelinated axons with P0 type myelin and formed intact nodes of Ranvier (Sasaki et al., 2006).

1.5.5 Interaction with astrocyte/CNS

OECs remain associated with newly generated axons while these traverse the boundary between the PNS/CNS allowing their entrance into the olfactory bulb (Franklin et al., 2000); here the glia limitans is not composed of astrocytes but OECs with an astrocyte-like morphology (Raisman, 1985; Douchette, 1991). This is in contrast to what occurs to all other peripheral nerves when their axons reach the glia limitans. For example, within a dorsal root a regenerating axon of a dorsal root ganglia neuron is ensheathed by Schwann cells, but upon reaching the dorsal root entry zone (DREZ) where the glia limitans is located, growth comes to a halt (O'Brien et al., 2001). Glia limitans is made up primarily of astrocytes which under conditions of hypertrophy are thought to inhibit regeneration.

In support of these *in vivo* observations *in vitro* studies using strips of OECs and astrocytes allowed to grow towards each other have shown that OECs can migrate within the astrocytic environment and intermingle; on the contrary Schwann cells allowed to grow towards astrocytes segregated from the astrocytes into separated patches forming boundaries that resembled the DREZ margins (Lakatos et al., 2000). Our group has further confirmed this finding *in vivo* by demonstrating that astrocytes mingle with OECs but not Schwann cells after injection into normal spinal cord (Lakatos et al., 2003). Furthermore other studies have reported better interaction of OECs with the host tissue compared

to Schwann cells (Santos-Silva et al., 2007; Andrews and Stelzner, 2007; Lankford et al., 2008).

1.5.6 Growth factors expressed by OECs

It has been reported that OECs secrete many growth factors in an autocrine and paracrine fashion both *in vitro* and *in vivo*. This property may contribute to axonal regeneration when OECs are transplanted into the CNS. Cultured OECs have been shown to secrete nerve growth factor (NGF), brain derived neurotrophic factor (BDNF) and to express glial cell-line derived neurotrophic factor (GDNF) (Woodhall et al., 2001; Lipson et al., 2003). These neurotrophic factors have been reported to promote the survival of several neuron populations, including peripheral ganglionic neurons (Barde, 1994; Sasaki et al., 2006).

1.5.7 Human derived OECs

The clinical use of OECs is for many scientists the ultimate aim of their research performed on animal models. Autologous cell transplantation will be preferable for clinical use to prevent adverse host-graft reactions and increase the successful outcome of OEC transplantation. The ideal non-invasive source of OECs is the olfactory mucosa, thus this OEC containing tissue will need to be easily removed from patients with a spinal cord injury, grown in culture to rapidly expand cell numbers so as to supply a reasonable amount of OECs for autotransplantation. OECs seem to fit these requirements as it has been shown that OECs purified from human biopsy tissue and from cadavers can be grown successfully in tissue culture (Miedzybrodzki et al., 2006, Barnett et al., 2000). Furthermore these cultured OECs were able to re-myelinate axons following transplantation into a rat model of induced persistent demyelination of the spinal cord (Barnett et al., 2000).

1.5.8 Neuroprotective effect on the lesion

Human spinal cord injuries develop cavities which grow in size with time as a consequence of cell dieback. Cavity formation can be found in rat models of spinal cord injury but not mice, and thus rats may offer a good model of study of the human injury. One of the most beneficial effects OECs exert when transplanted in rat spinal cord is to fill partially or totally the lesion cavity (Ramon-Cueto et al., 2000; Lu et al., 2001, Toft et al., 2007, Bretzner et al., 2008) and to stabilize it (Li et al., 1998, Toft et al., 2007), thus preventing it from forming cavitations which are the consequence of the progressive dieback of the degenerating tissue. Angiogenesis has been reported to occur within a rat crush lesion transplanted with lamina propria OECs (Ramer et al., 2004a; Ramer et al., 2004b), in an electrolytic lesion transplanted with OECs (Li et al., 1998) and in a dorsal column wire knife lesion model transplanted with mixed or pure populations of OECs (Toft et al., 2007); these blood vessels that formed *ex novo* were coated with laminin-rich basal lamina (Ramer et al., 2004a; Toft et al., 2007) and smooth muscle actin (Toft et al., 2007). In addition OECs have been suggested to induce a neuroprotective effect on neurons and their processes that are damaged following the lesion or that are localised close to the injury (Ruitenbergh et al., 2005; Toft et al., 2007).

1.5.9 Association of OECs with fibres in the lesion

The cavitation within a lesion is a major barrier for axons to regenerate through. The formation of an OEC scaffold within the lesion where otherwise there would be a cavity allows axons that are located in close vicinity to the lesion borders to regenerate within it. Various types of axons have been reported to grow into the lesion following OEC transplantation including: serotonin positive brainstem axons (Ramon-Cueto et al., 2000; Ramer et al., 2004a), noradrenergic positive fibres (Ramon-Cueto et al., 2000), tyrosine hydroxylase positive axons (Ramer et al., 2004a), neurofilament positive fibres (Lu et al., 2001; Ruitenbergh et al., 2003; Lu et al., 2006; Toft et al., 2007), corticospinal tract traced fibres (Li et al., 1998; Ramon-Cueto et al., 2000), fluororuby tract traced brainstem neurons

(Lu et al., 2001), sensory CGRP positive axons (Andrews and Stelzner, 2007), sensory afferent axons tract traced with cholera toxin or BDA (Andrews et al., 2004; Toft et al., 2007) and BDA tract traced rubrospinal fibres (Bretzner et al., 2008). Conversely there have been reports that BDA tract traced rubrospinal tract axons do not regenerate into a transplant (Ruitenberget al 2003; Ramer et al., 2004a) and the same for BDA tract traced corticospinal tract axons (Lu et al., 2006).

1.5.10 Interaction of OECs and spinal cord astrocytes

OECs are thought to promote axonal ingrowth into the lesion not only by providing a scaffold for the axons to grow in but also by promoting the growth of axons through the glial scar that lies between the growing axons and the lesion core. The glial scar is in fact thought to be one of the main inhibitors to axonal growth after injury. This scar is composed of many cell types of which astrocytes make up the main cellular component. Astrocytes become hypertrophic following injury and secrete chondroitin sulphate proteoglycans which are highly inhibitory to axonal growth. The OECs can closely interact with astrocytes and it has been reported that OECs prevent astrocytes from developing a tight pericavity boundary around the lesion, while promoting the formation of a diffuse permeabilised scar where the astrocyte processes align with OECs (Ramer et al., 2004a; Toft et al., 2007). Similarly, it was found that in an electrolytic or in a wire knife lesion the hypertrophy of astrocytes in the scar seen in the absence of transplantation was reduced following transplantation of OECs (Li et al., 1998; Toft et al., 2007), however this could not be confirmed by others (Andrews et al., 2004). Along the same line of evidence, OECs intermingled *in vitro* with meningeal cells, another major component of the glial scar; on the contrary when co-cultured with Schwann cells, meningeal and Schwann cells clustered away from each other (Franssen et al., 2009). Furthermore, the transplantation of mixed populations of OECs and meningeal cells rather than pure OECs promoted myelination (Lakatos et al., 2003).

1.5.11 OEC effects on long distance regeneration (anatomy)

While there is general consensus on the capacity of OECs to promote fibre ingrowth into the lesion, there is much debate on whether OECs alone can promote long distance axonal regeneration. A number of studies have reported that after transplantation OECs distribute not only in the lesion site but also in the rostral and caudal spinal cord tissue (Li et al., 1998; Ramon-Cueto et al., 2000; Lu et al., 2001; Andrews et al., 2004; Ruitenberg et al., 2005; Lu et al., 2006; Toft et al., 2007). It is possible that this may create in the CNS an axon friendly environment resembling the PNS tissue (Li et al., 1998) which in turn may enhance axonal regeneration over long distances.

Results obtained from anatomical, electrophysiological and behavioural studies of regeneration after OEC transplantation do not yet provide a clear picture of the extent to which OECs may promote CNS repair. In fact there are many contradictory reports on this subject, and one of the main aims of this thesis is to understand the limitations of OEC transplantation at the anatomical level.

Anatomical assessment of long distance regeneration is a *sine qua non* to prove regeneration: without anatomical assessment it is not possible to understand whether the treatment that has been applied to the spinal cord injury is actually inducing other reparative mechanisms other than long distance regeneration *per se*, such as re-myelination or reinforcement of pre-existing pathways.

At the same time reports of regeneration from anatomical studies must be considered carefully as an increasing number of publications omit to provide sufficient evidence for their conclusions. Furthermore these reports often omit fundamental information necessary for the reader to understand the methodology and thus to be able to fully appreciate the relevance of the study and to then reproduce it. Of interest might be this personal communication from Oswald Steward (at a course I attended in 2007 in U.C.I., U.S.A.): “up to date no one has yet provided unequivocal evidence that long distance axonal regeneration in the CNS does indeed occur”; an important review describing “false resurrections” of fibres after injury in the literature has been written by Steward and colleagues (2003).

1.5.11.1 Dorsal root injuries.

The first report of the effects of OECs after transplantation was published in 1994 by Ramon-Cueto and colleagues. In this study relatively pure OECs were transplanted at the dorsal root entry zone at the thoracic level after dorsal root rhizotomy and anastomosing the root back to the same location. Three weeks after the operation the rats were perfused and a crystal of the fluorescent tract tracer carbocyanine Dil was placed at the tip of the dorsal root to reveal any regenerating axons in the spinal cord. It was reported that the dorsal root afferent axons effectively entered the spinal cord and regenerated to the contralateral side into the grey matter. The same group reported in 1999 that OECs transplantation following rhizotomy of the lumbar roots that were reapposed to the original entry zone location promoted CGRP positive axons to regenerate back into the spinal cord (Navarro et al., 1999). Finally, a report from the same group in 2002 claims to demonstrate that OECs allow afferents entering through the lumbar and sacral dorsal roots to project to the sacral parasympathetic nucleus and thus restore bladder activity following rhizotomy (Pascual et al., 2002). The anatomical evidence of this study using wheat-germ agglutinin coupled to HRP (WGA-HRP) tract tracing revealed the presence of presumptive regenerating fibres that reached their proper destinations in the grey matter in the OEC transplanted animals only.

The report from Ramon-Cueto and colleagues (1994), can be criticised by suggesting non-specific labelling of the Dil tract tracer rather than regeneration, as images of individual afferent profiles are difficult to distinguish in the images provided (Riddell et al., 2004). Furthermore in the report of Navarro and colleagues, CGRP labelling is not a strong evidence of regeneration as it is thought by many that intraspinal sprouting of intact fibres adjacent to the rhizotomy underlies this recovery of CGRP immunoreactivity (Belyantseva and Lewin, 1999; Riddell et al., 2004). Finally, with regards to the WGA-HRP tracing method described by Pascual and colleagues, fibre sparing cannot be excluded as a detailed study performed by our group could not confirm axonal regeneration past the DREZ after rhizotomy and OECs transplantation (Riddell et al., 2004). In this work olfactory bulb OECs with a purity of over 70% were

transplanted at the L4 DREZ of adult syngeneic rats following a prior dorsal root injury and reanastomosis. By means of BDA tract tracing, 1 to 6 months after the injury, it was possible to show that no significant regeneration of afferent fibres could be detected beyond the site of injury (Riddell et al., 2004). In confirmation of our findings Gomez et al. (2003) using CTB tract tracing and CGRP immunocytochemistry could not detect regeneration of axons across a rhizotomy lesion at the cervical level after transplantation with purified olfactory bulb OECs. Furthermore, Ramer and colleagues (2004b), using anterograde tract tracing, did not find any regeneration beyond the DREZ in cervical, thoracic and lumbar crushed dorsal roots 2 or 4 weeks after the lesion following transplantation of olfactory mucosa OECs. Taken together these studies on DREZ regeneration are in conflict with each other and certainly do not prove convincingly that OECs transplants promote long distance axonal regeneration from dorsal roots into the spinal cord.

1.5.11.2 Spinal cord injuries

In a very interesting pioneering study olfactory bulb OECs were injected into an electrolytic injury to the corticospinal tract (CST) at the thoracic level in rat (Li et al., 1998). In this study OECs promoted the regeneration of CST axons within the electrolytic lesion and their growth beyond the lesion into the caudal grey matter. Interestingly, the BDA labelled CST fibres in the caudal host spinal cord viewed by electron microscopy and immunohistochemistry were ensheathed by peripheral type myelin in a characteristic peripheral-type one to one myelinating relationship with the presumptive OECs and were devoid of CNS glia such as astrocytes or oligodendrocytes or microglia (Li et al., 1998). Even more interestingly, the article reported that the regenerating CST axons re-entered the host environment abandoning the PNS type environment provided by the transplant and giving rise to mixed nodes of Ranvier, formed on one side by peripheral myelin and on the other by central type myelin as identified by P0 and MOG combined immunohistochemistry. Although inspiring, and giving much hope to the SCI community, this work was never repeated by others making it difficult to build new constructive work from it. Being generous one could say either the authors were years ahead of anyone else in the field or the data

produced lacked strong evidence. A second report claiming long distance axonal regeneration after a complete transection of the spinal cord at the thoracic level was published by Ramon-Cueto and colleagues (2000). Serotonergic, noradrenergic and corticospinal-BDA labelled fibres were found up to 3 cm into the distal cord 11 months after injury only in those rats that received a concurrent transplantation of olfactory bulb-derived pure OECs, while no regeneration was observed in non-transplanted rats. All images provided showed close correlation between OEC distribution and fibre location, however no clear description is present in the paper regarding OEC distribution in the distal cord and regarding unusual fibre morphology. The fact that no description of unusual fibre appearance (i.e. end bulbs, enlargements) is reported in this paper and that fibres were located in areas normally innervated in un-injured animals leads to some doubt on the authenticity of the regenerating fibres. In another report, Imaizumi et al. (2000) indicated bridging axonal regeneration across a dorsal column transection lesion, however the only photographic evidence available is that of axons bridging the lesion in one animal in what seems an extremely lateral section where sparing could be involved, and the axonal morphology doesn't suggest otherwise. No indication of the relationship between transplanted cells and regenerating fibres is given either. At a similar time it was reported by Lu and colleagues (2001) that transplantation of mixed olfactory mucosa OECs produced a positive effect on long distance regeneration after a complete transection of the thoracic cord. Ten weeks after the injury regeneration was assessed by fluororuby retrograde transport and by serotonin labelling in the distal cord. Fluororuby labelled neurons were found in the brainstem motor nuclei after injection of the tracer in the distal spinal cord in rats that received OEC transplantation but not in control animals; in conformity with this observation serotonin positive axons were seen in white and grey matter of OECs transplanted rats at a distance of up to 6 mm from the transplant site. The same authors in a subsequent study with a similar lesion paradigm but involving delayed OEC transplantation reported similar findings (Lu et al., 2002). Importantly, this study was replicated by Steward et al. (2006) who did not detect extensive regeneration, thus raising scepticism on the validity and reproducibility of both the reports by Lu et al. (2001 and 2002). Furthermore, the relationship between transplanted OECs and distally regenerating axons was not addressed by Li et al. 2001. Finally, a report not

involving tract tracing but serotonin and tyrosine hydroxylase immunohistochemistry described long distance regeneration/sparing in a rat cervical dorsal funiculus crush model (Ramer et al., 2004a). The relation between OEC distribution and regenerating/spared axons on the other side of the lesion was investigated using p75 labelling, but no p75 labelling was detected above the cord at the survival time when regeneration was studied. It must be remembered anyhow that p75 labelling does not label myelinating OECs.

Reports on the lack of ability of OECs to promote regeneration after spinal cord injury have been provided by a number of groups including ours. It was shown that no BDA positive anterogradely tract traced rubrospinal tract axons crossed the proximal border of the lesion in rats transplanted with purified olfactory bulb OECs 4 months after a complete transection of RST projections at the cervical level (Ruitenbergh et al., 2003). Furthermore, no regeneration of tract traced rubrospinal tract axons was seen when 98%-100% pure olfactory mucosa OECs were transplanted 1 or 4 weeks after a cervical crush injury (Ramer et al., 2004a). In addition, lesions of the corticospinal tract grafted with 95-98% pure olfactory bulb OECs did not promote CST anterogradely BDA labelled fibres to extend beyond the cervical site of injury 3 months after the lesion (Ruitenbergh et al., 2005) or 1 month after a cervical dorsal column wire knife lesion and transplantation of 98% pure olfactory mucosa OECs (Lu et al., 2006). Similarly, when considering the ascending sensory DRG neurons, it was reported that 80% pure olfactory bulb OECs transplanted into a thoracic crush lesion severing the dorsal funiculi did not promote regeneration of sensory afferents tract traced with cholera toxin-HRP beyond the site of injury, after a survival time of between 2 days and 2 weeks (Andrews et al., 2004). There was no regeneration beyond the injury even when OECs were optimally distributed to allow bridging of the lesion. Our group in a thorough and detailed study involving transplantation of olfactory bulb mixed OECs or >98% pure OECs into a wire knife dorsal column injury performed at the L3-4 border were also not able to detect any significant growth of BDA nor CTB labelled axons beyond the lesion 2-3 months after the lesion (Toft et al., 2007).

Table 1 summarises these publications and their main findings with reference to OEC distribution, myelination and importantly regeneration. Taking all these reports together, the non uniformity of methods used by the different groups

such as the origin of OECs (olfactory mucosa/bulb), the cell purity (mixed/pure transplants of OECs), the type of lesion applied (contusion/ electrolytic/ transection/wire knife), the location of the lesion (cervical/ thoracic/lumbar), the tract lesioned (CST/RST/DRG axons), the tract tracer used (BDA/CTB), the survival period (days/weeks/months) and finally the assessment method are likely to have influenced the great diversity in outcome after OEC transplantations. In our view and that of others, those publications that do claim long distance regeneration do not provide sufficiently strong evidence that there was an absence of spared fibres (Steward et al., 2004; Lu et al., 2006). Furthermore it would be advisable for published works to give a description of unusual fibre morphology, location, absence of sparing or sprouting and possibly even photographic evidence. Part of the study carried out in this thesis will try to clarify these points.

| Publication | Tract | Spinal cord lesion type | OEC distribution | Myelination | Long distance axonal regeneration | Comments |
|----------------------------|--|-------------------------|-----------------------------------|-------------|-----------------------------------|---|
| Li et al., (1998) | CST | electrolytic | extensive both rostral and caudal | yes | yes | Poor clues to suggest regeneration rather than sprouting. Same type of electrolytic lesions associated with sparing (Keyvan-Fouladi et al., 2003). Long distance axonal regeneration here is not always associated with OECs. |
| Ramon-Cueto et al., (2000) | CST | complete transection | yes, no clear description | na | yes | Low resolution images of putative regenerating axons. Furthermore, no indication of unusual axon morphology. |
| Imaizumi et al., (2000) | DRG | Incomplete transection | yes, rostral and caudal | yes | yes | Images and text are suggestive of sparing but not axonal regeneration. Distal axon-OEC localization not studied. |
| Lu et al., (2001) | neurons of the raphe nuclei | complete transection | yes, rostral and caudal | na | yes | Steward et al., (2006) could not see regeneration after replication of Lu et al., (2002) (same method as Lu et al., (2001)). Distal axon-OEC localization not studied. |
| Ramer et al., (2004a) | neurons of the locus coeruleus/ raphe nuclei | crush injury | no | na | yes | p75 to detect transplanted OECs. Crush injury cannot rule out sparing/sprouting. No tract tracing involved. |
| | RST | | | | yes | |

| | | | | | | |
|--------------------------|-----|---------------------------------|-------------------------|----|----|--|
| Ruitenberget al., (2003) | RST | complete transection | no | na | no | p75 was used to detect transplanted OEC. |
| Ruitenberget al., (2005) | CST | unilateral transection | no | na | no | p75 was used to detect transplanted OEC. |
| Lu et al., (2006) | CST | dorsal column wire knife lesion | yes | no | no | the presence of optimally distributed tracts of OECs proximal to the corticospinal axons was not enough to promote regeneration. |
| Andrews et al., (2004) | DRG | dorsal column lesion | yes, rostral and caudal | na | no | the presence of optimally distributed tracts of OECs was not enough to promote bridging regeneration. |
| Toft et al., (2007) | DRG | dorsal column wire knife lesion | yes, rostral and caudal | na | no | the presence of optimally distributed tracts of OECs was not enough to promote bridging regeneration. |

Table 1. Summary of studies performed on OEC transplantation focusing on OEC distribution, myelination and promotion of long distance axonal regeneration.

As it can be observed in the table, these studies mostly investigated descending systems, used the term regeneration even in crush injury type lesions, did not provide sufficient evidence for regeneration and did not investigate thoroughly the relation between OEC distribution and long distance axonal regeneration.

1.5.12 *Effects of OECs on functional recovery*

Following OEC transplantation into the spinal cord injury, behavioural tests of functional recovery have so far provided the field with inconsistent results (Toft et al., 2007). Behavioural functional recovery was described by Li et al. (1997) after electrolytic lesions of the corticospinal tract; by Ramon-Cueto et al. (2000), Lu et al., (2001, 2002) and Lopez-Vales (2006) after complete transection of the spinal cord and by Plant et al. (2003) after contusion lesion. However, these results were not confirmed in other studies that involved spinal cord contusion and transplantation of OECs into the lesion (Takami et al., 2002), nor in a study involving complete transection of the spinal cord by Steward et al. (2006), an investigation that aimed to replicate the study of Lu et al. (2002). One mechanism commonly proposed to foster the improved functional recovery observed is long distance axonal regeneration and functional connection, however strong evidence supporting the existence of functional connection following regeneration is not yet available. Other mechanisms that may explain the functional improvements include reduction of inflammation, remyelination, synaptic plasticity and sprouting (Priestley, 2007). It is possible that OEC transplantation may enhance any of these processes or that OEC transplantation might promote neuroprotection of the tissue in the lesion vicinity so that once the above restorative processes occur and functional connectivity is restored in animals transplanted with OECs will show a functional advantage over non-transplanted animals (Weidner et al., 2001; Andrews et al., 2004).

1.6 Sensory neuron anatomy – lumbar 4-5 DRG neurons and primary afferent fibres

Dorsal root ganglia neurons bring information from the somatic sensory receptors located in muscles, skin and viscera to the spinal cord and brain. Neurons in the DRG at the L4 and L5 level especially (on which we shall focus in subsequent chapters), but also at the L3 and L6 level convey information originating from the hind limb. Figure 1-1 depicts a DRG neuron and its axon. The soma of the DRG neuron is located in the DRG; each neuron in the DRG gives rise to a

pseudounipolar axon called a primary afferent axon which forms a peripheral branch and a central branch. The peripheral axons of L4 and L5 DRG neurons run through the corresponding spinal nerve and then through the sciatic nerve reaching finally the sensory receptors in the periphery. The central axon, instead, runs through the corresponding dorsal root and enters the spinal cord at the dorsal root entry zone. Upon entering the spinal cord each axon courses medially and divides in two branches: an axon that runs caudally and an axon that runs rostrally for varying distances, both giving rise to multiple axon collaterals that synapse with second order neurons in the dorsal horn, intermediate region and ventral horn in the spinal cord grey matter. Some of the axons upon entering the cord run rostral through the dorsolateral fasciculus (also known as tract of Lissauer) while most of the axons run through the dorsal column (also termed dorsal funiculus) within the fasciculus gracilis and some of these project to as far as the gracile nucleus, that is part of the dorsal column nuclei in the brain stem (Willis and Coggeshall, 2004). Two main classifications exist to group sensory afferents and these were classified based on electrophysiology using Greek letters (Erlanger and Gasser, 1937) and on fibre diameter using Roman letters (Lloyd, 1943). The two classifications correspond so that it is possible to divide the afferents into large very fast conducting myelinated muscle afferents (A α or group I), medium size fast conducting myelinated muscle and cutaneous afferents (A β or group II), thin slow conducting myelinated muscle and cutaneous afferents (A δ or group III) and very thin slow conducting non-myelinated muscle and cutaneous afferents (C or group IV). Subsequently, Lawson and Waddell (1991) studied neurofilament expression and electrophysiology of the neurons and found that almost all A fibre somata expressed neurofilament while almost all somata of C fibres did not. The fibres that run through Lissauer's tract are comprised mainly of thin III/A δ and IV/C fibres that terminate within 1-2 segments rostral (Willis and Coggeshall, 2004). The fibres running through the dorsal columns instead are comprised mainly of large and medium A α /I AB/II fibres that terminate rostrally within 4-12 segments. Only 15% of L4 primary afferents in rat project up to the gracile nucleus (Giuffrida and Rustioni, 1992), consisting only of the cutaneous type II/AB afferents.

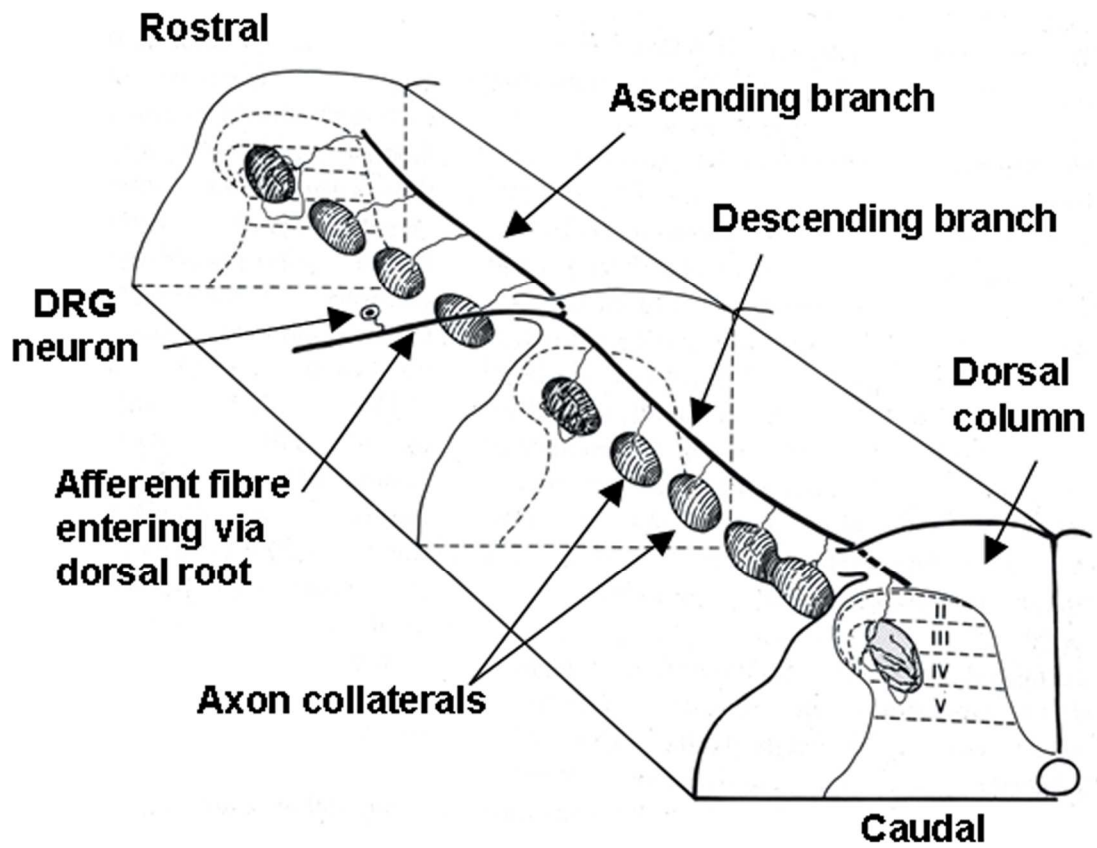


Figure 1-1. The anatomy of primary sensory afferents.

The primary sensory afferent fibre enters the spinal cord and sends a branch caudally and one rostrally running through the dorsal columns. Each fibre then branches, forming multiple collaterals into the grey matter (modified from Brown et al., (1978)).

1.7 Conditioning lesion

Gutmann's finding that the regeneration rate of the peroneal nerve was greater after two rather than one peripheral crush lesion was ignored for many decades (Gutmann, 1942). "This strange phenomenon" as described at the time by Gutmann was later named the "conditioned lesion effect" (McQuarrie and Graftstein, 1973). McQuarrie and Graftstein discovered that when a peripheral nerve received a "conditioning or priming lesion" and one or two weeks later the same nerve was crushed at a more proximal position ("test lesion") the rate of regeneration at the test site was significantly increased as a result of the prior conditioning lesion. They suggested that the conditioning lesion might produce a retrograde response that in turn initiates specific macromolecular synthesis necessary for regeneration so that primed neurons are prepared to respond without delay by the time the test lesion is made.

Richardson and Issa described in 1982 a similar yet different effect by which not only the temporal but also the spatial separation between the priming and test lesions enhanced the regeneration properties of the test lesion itself (Richardson and Issa, 1982). They injured the peripheral processes of the L4 and L5 DRG neurons of adult rats by transecting the sciatic nerve at different time points before, after or at the time of the spinal cord injury. The dorsal columns were incised bilaterally at the cervical level and a piece of sciatic nerve was placed into the spinal cord lesion to provide a suitable environment for regeneration to occur. Two to three months after the spinal cord injury the beta subunit of cholera toxin conjugated to HRP was injected in the transplanted nerve stump and the HRP positive DRG neurons were counted. Surprisingly, the result was a potent and comparable increase in regeneration of neurons that were primed 1 or 4 weeks before (pre-priming) or at the time of the spinal cord injury compared to un-primed neurons. In particular when the priming was concurrent with the central lesion the regeneration levels into the stump were increased by 100 fold. When the neurons received a priming lesion 1 or 4 weeks after (post-priming) the central lesion, a strong but yet significantly less potent regenerative effect in the nerve stump was registered as compared to the pre-priming paradigms. Such results indicated for the first time that the injury to the periphery of the DRG processes enhances the regenerative properties of the

central processes. Their methodology did not ascertain though whether any regenerating fibres had grown beyond the transplant into the distal spinal cord, because their main aim was to ascertain whether in optimal conditions (peripheral nerve stump rather than inhibitory milieu of the spinal cord) peripheral priming would increase central regeneration.

Similar experiments were carried out in greater detail by Oudega and colleagues (1994) confirming that inserting a peripheral nerve graft into the thoracic spinal cord of adult rats produced very little regeneration in the graft unless a conditioning lesion was performed on the peripheral process of the DRG neurons. Moreover this work showed that it was preferable to perform the conditioning lesion 1 week before rather than concurrently with the central lesion. The use of a pre-degenerated peripheral nerve graft rather than of a fresh one strongly potentiated the regenerative response of both conditioning lesion time point paradigms, also greatly increasing the difference between the two. However, regenerating fibres stopped abruptly at the distal transition zone between the nerve stump and the cord and no regeneration was ever observed in the distal spinal cord.

Importantly, Woolf's group reported regeneration beyond the spinal cord injury following a conditioning lesion without the necessity of modifying the trophic support of the lesion site (Neumann et al., 1999). The dorsal columns of adult rats were cut at the thoracic level using microscissors. Following B-HRP injection in the sciatic nerve to trace ascending sensory fibres no regeneration could be detected in or beyond the lesion site 7 to 9 weeks after the spinal cord injury. However, performing a sciatic nerve transection concurrently with the spinal cord lesion resulted in great axonal growth into the injury site. In addition, if the sciatic nerve was sectioned 1 or 2 weeks prior to the spinal cord lesion the response was even greater and many axons could be seen to grow through the injury site or around it and for long distances within the spinal cord grey matter and to a limited extent in the white matter. These axons could be followed for up to a distance of 4 mm from the lesion site, however no terminal or collateral connections were detected in the dorsal horn grey matter. In light of this study, regeneration after a complete transection of the dorsal columns can take place without provision of any permissive growth environment in the lesion site if a conditioning lesion is performed prior to or at the time of the central lesion.

However these results were not confirmed by Andrews et al. (2004) who injured the sciatic nerve one week prior to the spinal cord crush lesion and found that transganglionic CTB tract tracing revealed regeneration into the injury site but not beyond into the distal cord.

1.7.1 *Modus operandi*

As seen in other neuronal cell types, damage to the peripheral branch of DRG neurons has been shown to elicit a strong response in their cell body. These comprise the modification of the expression of multiple genes that are associated with axonal growth such as GAP43 and tubulin (Hoffman, 1989). In contrast, when the same axons are damaged on their central branch the expression of the same set of genes is not modified (Bulsara et al., 2002). In conformity with this the peripheral but not the central branch is able to regenerate following a lesion (Ramon y Cajal, 1928). As described in the previous section, a lesion performed on the peripheral branch enables the central branch to regenerate.

One of the main components involved in the signal transduction pathway that occurs following a conditioning lesion is thought to be cAMP concentration. The cAMP levels in the DRG and other neurons are thought to be tightly related to the growth state of the neuron. The levels of cAMP in rat DRG are high in the embryonic phase and decrease dramatically during development; this switch of expression soon after birth is temporally correlated to the switch from promotion to inhibition that myelin exerts on cultured DRG neurons (Cai et al., 2001). It was shown that pharmacological intervention to modify the cAMP levels in *Xenopus Laevis* cultured spinal cord neurons could switch their repulsion to myelin associated glycoprotein (MAG) into attraction (Song_Poo et al., 1998). Accordingly, neurotrophin treatment, which overcomes MAG inhibition, was reported to increase cAMP levels in rat cultured DRG and cerebellar neurons if the neurotrophins were supplied before exposing the neurons to the MAG inhibition (Cai et al., 1999). Moreover increasing the levels of cAMP or its permeable analogs *in vitro*, has been shown to enhance the growth capacity of embryonic and adult rat DRG neurons in the absence of inhibitory substrates

(Rydel and Green, 1988; Andresen et al., 2000). By means of specific binding to the neurofilament antibody this observation was confirmed also when considering only the medium and large diameter myelinated populations of sensory neurons that project to the dorsal columns (Neumann et al., 2002). Neurofilament positive fibres *in vitro* were also able to grow on a myelin coated surface if before dissection the DRG were primed with a c-AMP analog (Neumann et al., 2002).

To what extent do these findings translate *in vivo*? A cAMP analog, db-cAMP, was delivered in adult rats to the L4 and L5 DRG 48 hours before lesioning the dorsal columns at the T6-T7 level (Neumann et al., 2002). Six to eight weeks following this procedure regeneration was assessed and a large number of axons were seen to regenerate into the lesion site, however no fibres bridged the lesion to the other side. The extent of regeneration achieved was comparable to that observed following a single conditioning lesion made at the same time as the central lesion as described above in the report by Neumann et al. (1999). As expected, no fibres entered the lesion in untreated animals and in saline injected controls (Neumann et al., 2002). Similar results were published by Filbin's research group after injecting db-cAMP into adult rat L4 and L5 DRG one week prior to the dorsal column injury at the T7 level. Transganglionic labelling of HRP coupled with beta cholera toxin showed that 9-17 days after the spinal cord injury in all animals regenerating axons grew within and beyond the lesion for several millimetres. On the contrary saline injected animals showed no signs of regeneration at or beyond the lesion site (Qiu et al., 2002). These two works differ considerably in the timing of the experimental procedures, yet they describe similar regeneration outcome, suggesting that *in vivo* intervention to alter cAMP levels may be a reasonable direction to take for maximizing axonal regeneration.

Elevated levels of cAMP are associated with an elevation of the intrinsic growth state of the DRG neuron. Conditioning lesions might act on the same intracellular signal transduction pathways neurotrophins act on and to elevate the growth response in a similar mechanism. In fact conditioning lesions increase the cAMP levels in adult DRG (Qiu et al., 2002). Furthermore, priming neurons with conditioning lesions or with neurotrophins or with cAMP blocks the inhibition exerted by MAG and myelin on DRG cultures (Cai et al., 1999; Qiu et

al., 2002). Importantly, when DRG neurons are primed by conditioning lesions, NGF or BDNF in the presence of an inhibitor to protein kinase A, MAG or myelin inhibit DRG extension (Cai et al., 1999; Qiu et al., 2002). PKA inhibition, though, had no effect when DRG or cerebellar neurons received neurotrophic factor 3 (NT3) stimulation (Cai et al., 1999) which may follow a cGMP dependent pathway (Song et al., 1998). If DRG cells were exposed simultaneously to neurotrophins and MAG/myelin then DRG neuronal extension was inhibited, but if also the G_i protein inhibitor, pertussis toxin, was added then MAG/myelin inhibition was abrogated and cAMP levels increased (Cai et al., 1999). Considering that the Rho GTPase is a downstream effector of the inhibition exerted by MAG, Nogo and also chondroitin sulphate proteoglycans and semaphorins (Fawcett et al., 2006) and that PKA can phosphorylate and inactivate the G protein RhoA it is possible that conditioning lesions exert their effect through elevation of cAMP and consequent activation of PKA which in turn phosphorylates its target proteins, amongst which stands the Rho GTPase. Inactivation of Rho would ultimately override the inhibitory signals initiated by the scar and by myelin (Cai et al., 2001). The expression of tubulin, a growth associated protein, has been shown to increase strongly in DRG following intraganglionic injection of db-cAMP or conditioning lesions in adult rats when compared to saline injection animals. Interestingly, tubulin expression augmentation was stronger and the duration longer following a cAMP injection when compared to a conditioning lesion and lasted up to 28 days post-injection before returning to baseline levels (Han et al., 2004). Expression of other growth associated proteins such as GAP43 and CAP23 has been shown to increase following a lesion of the peripheral but not the central branch of DRG, however no studies have yet linked these proteins to the above signal transduction mechanisms.

1.8 Aims of the study

Despite extensive research, some of the important aspects on the effects carried out by OEC, Schwann cell and fibroblast transplantation on a spinal cord lesion are still unclear. The aims of the present study are outlined beneath in the following sections.

1.8.1 Aims of Chapter 3

- 1) Injections of the tract tracer BDA have previously been performed into the DRG, but never into the spinal nerves. However in studies of axonal regeneration, to reduce the possibility of BDA uptake into ascending sensory axons in other dorsal roots other than the L4 and L5, injection into the L4 and L5 spinal nerves should be of advantage compared to injection into the L4-L5 DRG. Therefore, BDA was injected into the L4 and L5 spinal nerves to characterise this novel methodology with the use of streptavidin conjugated to a fluorescent dye and confocal and epifluorescence microscopy.
- 2) The wire knife lesion of the dorsal columns is a transection type injury that was performed in our study in order to ablate all ascending sensory axons entering through the L4-L5 dorsal roots. The characterisation the wire knife lesion morphology 6 weeks after the injury in the absence of any treatment involved light microscopy and the use of GFAP antibody coupled with epifluorescent microscopy. Fluorescent microscopy was also adopted to determine the effects of the lesion on the interruption of the tract traced L4-L5 ascending sensory axons labelled with BDA.
- 3) Following the wire knife lesion, only axons located to the far left of the dorsal columns were detected in the lesioned animals. To understand if these axons were spared following the wire knife lesion technique, firstly, the morphology of these tract traced axons was studied; secondly, some animals received an extended wire knife lesion that was meant to ablate even very left hand side located axons.

- 4) OECs have been previously reported to reduce lesion cavity formation. To confirm this in our wire knife lesion model, the size of the lesion cavity was determined in animals transplanted acutely with OECs by using light microscopy. Furthermore, to determine the size of the astrocytic glial scar, GFAP labelling was used in conjunction with confocal microscopy.
- 5) After the wire knife lesion the central canal developed a cavity. To understand if OEC transplantation would reduce the level of cavitation the size of the central canal was measured on all animals with and without OEC transplantation.
- 6) No published research papers have determined so far the effects of OEC transplantation on ascending axonal regeneration after a transection type lesion. To determine the extent of regeneration 6 weeks after the lesion and after acute OEC transplantation, the number of axons was counted at increasing distances from the lesion.
- 7) A common limitation other works published in the literature have is the insufficiency of evidence to support the regenerative nature of the axons analysed. For this purpose, all processed material in the present work was carefully analysed and an over-conservative approach was used to study regeneration and distinguish it from sprouting or sparing. Furthermore, to confirm the regenerative nature of the axons some OEC transplanted animals were lesioned with an extended injury.
- 8) The spatial relationship between OECs and regenerating or sprouting axons has so far been investigated only qualitatively and to a very limited extent. To understand if BDA labelled axons grew preferentially through OEC seeded tracks, double labelling for GFP-OECs and BDA tract traced axons was adopted and axons located within or outwith regions of OEC distribution were counted.
- 9) Genuine regeneration of axons has never been studied following a combined treatment involving OECs transplantation and conditioning lesions of the sciatic nerve. To determine if axonal growth was boosted by

this combined method conditioning lesions were performed before and at the time of the central injury.

- 10) To understand the time course of OECs distribution animals transplanted acutely with OECs were given survival times of 2 days, 2, 6 and 17 weeks.
- 11) To understand how the number of sprouting/regenerating and genuine regenerating axons varied over time, conditioned lesioned animals were transplanted with OECs and were given 2, 6 and 17 weeks survival times.

1.8.2 Aims of Chapter 4

- 1) Schwann cells are an optimal candidate for cell transplantation. No convincing study has so far compared directly OEC and Schwann cell transplantation in the same lesion paradigm to determine their regenerative promoting properties. For this purpose Schwann cells were injected into the wire knife lesion using the same methodologies applied to OEC transplantation.
- 2) To determine whether fibroblasts were able to reproduce the results obtained following OECs and Schwann cell transplantation (i.e. to ascertain if the effects of OECs and Schwann cells is specific to these cells only), fibroblasts were transplanted in the same lesion paradigm.
- 3) Dorsal column wire knife lesions were also transplanted with Schwann cells to compare their level of integration and compare lesion and central canal preservation compared to OECs.

1.8.3 Aims of Chapter 5

- 1) Delayed transplantation is the necessary stepping stone for any spinal cord lesion treatment to reach clinical trial. OECs were transplanted 4

weeks after the dorsal column lesion to assess cell integration into the spinal cord 6 weeks later.

- 2) While there is evidence of axonal growth into the transplanted lesion, no convincing evidence is present on long distance axonal regeneration after a delayed OEC transplant. To understand whether axons could bridge the lesion and grow on the other side, BDA tract tracer was injected after the delayed transplantation 2 weeks prior to perfusion.
- 3) To understand whether OEC tracks were necessary to allow growth or regeneration of axons distal to the lesion as seen in the third chapter for acute transplanation, the colocalization of BDA and GFP-OEC was studied.
- 4) Finally, to understand whether delayed conditioning lesions would be effective at boosting axonal growth after OEC transplantation, the sciatic nerve was cut 4 weeks after the central lesion concurrently with the transplant.

2 Materials and Methods

2.1 Cell culture

Olfactory ensheathing cells, Schwann cells and fibroblasts were cultured and transplanted into the injured spinal cord to study the effects these cells exerted following the same lesion paradigm.

2.1.1 Preparation of the olfactory ensheathing cells from the olfactory bulb

In this study olfactory ensheathing cells (OECs) for transplantation were prepared from the olfactory bulb. The cellular population of the olfactory bulb consists of a mixture of cell types including oligodendrocytes, astrocytes, OECs and neurons. To purify OECs from this mixture of cell types fluorescence activated cell sorting (FACS) and cell type antibodies were used. The principle by which this separation is achieved is relatively simple: dissociated cells tagged with appropriate fluorescent markers flow one at a time through a small nozzle. The cells travel down the nozzle which is vibrated at an optimal frequency to produce drops at a fixed distance from the nozzle. As the cells flow down the stream of liquid, they are scanned by a laser. Some of the laser light is scattered by the cells and this is used to count the cells but also can be used to measure the size of the cells. The laser light also excites the fluorochrome attached to the cells which emits light at a frequency that is detected by a photomultiplier tube. By collecting the information from the light (scatter and fluorescence) a computer can determine which cells are to be separated and collected. The FACS machine applies an electromagnetic field which deviates the cell trajectory and redirects the selected cells to a specific collecting tube while excluding all other cells, dead cells, debris and auto-fluorescent material. Our laboratory has shown that OECs express the O4 antigen *in vivo* (Franceschini

and Barnett, 1996), however the O4 antigen is also expressed by oligodendrocytes (Sommer and Schachner, 1981). Galactocerebroside is the major galactosphingolipid in myelin; and it has been shown that anti-galactocerebroside antibody specifically binds to oligodendrocytes but not OECs (Ranscht et al., 1982). Therefore it is possible to discriminate and purify OECs from the other cell types present in the olfactory bulbs by using FACS coupled with O4 and GalC monoclonal antibodies (Barnett et al., 1993). The protocol followed to purify the OECs was a modification of that designed by Barnett and colleagues (1993) and is described below.

2.1.1.1 Dissection

Olfactory ensheathing cells were purified from the olfactory bulbs of post natal day 7 Fisher 344 rats, typically from 4-5 animals. Rats were sacrificed with an overdose of Euthatal (sodium pentobarbital, 200 mg/ml, Vericore Ltd, UK) in accordance with UK Animals Scientific Procedures Act of 1986 under the restrictions and regulations of the schedule 1 killing method.

After death, rats were placed on ice to maintain cell viability. The dissection was carried out on a polystyrene box top covered with tin foil in non sterile conditions; however animals, instruments and working surface were disinfected with ethanol to reduce the risk of microbial infection. The head was cut and immobilized with a needle and the skin was cut away to uncover the skull. Using forceps and scissors the olfactory bulbs were exposed, excised and placed in a 7 ml bijoux tube containing 1-2 ml of L15 and 25 µg/ml gentamicin. Samples were then transported from the animal house to the tissue culture facility in the Beatson. From this step onwards all procedures were carried out in a vertical laminar flow bench with the use of sterile material.

2.1.1.2 Dissociation

The sample containing the olfactory bulbs was maintained on ice as much as possible throughout the purification procedure in order to promote cell viability. Within 2 hours from dissection the olfactory bulbs were transferred to a 90mm Petri dish and all media was removed with a Pasteur pipette. The tissue was dissociated by chopping it into small pieces using a scalpel, followed by enzymatic dissociation by placing the sample in a 7 ml bijou tube containing 0.5 ml of a 1.33% collagenase solution for 30 min at 37°C. Subsequently 0.5 ml of a mix (SD) of soya bean trypsin inhibitor (0.52 mg/ml) and DNase1 (0.04 mg/ml) were added mainly to prevent cell clumping from the DNA released from dead cells.

The sample was finally fully dissociated into a cell suspension using a syringe attached to needles of decreasing diameter: starting with a needle sized 18 gauge, switching to a needle sized 23 gauge and ending with a needle sized 26 gauge. It was vital during this second step of mechanical dissociation to be gentle and not to pull or push the syringe plunger too hard as this would have produced strong negative or positive pressures that would have had a detrimental effect on cell viability.

Subsequently the sample was transferred into a 15 ml falcon centrifuge tube and washed in 4 ml of DMEM containing sorting media and centrifuged at a g-force of 306 m/sec^2 , discarding the supernatant and leaving the pellet in a small volume of liquid. This allowed the pellet to be easily resuspended in the remaining solution by flicking the tip of the tube.

2.1.1.3 Cell purification step

The sample contained in the tube was gently resuspended in filtered primary antibodies and left 30 minutes on ice: the solution of primary antibodies was a mixture comprised of the O4 antibody (mouse monoclonal IgM, 1:4) and anti-galactocerebroside (mouse monoclonal IgG3, 1:2) antibodies, diluted in sorting media to a final volume of 2 ml.

The excess of primary antibodies was removed by two washes and the sample was resuspended and incubated with a mix of secondary antibodies for 15 minutes on ice: goat anti-mouse IgM Phycoerythrin (1:100, Southern Biotech) and goat anti mouse IgG3 Fluorescein (1:100, Southern Biotech) or the inverse, diluted in sorting media to a final volume of 2 ml. The secondary antibodies were removed with 2 washes. The resulting cell sample was finally resuspended in 1 ml of sorting media, filtered through a 40 μm sieve and transferred to a FACS machine purification tube. The filtration process was necessary in order to remove cell clumps which would block the nozzle of the FACS machine.

A negative control to set up and standardise the FACS machine was a small aliquot of cells taken from the sample before incubation with the secondary antibodies. Once the FACS machine settings were optimized the cells were separated as an O4 positive and Galc negative cell population and collected in a new tube. The cells were centrifuged, the supernatant discarded and the sample centrifuged again for 1 second at 306 m/sec^2 to get rid of the thin film of sorting media present on the tube inner side surface (as this can occasionally cause bacterial or fungal contamination). A Gilson pipette was inserted in the tube and the sample was transferred to a 12.5 cm^2 poly -L-lysine (PLL, $13 \mu\text{g/ml}$) coated flask. The flask was placed into a 37°C incubator in a humidified atmosphere of 7% CO_2 and 93% air. After 10 minutes, the time required for viable cells to adhere to the flask surface, the flask was topped up with cell culture media.

The FACS machine was fully operated by Thomas Gilbey and occasionally by Margaret O'Prey, two specialized technicians in the Beatson institute.

All centrifuging steps in the 15 ml falcon tubes involving OECs, Schwann cells and fibroblasts were carried out at g-force of 306 m/sec^2 for a time that was determined by multiplying the sample volume (ml) by 30 sec/ml.

2.1.1.4 GFP lentiviral transduction

One or two days after OEC purification, if cell numbers and viability looked good the cells would be transduced with a lentiviral vector expressing a gene that

encodes the enhanced green fluorescent protein (GFP, virus kindly donated by Dr George Smith, University of Kentucky, USA). The procedure was carried out in a category 2 hood and involved adding concentrated GFP lentivirus to the cultured cells and leaving for 1-2 days. This time allowed the GFP gene to become integrated into the nuclear DNA of a high proportion of cells. Media was then changed and the transduction efficacy was confirmed by placing the flask under an inverted UV microscope (Olympus, CKX41) with the appropriate filter set and counting the number of GFP expressing cells.

2.1.1.5 OEC propagation

After the GFP lentiviral transduction procedure, cells were passaged every 2-3 days once they reached confluency. To passage OECs the culture media was removed from the tissue culture flasks and washed with PBS. This step was repeated once more and a PBS solution containing 0.025% trypsin was added, the flask placed in the incubator at 37°C and monitored under the phase microscope (Olympus CK2) to confirm cell detachment. To stop the trypsin reaction a solution containing foetal bovine serum (DMEM-10% FBS) was added and the cells transferred to a centrifuge tube and placed on ice. At this point cells were often counted with a haemocytometer (Weber Scientific). Then the sample was centrifuged and the supernatant discarded; and the cells resuspended in cell culture media and diluted in order to be plated into a new flask at 1/2-1/3 of their confluency. The amount of media used to plate cells in the 12.5 cm² flasks, 25 cm² flasks and 75 cm² flasks was approximately 0.12 ml/cm² of flasks surface area.

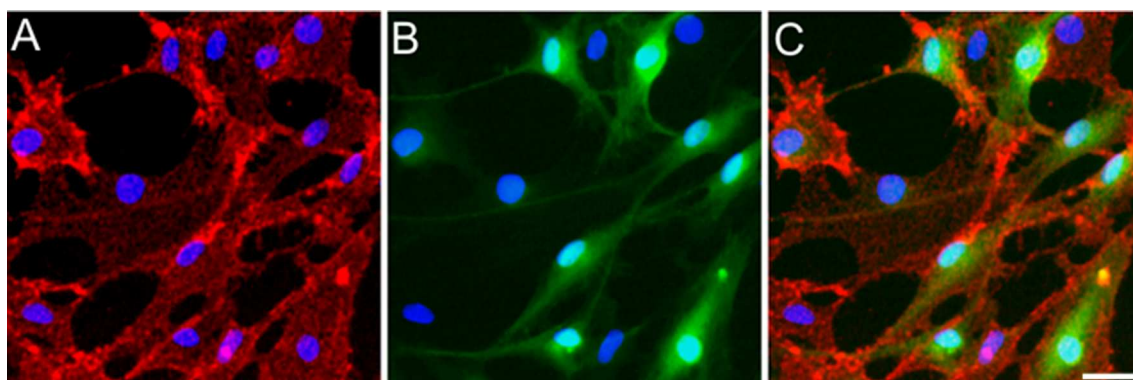
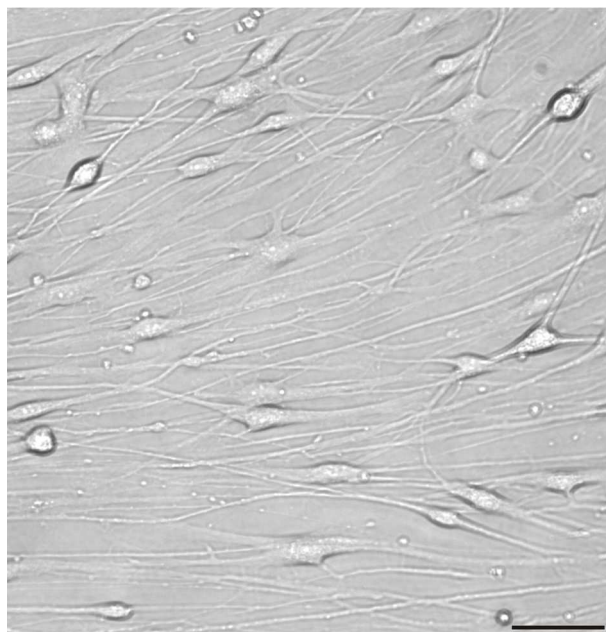
Information on the daily growth rate of OECs in culture was recorded on 19 populations of OECs, each deriving from different animals and different purification dates. The average value was calculated and was 0.85 (StErr= 0.06). In other words the number of cultured OECs doubled on average every 57 hours. The number of OECs per cultured surface area were calculated when the cells were fully confluent on cell populations from 19 independent olfactory bulb purifications after a varying number of passages: OEC density was of 21080 cells/cm² (StErr=1347 cells/cm²).

Figure 2-1. Cell culture of rat olfactory bulb FACS purified OECs.

Image of cultured OECs taken with QCapture (Media Cybernetics) camera and software on a Olympus CKX41 microscope using light coupled with a phase contrast filter. OECs in this example were FACS purified and transferred to tissue culture 19 days earlier and then passaged 6 times. Scale bar: 50 μm .

Figure 2-2 Antigenic profile of cultured OECs derived from rat olfactory bulb.

Image taken with Zeiss Axioplan2 microscope coupled with a ISIS camera and software using a 100 W mercury bulb coupled with the appropriate fluorescence filter sets to see p75 in red, GFP in green and nuclear labelling with DAPI in blue. The OECs in this example were FACS purified and transferred to tissue culture 18 days earlier. All cells in this example express p75, while approximately half express GFP marker. Scale bar: 30 μm .



2.1.2 Preparation of Schwann cells and fibroblasts from the sciatic nerve

2.1.2.1 Dissection

Schwann cells and fibroblasts were purified from the sciatic nerves of post natal day 7 Fisher 344 rats, typically from 4 or 5 animals, normally the same animals from which the olfactory bulbs were dissected. The rats were sacrificed by overdose of sodium pentobarbital and placed on ice to decrease cell mortality. The dissection was carried out on a dissecting board created from a polystyrene box top covered with tin foil in non-sterile conditions. The hind paws and the neck of each rat were pinned by a needle to the board to immobilize and stretch the leg for ease of dissection. After spraying the whole animal with ethanol, the skin over the sciatic nerve of the hind legs was removed with scissors. By using a pair of forceps and a pair of scissors, each sciatic nerve was exposed from beneath the leg muscles, excised and placed in a 7 ml bijoux tube containing 1-2 ml of L15 and 25 µg/ml gentamicin.

2.1.2.2 Dissociation

Once all the sciatic nerves were removed, the tube containing the nerves was transferred to a vertical laminar flow bench and all subsequent steps were carried out under sterile conditions. The sample was kept on ice as much of the time as possible throughout the purification procedure in order to increase cell viability. Within 2 hours of dissection the sciatic nerves were transferred to a 90 mm Petri dish and all media was removed with a Pasteur pipette. The cell dissociation was carried out as described for the olfactory bulb in section 2.1.1.2. Subsequently the sample was transferred into a centrifuge tube and washed as described in section 2.1.1.3.

The cells were resuspended in DMEM-10% FBS solution and plated in two PLL coated 75 cm² flasks.

2.1.2.3 Purification and culture of Schwann cells and fibroblasts

Two main cell populations from the dissociated sciatic nerves grew in the culture flasks: Schwann cells and fibroblasts. These were monitored using light microscopy. One or two days after being plated the Schwann cells and fibroblasts had assumed their typical morphology and had begun to proliferate (Figure 2-3).

The protocol which I initially tried to use to purify Schwann cells from fibroblasts was based on a method that used a fibroblast complement kill approach (Brookes et al., 1979), but unfortunately this method was not successful in my hands. After numerous attempts I tried another method that uses an ice cold step in the purification (Jirsova et al., 1997), also without success. Finally, I designed a method of purification based on light trypsinization of the cultured sciatic nerve cells. With this successful method it was possible to obtain highly pure populations of Schwann cells; importantly, from the same sample it was possible to obtain also highly pure populations of fibroblasts.

The new purification method used was as follows. One or two days after plating the sciatic nerve cells the culture flasks were washed twice with PBS. Then a PBS solution containing a low concentration of trypsin (0.017%) was added to each flask. Flasks were maintained at room temperature and the cells monitored under the microscope. The flasks were flicked very gently at a time point when most of the Schwann cells had started to detach from the flask surface but most of the fibroblasts were still strongly attached and the trypsin reaction was immediately stopped by adding DMEM-10% FBS. The resulting media containing a population of cells enriched for Schwann cells was transferred to a centrifuge tube and placed on ice while the flask was washed twice with PBS. At this point the cells remaining in the flask consisted primarily of a population of fibroblasts-like cells. To purify also fibroblasts, a PBS solution containing a high concentration of trypsin (0.083%) was added and the flasks were placed in the 37° C incubator. The cells in the flasks were monitored under the microscope and were flicked energetically after the fibroblasts started to detach. DMEM-10% FBS was added and this media containing an enriched population of fibroblasts

was transferred from each flask to a centrifuge tube. At this stage the original mixed population of Schwann cells and fibroblasts was divided into two separate tubes, one enriched with Schwann cells and the other with fibroblasts.

The tube containing the enriched population of Schwann cells was centrifuged and a small sample was taken and resuspended in the same culture media used for OECs and plated in a 12.5 cm² PLL coated flask. The same procedure was carried out with the sample enriched with fibroblasts and a small sample was resuspended in DMEM-10% FBS and plated in a 12.5 cm² PLL coated flask. One or two days later both the Schwann cells and the fibroblasts were infected with GFP-lentivirus. The cells were passaged when they reached confluency until a suitable number for transplantation was reached.

Schwann cell purification was continued at each passage by partial trypsinization. In this way any contaminating fibroblasts remained attached to the flask and the purity of Schwann cells increased after each passage (Figure 2-4 A, C and Figure 2-5 A-C). Importantly, it was necessary to passage the Schwann cells frequently, as soon as they grew to confluency (on average every 2-3 days), because fibroblasts could overtake the Schwann cells if passages were performed less frequently (every 4-5 days or more). Fibroblast purity was increased following each passage (Figure 2-4 B, D and Figure 2-5 D-F) by making sure all attached cells were detached following each trypsin treatment, and by making sure cells were given a longer time to reach confluency (on average every 4-5 days).

Preliminary work carried out by Edina Silajdzic in our laboratory showed that Schwann cells proliferate as well when cultured in DMEM-10% FBS as in the media used to culture OECs. For this reason and because transplantation efficiency of Schwann cells and OECs were to be compared it was felt appropriate to culture the Schwann cells and OECs in the same media: OECs culture media.

The daily growth rate of cultured Schwann cells was calculated on 11 populations of Schwann cells each deriving from different animals and different purification days and equalled 1.05 (StErr= 0.11). This means that the number of Schwann cells in culture doubled on average every 46 hours. The growth rate of

Schwann cells was not significantly different from that described in section 2.1.1.5 for OECs ($P=0.22$).

The number of purified Schwann cells attached to a culture flask at confluency was measured on 12 independent cell populations and equalled 45669 cells/cm² (StErr=6446 cells/cm²) which was more than double that calculated for OECs in section 2.1.1.5. Based on this finding it is evident that the two cell types cultured in this work had extremely different densities at confluency and this difference was significant ($P<0.0001$). This difference was not correlated with the passage number or with the number of days passed from purification.

Figure 2-3 Culture of cells from the sciatic nerve one day after dissociation.

Image of cultured cells in a tissue flask one day after dissociation from the sciatic nerves of 7 day old F344 rats, before starting the purification method. At this stage the cultured cells are comprised of fibroblasts and Schwann cells. These can already be recognised by their typical morphology: spindle like shape for Schwann cells (full arrow heads) and flattened shape for fibroblasts (empty arrowheads). This image was taken with QCapture camera and software on a Olympus CKX41 microscope using light coupled with a phase contrast filter. Objective: 10x. Scale bar: 60 μm .

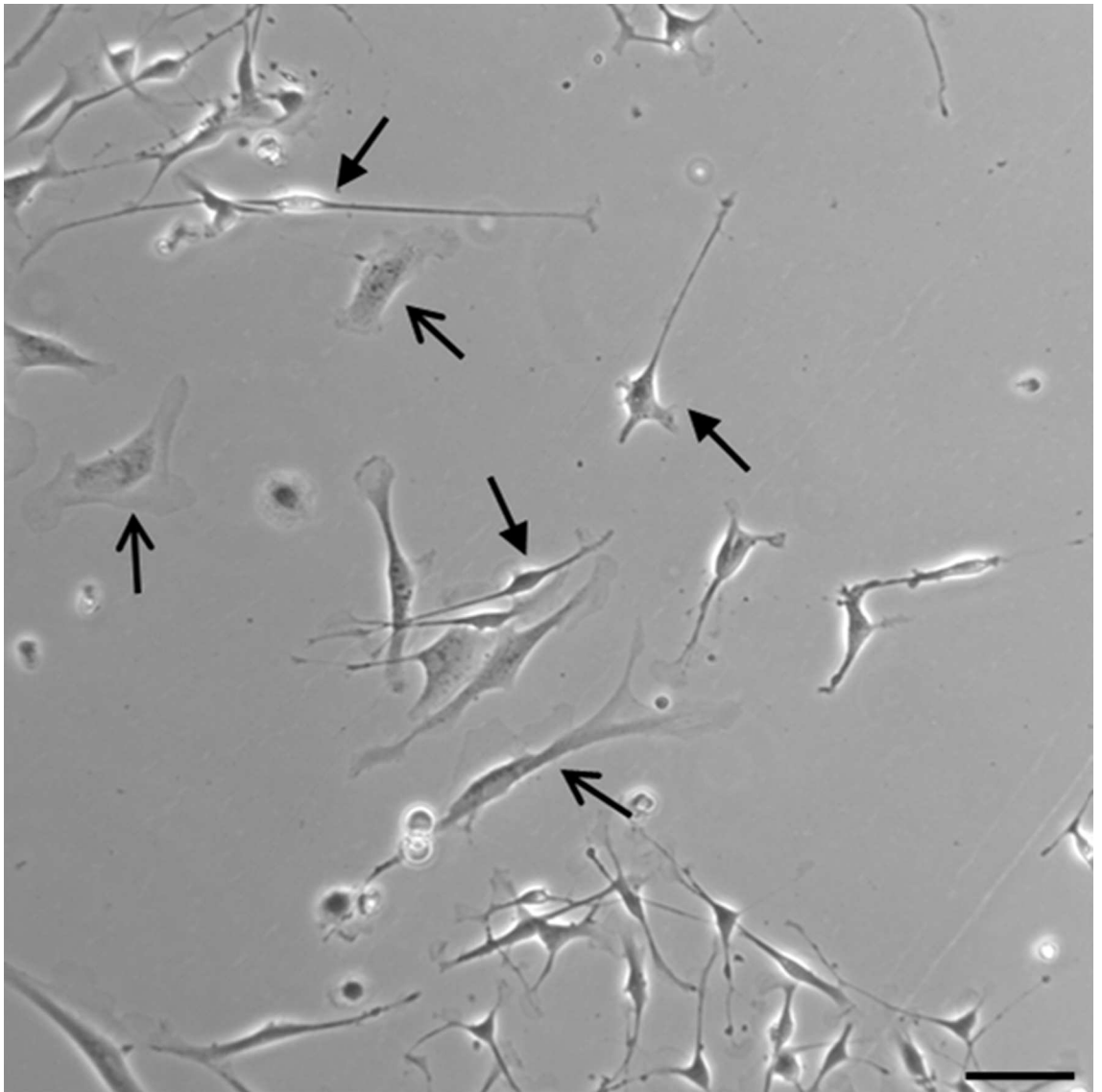


Figure 2-4. Purification of Schwann cells and fibroblasts by partial trypsinization. Image of cultured sciatic nerve derived cells to show together with Figure 2-3 the gradual purification of Schwann cells or fibroblasts over time. A) Population of enriched Schwann cells 4 days from dissociation and 3 days from the first passage. This example shows how after one passage using partial trypsinization Schwann cells had already outnumbered fibroblasts; however, many fibroblasts can still be seen (empty arrowheads). C) This image shows a Schwann cell enriched population 17 days and 5 passages after dissociation. In this example no fibroblast-like cells can be seen, indicating that frequent and multiple passages using partial trypsinization were effective for purifying Schwann cells. B) Population of enriched fibroblasts 4 days from dissociation and 3 days from the first passage. This example shows that after 1 passage most cells comprised of fibroblasts and only occasional Schwann cells could be seen (full arrow head). D) Example of an enriched population of fibroblast after 33 days in culture and 7 passages. Images taken with QCapture (Media Cybernetics) camera and software on an Olympus CKX41 microscope using light coupled with a phase contrast filter. Objectives: 20x in A-B, 10x in C-D. Scale bars: 30 μm in A-B, 60 μm in C-D.

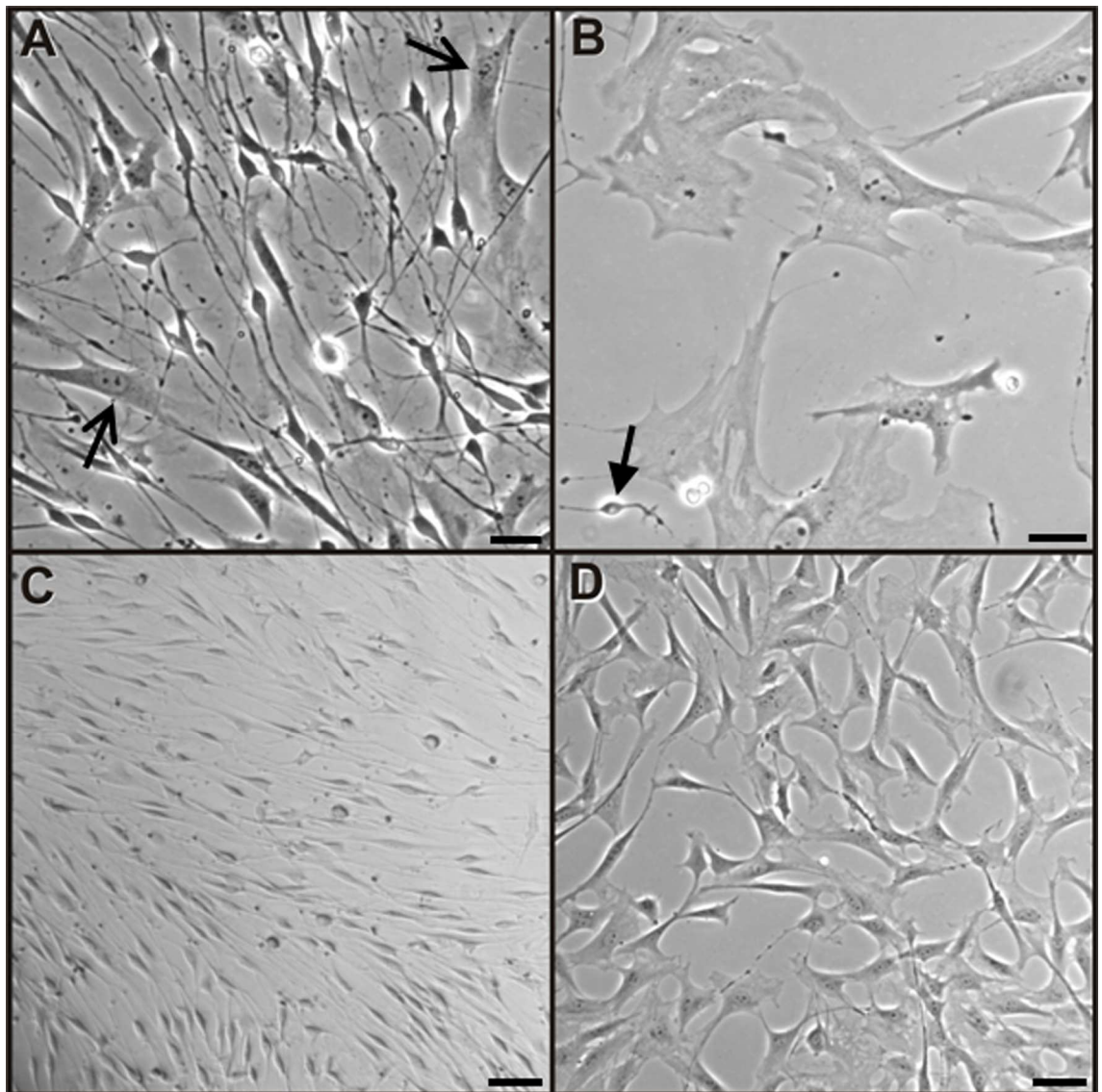
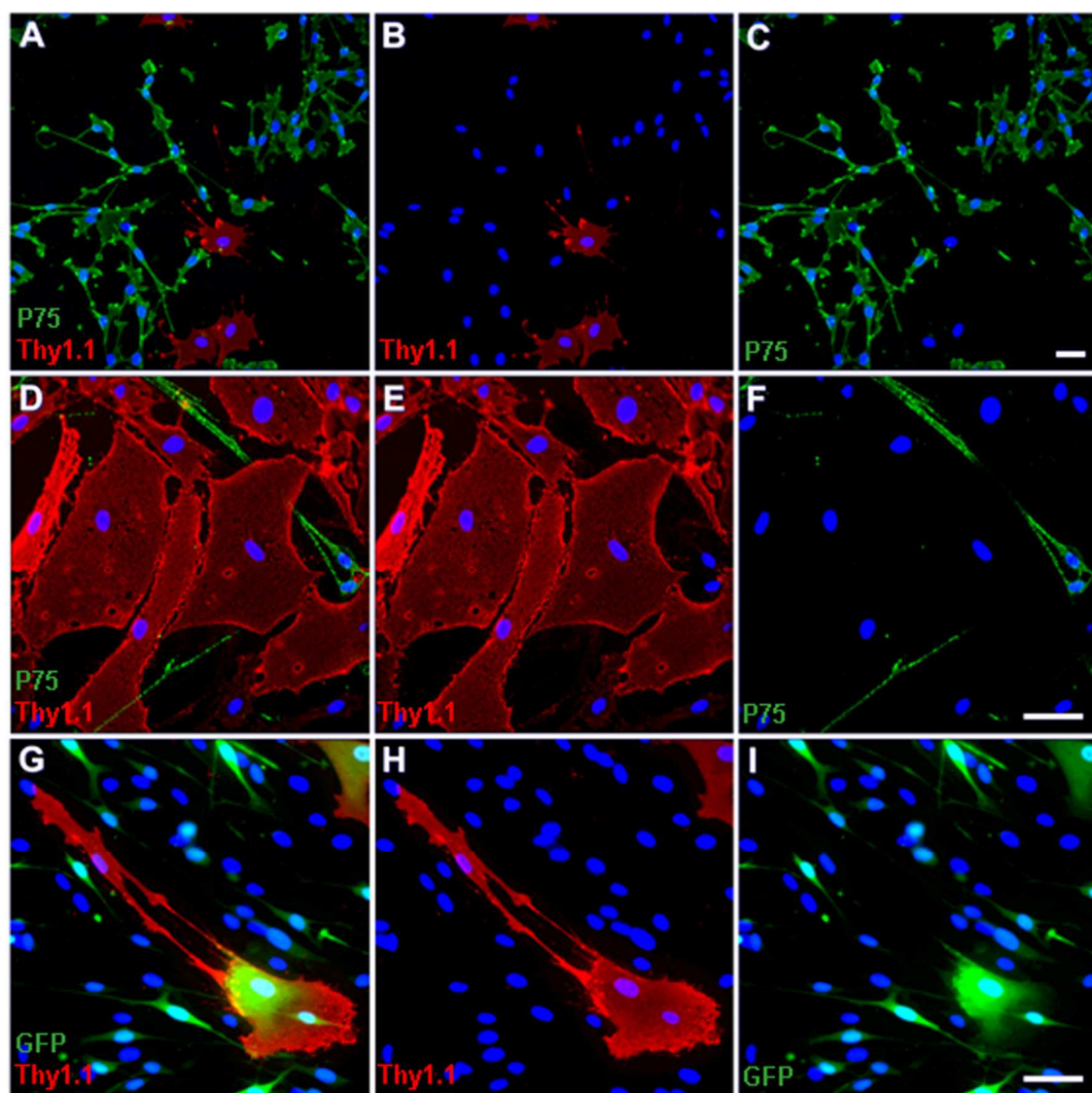


Figure 2-5 Antigenic profile of cultured Schwann cells and fibroblasts derived from rat sciatic nerve.

Images taken with a Zeiss Axioplan2 fluorescence microscope and ISIS camera and software. A-C) Example of a Schwann cell enriched population showing that after 4 passages and 10 days from dissociation from the sciatic nerve most of the cells identified by their nucleus stained with DAPI (blue) expressed the Schwann cell characteristic p75 receptor but not Thy1.1, specific to fibroblasts; only few fibroblasts were present as shown by Thy1.1 specific labelling. D-F) In these images taken from a fibroblast enriched cell population 27 days after dissociation it is possible to see that most cells were comprised of large flattened Thy1.1 positive fibroblasts and only few p75 positive Schwann cells, G-I) Both fibroblasts and Schwann cells expressed GFP after lentiviral transduction. These images taken on a Schwann cell enriched population 13 days after dissociation show that many cells identified by DAPI staining expressed GFP, including Thy1.1 fibroblasts. In all images DAPI is blue. Objectives used: 10x in A-C, 20x in D-I. Scale bars: 50µm.



2.1.3 Long-term freezing of OECs, Schwann cells and fibroblast in liquid nitrogen

During cell culture unpredictable and uncontrollable events could affect the growth of OECs, Schwann cells or fibroblasts: e.g. 7 day old rats were not necessarily available at the appropriate time, the cells plated after an olfactory bulb sort were not always viable, fungal or bacterial infections were unexpected and unwanted guests. These unpredictable events were incompatible with planning in advance for the surgical procedures in the knowledge that a source of cells could be available at any time. Planning for surgical procedures was done well in advance because for example recipient animals had to be ordered; the date for surgery had to be negotiated well in advance between all the people involved in the surgery; the surgery room had to be booked. It proved to be more convenient and certainly more controllable to make the timing of cell purification independent from the timing of cell transplantation; this was possible by freezing a stock of purified GFP positive cells. After purification and GFP infection of OECs, Schwann cells or fibroblasts and, once cells had reached a sufficient number, cells were frozen in liquid nitrogen to be retrieved and cultured when needed. It has been reported that no obvious differences in morphology or antigenic phenotype were found in cultured mouse OECs before and after storage in liquid nitrogen (Ramer et al., 2004b). Furthermore, transplanted cryopreserved OECs from canine olfactory bulb were shown to retain their ability to myelinate demyelination axons *in vivo* (Smith et al., 2002).

2.1.3.1 Cell freezing

Cells were detached from the culture flasks with trypsin, DMEM-10% FBS was then added to inactivate trypsin and a cell count was made with a haemocytometer. Following centrifugation, the supernatant was discarded and cells were resuspended in freezing media that contained DMSO (dimethyl sulfoxide) and aliquoted in cryotubes (this was completed as quickly as possible because DMSO is toxic to cells). Cryotubes were covered with cotton wool and

placed in the -80°C freezer for a few hours or up to a few days prior to storage in the liquid nitrogen freezer for an indefinite amount of time.

2.1.3.2 Cell thawing

Cells were normally thawed about a week before they were required for transplantation. A cryotube was collected from the liquid nitrogen and placed in a 37°C water bath to thaw the cells quickly prior to centrifugation in a falcon centrifuge tube containing DMEM-10% FBS to dilute residue DMSO. Following centrifugation the supernatant was discarded and the cells were resuspended in culture medium and plated at the required confluency.

2.1.4 Cell preparation for transplantation

The phase contrast microscope was used to assess the general appearance and confluency of the cells and to check lack of bacterial or fungal infection. The FBS present in the media was removed from the flasks and a PBS solution containing trypsin added. The flasks were placed in the 37°C incubator and monitored until cell detachment took place. The trypsin reaction was stopped by incubation in DMEM-10% FBS also containing approximately $2\ \mu\text{g}/\text{ml}$ DNase: DNase prevented the cells from forming clumps that would block the injection cannula during the transplantation process. The content of the flasks was transferred into a 15 ml falcon centrifuge tube and placed on ice. After counting the cells with a haemocytometer the tubes were centrifuged and the supernatant discarded. A second but brief centrifugation was necessary to get rid of any medium present on the inner surface of the falcon tube and to avoid contamination when inserting the Gilson to transfer the concentrated cells to a 0.2 ml PCR sterile tube. The PCR tube was placed inside a larger tube in ice, transported from the Beatson Institute to the University main campus animal house. Before starting the transplantation, the tube containing the cells was centrifuged on a bench centrifuge to remove excess medium.

The average density of the OECs and Schwann cells at the time of transplantation differed and was 229322 cells/ μ l (StErr=10544 cells/ μ l) and 394210 cells/ μ l (StErr=39960 cells/ μ l) respectively; this difference was significant ($P < 0.0001$).

Before being transplanted OECs were cultured for an average time of 29 days and passaged on average 8 times. Schwann cells instead yielded a larger amount of cells for transplantation in a shorter time and for this reason were cultured for a shorter time than OECs. Schwann cells were in fact cultured for an average time of 19 days and passaged on average 7 times before being transplanted.

2.1.5 Cell purity and GFP labelling

Cultured OECs, Schwann cells and fibroblasts possess a characteristic morphology when viewed under the phase contrast microscope (Brockes et al., 1979) giving an indication of cell type.

However to check for purity, markers were used that characterised each cell type and immunocytochemical techniques. OECs, Schwann cells or fibroblasts were seeded on PLL-coated cover slips for 2-3 days and then immunolabelled with cell surface markers. Purity of olfactory bulb OECs and sciatic nerve Schwann cells was determined by expression of the antibody to p75 neurotrophin receptor (p75, hybridoma supernatant, 1:2; IgG1, Yan and Johnson, 1988). Purity of sciatic nerve fibroblasts was determined using an antibody to the cell surface marker Thy1.1 (rabbit clone CD90 abcam, 1:800; IgG1) which is not expressed by Schwann cells (Brockes et al., 1979). Coverslips were incubated with the primary antibody diluted in DMEM for 15 min at room temperature, rinsed in PBS and then incubated in the goat secondary class specific antibody diluted 1:100 (Southern Biotechnologies) for 15 min at room temperature. Coverslips were rinsed in PBS and mounted in anti-fade containing DAPI (Vectashield, Vector Laboratories) to identify nuclei. On a few occasions OECs and Schwann cell cultures were incubated with Thy1.1 to quantify fibroblast contamination and conversely fibroblast cultures were assessed for Schwann cell contamination using anti-p75.

p75 expression was always detected on more than 98% of the cells in OECs cultures. In Schwann cell cultures cell purity varied with the passage number, however p75 always labelled more than 86% even at early cell culture stages and in some instances labelled as many as 98% of cells. Thy1.1 labelled as many as 10% of cells at early cell culture stages while labelled less than 5% after a few passages. Cultured fibroblasts were apparently composed only of Thy1.1 positive cells, but to confirm this more fibroblast cultures should be set up.

The presence of GFP expressing cells was determined on all cell populations before transplant by placing the tissue culture flask under a UV inverted microscope (Olympus, CKX41) and switching between the UV and the plain light source to confirm the expression of GFP in a reasonable proportion of cells. A more precise quantification was achieved on all cell populations that were transplanted by labelling the cells with a rabbit anti-GFP antibody (1:1000 AbCam). Cells were plated on PLL coated coverslips and fixed 2-3 days later with a solution of 4% paraformaldehyde; membranes were then permeabilised in a PBS 0.5% triton (Sigma) solution and non-specific antibody binding sites blocked with a PBS 0.2% porcine skin gelatine (Sigma) solution for 30 minutes. The GFP antibody was incubated with the cells for 30 minutes followed by donkey anti rabbit or anti goat Alexa 488 secondary antibody incubation for 10 minutes (Molecular Probes). Cells were incubated with primary and secondary antibodies in a PBS solution 0.1% Triton X-100 and 0.2% gelatine. Coverslips were mounted with DAPI containing Vectashield (Vector laboratories, Peterborough, UK) to visualize the nuclei. In some instances p75 or Thy1.1 and GFP immunolabelling were performed on the same coverslips (Figure 2-5G-I). GFP expression varied between individual OEC, Schwann cell and fibroblast cultures and was between 6% and 92%.

Images for both cell surface and intracellular staining were taken by fluorescence microscopy (Zeiss Axioplan2) coupled with ISIS camera and software (MetaSystems). Colour levels were adjusted with Photoshop (Adobe) and cell counting was performed with the Cell Counter plug-in on ImageJ (NIH, USA).

2.1.6 Cell culture materials

All cell culture formulations were filtered to reduce microbial contamination. Regular mycoplasma screening was performed to reduce the possibility mycoplasma infections.

2.1.6.1 OECs Media

OECs media was made up by adding to DMEM: 5% FBS, 48% DMEM-BS media, 25 ng/ml fibroblast growth factor (PeproTech, 100-18b), 25 ng/ml Heregulin (R&D systems, 396-HB) and 2.1 µg/ml Forskolin (Sigma, F-6886).

2.1.6.2 Bottenstein-Sato's Media (DMEM-BS)

This media was composed of DMEM, 5 ng/ml insulin (bovine pancreas, Sigma), 50 ng/ml transferrin (Sigma), 0.022% SATO mix (see below) and 100 mM glutamine (GIBCO, 25030) and was stored at 4° C.

2.1.6.3 SATO mix

Made up of: 200 ml PBS + 5.72 ml BSA path-o-cyte 5 (Bovine albumin path-o-cyte, MP biomedical 810111) mixed with 200 ml dH₂O + 322 mg Putrescine (Sigma P7505), and with 20 ml ethanol + 8.0 mg thyroxine T₄ (Sigma T-2501), and with 20 ml ethanol + 6.74 mg Tri-Iodo-Thyronine T₃ (Sigma T-2752). Once the above solutions were combined, 2 ml of each of the following were added: 20 ml ethanol + 12.46 mg Progesterone (Sigma P-0130) and then 20 ml dH₂O + 7.74 mg Selenium (Sigma S-1382). The resulting solution was filtered and stored at -20° C.

2.1.6.4 DMEM-10% FBS

Made up of 90% DMEM and 10% foetal bovine serum (FBS).

2.1.6.5 Sorting Media

Made up of 99% DMEM and 1% FBS.

2.1.6.6 DMEM

Once Dulbecco's Modified Eagle Medium (Gibco, 21885) was opened 25 µg/ml gentamicin (Gibco, 15750) was added to reduce risk of bacterial infections and stored at 4° C.

2.1.6.7 Leibovitz's L-15 Medium (L15)

Once Leibovitz's L-15 Medium (Gibco, 11415) was opened, 25 ug/ml gentamicin (Gibco, 15750) were added and stored at 4° C.

2.1.6.8 Collagenase

Collagenase was made up of L15 and 13.3 mg/ml collagenase (MP Biomedicals, 195109) and stored at -20° C.

2.1.6.9 Soya bean trypsin inhibitor and DNase (SD)

Made up of L15, 3.0 mg/ml bovine serum albumin (BSA) (Sigma A2153), 0.52 mg/ml Soya bean trypsin inhibitor (Sigma T-9003), 0.04 mg/ml bovine pancreas DNase (Sigma D-4263). Storage at -20° C.

2.1.6.10 Poly-L-lysine (PLL) coated flasks and coverslips

PLL (Sigma, MW>80,000) was dissolved to a final concentration of 13.3 µg/ml. 4 ml, 1 ml or 1 ml of this PLL solution were added to a 75 cm², a 25 cm² or a 12.5 cm² flask respectively, while 0.5 ml were added to each well containing a 13 mm diameter coverslip in a 24 multi-well plate. These were agitated to get PLL all over the surface. After incubation at 37° C for 30 min PLL was removed and washed away (as free PLL is toxic for cells) with sterile water.

2.1.6.11 Freezing media

Made up of 50% FBS, 40% DMEM and 10% DMSO (Fisher Chemicals, D/4121/PB08) and stored at 4° C.

2.1.6.12 O4, GalC and p75 hybridoma cell lines

O4 and GalC monoclonal antibodies were produced from the O4 and the galactocerebroside cell lines which were kindly donated by Mark Noble (University of Rochester). Hybridomas for the O4 antibody and galactocerebroside and p75 antibodies were maintained in liquid nitrogen in 1 ml cryotubes. Cryotubes were rapidly thawed in a 37° C water bath and transferred to a 15 ml falcon centrifuge tube. 10 ml of Optimem-50% FBS was added and the sample was centrifuged. The supernatant was discarded and the cells were resuspended in 5 ml of Optimem-50% FBS and counted with a haemocytometer. Cells were plated in non-PLL coated flasks at 30% of full confluency (full

confluency is approximately 2×10^5 cells/cm²) in a final volume of approximately 0.25 ml/cm² of Optimem-50% FBS. Two or three days later cells would be confluent and others formed floating clumps. The flasks were tapped strongly and any cell clumps dissociated using a pipette and then passaged. The cells in each flask were then transferred to new flasks and the volume of media adjusted to approximately 0.25 ml/cm² of Optimem-10% FBS in order to gradually reduce the FBS concentration from 50% to 10%.

2.1.6.13 Antibody production.

Following 2-3 more days in culture, cells were dissociated and transferred to a centrifuge tube. Following the centrifugation step the supernatant was discarded and cells were resuspended in Optimem-10% FBS and plated in new flasks. Three days later cells were dissociated and centrifuged. The supernatant was filtered, aliquoted and placed in the -20° C freezer for long storage. The titre of the hybridoma supernatant was tested on non-purified cultured olfactory bulb cells or on other CNS derived cultured cells.

An aliquot of the hybridoma was refrozen for future use into cryotubes. Each cryotube, containing approximately 2.5×10^6 hybridoma cells, was wrapped in cotton wool and placed in the -80° C freezer for a few hours or up to a few days and finally placed in liquid nitrogen for storage.

2.1.6.14 Optimem-50% FBS

Made up of 50% Optimem (Gibco 11415) with 25 µg/ml gentamicin and 50% foetal bovine serum; stored at 4° C.

2.1.6.15 Optimem-10% FBS

Made up of 90% Optimem (Gibco 11415) with 25 µg/ml gentamicin and 10% foetal bovine serum; stored at 4° C.

2.1.6.16 Hybridoma freezing medium

Made up of 90% FBS and 10% DMSO; stored at 4° C.

2.2 Operations on animals

All experimental procedures carried out on animals were approved by the Ethical Review Panel of the University of Glasgow and performed in accordance with the UK Animals Scientific Procedures Act 1986 under the restrictions and regulations stipulated by our Home Office personal, project and site licences. Excluding perfusion fixation, all operations were performed by Dr. John Riddell with the necessary assistance of my colleagues Tao Meng (PhD student) or Andrew Toft (research assistant) and the animal house staff. Tao Meng or Andrew Toft also prepared all the materials necessary excluding cells for transplantation.

2.2.1 Perioperative care

Buprenorphine (Vetergesic) was administered to relieve the animals from pain. It was administered subcutaneously before operations: 0.05 mg/kg (0.15 ml/100 g body weight).

Carprofen (Rimady1LA), an anti-inflammatory agent, was administered subcutaneously once before and once after each operation: 5 mg/kg body weight, delivered in a final volume of 0.1 ml/100 g body weight.

Saline was administered subcutaneously to prevent dehydration. A volume of 0.2-0.4 ml/100 g body weight of saline at body temperature was injected once before operation and for up to three days after the operation two or three times daily.

Amfipen, an antibiotic, was administered once before operations via a subcutaneous route: 0.1 ml/100 g of body weight.

Enrofloxacin (Baytril), an antibiotic, was administered subcutaneously twice daily for 7 days after operations: 5 mg/kg, injecting 0.02 ml/100 g body weight.

For spinal cord injury and delayed transplantation operations all the drugs above were administered, while for sciatic nerve transections and tract tracer injections all drugs were administered except the antibiotics.

After operations, animals were placed in a warmed environment and monitored regularly until they recovered. Food and water were always available. Soft mash and land pellets provided easy access to food at early recovery stages while a long spout provided easy access to water. Lighting was regulated in order to provide a 12 hour day and 12 hour night cycle.

Autotomy was observed on some animals following sciatic nerve transection. When the autotomy affected soft tissue the animal would be humanely sacrificed and where possible included in the study.

After operations animals were housed in twos as this improves recovery and reduces autotomy incidence.

2.2.2 Wire knife dorsal column lesion

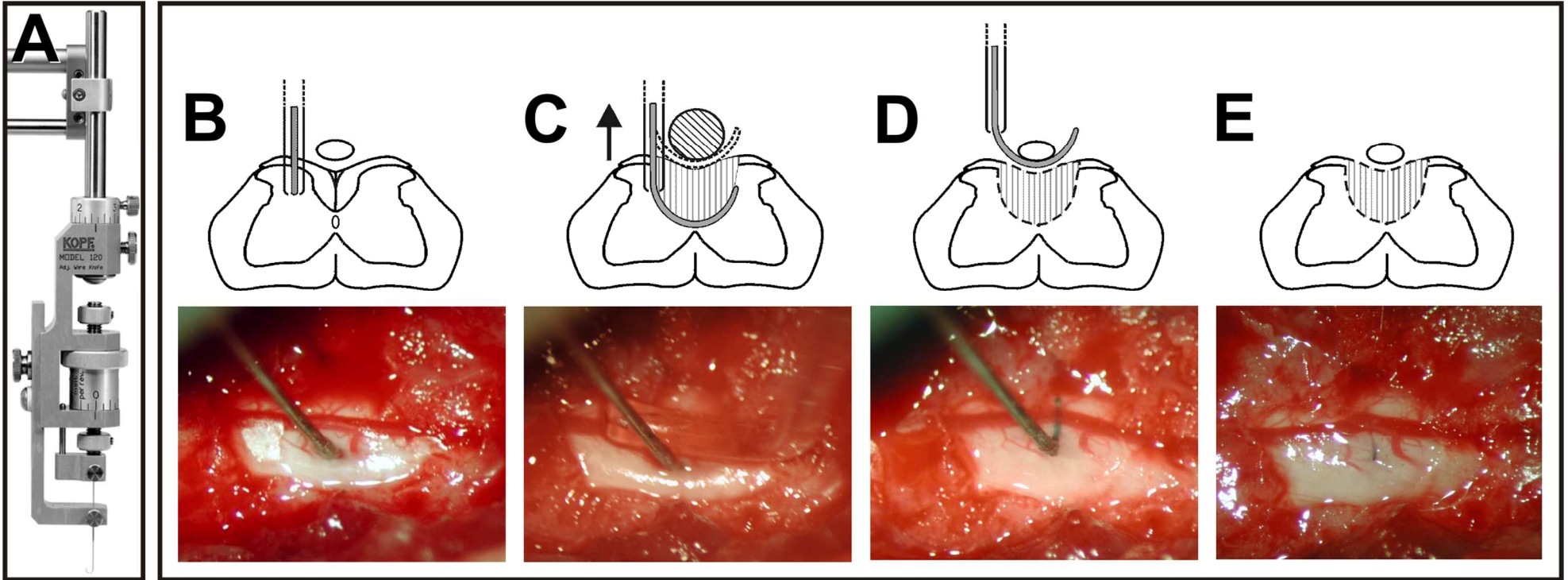
A total of 151 adult male Fischer 344 rats (Harlan, Loughborough, UK, weighing 200-250 g) were subjected to a bilateral dorsal column lesion. Surgical instruments were sterilised and precautions were taken to reduce the risk of wound infection. Rats were anaesthetised with halothane or isoflurane vapours

at an initial concentration of 4%, 96% O₂. Once the animals were deeply anaesthetised the concentration was lowered and typically maintained at 1.5-2% throughout the operation. The lumbar spinal cord was exposed by laminectomy at the T13/L1 vertebral junction. Then the dorsal columns were bilaterally injured close to the L3-4 spinal segmental level. This location was identified based on the vicinity to the T13 and L1 vertebral junction. The wire knife (shown in Figure 2-6A) (David Kopf Instruments, Tujunga CA, USA), made of a 100µm thick tungsten wire ensheathed within a Teflon cannula, is such that when the wire is protruded from the cannula, it coils to form an arc, the inner diameter of which can be precisely calibrated. The knife was mounted on a stereotactic device fitted with a stepper motor. In order to perform the lesion the wire knife was inserted through a slit in the dura, approximately 700 µm to the left of the spinal cord midline and lowered to a depth of 950 µm and then protruded to form a 1.5 mm diameter arc under the dorsal columns. A glass rod was placed on the surface of the cord and the wire knife was raised against it producing a clean repeatable transection of the dorsal columns (Figure 2-6). To ensure transection of the most superficial fibres while preserving the integrity of the dorsal vein located in the thickness of the meningi, the arc of the wire knife was also pressed for 20 seconds against the compacted head of a pointed cotton bud. Subsequently, the wire knife was retracted into its sheath. Finally, the L3 dorsal root was cut using scissors to prevent the tract tracer from being transported from the L4 root along anastomosing afferent fibres, which could potentially bypass the lesion and complicate analysis of regeneration.

A 10/0 ethicon suture was placed in the dura at the lesion site to mark it and wounds were closed in layers.

Figure 2-6 Diagram to illustrate the phases of the wire knife lesion operation.

A) The wire knife protruded from the cannula and formed an arc. B) The wire knife ensheathed in its cannula was inserted through a slit in the dura made to the left of the dorsal columns up to a depth of 950 μm . C) The wire knife was then protruded from the cannula, forming an arc encompassing the dorsal columns and raised against a glass rod resting on the surface of the cord and immediately after against a pointed cotton bud. D) This lesion resulted in the transection of the dorsal columns while preserving the dorsal vein integrity. E) Finally, the wire knife was retracted in its ensheath and raised out of the cord. Images B-E were modified from original ones designed by Dr. John Riddell.



2.2.3 Extended wire knife dorsal column lesion

In seven animals the dorsal column lesion was extended to ablate all primary sensory afferents in the left dorsal column at the L3-4 level. After retracting the wire knife into its sheath and raising it out of the spinal cord, the wire knife was rotated 180 degrees. The wire knife was then inserted again into the spinal cord through the same slit in the dura and a second wire knife lesion was performed extending the original dorsal column lesion to include the extreme left portions of the dorsal columns.

2.2.4 Acute cell transplantation

Ninety rats were transplanted with cells immediately after the spinal cord injury. The injections were performed with a glass pipette pulled to a fine taper and bevelled at the tip (inside and outside diameter 60-80 μm and 80-110 μm respectively). The pipette was filled with cells, mounted on a stereotactic arc, inserted into the lesion at an angle of 20° on each side through a slit in the dura with the tip pointing to the lesion centre and was lowered to a depth of approximately 1000 μm . Cells were then injected by applying brief (40 ms) pressure pulses (Picoinjector, WPI, Sarasota FL, USA) over the course of several minutes, during which the pipette was gradually raised to the surface. The cell injection process was ended when the transplanted cells, which appeared as a dense mass, overflowed from the lesion surface.

A 10/0 Ethicon suture was placed in the dura at the lesion site to mark it and wounds were closed in layers. There was no need for immune suppression as donors and receivers were from the same inbred F344 rat colony.

2.2.5 Delayed cell transplantation

Delayed transplants were performed on 31 animals four weeks after the dorsal column transection. By this time a fibrous scar had developed above the lesion

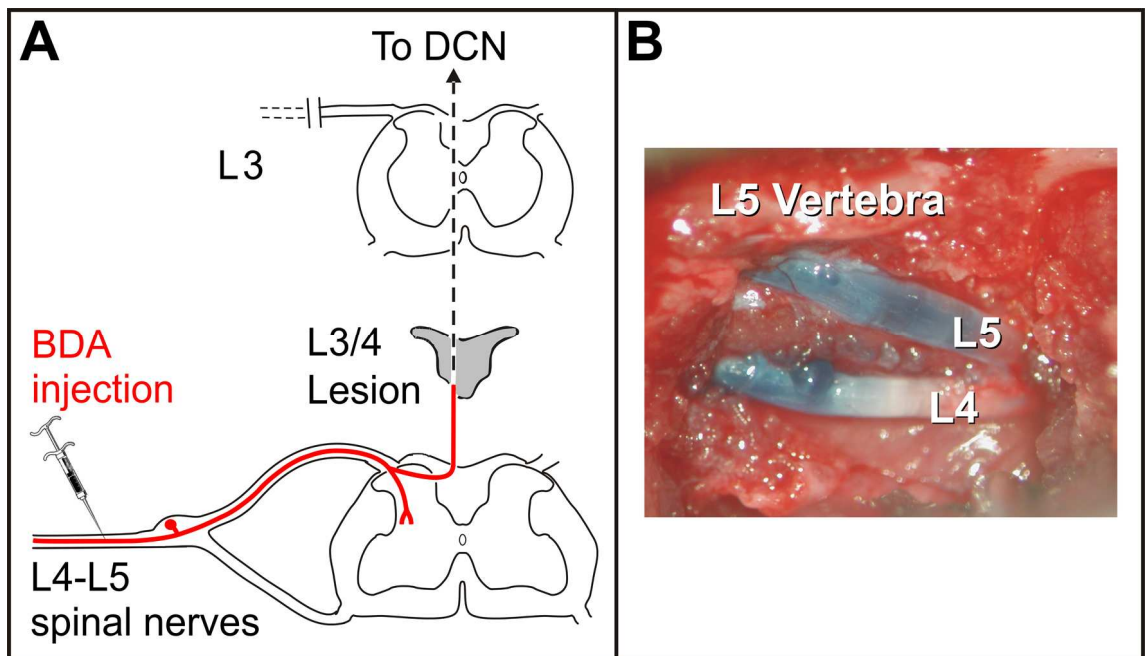
and a great technical skill was necessary to find the original wire knife lesion location. To help localise the lesion, 10/0 non absorbable (silk) sutures were placed on either side of the lesion and sutures on the back muscles were placed exactly in line with the rostral and the caudal ends of the laminectomy at the time of the wire knife transection. Further more, the lesion site was sometimes visible as a darker area. On a few instances, where stated, by mistake the cells were not injected into the lesion cavity and no GFP labelled cells were present in the spinal cord after examination. Those animals were excluded from the delayed cell transplantation paradigm and considered non-transplanted animals. The injection process was carried out under anaesthesia following the same steps described in section 2.2.3.

2.2.6 Tract tracer injection

Two weeks before perfusion 132 animals were anaesthetised with isofluorane and underwent an operation to inject the L4 and L5 spinal nerves with the tract tracer biotin dextran amine (BDA; 10,000 MW, product no. D-1956, Molecular Probes). The L4 and L5 spinal nerves were exposed outside the vertebral column at the level of the tip of the iliac crest. A solution of 20% BDA dissolved in 0.1 M phosphate buffer (PB) with 2% fast green dye (to detect spillage; R.A. Lamb Supplies, UK; product 42053) was injected into each spinal nerve through a glass pipette with a bevelled tip (internal diameter approximately 45 μm). A total of 3-4 μl was injected into each nerve using repeated 40 ms pressure pulses. Wounds were closed in layers and post-operative analgesia was routinely administered.

Figure 2-7 Injection of BDA tract tracer into the L4/5 spinal nerves.

A) Two weeks before perfusion fixation, the L4 and L5 spinal nerves were exposed and BDA neuronal tracer was injected into the two spinal nerves. By travelling through the dorsal root ganglia peripheral and central branch, the neuronal tracer allowed for the detection of any tract traced fibre rostral to the L3-4 dorsal column lesion site. The left L3 dorsal roots were cut to prevent the BDA tracer from locating in the spinal cord rostral to the lesion due to anastomosis with the L4 root. B) A solution containing fast green was mixed with the tracer in order to confirm the injection of the tracer into the spinal nerves and detect spillage. Images were modified from original ones made by Dr John Riddell.



2.2.7 Conditioning lesions

In 88 animals, under halothane/isoflurane anaesthesia, the left sciatic nerve was exposed at mid thigh level and freed from surrounding tissues. It was tightly ligated using 5-0 silk thread (Ethicon, UK), taking care that all branches were included within the ligature. The nerve was then cut approximately 2-3 mm distal to the ligature and the overlying muscle and skin closed with 3-0 vicryl sutures (Ethicon, UK).

A second conditioning lesion was performed on 47 animals; this was carried out as the previous one. The second ligation and transection was made 1-2 cm more proximal to the first conditioning lesion.

Conditioning lesion will be referred to in the present work also with the terms priming, sciatic nerve transection and peripheral lesion.

2.2.8 Perfusion and manipulation of spinal cord tissue

Of the 172 rats that entered procedure for the present study, 23 rats died or were humanely killed as a result of technical difficulties arising during the operations or following autophagy of the hind limb after conditioning lesion. Of the remaining animals, 18 were processed by Andrew Toft (research assistant in the lab) while 133 by me. After induction of anaesthesia animals were intraperitoneally injected with an overdose of 1.5 ml of Euthatal (sodium pentobarbital, 200 mg/ml, Vericore Ltd, UK). Animals were perfused through the left ventricle with gravity fed mammalian Ringer's solution containing 0.1% lidocaine for approximately 10 seconds until the liver changed colour. That was immediately followed by perfusion fixation with 1 l of 4% paraformaldehyde in 0.1 M phosphate buffer, pH 7.4. Dehydration and post-fixation of the cord were achieved by placing the cord in the same fixative solution with the addition of 30% sucrose. From all rats, a block of spinal cord of approximately 4 mm in length spanning the lesion site was prepared. It was described above that the lesion was performed approximately at the L3-4 level. The precise injury site was located to confirm that the lesion was not situated below the L4 dorsal root

entry zone where tract traced axons entered the spinal cord. This was possible by locating the L4 and L5 dorsal root ganglia and by following the L4 and L5 dorsal roots up to the L4 and L5 spinal cord segments. The lesion site was easily identified by a distinct scar on the dorsal surface of the cord. The lesion of all rats was located above the L4 dorsal root entry zone between the L3-4 border and the L3 segment. Throughout the thesis, the block of tissue comprising the lesion is referred to as the lesion block.

In initial experiments only the lesion block was extracted. In subsequent experiments caudal and rostral blocks were removed in order to provide more information on the distribution of transplanted cells and tract traced axons. The block immediately caudal to the lesion block is called the caudal block; the one immediately rostral is called the rostral block and the block removed at the T12-13 level is called the thoracic block.

Blocks were cut into 70 μm parasagittal sections on a freezing microtome, washed in phosphate buffered saline 0.3 M (PBS double salt), and then incubated for 30 min in 50% ethanol to permeabilise cell membranes. After washing 3 times for 10 minutes each in PBS, sections were incubated for 72 hours at 4° C with primary antibodies. Primary antibodies were mouse anti-Nf200 (1:1000 Sigma) to label axons (called neurofilament throughout the thesis), rabbit anti-GFP (1:1000, Abcam) to label transplanted cells and anti-GFAP (1:1000 rabbit anti-GFAP Dako or 1:1000 mouse anti-GFAP Sigma) to label astrocytes. Following primary antibody incubation sections were washed 3 times for 10 minutes each in PBS and incubated for 5 hours at room temperature with the appropriate species specific secondary antibodies raised in donkey: Alexa 488 1:500, Cy5 1:100, Rodamine 1:100. The tract tracer BDA was revealed by incubating sections for 72 hours at 4° C with a fluorophore conjugated to streptavidin (Alexa Fluor 568, Molecular Probes S-11226). Streptavidin and all antibodies were made up in PBS double salt with 0.3% Triton X-100. Excess of streptavidin and primary antibodies and excess of secondary antibodies were washed away from the sections by rinsing them 3 times for 10 minutes each in PBS double salt. No donkey serum or other blocking agents were needed to reduce non-specific binding because PBS double salt solution alone is used to drastically decrease the affinity of antibodies for non-specific binding targets (Polgar et al., 1999). On completion of reactions, sections were mounted on glass slides in anti-fade

medium (Vectashield; Vector Laboratories) and stored at -20°C where the fluorescence decays extremely slowly.

2.3 Post-processing analysis

2.3.1 Quantification of lesion cavity size

To understand whether the process of lesion cavitation was differently affected by different treatment conditions the degree of cavitation in the lesion was measured in each animal. The lesion cavity was normally present on multiple parasagittal sections of the lesion block in each animal. To compare the cavity size between different animals the lesion cavity was measured on the section with the largest lesion cavity in each animal. To do this, all the sections in the lesion block of an animal were analysed with a 1x objective under light microscopy with a Nikon Eclipse microscope. The section that appeared to contain the largest cavity was selected and an image of it was taken with a digital camera (Zeiss Axiocam) mounted on the microscope with a 1x objective. The image was subsequently used for measuring the size of the cavity it contained (Figure 2-8A) with Measure and Label, a plug-in of ImageJ (NIH, USA). The unit of the measurement obtained was square pixels; the measurement was multiplied for a correcting factor of $1226028\ \mu\text{m}^2/\text{pixel}^2$ to have a measurement unit in square microns. Finally the data between animals and between groups was compared.

2.3.2 Quantification of lesion size

The lesion size was quantified by using as a landmark the internal perimeter of the lesion glial scar defined by GFAP labelling. In the majority of animals GFAP antibody was coupled with a secondary antibody attached to the fluorophore Cy5. As the Nikon microscope used for the quantification of the lesion cavity size

in section 2.3.1 did not have an epifluorescence filter set for viewing Cy5 it was not possible to compare the lesion cavity size and lesion size on the same microscope by switching between light and epifluorescence view. Therefore to measure the lesion size using GFAP labelled with Cy5 it was necessary to use confocal microscopy. In each animal, the size of the lesion was measured using the parasagittal section that appeared to have the largest lesion as defined by GFAP labelling. The section was selected by scrolling all the sections from the lesion block of an animal under a 4x objective with the confocal microscope. Subsequently, a confocal image of the selected section was taken with a 4x objective in the middle of the depth of the section with a fully open iris. The image was then converted to a Tiff file using Confocal Assistant and the lesion size was measured (Figure 2-8B) with Measure and Label, a plug-in of ImageJ (NIH, USA). The unit of the measurement obtained was square pixels; the measurement was multiplied by a correcting factor of $58.08 \mu\text{m}^2/\text{pixel}^2$ to have a measurement unit in square microns. It must be noted that sections used for the quantification of the lesion size and lesion cavity sizes were not necessarily the same, as the section selection was independent in the two quantification procedures.

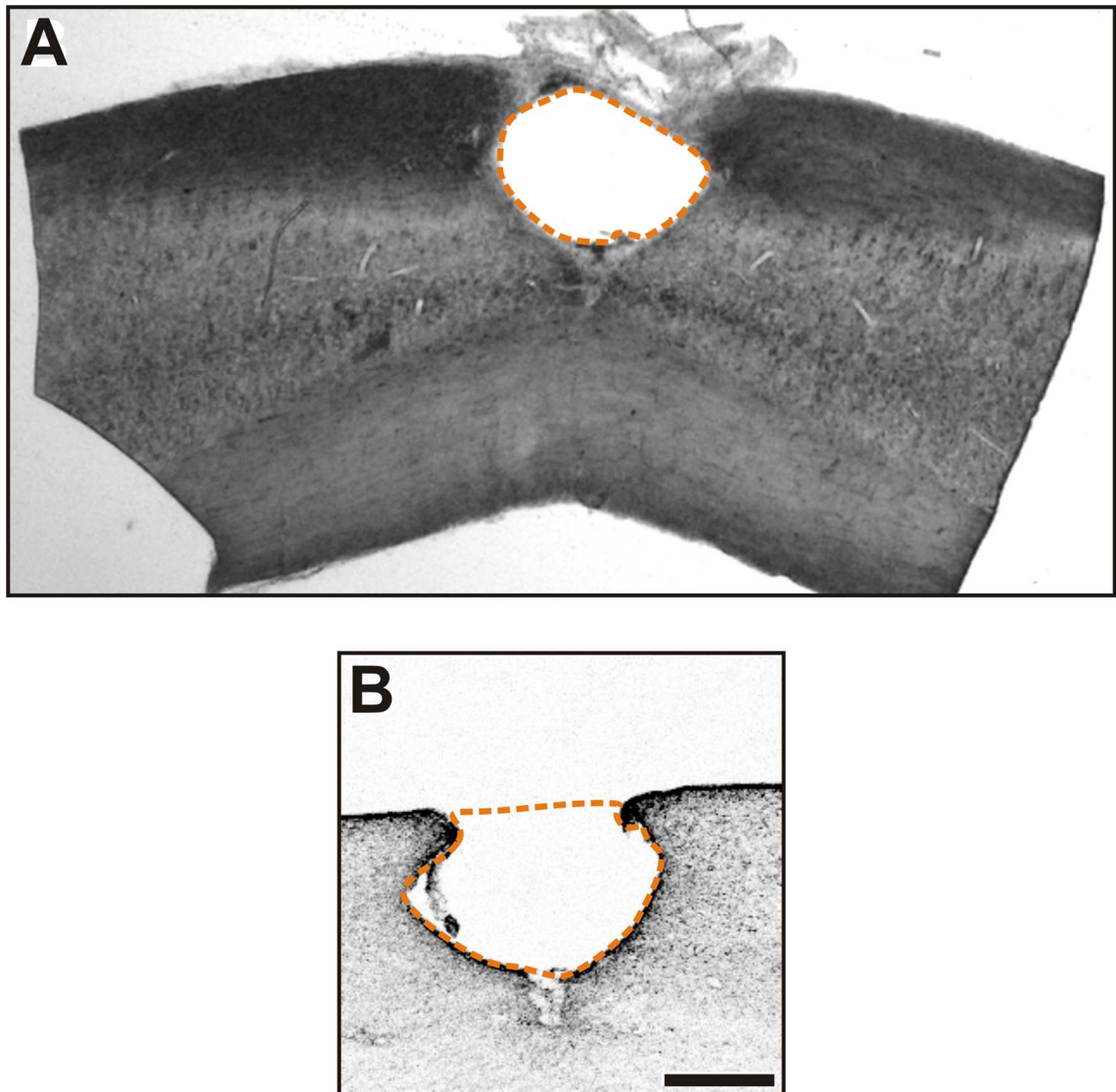


Figure 2-8. Designing the contour of the lesion cavity and of the lesion.

The lesion cavity size and the lesion size were measured in each rat on the section with the largest cavity and largest lesion respectively. A) Once the section with the largest lesion cavity was selected using light microscopy, a picture was taken using light microscopy (1x objective) and the contour of the cavity was delineated using ImageJ as shown in this example by the orange dotted line. ImageJ then calculated the surface area enclosed within the selection. B) Using confocal microscopy, once the section with the largest lesion defined by GFAP labelling was selected, a confocal image of the GFAP labelling was taken (objective 4x). Using ImageJ, a contour of the internal perimeter of the lesion defined by the GFAP positive astrocytes was designed and the surface area enclosed in the section was measured. Note that the sections selected to quantify the largest lesion cavity and the largest lesion were often different as in this example because the selection process was carried out independently in the two quantifications. Scale bar: 500 μm .

2.3.3 Quantification of central canal cavitation

The central canal cavity developed in the lesion block, rostral block and thoracic block. The central canal enlargement was often present on multiple sections in the same lesion block. For this reason to compare the cavity size between different animals the parasagittal section with the largest central canal cavity in each spinal cord block was selected under a Nikon microscope with a 1x objective and an image was taken with Zeiss AxioCam. The central canal borders were traced and measured using Measure and Label, a plug-in of ImageJ (NIH, USA) (Figure 2-9). The same steps were followed in order to quantify the central canal in the rostral block and the thoracic block. In order to compare the measurements obtained from the three spinal cord blocks, it was necessary to standardise the measurements to the length of the segment where the measurement was performed. In fact, the rostral end of the lesion block was approximately 2 mm long while the rostral and thoracic blocks were approximately 4 mm long. This meant dividing the surface of the central canal by the length of the block; in particular, for the lesion block only it was necessary to divide by the length of the rostral or caudal end of the lesion block respectively. The length was measured using NeuronJ, a plug-in of ImageJ (Figure 2-9). The value obtained by dividing the surface by the length was an estimate of the average central canal diameter. The measurement was finally multiplied by a correcting factor of 1241.673 $\mu\text{m}/\text{pixel}$ in order to have the average diameter of the central canal unit measurement in μm .

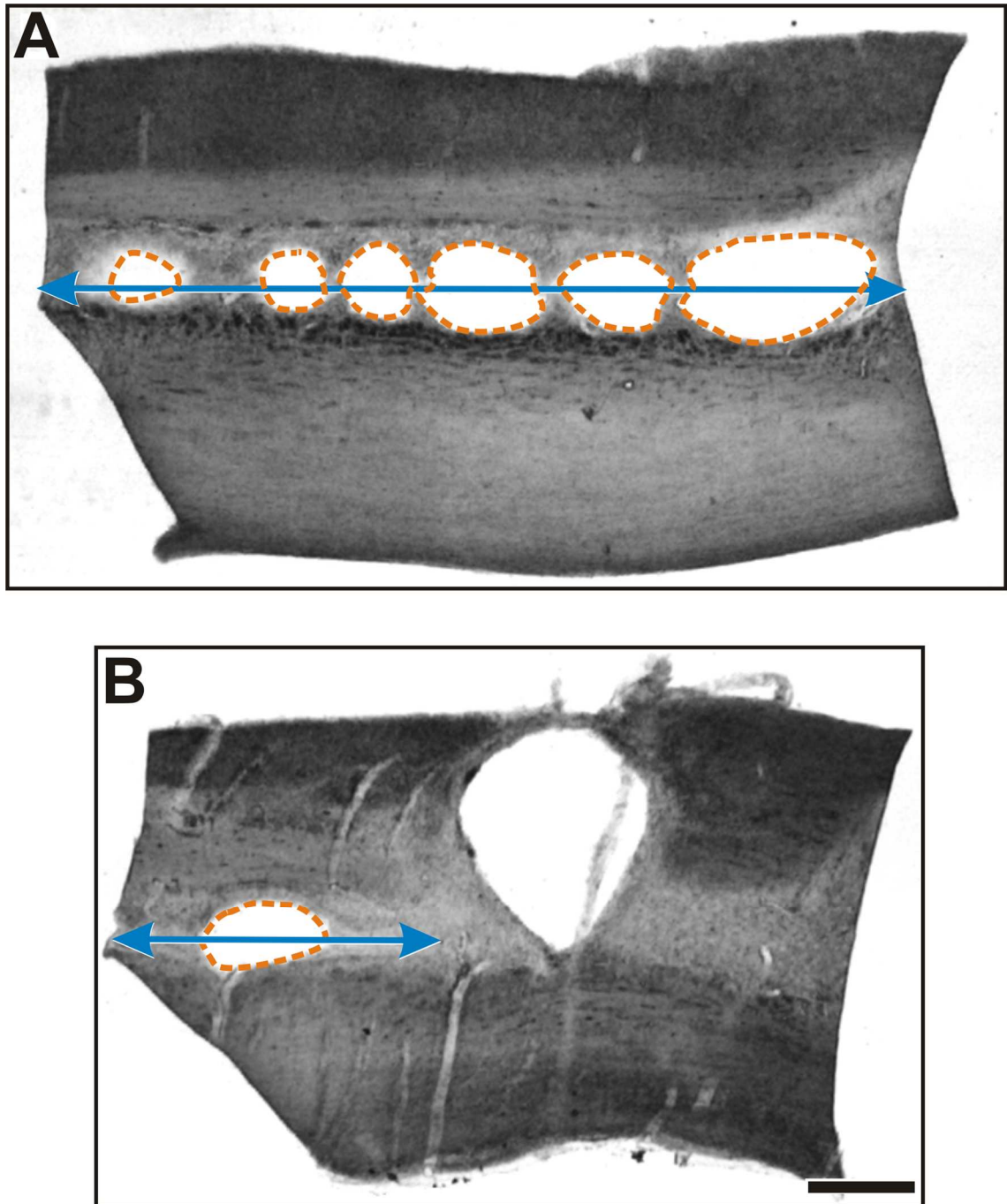


Figure 2-9. Quantification of central canal cavitation.

Two examples to show how the central canal was measured in the spinal cord lesion block and in the rostral block. A) This section from the rostral block of an animal contained the largest central canal cavitation amongst the sections from that block. A picture of the section was taken with light microscopy, and using ImageJ the contour (orange dotted line) of the central canal cavities was drawn. ImageJ then calculated the sum of the surface area enclosed within the selections. With ImageJ it also was possible to measure the length of the section (blue arrow). By dividing the cavitation area in that section by the length of the section it was possible to calculate the average cavitation diameter in that section. B) In this second example, central canal cavitation rostral to the lesion was measured on the section containing the largest central canal cavitation in the lesion block. The procedure was similar to that described in A), however it must be noted that to obtain the average central canal cavitation diameter in the rostral end of the lesion block, it was necessary to measure the length of the rostral portion of the section only; for this reason the blue arrow began immediately rostral to the lesion cavity.

2.3.4 Preliminary analysis on all sections

All parasagittal sections from the lesion, rostral and thoracic blocks (>6000 sections) in all animals were inspected to determine whether any axons labelled with BDA could be detected above the injury. The analysis was performed using a Zeiss Axioplan 2 epifluorescence microscope with a filter set optimal for viewing even extremely thin axons (<1 μm thick) labelled with BDA-Alexa568 (excitation HQ 581/10, BS Q593LP, emission HQ617/40). Those sections that displayed BDA labelling above the injury were subsequently used for quantification as described in section 2.3.6.

2.3.5 Distribution of transplanted cells

For each section information regarding the distribution of transplanted cells was obtained using a Zeiss Axioplan 2 epifluorescence microscope coupled with a filter set ideal to view GFP-Alexa488 (excitation HQ493/16, BS Q507LP, emission HQ 527/30) and dark field illumination. Sections were analysed to obtain information on the location of the GFP labelled OECs, Schwann cells or fibroblasts. This information included where they were situated, the presence of cell tracts or of isolated cells and how the GFP expressing cells had spread from the injection site.

2.3.6 Quantification of fibre numbers in the distal spinal cord

Quantification of the number of fibres was performed with a Zeiss Axioplan 2 microscope fitted with a 63x oil lens and coupled with a 100 W epifluorescence mercury lamp and filter sets optimal for viewing Alexa 568 labelled axons and Alexa 488-GFP labelled OECs. The quantification was performed by counting the number of axons crossing dorso-ventral oriented imaginary lines that were located at increasing distances from the lesion (Figure 2-10). The imaginary line along which the axons were counted passed through the crosshair located in the middle of the field of view. With regards to sections from the lesion block the

quantification process started close to the rostral border of the lesion site. This was not identified by GFAP labelling as GFAP was conjugated to the Cy5 fluorophore which was not visible with the filter sets present on the microscope. The lesion location was identified instead on the basis of BDA background labelling and where applicable labelling of the transplanted cells which normally formed a denser agglomeration in the injection site. The centre of the field of view was placed approximately on the middle of the rostral half of the lesion and was moved from there 200 μm (half a field of view) rostral. That was the first measurement distance and was located approximately 200 μm above the rostral lesion border. The axons passing across that imaginary line were counted by moving the field of view along the dorso-ventral direction and by focusing up and down to follow and count individual axons. Once the measurement along the imaginary line was complete the field of view was moved 200 μm further rostral and a new measurement took place. The process was repeated until reaching the end of the section. On lateral sections of the lesion block where the lesion was not visible it was not possible to identify the location to place the first imaginary line with the method described above. Instead, the location was estimated by calculating the distance of the imaginary line from the rostral end of the section on two or more sections of the same block where the lesion location was easily determined.

With reference to sections from rostral and thoracic blocks, the process of measurement was similar; except that measurements were made starting from an imaginary line located immediately above the caudal end of each section and moved 400 μm (one field of view) thereafter.

During the process of counting axons crossing the imaginary lines it was necessary to switch between the green and red filter sets to note whether or not the axons were located in close vicinity to GFP expressing cells.

2.3.6.1 Inclusion criteria for quantification

The method described in this section to quantify axons rostral to the lesion was designed only after a great number of rats had already been processed. This is why in a relatively high number of rats not enough sections were cut to cover all the areas where BDA labelled fibres normally distributed. Tissue blocks that did

not include medial or sufficiently lateral areas were not used for quantification. The inclusion was done blinded, without knowing the group of which the animals were part of. The inclusion criteria was the following: 1) the lesion block, rostral block or thoracic block were included only if they spanned at least all of the LHS and part of the RHS dorsal columns; 2) the lesion block was included only if 12 or more sections were present to the left of the border between the medial dorsal columns and the nearby grey matter (an example of this border is shown in Figure 3-29); 3) the rostral block or the thoracic block were included only if 10 sections were present to the left of the border between the medial dorsal columns and the nearby grey matter; 4) the inclusion criteria on all blocks was not performed on the block as a whole but considering each distance from the lesion independently. For this reason, for this quantification in the results sections in all tables (except in Table 4) blank cells were used to indicate that the quantification did not meet the inclusion criteria.

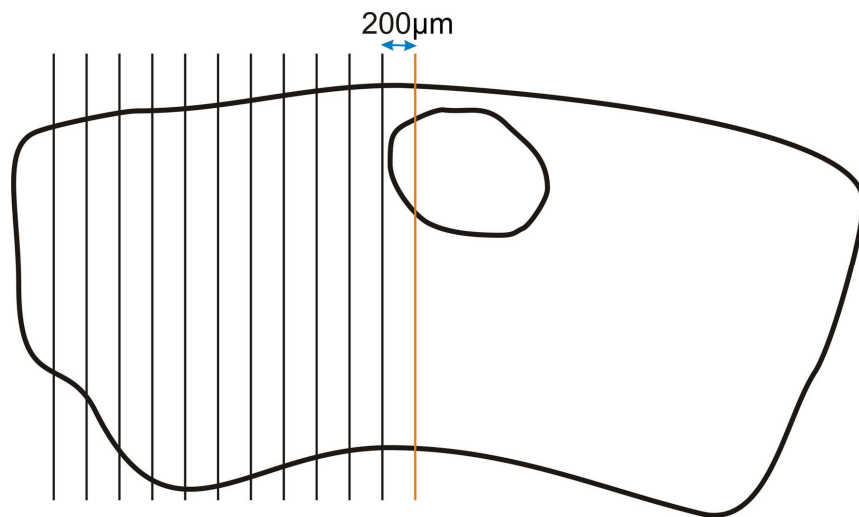


Figure 2-10. Schematic representation of the quantification of the number of fibres labelled with BDA rostral to the lesion.

The quantification was performed using an epifluorescence microscope with a 63x lens. The centre of the field of view (defined by a crosshair on the eye piece) was placed along a dorso-ventral oriented imaginary line passing along the middle of the rostral half of the lesion, here represented in orange. The field of view was then moved 200 μm (half a field of view) rostral defining a new dorso-ventral line passing across the middle of the crosshair here represented by the first black vertical line from the right. By moving the crosshair of the field of view along this line and by focus up and down, the number of BDA labelled axons crossing the imaginary line was counted. After the count was complete the field of view was positioned 200 μm further rostral repeating the same steps.

2.3.7 Determination of section order

To interpret the location of axons and OECs seen in individual sections it was important to know their original topographic position within the spinal cord. For this purpose sections were analysed under the microscope with a dark field view condenser and sections were placed in serial order based on the location of white matter and grey matter. For the lesion blocks only, it was also possible to take advantage of the presence of BDA labelling in the caudal portion of the sections on the LHS of the spinal cord.

2.3.8 Method of recording data on the distribution and axon numbers

An excel spreadsheet was used to register the order of sections, the presence/absence of BDA and GFP labelling and the number of fibres at increasing distances from the lesion on each section. This information was recorded from each section of the lesion, rostral and thoracic blocks for each animal (see the example in Figure 2-11). The information gained and recorded in this type of spreadsheet was easily accessible and allowed complex qualitative and quantitative comparisons of the distribution of transplanted cells and fibre distribution and number.

Figure 2-11 Simplified example of spreadsheet used to record observations made when examining individual spinal cord sections.

This is an example of data recorded from the sections of the lesion block of a rat receiving a wire knife dorsal column lesion and transplanted with Schwann cells. The sections are ordered from left to right of the spinal cord (top to bottom in this example) with the section number indicated in column J. The presence or absence of BDA labelling rostral to the lesion is shown in column A. In sections where BDA was present rostral to the lesion, the number of BDA labelled axons was quantified as explained in section 2.3.6 and shown in columns B-I. If the BDA labelled axons were associated with green GFP labelled cells then the box was given a green background (e.g. cell in column B and row 20), while it was given a red background if no association was detected (e.g. cell in column B and row 8). This method provided a picture of how the axons were distributed along the rostro-caudal and lateral axes. For each section the location of the GFP labelled cells was determined with reference to the white and grey matter; for example GFP labelled cells were present in the white matter of section 118 as shown in the cell in column K and row 20 with a green colour. Furthermore, the presence of large assemblies of GFP labelled cells and their location was registered; for example large assemblies of GFP labelled cells were present in the white matter of section 118 as shown in the cell in column P and row 20. By scrolling through all sections in a block it was also possible to determine whether GFP labelled cells formed virtually continuous cell tracks through the block: this information is shown in row 1 between columns B and I (in this example the Schwann cells formed a continuous track exiting the lesion and continuing for at least 1600 μm rostral). By using light microscopy coupled with a dark field view condenser it was possible to define where the border between the left dorsal column and the grey matter to its left was located; in this example it was located between section 120 and section 112 and in the rostral portion of the section between section 117 and section 120 (see section 3.2.3.6 and Figure 3-29 to better comprehend the necessity of defining the location of this border).

2.3.9 Quantification of fibres in OEC tracts caudal to the lesion

In preliminary observations it was noted that where transplanted OECs had spread caudal to the lesion in large enough tracts, there were often more BDA labelled fibres in the tracts of OECs than in the surrounding cord devoid of OECs. In order to determine whether there was a greater density of fibres within OEC tracts compared to areas devoid of OECs and whether the numbers of axons were affected by conditioning lesions, animals with a survival time of 6 weeks following the dorsal column injury and receiving an acute transplant of OECs with or without combined treatment of conditioning lesions were evaluated for quantification inclusion. Rats that were chosen for inclusion were those with a prominent cell tract extending caudal to the lesion in at least one parasagittal section of the lesion block. For those animals possessing large tracts of OECs in more than one section, two sections with the largest tracts were included. The selection was performed by using the epifluorescence microscope on the green channel. To avoid bias during the selection process and subsequent quantification steps this was done blinded; furthermore the red channel was not used during these selection steps.

Quantification of the numbers of fibres within OEC tracts was performed with a confocal microscope coupled with light and U.V. sources. By using light microscopy the centre of the field of view with a 20x lens was placed at the centre of the lesion, then moved caudal by a distance equivalent to one field of view. The field of view was then moved along the dorso-ventral axis so that the top of the field of view included the dorsal border of the spinal cord section. The filter set was then switched to epifluorescence with the green channel: if an OEC tract was not present at this location the field of view was moved ventrally until an OEC tract was located. If an OEC tract was still not present the field of view was moved along the rostral-caudal direction to localise one. Normally the image was taken very near to the original intended location. Then the lens was switched to 60x oil and took with the confocal a stack of images 1 μm apart that included the whole thickness of the OEC tract. Because a short pilot study it was previously shown that projecting the whole stack often produced a projected image possessing too many axons that was too complex to be quantifiable, it was necessary to reduce the density of axons in the projected image. This was

possible by sampling the original stack and projecting no more than 3 stacked images at a time (Figure 2-12). For this purpose each stack of images for both channels was projected with Confocal Assistant from 3 locations within the stack into 3 independent projected images for each channel to sample the whole of the stack as uniformly as possible and reduce the density of axons in the image. The 3 projections of the stack were each made of 3 images 1 μm apart selected by a formula as shown in Figure 2-12.

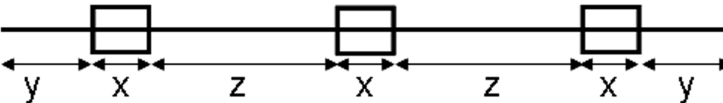
$$\begin{aligned}
 x &= 3; \quad y = 1/2z; \\
 a &= y + x + z + x + z + x + y = 1/2z + 1/2z + z + z + x + x + x = \\
 &= 3z + 3x = 3z + 9; \quad \rightarrow z = (a - 9) / 3
 \end{aligned}$$


Figure 2-12 Method to determine which stacked images to project.

After making a confocal image stack of BDA and GFP labelling of the whole thickness of a section, 3 locations within the stack were selected and projected for subsequent quantification of axonal density. To determine which images within the stack were to be projected this formula was followed where “a” was the total number of images in the stack, “x” was the number of images to be projected and was a fixed value (3 images), “z” was the number of images between two “x” locations and “y” was the number of images between the most external image in the stack and the closest “x” location. By knowing the total number of images in the stack it was possible to calculate the values for “y” and “z”.

The red and green channels were subsequently merged. With Photoshop the regions where green OECs were present were manually delimited by a thick red line before removing the green channel. Then the red channel was converted into greyscale and greyscale grading was inverted to visualize the axons in greyscale: BDA labelled axons were best visualised in shades of grey on a white background compared to the original red/black colour settings. The contrast and luminosity were modified to optimally highlight the axonal profiles (see example in Figure 3-23). The surface delimited by the line drawn on Photoshop was measured with ImageJ. The axons were traced with NeuronJ (Meijering et al., 2004), a plug-in of ImageJ. NeuronJ allows the user to trace the axons on an image precisely and rapidly and to quantify the total axon tracing. Axon tracing was performed on each projected image 3 times 1 week apart to reduce the error associated with the measurement. Average fibre density in each projected

image was calculated by dividing the length of tracing in each image by the surface of that image. Fibre density of each section was then obtained by averaging the densities of the 3 projected images. Fibre density for each animal was calculated from the average of the density in each section. The densities were multiplied by a conversion factor ($0.79 \text{ pixel}/\mu\text{m}^2$) that introduced the 3rd dimension ($5 \mu\text{m}$ thickness for each projection: $3 \mu\text{m} + 1 \mu\text{m}$ on either side due to the confocal iris size) and introduced the metric system in place of pixels.

Confocal stacks of images were also taken in regions devoid of GFP labelled OECs to quantify the density of BDA labelled axons out of the OEC tracts and compare this to the density of BDA labelled fibres in the OEC tracts. The field of view of the microscope was positioned following the same procedure described above except that areas devoid of GFP OECs were selected. The sections that were utilised for this purpose were both the LHS and RHS sections adjacent to the section utilised for quantification in the OEC tracts. Subsequent image manipulations and measurements were performed following the same rules described above.

BDA labelled axons associated with OEC tracts were often so dense even in the projection of only 3 stack image projections that it wasn't possible with NeuronJ to trace all axons: as a consequence the measured fibre length for these projections was an underestimate of the actual length.

2.3.10 *Quantification of fibre density in the injury*

The fibre density within the tracts of transplanted OECs caudal to the injury gave an indication of the growth state of the lesioned sensory BDA labelled axons. It would have been interesting to quantify also the density of fibres within the lesion site itself as it would have given an indication of the permeability of the glial scar to regenerating fibres; but the quantification of fibre density within the lesion site was not possible because it proved to be extremely time consuming. There was too much fibre ingrowth variability in the lesion between different animals and even amongst different sections within the lesion block of the same animal. The variability was likely due to the following:

a non uniform distribution of OECs in the lesion so that some sections ended up displaying great ingrowth in the transplant while others did not; the facility with which the lesion site was damaged during processing; the fact that BDA labelled axonal ingrowth in each animal even within the same treatment group appeared highly variable. Because of these points it would have been necessary to measure BDA labelled fibre ingrowth in the lesion on all sections encompassing the lesion rather than in a sample of sections per animal. Unfortunately, this type of approach proved to be incompatible with the time scale of this project.

2.3.11 *Quantification of fibre number in non-lesioned animals*

In non-lesioned animals tissue blocks were taken at the L3-4 level, at the T12-13 level, at the C4-5 level and at the dorsal column nuclei level. While the number of labelled axons in the spinal cord at increasing distances from the injection site in the L3-4 spinal nerves was measured in all lesioned animals as described in section 2.3.6, this method wasn't applicable for non-lesioned animals. In fact, in non-lesioned animals, due to the high number of axons present, it was impossible to discriminate traced fibres one from the other with that quantification method. Consequently, it was necessary to count the profiles of traced axons on transverse sections. Traced axons from the L4 and L5 dorsal roots travel in the ipsilateral dorsal columns and send projections to the grey matter, especially in the segments closer to the dorsal root entry zone. On transverse sections, collateral branches descending into the grey matter can be easily distinguished from axons running in the dorsal columns: the first appear near to parallel to the plane of the section in a transverse section, while the latter are near to perpendicular to the plane of a transverse section. One single section that exhibited typical BDA labelling was chosen from the L3-4 level, the T12-13 level and the C4-5 level for each animal. Multiple confocal projected image stacks were made with a 40x oil objective to include the whole left hand side dorsal column of each section and were used to count the number of BDA labelled axons. For this purpose, firstly, each stack of images was merged into a projection image; secondly, all projected images were united in one composite image that spanned the whole left hand side dorsal column (examples at the

lumbar, thoracic and cervical level are shown in section 3.2.1). Luminosity and contrast were then adjusted to optimize the view of individual axons and finally counts were made with the Cell Counter plug-in on ImageJ (NIH, USA).

2.3.12 *Statistical analysis*

All statistical analysis was performed using GraphPad software. Each measurement group was analysed using the Kolmogorov-Smirnov test with Dallal-Wilkinson-Lilliefors P value to understand if data followed a Gaussian distribution: data was considered to be normally distributed when P was greater than 0.05. Paired or unpaired data sets were compared with the two tailed t test when both data sets followed a normal distribution. When one or both of the groups to be compared did not fit the normality requirements paired or unpaired data was compared with a two tailed Mann-Whitney test. Two measurement groups were considered significantly different if the t test or the Mann-Whitney test gave a P value smaller than 0.05. All error bars shown in graphs were represented by the standard error (StErr) of the average value.

2.3.13 *Confocal microscopy imaging*

All confocal images were taken with a Bio-Rad confocal coupled with a Nikon microscope. Images shown in the results sections consisted of either image stacks or of individual images. Image stacks were typically taken through the whole depth of the 70 μm thick sections with spacing between each image of 2 μm when using 40x oil objective and 5 μm when using the 10x objective. Stacked images were projected using Confocal Assistant (Todd Clark Brelje). Where applicable multiple channels were merged after projection into one image with Confocal Assistant and then converted to Tiff file format. Composite images of projected image stacks or composite images of individual images were made where necessary to show larger views of the section of interest. Composite images were assembled using Adobe Photoshop CS2. All images of parasagittal

sections shown in the results sections are oriented with the rostral end to the left and caudal to the right.

3 Transplantation of OECs and conditioning lesions

3.1 Introduction

Transplantation of OECs and conditioning lesions have already been introduced extensively in the general introduction. The field is still lacking sufficient information on the regeneration promoting properties of OECs after injury, particularly with reference to ascending systems such as DRG neurons. Furthermore, it is not clear whether OECs need to localize in the distal spinal cord to allow long distance axonal regeneration or whether it is enough for them to remain confined to the lesion site. Once these two questions have been answered it would be interesting to find out whether combination of OEC transplantation with conditioning lesion might boost the regenerative effect seen with OEC transplantation alone.

3.2 Results

3.2.1 Biotinylated dextran amine tract tracing in non-lesioned rats

The aim of this first section is to describe the distribution and intensity of biotinylated dextran amine (BDA) tract tracer labelling in the non-lesioned spinal cord to form the base line for future experiments. For this purpose BDA was injected in the L4-5 spinal nerves of three rats and perfusion fixation was performed two weeks later as shown in Figure 3-1. Transverse sections of the spinal cord tissue were cut from two rats while parasagittal sections were cut from a third animal.

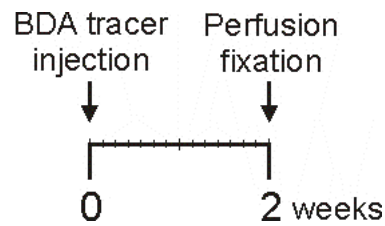


Figure 3-1. Time course of operations performed on the animals used to characterise tract tracer labelling.

Labelling was detected in sections cut from the spinal cord block at the L3-4 level as shown in Figure 3-2. BDA labelling was found also at the thoracic and cervical levels and in the brain stem dorsal column nuclei, to which some of the L3-4 sensory neurons are known to project (Figure 3-3, Figure 3-4 and Figure 3-5). The number of labelled fibres decreased dramatically at increasing distances from the tracer injection site and very few axons were labelled at the cervical level and in the dorsal column nuclei. Most of the fibres were located in the medial portion of the dorsal columns, however many axons sent collaterals to the grey matter (Figure 3-2). The collaterals that descended to the grey matter were mostly located at the lumbar level and very few were detected in the segments above (compare Figure 3-2, Figure 3-3 and Figure 3-4). As expected BDA labelling was ipsilateral to the injection and was never found on the contralateral side of the spinal cord. Images of BDA labelling from transverse sections at the lumbar, thoracic, cervical and brain stem level of the same animal are shown in Figure 3-2, Figure 3-3, Figure 3-4 and Figure 3-5 respectively.

To confirm these observations quantitatively, the number of axons in the dorsal columns was counted in transverse sections of 2 non-lesioned rats and is shown in Table 2 (for methodology see section 2.3.11). On average the number of axons present at the thoracic level was 77% of those present at the lumbar level; while at the cervical level only 15% of the fibres found at the lumbar level were present.

Figure 3-2. Labelling at the L3-L4 spinal cord level in a non-lesioned animal following injection of BDA tracer in the left L4-5 spinal nerves. **A)** Composite of confocal images taken on a transverse section at the L3-4 level in a non-lesioned animal with a 10x objective lens; the image shows the normal location of BDA labelled axons close to their dorsal root entry zone. **B)** 40x composite image of confocal stacks from the area boxed in blue in image **A** showing the distribution of axons; fibres running perpendicular to the image plane through the dorsal column white matter sent many projections down to the grey matter. Scale bars: 400 in **A** and 100 μm in **B**.

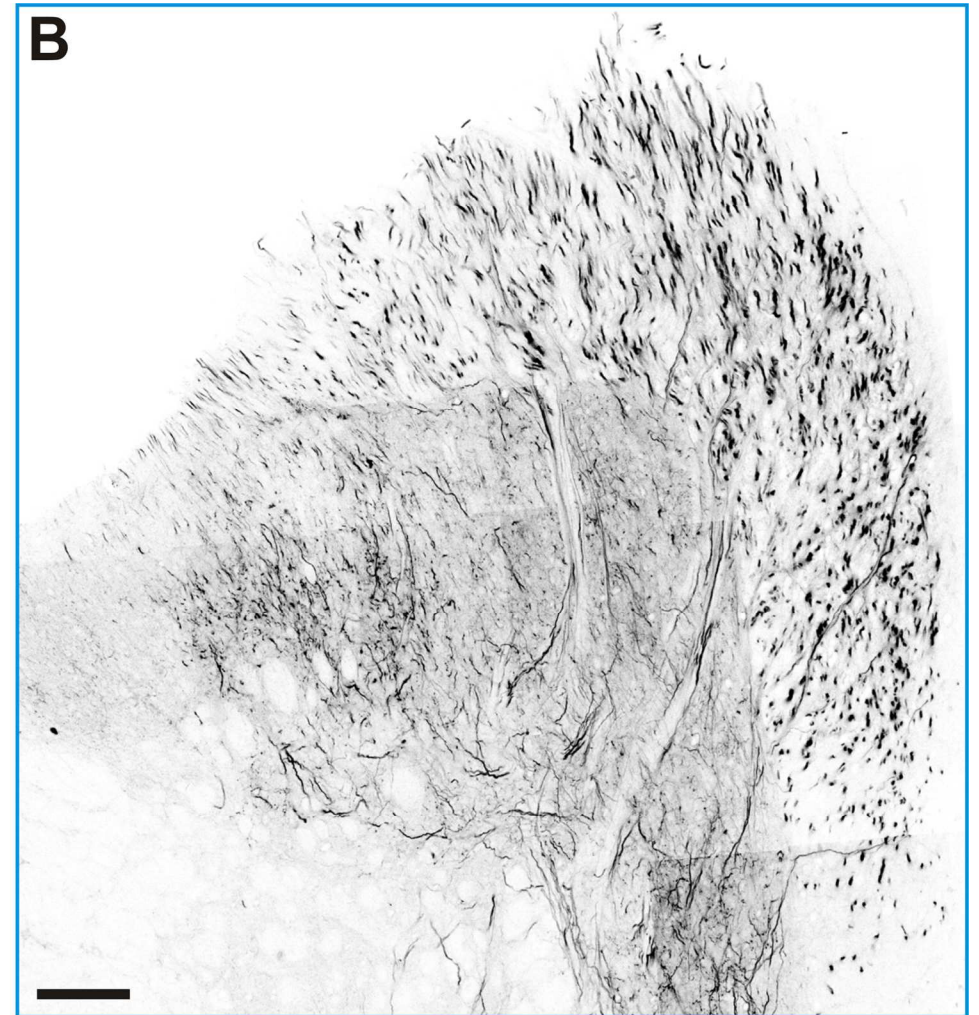
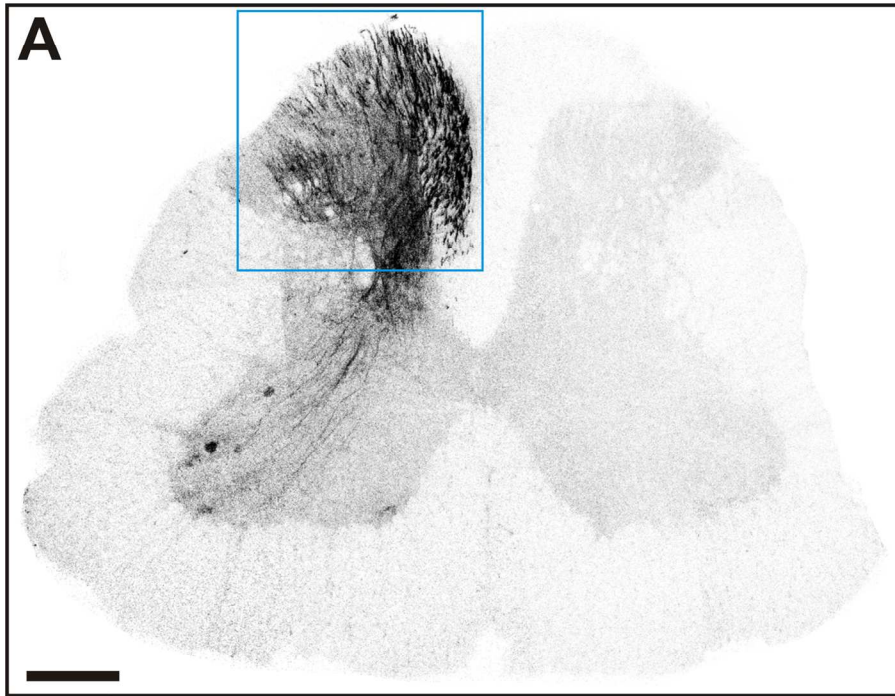


Figure 3-3. BDA labelling at the thoracic level in a non-lesioned animal.

A) Composite of confocal images taken on a transverse section with a 10x objective; the image shows that BDA labelling of axons belonging to L4-5 dorsal root ganglia neurons at the T12-13 level was mainly restricted to the medial portion of the dorsal columns; the labelling also appeared less intense than that detected at the lumbar level. **B)** In this 40x composite image of confocal stacks taken on the area boxed in blue in image **A** it is possible to see that only a small number of axons sent collaterals to the grey matter in the region of Clarke's column; note also that most axons were located in the medial portion of the dorsal columns but some were still detected in lateral portions of the dorsal columns (arrow head) above the left dorsal horn. Scale bars: 400 in **A** and 100 μm in **B**.

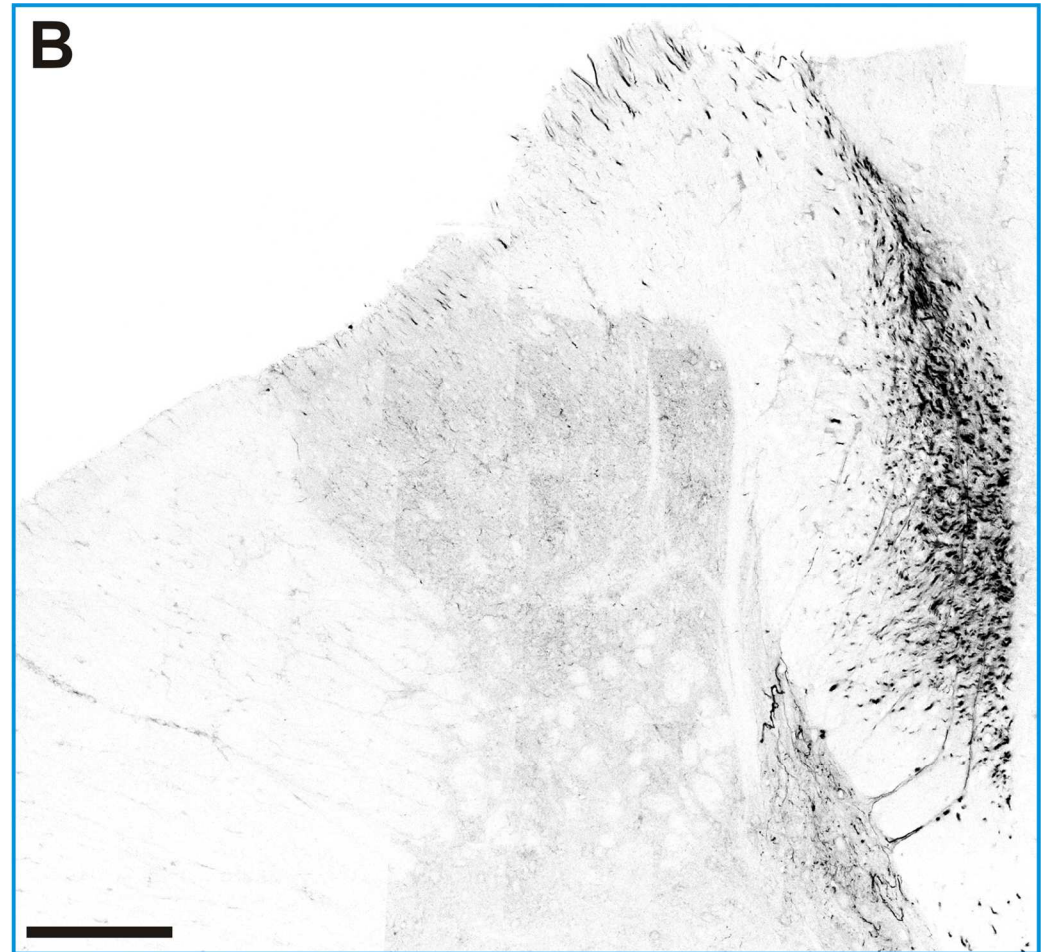
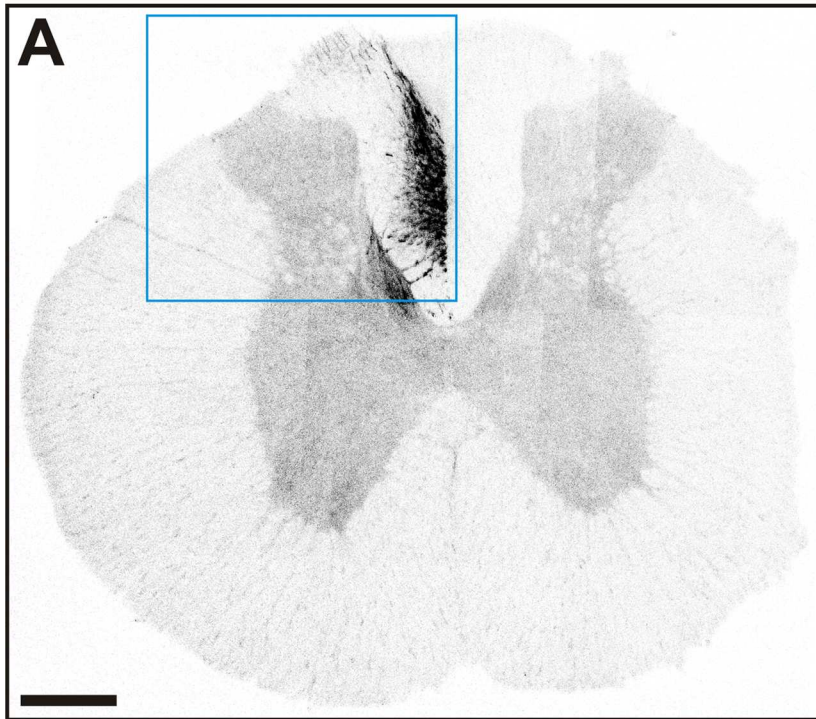


Figure 3-4. BDA labelling at the cervical level in a non-lesioned animal.

A) Composite of confocal images taken on a transverse section at the C4-5 level with a 10x objective; the image shows that the number of axons was clearly diminished compared to caudal segments. **B)** In this 40x composite image of confocal stacks taken on the area boxed in blue in image **A** it is possible to notice that all labelled axons were concentrated in the dorso-medial portion of the medial dorsal columns corresponding with the fasciculus gracilis. Scale bars: 400 in **A** and 50 μm in **B**.

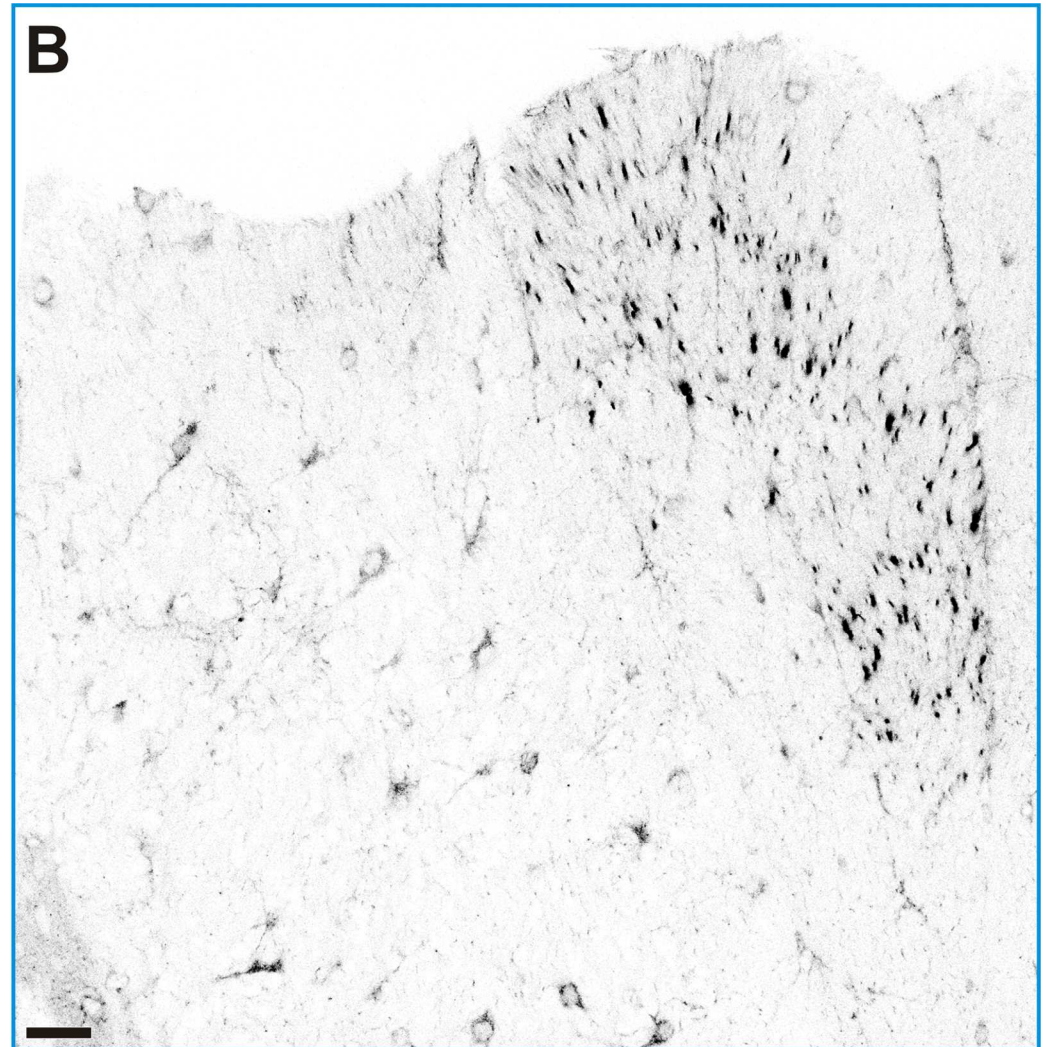
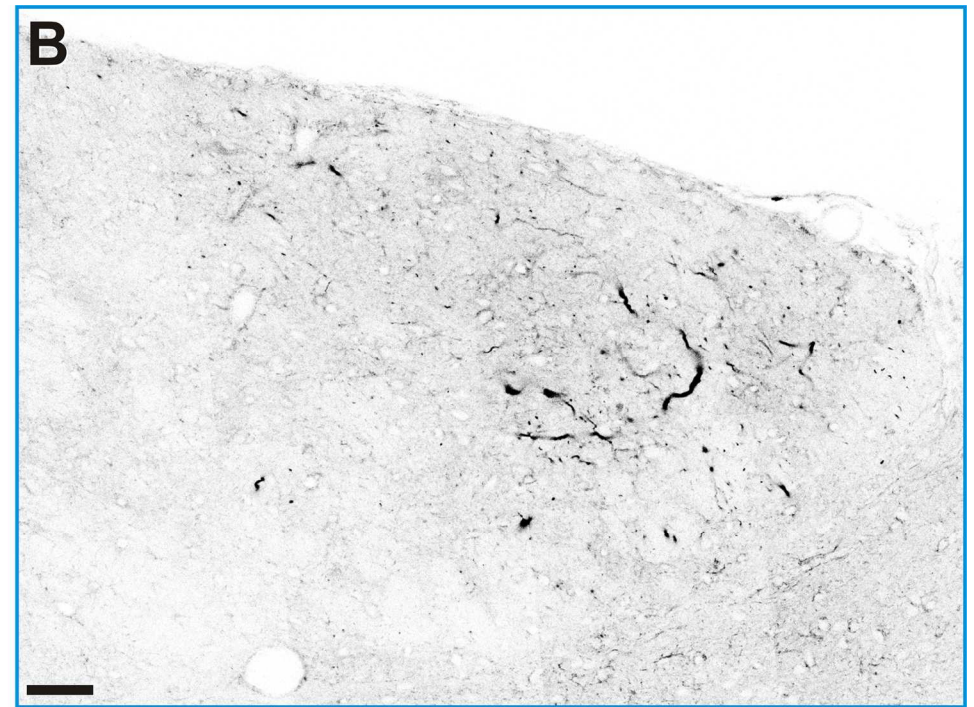
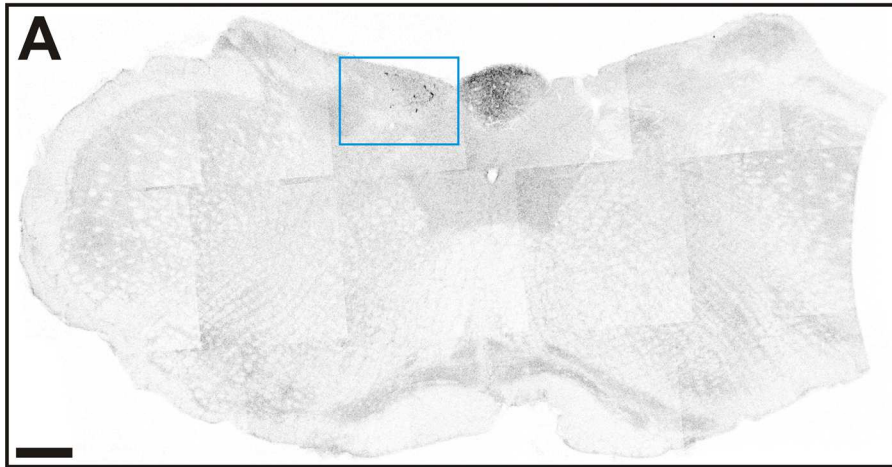


Figure 3-5. Labelling of BDA at the brain stem level in a non-lesioned animal.

A) Composite of confocal images taken on a transverse section of the gracile nucleus with a 10x objective; the image shows that BDA was detected even in the brain stem where dorsal root ganglia project, however very few axons were labelled as shown in image **B**. The area with dark non-specific background labelling located out of the blue box was the area postrema. **B)** 40x composite image of confocal stacks showing the boxed area in **A** at higher magnification. Scale bars: 400 in **A** and 50 μm in **B**.



| | L3-L4 | T12-13 | C4-C5 |
|---------|--------|--------|-------|
| R17907 | 1225 | 856 | 225 |
| R2608 | 1247 | 1053 | 48 |
| average | 1236.0 | 954.5 | 136.5 |

Table 2. Quantification of BDA labelled axonal numbers in non-lesioned animals.

Quantification was performed on transverse sections of the lumbar, thoracic and cervical cord. Quantification was performed on composites of confocal projected images stacks taken with a 40x oil lens that covered the whole left dorsal columns. The number of labelled axons dramatically decreased in both rats analysed at increasing distances from the BDA injection point.

3.2.2 Dorsal column wire knife lesion

To determine the characteristics of the dorsal column lesion produced using a wire knife in animals that did not receive a transplant seven rats were lesioned at the L3-L4 spinal cord level and sacrificed six weeks later. These animals were also injected with BDA in order to assess the effects of the lesion on the projection of axons of sensory dorsal root ganglia neurons in the dorsal columns. The time course of the operations is shown in Figure 3-6. The spinal cord block containing the lesion site was cut into parasagittal sections in six animals and into transverse sections in one animal.

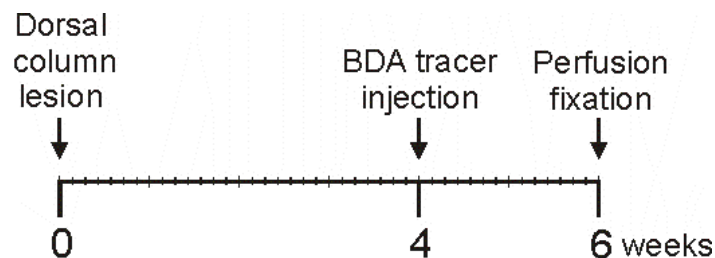


Figure 3-6. Time course of operations performed on spinal cord lesioned untreated animals.

3.2.2.1 Dorsal column wire knife lesion size and morphological characterization

By examining the lesion site with light microscopy it was possible to note that all seven rats developed a cavity during the intervening period of six weeks following the injury. In all animals the cavity had a rounded shape and encompassed all or nearly all of the width of the dorsal columns. The cavity was located where the original lesion was performed, as defined by a stitch placed in the dura at the time of the injury. The cavity enveloped the central canal but it was not clear if it was continuous with it. The cavity was delimited dorsally by a thin rim of connective tissue attached to the pia mater that was spared at the time of the injury along with the overlying dorsal vein. As the cavity spanned a number of parasagittal sections, the cavity size was measured in each rat from the parasagittal section containing the largest cavity and calculated as the

cavity cross sectional area. Quantification is shown in Figure 3-9A (for details see methods, section 2.3.1).

It is well established that a glial scar develops following a spinal cord injury. By means of confocal microscopy and the specific recognition of astrocytic cells using the GFAP antibody, it was possible to identify the glial scar at the lesion site (Figure 3-7). As described in methods, section 2.3.2, the lesion size in each animal was measured from the section containing the largest lesion as defined by the internal borders of the GFAP labelling and measured as the lesion cross sectional area (Figure 3-9A). As expected the difference between the mean lesion and mean cavity size was not significant ($P=0.54$); in fact in all animals a GFAP positive rim of tissue enclosed the cavity so that the borders of the lesion defined by GFAP labelling actually corresponded with the cavity borders. Neither GFAP positive processes nor any processes visible with light microscopy were observed in the cavity connecting one side of the lesion with the other except occasionally on very lateral portions of the cavity where its dimension decreased. Although unlikely, it cannot be excluded that the tissue processing steps might have destroyed any such tissue connections if these were present originally.

3.2.2.2 Characterization of central canal cavitation

The lesion cavity wasn't the only cavity that developed. Of the 7 rats analysed at 6 week survival all developed a cavitation of the central canal (Figure 3-8), known as syringomyelia (Radojicic et al., 2007). Such cavitation was always observed in the rostral half of the lesion block, in the rostral block and in the thoracic block, but never in the caudal half of the lesion block. The cavitation appeared as consecutive enlargements and constrictions of the central canal. These were of variable size and their diameter surpassed in some cases that of the lesion cavity. Because the central canal enlargements would span a number of parasagittal sections, the average central canal diameter was quantified in each rat on the parasagittal section containing the largest enlargements and calculated as follows: the central canal cavity cross sectional area divided by the

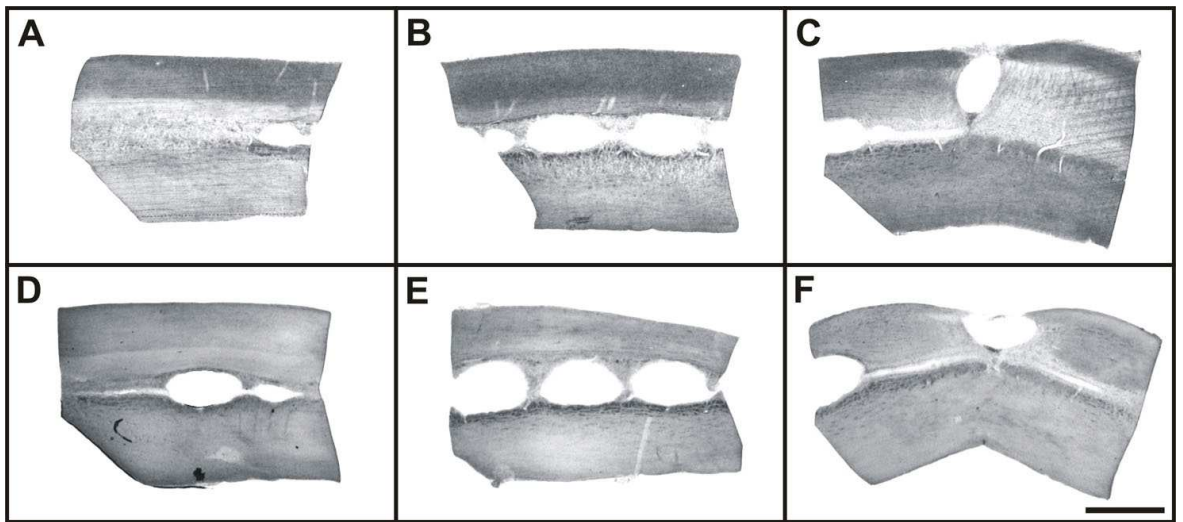
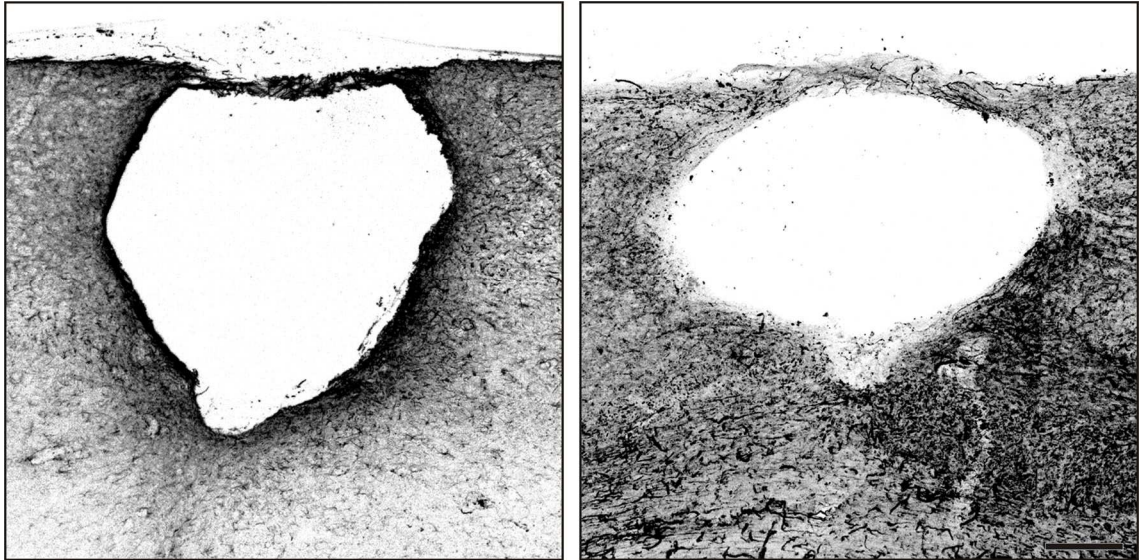
length of the section (see methods, section 2.3.3). Quantification is shown in Figure 3-9 B.

Figure 3-7. Dorsal column wire knife lesion morphology in non-transplanted animals with a survival time of 6 weeks.

Composites of confocal images of GFAP immunoreactivity of parasagittal sections spanning the lesion site from two animals. The lesion developed as a rounded acellular structure surrounded by a GFAP positive glial scar. The lesion was capped by a thin rim of tissue. No GFAP processes nor other structures were found to extend within the lesion or connect opposite sides of the lesion. Objective 10x. Scale bar 200 μ m.

Figure 3-8. Central canal cavitation rostral to and caudal to the lesion.

Light microscopy images taken with a darkfield view condenser from parasagittal sections of two animals of the lesion block (**C, F**), rostral block (**B, E**) and thoracic block (**A, D**). The cavitation was absent caudal to the lesion level, while it developed above the injury in the form of consecutive enlargements and constrictions presumably filled with cerebrospinal fluid in place of the grey matter. Objective 1x. Scale bar: 1mm.



3.2.2.3 Tract traced fibres caudal to the lesion

In six of the seven rats lesioned with the wire knife BDA was injected into the L4-5 spinal nerves two weeks before perfusion. In the spinal cord of these rats a large number of ascending sensory axons were labelled with the BDA tract tracer. Tracer labelling was observed in the medial and lateral dorsal columns on transverse sections of the caudal block (Figure 3-10) and on parasagittal sections of the lesion block (Figure 3-11). In the region immediately caudal to the lesion cavity in all rats analysed some axons presented enlargements, end bulbs and retraction bulbs typical of axotomised fibres.

3.2.2.4 Tract traced fibres rostral to the lesion

BDA labelled fibres were found rostral to the lesion in 3 of the 7 rats that were injected with tract tracer. Axonal labelling was quantified by counting in parasagittal sections the number of tract traced axons at increasing distances from the lesion as described in methods, section 2.3.6, and results are shown in Table 3. In order to understand the origin and location of these fibres, serially ordered parasagittal sections as well as transverse sections of the lesion, rostral and thoracic blocks were analysed. In all animals tract traced fibres were virtually absent within the medial dorsal columns of parasagittal sections (Figure 3-11) and transverse sections (Figure 3-12). This observation indicated that the lesion was effective in ablating all fibres running through the medial dorsal columns and that no axons were spared or regenerating through the dorsal cap of connective tissue that formed adjacent to the dorsal vein which remained intact after the injury. Fibres were also absent in the grey matter ventral to the medial dorsal columns indicating that no sparing or regeneration occurred beneath the lesion. Finally, as expected labelled axons were absent on the contralateral side to the right of the injury in the lesion, rostral and thoracic blocks.

In 3 of the 7 rats, however, tract traced axons were located in the lateral portions of the left dorsal columns at the lesion level and rostral to the injury in the lesion block, rostral block and thoracic block. The most lateral axons were located in the dorsolateral fasciculus, a portion of the lateral dorsal columns. The morphology and trajectory of labelled axons located beyond the lesion site appeared similar to those of intact axons. Furthermore, these fibres were found to give rise to collateral branches to the grey matter and this occurred more and more sporadically at increasing distances from the lesion. This is in accordance with the fact that non-lesioned sensory muscle and cutaneous L4 and L5 afferents are known to branch most collaterals within the first couple of segments from the dorsal root entry zone (Shortland et al., 1989; Shortland and Woolf, 1993).

Figure 3-10. BDA labelling caudal to the lesion in a transverse section of the caudal block.

Composite of confocal images taken approximately 2 mm caudal to the lesion level. Labelling of injured axons was intense and encompassed most of the left dorsal columns. Labelled axons also sent collaterals to the grey matter. Scale bar: 200 μm .

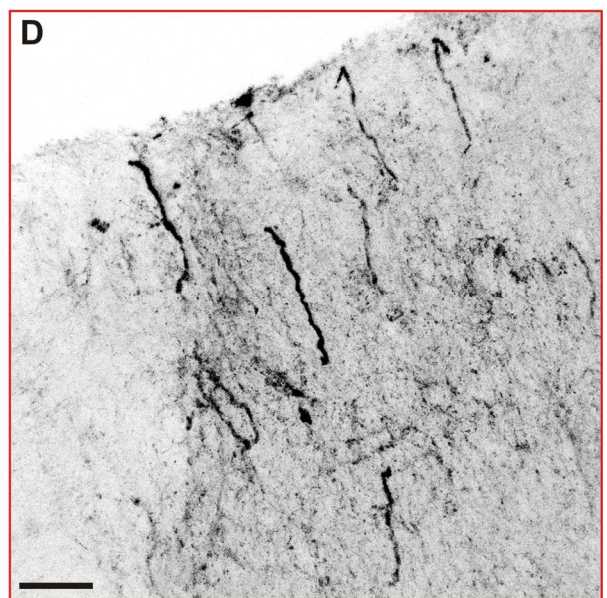
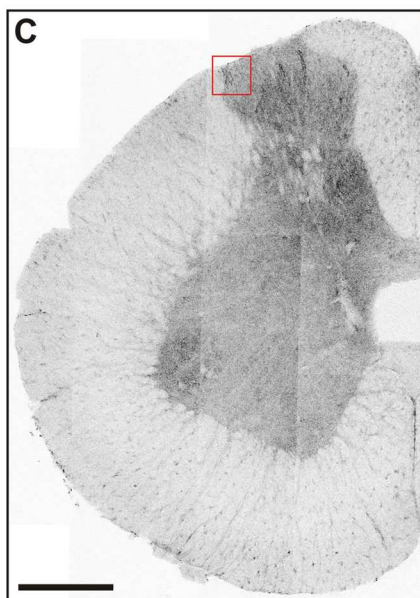
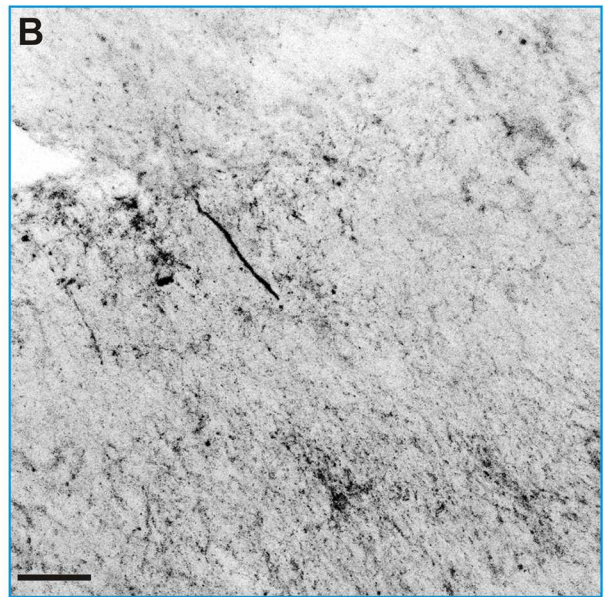
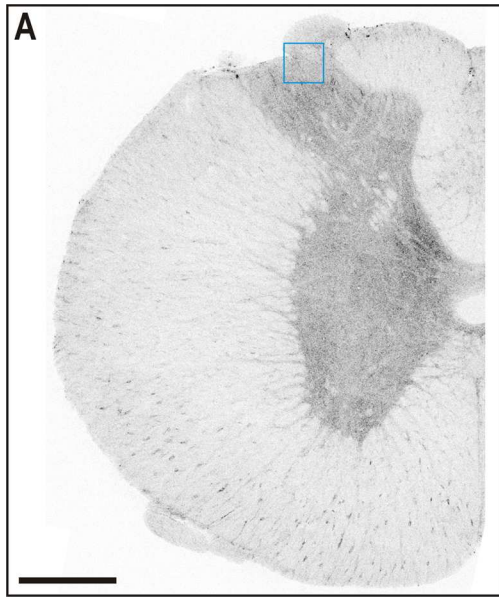


Figure 3-11. BDA labelling was interrupted at the lesion level in medial dorsal columns.

Composite of confocal images of a parasagittal section from a dorsal column lesioned rat showing BDA labelling interrupted by the lesion. While extensive labelling was detected caudal to the lesion as seen in Figure 3-10, no axons were detected in the medial dorsal columns rostral to the lesion. Objective: 20x. Scale bar: 100 μ m.



Figure 3-12. Tract tracing in transverse sections rostral to the dorsal column lesion. Composites of confocal images were taken from the same animal also depicted in Figure 3-11 from transverse spinal cord sections to show BDA labelling at the caudal end of the rostral block (**C-D**) (approximately 2 mm rostral to the lesion) and thoracic block (**A-B**) (approximately 10 mm rostral to the lesion). **A** and **C**) No BDA labelling was detected in the medial dorsal columns or in the medial grey matter ventral to the dorsal columns (10x objective). The boxed areas in **A** and **C** demarcate all the BDA labelled axons detected and these are shown at a higher magnification in **B** and **D** respectively. **B** and **D**) Projections of confocal images taken with a 40x oil lens demonstrate the presence of tract traced fibres rostral to the injury level located in the lateral dorsal columns. Scale bars: 500 μm in **A** and **C**; and 25 μm in **B** and **D**.



3.2.2.4.1 *Tract traced axons passing the lesion level*

In rats possessing labelled axons rostral to the lesion, bundles of fibres were seen to cross the lesion level on parasagittal sections lateral to the lesion (Figure 3-13A). The location of these fibres was in the extreme lateral portions of the dorsal columns which was lateral enough not to be damaged by the dorsal column lesion. The size and trajectory of the fibres appeared normal when compared to fibres located caudal to the lesion level. Instead, in rats that did not possess any labelled fibres rostral to the lesion, all axons ended at the lesion level even on very lateral sections. Arborisations and collaterals to the grey matter were observed originating from these extremely lateral axons both rostral and caudal to the dorsal column transection level (Figure 3-14).

Furthermore, it was possible to confirm that terminal boutons could be seen because they occurred in the centre of a confocal image stack connected to the axon on one side only. In the light of these findings the most likely hypothesis to explain the origin of the axonal labelling detected rostral to the lesion involves fibre sparing: some axons must have been located to the left of the wire knife and were not ablated by it. To confirm this hypothesis a more extensive wire knife dorsal column lesion was performed on some animals as described in the following section.

Figure 3-13. Tract traced axons at and rostral to the lesion level on lateral sections from animals receiving a dorsal column lesion.

A) Composite of projections of confocal stacked images of a section of intact spinal cord tissue to the left of the lesion in the lesion block (20x objective); lesion level is indicated by a dashed line. It is possible to follow individual axons crossing the lesion level. **B-D)** Confocal projected images (40x objective) that show BDA labelled fibres rostral to the transection level in the lesion block (**D**) (blue boxed area), rostral block (**C**) and thoracic block (**B**). Scale bars: 100 μm in **A**; 50 μm in **B-D**.

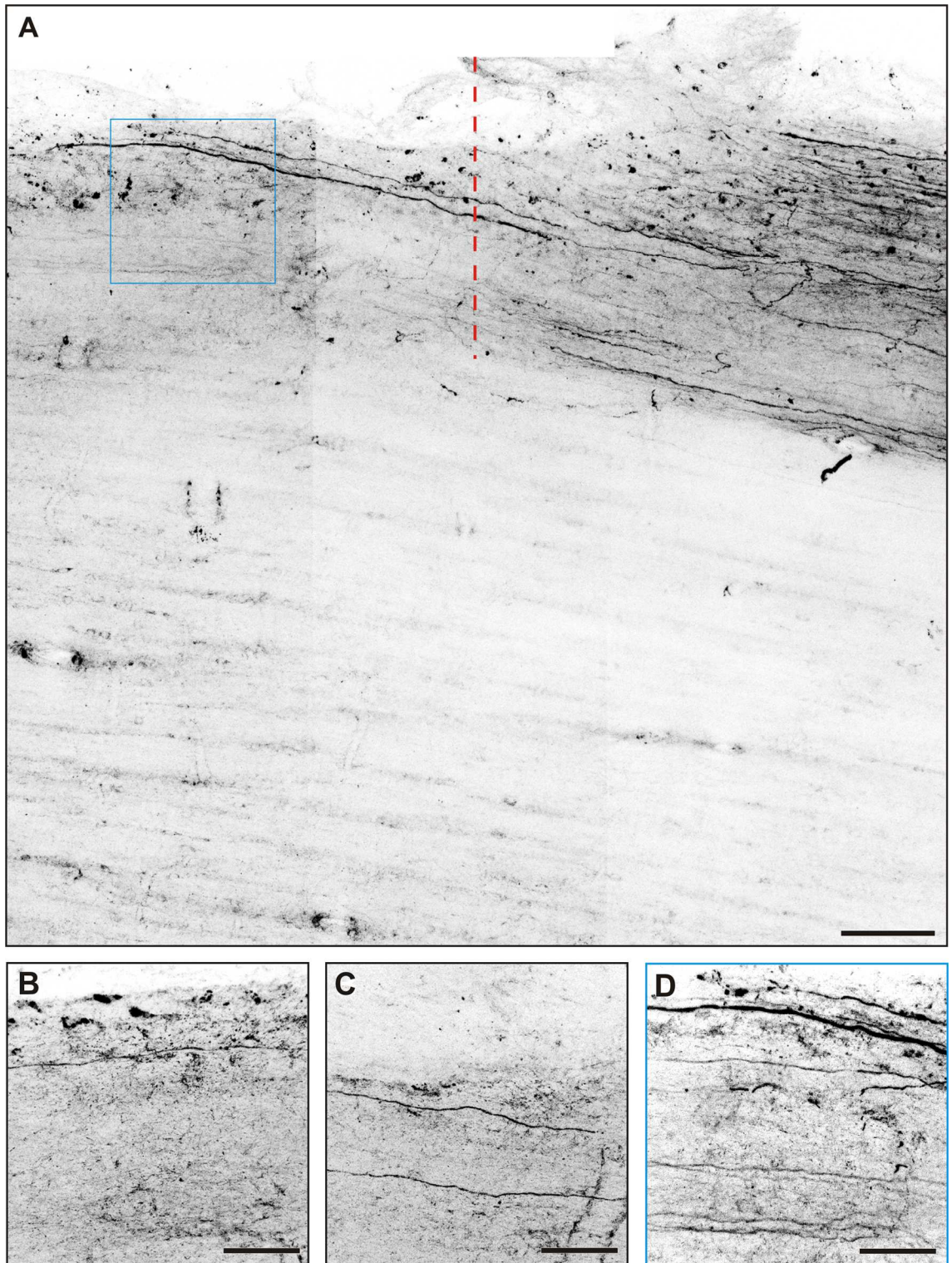
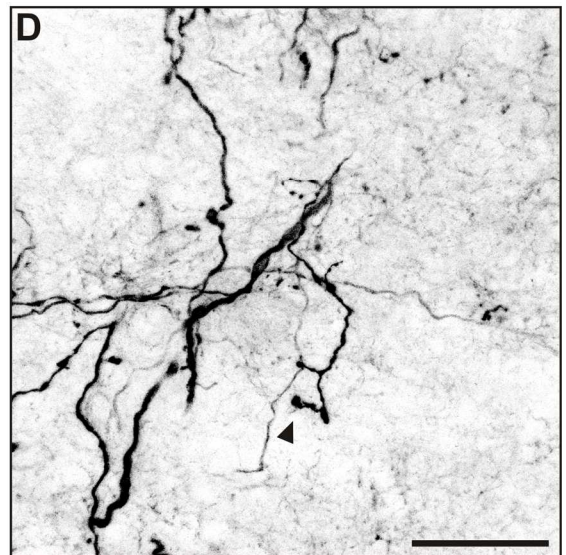
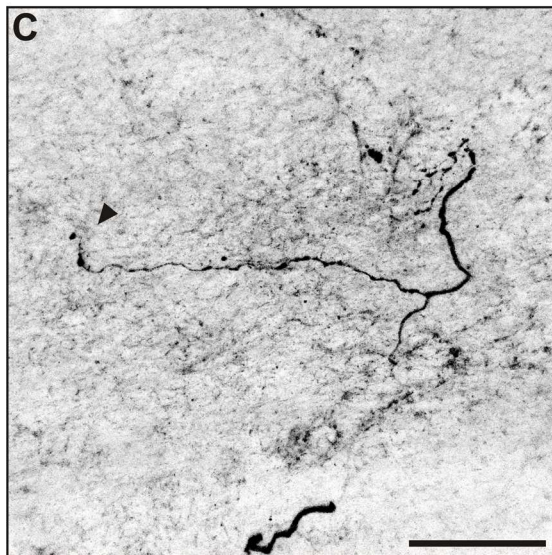
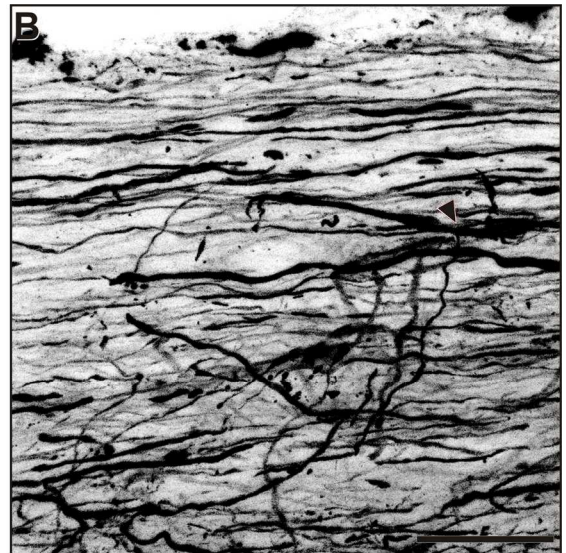
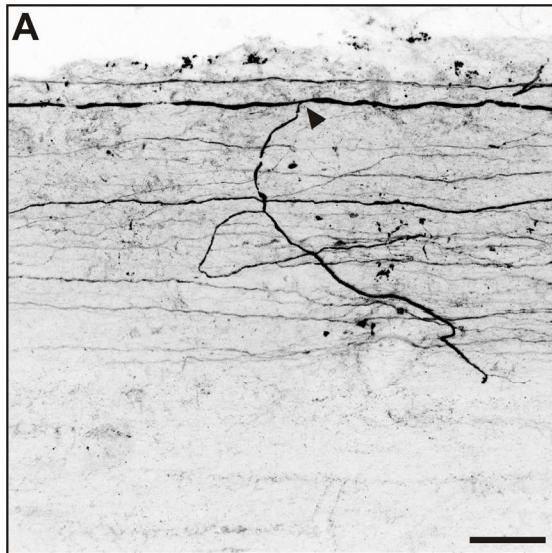


Figure 3-14. Branching of axons in the most lateral dorsal columns in a rat 6 weeks after a dorsal column lesion.

A-D) Projections of confocal image stacks. **A)** BDA labelled axons rostral to the lesion level in the white matter of the lateral dorsal column have collateral branches (arrowhead). This suggests that these fibres are spared rather than regenerating: compare with image **B** where branching caudal to the lesion level is shown (arrowhead). **C)** Furthermore, BDA labelled axon collaterals formed terminal arborisations in the grey matter ending with synaptic boutons well within the stack of images (arrowhead): compare with terminal arborisations and synaptic boutons caudal to the lesion shown in image **D** (arrowhead). 40x oil objective in all images. Scale bars: 50 μm .



| | | Number of axons | | | | | | | | Average | St. Error |
|--|--------------|-----------------|-------|--------|--------|--------|--------|------------|-------------|------------|-----------|
| | | R8508 | R8608 | R14908 | R15208 | R24108 | R24208 | R24508 | | | |
| Distance from the lesion (μm) | 200 | - | 18 | - | 30 | - | 0 | 1 | 12.0 | 7.2 | |
| | 400 | - | 33 | - | 27 | - | 0 | 1 | 15.3 | 8.6 | |
| | 600 | - | 28 | - | 23 | - | 0 | 1 | 13.0 | 7.3 | |
| | 800 | - | 26 | - | 15 | - | 0 | 1 | 10.5 | 6.2 | |
| | 1000 | - | 12 | - | 16 | - | 0 | 1 | 7.3 | 4.0 | |
| | 1200 | - | 10 | - | 12 | - | 0 | 2 | 6.0 | 2.9 | |
| | 1400 | - | 15 | - | 11 | - | 0 | 2 | 7.0 | 3.6 | |
| | 1600 | - | 24 | - | 14 | - | 0 | 0 | 9.5 | 5.9 | |
| | | | | | | | | | | | |
| | 3200 | - | 7 | - | 5 | 0 | 0 | 0 | 1.0 | 1.0 | |
| | 3600 | - | 4 | - | 3 | 0 | 0 | 0 | 0.6 | 6.0 | |
| | 4000 | - | 1 | - | 2 | 0 | 0 | 0 | 0.4 | 4.0 | |
| | 4400 | - | 5 | - | 1 | 0 | 0 | 0 | 0.2 | 2.0 | |
| | 4800 | - | 6 | - | 1 | 0 | 0 | 0 | 0.2 | 2.0 | |
| | | | | | | | | | | | |
| | 10000 | - | - | - | - | 0 | 0 | 0 | 0.0 | 0.0 | |
| 10400 | - | - | - | - | 0 | 0 | 0 | 0.0 | 0.0 | | |
| 10800 | - | - | - | - | 0 | 0 | 0 | 0.0 | 0.0 | | |
| 11200 | - | - | - | - | 0 | 0 | 0 | 0.0 | 0.0 | | |
| 11600 | - | - | - | - | 0 | 0 | 0 | 0.0 | 0.0 | | |

Table 3. Number of fibres at increasing distances from the lesion in seven rats six weeks after the dorsal column lesion.

Quantification of axon number rostral to the lesion performed with an epifluorescence microscope and 63x lens on parasagittal sections of the lesion block, rostral block and thoracic block. Where blank cells are present data was excluded from the quantification based on the criteria described in methods, section 2.3.6.1.

3.2.2.4.2 *Extended wire knife injury of dorsal columns*

In order to confirm that the tract traced fibres rostral to the lesion level were spared fibres located in the lateral dorsal columns, further experiments were performed in which the usual dorsal column lesion was extended laterally on the left side. Three rats underwent the normal wire knife lesion of the dorsal columns and this was extended to include the left dorsolateral fasciculus. The animals were then injected after 4 weeks with BDA and finally perfused two weeks later.

Light microscopy examination of parasagittal sections from the animals revealed a cavity with a size and shape similar to that observed in rats that had received a standard dorsal column lesion, however the cavity extended more laterally on the left hand side.

When sections were examined using epifluorescence microscopy, traced fibres were detected caudal to the lesion (Figure 3-15) but no traced fibres were detected rostral to the lesion in sections cut from the lumbar and thoracic cord (Figure 3-16 and Figure 3-17). Furthermore no fibres were found crossing the lesion level on lateral sections (Figure 3-17). This result confirms that the fibres found rostral to the transection in animals lesioned using the standard wire knife lesion procedure were spared fibres.

Figure 3-15. BDA labelling caudal to a laterally extended wire knife dorsal column lesion.

Composite of confocal images taken from a transverse section approximately 2 mm caudal to the lesion level. Labelling of injured axons was intense in the dorsal columns and grey matter. Scale bar: 200 μm .

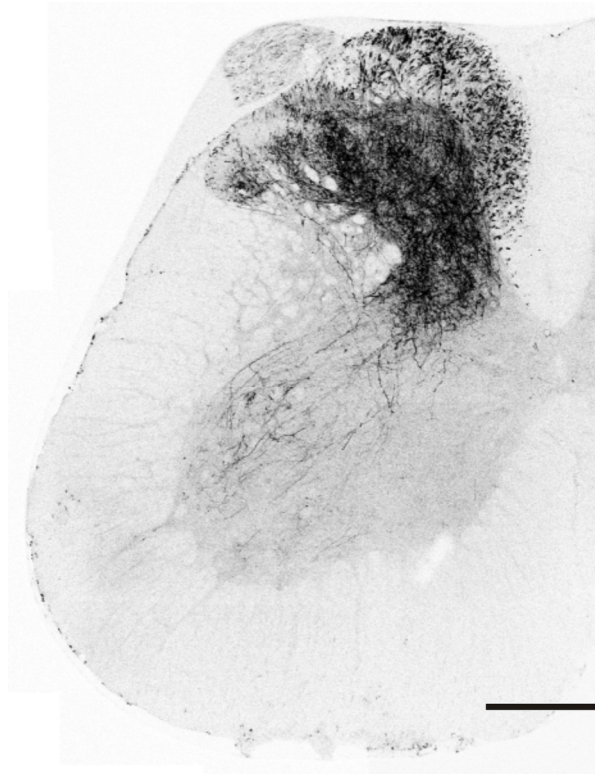


Figure 3-16. Tract tracing rostral to a laterally extended dorsal column lesion in transverse sections.

Composites of confocal images were taken from the same animal in Figure 3-15. The images are of transverse spinal cord sections to show BDA labelling in the rostral block (**A-B**) and thoracic block (**C-D**). **A** and **C**) No BDA labelling was detected in the medial or lateral dorsal columns nor in the grey matter ventral to the dorsal columns (10x objective). The boxed areas in **A** and **C** are shown at a higher magnification (40x) in **B** and **D** respectively. **B** and **D**) projections of confocal images demonstrate the absence of tract traced fibres rostral to the injury level even in the lateral dorsal columns confirming complete ablation of the dorsal columns with the extended dorsal column lesion procedure. Scale bars: 500 μm in **A** and **C**; 25 μm in **B** and **D**.

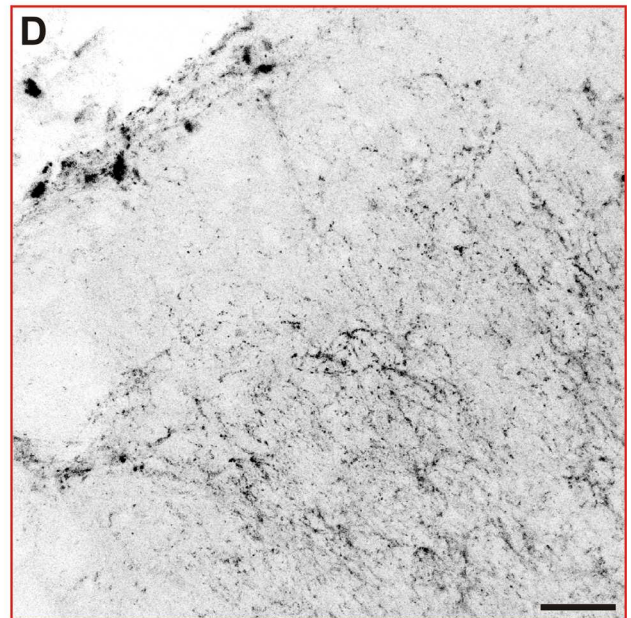
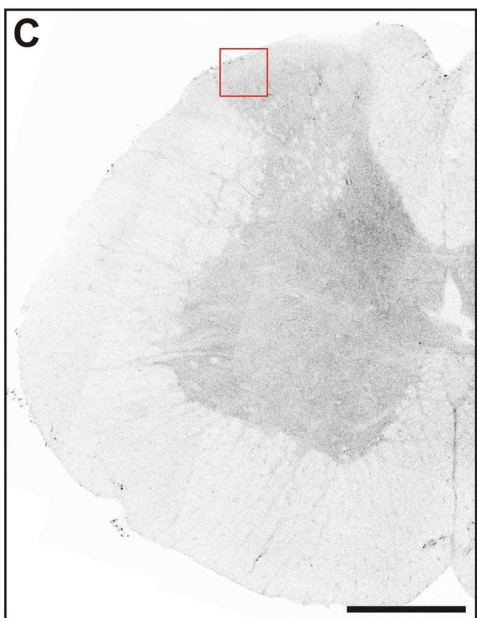
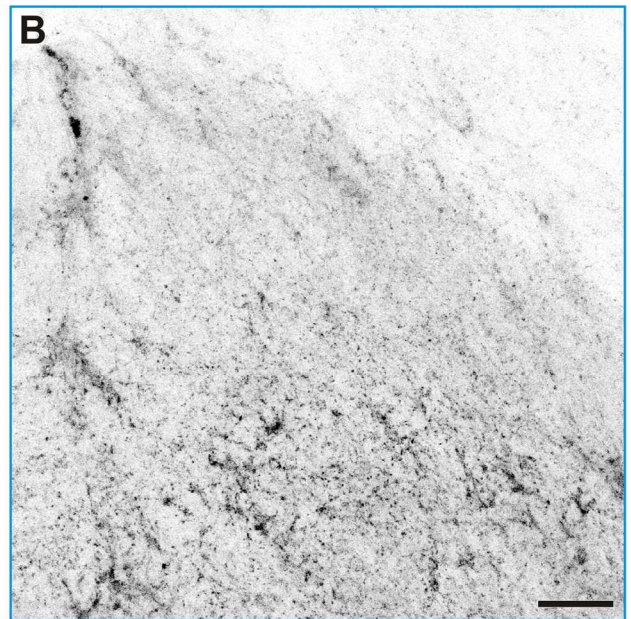
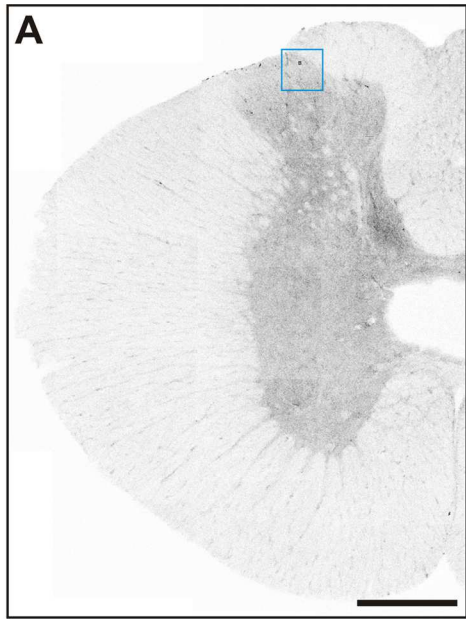
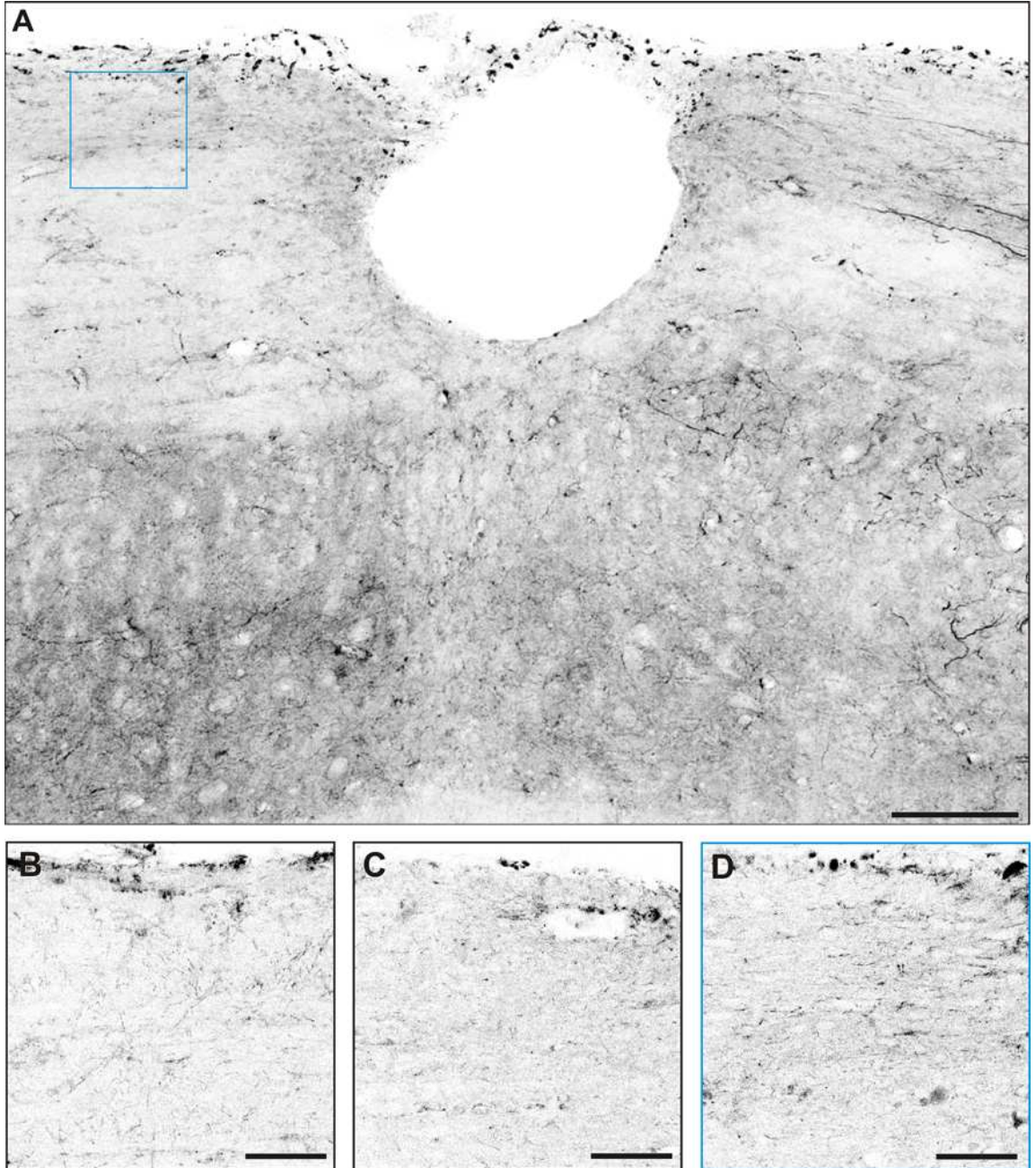


Figure 3-17. Ablation of all axons in the lateral dorsal columns in a rat receiving a laterally extended dorsal column lesion in parasagittal sections.

A) Composite of projections of confocal stacked images of a section of intact spinal cord tissue from the extreme left of the dorsal columns; although axons were detected caudal to the lesion level, none were found rostral to it. Boxed area in **A** (20x objective) is depicted at higher magnification in **D**. **D**, **C** and **B**) These images (40x oil objective) show the absence of BDA labelled fibres rostral to the transection level in sections from the lesion block, rostral block and thoracic block respectively. Scale bars: 200 μm in **A**; 50 μm in **B-D**.



3.2.3 OEC transplantation

In order to investigate the neuroprotective and axonal growth promoting effects of an OEC transplant after a dorsal column lesion, twenty seven rats were transplanted with OECs at the time of the wire knife dorsal column injury. Four weeks later BDA was injected in the L4/5 spinal nerves and two weeks later they were perfused and processed (Figure 3-18).

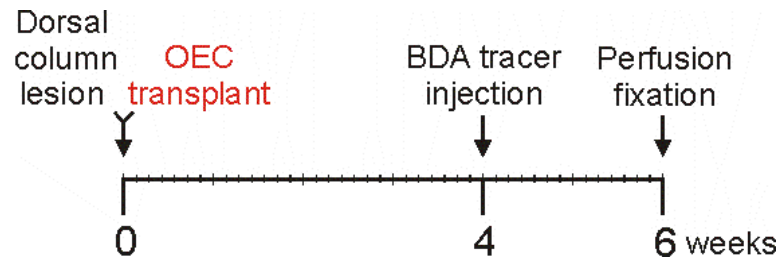


Figure 3-18. Time course of procedures performed on spinal cord lesioned animals transplanted with OECs.

3.2.3.1 Characterization of the lesion after transplanting OECs

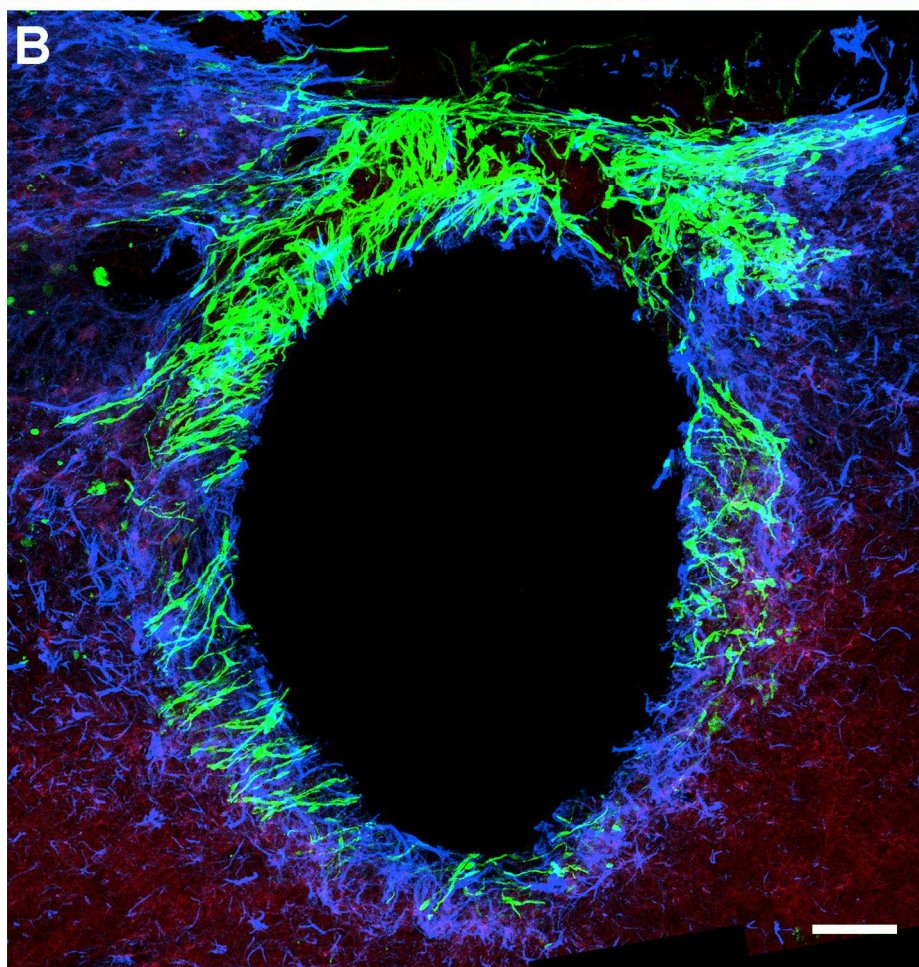
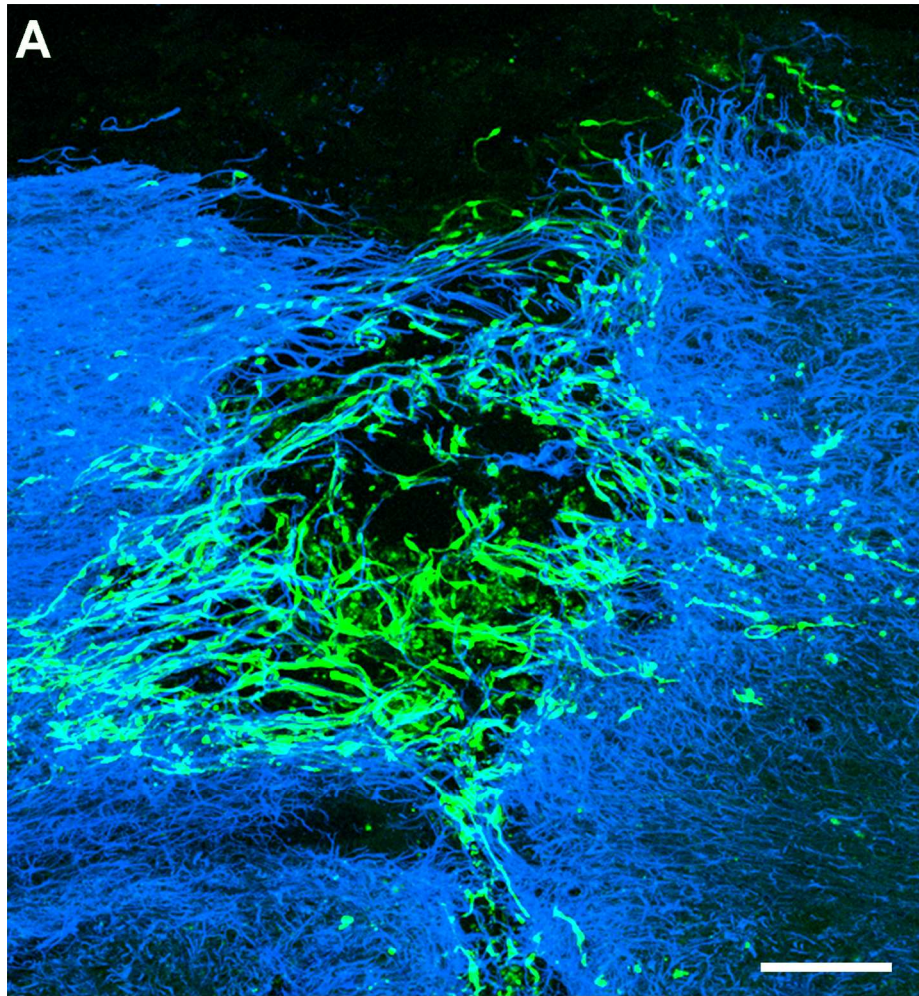
Transplanted GFP expressing cells were detected in the lesion of all the rats in this experimental group. In some animals a small cavity or no cavity at all was present within the lesion and the transplanted cells wholly or partially filled the lesion cavity bridging opposite ends. In other animals the lesion cavity shape and size was not dissimilar to that of non-transplanted animals: a single rounded large cyst; in this second subset of animals the OECs were localised mainly in the GFAP labelled lesion walls and not in the cavity.

Importantly, in those animals where the localisation of labelled OECs was restricted to the lesion walls, GFAP positive astrocytes formed an even surface surrounding the cavity with no GFAP positive processes directed into the cavity (Figure 3-19B). On the other hand, in the subset of animals with an extensive distribution of OECs in the lesion the GFAP borders instead of constituting a thick rim around the lesion formed a more open mesh, in which the astrocytes extended processes of varying size towards the centre of the injury intermingling with the OECs (Figure 3-19A).

To quantify the lesion size defined by the area delimited by the internal perimeter of the GFAP labelling, the section with the largest lesion was selected for each animal and measured from confocal images. In addition, the lesion cavity size was measured from light microscope images taken from the section with the largest lesion cavity in each animal. The results from individual animals are shown in the graph in Figure 3-20A. The lesion size was 1.4 times larger than the lesion cavity size and this difference was significant ($P=0.0049$) (Figure 3-20A). This indicates that, unlike the non-transplanted animals where the lesion size was not significantly different from the lesion cavity size, the cavity size was significantly smaller than the lesion in animals that received a transplant. The lesion size was 1.4 times smaller than that measured in non-transplanted animals, however the difference was not significant ($P=0.12$). In OEC transplanted animals the lesion cavity size was reduced significantly of 1.9 times compared to non-transplanted animals ($P=0.017$) (Figure 3-21A): in over 25% of the 26 animals suitable for the analysis the lesion cavity size was reduced at least fivefold when compared to lesioned rats that did not receive a transplant; in even more animals, over half, the lesion cavity size was reduced at least twofold; in particular, in two rats the cells completely filled the lesion site and no cavity was present.

Figure 3-19. Examples of lesion morphology and size after an OEC transplant.

Composites of confocal projected image stacks that depict the lesion of two different animals. **A)** Lesion with a small cavity largely filled with OECs (green). The in-growing astrocyte (blue) processes that formed trabeculae connecting opposite sides intermingled with OECs. **B)** Large lesion with a large cavity devoid of both OECs and astrocytic processes; the OECs were located mainly in the GFAP positive lesion walls and were not filling the cavity. Compare both images with the lesions of non-transplanted animals in Figure 3-7 and find similarities between those and **B**. Scale bars: 100 μm .



3.2.3.2 Characterization of the central canal cavitation after an OECs transplant

While no cavitation of the central canal caudal to the lesion was seen in any of the 26 animals examined, central canal cavitation was observed rostral to the lesion in the lesion block, rostral block and thoracic block. Quantification of the average central canal diameter and comparison with that of non-transplanted animals showed that OEC transplantation reduced cavitation of the central canal in the lesion, rostral and thoracic blocks. In particular 13/26 (50%) of the animals did not develop a cavitation of the central canal at the rostral end of the lesion block while one developed in all non-transplanted animals. There was a 2.4 times reduction of average cavity size on the rostral side of the lesion block compared to non-transplanted animals and this difference was significant ($P=0.013$) (Figure 3-20 and Figure 3-21). The OECs thus exerted a neuroprotective effect on the spinal cord lesion by reducing the lesion cavitation but also by reducing central canal cavitation thus preserving the grey matter that would have otherwise been lost in place of a cavity.

There was no significant difference when the same comparison was performed for the rostral block and the thoracic block, however much less material was available for comparison.

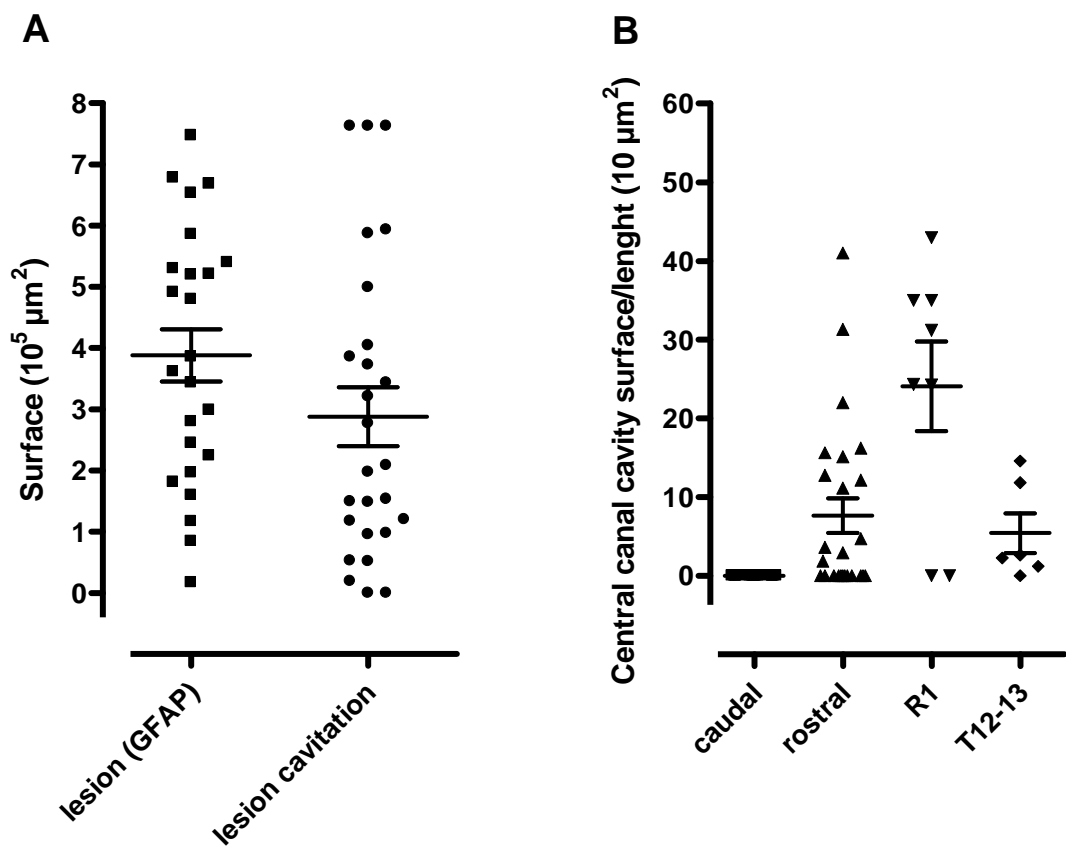


Figure 3-20. Lesion and central canal characterization 6 weeks after a dorsal column injury and OEC transplantation.

A) Scatter dot plot showing that the size of the lesion defined by the GFAP positive glial scar surrounding the site of injury was significantly larger compared to the size of the lesion cavitation ($P=0.0049$). **B)** Cavitations formed in the central canal rostral to but not caudal to the injury level. No significant difference was found between the rostral end of the lesion block and the rostral block ($P=0.35$), nor between these and the thoracic block ($P=0.46$ and $P=0.33$ respectively).

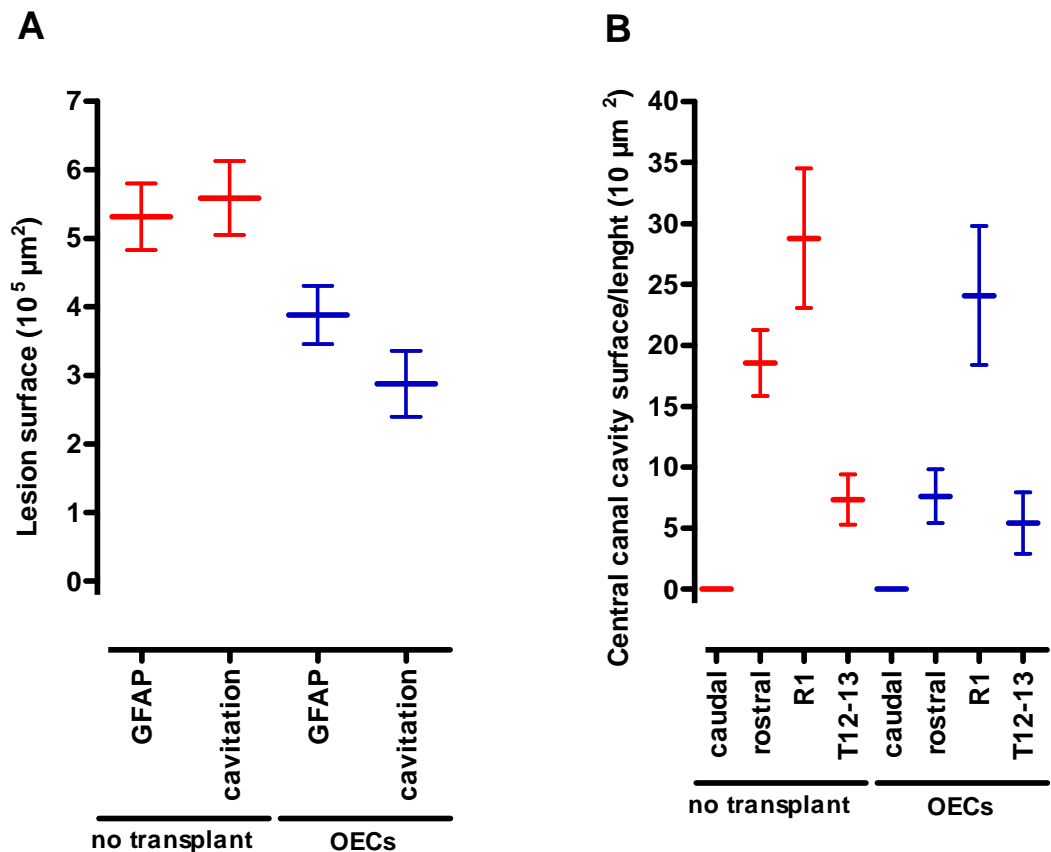


Figure 3-21. Comparison of lesion, lesion cavity and central canal cavity size between OEC transplanted and non-transplanted rats.

A) OEC transplantation reduced the lesion size, however not significantly ($P=0.21$), while the reduction in the lesion cavity size was significant ($P=0.017$). **B)** OEC transplantation significantly reduced the central canal cavitation in the rostral portion of the lesion block ($P=0.013$) while the reduction was not significant in the rostral block and thoracic block ($P=0.58$ and $P=0.39$ respectively). A comparison that takes into consideration all the animals receiving OEC transplantation and non-transplanted animals including those that also received a conditioning lesion is shown in Figure 3-46.

3.2.3.3 Distribution of OECs in the spinal cord

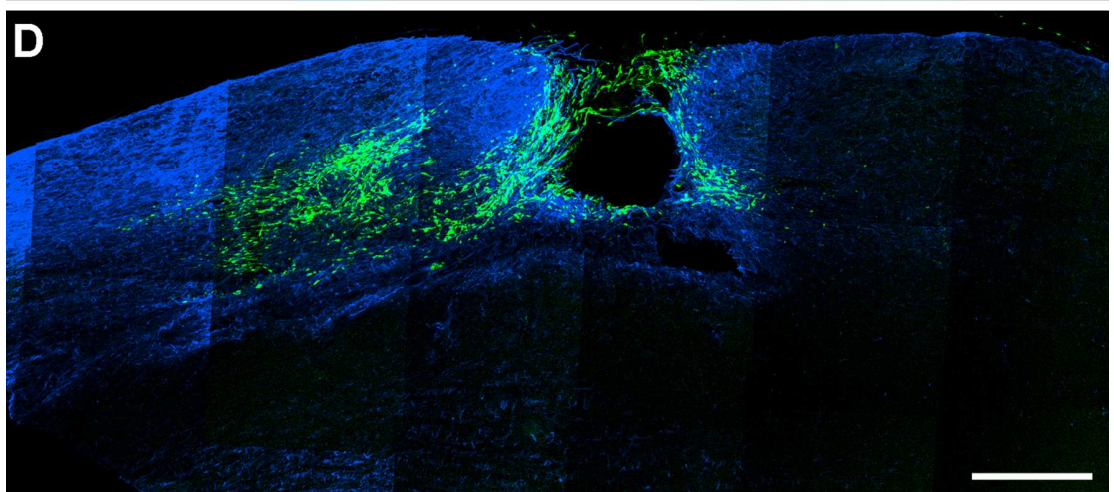
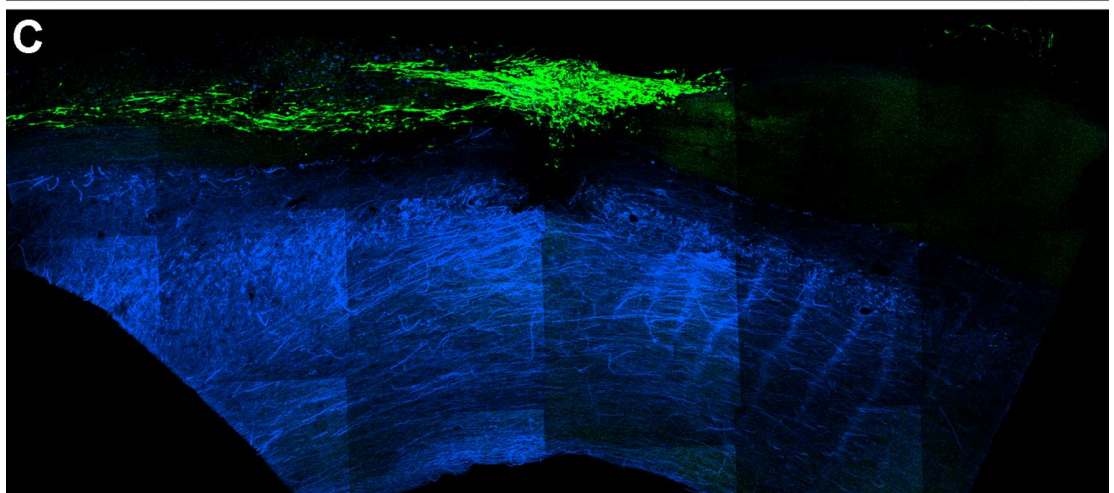
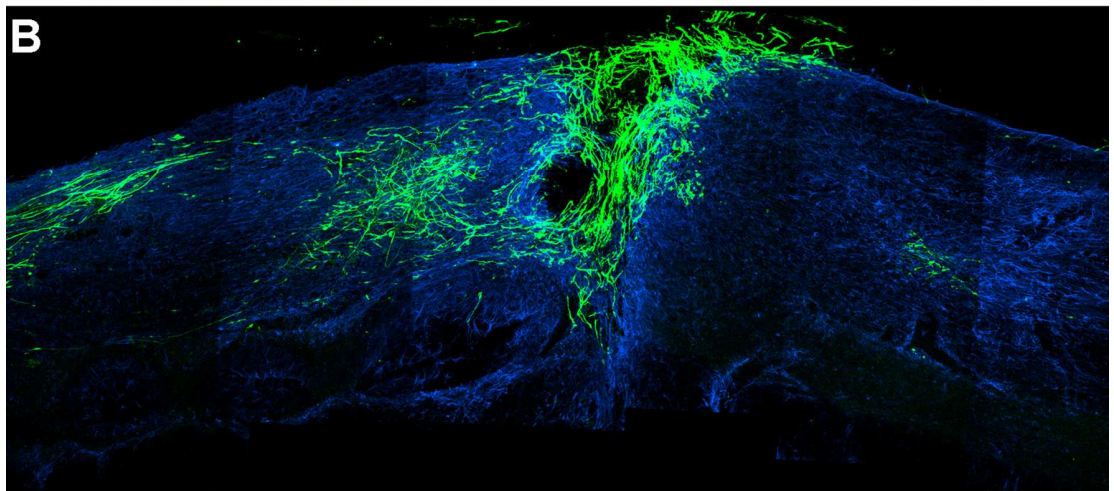
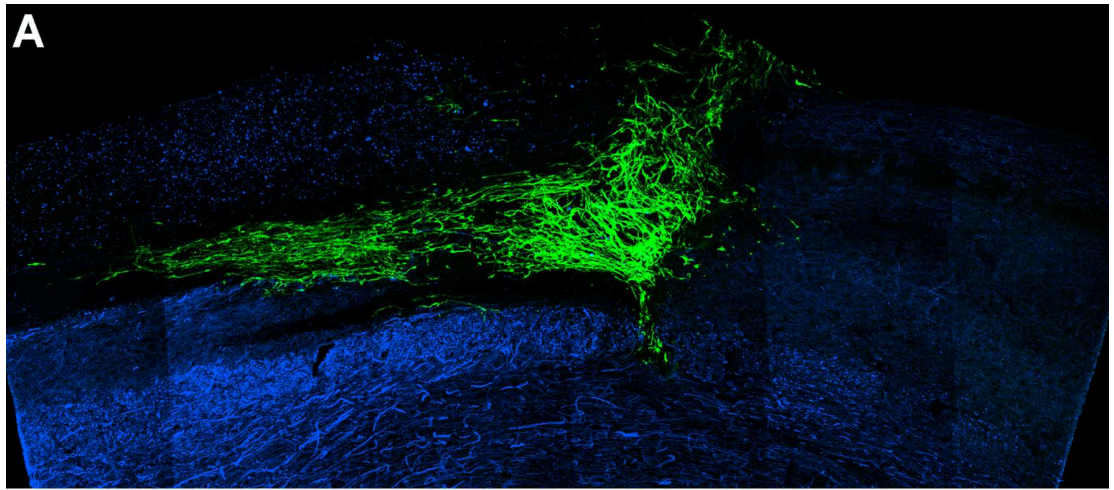
GFP labelled OECs injected inside the lesion cavity generated by the wire knife were frequently found not only at the injection site but also beyond the lesion as shown in some examples in Figure 3-22. In 89% of rats (24/27) some degree of OEC distribution was observed both rostral and caudal to the lesion. In the remaining 3 rats no OECs had distributed beyond the lesion site. In a number of animals the transplanted cells were observed at long distances from the transplant site extending into the rostral and thoracic blocks, even as far as 12 mm from the lesion, the furthest distance analysed in this study. Transplanted cells were distributed in different ways. OECs were either i) isolated one from each other, ii) organised in clusters or iii) formed long continuous tracts. In 78% of the animals (21/27) OECs formed continuous tracts that were in continuity with the OECs in the lesion and extended for varying distances from the lesion. These tracts did not end in the lesion block in 15% (4/27) of animals extending into the rostral block. For 8 of the 27 animals where the rostral block had been taken from the spinal cord the average length of the OEC continuous tracts rostral to the lesion was 1550 μm .

Rostral to the injury, in the majority of cases, OECs were distributed in the medial dorsal columns (82%, 22/27), often on the border between the medial dorsal column white matter and the underlying grey matter (44%, 12/27) and less often only in the underlying grey matter (30%, 8/27).

OECs located in the white and grey matter were found to be densest in the lesion block becoming noticeably less dense at increasing distances from the lesion (i.e. in the rostral and thoracic blocks). In all rats in which OECs were seen in the rostral and thoracic blocks, they were also present in the lesion block. In some animals where OECs were located in the grey matter they also invaded the central canal at the lesion level and distributed rostrally within the canal, being detected even in the thoracic block, forming a thin non continuous tract of cells.

Both in the white matter and in the grey matter OECs were generally aligned with each other and parallel to the rostro-caudal direction of the spinal cord. Nonetheless, in most animals it was normal to see a small proportion of OECs oriented differently. In particular, in the vicinity of blood vessels, OECs often oriented themselves parallel to these.

Figure 3-22. Distribution of OECs after transplantation into spinal cord lesions. Composite confocal projected image stacks of parasagittal sections of the lesion block from four animals that showed widespread distribution of OECs (green) rostral to and caudal to the injection site. OECs partially filled (**B** and **D**) or even entirely filled (**A** and **C**) the lesion (located in the middle of each section) in these sections and formed continuous cell tracts leading out of the lesion rostral to and caudal to the injection point. In **A** and **C** blue is neurofilament, while in **B** and **D** is GFAP. Scale bar: 500 μm .

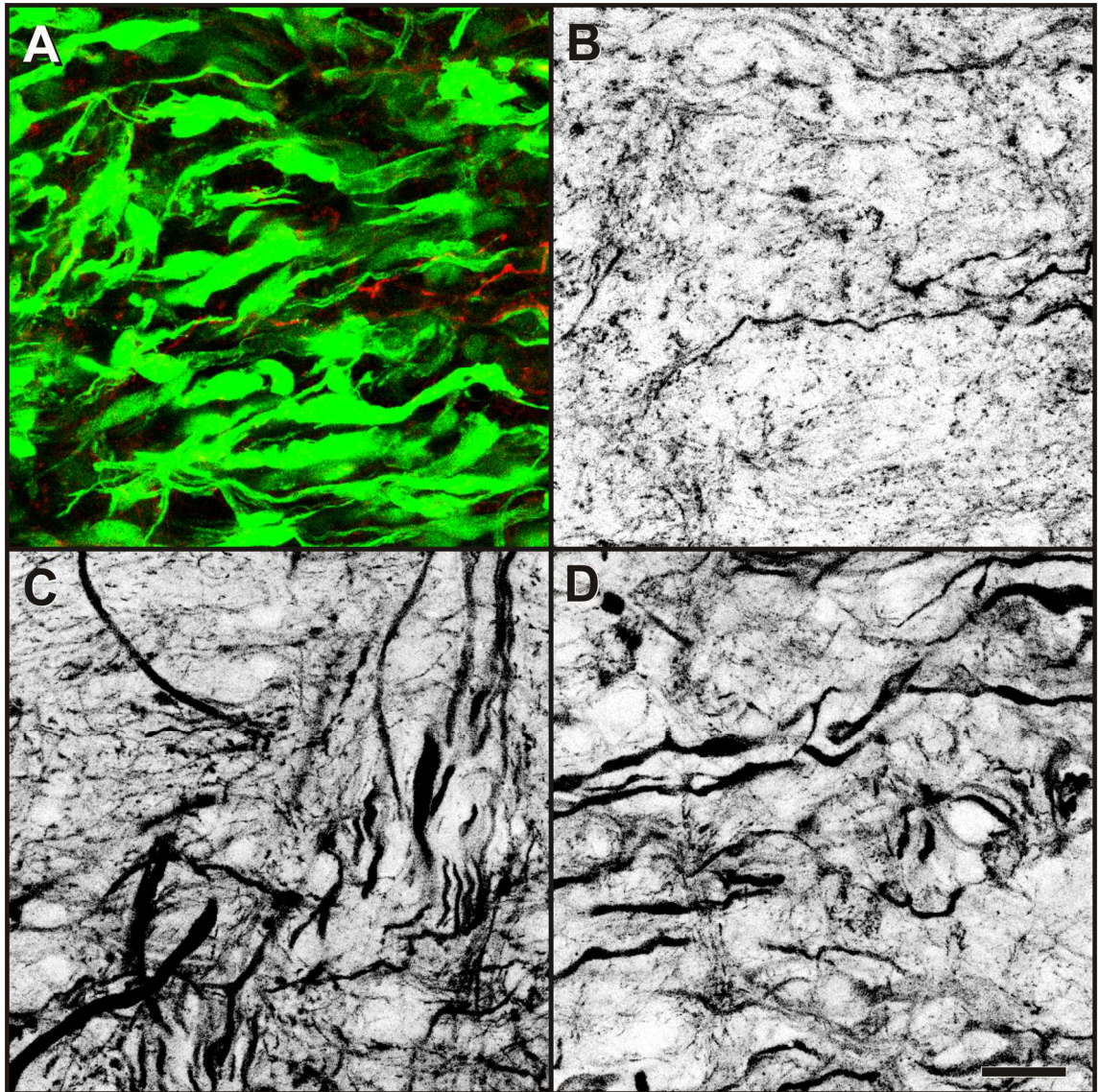


3.2.3.4 Density of BDA labelled fibres in areas containing OECs compared to those devoid of OECs caudal to the lesion

In animals where OECs had spread caudally there appeared to be differences in the density of tract traced fibres within tracks of GFP labelled transplanted cells compared to surrounding areas. The areas of distribution of OECs seemed to be devoid of the resident BDA labelled fibres, as if these had been displaced by the transplanted cells. In accordance with this, the density of axons within the OEC tract appeared lower than that in normal tissue. The appearance of the fibres present within these caudal OEC tracts was different from that of the BDA labelled fibres present in surrounding areas devoid of OECs (Figure 3-23). In particular, the orientation of fibres associated with OECs followed closely that of the transplanted cells and fibre diameter appeared smaller than that of fibres in intact surrounding tissue. The fibre density within the OEC tract and surrounding areas was quantified in 12 animals selected according to the criteria described in the methods (section 2.3.9); an example from one animal is shown in Figure 3-23. This quantification showed that the presence of OECs was associated with a 1.4 times reduction of fibre density however the difference was not significant due to a high variability between animals ($P=0.35$).

Figure 3-23. Examples of tract traced fibres among tracts of OECs caudal to the lesion site compared to tract traced fibres in immediately adjacent tissue.

The axonal density of BDA labelled axons caudal to the injury was higher in intact spinal cord tissue compared to neighbouring tissue infiltrated by OECs, however not significantly ($P=0.35$). **A**) Image of a tissue section where a tract of OECs distributed caudal to the lesion (OEC-GFP in green, traced axons in red). **B**) Same image as depicted in **A** displaying only labelled axons in greyscale mode. **C-D**) Images taken from the sections to the LHS and RHS respectively of the section depicted in **A** and **B** to show denser BDA labelling (greyscale) in areas where OECs were absent. All images are projections of confocal stacks of 3 images taken 1 μm apart. Scale bar: 20 μm .



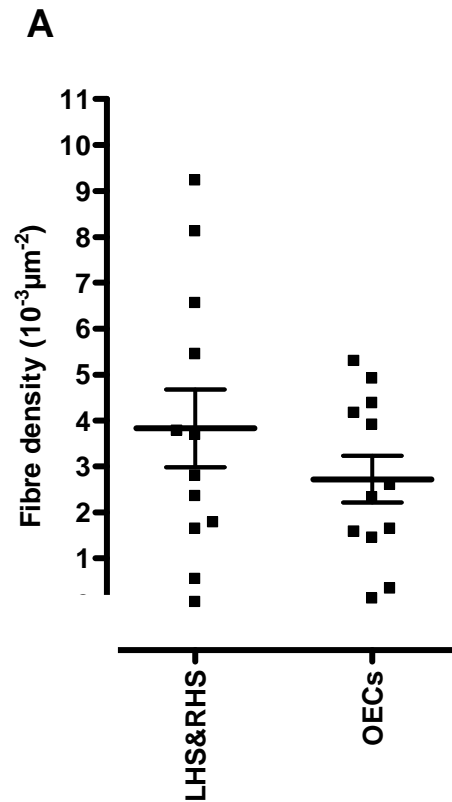


Figure 3-24. Quantification of BDA labelled fibres in sections containing OECs compared to adjacent sections devoid of OECs.

The density of BDA labelled fibres caudal to the lesion was decreased where the GFP labelled OECs had distributed compared to the average density of BDA labelled axons in areas devoid of GFP labelling on the left hand side (LHS) and right hand side (RHS) of the section where the fibre density in association with GFP labelling was measured, however this difference was not significant ($P=0.35$).

3.2.3.5 Regeneration within the lesion transplant

Most of the ascending sensory axons entering through the L4 and L5 spinal nerves and labelled with BDA ended abruptly caudal to the lesion, in a similar manner to that observed in non-transplanted animals with a dorsal column lesion. However, some BDA labelled fibres were found amongst the OECs within the lesion of all 24 transplanted and tract traced animals (Figure 3-25). The amount of fibres in the lesion was highly variable between individual sections of the same animals and amongst different animals. These fibres were most likely regenerating because no fibres were found in the lesion cavity of non-transplanted animals. Orientation of the regenerating fibres followed closely that of the transplanted cells and was variably and randomly directed.

Although regenerating axons in the lesion were in close vicinity to OECs they were only very rarely ensheathed by them. An example of a fibre ensheathed by transplanted OECs is shown in Figure 3-26.

The lesion was also a permissive environment for the regeneration of neurofilament labelled axons. Neurofilament is a marker of large myelinated dorsal root ganglia neurons and of spinal cord interneurons. In all rats (n=7) for which sections were processed with the neurofilament antibody, neurofilament positive fibres were found to have grown within the lesion site amongst GFP labelled transplanted cells. Some of the BDA labelled axons were double labelled also for neurofilament indicating that these were myelinated sensory axons, however the majority of neurofilament labelled axons did not double label indicating that regeneration of primary sensory afferents into the lesion was a minor component of the ongoing regenerative process.

Figure 3-25. Axonal regeneration in a lesion transplanted with OECs.

A) Composite of confocal projected images that depict regenerating BDA labelled axons (red) in a lesion (outlined by GFAP labelling in blue) filled with OECs (green). **B)** After deleting the green channel it is possible to see that axons had grown into the lesion crossing the caudal border of the lesion. Objective: 20x. Scale bar 100 μm .

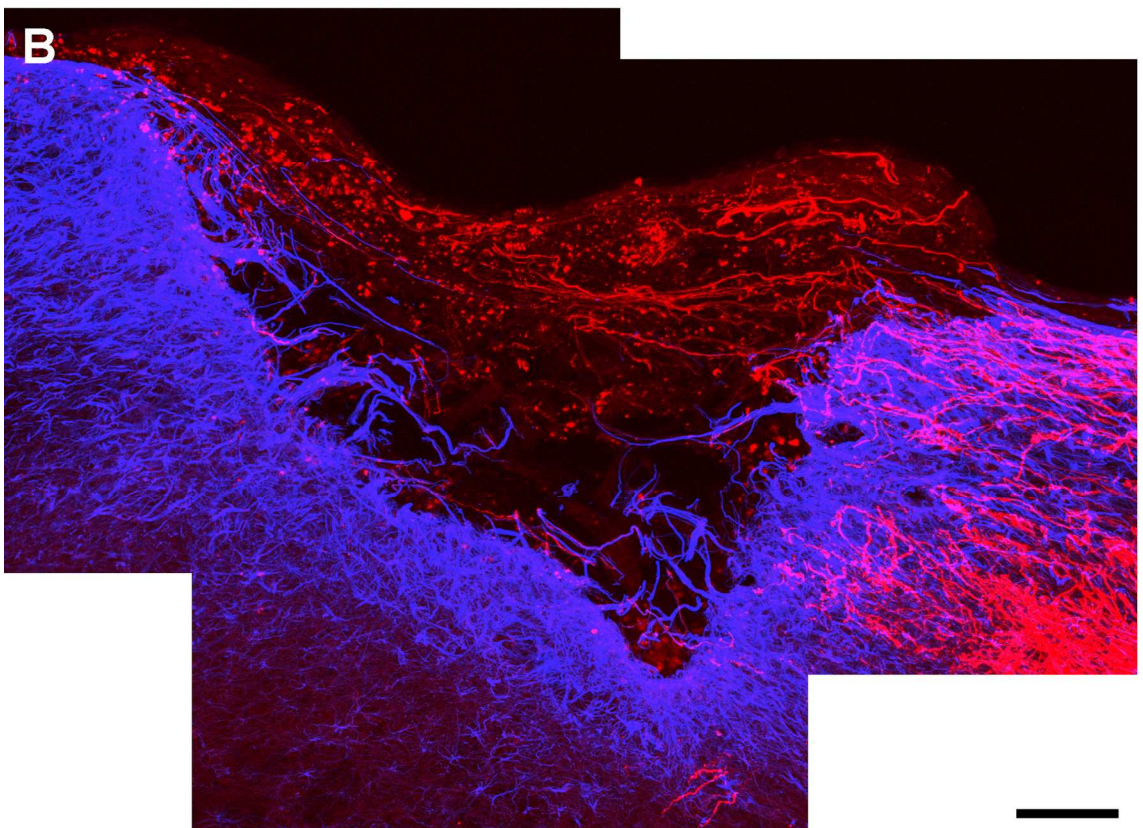
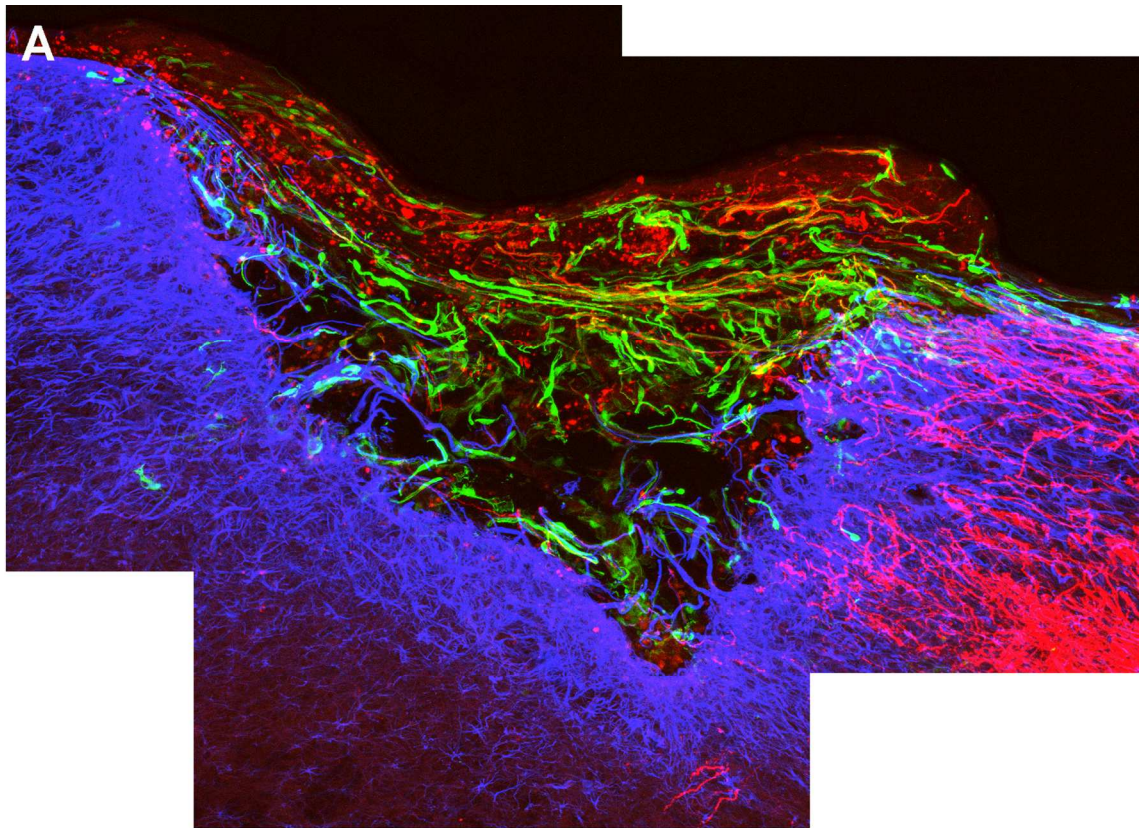


Figure 3-26. OEC association with tract traced fibres in the lesion.

A) Composite of confocal projected images that depict regenerating BDA labelled axons in red, GFP-OECs in green and astrocytes in blue. Tract traced axons were mainly located in association with GFP-OECs, however only few axons were ensheathed by the OECs. **B)** Higher magnification of boxed area depicted in **A** showing a BDA labelled axon ensheathed by OECs, while a nearby tract traced axon running close to OECs wasn't ensheathed by them. Objective 20x. Scale bars: 50 μm in **A** and 20 μm in **B**.

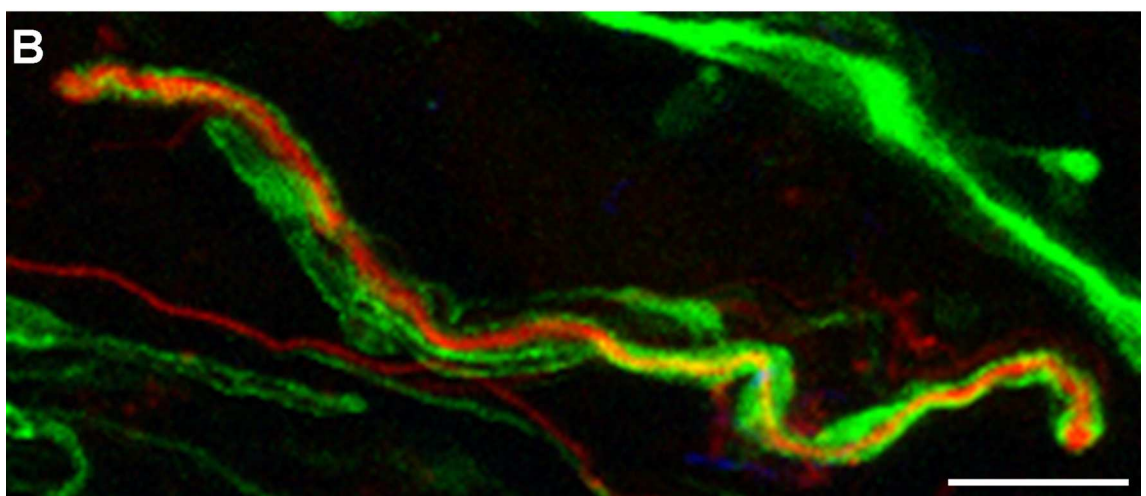
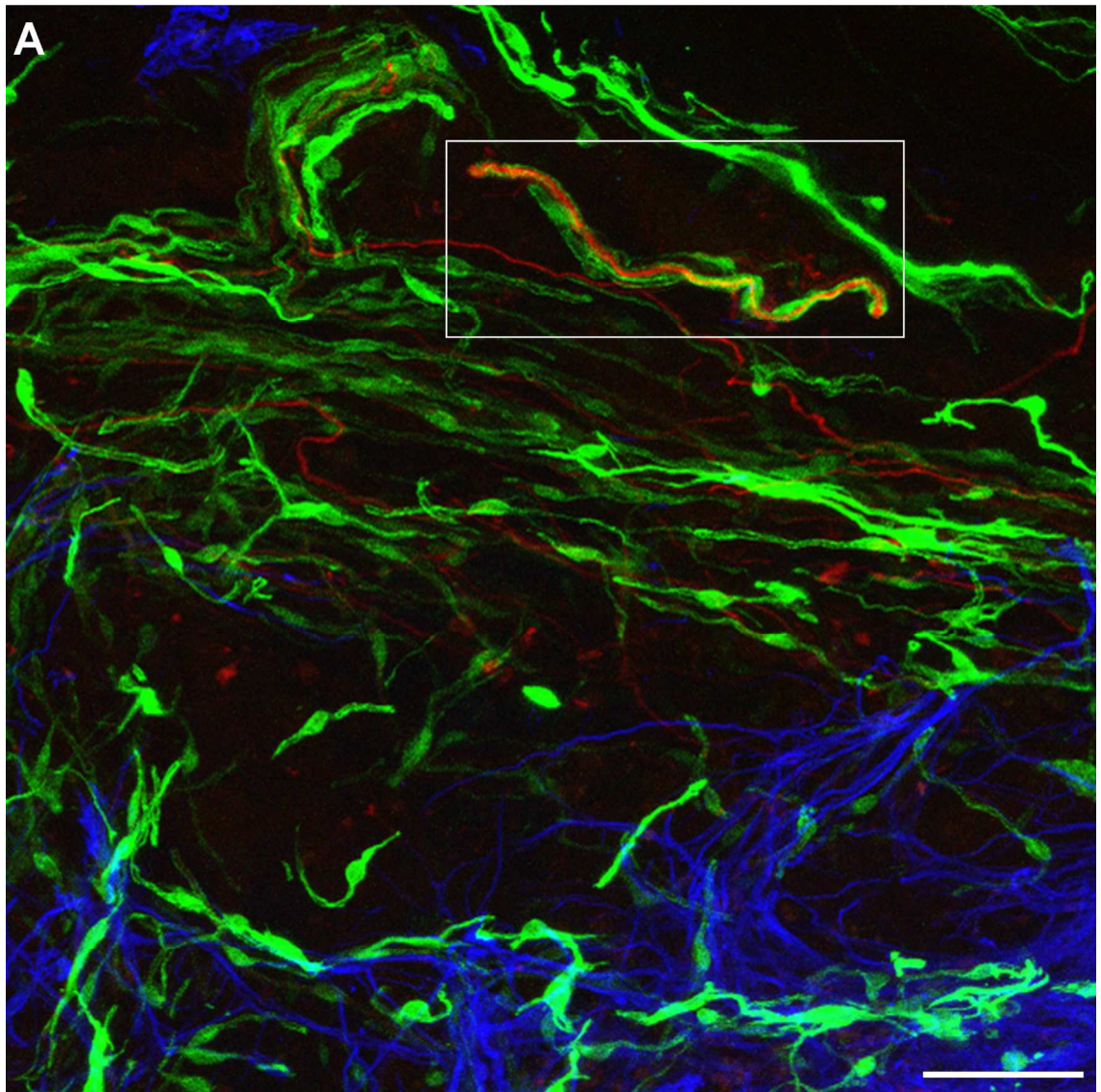
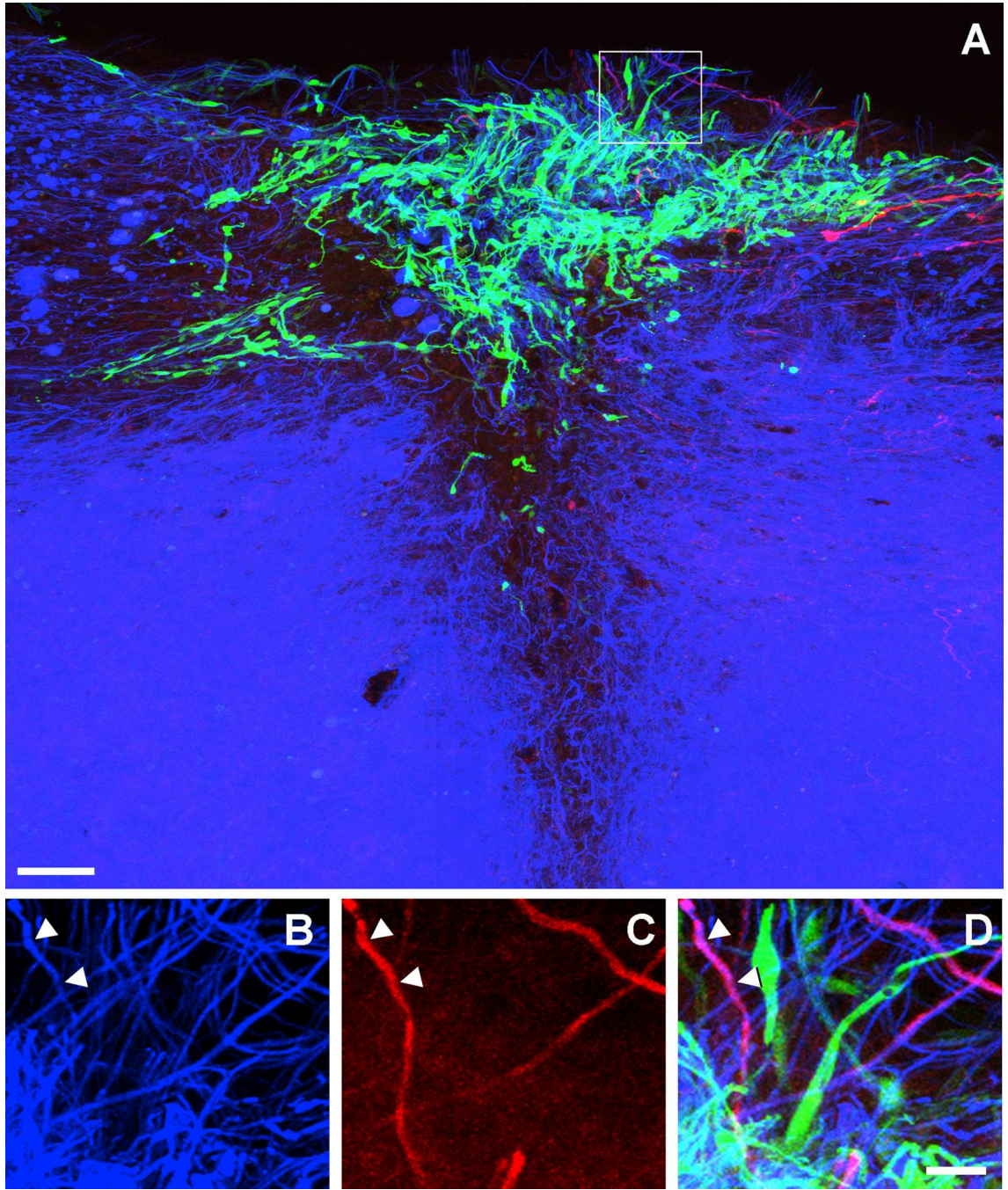


Figure 3-27. Neurofilament labelling in a lesion transplanted with OECs.

A) Neurofilament (blue) labelled intensely the spinal cord. Profuse labelling of neurofilament labelled axons was also found in the lesion indicating regeneration of interneurons and/or myelinated dorsal root ganglia axons. Boxed area in **A** is enlarged in **B-D** to show occasional axonal double labelling for neurofilament and BDA tract tracer (red) (for example see arrow heads) indicating regeneration of myelinated dorsal root ganglia neurons. OECs are shown in green. Objective: 20x. Scale bars: 100 μm in **A** and 25 μm in **B-D**.



3.2.3.6 BDA labelled fibres rostral to the lesion

Tract traced fibres were detected rostral to the lesion in at least 16/21 animals. Axons were located in the lesion block but also in the rostral and thoracic blocks. Fibres were found in the most lateral portions of the dorsal columns (Figure 3-28A,B) and underlying grey matter (Figure 3-28A,C) as already described for non-transplanted lesioned animals. However, an extremely important and interesting difference was found. Whereas in non-transplanted animals labelling of BDA was not found in the medial portion of the dorsal columns or underlying grey matter, in the transplanted animals fibres were detected not only in the most lateral portion of the dorsal column but also in the medial portion of the dorsal columns (Figure 3-28A,D) and in underlying grey matter. These fibres were mostly associated with tracts of OECs.

As the main difference between transplanted and non-transplanted rats was the presence of axons in the medial dorsal columns of transplanted animals, tract traced fibres rostral to the lesion were divided in two groups: 1) axons in the most lateral dorsal columns and underlying dorsal horn grey matter (termed hereafter lateral axons, or axons in the lateral cord) and 2) axons in the medial dorsal columns and underlying grey matter (termed hereafter medial axons, or axons in the medial cord). In some animals these two populations of fibres formed a continuous distribution from lateral to medial, while in other animals the two populations were spatially separated by an area where no labelled axons were present. Where it occurred, this gap between the lateral and medially located fibres corresponded to the border between the white matter of the dorsal columns and the grey matter of the dorsal horn. An example of this border and how it is defined is shown in Figure 3-29.

Figure 3-28. Location of tract traced fibres rostral to a dorsal column lesion in an OEC transplanted animal.

A) Composite of confocal images of a transverse section from the spinal cord of an animal transplanted with OECs. BDA labelling (greyscale) was seen in the medial spinal cord in the area boxed in blue, and in the lateral spinal cord in the areas boxed in yellow and pink. **B)** Higher magnification of the yellow boxed area to show BDA labelled axons located in the lateral dorsal columns. **C)** Higher magnification of the pink boxed area to show BDA labelled fibres in the dorsal horn grey matter. **D1)** Higher magnification of the area boxed in blue showing colocalization between tract traced axons (red) and an OEC cell tract (green). BDA axonal labelling in **D1** is also shown in greyscale in **D2**. Objectives used: 10x in **A**, 40x in **B-D**. Scale bars: 200 μm in **A**; 50 μm in **B-D**.

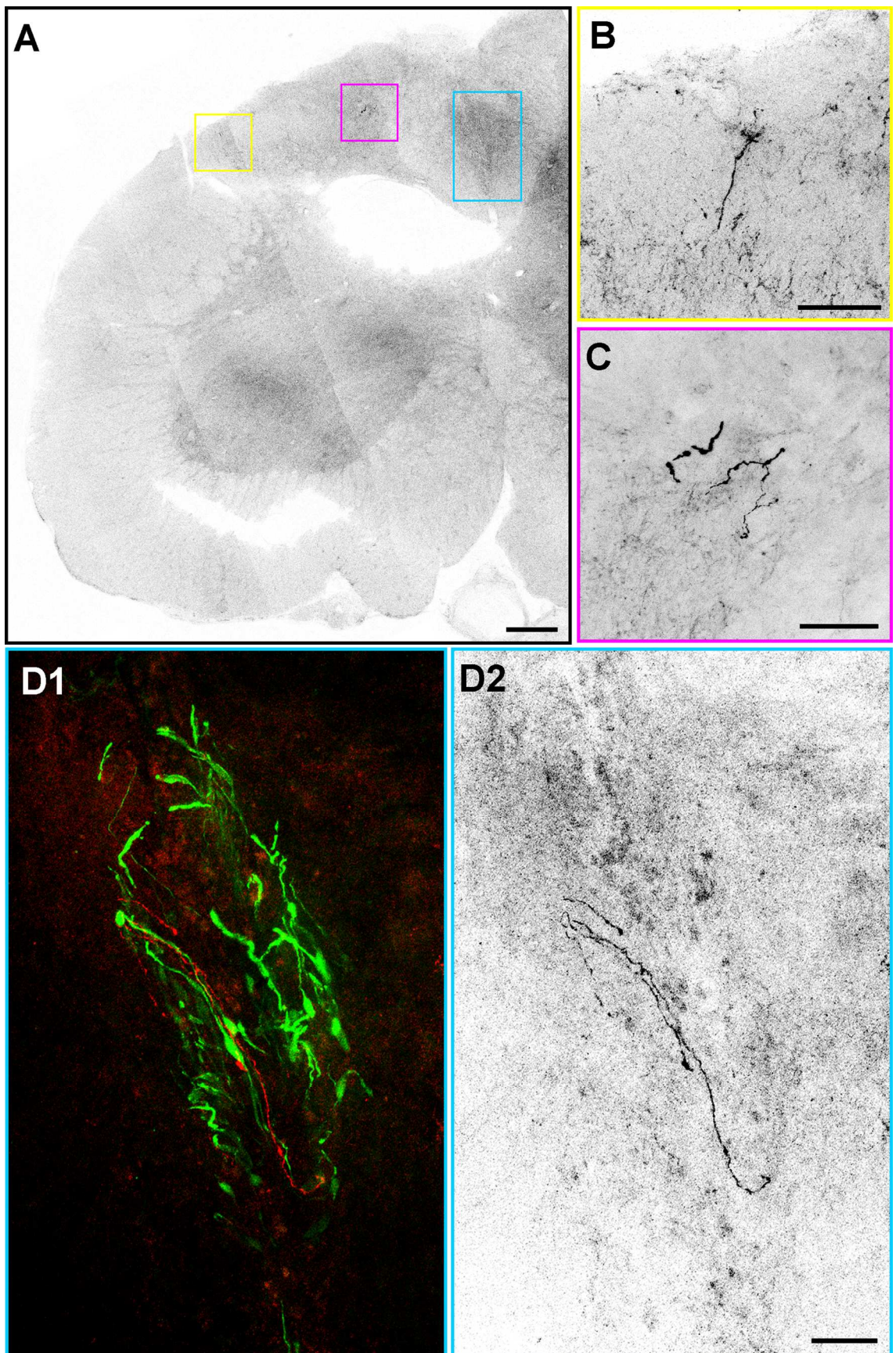
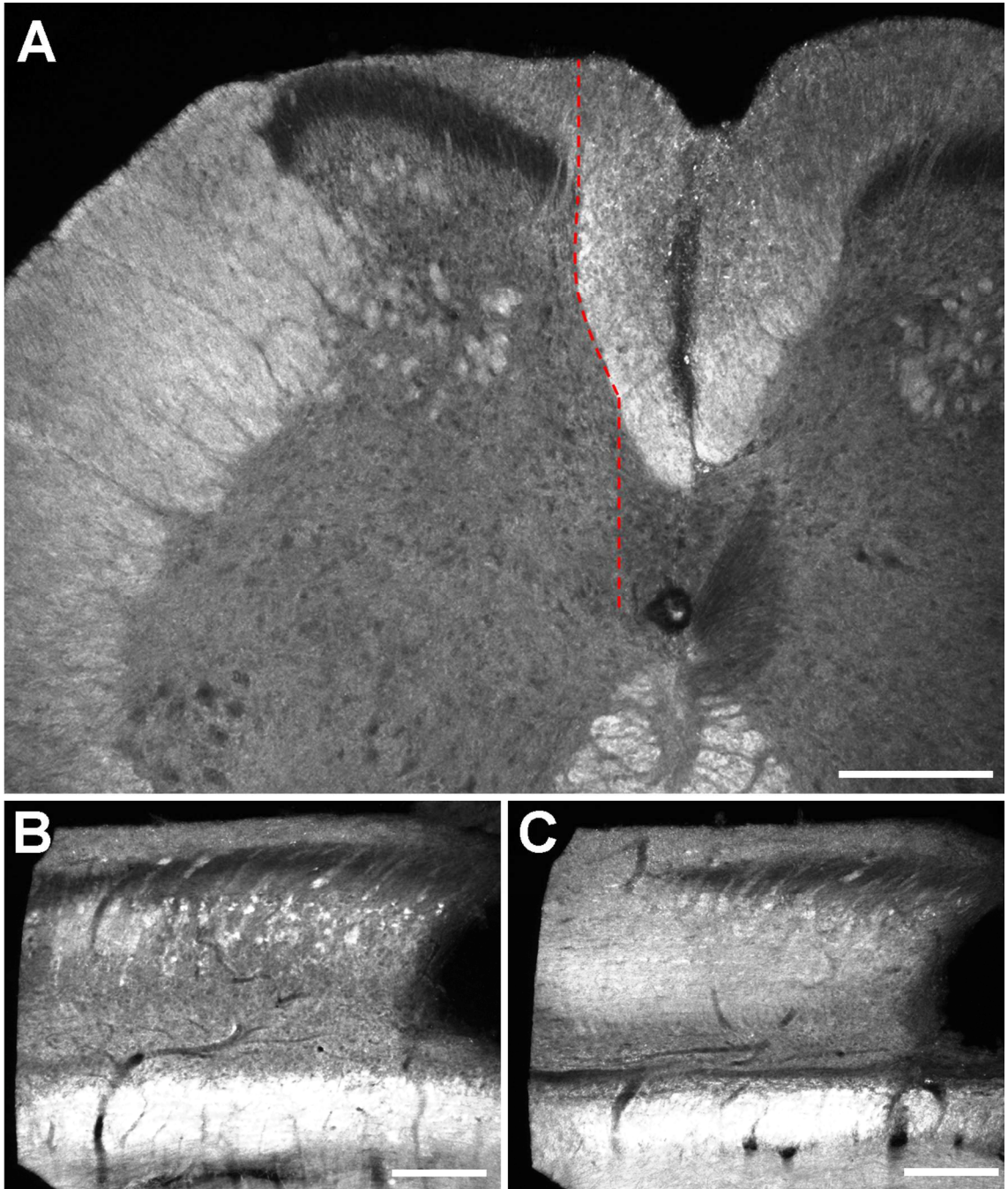


Figure 3-29. Definition of the border between medial spinal cord and lateral spinal cord.

For analysis purposes axons detected rostral to the lesion were divided in two populations depending on their location with respect to an imaginary borderline passing along the border between the left dorsal column and the grey matter to its side. **A-C**) Light microscopy images using a dark field view condenser to differentiate between white and grey matter. **A**) Image of a transverse section ~2 mm rostral to the lesion where the position of the dividing line used to differentiate between lateral and medial fibres is shown (red dashed line). **B-C**) Images of the rostral end of two consecutive parasagittal sections of lesion block to show how straightforward it was to decide whether an axon was in the lateral or in the medial cord. An axon located on the section depicted in **B** would have been defined lateral, while an axon located in the areas where white matter was present in the section shown in **C** would have been defined medial. Scale bars: 200 μm in **A**; 400 μm in **B-C**.



3.2.3.7 BDA labelling in the lateral spinal cord

A large number of fibres were observed in the lateral spinal cord. These fibres possessed the same properties as those present in similar areas in non-transplanted rats: the fibres could be seen crossing the lesion level on lateral undamaged parasagittal sections; these fibres sent collaterals to the grey matter and the trajectory and size of these axons was similar to those observed in similar areas in non-transplanted animals. Quantification of these fibres is shown in Table 4. The quantification was performed on 11 animals selected randomly amongst those available in this group. Comparison with non-transplanted rats indicates that the number of spared fibres was increased following an OEC transplant and is shown in Figure 3-30. The difference between the two treatment groups was significant at 3200 μm , 3600 μm and 4000 μm rostral to the lesion ($P < 0.05$).

| | | Number of axons | | | | | | | | | | | | | | | | | | | | | | |
|--|-------|-----------------|-------|-------|-------|-------|-------|-------|-------|--------|--------|--------|--------|--------|--------|--------|--------|--------|--------|--------|--------|------------|-------------|-------------|
| | | R4204 | R0705 | R2805 | R2905 | R8105 | R8205 | R0506 | R0706 | R16606 | R21106 | R21406 | R30906 | R31006 | R16907 | R17007 | R17707 | R17807 | R22908 | R23008 | R23108 | R23208 | Average | St. Error |
| Distance from the lesion (μm) | 200 | - | - | 0 | 0 | - | - | - | - | - | - | - | 16 | - | 99 | 48 | 37 | 9 | 11 | - | 1 | 12 | 23.0 | 9.8 |
| | 400 | - | - | 0 | 0 | - | - | - | - | - | - | - | 16 | - | 82 | 59 | 25 | 8 | 14 | - | 4 | 7 | 21.5 | - |
| | 600 | - | - | 0 | 0 | - | - | - | - | - | - | - | 20 | - | 93 | 41 | 75 | 8 | 18 | - | 1 | 8 | 26.4 | 10.5 |
| | 800 | - | - | 0 | 0 | - | - | - | - | - | - | - | 24 | - | 109 | 64 | 121 | 7 | 5 | - | 0 | 5 | 33.5 | - |
| | 1000 | - | - | 0 | 0 | - | - | - | - | - | - | - | 18 | - | 72 | 67 | 106 | 5 | 5 | - | 2 | 9 | 28.4 | 12.2 |
| | 1200 | - | - | 0 | 0 | - | - | - | - | - | - | - | 19 | - | 77 | 60 | 65 | 3 | 7 | - | 8 | 11 | 25.0 | - |
| | 1400 | - | - | 0 | 0 | - | - | - | - | - | - | - | 19 | - | 60 | 58 | 58 | 4 | 8 | - | 2 | 6 | 21.5 | 8.3 |
| | 1600 | - | - | 0 | 0 | - | - | - | - | - | - | - | 22 | - | 53 | 53 | 53 | 3 | 5 | - | 12 | 5 | 20.6 | - |
| | 3200 | - | - | - | - | - | - | - | - | - | - | - | - | - | 48 | 6 | 18 | 4 | 6 | 19 | 0 | 6 | 13.4 | 5.5 |
| | 3600 | - | - | - | - | - | - | - | - | - | - | - | - | - | 41 | 5 | 14 | 2 | 3 | 12 | 0 | 2 | 9.9 | 4.8 |
| | 4000 | - | - | - | - | - | - | - | - | - | - | - | - | - | 29 | 4 | 15 | - | 1 | 9 | 0 | 3 | 8.7 | 3.9 |
| | 4400 | - | - | - | - | - | - | - | - | - | - | - | - | - | - | - | 16 | - | 0 | 10 | 0 | 1 | 5.4 | 3.3 |
| | 4800 | - | - | - | - | - | - | - | - | - | - | - | - | - | - | - | 14 | - | 0 | 12 | 0 | 2 | 5.6 | 3.1 |
| | 1000 | - | - | - | - | - | - | - | - | - | - | - | - | - | - | 1 | 5 | - | - | 1 | 0 | 1 | 1.6 | 0.9 |
| | 1000 | - | - | - | - | - | - | - | - | - | - | - | - | - | - | 1 | 4 | - | - | 2 | 0 | 1 | 1.6 | 0.7 |
| | 10800 | - | - | - | - | - | - | - | - | - | - | - | - | - | - | 0 | 4 | - | - | 1 | 0 | 2 | 1.4 | 0.8 |
| | 11200 | - | - | - | - | - | - | - | - | - | - | - | - | - | - | 0 | 3 | - | - | 1 | 0 | 0 | 0.8 | 0.6 |
| 11600 | - | - | - | - | - | - | - | - | - | - | - | - | - | - | 0 | 3 | - | - | 1 | 0 | 1 | 1.0 | 0.6 | |

Table 4. Number of spared fibres at increasing distances from the lesion in the lateral spinal cord of OEC transplanted animals.

Quantification of axon number rostral to the lesion performed with an epifluorescence microscope and 63x lens on parasagittal sections of the lesion block, rostral block and thoracic block. Blank cells are used to indicate that data did not meet the inclusion criteria or that the quantification was not performed (see methods, section 2.3.6.1 for further clarification).

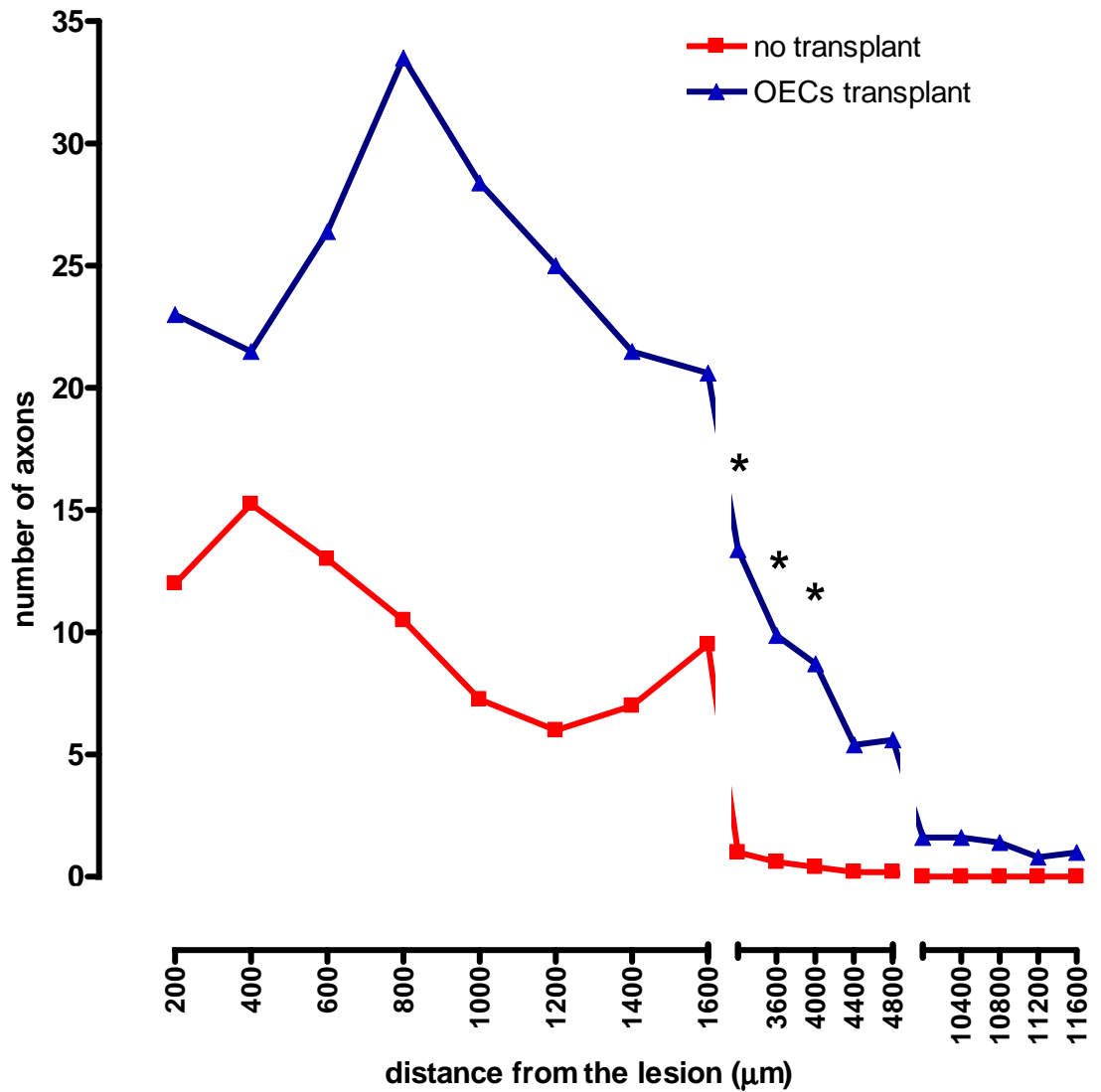


Figure 3-30. Comparison of the average number of BDA labelled fibres in the lateral cord between OEC transplanted and non-transplanted rats.

Overall OEC transplants were associated with an increase in the number of axons in the lateral cord compared to non-transplanted animals. In particular this difference was significant between 3200 and 4000 µm. *: $P < 0.05$.

3.2.3.8 BDA labelled fibres in the medial spinal cord

In this section all BDA labelled fibres in the medial spinal cord irrespective of whether they were in continuity or not in continuity with fibres in the lateral cord shall be considered. Continuity with spared fibres in the lateral cord could in fact underlie sprouting of spared fibres into the OEC tracts, a phenomenon that is different from regeneration. The following section, instead, will focus only on regenerating fibres in the medial spinal cord by subtracting from the analysis all fibres or entire animals where discontinuity between medial and lateral fibres was not found.

The presence of OEC tracts rostral to the lesion in the dorsal columns and in the grey matter caudal to the dorsal columns set up the ideal conditions to question whether OECs could promote fibres to sprout/regenerate rostral to the lesion. Importantly, as already mentioned above, the frequent distribution of OECs rostral to the lesion allowed for the possibility for a number of BDA labelled axons to grow beyond the lesion for relatively long distances. The majority of sprouting/regenerating fibres in the medial spinal cord of the lesion block were found in association with OECs (examples from two animals are shown in Figure 3-31 and Figure 3-32). Only a small number of fibres in the medial spinal cord (10%) were not associated with the transplanted cells (Table 5 and Table 6; graph in Figure 3-33). The difference in number between fibres associated with OECs and fibres that were not was significant at 200 μm and 400 μm distances rostral to the lesion (Figure 3-33). The BDA labelled axons that were not associated with OECs were in most cases located close to the border between the medial and the lateral cord (position indicative of sparing); while those that were associated with OECs were normally in the centre of the medial dorsal columns on the ipsilateral and contralateral side or beneath the medial portion of the dorsal columns in the grey matter and even in the central canal. An example of fibres sprouting/ regenerating in the central canal is shown in Figure 3-32.

The orientation of medial fibres followed closely that of the GFP labelled cells so that normally they were aligned with the rostro-caudal spinal cord.

Nonetheless, if OECs were oriented differently (e.g. dorso-ventral direction) it was common to see the BDA labelled fibres having that same orientation.

Figure 3-31. Sprouting/regenerating axons rostral to the lesion in the medial spinal cord following OEC transplantation.

Axons found rostral to the dorsal column lesion were mostly associated with OEC tracts. **A)** Confocal image taken with a low power objective (10x) of a parasagittal section of the lesion block in a rat transplanted with OECs; boxed area is depicted at higher magnification (40x) in **B**. **C1-C2)** Enlarged images of the boxed area in **B** to show that BDA labelled axons were mostly associated with OECs; **C2)** BDA axonal labelling in greyscale. **A-C)** Composites of confocal projected image stacks. Colour codes: red (axons), green (OECs), blue (astrocytes). Scale bars: 500 μm in **A**; 100 μm in **B**; 25 μm in **C**.

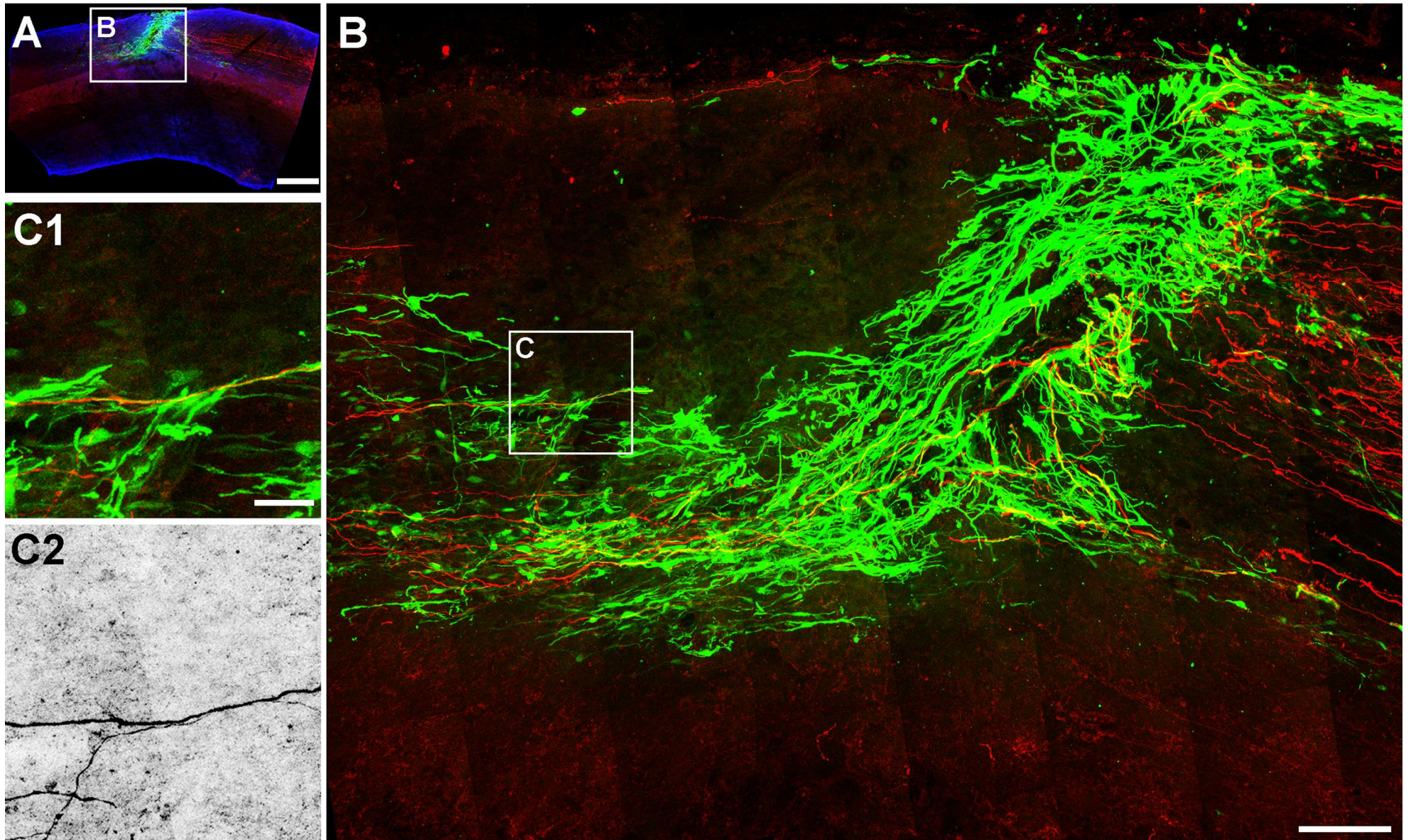
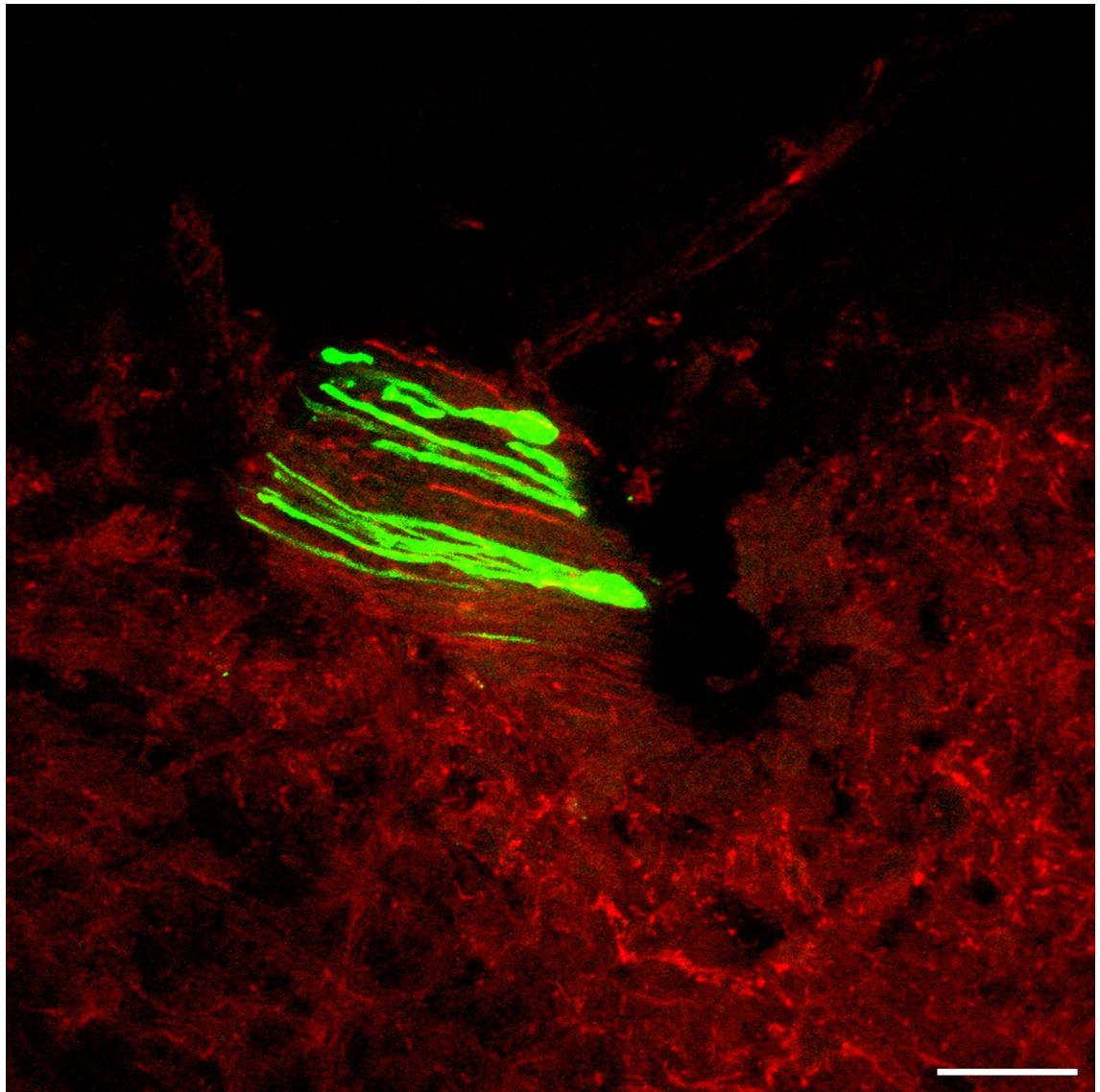


Figure 3-32. BDA labelling of sprouting/regenerating axons in the central canal following OEC transplantation.

Aberrant BDA labelling in the central canal was observed only in animals where OECs had distributed in the central canal. In this projection of confocal stacked images tract traced axons (red) were closely associated with OECs (green). Both OECs and axons were oriented along the rostro-caudal direction running through the central canal. Objective: 40x. Scale bar: 25 μ m.



| | | Number of axons | | | | | | | | | | | | | | | | | | | | | | | |
|--|-------|-----------------|-------|-------|-------|-------|-------|-------|-------|--------|--------|--------|--------|--------|--------|--------|--------|--------|--------|--------|--------|--------|---------|-----------|-----|
| | | R4204 | R0705 | R2805 | R2905 | R8105 | R8205 | R0506 | R0706 | R16606 | R21106 | R21406 | R30906 | R31006 | R16907 | R17007 | R17707 | R17807 | R22908 | R23008 | R23108 | R23208 | Average | St. Error | |
| Distance from the lesion (μm) | 200 | - | - | 0 | 0 | 0 | 32 | 43 | 8 | 0 | 0 | 0 | - | 3 | 0 | 8 | 18 | 0 | 60 | 1 | 4 | 1 | 9.9 | 4.1 | |
| | 400 | - | - | - | - | 0 | 9 | 24 | 10 | 0 | 0 | 0 | - | 2 | 0 | 1 | 26 | 0 | 34 | 2 | 2 | 2 | 7.0 | 2.8 | |
| | 600 | - | - | - | - | 0 | 3 | 19 | 18 | 0 | 0 | 0 | - | 0 | 0 | - | 10 | 0 | 22 | 0 | 3 | - | 5.4 | 2.2 | |
| | 800 | - | - | - | - | 0 | 3 | 8 | 2 | - | 0 | - | - | 0 | 0 | - | 5 | 0 | 27 | 0 | 3 | - | 4.0 | 2.2 | |
| | 1000 | - | - | - | - | 0 | 0 | 10 | 1 | - | - | - | - | - | 0 | - | 4 | 0 | 20 | 0 | 3 | - | 3.8 | 2.1 | |
| | 1200 | - | - | - | - | 0 | 0 | - | 1 | - | - | - | - | - | - | - | 4 | 0 | 21 | 1 | 1 | - | 3.5 | 2.5 | |
| | 1400 | - | - | - | - | 0 | 0 | - | - | - | - | - | - | - | - | - | 1 | 0 | 8 | 1 | 0 | - | 1.4 | 1.1 | |
| | 1600 | - | - | - | - | 0 | 0 | 0 | - | - | - | - | - | - | 0 | - | - | 3 | 0 | 10 | - | 1 | - | 1.8 | 1.2 |
| | 3200 | - | - | - | - | - | - | - | - | - | - | - | - | - | - | - | 0 | - | - | 0 | - | - | - | 0.0 | 0.0 |
| | 3600 | - | - | - | - | - | - | - | - | - | - | - | - | - | - | - | - | - | - | - | - | - | - | - | - |
| | 4000 | - | - | - | - | - | - | - | - | - | - | - | - | - | - | - | - | - | - | - | - | - | - | - | - |
| | 4400 | - | - | - | - | - | - | - | - | - | - | - | - | - | - | - | - | - | - | - | - | - | - | - | - |
| | 4800 | - | - | - | - | - | - | - | - | - | - | - | - | - | - | - | - | - | - | - | - | - | - | - | - |
| | 10000 | - | - | - | - | - | - | - | - | - | - | - | - | - | - | - | - | - | - | - | - | - | - | - | - |
| | 10400 | - | - | - | - | - | - | - | - | - | - | - | - | - | - | - | - | - | - | - | - | - | - | - | - |
| | 10800 | - | - | - | - | - | - | - | - | - | - | - | - | - | - | - | - | - | - | - | - | - | - | - | - |
| | 11200 | - | - | - | - | - | - | - | - | - | - | - | - | - | - | - | - | - | - | - | - | - | - | - | - |
| 11600 | - | - | - | - | - | - | - | - | - | - | - | - | - | - | - | - | - | - | - | - | - | - | - | - | |

Table 5. Number of tract traced fibres associated with OECs at increasing distance from the lesion in the medial spinal cord.

Quantification of axon number rostral to the lesion performed with an epifluorescence microscope and 63x lens on parasagittal sections of the lesion block, rostral block and thoracic block. Blank cells are used to indicate that data did not meet the inclusion criteria.

| | | Number of axons | | | | | | | | | | | | | | | | | | | | | | | |
|--|-------|-----------------|-------|-------|-------|-------|-------|-------|-------|--------|--------|--------|--------|--------|--------|--------|--------|--------|--------|--------|--------|--------|---------|-----------|-----|
| | | R4204 | R0705 | R2805 | R2905 | R8105 | R8205 | R0506 | R0706 | R16606 | R21106 | R21406 | R30906 | R31006 | R16907 | R17007 | R17707 | R17807 | R22908 | R23008 | R23108 | R23208 | Average | St. Error | |
| Distance from the lesion (μm) | 200 | . | . | 0 | 0 | 0 | 0 | 0 | 2 | 0 | 0 | 2 | 0 | 0 | 0 | 0 | 0 | 0 | 0 | 0 | 0 | 0 | 0 | 0.2 | 0.1 |
| | 400 | . | . | 0 | 0 | 0 | 3 | 0 | 0 | 0 | 0 | 1 | 0 | 0 | 0 | 0 | 0 | 0 | 0 | 0 | 0 | 0 | 0 | 0.2 | 0.2 |
| | 600 | . | . | 0 | 0 | 0 | 2 | 0 | 0 | 0 | 0 | 1 | 0 | 0 | 0 | 0 | 0 | 0 | 1 | 0 | 0 | 0 | 0 | 0.2 | 0.1 |
| | 800 | . | . | 0 | 0 | 0 | 1 | 0 | 2 | 0 | 0 | 1 | 0 | 0 | 0 | 0 | 0 | 0 | 4 | 0 | 0 | 0 | 0 | 0.4 | 0.2 |
| | 1000 | . | . | 0 | 0 | 1 | 1 | 0 | 3 | 0 | 0 | 0 | 0 | 0 | 0 | 0 | 0 | 0 | 3 | 0 | 0 | 0 | 0 | 0.4 | 0.2 |
| | 1200 | . | . | 0 | 0 | 0 | 0 | 0 | 2 | 0 | 0 | 0 | 0 | 0 | 0 | 0 | 0 | 0 | 3 | 0 | 0 | 0 | 0 | 0.3 | 0.2 |
| | 1400 | . | . | 0 | 0 | 0 | 0 | 0 | 2 | 0 | 0 | 0 | 2 | 0 | 0 | 0 | 0 | 0 | 1 | 0 | 0 | 0 | 0 | 0.3 | 0.1 |
| | 1600 | . | . | 0 | . | 0 | 0 | 0 | 15 | 0 | 0 | 0 | 3 | 0 | 0 | 0 | 0 | 0 | 1 | 0 | 0 | 0 | 0 | 1.1 | 0.8 |
| | 3200 | . | . | . | . | . | . | . | . | . | . | . | . | . | . | 9 | 0 | 0 | 0 | 1 | 3 | 0 | 0 | 1.6 | 1.1 |
| | 3600 | . | . | . | . | . | . | . | . | . | . | . | . | . | . | 10 | 0 | 1 | 0 | 0 | 0 | 0 | 0 | 1.4 | 1.2 |
| | 4000 | . | . | . | . | . | . | . | . | . | . | . | . | . | . | 13 | 0 | 1 | 0 | 0 | 0 | 0 | 0 | 1.8 | 1.6 |
| | 4400 | . | . | . | . | . | . | . | . | . | . | . | . | . | . | . | 0 | 0 | 0 | 0 | 0 | 0 | 0 | 0.0 | 0.0 |
| | 4800 | . | . | . | . | . | . | . | . | . | . | . | . | . | . | . | 1 | 0 | 0 | 0 | 0 | 0 | 0 | 0.2 | 0.2 |
| | 1000 | . | . | . | . | . | . | . | . | . | . | . | . | . | . | . | 1 | 0 | . | 0 | 0 | 0 | 0 | 0.2 | 0.2 |
| | 1000 | . | . | . | . | . | . | . | . | . | . | . | . | . | . | . | 1 | 0 | . | 0 | 0 | 0 | 0 | 0.2 | 0.2 |
| | 10800 | . | . | . | . | . | . | . | . | . | . | . | . | . | . | . | 1 | 0 | . | 0 | 0 | 0 | 0 | 0.2 | 0.2 |
| | 11200 | . | . | . | . | . | . | . | . | . | . | . | . | . | . | . | 1 | 0 | . | 0 | 0 | 0 | 0 | 0.2 | 0.2 |
| 11600 | . | . | . | . | . | . | . | . | . | . | . | . | . | . | . | 1 | 0 | . | 0 | 0 | 0 | 0 | 0.2 | 0.2 | |

Table 6. Number of tract traced fibres, that were not associated with OECs, at increasing distance from the lesion in the medial spinal cord. Quantification of axon number rostral to the lesion performed with an epifluorescence microscope and 63x lens on parasagittal sections of the lesion block, rostral block and thoracic block. Blank cells are used to indicate that data did not meet the inclusion criteria.

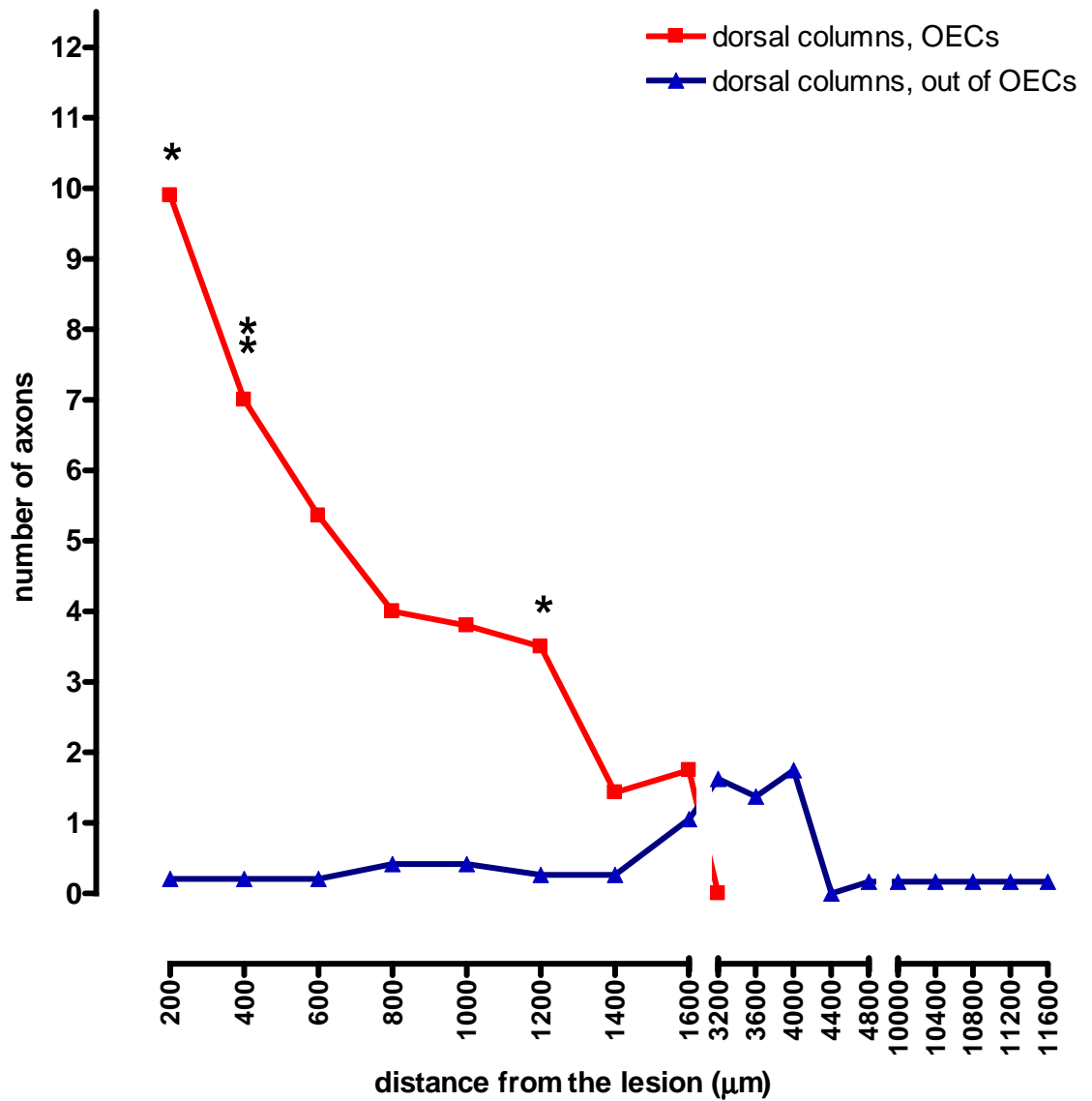


Figure 3-33. Comparison of the average number of BDA labelled fibres associated and not associated with OECs in the medial spinal cord.

The vast majority of tract traced axons were located in close vicinity to OECs. The difference in number between the two fibre groups was significant. *: $P < 0.05$; **: $P < 0.005$.

3.2.3.9 Genuine regenerating BDA labelled fibres rostral to the lesion level

When the quantification of the number of axons associated with OECs was estimated as described in the previous section, it potentially included spared and sprouting fibres. To carry out quantification of regeneration rostral to the lesion, a more conservative analysis of the number of BDA labelled fibres was performed and all necessary steps were undertaken to subtract from the analysis of quantification of regeneration any fibres that were not convincingly regenerating. The sophisticated way all data was organised (for an example of data recording see Figure 2-11 in the methods chapter), including qualitative and quantitative information on OEC distribution and fibre number for each section from each spinal cord block from each rat, allowed me to easily pick out all those fibres associated with OECs that were not convincingly genuine regenerating fibres and to exclude them, or when necessary exclude all data from an animal. The definition of a convincingly regenerating fibre followed 3 criteria: 1) only fibres within the medial dorsal columns and underlying grey matter could be considered regenerating; 2) to be considered regenerating, fibres had to be in discontinuity with fibres located in the lateral spinal cord (a condition suggestive of sprouting); 3) discontinuity was met when no fibres were detected in 3 sections (~210 μm) or more to the left of the putative regenerating fibres. Other attributes that are suggestive of regeneration were often met by the fibres termed as regenerating in this thesis, such as unusual morphology (growth cones, orientation) and location (contralateral), but were not used in the inclusion criteria because these attributes are also typical of sprouting.

After this stringency was applied to the data, convincing regeneration was detected only in 6 of the 16 animals which showed BDA labelling in the medial spinal cord rostral to the lesion. These axons, quantified in Table 7, were mostly (93.5% of fibre counts) localised within tracts of OECs. An example is shown in Figure 3-35.

Interestingly, OEC tracts rostral to the lesion and in continuity with the lesion were not only present in those animals where regeneration was detected, but were also present in 7 more animals where regeneration was not detected.

Importantly, in these 7 animals although OEC tracts were present these were not sufficient to promote regeneration beyond the lesion as it is shown in the example depicted in Figure 3-34.

On the other hand, in 3 of the 6 animals where regeneration was detected in the OEC tracts rostral to the dorsal column lesion, the axons were not detected the full length of the OEC tract, but ended more caudally than the rostral end of the cell tract (Figure 3-36). Consistent with this observation, the average length of the OEC tracts rostral to the lesion in these animals was 1070 μm while the average length of the furthest regenerating fibre detected in each animal rostral to the lesion was 380 μm .

Using BDA tract tracing it was not possible to determine with confidence whether synaptic boutons were associated with the regenerating axons in any of the animals analysed. This was because with BDA labelling synaptic boutons and growth cones of extremely thin axons in the OEC tract cannot be easily distinguished, so it would be necessary to use specific antibodies against synapse formation. Regenerating axons were observed in an area devoid of GFP labelling which was rostral to the end of an OEC tract only in one animal; however it cannot be excluded that these fibres were associated with non-labelled OECs.

Figure 3-34. OEC tracts in continuity with the lesion were not sufficient to promote regeneration rostral to the lesion in some animals. **A)** Confocal image taken with a low power objective (10x) of a parasagittal section of the lesion block in a rat transplanted with OECs; boxed area is depicted at higher magnification (40x) in **B**. **B)** Axons approached the caudal end of the lesion but none were found to bridge the lesion to the other side in the OEC tract. **C1-C2)** Enlarged images of the boxed area in **B** to show the absence of axonal BDA labelling in a track of OECs distributed rostral to the lesion. **C2)** This image depicts BDA labelling in greyscale. **A-C)** Composite of confocal projected image stacks. Colour codes: red (axons), green (OECs), blue (astrocytes). Scale bars: 500 μm in **A**; 100 μm in **B**; 25 μm in **C**.

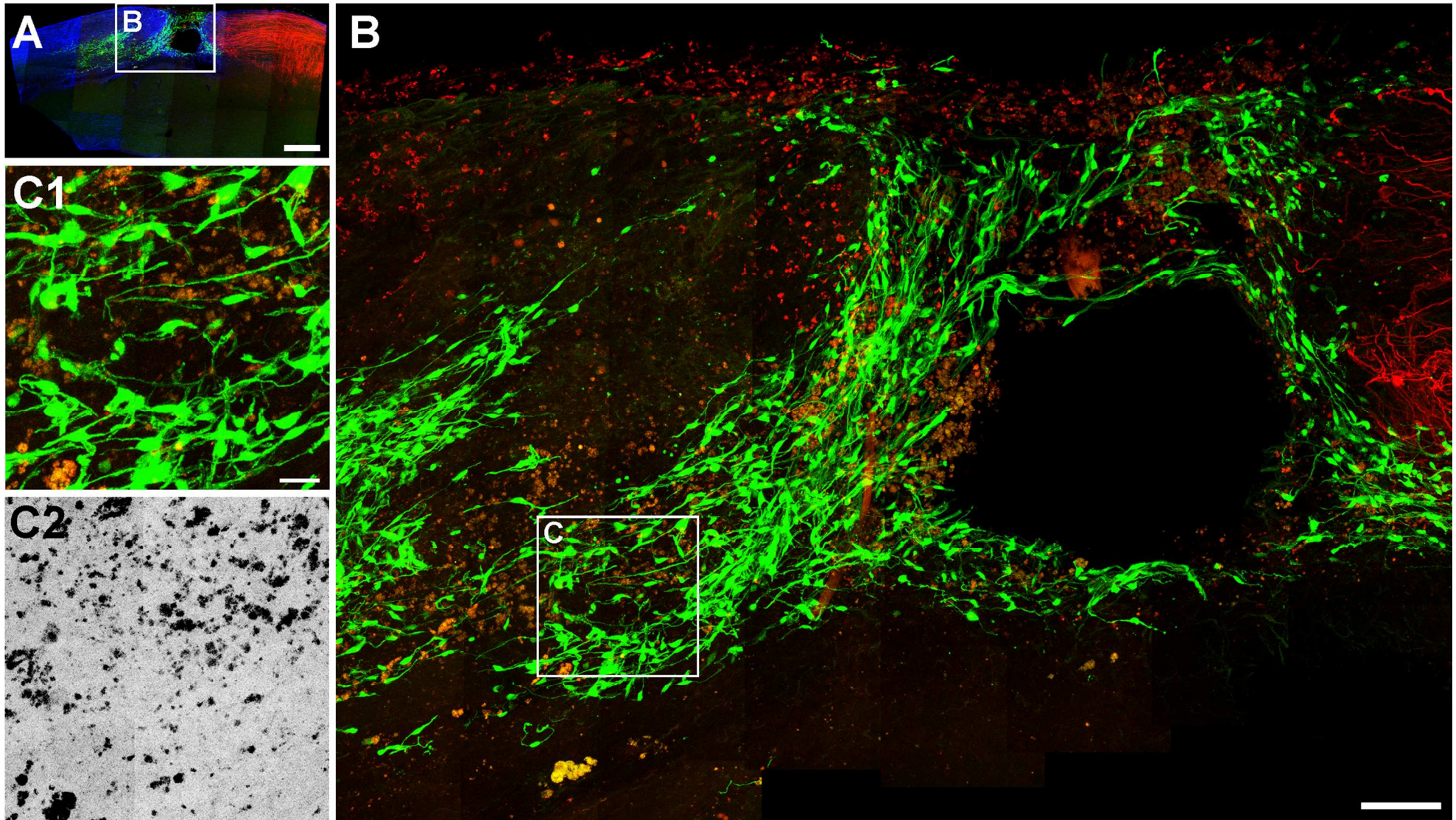
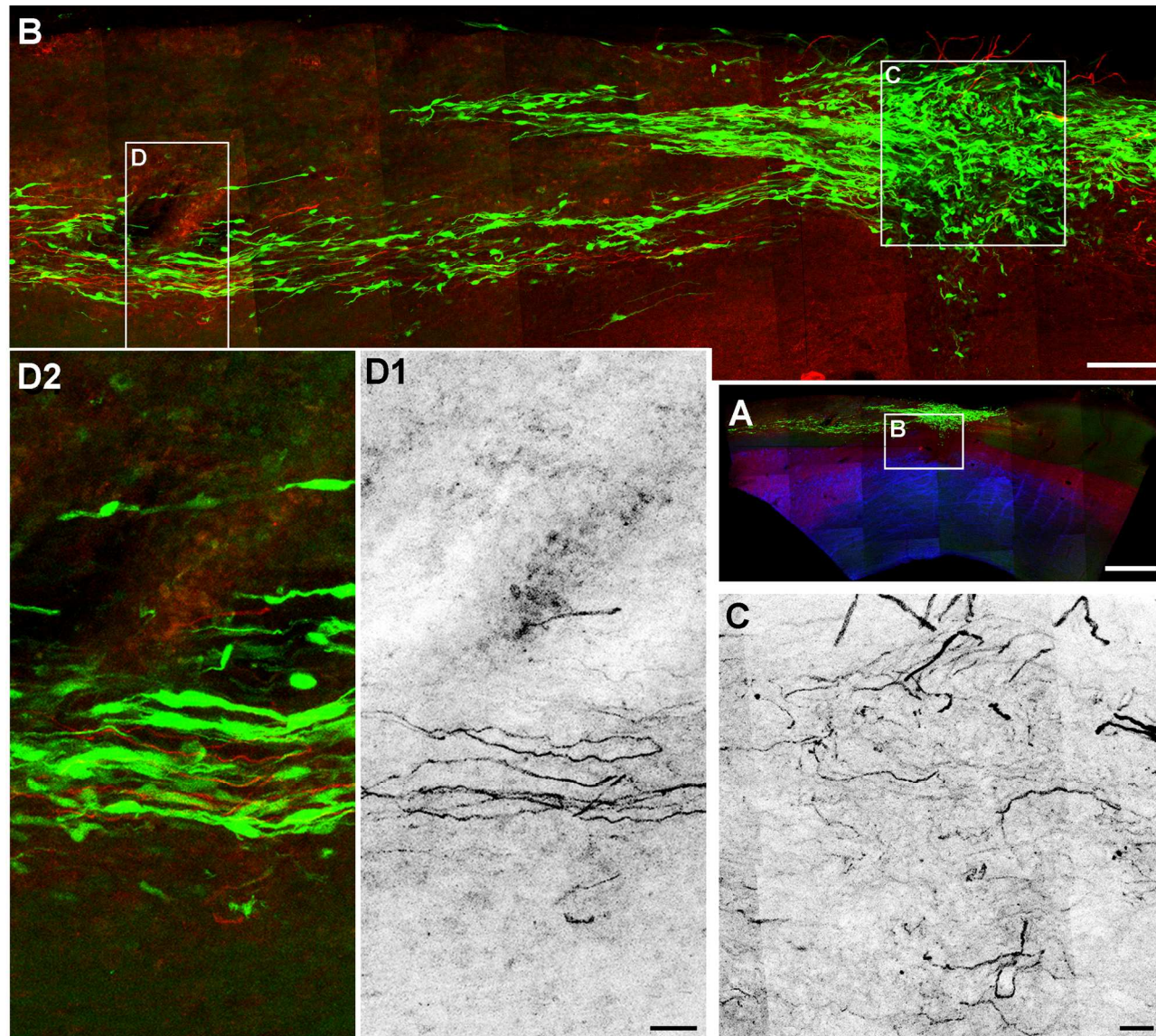


Figure 3-35. Regeneration of BDA labelled axons in OEC tracts rostral to the lesion.

A) Confocal images taken with a low power objective (10x) of a parasagittal section of the lesion block in a rat transplanted with OECs; boxed area is depicted at higher magnification (40x oil) in **B**. **B)** Axons approached the caudal end of the dorsal column transection and bridged the lesion to the other side within the OEC tract. **C:** enlarged image of the boxed area shown in **B** that shows the axons regenerating in the lesion. **D1-D2)** Images of the boxed area shown in **B** are depicted here at higher magnification (40x oil) to show axons regenerating in rostral tracks of OECs in continuity with the lesion. It is also possible to see that axons were closely associated with OECs. **D1)** BDA axonal labelling in greyscale. **A-D)** Composite of confocal projected image stacks. Colour codes: red (axons), green (OECs), blue (astrocytes). Scale bars: 500 μm in **A**; 100 μm in **B**; 25 μm in **C-D**.



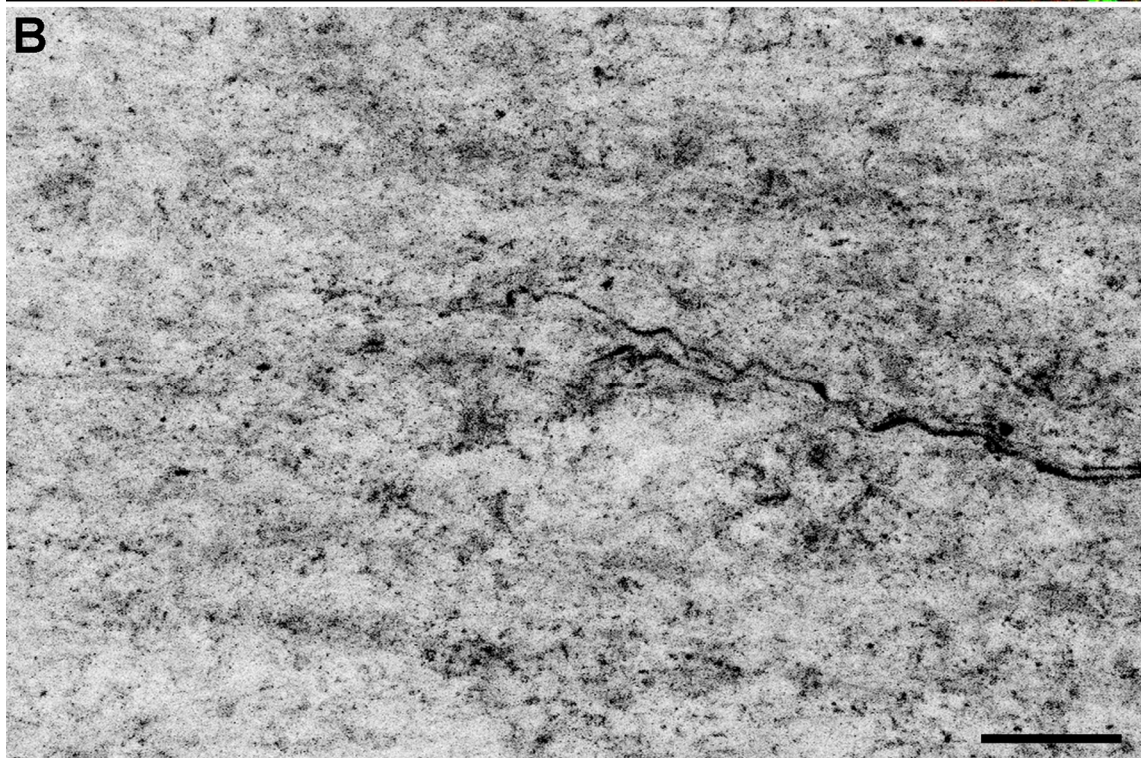
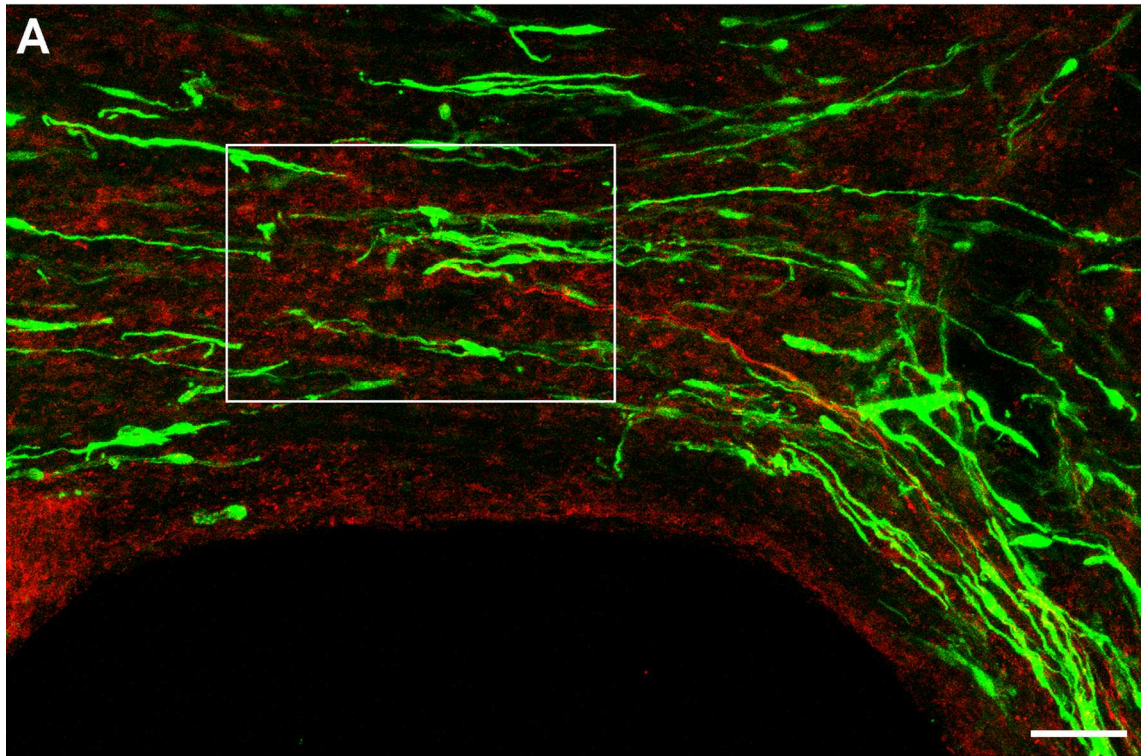
| | | Number of axons | | | | | | | | | | | | | | | | | | | | | | |
|--|-------|-----------------|-------|-------|-------|-------|-------|-------|-------|--------|--------|--------|--------|--------|--------|--------|--------|--------|--------|--------|--------|--------|------------|------------|
| | | R4204 | R0705 | R2805 | R2905 | R8105 | R8205 | R0506 | R0706 | R16606 | R21106 | R21406 | R30906 | R31006 | R16907 | R17007 | R17707 | R17807 | R22908 | R23008 | R23108 | R23208 | Average | St. Error |
| Distance from the lesion (μm) | 200 | - | - | 0 | - | 0 | 32 | - | - | 0 | 0 | 0 | - | 3 | 0 | 8 | - | 0 | - | 1 | 4 | 1 | 3.8 | 2.4 |
| | 400 | - | - | - | - | 0 | 9 | - | - | 0 | 0 | 0 | - | 2 | 0 | 1 | - | 0 | - | 2 | 2 | 2 | 1.5 | 0.7 |
| | 600 | - | - | - | - | 0 | 3 | - | - | 0 | 0 | 0 | - | 0 | 0 | - | - | 0 | - | 0 | 3 | - | 0.6 | 0.4 |
| | 800 | - | - | - | - | 0 | 3 | - | - | - | 0 | - | - | 0 | 0 | - | - | 0 | - | 0 | 3 | - | 0.8 | 0.5 |
| | 1000 | - | - | - | - | 0 | 0 | - | - | - | - | - | - | - | 0 | - | - | 0 | - | 0 | 3 | - | 0.5 | 0.5 |
| | 1200 | - | - | - | - | 0 | 0 | - | - | - | - | - | - | - | - | - | - | 0 | - | 1 | 1 | - | 0.4 | 0.2 |
| | 1400 | - | - | - | - | 0 | 0 | - | - | - | - | - | - | - | - | - | - | 0 | - | 1 | 0 | - | 0.2 | 0.2 |
| | 1600 | - | - | - | - | 0 | 0 | - | - | - | - | - | - | - | - | - | - | 0 | - | - | 1 | - | 0.3 | 0.3 |
| | 3200 | - | - | - | - | - | - | - | - | - | - | - | - | - | - | - | - | - | - | - | - | - | - | - |
| | 3600 | - | - | - | - | - | - | - | - | - | - | - | - | - | - | - | - | - | - | - | - | - | - | - |
| | 4000 | - | - | - | - | - | - | - | - | - | - | - | - | - | - | - | - | - | - | - | - | - | - | - |
| | 4400 | - | - | - | - | - | - | - | - | - | - | - | - | - | - | - | - | - | - | - | - | - | - | - |
| | 4800 | - | - | - | - | - | - | - | - | - | - | - | - | - | - | - | - | - | - | - | - | - | - | - |
| | 1000 | - | - | - | - | - | - | - | - | - | - | - | - | - | - | - | - | - | - | - | - | - | - | - |
| | 1000 | - | - | - | - | - | - | - | - | - | - | - | - | - | - | - | - | - | - | - | - | - | - | - |
| | 10800 | - | - | - | - | - | - | - | - | - | - | - | - | - | - | - | - | - | - | - | - | - | - | - |
| | 11200 | - | - | - | - | - | - | - | - | - | - | - | - | - | - | - | - | - | - | - | - | - | - | - |
| 11600 | - | - | - | - | - | - | - | - | - | - | - | - | - | - | - | - | - | - | - | - | - | - | - | |

Table 7. Number of regenerating fibres at increasing distance from the lesion in the medial spinal cord associated with OECs.

Quantification of axon number rostral to the lesion performed with an epifluorescence microscope and 63x lens on parasagittal sections of the lesion block, rostral block and thoracic block. Blank cells are used to indicate that data did not meet the inclusion criteria or fit the stringency applied.

Figure 3-36. Axons did not regenerate for the full length of the OEC tract.

Confocal projected image stacks of a parasagittal section of the lesion block above the lesion level. **A)** OEC tract (green) above the lesion associated with few regenerating BDA labelled (red) axons (arrow). **B)** Higher magnification (40x) of boxed area in **A** showing BDA labelling in grey scale; a regenerating axon (~1 μ m diameter) can be seen ending in the depth of the section thickness (arrow head). Scale bars: 50 μ m in **A**; 25 μ m in **B**.



3.2.4 Conditioning lesions coupled with OECs transplant

To question whether a combined treatment paradigm could boost the limited axonal regeneration observed in the OEC transplanted animals in the previous section, here OEC transplantation was combined with conditioning lesions of the sciatic nerve. A total of 24 rats underwent a treatment procedure that included transplanting OECs into the lesion and either single or double conditioning lesions of the sciatic nerve (Figure 3-37).

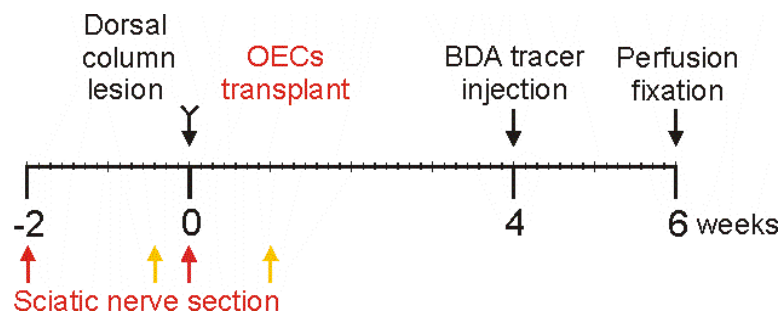


Figure 3-37. Time course of procedures performed on lesioned animals receiving an OEC transplant and conditioning lesions.

Conditioning lesions combined with OEC transplantation were performed following 3 different paradigms: i) one conditioning lesion two weeks before the spinal cord injury; ii) two conditioning lesions performed two weeks before and at the time of the dorsal column injury; or iii) two conditioning lesions performed three days before and seven days after the spinal cord injury.

3.2.4.1 OEC distribution in the spinal cord

Transplanted GFP expressing OECs were found in the lesion of all the rats in this conditioning lesioned experimental group. The distribution of OECs in the lesion and in the spinal cord tissue was similar to that of non-conditioned OEC transplanted rats. OECs were found to partially fill the lesion of all animals and to distribute rostral to the lesion in 96% (23/24) of rats and caudal in 96% (23/24) of rats. Cells formed continuous tracts rostral to the injury in 83% (20/24) of animals; these continuous tracts varied in length and ended on average 1800 μm from the injury. On average the length of the OEC continuous

tracts rostral to the lesion was 2150 μm in 5 of the 24 animals where the rostral block had also been taken from the spinal cord.

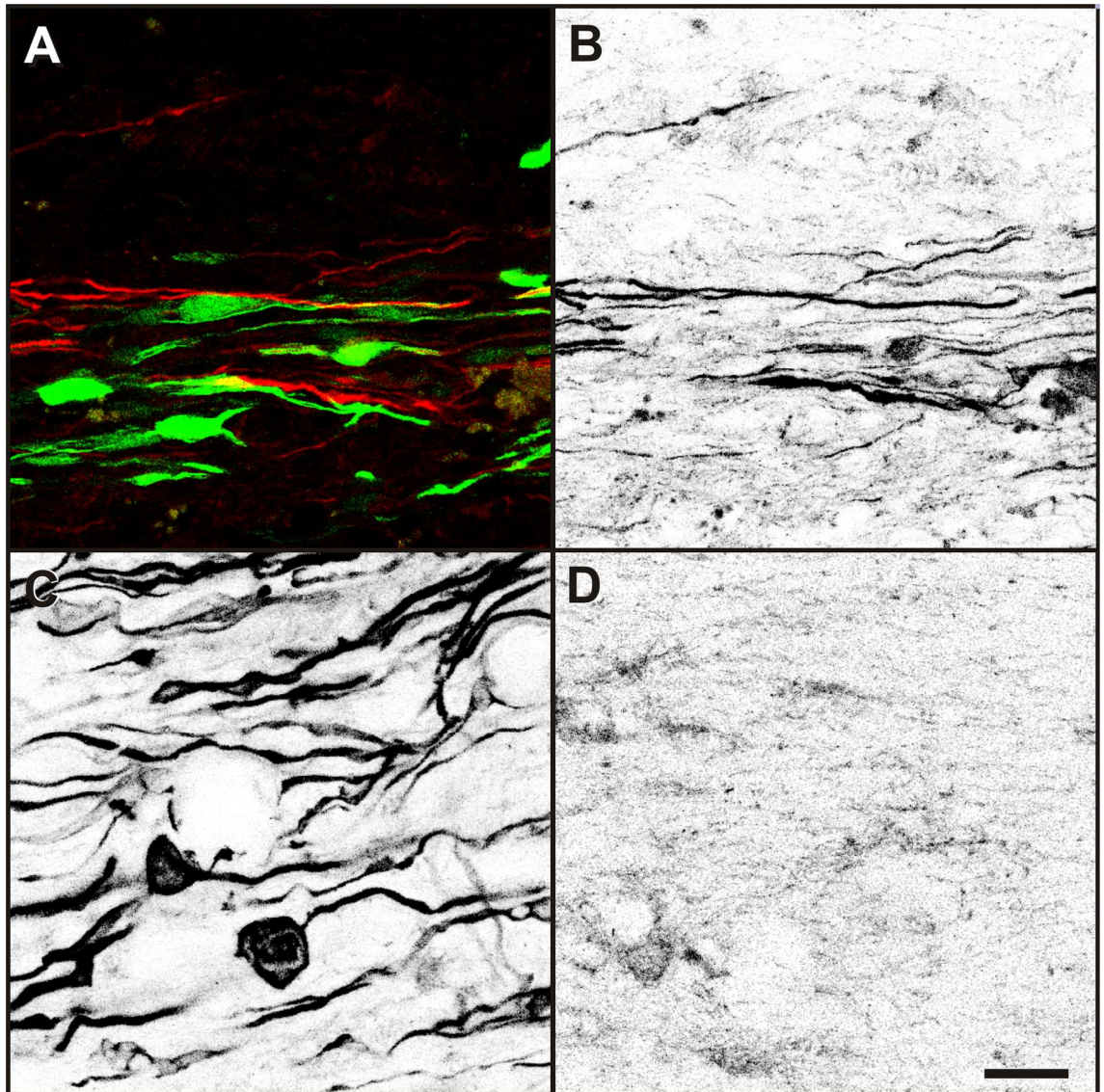
3.2.4.2 BDA labelled fibres sprouting within caudally distributed OECs

In those animals where OECs had formed tracts caudal to the lesion it was possible to notice that the areas of distribution of OECs contained denser BDA labelled axons compared to neighbouring areas devoid of OECs (Figure 3-38). A quantification of the fibre density within the OEC tracts and in neighbouring areas devoid of OECs was performed and is shown in Figure 3-39A. The density of axons within the transplant was significantly higher than that in areas devoid of OECs ($P=0.042$). This result and the fact that fibres were mostly aligned with the OECs might indicate that sprouting occurred, and that OECs provided a more favourable environment for sprouting fibres to grow in than that provided by host spinal cord tissue.

As shown in Figure 3-39B the level of sprouting in tracts of OECs distributed caudal to the transplant site in conditioning lesioned animals was double that observed in animals which did not receive a conditioning lesion, however the difference between the two was not significant ($P=0.065$). It is important to note that the high density of sprouting in some conditioned animals was possibly underestimated in the quantification process because labelled axons overlapped. This axon overlapping might have reduced the difference between the two experimental groups.

Figure 3-38. Examples of tract traced fibres among tracts of OECs caudal to the lesion site compared to tract traced fibres in immediately adjacent tissue in conditioning lesioned animals.

The axonal density of BDA labelled axons caudal to the injury was higher in areas where OECs were distributed compared to neighbouring tissue devoid of OECs. **A)** Image of a tissue section where a tract of OECs distributed caudal to the lesion (OEC-GFP in green, traced axons in red). **B)** Same image as depicted in **A** displaying only labelled axons in greyscale mode. **C-D)** Images taken from the sections to the LHS and RHS respectively of the section depicted in **A-B** to show denser BDA labelling (greyscale) in areas where OECs were distributed. All images are projections of confocal stacks of 3 images taken 1 μm apart. Scale bar: 20 μm .



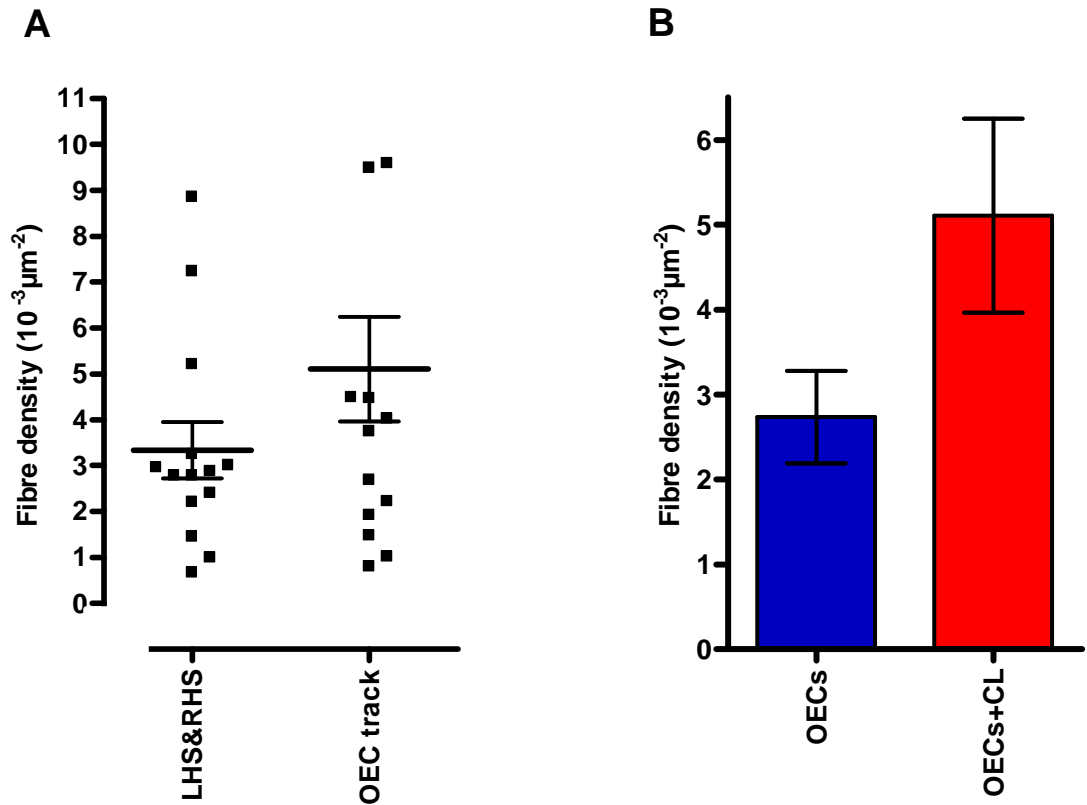


Figure 3-39. Axonal density in caudal tracts of OECs transplanted into a dorsal column lesion in animals receiving conditioning lesions.

A) Scatter plot depicting the fibre density. The tract traced axons in conditioning lesioned animals were significantly denser in the tracts of OECs that had distributed caudally compared to neighbouring areas devoid of OECs ($P=0.042$). **B)** Comparison of fibre density in OEC tracts distributed caudal to the lesion in animals that received only an OECs transplant and in animals treated with a combination of OEC transplant and conditioning lesions. Conditioning lesions doubled the axonal density, however the difference was not significant ($P=0.065$).

3.2.4.3 Regeneration within the transplant

BDA labelling was detected in the lesion of all (n=24) animals however this was highly variable amongst sections of the same animals and between different animals. The amount of fibres in the lesion was not quantified so no quantitative comparison could be made with rats receiving an OECs transplant only.

3.2.4.4 BDA labelled fibres rostral to the lesion

Parasagittal and transverse sections were analysed for the presence of BDA labelled axons rostral to the injury level. Following the same methodology (section 3.2.3.6) applied with OEC transplanted only rats these fibres were subdivided for practical purposes in to 2 main categories: axons in the medial cord and axons in the lateral cord.

BDA labelled fibres rostral to the injury in the medial spinal cord were detected in 13 animals. These fibres were likely regenerating or sprouting fibres as their orientation followed closely the orientation of the OECs. Quantification of axonal numbers is shown in Table 8 and Table 9 and is expressed graphically in Figure 3-40. It was found that 90% of axons were in close vicinity to OECs while only 10% were not, and the difference between the two groups of fibres was significant. Fibres that were located in areas devoid of OECs were mostly found in sections close to the border of the dorsal columns and they presumably were spared fibres in continuity with spared fibres in the lateral cord. Figure 3-41 shows a comparison between the number of axons in the medial spinal cord in OEC transplanted animals and in OEC transplanted and conditioning lesioned animals. The difference in number was significant between 600 μm and 1400 μm . The average increase in fibre number seen in the lesion block after combining OEC transplantation with conditioning lesions was 9 fold (Figure 3-41B).

| | | Number of axons | | | | | | | | | | | | | | | | | | | | |
|--|-------|-----------------|-------|-------|-------|-------|-------|-------|--------|--------|--------|--------|--------|--------|--------|--------|--------|--------|--------|--------|---------|-----------|
| | | R3304 | R5704 | R5904 | R7205 | R1406 | R2806 | R3906 | R15806 | R15906 | R17906 | R19506 | R19606 | R20506 | R30606 | R30706 | R30806 | R16707 | R16807 | R17607 | Average | St. Error |
| Distance from the lesion (μm) | 200 | - | - | 82 | 2 | 0 | 29 | 1 | 2 | 98 | 0 | 5 | 96 | 38 | 30 | 0 | 0 | 0 | 27 | - | 26.0 | 8.9 |
| | 400 | - | - | 80 | 2 | 0 | 28 | 3 | 2 | 77 | 0 | 4 | 87 | 28 | 25 | 0 | 0 | 0 | 24 | - | 22.5 | 7.8 |
| | 600 | - | - | 67 | 5 | 0 | 24 | 3 | 0 | 24 | 0 | 2 | 82 | 15 | 27 | 0 | 4 | 0 | 29 | - | 17.6 | 6.2 |
| | 800 | - | - | 49 | 12 | 0 | 30 | 6 | 0 | 10 | 0 | 1 | 84 | 7 | 20 | 0 | 5 | 0 | 34 | - | 16.1 | 5.8 |
| | 1000 | - | - | 47 | 7 | 0 | 30 | 1 | 0 | 9 | 2 | 1 | 61 | 6 | 20 | 0 | 5 | 0 | 23 | - | 13.3 | 4.6 |
| | 1200 | - | - | 40 | 6 | 0 | 48 | 3 | 0 | 0 | 5 | 5 | 57 | 12 | 13 | 0 | 6 | 0 | 21 | - | 13.5 | 4.6 |
| | 1400 | - | - | 41 | 10 | - | 29 | 3 | 0 | 0 | 4 | 1 | 46 | 12 | 19 | 0 | 5 | 0 | 15 | - | 12.3 | 3.9 |
| | 1600 | - | - | 19 | - | - | 32 | 2 | 0 | 0 | 3 | - | 49 | 9 | 19 | 0 | 3 | 0 | 13 | - | 11.5 | 4.2 |
| | 3200 | - | - | - | - | - | - | - | - | - | - | - | - | - | 0 | 9 | 0 | 5 | - | - | 2.8 | 1.8 |
| | 3600 | - | - | - | - | - | - | - | - | - | - | - | - | - | 0 | 15 | 0 | 5 | - | - | 4.0 | 2.9 |
| | 4000 | - | - | - | - | - | - | - | - | - | - | - | - | - | 0 | 20 | 0 | 6 | - | - | 5.2 | 3.9 |
| | 4400 | - | - | - | - | - | - | - | - | - | - | - | - | - | 0 | 7 | - | 6 | - | - | 3.3 | 1.9 |
| | 4800 | - | - | - | - | - | - | - | - | - | - | - | - | - | 0 | 9 | - | 0 | - | - | 2.3 | 2.3 |
| | 10000 | - | - | - | - | - | - | - | - | - | - | - | - | - | - | - | - | 0 | - | - | 0.0 | 0.0 |
| | 10400 | - | - | - | - | - | - | - | - | - | - | - | - | - | - | - | - | 0 | - | - | 0.0 | 0.0 |
| | 10800 | - | - | - | - | - | - | - | - | - | - | - | - | - | - | - | - | 0 | - | - | 0.0 | 0.0 |
| 11200 | - | - | - | - | - | - | - | - | - | - | - | - | - | - | - | - | 0 | - | - | 0.0 | 0.0 | |
| 11600 | - | - | - | - | - | - | - | - | - | - | - | - | - | - | - | - | 0 | - | - | 0.0 | 0.0 | |

Table 8. Number of fibres associated with OECs at increasing distance from the dorsal column lesion in the medial spinal cord in OEC transplanted and conditioning lesioned animals.

Quantification of axon number rostral to the lesion performed with an epifluorescence microscope and 63x lens on parasagittal sections of the lesion block, rostral block and thoracic block. Blank cells are used to indicate that data did not meet the inclusion criteria.

| | | Number of axons | | | | | | | | | | | | | | | | | | | | | |
|--|-------|-----------------|-------|-------|-------|-------|-------|-------|--------|--------|--------|--------|--------|--------|--------|--------|--------|--------|--------|--------|---------|-----------|-----|
| | | R3304 | R5704 | R5904 | R7205 | R1406 | R2806 | R3906 | R15806 | R15906 | R17906 | R19506 | R19606 | R20506 | R30606 | R30706 | R30806 | R16707 | R16807 | R17607 | Average | St. Error | |
| Distance from the lesion (μm) | 200 | - | - | - | 0 | 0 | 0 | 0 | 0 | 0 | 2 | 0 | 0 | 0 | 0 | 10 | 0 | 0 | 0 | 0 | 0.8 | 0.6 | |
| | 400 | - | - | - | 0 | 3 | 0 | 0 | 2 | 0 | 0 | 0 | 0 | 0 | 0 | 15 | 0 | 0 | 0 | 0 | 1.3 | 0.9 | |
| | 600 | - | - | - | 0 | 7 | 0 | 0 | 2 | 0 | 0 | 0 | 0 | 0 | 0 | 22 | 0 | 0 | 0 | 0 | 1.9 | 1.4 | |
| | 800 | - | - | - | 0 | 8 | 0 | 1 | 2 | 0 | 0 | 0 | 0 | 0 | 0 | 24 | 0 | 0 | 0 | 0 | 2.2 | 1.5 | |
| | 1000 | - | - | - | 0 | 11 | 0 | 0 | 0 | 0 | 2 | 0 | 0 | 0 | 0 | 22 | 0 | 0 | 0 | 0 | 2.2 | 1.5 | |
| | 1200 | - | - | - | 0 | 8 | 0 | 0 | 0 | 0 | 3 | 0 | 0 | 0 | 0 | 28 | 0 | 0 | 0 | 0 | 2.4 | 1.8 | |
| | 1400 | - | - | - | 0 | 6 | - | 0 | 0 | 0 | 7 | 0 | 0 | 0 | 0 | 26 | 0 | 0 | 0 | 0 | 2.6 | 1.8 | |
| | 1600 | - | - | - | 0 | - | - | 0 | 0 | 0 | 5 | 0 | - | 0 | 0 | 22 | 0 | 0 | 0 | 0 | 2.1 | 1.7 | |
| | 3200 | - | - | - | - | - | - | - | - | - | - | - | - | - | 0 | 3 | 0 | 0 | 0 | 0 | - | 0.6 | 0.6 |
| | 3600 | - | - | - | - | - | - | - | - | - | - | - | - | - | 0 | 5 | 0 | 0 | 0 | 0 | - | 1.0 | 1.0 |
| | 4000 | - | - | - | - | - | - | - | - | - | - | - | - | - | 0 | 2 | 0 | 0 | 0 | 0 | - | 0.4 | 0.4 |
| | 4400 | - | - | - | - | - | - | - | - | - | - | - | - | - | 0 | 0 | - | 0 | 0 | 0 | - | 0.0 | 0.0 |
| | 4800 | - | - | - | - | - | - | - | - | - | - | - | - | - | 0 | 0 | - | 0 | 0 | 0 | - | 0.0 | 0.0 |
| | 10000 | - | - | - | - | - | - | - | - | - | - | - | - | - | - | - | 0 | 0 | 0 | 0 | - | 0.0 | 0.0 |
| | 10400 | - | - | - | - | - | - | - | - | - | - | - | - | - | - | - | 0 | 0 | 0 | 0 | - | 0.0 | 0.0 |
| | 10800 | - | - | - | - | - | - | - | - | - | - | - | - | - | - | - | 0 | 0 | 0 | 0 | - | 0.0 | 0.0 |
| | 11200 | - | - | - | - | - | - | - | - | - | - | - | - | - | - | - | 0 | 0 | 0 | 0 | - | 0.0 | 0.0 |
| 11600 | - | - | - | - | - | - | - | - | - | - | - | - | - | - | - | 0 | 0 | 0 | 0 | - | 0.0 | 0.0 | |

Table 9. Number of fibres not associated with OECs at increasing distance from the dorsal column lesion in the medial spinal cord of OEC transplanted and conditioning lesioned animals.

Quantification of axon number rostral to the lesion performed with an epifluorescence microscope and 63x lens on parasagittal sections of the lesion block, rostral block and thoracic block. Blank cells are used to indicate that data did not meet the inclusion criteria.

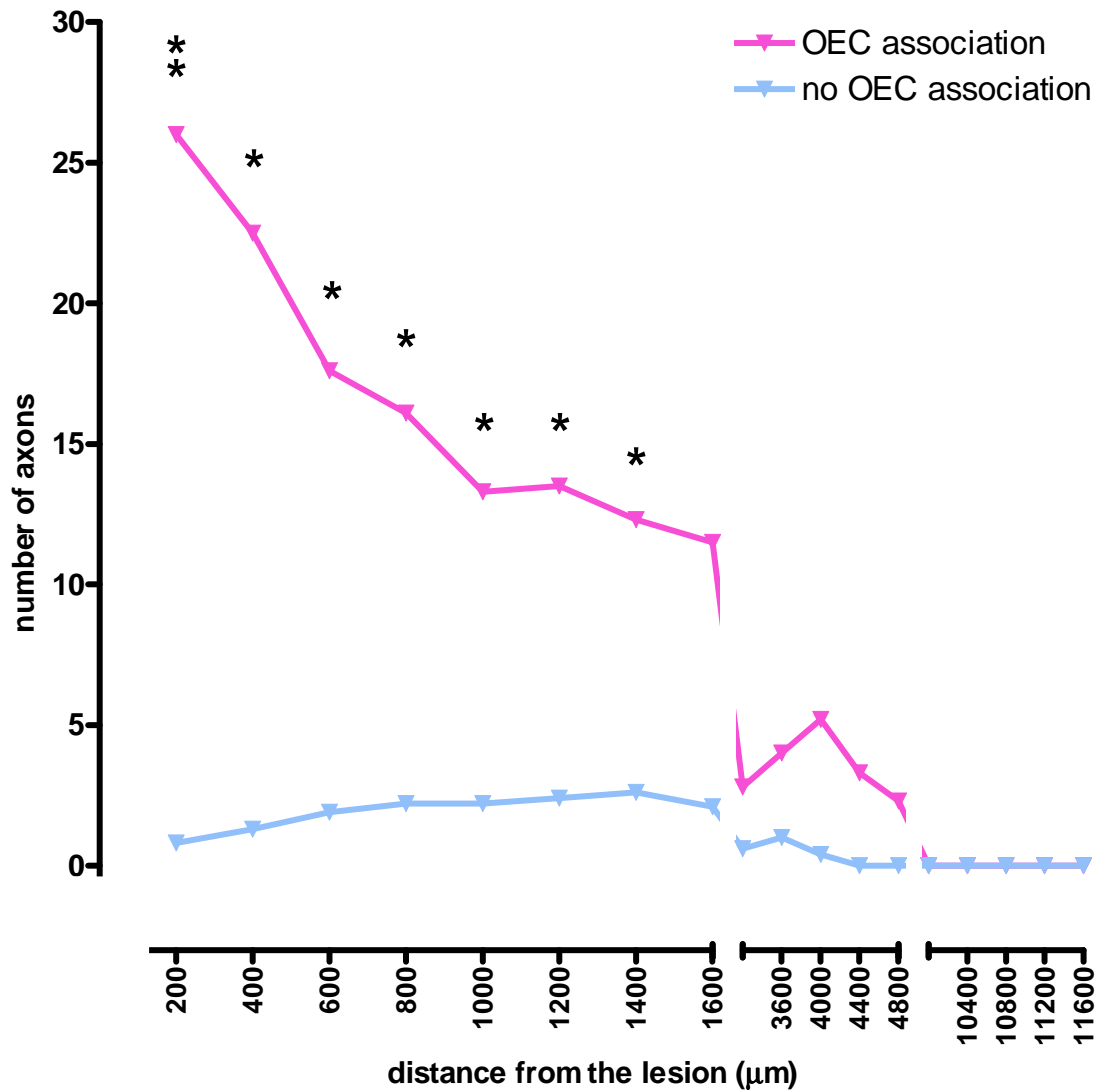


Figure 3-40. Comparison of the average number of BDA labelled fibres associated and not associated with OECs in the medial spinal cord of conditioned animals.

The majority of tract traced axons were located in close vicinity to OECs. The difference was significant between 200 µm and 1400 µm. *: P<0.05; **: P<0.005.

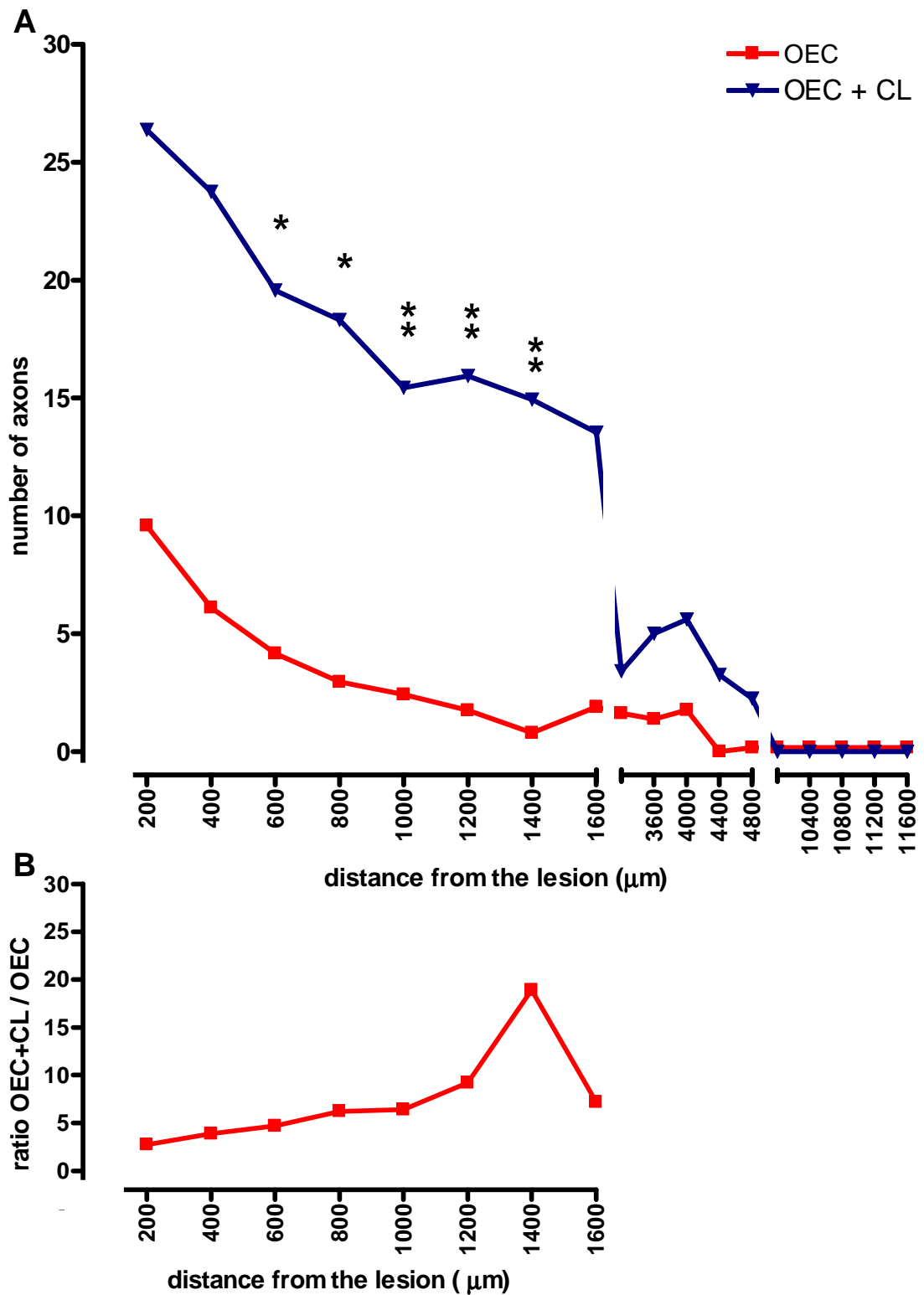


Figure 3-41. Comparison of sprouting/regeneration rostral to the lesion associated with OECs in the medial spinal cord of conditioned and non-conditioned animals. **A)** The average number of BDA labelled fibres in rats that received an OECs transplant and conditioning lesions was significantly greater than that in OEC transplanted animals without conditioning lesions. *: $P < 0.05$; **: $P < 0.005$. Ratio between the two curves in the lesion block only is shown in **B**. **B)** Conditioning lesions coupled with OEC transplantation enhanced growth rostral to the lesion from a minimum of 3 fold at 200 μm up to 19 fold at 1400 μm compared to animals treated only with OEC transplantation; on average the increase was nine fold in the lesion block.

3.2.4.5 Genuine regenerating BDA labelled fibres rostral to the lesion level

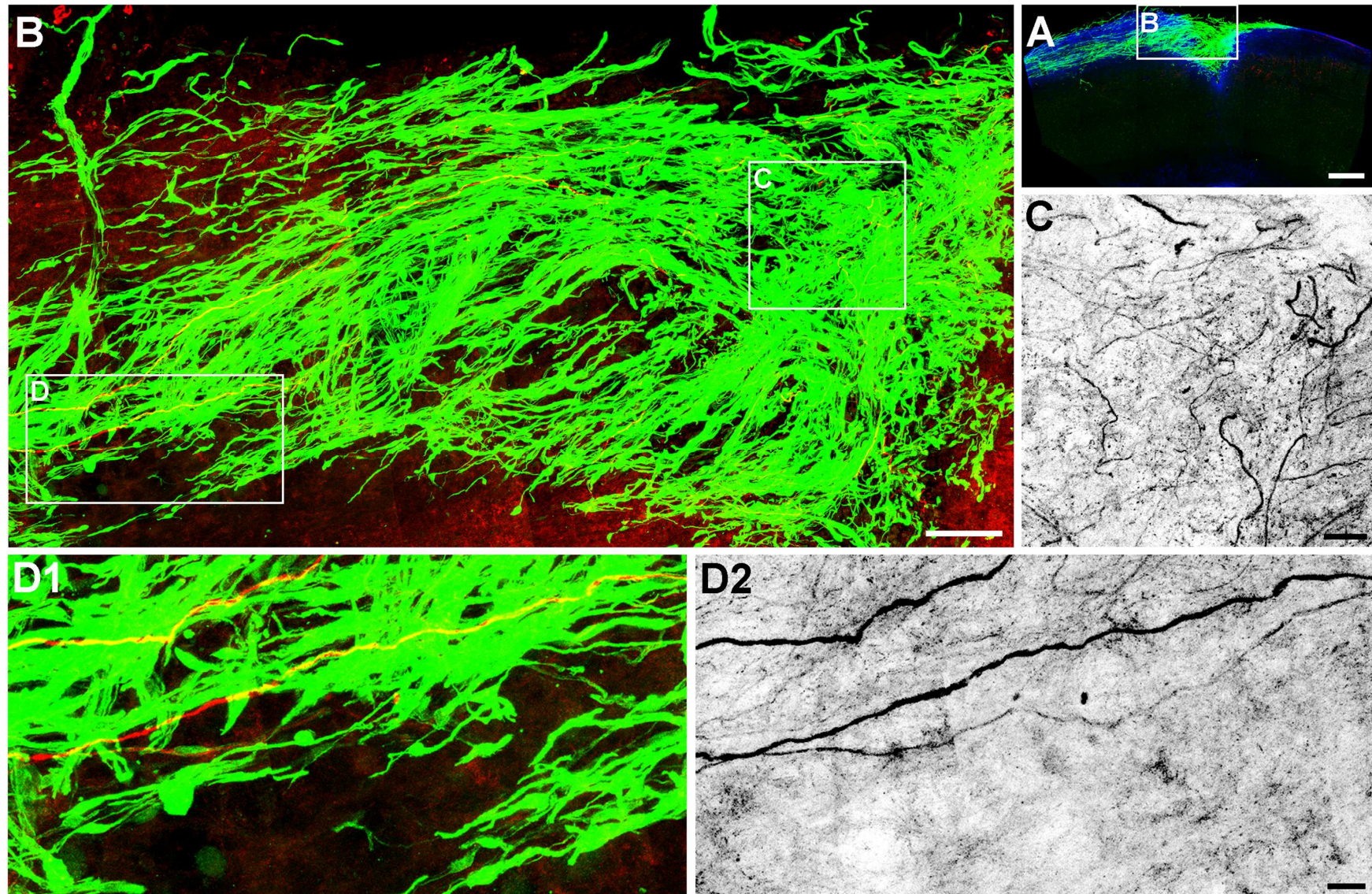
To include in the analysis only convincing regeneration the same stringency criteria applied in section 3.2.3.9 was also performed on the group of animals receiving conditioning lesions.

After this stringency was applied, convincing regeneration was detected only in 5 of the 13 animals where BDA labelling was originally found in the medial spinal cord rostral to the lesion. These axons were mostly localised within tracts of OECs (98% of fibre counts) as it can be seen in the example depicted in Figure 3-42. Quantification of these axons is shown in Table 7. There was a significant increase in the number of regenerating axons in OEC transplanted animals following conditioning lesions compared to OEC transplanted animals in the absence of conditioning lesions as shown in Figure 3-43; the increase was on average 58 fold (Figure 3-43B).

Also as observed also for rats that did not receive a conditioning lesion, not all the animals with continuous tracts of OECs exiting the lesion and distributing rostral to it, possessed regenerating axons within the transplanted cell tracts. In 4 animals out of 9, lack of axonal regeneration was detected. Importantly, no obvious correlation was found between the lesion size and the number of regenerating axons. Importantly, in all of the remaining 5 animals where regeneration was detected in the OEC tracts rostral to the wire knife dorsal column lesion, regeneration proceeded until the very end of the cell tracts (see the example in Figure 3-44). This is a clear difference from what was observed in non conditioning lesioned animals (Figure 3-34). Consistent with this observation the average length of the OEC tracts rostral to the lesion in these animals was 1480 μm as also the average length of the furthest regenerating tract traced axons detected in each animal rostral to the lesion was 1480 μm , including also blocks rostral to the lesion if available. Only in one animal some regenerating axons were not associated with the GFP labelled OEC tract; these axons exited the GFP labelled tract and branched in what appeared to be host tissue devoid of OECs, however it cannot be excluded that OECs which were not expressing GFP were distributed near these axons.

Figure 3-42. Regenerating axons in a tract of OECs rostral to the dorsal column lesion following conditioning lesions.

A) Confocal image taken with a low power objective (10x) of a parasagittal section of the lesion block in a rat transplanted with OECs; boxed area is depicted at higher magnification (40x) in **B**. **B)** Axons bridged the lesion and grew rostral to the lesion within the OEC tract. **C)** Enlarged image of the boxed area shown in **B** that shows axons in greyscale regenerating in the lesion. **D1-D2)** Enlarged images of the boxed area shown in **B** to show regenerating axons in the rostral track of OECs ; **D2)** BDA labelled regenerating axons in greyscale. **A-D)** Composite of confocal projected image stacks. Colour codes: red (axons), green (OECs), blue (astrocytes). Scale bars: 500 μm in **A**; 100 μm in **B**; 25 μm in **C-D**.



| | | Number of axons | | | | | | | | | | | | | | | | | | | | | |
|--|-------|-----------------|-------|-------|-------|-------|-------|-------|--------|--------|--------|--------|--------|--------|--------|--------|--------|--------|--------|--------|---------|-----------|---|
| | | R3304 | R5704 | R5904 | R7205 | R1406 | R2806 | R3906 | R15806 | R15906 | R17906 | R19506 | R19606 | R20506 | R30606 | R30706 | R30806 | R16707 | R16807 | R17607 | Average | St. Error | |
| Distance from the lesion (μm) | 200 | - | - | - | - | - | 0 | - | - | 2 | 98 | 0 | - | 96 | 38 | - | - | 0 | 0 | 27 | 29.0 | 14.0 | |
| | 400 | - | - | - | - | - | 0 | - | - | 2 | 77 | - | - | 87 | 28 | - | - | 0 | - | 24 | 31.1 | 13.9 | |
| | 600 | - | - | - | - | - | 0 | - | - | - | 24 | - | - | 82 | 15 | - | - | - | - | 29 | 30.0 | 13.9 | |
| | 800 | - | - | - | - | - | - | - | - | - | 10 | - | - | 84 | 7 | - | - | - | - | 34 | 33.8 | 17.8 | |
| | 1000 | - | - | - | - | - | - | - | - | - | 9 | - | - | 61 | 6 | - | - | - | - | 23 | 24.8 | 12.6 | |
| | 1200 | - | - | - | - | - | - | - | - | - | - | - | - | 57 | 12 | - | - | - | - | 21 | 30.0 | 13.7 | |
| | 1400 | - | - | - | - | - | - | - | - | - | - | - | - | 46 | 12 | - | - | - | - | 15 | 24.3 | 10.9 | |
| | 1600 | - | - | - | - | - | - | - | - | - | - | - | - | 49 | 9 | - | - | - | - | 13 | 23.7 | 12.7 | |
| | 3200 | - | - | - | - | - | - | - | - | - | - | - | - | - | - | - | - | - | - | - | - | - | - |
| | 3600 | - | - | - | - | - | - | - | - | - | - | - | - | - | - | - | - | - | - | - | - | - | - |
| | 4000 | - | - | - | - | - | - | - | - | - | - | - | - | - | - | - | - | - | - | - | - | - | - |
| | 4400 | - | - | - | - | - | - | - | - | - | - | - | - | - | - | - | - | - | - | - | - | - | - |
| | 4800 | - | - | - | - | - | - | - | - | - | - | - | - | - | - | - | - | - | - | - | - | - | - |
| | 10000 | - | - | - | - | - | - | - | - | - | - | - | - | - | - | - | - | - | - | - | - | - | - |
| | 10400 | - | - | - | - | - | - | - | - | - | - | - | - | - | - | - | - | - | - | - | - | - | - |
| | 10800 | - | - | - | - | - | - | - | - | - | - | - | - | - | - | - | - | - | - | - | - | - | - |
| | 11200 | - | - | - | - | - | - | - | - | - | - | - | - | - | - | - | - | - | - | - | - | - | - |
| 11600 | - | - | - | - | - | - | - | - | - | - | - | - | - | - | - | - | - | - | - | - | - | - | |

Table 10. Number of regenerating fibres at increasing distance from the lesion in the medial spinal cord of OEC transplanted and conditioned animals.

Quantification of axon number rostral to the lesion performed with an epifluorescence microscope and 63x lens on parasagittal sections of the lesion block, rostral block and thoracic block. Blank cells are used to indicate that data did not meet the inclusion criteria or fit the stringency applied.

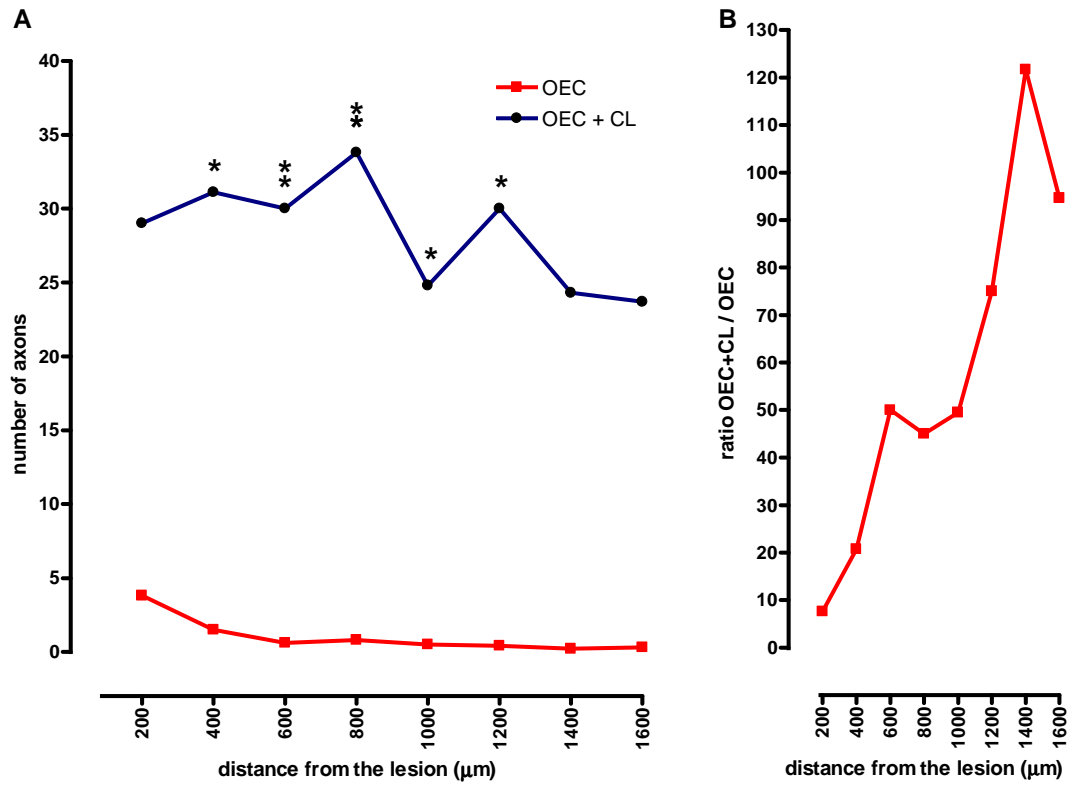
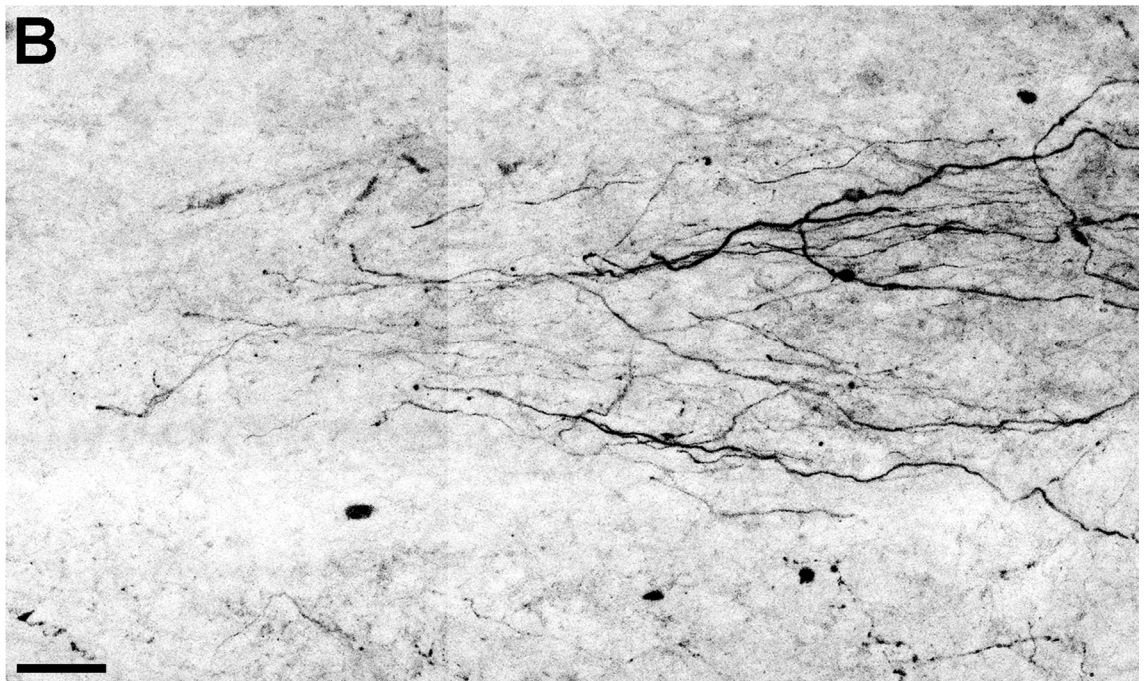
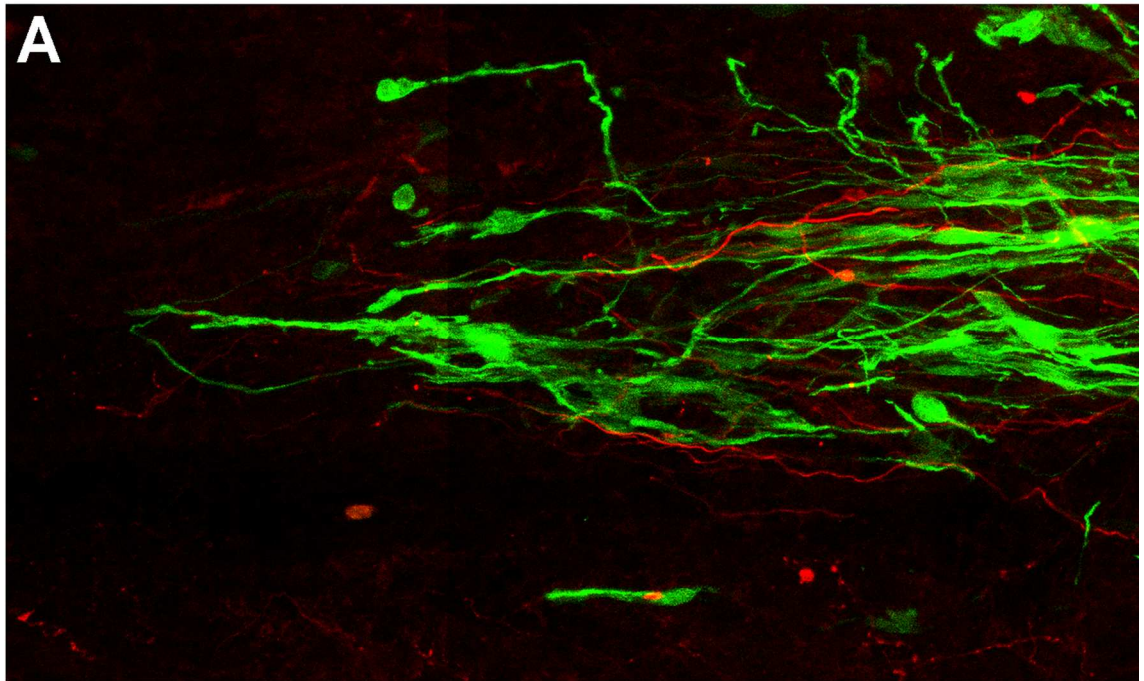


Figure 3-43. Regeneration in OEC transplanted animals with and without conditioning lesion.

A) The average number of regenerating axons in OEC tracts of conditioned animals was significantly greater than that of transplanted only animals. The ratio between the two curves is shown at increasing distances from the lesion in **B**. **B)** Conditioning lesions potentiated regeneration a minimum of 8 times 200 μm rostral to the lesion and a maximum of 122 times at 1400 μm rostral to the lesion; on average the increase was 58 fold. *: $P < 0.05$; **: $P < 0.005$.

Figure 3-44. Following conditioning lesions, axons regenerated the full length of the OEC tract rostral to the dorsal column lesion, with profuse regeneration of sensory afferent axons.

A) Composite of confocal projected image stacks of a parasagittal section of the lesion block that illustrates the profuse regeneration of BDA labelled axons (red) even near the end of a tract of OECs (green) approximately 1 mm rostral to the lesion. **B)** Image in **A** was deprived of the green channel and BDA labelling is here depicted in greyscale; BDA labelled axons regenerating through the tract present end bulbs near the end of the OEC tract. Objective: 40x. Scale bar: 25 μ m.



3.2.5 Conditioning lesions

The experiments described above and carried out on animals transplanted with OECs indicated that the conditioning lesion growth promoting properties in the medial spinal cord were expressed only when these axons were associated with OECs and rarely otherwise. To understand whether conditioning lesions alone were promoting such a degree of regeneration, five rats were treated with conditioning lesions in the absence of cell transplantation. The sciatic nerve containing the peripheral branch of the L4-5 dorsal root ganglia axon was cut before the dorsal column injury in order to increase the growth state of the central branch before this was injured and was cut a second time after the dorsal column injury in order to maintain the growth state at high levels, as seen in the previous sections with the combined treatment paradigm. Four weeks after the spinal cord injury the BDA tracer was injected and finally perfusion fixation took place two more weeks later (Figure 3-45).

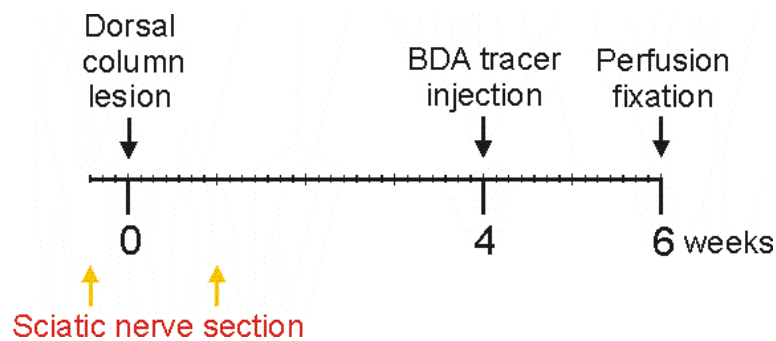


Figure 3-45. Time course of procedures performed on spinal cord injured animals receiving conditioning lesions but not transplantation.

3.2.5.1 Lesion and central canal cavity size

No significant differences were found in the size of the lesion, of the lesion cavity and of the central canal cavity size between this group of animals and non-transplanted and non-conditioned rats. No significant differences were found between OEC transplanted animals and animals receiving both OEC transplantation and conditioning lesions. For this reason data from all non-transplanted animals was pooled together and compared to data from all OEC transplanted animals and is shown in Figure 3-46. This data shows that the lesion

size was significantly reduced by 1.4 times after OEC transplantation ($P=0.0088$). Lesion cavity was partially prevented from developing with OEC transplantation and was significantly reduced by 2.1 times ($P=0.0002$). Enlargement of the central canal was also analysed. It did not occur in the caudal end of the lesion block of most rats analysed while it normally developed rostral to the lesion in the lumbar and thoracic cord. The central canal in the rostral end of the lesion block developed a cavity that was 2.6 times smaller than that detected in non-transplanted rats ($P=0.0012$); the central canal in the rostral block was 1.5 times smaller in OEC transplanted animals ($P=0.25$) and finally the central canal in the thoracic block was 2.9 times smaller ($P=0.019$). Taken together syringomyelia development was significantly reduced in the central canal rostral to the lesion level in the lumbar and thoracic cord. These findings, obtained on a larger sample of animals, strengthen those described in sections 3.2.3.1 and 3.2.3.2.

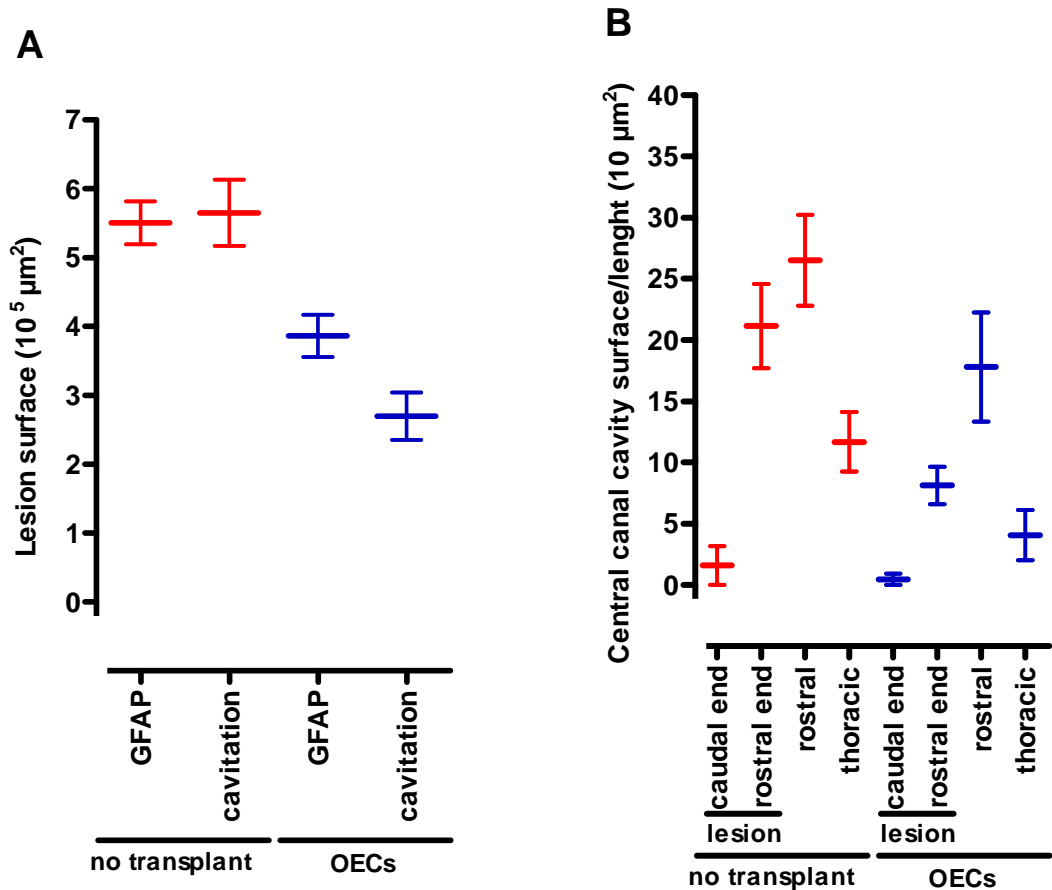


Figure 3-46. Comparison of the lesion size, lesion cavity size and central canal cavity size between all OEC transplanted and all non-transplanted animals (including conditioning lesioned animals).

Average lesion size and cavity size were significantly reduced after OECs transplantation ($P=0.0088$ and $P=0.0002$ respectively). Average central canal size following OEC transplantation was also diminished at the rostral end of the lesion block and in the rostral and thoracic blocks ($P=0.0012$, $P=0.25$ and $P=0.019$ respectively).

3.2.5.2 BDA labelling in the medial cord

It was possible to note through the use of epifluorescence microscopy that the majority of fibres in the medial dorsal columns labelled with BDA ended at the lesion level. Many fibres showed typical signs of damage such as end bulbs and retraction from the lesion.

By analysing the lesion block, the rostral block and the thoracic block, BDA labelling was detected rostral to the wire knife dorsal column lesion in the medial spinal cord in 3 of the 5 rats analysed, however these were extremely few axons (Table 11, Figure 3-47). These axons in the medial spinal cord were all located near the border with the lateral cord, and were presumably in continuity with axons in the lateral cord and did not appear to be regenerating; rather these axons were likely to be spared. Importantly, no axons were found crossing the dorsal cap of spared connective tissue located above the lesion in the middle of the dorsal columns nor any axons were detected passing beneath the dorsal column lesion. Taken together it was shown that conditioning lesions alone could not promote sprouting nor regeneration in the medial spinal cord.

3.2.5.3 BDA labelling in the lateral cord

A large number of BDA labelled axons were detected rostral to the lesion in the lesion block, rostral block and thoracic block: 97% of fibres labelled rostral to the lesion were located in the lateral dorsal columns. The quantification of the number of fibres at increasing distances from the lesion in the lateral spinal cord is shown in Table 12 and is compared to untreated rats and OEC transplanted rats in Figure 3-47. From the graph it is possible to understand that the number of fibres in the group receiving the conditioning lesions or receiving an OEC transplant was higher than that in the untreated group, in particular conditioning lesions were associated with a 22 fold average increase in the number of fibres in the lateral cord compared to untreated animals.

Interestingly, the conditioning lesion was approximately twofold more effective than OEC transplantation at promoting sparing in the lateral cord.

| | | Number of axons | | | | | | Average | St. Error |
|--|-------|-----------------|--------|--------|--------|-------|-------|---------|-----------|
| | | R5804 | R17507 | R18707 | R18807 | R8308 | R8408 | | |
| Distance from the lesion (μm) | 200 | - | 1 | 0 | 1 | 0 | 0 | 0.4 | 0.2 |
| | 400 | - | 1 | 0 | 3 | 0 | 0 | 0.8 | 0.6 |
| | 600 | - | 1 | 0 | 0 | 0 | 0 | 0.2 | 0.2 |
| | 800 | - | 1 | 0 | 1 | 0 | 0 | 0.4 | 0.2 |
| | 1000 | - | 1 | 0 | 1 | 0 | 0 | 0.4 | 0.2 |
| | 1200 | - | 1 | 0 | 1 | 0 | 0 | 0.4 | 0.2 |
| | 1400 | - | 1 | 0 | 1 | 0 | 0 | 0.4 | 0.2 |
| | 1600 | - | - | 0 | 1 | - | 0 | 0.3 | 0.3 |
| | | | | | | | | | |
| | 3200 | - | 8 | 1 | 0 | 0 | 0 | 1.8 | 1.6 |
| | 3600 | - | 5 | 0 | 0 | 0 | 0 | 1.0 | 1.0 |
| | 4000 | - | 4 | 1 | 0 | 0 | 0 | 1.0 | 0.8 |
| | 4400 | - | 3 | 0 | 0 | 0 | 0 | 0.6 | 0.6 |
| | 4800 | - | 0 | 0 | 0 | 0 | - | 0.0 | 0.0 |
| | | | | | | | | | |
| | 10000 | - | 3 | 0 | 0 | 0 | 0 | 0.6 | 0.6 |
| | 10400 | - | 2 | 0 | 0 | 0 | 0 | 0.4 | 0.4 |
| | 10800 | - | 3 | 0 | 0 | 0 | 0 | 0.6 | 0.6 |
| 11200 | - | 2 | 0 | 0 | 0 | 0 | 0.4 | 0.4 | |
| 11600 | - | 2 | 0 | 0 | 0 | 0 | 0.4 | 0.4 | |

Table 11. Number of fibres at increasing distances from the lesion in the medial spinal cord of conditioning lesioned animals that did not receive a transplant. Quantification of axon number rostral to the lesion performed with an epifluorescence microscope and 63x lens on parasagittal sections of the lesion block, rostral block and thoracic block. Blank cells are used to indicate that data did not meet the inclusion criteria.

| | | Number of axons | | | | | | | Average | St. Error |
|--|--------------|-----------------|--------|--------|--------|-------|------------|-------------|-------------|-----------|
| | | R5804 | R17507 | R18707 | R18807 | R8308 | R8408 | | | |
| Distance from the lesion (μm) | 200 | - | 88 | 43 | 38 | 5 | - | 44.0 | 17.0 | |
| | 400 | - | 87 | 38 | 38 | 2 | - | 41.3 | 17.5 | |
| | 600 | - | 95 | 35 | 54 | 2 | - | 46.5 | 19.4 | |
| | 800 | - | 74 | 38 | 46 | 4 | - | 40.5 | 14.4 | |
| | 1000 | - | 73 | 39 | 40 | 4 | - | 39.0 | 14.1 | |
| | 1200 | - | 63 | 34 | 53 | 5 | - | 38.8 | 12.8 | |
| | 1400 | - | 52 | 37 | 38 | 6 | - | 33.3 | 9.7 | |
| | 1600 | - | - | 34 | 30 | - | - | 32.0 | 2 | |
| | | | | | | | | | | |
| | 3200 | - | 63 | 19 | 15 | - | 0 | 24.3 | 13.5 | |
| | 3600 | - | 53 | 15 | 8 | - | 0 | 19.0 | 11.7 | |
| | 4000 | - | 48 | 12 | 5 | - | 0 | 16.3 | 10.9 | |
| | 4400 | - | 40 | 7 | 10 | - | 0 | 14.3 | 8.8 | |
| | 4800 | - | 41 | 4 | 7 | - | - | 17.3 | 11.9 | |
| | | | | | | | | | | |
| | 10000 | - | 14 | 4 | 2 | - | 0 | 5.0 | 3.1 | |
| 10400 | - | 10 | 4 | 1 | - | 0 | 3.8 | 2.3 | | |
| 10800 | - | 5 | 4 | 2 | - | 0 | 2.8 | 1.1 | | |
| 11200 | - | 8 | 2 | 1 | - | 0 | 2.8 | 1.8 | | |
| 11600 | - | 5 | 3 | 1 | - | 0 | 2.3 | 1.1 | | |

Table 12. Number of fibres at increasing distances from the lesion in the lateral spinal cord of conditioning lesioned animals that did not receive a transplant. Quantification performed with an epifluorescence microscope and 63x lens on parasagittal sections of the lesion block, rostral block and thoracic block. Blank cells are used to indicate that data did not meet the inclusion criteria.

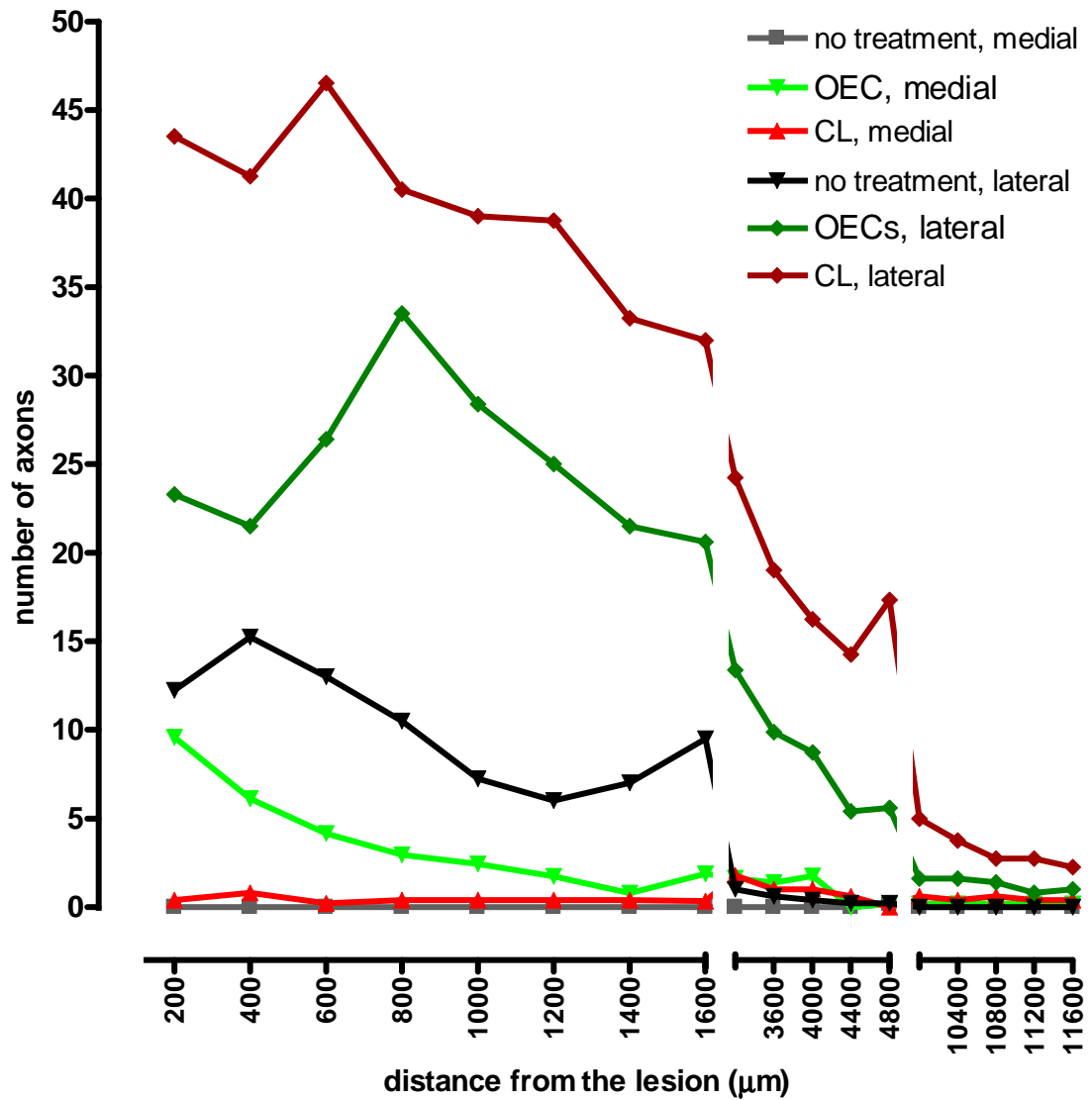


Figure 3-47. The effect of OEC transplantation and conditioning lesions on the number of fibres rostral to the lesion after lesion.

OECs in contrast to conditioning lesions were effective at allowing sprouting/regeneration in the medial spinal cord while conditioning lesions were not. On the other hand sciatic nerve transections were more effective than transplantation of OECs at promoting fibre sparing in the lateral cord.

3.2.6 Combined OEC transplant and sciatic nerve transection in rats receiving an extended wire knife dorsal column lesion.

Regeneration of tract traced ascending sensory axons was described in previous sections of this chapter for OEC transplanted animals and for combined OEC transplanted and conditioning lesioned animals. The aim of the present section is to confirm using a different approach from that used for the stringency criteria described in section 3.2.3.9 to assess that the axons located in the medial spinal cord can appropriately be termed regenerating. For this purpose four rats received an extended lesion of the dorsal columns and a combined treatment of OEC transplant and conditioning lesions. The extended lesion was meant to ablate all primary sensory afferents in the dorsal columns including those axons that were localised to the far left of the dorsal columns. The extended wire knife lesion was carried out by performing the normal dorsal column wire knife lesion and then immediately extending it with a second wire knife lesion that ablated the remaining axons in the lateral dorsal columns. Four weeks later animals were injected with the tract tracer and were perfusion fixed two weeks later.

Importantly, no fibres were found rostral to the lesion in the lateral cord in any of the animals confirming the completeness of the injury to the lateral dorsal columns. Examples from transverse section and parasagittal sections taken from the lesion block, rostral block and thoracic block to show the absence of any detectable BDA labelled axon in the lateral cord are depicted in Figure 3-48 (A-B), Figure 3-49 and Figure 3-50. On the other hand, in the medial portion of the spinal cord fibres labelled with BDA were detected rostral to the injury in all animals in this group. Examples are shown in in Figure 3-48A-C and Figure 3-51. These fibres were mostly associated with OECs (99.5% of axons counted) while only a few axons in one animal were found to exit and re-enter regions in which OECs were distributed. OECs formed continuous tracts that exited the lesion and were distributed rostrally generating the ideal conditions for the axons to grow out of the lesion. Quantification of fibre number in the medial portion of the dorsal columns is shown in Table 13.

Figure 3-48. Absence of sparing in the lateral spinal cord and regeneration after OEC transplantation into an extended dorsal column lesion of conditioning lesioned animals.

A) Composite of confocal images (10x) of a transverse section in the rostral block of an animal transplanted with OECs and treated with conditioning lesions. No fibres were located in the lateral spinal cord as shown in the red boxed area depicted at higher magnification in **B** (40x) indicating that sparing was not occurring after the extended wire knife lesion. Regenerating axons were detected in the medial dorsal columns in association with transplanted OECs as shown in the blue boxed area and at higher magnification (40x) in **C1** and **C2**. **C1)** Tract traced axons (red) were in close vicinity to OECs (green); **C2)** BDA labelled axons shown in greyscale. Scale bars: 200 μm in **A**; 25 μm in **B-D**.

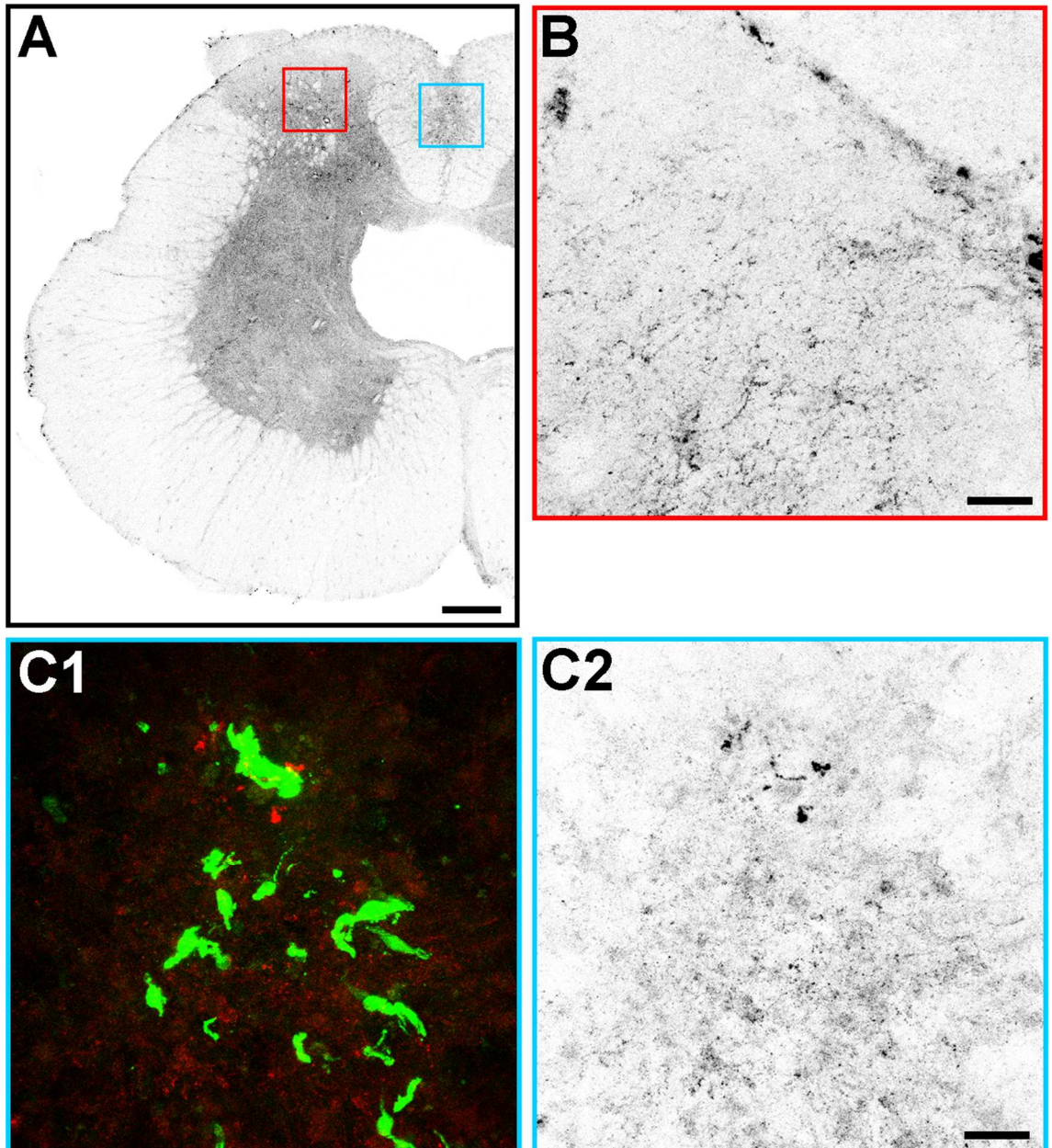


Figure 3-49. No sparing at the thoracic level following OEC transplantation into an extended lesion of the dorsal columns of conditioning lesioned rats.

A) Composite of confocal images (10x) of a transverse section in the thoracic block of the same animal depicted in Figure 3-48. No tract traced fibres were detected in the lateral cord (**B**) or in the medial cord at the thoracic level either. This confirms also that the axons in the medial dorsal columns observed in association with OECs in the rostral block were not spared. Scale bar: 200 μm in **A** and 30 μm in **B**.

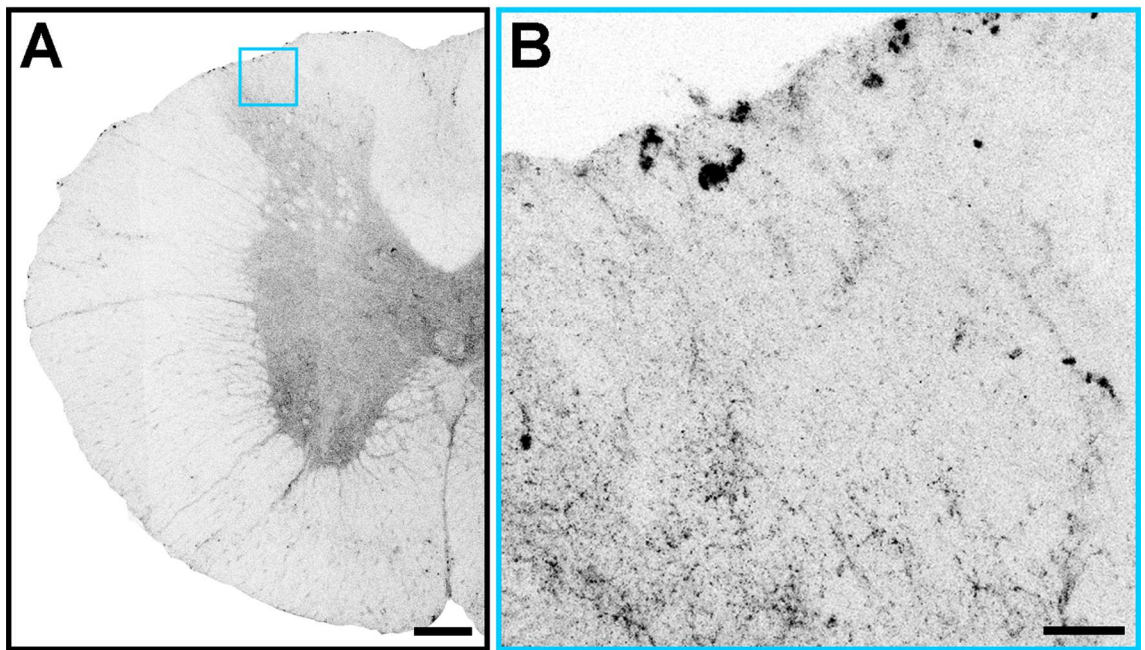


Figure 3-50. Tract traced axons at and rostral to the lesion level in the lateral cord following OEC transplantation into an extended lesion of the dorsal columns of conditioning lesioned animals.

A) Composite confocal images (10x) in a parasagittal section that shows an extended wire knife dorsal column lesion cavity that ablated lateral axons in the lateral dorsal columns. No axons can be seen crossing the lesion level. Furthermore, no axons were found rostral to the lesion in the lesion block (**D**), rostral block (**C**) and thoracic block (**B**). **B-C)** Projections of confocal stacked images taken in the same animal with a 40x objective. Scale bars: 100 μm in **A** and 25 μm in **B-D**.

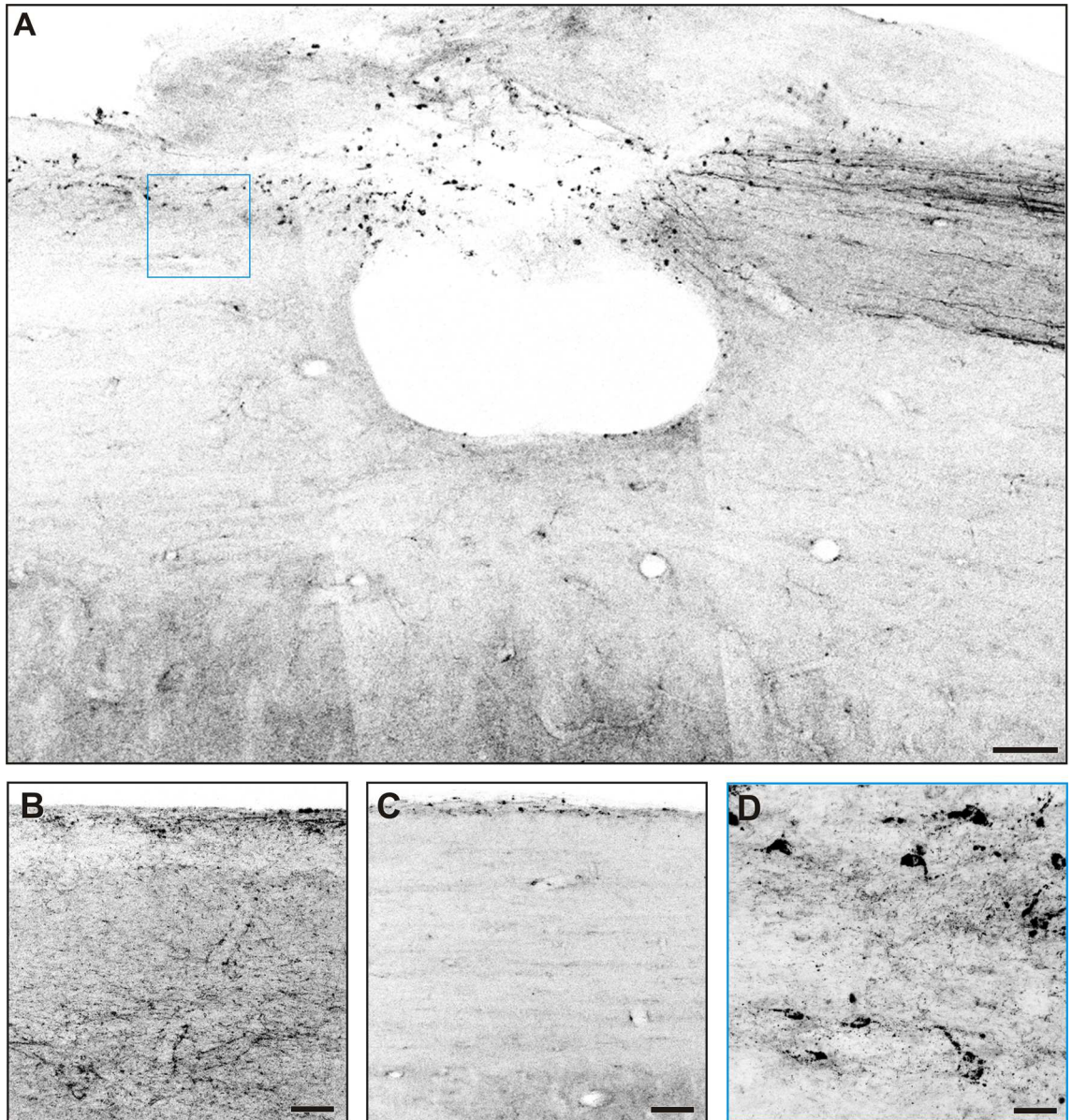
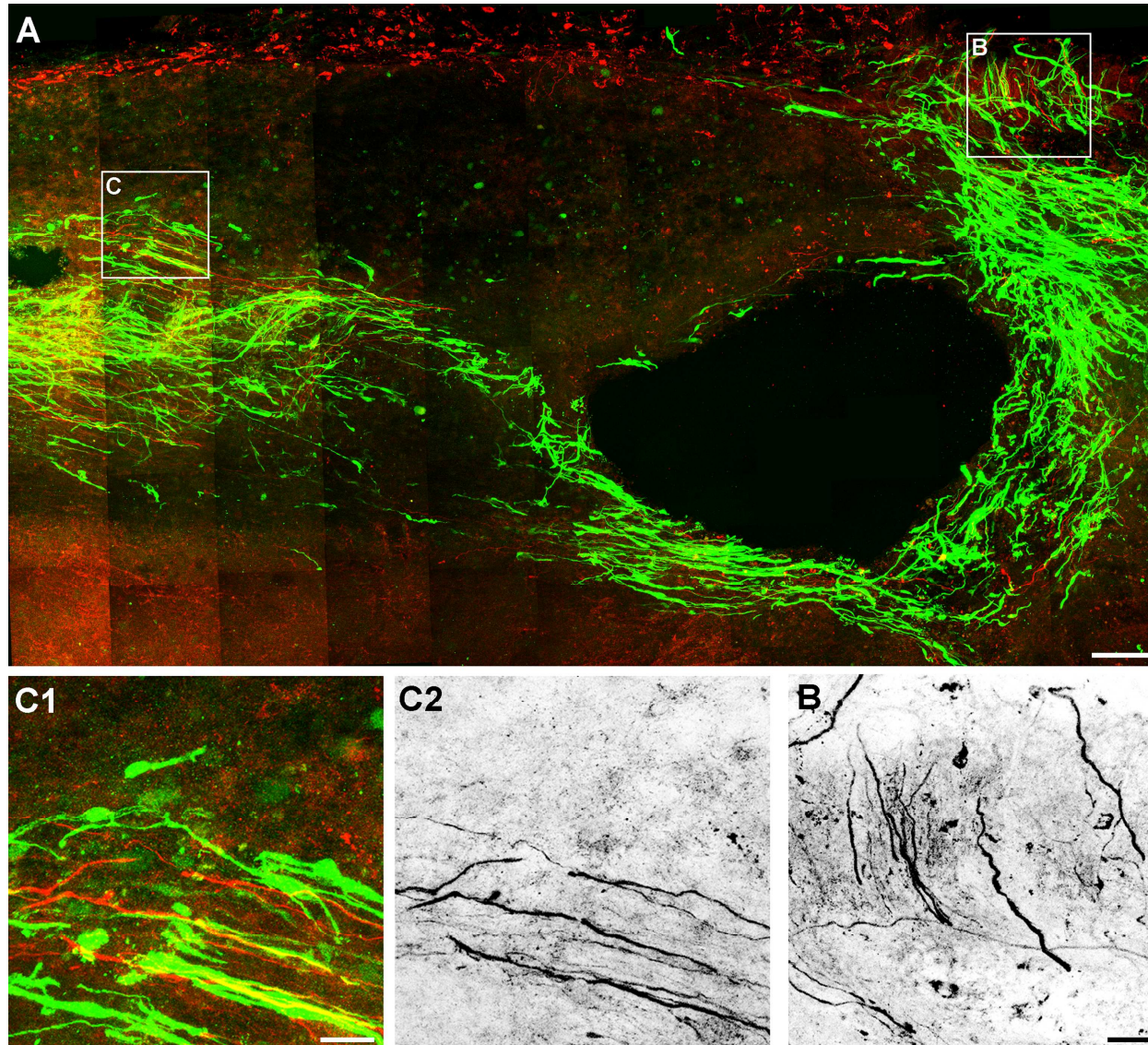


Figure 3-51. Long distance axonal regeneration occurred after an extended dorsal column lesion transplanted with OECs after conditioning lesions.

A) Confocal image taken with a 40x objective of a parasagittal section of the lesion block in a rat transplanted with OECs; axons bridged the lesion to and regenerated within the OEC tract rostral to the lesion. **B)** Enlarged image of the boxed area depicted in **A** that shows axons in greyscale regenerating in the lesion. **C1-C2)** Enlarged images of the boxed area shown in **B** where it is possible to see tract traced axons regenerating through a rostral track of OEC; **C2)** BDA labelled regenerating axons in greyscale. **A-C)** Composite of confocal projected image stacks. Colour codes: red (axons), green (OECs). Scale bars: 100 μm in **A** and 25 μm in **B-C**.



| | | Number of axons | | | | | |
|--|--------------|-----------------|-------|-------|------------|-------------|-------------|
| | | R0509 | R0609 | R0709 | R0809 | Average | St. Error |
| Distance from the lesion (μm) | 200 | 6 | 30 | 1 | 46 | 20.8 | 10.5 |
| | 400 | 2 | 40 | 1 | 27 | 17.5 | 9.6 |
| | 600 | 4 | 42 | 1 | 44 | 22.8 | 11.7 |
| | 800 | 3 | 27 | 2 | 56 | 22.0 | 12.7 |
| | 1000 | 2 | 23 | 3 | 68 | 24.0 | 15.4 |
| | 1200 | 0 | 20 | 3 | 67 | 22.5 | 15.5 |
| | 1400 | 0 | 18 | - | 79 | 32.3 | 23.9 |
| | 1600 | 1 | 11 | - | 40 | 17.3 | 11.7 |
| | | | | | | | |
| | 3200 | 0 | 4 | 5 | - | 3.0 | 1.5 |
| | 3600 | 0 | 8 | 2 | - | 3.3 | 2.4 |
| | 4000 | 0 | 8 | 2 | - | 3.3 | 2.4 |
| | 4400 | 0 | 8 | 2 | - | 3.3 | 2.4 |
| | 4800 | 0 | 3 | - | - | 1.5 | 1.5 |
| | | | | | | | |
| | 10000 | 0 | - | - | 21 | 10.5 | 10.5 |
| | 10400 | 0 | - | - | 18 | 9.0 | 9.0 |
| 10800 | 0 | - | - | 17 | 8.5 | 8.5 | |
| 11200 | 0 | - | - | 14 | 7.0 | 7.0 | |
| 11600 | 0 | - | - | 7 | 3.5 | 3.5 | |

Table 13. Number of fibres at increasing distances from the lesion in the medial dorsal columns after OEC transplantation into an extended lesion of the dorsal columns of conditioning lesioned animals.

Quantification performed with an epifluorescence microscope and 63x lens on parasagittal sections of the lesion block, rostral block and thoracic block. Blank cells are used to indicate that data did not meet the inclusion criteria.

3.2.7 Transplantation of OECs into a dorsal column lesion combined with sciatic nerve transection with a 2 week survival

The main aim of this section was to determine whether axonal regeneration occurred sooner than the 6 week survival time point used in the experiments carried out in the previous sections of this chapter. To assess this, four rats were transplanted with OECs into the dorsal column lesion and sacrificed 2 weeks later. To trace the axons BDA was injected into the spinal nerves 2 days after the dorsal column lesion and 12 days later animals were perfusion fixed (Figure 3-52). Two week survival was the shortest time point that could be considered for analysis as it was necessary to allow enough time for the BDA tract tracer to travel sufficiently in the axons. A conditioning lesion was performed two weeks before the spinal cord lesion and a second one concurrently with the spinal cord lesion.

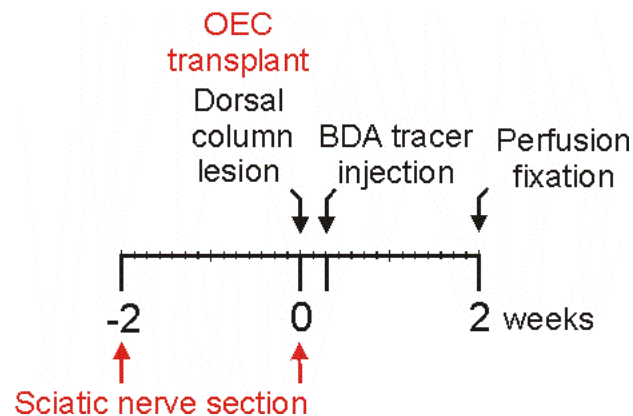


Figure 3-52. Time course of procedures performed on short survival animals transplanted with OEC and subjected to conditioning lesions.

3.2.7.1 OEC distribution

OECs distributed rostral to and caudal to the injection site. The density of the transplanted cells was far greater than that observed at a 6 week survival time

point. For example the confocal settings to capture images of GFP labelling had to be completely changed not to have signal saturation. Even the distribution of OECs was different and GFP labelled cells were detected on a clearly larger number of sections per animal compared to OEC transplanted 6 week survival animals. The distribution of OECs was quantified by counting the number of sections in each animal where OECs had distributed rostral to the lesion. The average number of sections per animal containing OECs distributed rostral to the lesion pooling together all 6 week survival OEC transplanted rats was 3 sections per rat, while in the two week survival animals it was 10 sections per animal. This is an indication that most of the OECs transplanted were lost by the 6th week after transplantation.

3.2.7.2 Axonal labelling rostral to the lesion

BDA labelling was detected rostral to the lesion in the lateral and medial spinal cord of all four animals. The axons detected in the medial cord were quantified on parasagittal sections and an extraordinary high number of fibres were counted in all of the four animals (Table 14). These were significantly more than those present in OEC transplanted rats 6 weeks post lesion as shown in the graph in Figure 3-53. All fibres were associated with OECs.

Analysis of regeneration was then carried out on these animals following the same stringency used in section 3.2.3.9 and was detected in 2 of the 4 animals of this group. An example of long distance axonal regeneration 2 weeks after transplantation is shown in Figure 3-54. The quantification of regeneration rostral to the lesion is shown in Table 15, while comparison with the regeneration occurring in OEC transplanted animals with the same lesion paradigm but with a 6 week survival is shown in Figure 3-55. The number of regenerating axons was greater at the 2 week survival point; however the difference with the 6 week survival OEC transplanted and conditioning lesioned animals was not significant.

| | | Number of axons | | | | | |
|--|--------------|-----------------|-------|-------|------------|--------------|-------------|
| | | R2209 | R2309 | R2409 | R2609 | Average | St. Error |
| Distance from the lesion (μm) | 200 | 87 | 199 | 45 | 235 | 141.5 | 45.0 |
| | 400 | 96 | 140 | 47 | 203 | 121.5 | 33.1 |
| | 600 | 62 | 88 | 68 | 181 | 99.8 | 27.6 |
| | 800 | 12 | 48 | 67 | 192 | 79.8 | 39.1 |
| | 1000 | 4 | 15 | 82 | 169 | 67.5 | 38.0 |
| | 1200 | 1 | 44 | 85 | 158 | 71.8 | 33.6 |
| | 1400 | 0 | 60 | 60 | 142 | 65.5 | 29.2 |
| | 1600 | 0 | 21 | 66 | 108 | 48.8 | 24.1 |
| | | | | | | | |
| | 3200 | 0 | 0 | 24 | 49 | 18.3 | 11.7 |
| | 3600 | 0 | 0 | 17 | 56 | 18.3 | 13.2 |
| | 4000 | 0 | 0 | 6 | 48 | 13.5 | 11.6 |
| | 4400 | 0 | 0 | 5 | 34 | 9.8 | 8.2 |
| | 4800 | 0 | 0 | 0 | 21 | 5.3 | 5 |
| | | | | | | | |
| | 10000 | 0 | 0 | 0 | 12 | 3.0 | 3.0 |
| | 10400 | 0 | 0 | 0 | 8 | 2.0 | 2.0 |
| 10800 | 0 | 0 | 0 | 8 | 2.0 | 2.0 | |
| 11200 | 0 | 0 | 0 | 11 | 2.8 | 2.8 | |
| 11600 | 0 | 0 | 0 | 3 | 0.8 | 0.8 | |

Table 14. Number of regenerating/sprouting fibres at increasing distances from the lesion following OEC transplantation and conditioning lesions in the 2 week survival animals.

Quantification performed with an epifluorescence microscope and 63x lens on parasagittal sections of the lesion block, rostral block and thoracic block. Blank cells are used to indicate that data did not meet the inclusion criteria.

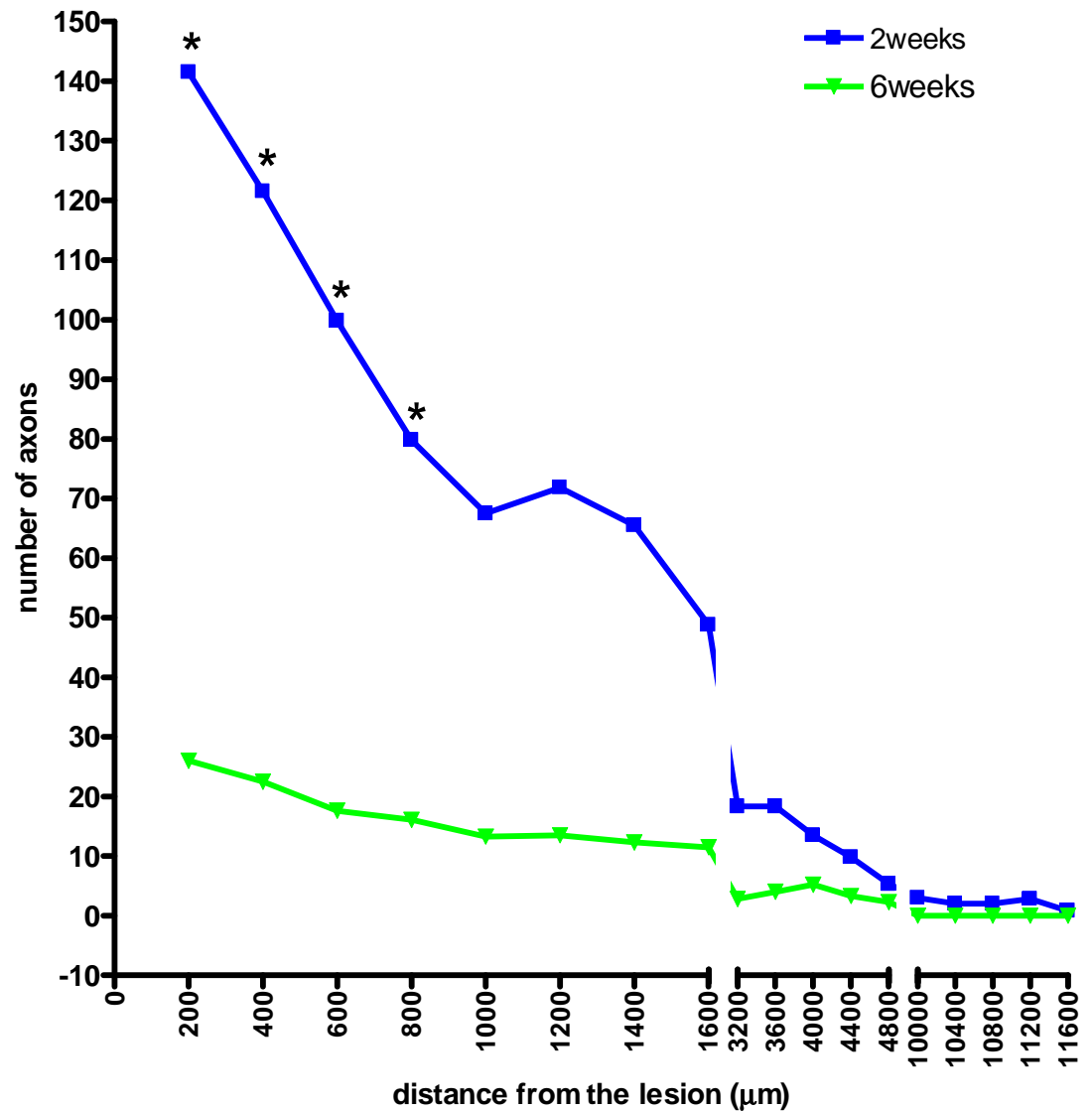
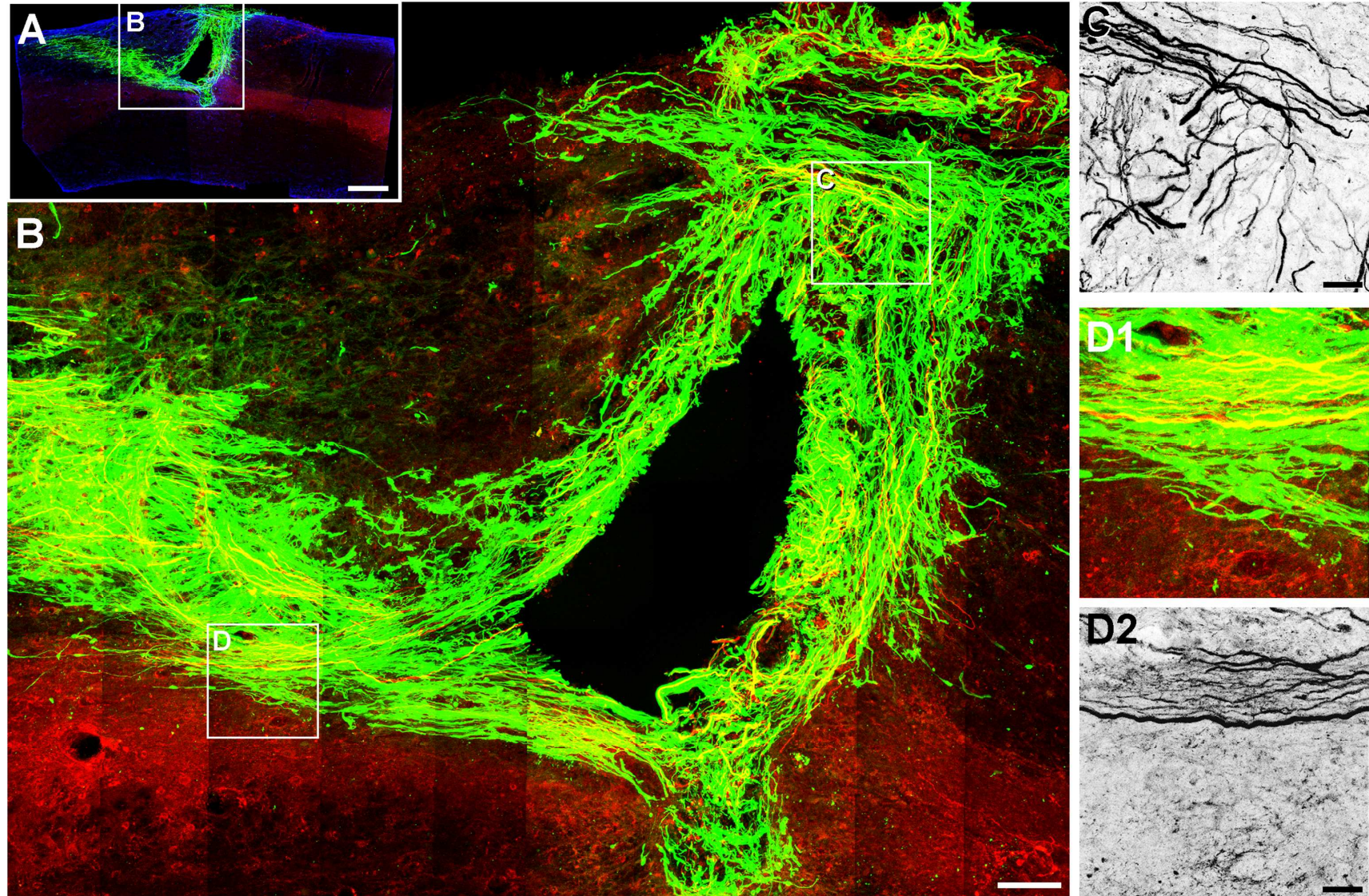


Figure 3-53. Comparison of sprouting/regeneration rostral to the lesion associated with OECs in the medial spinal cord in the 2 weeks and the 6 week survival animals after OEC transplantation and conditioning lesions.

The average number of BDA labelled fibres in rats that received an OECs transplant and conditioning lesions and sacrificed 2 weeks later was significantly greater than that in animals with the same treatment paradigm but with a 6 week survival. *: P<0.05.

Figure 3-54. Regeneration occurred as early as 2 weeks after a dorsal column lesion.

A) Confocal image taken with a low power objective (10x) of a parasagittal section of the lesion block in a rat transplanted with OECs; boxed area is depicted at higher magnification (40x) in **B**. **B)** Axons bridged the lesion and regenerated through the OEC tract. **C:** enlarged image of the boxed area depicted in **B** that shows axons in greyscale regenerating in the lesion. **D1-D2)** Enlarged images of the boxed area in **B** showing regenerating axons associated with a rostral tract of OECs. **D2)** BDA labelled regenerating axons in greyscale. **A-D)** Composite of confocal projected image stacks. Colour codes: red (axons), green (OECs), blue (astrocytes). Scale bars: 500 μm in **A**, 100 μm in **B** and 25 μm in **C-D**.



| | | Number of axons | | | | | |
|--|--------------|-----------------|-------|-------|------------|--------------|-------------|
| | | R2209 | R2309 | R2409 | R2609 | Average | St. Error |
| Distance from the lesion (μm) | 200 | - | 199 | 45 | - | 122.0 | 77.0 |
| | 400 | - | 140 | 47 | - | 93.5 | 46.5 |
| | 600 | - | 88 | 68 | - | 78.0 | 10.0 |
| | 800 | - | 48 | 67 | - | 57.5 | 9.5 |
| | 1000 | - | 15 | 82 | - | 48.5 | 33.5 |
| | 1200 | - | 44 | 85 | - | 64.5 | 20.5 |
| | 1400 | - | 60 | 60 | - | 60.0 | 0.0 |
| | 1600 | - | 21 | 66 | - | 43.5 | 22.5 |
| | | | | | | | |
| | 3200 | - | 0 | 24 | - | 12.0 | 12.0 |
| | 3600 | - | 0 | 17 | - | 8.5 | 8.5 |
| | 4000 | - | 0 | 6 | - | 3.0 | 3.0 |
| | 4400 | - | 0 | 5 | - | 2.5 | 2.5 |
| | 4800 | - | - | - | - | - | - |
| | | | | | | | |
| | 10000 | - | 0 | - | - | 0.0 | - |
| 10400 | - | 0 | - | - | 0.0 | - | |
| 10800 | - | 0 | - | - | 0.0 | - | |
| 11200 | - | 0 | - | - | 0.0 | - | |
| 11600 | - | 0 | - | - | 0.0 | - | |

Table 15. Number of convincing regenerating fibres at increasing distances from the lesion following OEC transplantation and conditioning lesions in the 2 week survival animals.

Quantification performed with an epifluorescence microscope and 63x lens on parasagittal sections of the lesion block, rostral block and thoracic block. Blank cells are used to indicate that data did not meet the inclusion criteria.

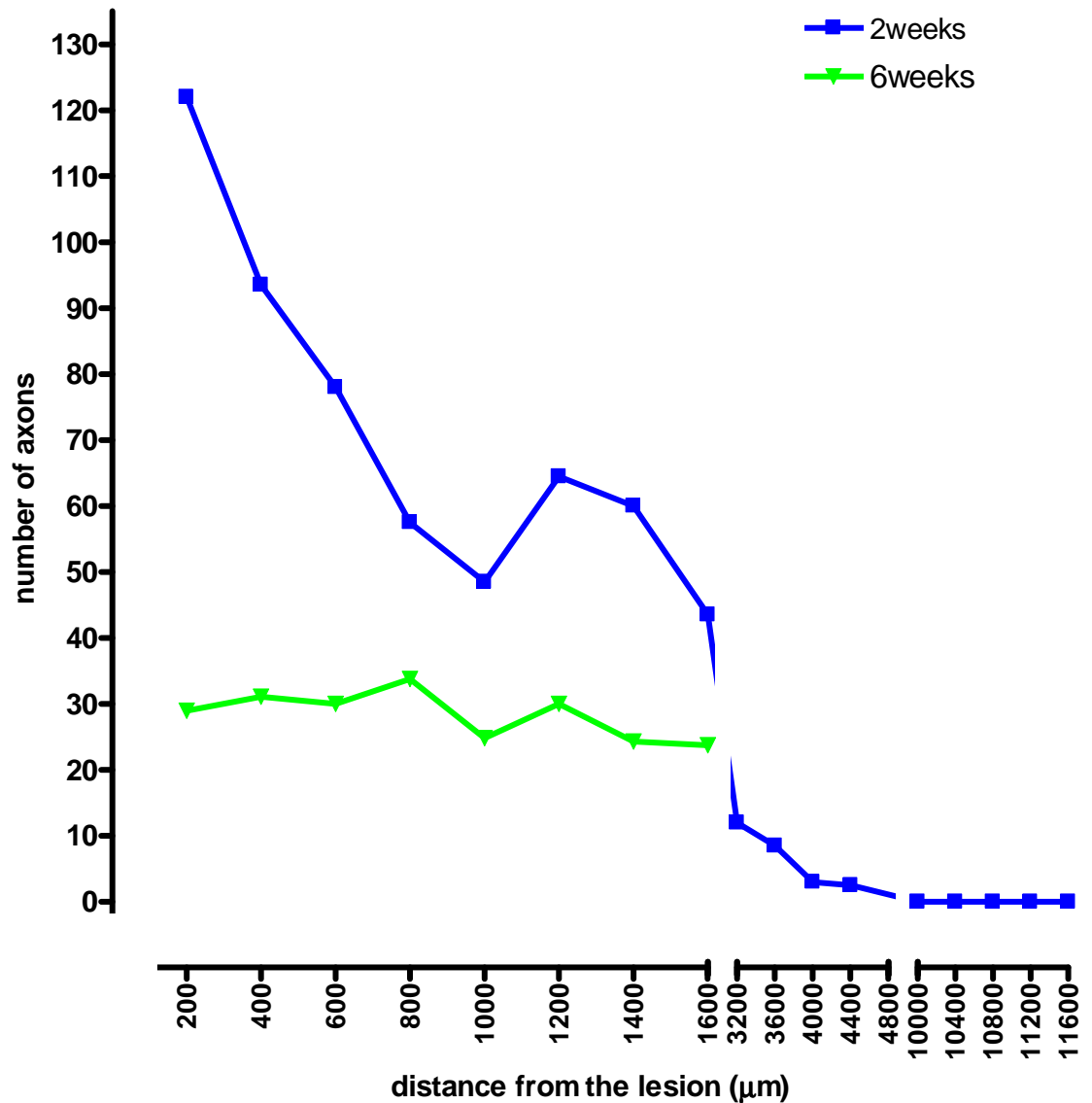


Figure 3-55. Comparison of axonal regeneration rostral to the lesion in the medial spinal cord in the 2 weeks and 6 week survival animals after OEC transplantation and conditioning lesions.

The average number of BDA labelled fibres in rats that received an OECs transplant and conditioning lesions and sacrificed 2 weeks later was greater than that in animals with the same treatment paradigm but 6 week survival, however the difference was not significant.

3.2.8 OECs transplant and conditioning lesion with 17 week survival

Having determined in the previous sections that the amount of OECs rostral to the lesion greatly decreased in the first 6 weeks after transplantation and that there was a concurrent decrease in long distance axonal regeneration, we questioned whether at a longer survival time the number of transplanted cells decreased and whether this decrease was associated with a decrease of axon regeneration. Three rats were transplanted with OECs into the lesion site and sacrificed 17 weeks later. To trace the axons the BDA tract tracer was injected into the spinal nerves and perfusion fixation was performed 2 weeks later. A conditioning lesion was performed two weeks before the spinal cord lesion and a second one concurrently with the spinal cord lesion (Figure 3-56).

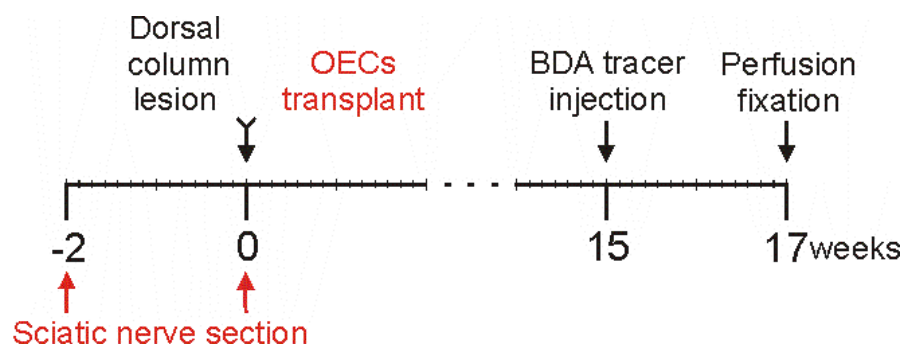


Figure 3-56. Time course of procedures performed on animals with 17 week survival subjected to OEC transplantation and conditioning lesions.

3.2.8.1 OEC distribution

OECs were distributed rostral to and caudal to the injection site. Under epifluorescence microscopy examination similar levels of GFP labelling were visible compared to the 6 week survival time point and OECs were distributed in approximately 6 sections per animal.

3.2.8.2 Axonal labelling rostral to the lesion

BDA labelling was detected rostral to the lesion in all three animals. The axons detected in the medial cord were quantified on parasagittal sections and a similar number of axons were present compared to the 6 week survival animals (Figure 3-57). The difference between the 17 weeks time point and the 6 week survival were not significant at any distance considered. Most of the axons, 91%, were localised in the vicinity of GFP labelled cells while the remaining axons were located in areas devoid of OECs. Axons could be detected in all three animals: in two animals they were located near the border with the lateral dorsal columns; however, in one animal they were located in the centre of the medial dorsal columns and all evidence suggested they were regenerating. Quantification of axonal number is shown in Table 16 and comparison with axonal number of 6 weeks survival animals is shown in Figure 3-57.

Analysis of axonal regeneration was then carried out and the axons that appeared potentially spared or sprouting were excluded from the quantification. The results are shown in Table 17 and Figure 3-59. Importantly, these results indicate that regeneration was lower after longer survival time points but was still detectable 17 weeks after the lesion (an example is shown in Figure 3-58). More experiments will be needed however to study the significance of the difference observed here.

| | | Number of axons | | | | |
|--|--------------|-----------------|--------|----------|-------------|-------------|
| | | R21608 | R21708 | R21808 | Average | St. Error |
| Distance from the lesion (μm) | 200 | 15 | 1 | - | 8.0 | 7.0 |
| | 400 | 23 | 1 | - | 12.0 | 11.0 |
| | 600 | 28 | 1 | - | 14.5 | 13.5 |
| | 800 | 37 | 2 | - | 19.5 | 17.5 |
| | 1000 | 27 | 1 | - | 14.0 | 13.0 |
| | 1200 | 30 | 1 | - | 15.5 | 14.5 |
| | 1400 | 33 | 0 | - | 16.5 | 16.5 |
| | 1600 | 34 | 0 | - | 17.0 | 17.0 |
| | | | | | | |
| | 3200 | 15 | 0 | 22 | 11.3 | 6.4 |
| | 3600 | 9 | 0 | 10 | 6.0 | 3.1 |
| | 4000 | 9 | 0 | 18 | 7.7 | 4.3 |
| | 4400 | 1 | 0 | 8 | 2.0 | 2.0 |
| | 4800 | 1 | 0 | 1 | 0.0 | 0.0 |
| | | | | | | |
| | 10000 | - | 0 | 0 | 0 | 0 |
| | 10400 | - | 0 | 0 | 0 | 0 |
| 10800 | - | 0 | 0 | 0 | 0 | |
| 11200 | - | 0 | 0 | 0 | 0 | |
| 11600 | - | 0 | 0 | 0 | 0 | |

Table 16. Number of regenerating/sprouting fibres at increasing distances from the lesion 17 week survival after OEC transplantation.

Quantification performed with an epifluorescence microscope and 63x lens on parasagittal sections of the lesion block, rostral block and thoracic block. Blank cells are used to indicate that data did not meet the inclusion criteria.

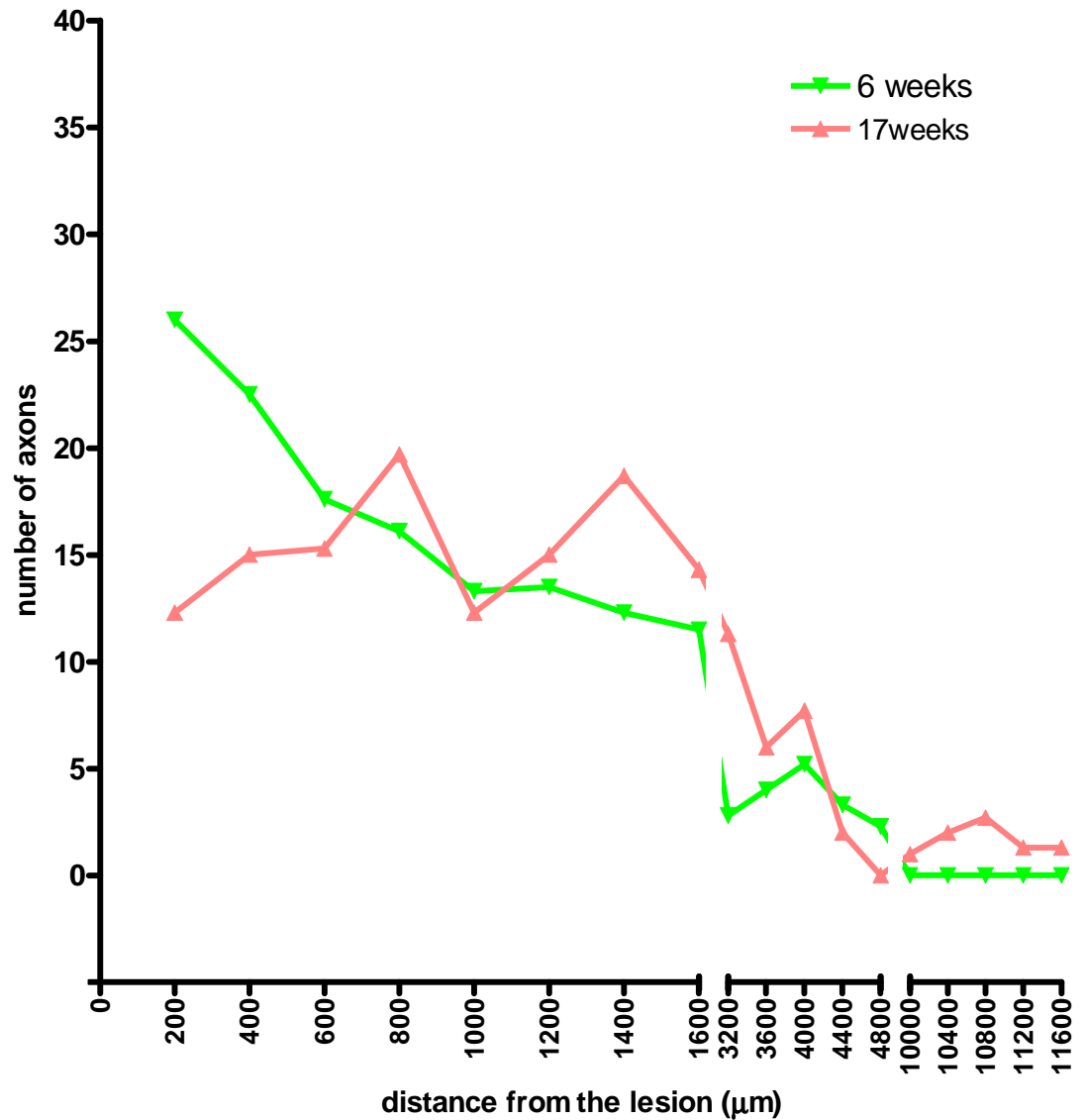
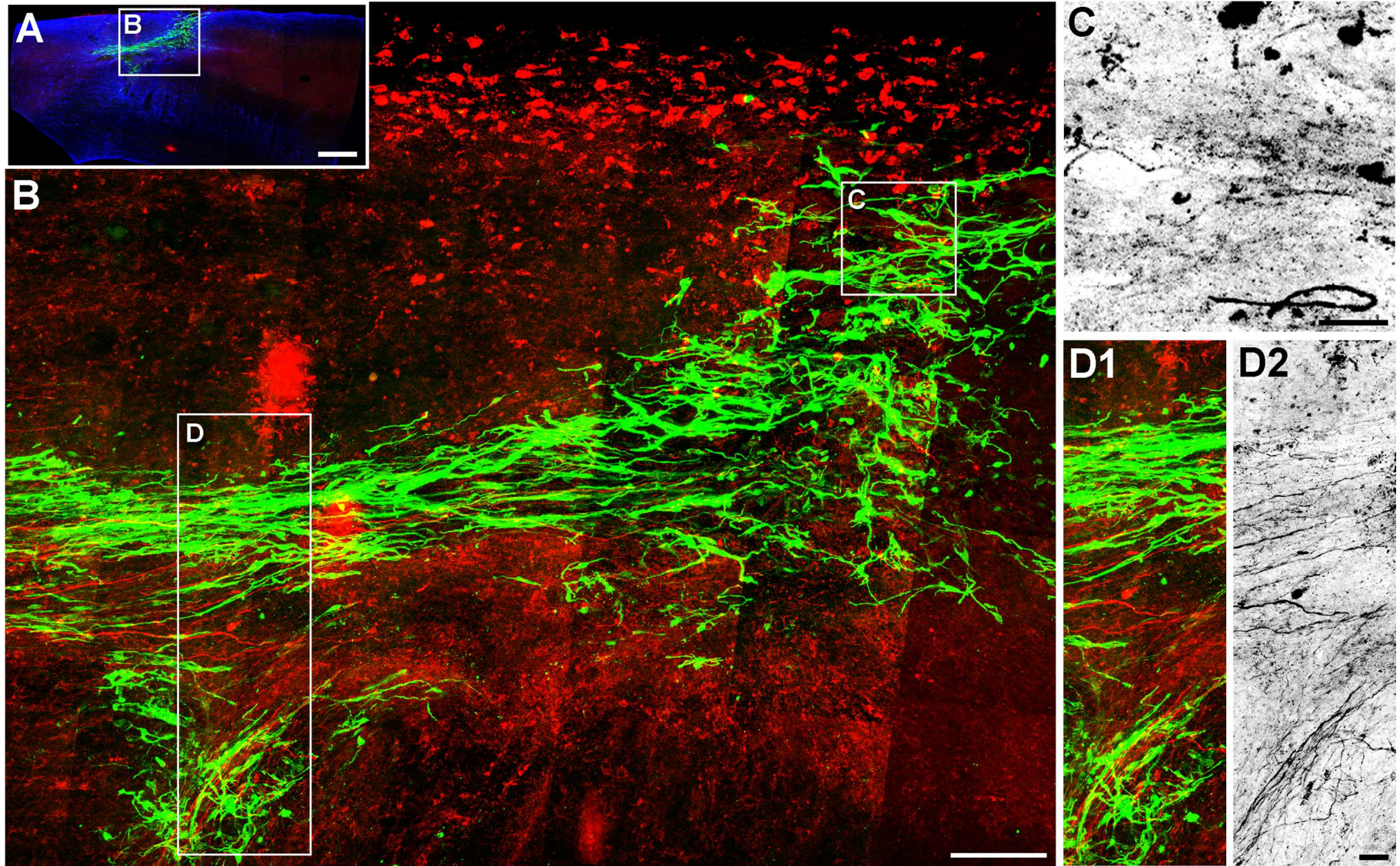


Figure 3-57. Comparison of sprouting/regeneration rostral to the lesion associated with OECs in the medial spinal cord 6 and 17 weeks after OEC transplantation. The average number of BDA labelled fibres in rats that received an OECs transplant and conditioning lesions and sacrificed 17 weeks later overlapped that of animals with the same treatment paradigm but 6 week survival. No significant difference between the two groups was found.

Figure 3-58. Long distance regeneration was detected 17 weeks after a dorsal column wire knife lesion.

A) Confocal image taken with a low power objective (10x) of a parasagittal section of the lesion block in a rat transplanted with OECs; boxed area is depicted at higher magnification (40x) in **B**. **B)** Regenerating axons were detected in association with the continuous tract of OECs rostral to the lesion. **C)** Enlarged image of the boxed area depicted in **B** that shows axons regenerating in the lesion in greyscale. **D1-D2)** Enlarged images of the boxed area in **B** showing long distance axonal regeneration occurring mainly in association with OECs; **D2)** BDA labelled regenerating axons in greyscale. **A-D)** Composites of confocal projected image stacks. Colour codes: red (axons), green (OECs), blue (astrocytes). Scale bar: 500 μm in **A**, 100 μm in **B** and 25 μm in **C-D**.



| | | Number of axons | | | | |
|--|-------|-----------------|--------|--------|---------|-----------|
| | | R21608 | R21708 | R21808 | Average | St. Error |
| Distance from the lesion (μm) | 200 | - | 1 | 21 | 11.0 | 10.0 |
| | 400 | - | 1 | 21 | 11.0 | 10.0 |
| | 600 | - | 1 | 17 | 9.0 | 8.0 |
| | 800 | - | 2 | 20 | 11.0 | 9.0 |
| | 1000 | - | 1 | 9 | 5.0 | 4.0 |
| | 1200 | - | 1 | 14 | 7.5 | 6.5 |
| | 1400 | - | - | 24 | 24.0 | - |
| | 1600 | - | - | 10 | 10.0 | - |
| | | | | | | |
| | 3200 | - | - | 22 | 22.0 | - |
| | 3600 | - | - | 10 | 10.0 | - |
| | 4000 | - | - | 15 | 15.0 | - |
| | 4400 | - | - | 6 | 6.0 | - |
| | 4800 | - | - | - | - | - |
| | | | | | | |
| | 10000 | - | - | - | - | - |
| | 10400 | - | - | - | - | - |
| 10800 | - | - | - | - | - | |
| 11200 | - | - | - | - | - | |
| 11600 | - | - | - | - | - | |

Table 17. Number of regenerating fibres at increasing distances from the lesion 17 weeks after OEC transplantation.

Quantification performed with an epifluorescence microscope and 63x lens on parasagittal sections of the lesion block, rostral block and thoracic block. Blank cells are used to indicate that data did not meet the inclusion criteria or fit the stringency applied..

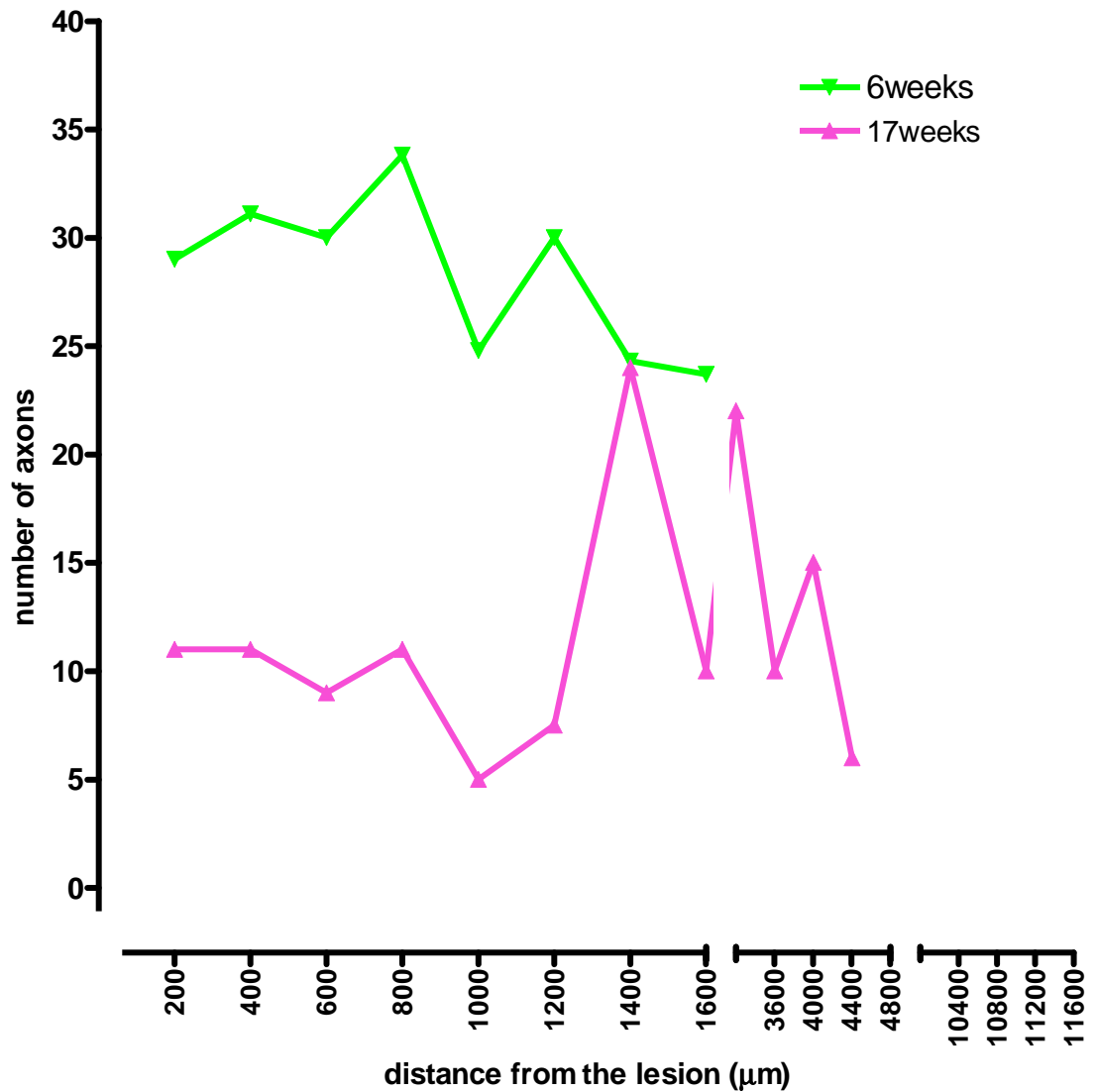


Figure 3-59. Comparison of regeneration 6 and 17 weeks after the dorsal column lesion.

Regeneration was detected 17 weeks after the dorsal column lesion and OEC transplantation in animals receiving conditioning lesions. The average number of axons was lower than those measured in conditioned and OEC transplanted animals with a 6 week survival, however differences were not significant.

3.2.9 OECs transplant with 2 days survival

OEC distribution was characterised in two animals with a short two day survival time point. The rats were sacrificed only two days after cell transplantation and spinal cord lesion (Figure 3-60). No BDA tract tracing could be performed, as we found that approximately two weeks are necessary for the tracer to travel through the sensory afferents and well into the spinal cord.

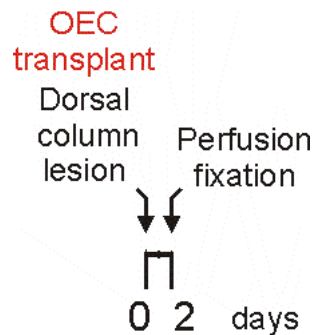
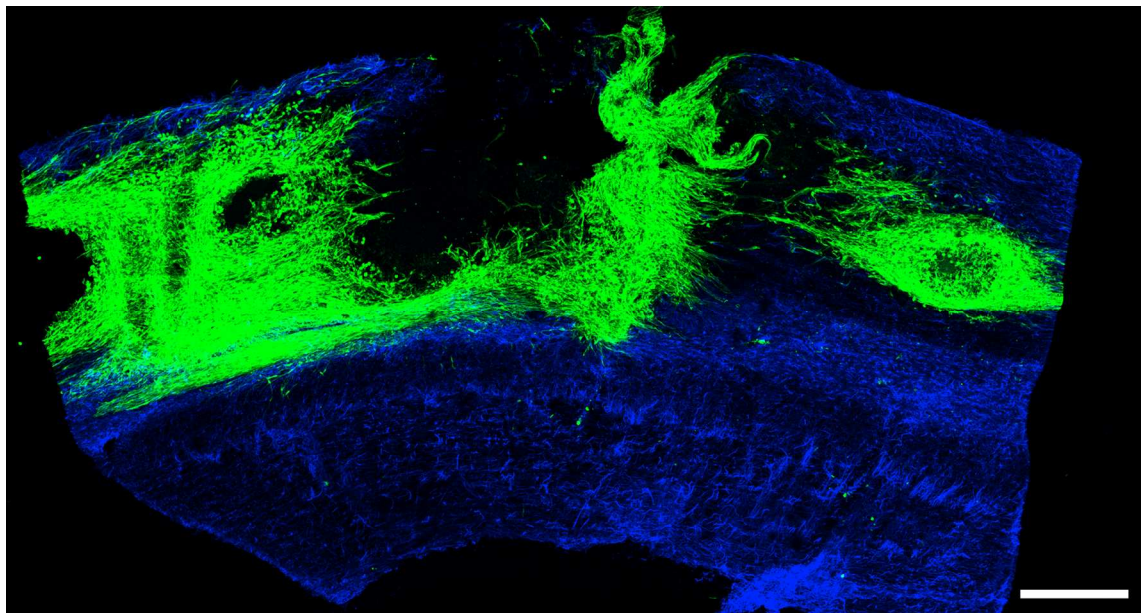


Figure 3-60. Time course of procedures performed on animals with 2 days survival.

Extensive OEC distribution in the lesion and rostral and caudal to the lesion was observed (Figure 3-61). GFP labelled cells were distributed on an average of 12 parasagittal section per animal. The OEC density was higher compared to the 2 week survival animals and extremely high compared to that at survival times of 6 weeks and 17 weeks. The widespread distribution of OECs and the fact that they density was so great made it impossible to place the sections in serial order; in fact with the light microscope coupled with dark field view condenser it was not possible to recognise the white-grey matter borders that were shaded by the OECs extensive distribution. OECs mainly distributed in the dorsal columns however some were distributed beyond the border with the lateral cord. Interestingly, while 2, 6 or 17 weeks after transplantation the GFP-OECs appeared as differentiated and elongated cells, here a large proportion of cells was rounded and appeared undifferentiated.

Figure 3-61. OEC distribution in the spinal cord two days after transplantation. Composite of confocal projected stacked images showing the widespread distribution of OECs in a parasagittal section of the lesion block. Objective: 10x. Scale bar: 500 μm .



3.3 Discussion

3.3.1 *Characterization of the BDA labelling*

BDA has previously been shown to produce efficient anterograde labelling of long spinal pathways in adult rat spinocerebellar tracts (Matsushita, 1999), corticospinal tract (Ruitenberget al., 2003) and when injected in the dorsal root ganglia to label sensory axons (Novikov, 2001). BDA labelling of L5 DRG afferents was shown to be superior to neurobiotin and Phaseolus vulgaris-leucoagglutinin with respect to intensity of staining and distance of labelling (Novikov, 2001). BDA is known for distributing uniformly along the axon length and its terminals: for this reason BDA was preferred to cholera toxin in this study because cholera toxin has been shown by us and others to localise preferentially in fibre terminals and yields inferior visualization of axons (Dent et al., 1996; Taylor et al., 2006; Toft et al., 2007).

In this present study biotinylated dextran amine injections into the L4 and L5 spinal nerves were performed two weeks prior to perfusion fixation to detect labelling of the L4 and L5 dorsal root ganglia neurons, thus allowing probing for the presence of regeneration rostral to the injury. Importantly, the injection of BDA directly into the spinal nerves rather than in the dorsal root ganglia is a novel approach and has not been published by others in the literature.

To assess the intensity of labelling and the distribution of BDA in the present tracer injection paradigm non-lesioned animals were injected with the tract tracer. A large number of axons were labelled with BDA in the lumbar cord. BDA labelling however decreased with distance when counting the number of axons in transverse sections of non-lesioned animals at the lumbar, thoracic, cervical and dorsal column nuclei levels. This observation is consistent with a previous study on BDA distribution efficiency after injections into the L5 rat dorsal root ganglia (Novikov, 2001) and may be explained by the fact that only a proportion of axons project to the dorsal column nuclei (Giuffrida and Rustioni, 1992).

The labelling appeared uniform throughout the length of the axons and it was possible to follow individual axons for relatively long distances if these were parallel to the section plane. Strong BDA labelling was detected both in sensory afferents travelling in the dorsal columns and in collaterals in the grey matter where it was possible to see arborisation of fibre terminals and synaptic boutons. BDA labelling allowed for the detection of large but also extremely thin diameter axons (~1 μm diameter) such as those sprouting or regenerating. Although it is likely that the efficiency of labelling varied between experiments, the variability in labelling between all the animals did not appear striking overall under epifluorescence microscope examination indicating that the technique is highly reproducible. Importantly, BDA tract tracing allowed for the use of other fluorescent markers, so that for example studies of colocalization between regenerating axons and OECs could be determined. Overall the present tract tracing injection paradigm technique proved to be extremely advantageous for studies of axonal regeneration compared to the other tracing techniques available in the field.

3.3.2 OEC transplantation

The interpretation of transplantation paradigms depends on the ability to identify the transplanted cells within the host spinal cord. Many studies have in the past used methods to identify OECs that are no longer considered reliable. For example transplanted OECs cannot be distinguished from host Schwann cells with p75 immunoreactivity or the use of the electron microscope (Li et al., 1998). Furthermore p75 will only label non-myelinating OECs and if any of the transplanted cells do myelinate they will not be detected with p75. Hoechst staining of OECs has been shown to form artifactual distribution leading to erroneous interpretations (Iwashita et al., 2000; Ruitenbergh et al., 2002; Andrews et al., 2004). In recent years technology has allowed researchers to manipulate cells to express markers that when transplanted distinguish them reliably from the surrounding environment.

The use in our work of genetically modified OECs to express green fluorescent protein allowed us to follow the distribution of OECs in the host spinal cord.

Highly pure neonatal olfactory bulb derived OECs were transplanted acutely into the cavity generated by a wire knife injury of the dorsal columns of syngeneic adult rats. GFP expression was observed in all the animals injected with OECs including those with a survival time of 17 weeks, thus showing for the first time with a reliable labelling method, that the transplanted OECs can survive in the host spinal cord for such lengthy times. This long survival was probably also due to the fact that recipients and donors were syngeneic and therefore shared the same genetic material strongly reducing the possibility of transplant rejection after allo/xenotransplantation (Andrews et al., 2004; Ramer et al., 2004a; Richter et al., 2005; Steward et al., (2006); Andrews and Stelzner, 2007).

3.3.2.1 OEC distribution in the lesion

OECs were found to partially fill the injection site of all transplanted animals. This is consistent with previous findings reported for electrolytic injuries (Li et al., 1998), crush injuries (Ramer et al., 2004a), contusion injuries (Collazos-Castro et al., 2005) and wire knife injuries (Toft et al., 2007) transplanted with OECs into the lesion site.

Following transplantation the animals were given recovery times of 44 hours, 2 weeks, 6 weeks or 17 weeks. GFP labelled cells were found to partially fill the lesion site in all conditions considered, however there was a noticeable reduction in the number of GFP labelled cells when the survival time was increased. This observation seems to be in contradiction with a work that reported an expansion of OEC number over time (Lu et al., 2006). It is possible though that the limited timescale considered by Lu and colleagues, between 1 hour and 7 days, might explain the diverging outcomes.

3.3.2.2 OEC protective effect on the lesion

We found that OEC transplanted animals developed a lesion cavity that appeared smaller compared to that of non-transplanted animals as previously shown (Toft

et al., 2007). In other reports, quantification of the lesion cavity showed cavity reduction after OEC transplant into a rat crush injury model (Ramer et al., 2004a; Bretzner et al., 2008) and a rat contusion injury (Plant et al., 2003) compared to non-transplanted animals. Moreover, in agreement with this finding, cavity quantification in our dorsal column wire knife injury model was significantly reduced after OEC transplantation compared to non-transplanted animals while no evident difference was found between animals with the same transplantation paradigm that received a conditioning lesion. Thus, the reduction of cavity formation was confirmed in our wire knife lesion model and the OEC graft affected the degree of cavitation. Furthermore we also found that even the lesion size, as defined by the internal perimeter of the GFAP positive glial scar was significantly decreased following OEC transplantation. A likely interpretation to explain this finding is that either OECs kept together opposite ends of the spinal cord and prevented them from moving apart or that OECs prevented astrocytes that surrounded the lesion from dying.

The GFAP boundary in the absence of a transplantation coincided with the lesion cavity borders and it surrounded a single large rounded cyst, devoid of cells. In the presence of OECs the GFAP borders were not so clearly defined as in non-transplanted rats and many GFAP trabeculae extended into the injury site and intermingled with GFP expressing OEC. This observation is in accordance with others and our group who found a reduction in astrogliosis and the formation of GFAP positive evaginations into the lesion (Ramer et al., 2004a; Collazos-Castro et al., 2005) (Toft et al., 2007).

Taken together, our findings show that reports published using other lesion models are true even for a wire knife lesion that ablates the dorsal columns: 1) wire knife lesions produced a cavity surrounded by a glial scar; 2) following cell transplantation both the cavity and the lesion size were significantly diminished; 3) in the presence of an OEC transplant the glial scar did not form an impenetrable barrier but permitted astrocytes to intermingle with the environment of the lesion core.

The lesion cavity develops both in humans and in rats (Radojicic et al., 2005) making the rat an ideal species to study cavity formation. The cavity appears a few hours after the injury due to necrosis of the insulted area and expands in

the following weeks due to a process of apoptosis (Crowe et al., 1997). OECs are thought to stabilize the lesion and consequently reduce cavitation (Ramer et al., 2004a; Toft et al., 2007). A mechanism that has been suggested to induce apoptosis in this context, is the migration of astrocytes away from the lesion, a process that could exacerbate the undergoing degeneration and consequently cause cavity enlargement (Fitch et al., 1999). The finding in our and others work that astrocytes do not abandon the lesion cavity, but instead are found to penetrate it and widely intermingle with the transplanted cells, could suggest that OECs ameliorate the lesion milieu and inhibit cavitation by reducing the migration of astrocytes away from the injury, consequently reducing grey matter loss.

3.3.2.3 OEC neuroprotective effect on the grey matter surrounding the central canal

Central canal cavitation, also known as syringomyelia, has been extensively described in the human spinal cord lesion pathology (Klekamp, 2002). Rats also develop central canal cavitation and are now being used as clinical models to study this pathology (Beattie et al., 1997; Akesson et al., 1998; Radojicic et al., 2007). Cavitation of the central canal is part of the secondary effects that contribute to worsening the severity of the injury and disability by destroying grey matter tissue even many segments away from the site of initial injury (Klekamp, 2002). In our present work, central canal cavitation occurred in most animals receiving a dorsal column injury. Interestingly, the cavity developed in the central canal rostral to but rarely caudal to the lesion. This finding is in agreement with a previous report by Radojicic and colleagues (2007) who described syringomyelia developing more in the rostral spinal cord than caudal to a contusion injury in rat. This may be a consequence of the scarring at the injury site which could obstruct the flow of the cerebrospinal fluid and build up the pressure in the central canal compartment (Klekamp et al., 2001). We found that the central canal appeared as consecutive enlargements and restrictions that often took over the whole grey matter located caudal to the central portion of the medial dorsal columns. The same ultrastructure has been described in human and rat central canal dilatation (Radojicic et al., 2007).

We report here an extremely interesting finding: that OECs transplanted into the spinal cord lesion was associated with a reduction of syringomyelia in the lumbar and thoracic cord. In particular the reduction was significant in the rostral end of the lesion block and in the thoracic cord. The lesion and central canal size did not correlate suggesting that the mechanism underlying neuroprotection of the central canal was different from that involved in the lesion cavity development. Probably the cytoarchitecture of the lesion following OEC transplantation prevented the obstruction of the central canal and the pressure of the cerebrospinal fluid did not build up. This result suggests that OEC transplantation can reduce tissue dieback in the grey matter. This property might be extremely relevant as preserving multiple segments of the spinal cord from the destruction of the grey matter that occurs during syringomyelia, could prevent people with spinal cord injury from developing autonomic dysfunctions, neuropathic pain and sensory and motor dysfunctions (Seki et al., 2008). Interestingly, the reduction of cavity formation was not a consequence of OECs completely filling the central canal, as in most animals OECs were not normally distributed along the length of the central canal.

These findings reinforce a single previous report on central canal size reduction following transplantation of human embryonic spinal cord grafts into rat lumbar spinal cord (Akesson et al., 1998). In this study, Akesson and colleagues reported that the central canal dilation rostral to the site of lesion and transplantation into nude athymic rats was reduced in all animals compared to the central canal size of non-transplanted Sprague-Dawley rats. In our present study we confirm these findings using control animals of the same strain as those transplanted. In fact it is possible that the differences observed by Akesson et al., (1998) were due to rat strain variation. In particular, the absence of an immune response in the nude athymic rats, rather than cell transplantation *per se*, could have prevented the central canal cavity from dilating. Furthermore, we show that autotransplantation of adult differentiated cells (e.g. OECs) have the potential to reduce central canal cavitation without the need for using tissue from the human embryo, a practice that involves many ethical issues.

3.3.3 OEC distribution beyond the transplant site

The use of GFP expressing OECs allowed us to study the distribution of OECs beyond the lesion site. In most animals OECs distributed rostral to and caudal to the injection level as single cells or in large groups. OECs were found mostly in the dorsal column white matter, but also in the grey matter caudal to the dorsal columns, in the central canal and at the border between white matter and grey matter. In many rats OECs formed continuous tracts that exited the lesion through the glial scar and extended for considerable distances.

The amount of OECs distributed in the spinal cord strongly decreased with time when comparing animals of varying survival times. The reduction of OEC number was already striking 6 weeks after the OEC injection, the most likely explanation being that the majority of transplanted cells had died in the intervening time.

While in the lesion OECs were randomly oriented, the direction of OECs outside of the lesion was normally rostro-caudal as observed previously by Lu et al. (2006), however often OECs aligned themselves along alternative directions, especially in the immediacy of blood vessels. In particular, in dorsal column white matter regions of animals that were mostly devoid of OECs, it was not infrequent to observe a denser OEC distribution around blood vessels. Along blood vessels trophic support might have been greater allowing OECs to survive longer or to preferentially locate there.

In the literature the distribution of OECs beyond the site of spinal cord injury has always been referred to as migration. This was questioned in a study from Mark Tuszynski's group in which it was suggested that OECs injected in the spinal cord underwent passive fluid flow distribution rather than migration (Lu et al., 2006), a finding later confirmed by Andrews et al. (2007). We observed OEC distribution away from the lesion at all survival time points considered after cell transplantation, including 2 days (which is the earliest time point our Home Office animal license allowed us to perform this experiment). These results could indicate that OECs underwent passive dispersion at the injection time as suggested by Lu and colleagues, yet the distribution and orientation of the cells observed in our present work does not entirely confirm these studies and in fact would suggest otherwise. Lu et al. (2006) and Andrews et al. (2007) showed that

the OEC distribution hours after transplantation rostral to and caudal to the injury were restricted to a thin tract that was likely to have formed along the breaking point of the spinal cord tissue as a consequence of the pressure generated during the injection. Instead, in our present study, at all time points, OECs were found to form continuous tracts leading out of the lesion. These tracts were not limited to thin bridges but often also extended to include large widths of the dorsal columns as also observed one week after transplantation by Lu et al. (2006). This would suggest that migration took place. Secondly, the injections performed by Lu et al. (2006) on a wire knife dorsal column injury were not directed into the lesion cavity but into intact tissue 1 mm rostral to or caudal to the injury, areas where pressure is likely to build up at the time of the injection. It is unlikely that similar pressures would be generated also in a lesion cavity; on the contrary, the excess of cells would be expected to exit at the top of the lesion, an occurrence that we observed during each cell injection. Moreover, the strong evidence that others have reported recently on the inability of Schwann cells to migrate after an X-irradiation of the spinal cord (Lankford et al., 2008) when compared to the ability of OECs to distribute many millimetres away from the site of injection (Sasaki, 2006; Lankford et al., 2008) supports the concept that OECs may have the potential to migrate through the CNS. Cell migration away from the site of injection might be however strongly dependant on the type of lesion involved (X-irradiation / electrolytic / transection / contusion). It is possible that the OEC distribution observed in the present work was due to a combination of passive cell dispersal and active cell migration.

3.3.4 Neurofilament labelling in the lesion

Neurofilament labelled fibres were found in the lesion of all animals that received an OEC transplant with and without combined treatment of conditioning lesions. Fibres appeared randomly orientated, generally aligning themselves with the OECs. In the absence of transplantation, no neurofilament was detected in the lesion while its distribution around the injury site appeared normal. This finding agrees with previous reports that described the presence of

neurofilament ingrowth in an OEC transplant (Ruitenberget al., 2003; Lu et al., 2006; Toft et al., 2007) but none in the absence of a cell transplant (Lu et al., 2001).

3.3.5 Regeneration of BDA labelled fibres in the lesion

The wire knife dorsal column lesion interrupted almost all of the ascending sensory fibres. This observation was true even after OEC transplantation and or conditioning lesions. Fibres showed typical signs of damage such as retraction from the injury and the presence of end bulbs and sprouts, features that have been extensively described by others (Kerschensteiner et al., 2005; Al-Jahdari et al., 2008; Ylera et al., 2009).

In all animals that were transplanted with OECs a variable number of BDA labelled fibres had grown into the injury. This observation is consistent with previous tract tracing reports of axonal growth in lesions of various nature transplanted with OECs of varying source and purity (Ramon-Cueto et al., 2000; Ruitenberget al., 2003; Bretzner et al., 2008).

Axonal growth in the lesion was likely to be regeneration rather than sparing: while fibres in the dorsal columns were mostly oriented along the spinal cord main axis, the fibres in the lesion followed the random orientation of the OECs. Furthermore, fibres in the dorsal columns could be followed for considerable distances, while it was virtually impossible to follow individual axons in the lesion environment even for short distances because each axon passed from one section to the next.

Fibres in the lesion possessed variable diameters and their orientation mirrored that of the OECs. Rats had a variable abundance of large to thin fibres regenerating in the lesion, however in general there was a larger amount of thin fibres. It has been shown that the ability to regenerate varies amongst different neuronal types in the laryngeal nerve (Nahm et al., 1992). An open question is whether the diameter of regenerating axons in a spinal cord lesion mirrored the type of DRG neuron regenerating: A α , A β , A δ or C fibres if using the distinction

by Erlanger and Gasser (1937) / I, II, III, IV fibres using the distinction by Lloyd (1943) / A type and c type fibres using the distinction by Lawson et al., (1991); or mirrored the regeneration rate of the fibres: fast regenerating axons are known to be very thin compared to slower regenerating axons at least in early stages of regeneration and become larger in later stages (Cajal, 1928).

Colocalization of BDA and the appropriate axonal markers to recognise the neuronal type should be used to answer this question. The question was partially addressed by studying the double labelling of neurofilament 200 which labels myelinated type A neurons (Lawson et al., 1991; Neuman et al., 2002) and BDA. We found that only occasional BDA labelled fibres displayed colocalization with neurofilament antibody even though a great number of neurofilament positive fibres were present in the transplant. This means that either the neurofilament levels decreased after injury in the type A fibres (Rosenfeld et al., 1997; Wong and Oblinger, 1987) that were labelled with the BDA tract tracer or that most regenerating fibres in the transplant were small C fibres not expressing neurofilament. This second possibility is unlikely as most C fibres enter Lissauer's tract which was not lesioned by the dorsal column lesion.

In non-transplanted animals, fibres were absent from the lesion site and only approached the caudal glial scar. This finding was similar to other reports involving transection or crush injury of DRG sensory axons in the spinal cord (Neumann et al., 1999; Andrews et al., 2004). Also studies involving transection of corticospinal tract axons showed that no axons could bypass the scar and enter the lesion (Li et al., 1998; Ramon Cueto et al., 2000) nor could tract traced rubrospinal axons enter a crush injury (Ramer et al., 2004a).

We also found that conditioning lesions performed 2 weeks before and at the time of the dorsal column lesion or 3 days before and 7 days after did not promote regeneration in the lesion either. Instead in all other studies involving conditioning lesion some degree of regeneration in the injury was observed (Andrews et al., 2004; Neuman et al., 1999). Differing lesion paradigms might explain differing outcomes of regeneration into the lesion. It must be noted, however, that the lesion appearance as reported in these published works was not as neat and self contained as in the dorsal column wire knife injury model as demonstrated by us in the present study. This difference might be explained by the fact that the wire knife lesion is a relatively small defined lesion when

compared to that generated with other lesioning techniques such as contusion or compression or complete transection. For this reason the wire knife dorsal column lesion site consisted of a well defined area easily identifiable from the remaining spinal cord tissue with GFAP staining. In particular, the axons ended quite abruptly behind the lesion site, while in other lesion models axons might be damaged caudal to the lesion but also at different levels within the lesion and consequently sparing might be misunderstood for regeneration. Anyhow, it must be considered that in our studies the wire knife dorsal column lesion was constituted by thin walls surrounding the cavity. As the lesion walls were very thin, it cannot be excluded that some regeneration occurred into the lesion walls of conditioned animals, but this was hard to detect. For certain, no regeneration was present in the core of the lesion and in the rostral lesion walls as observed by Andrews and colleagues (2004) and Neuman and colleagues (1999).

3.3.6 BDA labelling rostral to the injury

3.3.6.1 Two different groups of tract traced fibres rostral to the injury

After analysing transverse sections rostral to and caudal to the lesion and after ordering serially parasagittal sections in each animal it was possible to discriminate two main populations of axons rostral to the injury level, in the lesion block, rostral block and thoracic block. One population of axons was present in all animal groups and was located to the left of a near-vertical imaginary line passing along the border between the left medial dorsal columns and the grey matter (example of the border is shown in the results section in Figure 3-29). The imaginary line continued ventral to exclude the grey matter surrounding the central canal. A second population of axons were instead present almost uniquely in animals receiving OEC transplantation and were located to the right of the imaginary line, including the grey matter surrounding the central canal where OECs often distributed. For ease, throughout this work

the first group of fibres were called lateral fibres or also fibres in the lateral cord while the latter were called medial fibres or fibres in the medial cord.

3.3.6.2 Spared fibres in the lateral cord

Evidence that lateral fibres were a result of sparing came from a number of facts: 1) BDA labelled fibres span the lesion from one side to the other in intact sections that were located on the LHS of the lesion in animals with and without a transplant; 2) lateral fibres possessed a normal morphology and orientation and sent collaterals to the grey matter rostral to the lesion level; 3) the profile of individual lateral fibres that had a normal morphology could be followed and crossed the lesion level; 4) no axons were detected in lateral portions of the dorsal columns in any of the transplanted or non-transplanted animals where the wire knife injury was extended to ablate even lateral portions of the dorsal columns.

In the present work we found a higher number of axons in the lateral cord of OEC transplanted and conditioned animals compared to untreated animals. This difference indicates that it was likely that sparing of axons near the lesion environment was increased following both OEC transplantation and sciatic nerve transection. This finding is in accordance with electrophysiological work carried out in our laboratory that suggested a neuroprotective effect of OECs on the spinal cord environment surrounding the lesion (Toft et al., 2007).

Tuszynski and co-workers reported axonal regeneration of L4-L5 DRG neurons rostral to the injury in the dorsal column wire knife injury model when transplants of bone marrow stromal cells were combined with neurotrophin delivery (Taylor et al., 2006). Unlike our results he did not find any spared fibres on lateral sections at the lesion level, even using our same wire knife device (David Kopf Instruments) with the same arc aperture (Taylor et al., 2006). The diverging outcomes can be explained if we take into consideration the different locations of the injury: their lesion was cervical and ours was lumbar. It is known that the most lateral primary afferents upon entry in the spinal cord are localised in the dorsolateral fasciculus and travel rostral only for a few segments

sending collaterals to the dorsal horn. These axons are lateral enough to bypass the lumbar wire knife lesion created in our animal models and as expected they do not reach the cervical level. This explains why a cervical wire knife dorsal column lesion will likely ablate all ascending sensory axons from L4-5 DRG. In our lesion paradigm the transection was performed so close to the L4 and L5 DREZ rather than in the thoracic or cervical regions due to the consequence of the use of BDA rather than CTB. BDA tract tracing in the DRG neurons labels a smaller proportion of fibres and travels more slowly along the axons compared to CTB which in contrast yields inferior visualization of the tract traced fibres. To maximise visualization of regeneration we maximised the number of fibres that were ablated by performing the lesion at the L3-4 level. In this way we maximised the number of fibres that were potentially involved in regeneration processes: including all sensory fibres rather than only sensory cutaneous A β axons that are the only axons that project all the way to the cervical level and brainstem. In addition, we wanted to make the lesion close to the normal target of the axotomised fibres in the spinal grey matter.

3.3.6.3 Axonal labelling rostral to the lesion in the medial cord after OEC transplantation

It is generally accepted that regeneration occurs in the injury site transplanted with OECs but it is an open question whether regenerating fibres may bridge the lesion and grow into the distal spinal cord. In fact contradictory evidence has been reported so far, which mostly involves descending rather than ascending tracts. Moreover, the majority of papers that have so far described long distance axonal regeneration after OEC transplantation have failed to show comprehensive understanding of the relationship between the distribution of OECs located in the distal cord and regenerating fibres (Ramon-Cueto et al., 2000; Lu et al., 2001; Ramer et al., 2004a). In the present study the distribution of OECs rostral to the injury and moreover the fact OECs formed continuous tracts leading out of the injury for considerable distances produced the ideal conditions to answer the above question. Importantly, in many animals BDA labelled fibres were effectively found rostral to the injury in medial portions of the spinal cord, the majority of which were in association with OECs.

3.3.6.3.1 *Regeneration/sprouting/sparing in the medial cord*

The fibres located in the medial portion of the dorsal columns were mostly associated with OECs, and since non-transplanted animals lacked these fibres, their presence was likely to be due mainly to regeneration and/or sprouting of spared fibres promoted by the transplanted OEC tracts. Sprouting associated with OECs similar to that described by Li et al. (1994) cannot be excluded because in a number of animals continuity of fibres was found between spared axons located in the lateral cord and axons located in the OEC tracts. In particular in OEC transplanted animals and in conditioned animals but not in untreated ones, we often found axons in the medial dorsal columns located near the border with the lateral cord. These fibres were not associated with OECs but were clearly in continuity with fibres in the lateral cord. This suggested that these medial fibres were spared and were not present in untreated animals because they degenerated after injury. However, they were present in treated animals probably because the neuroprotection provided by OEC transplantation or conditioning lesions prevented their death. To support this idea, as described in section 3.3.6.2, we detected both in OEC transplanted animals and in conditioned animals more axons in the lateral spinal cord compared to those in untreated animals.

3.3.6.3.2 *Convincing regeneration*

The presence of spared fibres crossing the lesion level in undamaged portions to the far left of the dorsal columns required the application of stringent criteria to exclude from quantification any unwanted spared and sprouting fibres from those that were included in the quantification of regeneration. After subtracting all fibres that were not convincingly of a regenerating nature it was still possible to show that a small, although relevant number of BDA labelled axons had regenerated within the OEC tracts rostral to the injury, while no convincing regeneration was observed in non-transplanted animals. This is an important finding, as it shows for the first time that in a dorsal column lesion model involving a lesion of the ascending sensory fibres, DRG neurons can regenerate their axons rostral to the injury when optimal OEC distribution is present without

the requirement of any combined treatment. This is in contrast to previous work by Andrews et al. (2004) who did not detect the presence of regenerating sensory fibres rostral to a crush injury even when OECs were optimally distributed rostral to the lesion. Our finding is in agreement with other studies that have reported regeneration of descending corticospinal, serotonergic and noradrenergic fibres into the caudal spinal cord (Li et al., 1998; Ramon-Cueto et al., 2000; Lu et al., 2001; Ramer et al., 2004a).

With the exception of Li et al. (1998) all reports on regeneration in OEC transplanted animals focused hardly any attention on the relationship between the distribution of the OECs in the distal spinal cord and the location of regenerating axons. In contrast, in the present study this relation is shown to be with few exceptions a *conditio sine qua non* for regeneration. In the light of the present finding and of the work carried out by Li et al. (1998) the absence of long distance regeneration reported for rubrospinal tract axons (Ruitenbergh et al., 2003; Ramer et al., 2004a) and for corticospinal tract axons (Ruitenbergh et al., 2005; Lu et al., 2006) could have been a consequence of poor OEC distribution out of the lesion, especially considering that these publications lacked of descriptive or photographic information to address the issue (Ruitenbergh et al., 2003; Ramer et al., 2004a; Ruitenbergh et al., 2005; Lu et al., 2006).

It must be noted that the animals in the present lesion paradigm, although not receiving a conditioning lesion before or at the time of the injury, were likely to receive some damage to the peripheral branches of the L4 and L5 DRG when these were injected with BDA in the spinal nerves. The injection of BDA could thus be considered a conditioning lesion performed 4 weeks after the spinal cord injury. Yet, Andrews et al. (2004), who even transected the sciatic nerve immediately before injecting the tract tracer in to it, did not detect any regeneration or sparing rostral to the injury even though OEC tracts were present and even though regeneration or sparing within the lesion transplant was detected in other treatment groups.

An interesting question is to understand how closely do the OECs, that have been shown to promote the long distance axonal bridging regeneration, interact with the axons. Some reports have found no direct contact between myelinated axons

and transplanted OECs in the spinal cord but found evidence of contact with infiltrating Schwann cells (Boyd et al., 2004; Ramer et al., 2004a; Lu et al., 2006). In particular Lu et al. (2006) suggested, after observing by means of immunocytochemistry using a supposed Schwann cell specific marker (personal communication by Wewetzer informed us that this antibody was not specific), that Schwann cells ensheathed neurofilament positive axons and were surrounded by GFP expressing OECs. On the other hand, the group directed by Geoffrey Raisman using electron microscopy saw peripheral type myelin ensheathing corticospinal axons after OEC transplantation into a spinal cord injury (Li et al., 1998) suggesting direct contact of OECs and axons. In another experimental approach that involved X-irradiation and ethidium bromide injection in the spinal cord, leading to a persistent demyelination lesion, GFP expressing OECs formed myelin sheaths and nodes of Ranvier around dorsal columns axon (Sasaki et al., 2006). In the present study, only occasional GFP labelled OECs were found to ensheath BDA labelled axons, while the majority of BDA labelled fibres that localised in the very vicinity of GFP expressing OECs were not ensheathed by GFP labelled OECs. On the other hand, the finding in the following chapter that even GFP expressing Schwann cells transplanted into the lesion only occasionally ensheathed BDA labelled axons indicates that probably in our lesion model paradigm myelination was not extensive. A possible explanation for the divergent observations in these studies is that some lesion models but not others allow endogenous Schwann cells to enter the lesion. Once in the lesion endogenous Schwann cells, rather than OECs, interact directly with the regenerating fibres and myelinate them as suggested by Beattie et al. (1997). Furthermore, some lesion models could be more favourable for myelination than others.

It is evident in our lesion model, that in the absence of OEC transplant, although endogenous Schwann cells have been shown previously to distribute into the dorsal columns of the injured spinal cord (Keyvan-Fouladi et al., 2005), these Schwann cells did not promote detectable levels of long distance axonal regeneration.

3.3.6.4 Conditioning lesions enhance regeneration/sprouting when combined with OEC transplants

To maximise the axonal growth response after OEC transplantation we used a combined approach of transplanting OECs together with conditioning lesions. Conditioning lesions alone have been shown to elicit long distance axonal regeneration rostral to the injury when performed 1 or 2 weeks prior to the spinal cord lesion (Neumann et al., 1999) or even when performed at the time and 1 week after the spinal cord lesion (Neumann et al., 2005).

After combining conditioning lesions and OEC transplants BDA labelling was detected rostral to the lesion. Quantification of the number of axons at increasing distances from the lesion showed that regeneration/sprouting/sparing surpassed significantly (7 fold) that of animals with an OEC transplant only. Importantly, the majority of fibres were located in regions containing OECs.

After excluding from the quantification all those fibres that were not convincingly regenerating, it was possible to affirm that a combination of OECs and conditioning lesions promoted long distance axonal regeneration within the continuous OEC tracts that were present rostral to the injury in the medial dorsal columns and in the medial grey matter. It was also possible to affirm that the amount of regeneration was significantly higher than in non conditioned rats. Moreover the location of the fibres (aberrant location: i.e. grey matter, central canal), their orientation and the presence of branching and end bulbs was further evidence of their genuine regenerative nature. Nevertheless, while the profile of individual BDA labelled fibres could be followed for relatively long distances (mm) in the spinal cord caudal to the lesion where axons travelled following a relatively straight trajectory, this was not possible in the lesion site where the fibres frequently changed direction and traversed consecutive parasagittal sections. Thus, continuity of single fibres bridging the lesion could not be proved definitively.

To remove any remaining doubts on the strength of the above findings, the dorsal columns in four rats were completely ablated by extending the transected portion of the dorsal columns with the wire knife device and ablating also those lateral regions of the dorsal columns that had been spared with the previous

standard wire knife dorsal column lesion model. Even in the absence of any spared fibres to the left of the lesion, regeneration was detected rostral to the lesion in the medial cord, where OECs were distributed and had formed continuous cell tracts. The level of regeneration even in this group was significantly higher than that detected in the absence of conditioning lesions and most axons were located in close vicinity to OECs. The present findings are in accordance with a previous publication by Andrews et al. (2004) who combined OECs transplants and conditioning lesions and pointed out how the combination of the two treatments promoted regeneration or sparing of sensory DRG neurons after a dorsal column crush injury at the T8/9 level.

However, our present study shows for the first time that conditioning lesions enhance genuine regeneration response observed after a transplant. Importantly, by applying a transection method that ablated all the ascending sensory fibres the present study is also a proof of principle that regeneration is possible in such a combined treatment paradigm. In lesion models that involve contusion or crush injury (Andrews et al. 2004) a doubt should always remain that the anatomical regeneration observed is due to other mechanisms such as enhanced sparing rather than regeneration.

It is unlikely that carrying out a conditioning lesion of the sciatic nerve might protect DRG neurons from death. On the contrary, peripheral ablation of the sciatic nerve leads to an increase of DRG neuron cell death (Tandrup et al., 2004) and reduces the potential number of axons that may regenerate beyond the injury. Anyhow, no neuron loss was found in the adult rat L5 DRG 4 weeks after sciatic nerve axotomy (Tandrup et al., 2004); neuronal death initiated only after 8 weeks when 14% of neurons died and death increased at 32 weeks when 37% of neurons had died (Tandrup et al., 2004).

3.3.6.5 Conditioning lesions did not promote regeneration

It was not clear whether the incapacity of axons to grow past an OEC graft in the spinal cord was due to reduced trophic support when passing from the graft to the host interface or an intrinsic limitation of the conditioning lesions to support

regeneration in the spinal cord. Furthermore, it was not clear whether the major driving force for regeneration in combined treatment paradigms was the OEC distribution rostral to the dorsal column lesion or the conditioning lesions themselves. To answer these points, conditioning lesions were performed in the absence of cell transplantation. Importantly, in the present study no regeneration was observed rostral to the injury when conditioning lesions were made 2 weeks and at the time of injury or 3 days before and 7 days after the spinal cord injury. Apparently contradicting previous findings by Neumann et al. (1999; 2005) we found that no regeneration could be detected in or rostral to the lesion. This indicated that in our dorsal column lesion model the growth response provided by conditioning lesions was sufficient to increase regeneration in a permissive environment, such as a tract of OECs, but was insufficient to allow axons to grow into a hostile one, while the growth response following an OECs alone was effective at promoting regeneration. In Neumann et al. (1999; 2005) the lesion was performed using microscissors which do not create a complete cavity but generate multiloculated cavities separated by spared trabeculae.

3.3.6.6 Significance of the level of regeneration observed for future studies

The final goal for any regenerative research project is to find a procedure that can translate to the clinic. For this purpose the significance of the numbers of regenerating axons quantified here is briefly considered below. To have a very rough estimate of the proportion of fibres labelled with BDA regenerating rostral to the injury within the OEC tracts, two non-lesioned rats, one year apart from each other were injected with BDA, and on analysis we counted on average 1236 axons at the L3/L4 level. The number of L4 and L5 DRG neurons in adult rat has been shown to be approximately 12000 and 15000 respectively (Schmalbruch, 1987; Tandrup, 2004). Considering that each DRG neuron possesses one axon that runs in the dorsal columns rostral to the dorsal root entry zone sending collaterals down to the grey matter it is acceptable for a rough estimate to consider the number of L4/L5 DRG neuron axons in the dorsal columns at the L3/L4 level equal to the number of neurons in the L4/L5 DRG. A rough calculation suggests that approximately $1236 / (12000 + 15000) = 5\%$ of the axons

were labelled with BDA. This would mean that the number of regenerating axons quantified with BDA labelling were only 1/20 of those actually regenerating! In consideration that spinal cord injured individuals with only 10% of white matter spared can recover antigravity strength (Little et al., 1999) the number of fibres regenerating in the present study ($\sim 10-100 \times 20 = 200-2000$) can be considered a promising result and an incentive for continuing studies.

3.3.6.7 Regeneration at 2 weeks

Using *in vivo* time-lapse imaging it was reported that dorsal root ganglia neurons start to regenerate as early as 6 hours after injury (Kerschensteiner et al., 2005). We detected regeneration 6 weeks after the lesion, so to understand whether this occurred at earlier time points we examined regeneration 2 weeks post lesion in animals receiving a transplant and conditioning lesions.

Importantly we found that regeneration could be detected as soon as two weeks after the lesion. The number of regenerating fibres detected at two weeks was more potent than at the 6 week survival time point; however the number of animals where regeneration was detected was too small to apply statistical analysis. Even at this time point regeneration occurred mainly within tracts of OECs. The distance covered by the regenerating axons after two weeks was 4.4 mm. This distance is compatible with what is considered to be a reasonable speed of axonal growth in optimal conditions which is approximately 1 mm per day (Steward et al., 2003). The presence of such a great number of axons comparable if not higher to those present at 6 weeks indicates that the regeneration process started very early after injury.

3.3.6.8 Regeneration at later time points

Cajal himself observed that following a lesion to the spinal cord, growth cones emerged from the cut fibres, grew and branched in a comparable way with those of the peripheral nerve stump. It is at a later stage, though, 10-14 days after the injury that the restoration process ended. Since then many have shown that

the regeneration response can be delayed by providing axons with trophic support. Oudega and colleagues (1994) found that the number of conditioned dorsal root ganglia axons regenerating into a peripheral nerve stump placed in the spinal cord was highest one month after the lesion and decreased significantly a month later. Regeneration did not extend beyond the peripheral nerve stump however at any time point considered (Oudega et al., 1994). To understand whether the axons that were regenerating through the OEC tracts in the host spinal cord in our lesion paradigm maintained a high growth response for long time periods or whether their number decreased we sacrificed animals 17 weeks after the injury. We found that regenerating axons were still present rostral to the lesion in animals sacrificed 17 weeks after the dorsal column lesion and were mostly located in association with OEC tracts. This result indicates that the combined treatment paradigm was sufficient to make the regenerative response within the host spinal cord stable for many weeks and possibly delay its decay.

4 Transplantation of Schwann cells and fibroblasts

4.1 Introduction

Based on extremely promising data obtained on the effects OECs seemed to have on the injured spinal cord following anatomical but especially behavioural assessments, more and more work has been carried out *in vitro* or *in vivo* on the biological and molecular properties of OECs. In particular, data that suggested OECs were able to migrate into the olfactory bulbs of the adult after a lesion to the olfactory nerve (Chua et al., 1995) led to the idea that OECs might also exhibit this property after transplantation into the spinal cord (Doucette et al., 1995). Anyhow, the idea that the OEC is the miracle cell and could repair any complex biological system may be too simplified. It has been subsequently shown that after injury of the olfactory nerve, in a similar manner to Schwann cells in other peripheral nerves, OECs remain in place and form conduits for newly generated axons to grow through (Williams et al., 2004; Li et al., 2005). Having said this, the two cell types also exhibit differences as the conduits formed by Schwann cells after peripheral nerve injury promote the regeneration of damaged axons into the peripheral system where the regenerating axons innervate the appropriate tissue, while the conduits formed by OECs promote the growth of newly differentiated olfactory receptor neurons from the PNS into the CNS where these synapse with second order neurons in the CNS. Therefore the main striking feature that differentiates the two cell types is the ability of OECs but not Schwann cells to promote growth of axons into the CNS environment and synaptogenesis with CNS neurons. These properties which OECs exhibit in the olfactory system might not be exhibited in a spinal cord injury model which is an ectopic location for OECs.

Transplantation of either OECs or Schwann cells into spinal cord injuries has been implicated in the repair of central nervous tissue (Takami et al., 2002; Garcia-Alias et al., 2004). Both cell types can i) form peripheral type myelin after transplantation into an experimentally created demyelinated lesion in the spinal cord (Franklin et al., 1996; Radtke et al., 2004; Keyvan-Fouladi et al.,

2005) and ii) promote axonal growth into a graft after transplantation into the damaged CNS (Li et al., 1998; Takami et al 2002). There is in any case an important feature differentiating OECs and Schwann cells after transplantation into spinal cord injury, and it is their ability to reduce astrocytosis.

Hardly any work has been carried out to make a direct comparison of the repair capabilities of the two cell types, to address if there is an advantage of one cell type over the other. Direct comparison is particularly important especially in the light of the fact that every research group uses different lesion models of central nervous system injury and different methodologies. Especially since only direct comparisons under the same experimental hands might bring into the light any differences between cell types, that might otherwise remain covered by experimental variability between research groups. We therefore compared the regenerative capacity of OECs directly with that of Schwann cells in the same lesion paradigm and provide evidence on the potential of these cells as candidates for transplant-mediated repair of spinal cord injury.

4.1.1 Direct comparison of the reparative capacity of OECs and Schwann cells after transplantation

In vitro and *in vivo* studies of astrocyte/OEC interactions and astrocyte/Schwann cell interactions suggest that in the same experimental conditions OECs mingle better with astrocytes than Schwann cells (Lakatos et al., 2003; Fairless et al., 2005; Santos-Silva et al., 2007). In particular the expression of chondroitin sulfate proteoglycans (CSPG) by astrocytes was increased following interaction with Schwann cells when compared to their interactions with OECs (Takami et al., 2002; Lakatos et al., 2003). This has relevance to regeneration after CNS injury because astrocytosis following a lesion results in the increased expression of CSPG that creates a barrier to axonal regeneration (Moon et al., 2001). This difference between OECs and Schwann cells might provide an advantage to OECs over Schwann cells as an optimal candidate for transplant-mediated repair of a

spinal cord lesion. However, in some studies differences in the repair capacity of OECs and Schwann cells were not overly apparent (see Table 18 for a summary). In models of spinal cord injury where direct comparison of axonal regeneration into OEC and Schwann cell transplants was made, contusion lesions contained GAP43 positive axons, neurofilament positive axons, ascending sensory CGRP positive axons and serotonergic axons (Takami et al., 2002); electrolytic lesions contained axons ensheathed by P0 type myelin (Keyvan-Fouladi et al., 2003, 2005) and crush lesions contained GAP43 and CGRP positive axons and serotonergic and noradrenergic axons (Andrews and Stelzner, 2007). Furthermore, both OECs and Schwann cells promoted cavity reduction when transplanted into a spinal cord contusion lesion (Takami et al., 2002; Keyvan-Fouladi et al., 2003, 2005). In addition it has been reported that both OECs and Schwann cells distributed beyond a transection lesion for several millimetres after transplantation (Imaizumi et al., 2000). Furthermore in studies involving X-irradiation of the spinal cord and subsequent transplantation of Schwann cell or OECs it was seen that transplanted cell types distributed extensively in the host cord tissue (Akyiama et al., 2006). On the other hand in a similar study where direct comparison was made of OECs and Schwann cell migration after X-irradiation of the spinal cord it was demonstrated that OECs could migrate extensively while Schwann cells in the same experimental conditions could not (Lankford et al., 2008). In line with this finding, studies of the migration properties of OECs and Schwann cells after delayed transplantation following a contusion injury showed that OEC distribution in host tissue was more extensive than that of Schwann cells (Andrews and Stelzner, 2007). In particular, OECs, but not Schwann cells, crossed the glial scar and distributed into the lesion area when transplanted in an area away from the lesion site (Andrews and Stelzner, 2007). Thus the inherent property of OECs to mingle with astrocytes might make OECs more advantageous for CNS transplantation.

4.1.2 Direct comparison of regeneration/sparing/sprouting beyond the site of injury after OECs and Schwann cells

Little work has been carried out to date to compare convincing genuine long distance axonal regeneration after the transplantation of OECs or Schwann cells in the same experimental paradigm as shown also in Table 18. The only information available is described as follows. Imaizumi et al. (2000) indicated that following OEC or Schwann cell transplantation into a dorsal column transection grossly similar amounts of sensory fibres labelled with BDA tract tracer were seen immediately above the lesion. The only evidence reported by Imaizumi et al. (2000) to suggest regeneration rather than sparing occurred is from an image in which BDA labelled axons can be seen crossing the lesion level on what appears a lateral section, a location that is indicative of sparing. Furthermore in this report a relatively large number of fibres were present above the lesion even in the absence of cell transplantation (Imaizumi et al., 2000). A subsequent report that involved a contusion injury indicated that Schwann cells promoted more sparing/regeneration compared to OECs, however this difference was not significant (Takami et al., 2002). Therefore, based on the scarce data available, it is important for the field of regenerative medicine to examine in more detail long distance regeneration qualitatively and quantitatively making direct comparison between transplantation of OECs and Schwann cells.

| Publication | Transplanted cells | Tract | Spinal cord lesion | Cell distribution | Myelination | Long distance regeneration | Comments |
|-------------------------------|--------------------|-------------------|----------------------------------|-------------------------|-------------|----------------------------|---|
| Takami et al., (2002) | OECs | brainstem neurons | contusion | not clear | yes | yes | contusions are associated with sparing and sprouting, not with genuine regeneration |
| | Schwann cells | | | not clear | yes | yes | |
| Keyvan-Fouladi et al., (2003) | OECs | CST | electrolytic | not clear | yes | yes | electrolytic lesions in this paper are associated with sparing |
| Keyvan-Fouladi et al., (2005) | Schwann cells | na | electrolytic | not clear | yes | na | long distance regeneration was not investigated |
| Imaizumi et al., (2000) | OECs | DRG | Incomplete transection | yes, rostral and caudal | yes | yes | images and text are suggestive of sparing rather than long distance axonal regeneration. Distal axon-OEC localization not studied |
| | Schwann cells | | | | yes | yes | |
| Akyiama et al., (2006) | OECs | na | x-irradiation / ethidium bromide | yes | yes | na | |
| | Schwann cells | | | yes | yes | | |
| Lankford et al., (2008) | OECs | na | x-irradiation / ethidium bromide | yes | yes | na | |
| | Schwann cells | | | no | no | | |
| Andrews and Stelzner, (2007) | OECs | na | contusion | yes | na | na | OECs crossed the glial scar, not Schwann cells |
| | Schwann cells | | | no | na | | |

Table 18. Summary of studies directly comparing OEC and Schwann cell transplantation focusing on distribution, myelination and promotion of long distance axonal regeneration.

As shown in the table no comparisons of convincing long distance axonal regeneration have so far been performed. In most studies OEC and Schwann cells were equally effective at myelinating axons in the transplant; while with regards to cell distribution from the injections site, in half of the studies OECs moved away from the injection site better than Schwann cells.

4.2 Results

4.2.1 Schwann cell transplantation

Sciatic nerve derived Schwann cells were injected into the wire knife dorsal column lesion at the L3-4 level of 18 animals; 10 of which were primed with conditioning lesions. All animals underwent a recovery period of 6 weeks from the dorsal column lesion. Data regarding lesion and central canal morphology from all Schwann cell transplanted animals regardless of whether they received a sciatic nerve transection or not was pooled to quantify lesion and central canal size on a larger number of animals. However the distribution of transplanted cells rostral and caudal to the lesion and the number of tract traced fibres were considered independently for each of the two treatment groups (Figure 4-1).

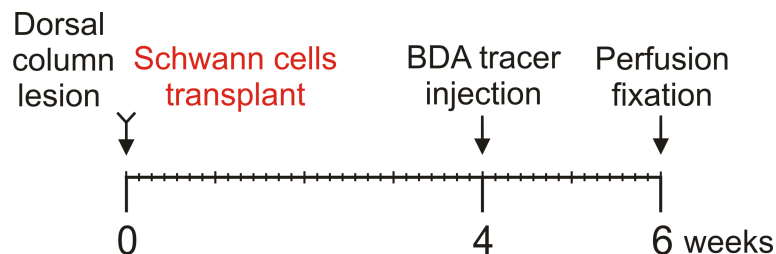


Figure 4-1. Time course of procedures performed on animals transplanted with Schwann cells.

Eight animals were transplanted with Schwann cells at the time of the dorsal column lesion. Seven of these were also tract traced with BDA to study the regeneration of L4-5 DRG neuron sensory axons.

4.2.1.1 Characterization of the lesion after a Schwann cell transplant

For the purpose of defining the lesion and central canal morphology on a larger number of animals and to compare this to non-transplanted animals and OEC

transplanted animals data was pooled together from animals receiving Schwann cell transplantation alone and from those where Schwann cell transplantation was combined with conditioning lesions. The distribution of Schwann cells in the spinal cord lesion and beyond the lesion closely resembled that seen in OEC transplanted rats, which was described in the previous chapter. In more detail, it was seen that in a subset of animals Schwann cells partially filled the lesion site (Figure 4-2A). These animals presented small lesions as defined by GFAP labelling and smaller or no lesion cavities. Within this subset of animals GFAP positive processes of varying size stretched towards the lesion centre in areas where transplanted cells were also located. However another set of animals presented with a large cavity and a large lesion (Figure 4-2B) that recapitulated the lesion size observed in non-transplanted rats. In this second group of lesions the Schwann cells were localised in the walls surrounding the lesion cavity and no GFAP processes extended into the lesion core.

As shown in Figure 4-3A, in Schwann cell transplanted animals the lesion cavity size was smaller compared to the lesion size defined by GFAP labelling, however the difference was not significant ($P=0.11$). Importantly, the lesion and lesion cavity sizes in Schwann cell transplanted animals (as shown in Figure 0-13) were 1.6 and 2.0 times respectively smaller than those in non-transplanted animals ($P=0.029$ and $P=0.0024$ respectively) indicating that Schwann cell transplantation not only reduced cavitation but also prevented the opposite sides of the lesion to separate, possibly by preventing tissue loss. This effect was comparable to that exhibited by OEC transplantation as shown for comparison purposes in Figure 0-13. In fact, when Schwann cell transplanted lesions were compared to those seen in OECs transplanted animals, they were 1.1 times smaller while lesion cavities were on average 1.1 times larger, differences that were not significant ($P=0.48$ and $P=0.82$ respectively).

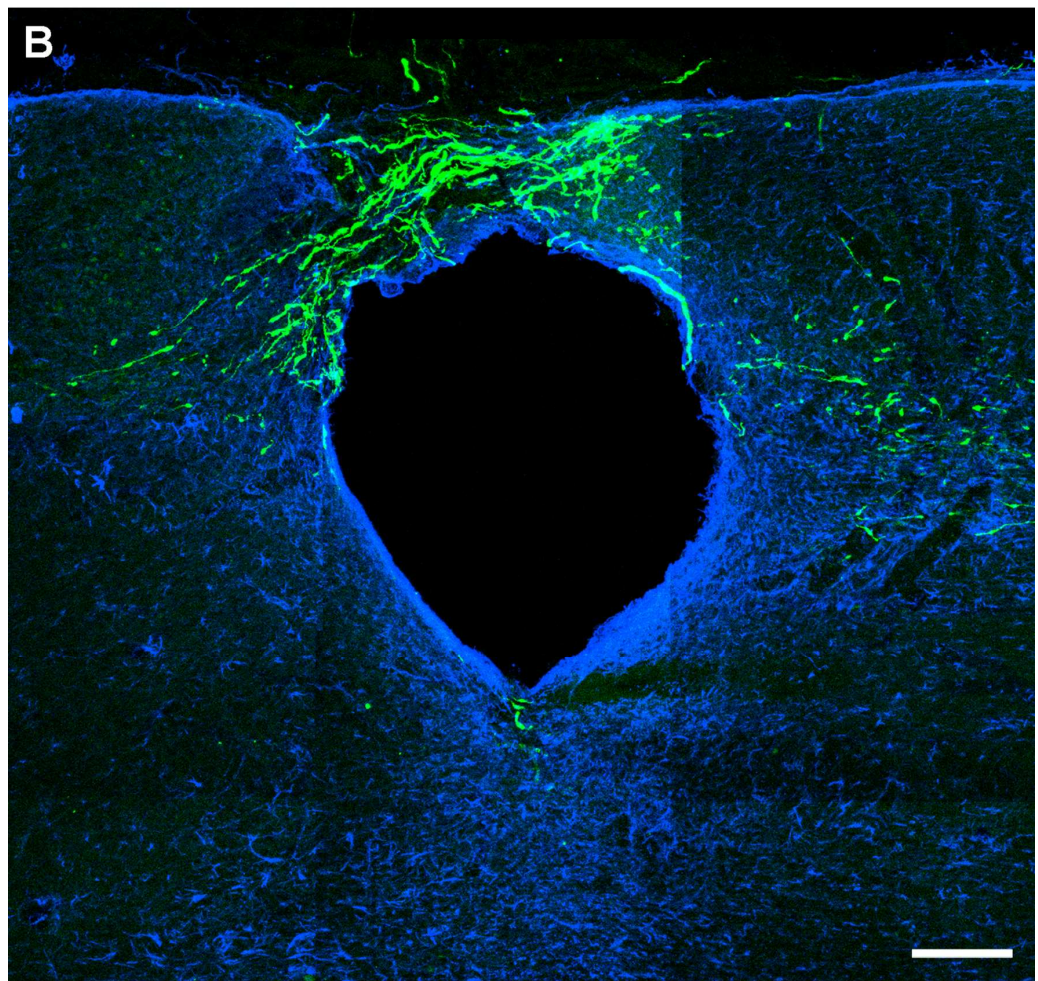
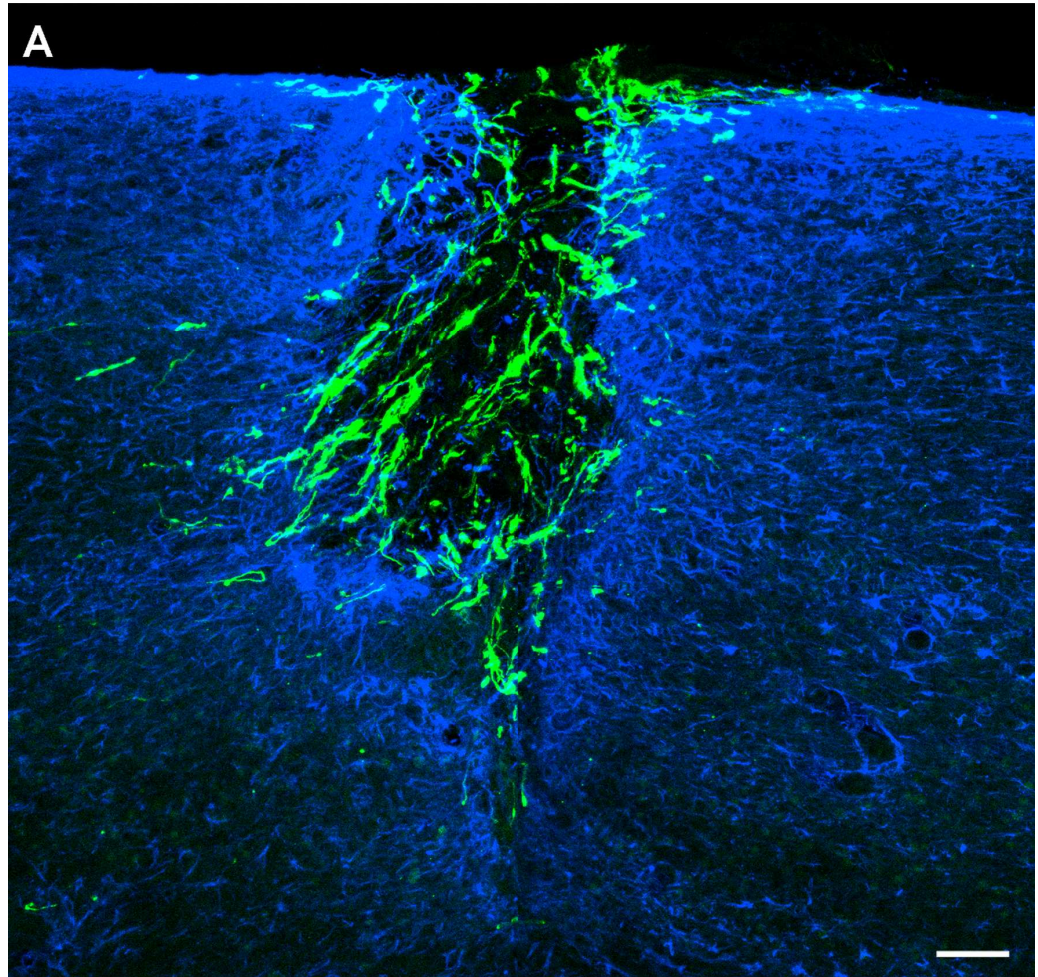
4.2.1.2 Characterization of central canal cavitation

In this section we combined the data from conditioned and non-conditioned animals receiving transplantation of Schwann cells: a total of 18 animals. A degree of central canal cavitation was observed in most animals receiving

Schwann cell injections into the dorsal column lesion (Figure 4-3B). Cavitation was detected only in one animal caudal to the lesion, while it was present in most of the animals rostral to the injury. No significant difference in the extent of cavitation was found between the rostral end of the lesion block, the rostral block and the thoracic block. However it must be noted that as also observed for non-transplanted and OEC transplanted animals, a trend could be observed where the central canal cavity size reached a peak in the rostral block before becoming smaller again at the thoracic level (Figure 4-14). Importantly, compared to non-transplanted animals, Schwann cell transplantation was associated with a 2.0 fold reduction of the average degree of cavitation in the rostral end of the lesion block ($P=0.015$), a 2.1 fold reduction of the cavitation in the rostral block ($P=0.014$) and a 1.6 fold reduction of the cavitation in the thoracic block ($P=0.056$) (Figure 4-14). Interestingly, in 17% (3/18) of animals the central canal did not contain any cysts. When comparing the level of central syringomyelia in Schwann cell transplantation with that seen in OEC transplantation it was found that there was no significant difference in all blocks analysed. This is consistent with the fact that also OECs were associated with a similar degree of preservation of grey matter around the central canal at all levels rostral to the lesion as shown for comparison purposes in Figure 4-14.

Figure 4-2. Schwann cell distribution in the lesion and lesion morphology 6 weeks after transplantation.

Composites of confocal projected image stacks that depict the lesion of two different animals (objective 10x). **A)** A lesion with a small cavity largely filled with Schwann cells (green) mixed with GFAP positive astrocytes (blue) processes that formed trabeculae extending through the lesion core. **B)** A large lesion with a large cavity devoid of both Schwann cells and astrocytic processes; the Schwann cells were located mainly in the GFAP labelled lesion walls and not in the cavity. Scale bars: 200 μm .



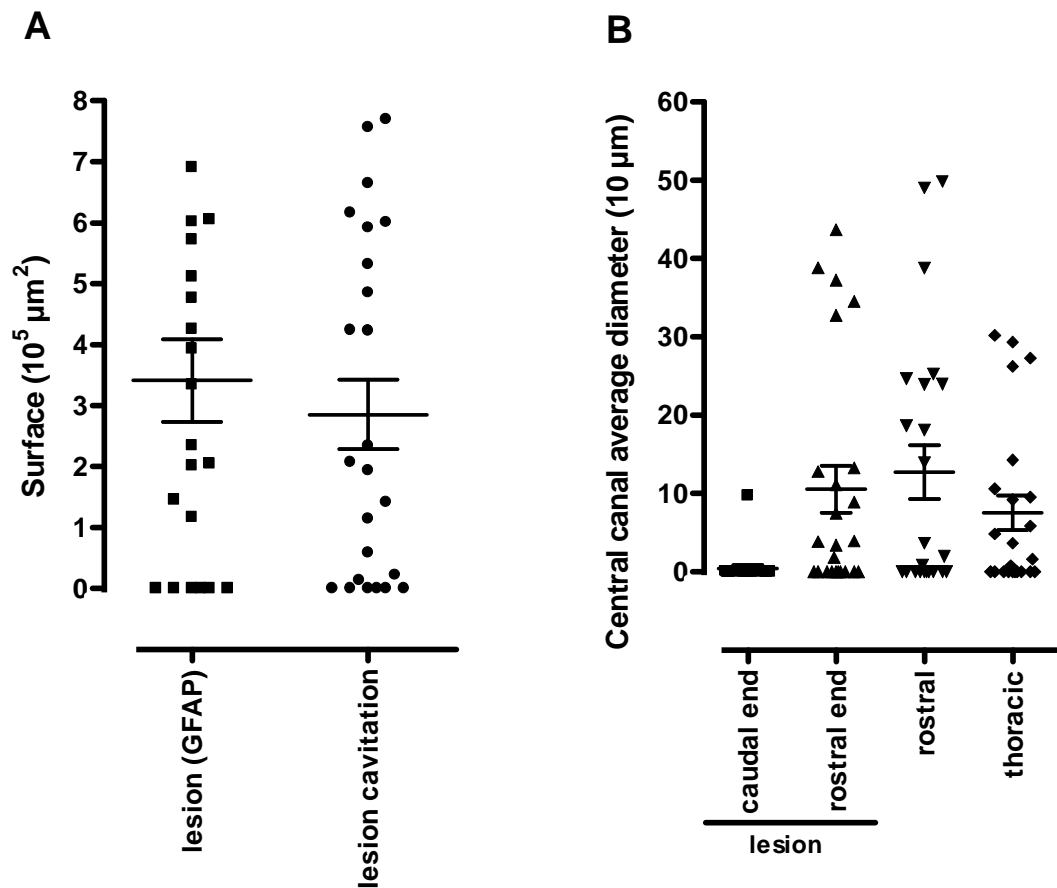


Figure 4-3. Lesion and central canal characterization 6 weeks after a dorsal column injury and Schwann cells transplantation.

A) Scatter dot plot showing that the size of the lesion defined by the GFAP positive glial scar surrounding the site of injury was larger than the size of the lesion cavitation however this was not significant ($P=0.11$) indicating that on average Schwann cells largely filled the lesion site. **B)** Cavitations formed in the central canal especially rostral to the injury level. No significant difference was found between the rostral end of the lesion block and the rostral block ($P=0.22$), nor between the rostral end of the lesion block and the thoracic block ($P=0.22$), nor between the rostral and thoracic blocks ($P=0.080$).

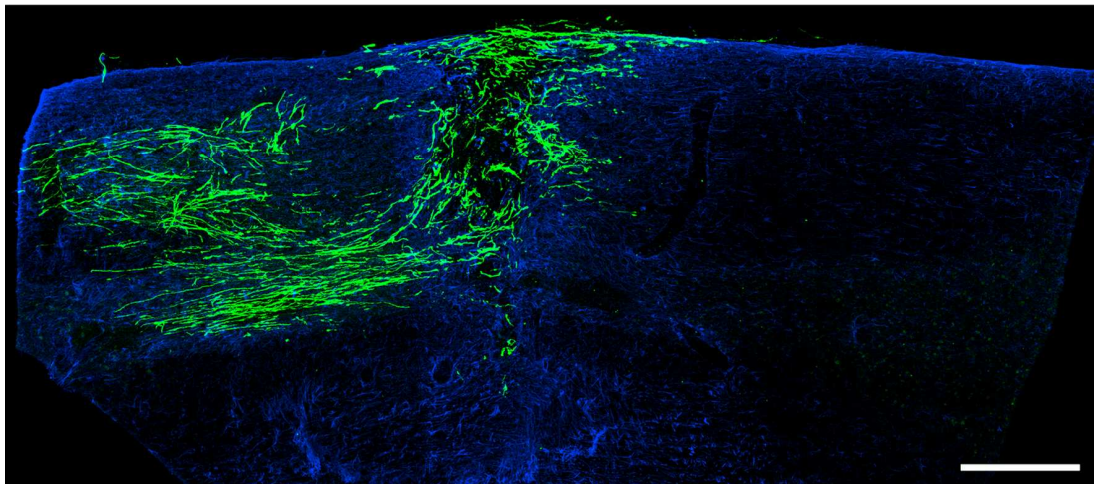
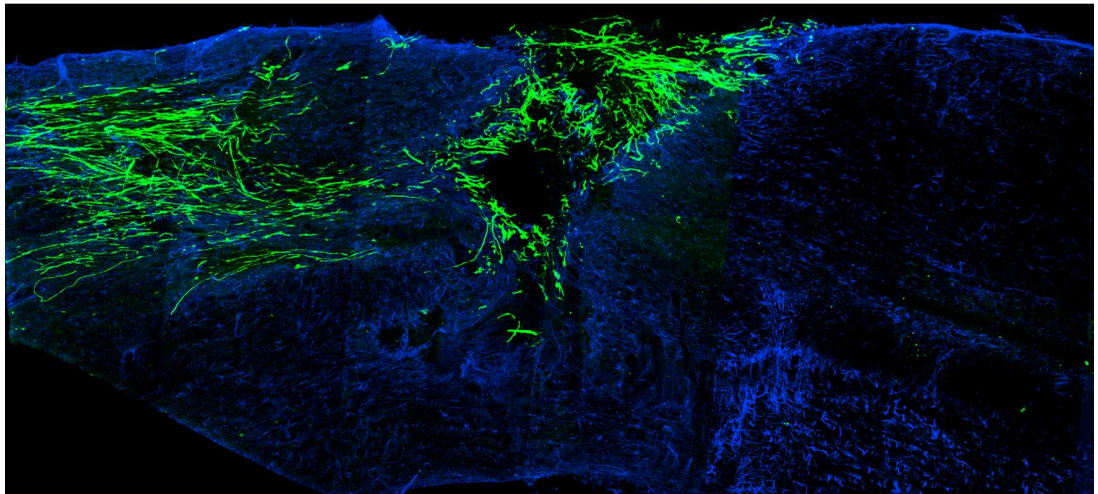
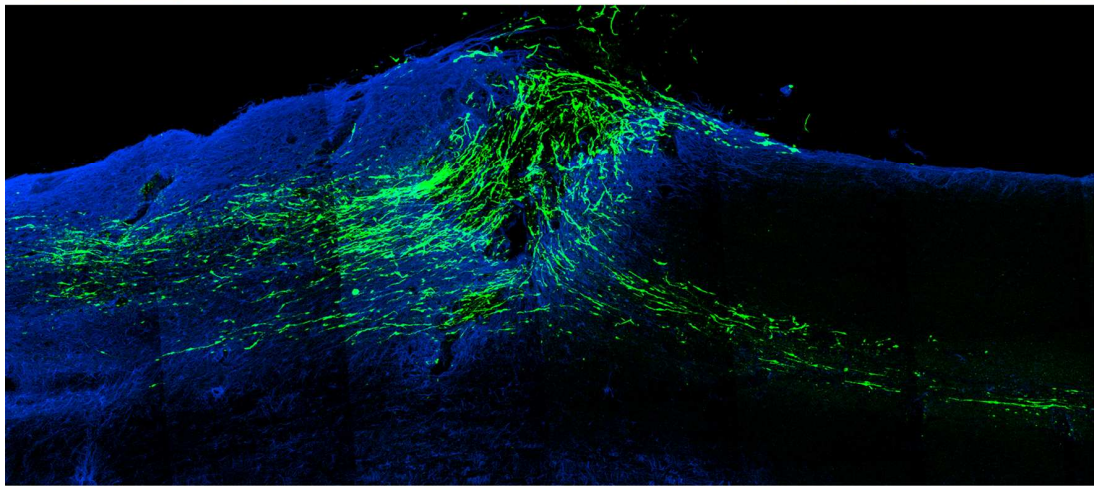
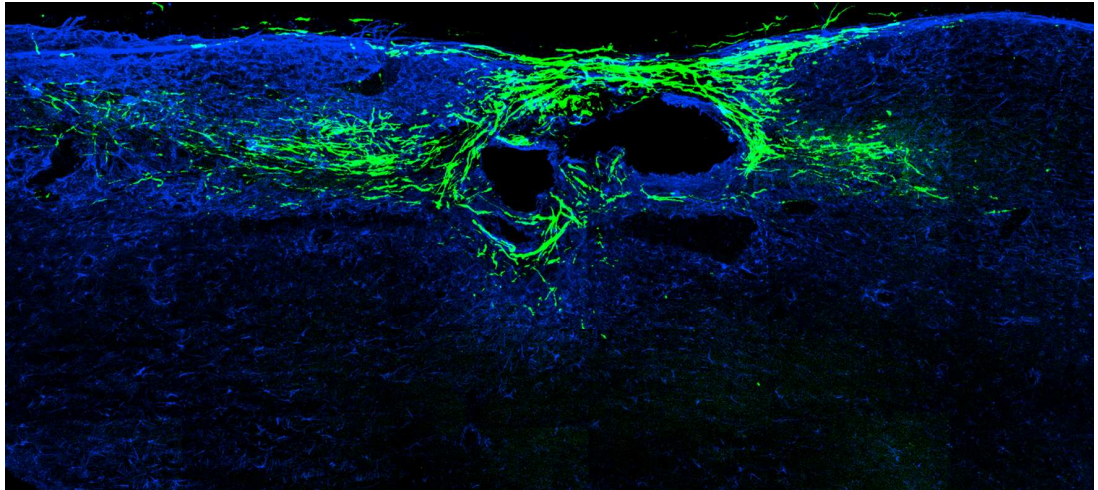
4.2.1.3 Distribution of Schwann cells in the spinal cord after transplantation

In animals that received a Schwann cell injection into the lesion site, transplanted cells distributed rostral in all (8/8) of the animals while they were distributed below the lesion in 75% (6/8) of them. Examples of cell distribution in the lesion block are shown in Figure 4-4. The cell distribution extended to the rostral block and even to the thoracic block. Schwann cells were located in the medial portion of the dorsal columns in all animals, and also in the grey matter located beneath the medial portion of dorsal columns in 38% (3/8) of animals and at the border between the two in 38% (3/8) of animals. In some rats the transplanted cells distributed along the central canal for considerable distances forming a non continuous column of cells. Schwann cells were distributed as isolated cells or more commonly in clusters, which often formed long tracts in continuity with the lesion. These findings were not dissimilar to those noted when analysing the distribution of OECs throughout the spinal cord.

Importantly, as also observed in the previous chapter for OECs, Schwann cells formed continuous tracts that lead out of the lesion and progressed into the spinal cord tissue for variable distances in 50% (4/8) of transplanted rats. The average length of the continuous tracts was 2600 μm .

Figure 4-4. Distribution of Schwann cells in the spinal cord.

Composite of confocal projected image stacks of parasagittal sections of the lesion block of four animals that show the widespread distribution of Schwann cells (green) in the spinal cord rostral to and caudal to the lesion/injection site. In particular, Schwann cells formed continuous cell tracts leading out of the lesion rostral to the injection point. Scale bar: 500 μm .



4.2.1.4 Regeneration of BDA labelled fibres within the Schwann cell transplant

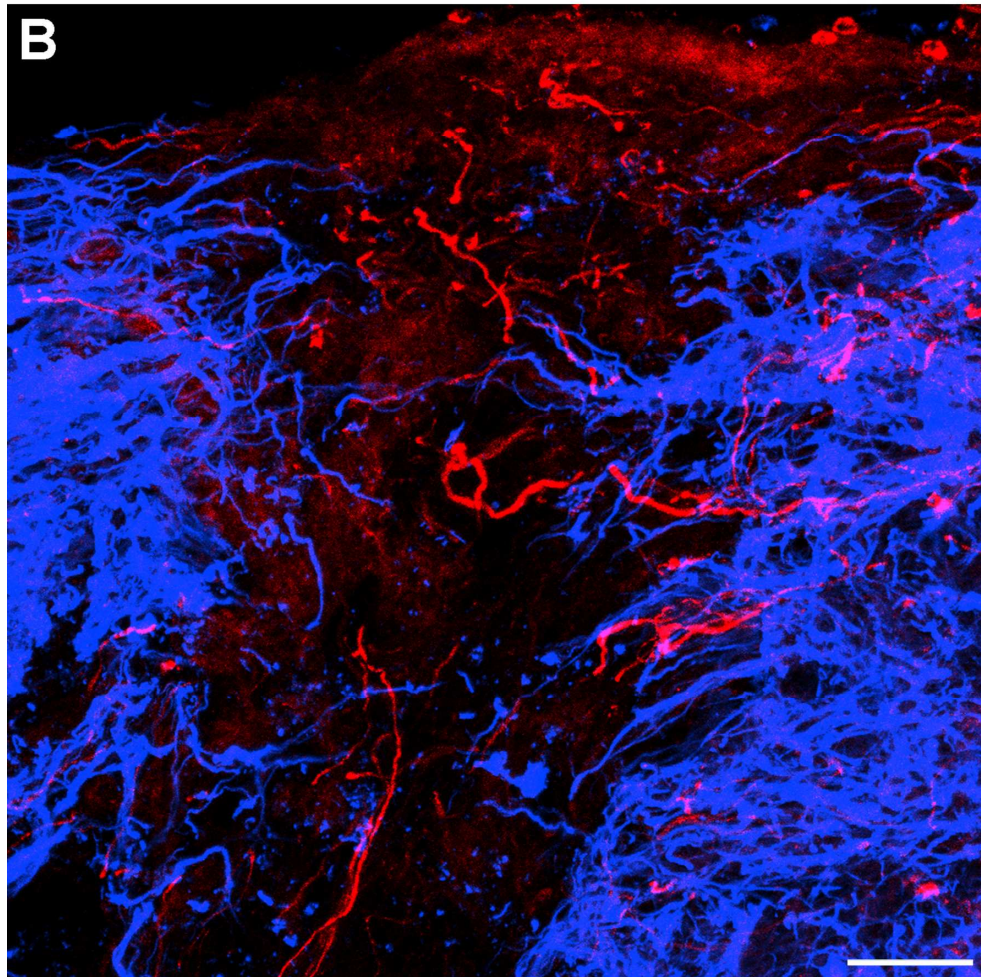
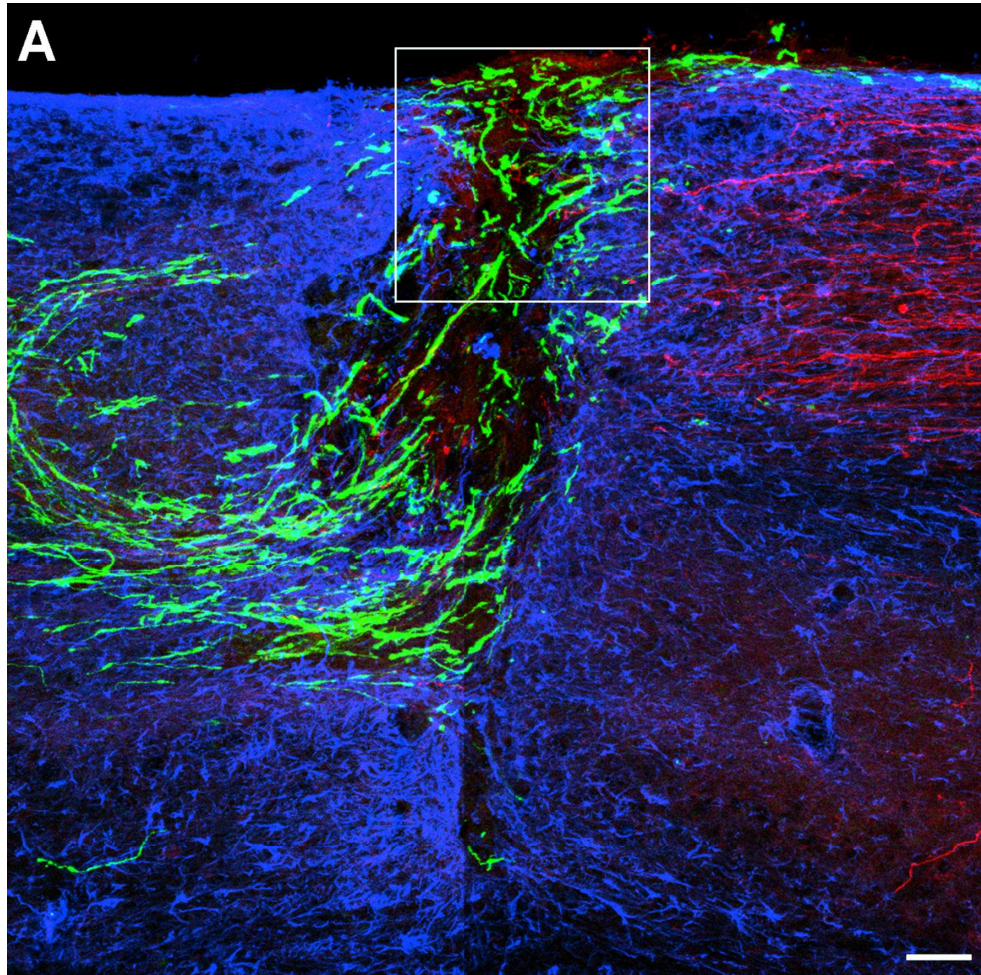
After transplantation with Schwann cells it can be seen that most of the ascending sensory axons labelled with BDA entering through the L4 and L5 spinal nerves terminated beneath the lesion. A variable amount of BDA labelled fibres were detected in association with Schwann cells within the lesion borders in all the animals tract traced with BDA (7/7). These fibres were likely to have regenerated as their orientation followed closely that of the transplanted cells (Figure 4-5).

4.2.1.5 BDA labelled axons rostral to the spinal cord lesion

Tract traced axons running along the lateral cord were detected in all animals except one. Axons labelled with BDA were also detected in the medial cord in all animals transplanted with Schwann cells (7/7). Following quantification on parasagittal sections using epifluorescence microscopy (Table 19 and Table 20) it was possible to note that 94% of axons counted were associated with Schwann cells. These axons followed closely the orientation of the transplanted cells. Axons were mostly oriented along the rostro-caudal direction, but where Schwann cells were for example oriented along the dorso-ventral direction, then the axons followed this same orientation. Only 6% of axons in the medial cord were located in areas devoid of Schwann cells and these were mostly situated near the border with the lateral cord, a location suggestive of sparing. The number of axons rostral to the lesion in rats transplanted with Schwann cells was on average 1.8 times greater than in rats transplanted with OECs, however this difference was not significant. A graph comparing the axonal quantification between Schwann cell and OEC transplanted animals is shown in Figure 4-16.

Figure 4-5. Axonal regeneration into a lesion transplanted with Schwann cells.

A) Composite of confocal projected images taken with a 20x objective that depicts BDA labelled axons (red) approaching the lesion site outlined by GFAP labelling (blue) filled with Schwann cells (green). **B)** Higher magnification (40x) of the boxed area in **A** without the green channel showing BDA labelled axons entering the lesion and regenerating within the lesion boundaries. Scale bars: 100 μm in **A** and 25 μm in **B**.



| | | Number of axons | | | | | | | | Average | St. Error |
|--|--------------|-----------------|-------|--------|--------|--------|--------|------------|-------------|------------|-----------|
| | | R4708 | R4808 | R13908 | R14008 | R14108 | R24608 | R24708 | | | |
| Distance from the lesion (μm) | 200 | 0 | 12 | 0 | 30 | 0 | 2 | 62 | 15.1 | 8.8 | |
| | 400 | 2 | 10 | 0 | 25 | 0 | 0 | 44 | 11.6 | 6.4 | |
| | 600 | 0 | 0 | 0 | 15 | 0 | 0 | 48 | 9.0 | 6.8 | |
| | 800 | 0 | 5 | 0 | 17 | 0 | 0 | 38 | 8.6 | 5.4 | |
| | 1000 | 0 | 4 | 0 | 9 | 0 | 0 | 25 | 5.4 | 3.5 | |
| | 1200 | 0 | 3 | 0 | 7 | 1 | 0 | 29 | 5.7 | 4.0 | |
| | 1400 | 0 | 4 | 0 | 1 | 1 | 0 | 16 | 3.1 | 2.2 | |
| | 1600 | 2 | 5 | 0 | 1 | 2 | 0 | 23 | 4.7 | 3.1 | |
| | | | | | | | | | | | |
| | 3200 | 0 | 1 | 0 | 10 | 1 | 0 | 10 | 3.1 | 1.8 | |
| | 3600 | 0 | 1 | 0 | 10 | 11 | 0 | 4 | 3.7 | 1.8 | |
| | 4000 | 0 | 3 | 0 | 0 | 8 | 0 | 3 | 2.0 | 1.1 | |
| | 4400 | 0 | 2 | 0 | 0 | 0 | 0 | 0 | 0.3 | 0.3 | |
| | 4800 | 0 | 1 | 0 | 0 | 0 | 0 | 0 | 0.1 | 0.1 | |
| | | | | | | | | | | | |
| | 10000 | 0 | 0 | 0 | 0 | 0 | 0 | 0 | 0.0 | 0.0 | |
| 10400 | 0 | 0 | 0 | 0 | 0 | 0 | 0 | 0.0 | 0.0 | | |
| 10800 | 0 | 0 | 0 | 0 | 0 | 0 | 0 | 0.0 | 0.0 | | |
| 11200 | 0 | 0 | 0 | 0 | 0 | 0 | 0 | 0.0 | 0.0 | | |
| 11600 | 0 | 0 | 0 | 0 | 0 | 0 | 0 | 0.0 | 0.0 | | |

Table 19. Number of tract traced fibres associated with Schwann cells rostral to the lesion in the medial spinal cord.

Quantification of axon number rostral to the lesion performed with an epifluorescence microscope and 63x lens on parasagittal sections of the lesion block, rostral block and thoracic block.

| | | Number of axons | | | | | | | | Average | St. Error | |
|--|-------|-----------------|-------|--------|--------|--------|--------|--------|-----|---------|-----------|--|
| | | R4708 | R4808 | R13908 | R14008 | R14108 | R24608 | R24708 | | | | |
| Distance from the lesion (μm) | 200 | 0 | 0 | 0 | 0 | 0 | 0 | 0 | 0 | 0.0 | 0.0 | |
| | 400 | 0 | 0 | 0 | 0 | 0 | 0 | 0 | 0 | 0.0 | 0.0 | |
| | 600 | 0 | 2 | 0 | 0 | 1 | 0 | 0 | 0 | 0.4 | 0.3 | |
| | 800 | 0 | 0 | 0 | 0 | 1 | 0 | 0 | 0 | 0.1 | 0.1 | |
| | 1000 | 0 | 0 | 0 | 0 | 0 | 0 | 0 | 0 | 0.0 | 0.0 | |
| | 1200 | 0 | 0 | 2 | 2 | 0 | 0 | 0 | 0 | 0.6 | 0.4 | |
| | 1400 | 0 | 0 | 1 | 5 | 0 | 0 | 0 | 0 | 0.9 | 0.7 | |
| | 1600 | 2 | 0 | 1 | 7 | 0 | 0 | 0 | 0 | 1.4 | 1.0 | |
| | | | | | | | | | | | | |
| | 3200 | 0 | 0 | 2 | 0 | 0 | 0 | 0 | 0 | 0.3 | 0.3 | |
| | 3600 | 0 | 0 | 3 | 0 | 0 | 0 | 0 | 0 | 0.4 | 0.4 | |
| | 4000 | 0 | 0 | 0 | 1 | 2 | 0 | 0 | 0 | 0.4 | 0.3 | |
| | 4400 | 0 | 0 | 0 | 0 | 0 | 0 | 0 | 0 | 0.0 | 0.0 | |
| | 4800 | 0 | 0 | 0 | 0 | 0 | 0 | 0 | 0 | 0.0 | 0.0 | |
| | | | | | | | | | | | | |
| | 10000 | 0 | 0 | 0 | 0 | 0 | 0 | 0 | 0 | 0.0 | 0.0 | |
| | 10400 | 0 | 0 | 0 | 0 | 0 | 0 | 0 | 0 | 0.0 | 0.0 | |
| 10800 | 0 | 0 | 0 | 0 | 0 | 0 | 0 | 0 | 0.0 | 0.0 | | |
| 11200 | 0 | 0 | 0 | 0 | 0 | 0 | 0 | 0 | 0.0 | 0.0 | | |
| 11600 | 0 | 0 | 0 | 0 | 0 | 0 | 0 | 0 | 0.0 | 0.0 | | |

Table 20. Number of tract traced fibres that were not associated with Schwann cells rostral to the lesion in the medial spinal cord.

Quantification of axon number rostral to the lesion performed with an epifluorescence microscope and 63x lens on parasagittal sections of the lesion block, rostral block and thoracic block.

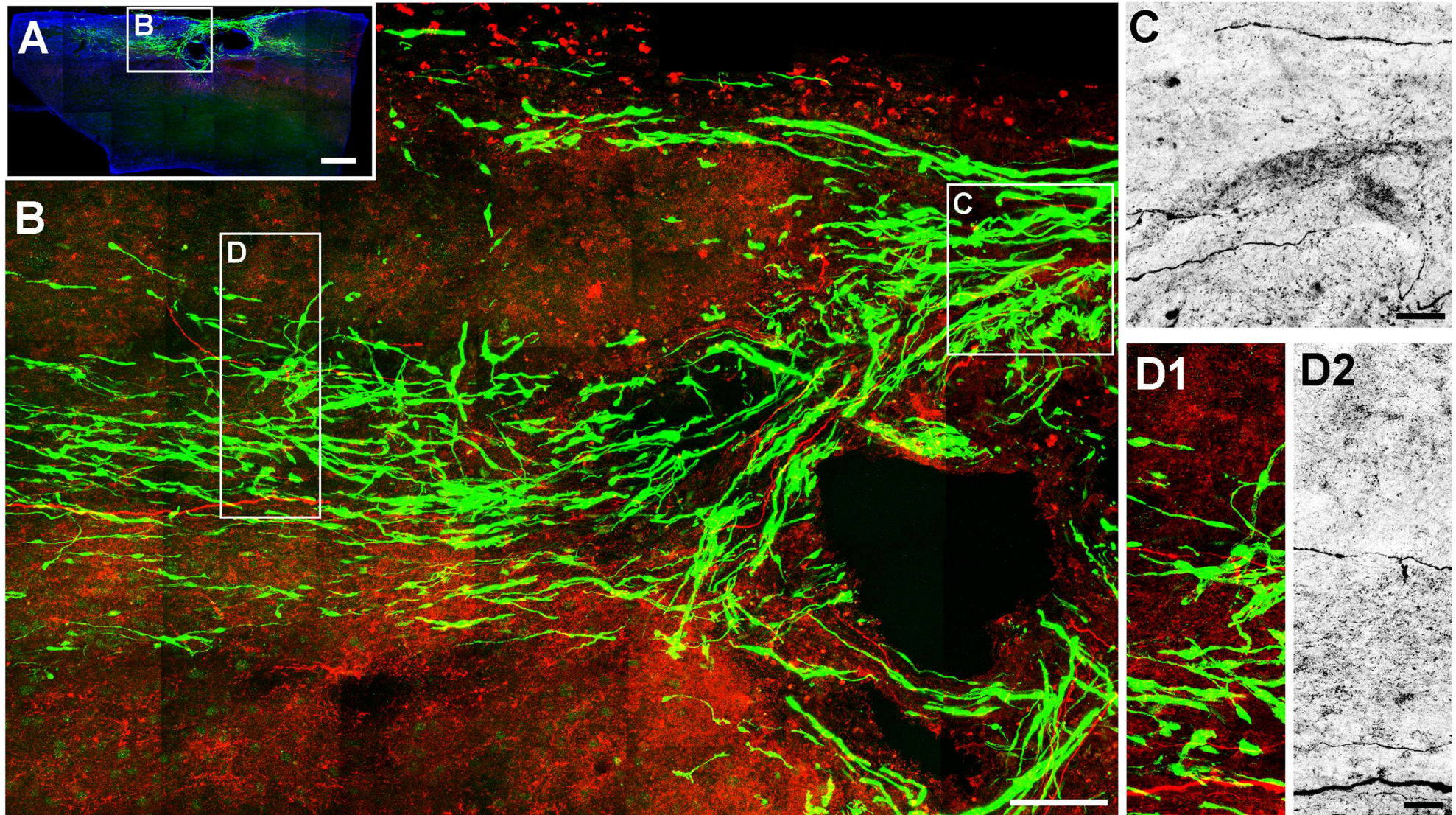
4.2.1.6 Genuine regenerating BDA labelled fibres rostral to the lesion level

To determine whether Schwann cells were promoting long distance axonal regeneration rostral to the lesion, all axons that were potentially spared or sprouting were removed from the quantification following the same stringent criteria applied to axons after OEC transplantation in the previous chapter (section 3.2.3.9). After application of this methodology, convincing regeneration could be confirmed only in 2 rats out of the 8 where BDA labelling was originally found in the medial cord. These axons, quantified in Table 21, were mostly localised within tracts of Schwann cells (99% of fibre counts). Furthermore, it could be seen that no animals contained continuous cell tracts exiting the lesion which were devoid of BDA labelling.

Importantly, in the 3 animals where regeneration was detected in the Schwann cell tracts rostral to the dorsal column lesion, regeneration proceeded up to the end of the cell tracts. Consistent with this observation, the average length of the Schwann cell tracts rostral to the lesion in these animals was 3000 μm and the average of the furthest regeneration detected in each animal rostral to the lesion was also 3000 μm .

Figure 4-6. Schwann cell tracts in continuity with the lesion were sufficient to promote regeneration rostral to the lesion.

A) Confocal image taken with a low power objective (10x) of a parasagittal section of a dorsal column lesion at the L3-4 level in a rat transplanted with Schwann cells; boxed area is depicted at higher magnification (40x oil) in **B**. **B)** Axons bridged the lesion to the other side and regenerated within the Schwann cell tracts. **C)** Enlarged image of the boxed area shown in **B** that shows the axons regenerating in the lesion with BDA labelling in greyscale. **D1-D2)** Images of the boxed area shown in **B** are depicted here at higher magnification (40x oil) and it is possible to see that axons had regenerated within the Schwann cell tracks. **D2)** BDA axonal labelling in greyscale. **A-D)** Composite of confocal projected image stacks. Colour codes: red (axons), green (Schwann cells), blue (astrocytes). Scale bars: 500 μm in **A**, 100 μm in **B** and 25 μm in **C-D**.



| | | Number of axons | | | | | | | | Average | St. Error |
|--|-------|-----------------|-------|--------|--------|--------|--------|--------|------|---------|-----------|
| | | R4708 | R4808 | R13908 | R14008 | R14108 | R24608 | R24708 | | | |
| Distance from the lesion (μm) | 200 | - | 12 | - | - | - | 2 | - | 7.0 | 5.0 | |
| | 400 | - | 10 | - | - | - | - | - | 10.0 | - | |
| | 600 | - | 2 | - | - | - | - | - | 2.0 | - | |
| | 800 | - | 5 | - | - | - | - | - | 5.0 | - | |
| | 1000 | - | 4 | - | - | - | - | - | 4.0 | - | |
| | 1200 | - | 3 | - | - | - | - | - | 3.0 | - | |
| | 1400 | - | 4 | - | - | - | - | - | 4.0 | - | |
| | 1600 | - | 5 | - | - | - | - | - | 5.0 | - | |
| | | | | | | | | | | | |
| | 3200 | - | 1 | - | - | - | - | - | 1.0 | - | |
| | 3600 | - | 1 | - | - | - | - | - | 1.0 | - | |
| | 4000 | - | 3 | - | - | - | - | - | 3.0 | - | |
| | 4400 | - | 2 | - | - | - | - | - | 2.0 | - | |
| | 4800 | - | 1 | - | - | - | - | - | 1.0 | - | |
| | | | | | | | | | | | |
| | 10000 | - | - | - | - | - | - | - | - | - | - |
| 10400 | - | - | - | - | - | - | - | - | - | - | |
| 10800 | - | - | - | - | - | - | - | - | - | - | |
| 11200 | - | - | - | - | - | - | - | - | - | - | |
| 11600 | - | - | - | - | - | - | - | - | - | - | |

Table 21. Number of genuine regenerating fibres rostral to the lesion in the medial spinal cord after Schwann cell transplantation.

Quantification of axon number rostral to the lesion performed with an epifluorescence microscope and 63x lens on parasagittal sections of the lesion block, rostral block and thoracic block. Blank cells are used to indicate that data did not meet the inclusion criteria.

4.2.2 Transplantation of Schwann cells combined with conditioning lesions

In order to assess whether a combined treatment paradigm could boost the extent of axonal regeneration observed in the Schwann cell transplanted animals we combined Schwann cell transplantation with sciatic nerve transection. A total of 10 rats underwent a treatment procedure that included Schwann cell transplantation into the lesion together with a double conditioning lesion of the sciatic nerve; 8 of these were injected with BDA to tract trace ascending dorsal column axons (Figure 4-7).

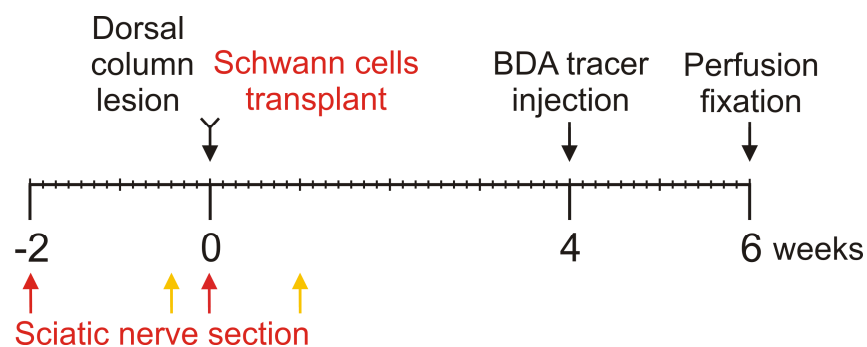


Figure 4-7. Time course of procedures in animals with combined Schwann cell transplantation and conditioning lesions.

Conditioning lesions combined with Schwann cell transplantation were performed following 2 different paradigms used also for OEC transplantation in the previous chapter: i) two conditioning lesions performed two weeks before and at the time of the dorsal column injury; or ii) two conditioning lesions performed three days before and seven days after the spinal cord injury. Results from these three groups were pooled together as no obvious differences were found between them.

4.2.2.1 BDA labelled axons rostral to the spinal cord lesion

BDA labelled fibres rostral to the injury in the lateral cord were detected in all of the animals in this group. Tract tracing was also detected in the medial portion of the spinal cord of all animals. Approximately 100% of fibre counts were associated with Schwann cells (Table 22 and Table 23). The number of

axons located in the medial spinal cord rostral to the lesion was on average 5 times that of non conditioned animals transplanted with Schwann cells as shown the graph depicted in Figure 4-16. This increase was significant and comparable to the 7 fold increase produced by combining conditioning lesions with OEC transplantation paradigm over OEC transplantation alone. Importantly, in addition the absolute number of axons in the Schwann cell and the OEC combined treatment paradigms involving conditioning lesions were similar and not significantly different (Figure 4-16).

| | | Number of axons | | | | | | | | Average | St. Error |
|--|--------------|-----------------|-------|-------|-------|-------|--------|------------|-------------|-------------|-----------|
| | | R0308 | R0408 | R2508 | R3808 | R3908 | R22508 | R22708 | | | |
| Distance from the lesion (μm) | 200 | 9 | 11 | 2 | 47 | 57 | 20 | 89 | 33.6 | 12.0 | |
| | 400 | 12 | 11 | 3 | 51 | 46 | 14 | 70 | 29.6 | 9.7 | |
| | 600 | 7 | 11 | 4 | 40 | 48 | 15 | 54 | 25.6 | 7.9 | |
| | 800 | 10 | 11 | 8 | 51 | 43 | 12 | 37 | 24.6 | 6.9 | |
| | 1000 | 6 | 8 | 5 | 42 | 63 | 8 | 19 | 21.6 | 8.5 | |
| | 1200 | 4 | 11 | 6 | 45 | 74 | 7 | 30 | 25.3 | 9.9 | |
| | 1400 | 3 | 11 | 1 | 47 | 51 | 10 | 22 | 20.7 | 7.7 | |
| | 1600 | 2 | 8 | 2 | 45 | 41 | 9 | 25 | 18.9 | 6.9 | |
| | | | | | | | | | | | |
| | 3200 | 2 | 2 | 2 | 10 | 26 | 1 | 7 | 7.1 | 3.4 | |
| | 3600 | 2 | 1 | 0 | 4 | 17 | 1 | 5 | 4.3 | 2.2 | |
| | 4000 | 0 | 3 | 0 | 7 | 2 | 0 | 1 | 1.9 | 1.0 | |
| | 4400 | 0 | 1 | 0 | 12 | 2 | 1 | 4 | 2.9 | 1.6 | |
| | 4800 | 0 | 1 | 0 | 18 | 0 | 3 | 0 | 3.1 | 2.5 | |
| | | | | | | | | | | | |
| | 10000 | 0 | 0 | 0 | 0 | 0 | 0 | 0 | 0.0 | 0.0 | |
| | 10400 | 0 | 0 | 0 | 0 | 0 | 0 | 0 | 0.0 | 0.0 | |
| 10800 | 0 | 0 | 0 | 0 | 0 | 0 | 0 | 0.0 | 0.0 | | |
| 11200 | 0 | 0 | 0 | 0 | 0 | 0 | 0 | 0.0 | 0.0 | | |
| 11600 | 0 | 0 | 0 | 0 | 0 | 0 | 0 | 0.0 | 0.0 | | |

Table 22. Number of fibres associated with Schwann cells rostral to the dorsal column lesion in the medial spinal cord in animals that received conditioning lesions.

Quantification of axon number rostral to the lesion performed with an epifluorescence microscope and 63x lens on parasagittal sections of the lesion block, rostral block and thoracic block.

| | | Number of axons | | | | | | | | Average | St. Error |
|--|-------|-----------------|-------|-------|-------|-------|--------|--------|-----|---------|-----------|
| | | R0308 | R0408 | R2508 | R3808 | R3908 | R22508 | R22708 | | | |
| Distance from the lesion (μm) | 200 | 0 | 0 | 0 | 0 | 0 | 0 | 0 | 0 | 0.0 | 0.0 |
| | 400 | 0 | 0 | 0 | 0 | 0 | 1 | 0 | 0.1 | 0.1 | |
| | 600 | 0 | 0 | 0 | 0 | 0 | 0 | 0 | 0.0 | 0.0 | |
| | 800 | 0 | 0 | 0 | 0 | 0 | 0 | 0 | 0.0 | 0.0 | |
| | 1000 | 0 | 0 | 0 | 0 | 0 | 0 | 0 | 0.0 | 0.0 | |
| | 1200 | 0 | 0 | 0 | 0 | 0 | 0 | 0 | 0.0 | 0.0 | |
| | 1400 | 0 | 0 | 0 | 0 | 0 | 0 | 0 | 0.0 | 0.0 | |
| | 1600 | 0 | 0 | 0 | 0 | 0 | 1 | 0 | 0.1 | 0.1 | |
| | 3200 | 0 | 0 | 0 | 0 | 0 | 0 | 0 | 0.0 | 0.0 | |
| | 3600 | 0 | 0 | 0 | 0 | 0 | 0 | 1 | 0.1 | 0.1 | |
| | 4000 | 0 | 0 | 0 | 0 | 0 | 0 | 0 | 0.0 | 0.0 | |
| | 4400 | 0 | 0 | 0 | 0 | 0 | 0 | 0 | 0.0 | 0.0 | |
| | 4800 | 0 | 0 | 0 | 0 | 0 | 0 | 1 | 0.1 | 0.1 | |
| | 10000 | 0 | 0 | 0 | 0 | 0 | 0 | 0 | 0.0 | 0.0 | |
| | 10400 | 0 | 0 | 0 | 0 | 0 | 0 | 0 | 0.0 | 0.0 | |
| | 10800 | 0 | 0 | 0 | 0 | 0 | 0 | 0 | 0.0 | 0.0 | |
| | 11200 | 0 | 0 | 0 | 0 | 0 | 0 | 0 | 0.0 | 0.0 | |
| | 11600 | 0 | 0 | 0 | 0 | 0 | 0 | 0 | 0.0 | 0.0 | |

Table 23. Number of fibres not associated with Schwann cells rostral to the dorsal column lesion in the medial spinal cord in animals that received conditioning lesions.

Quantification of axon number rostral to the lesion performed with an epifluorescence microscope and 63x lens on parasagittal sections of the lesion block, rostral block and thoracic block.

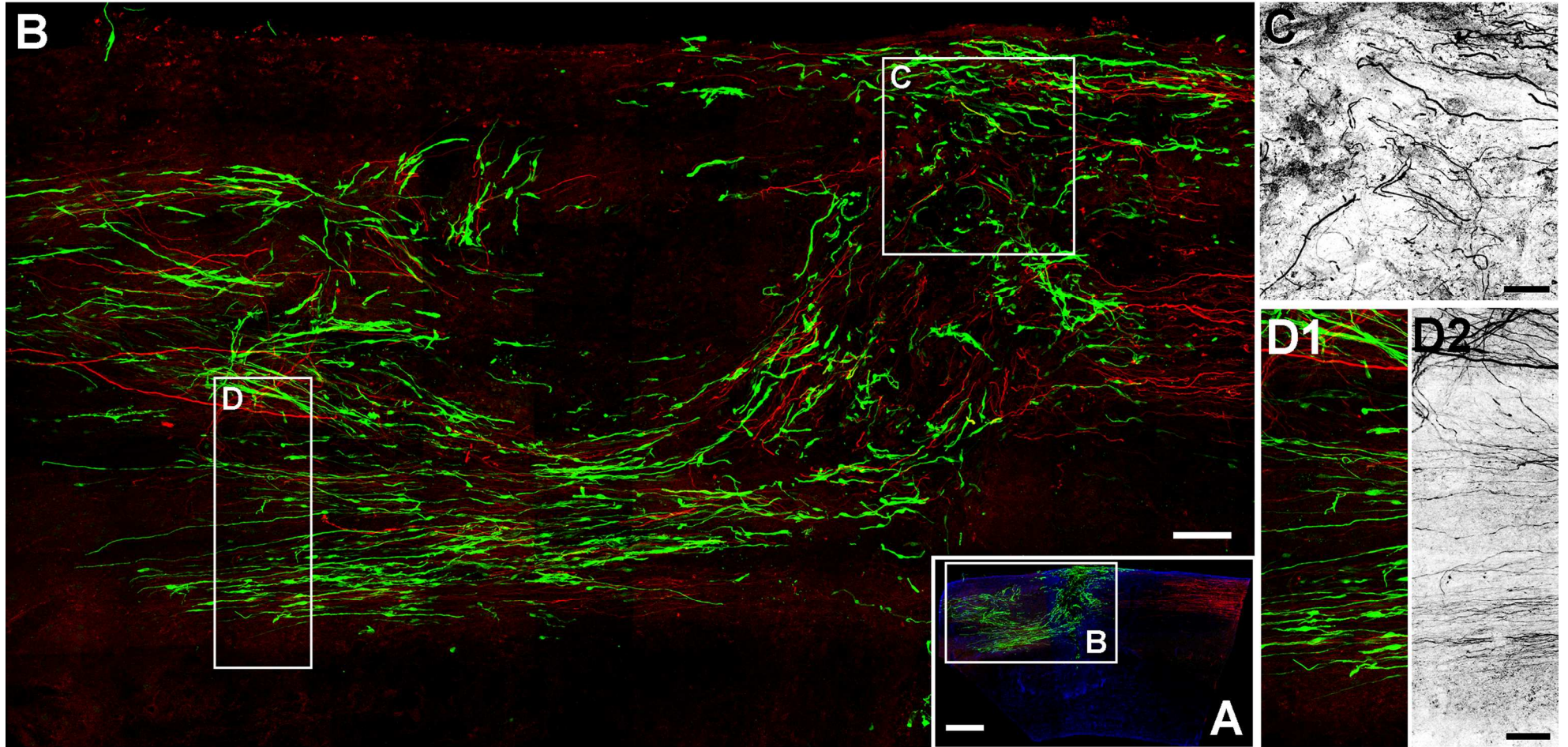
4.2.2.2 Genuine regenerating BDA labelled fibres rostral to the lesion level

To include in the analysis only convincing regeneration, axons located rostral to the lesion that were potentially spared or sprouting were excluded. The quantification is shown in Table 24 and shows that genuine regeneration was detected in 6 of the 7 animals where BDA labelling was originally found in the medial cord (an example is shown in Figure 4-17). Regenerating fibres were all located in the vicinity of GFP labelled Schwann cells. When combined with conditioning lesions, Schwann cell transplanted animals were associated with a comparable level of regeneration to that of OEC transplanted animals (Figure 4-18).

It was found that no rats possessed Schwann cell tracts that were devoid of BDA labelling. Furthermore, Schwann cells supported regenerating axons up to the end of the continuous cell tracts. On average the cell tracts were 4000 μm long and also the furthest rostral regenerating axons ended growing on average at 4000 μm rostral to the lesion.

Figure 4-8. Axons regenerating in a tract of Schwann cells rostral to the lesion following conditioning lesions.

A) Image taken with a low power objective (10x) of a parasagittal section of the lesion block in a rat transplanted with Schwann cells; boxed area is depicted at higher magnification (40x) in **B**. **B)** Axons approached the caudal end of the dorsal column transection and bridged the lesion to the other side within the Schwann cell tract. **C)** Enlarged image of the boxed area in **B** that shows axons regenerating in the lesion in greyscale. **D1-D2)** Enlarged images of the boxed area shown in **B** profuse regeneration within the GFP positive cell tract; **D2** depicts BDA labelled regenerating axons in greyscale. **A-D)** Composite of confocal projected image stacks. Colour codes: red (axons), green (Schwann cells), blue (astrocytes). Scale bar: 500 μm in **A**, 100 μm in **B** and μm 50 in **C-D**.



| | | Number of axons | | | | | | | | Average | St. Error |
|--|--------------|-----------------|-------|-------|-------|-------|--------|--------|-------------|-------------|-----------|
| | | R0308 | R0408 | R2508 | R3808 | R3908 | R22508 | R22708 | | | |
| Distance from the lesion (μm) | 200 | 9 | 11 | 2 | 47 | 57 | - | 89 | 35.8 | 14.0 | |
| | 400 | 12 | 11 | 3 | 51 | 46 | - | 70 | 32.2 | 11.1 | |
| | 600 | 7 | 11 | 4 | 40 | 48 | - | 54 | 27.3 | 9.2 | |
| | 800 | 10 | 11 | 8 | 51 | 43 | - | 37 | 26.7 | 7.8 | |
| | 1000 | 6 | 8 | 5 | 42 | 63 | - | 19 | 23.8 | 9.7 | |
| | 1200 | 4 | 11 | 6 | 45 | 74 | - | 30 | 28.3 | 11.2 | |
| | 1400 | 3 | 11 | 1 | 47 | 51 | - | 22 | 22.5 | 8.9 | |
| | 1600 | 2 | 8 | 2 | 45 | 41 | - | 25 | 20.5 | 7.9 | |
| | | | | | | | | | | | |
| | 3200 | 2 | 2 | - | 10 | 26 | - | 7 | 8.0 | 3.9 | |
| | 3600 | 2 | 1 | - | 4 | 17 | - | 5 | 5.0 | 2.5 | |
| | 4000 | 0 | 3 | - | 7 | 2 | - | 1 | 2.6 | 1.2 | |
| | 4400 | - | 1 | - | 12 | 2 | - | 4 | 4.8 | 2.5 | |
| | 4800 | - | 1 | - | 18 | - | - | - | 9.5 | 8.5 | |
| | | | | | | | | | | | |
| | 10000 | - | - | - | - | - | - | - | - | - | |
| 10400 | - | - | - | - | - | - | - | - | - | | |
| 10800 | - | - | - | - | - | - | - | - | - | | |
| 11200 | - | - | - | - | - | - | - | - | - | | |
| 11600 | - | - | - | - | - | - | - | - | - | | |

Table 24. Number of regenerating fibres rostral to the dorsal column lesion in the medial spinal cord associated with Schwann cells in animals treated with conditioning lesions.

Quantification of axon number rostral to the lesion performed with an epifluorescence microscope and 63x lens on parasagittal sections of the lesion block, rostral block and thoracic block. Blank cells are used to indicate that data did not meet the inclusion criteria or fit the stringency applied.

4.2.3 Sciatic nerve (SN) fibroblast transplantation combined with conditioning lesions

It has been suggested by Raisman that olfactory bulb fibroblast-like cells can aid OECs repair (Li et al., 1998). In some cases researches have used skin derived fibroblast for transplant mediated repair but comparison with fibroblast from the sciatic nerve has not been done except by Raisman's group (Keyvan-Fouldai et al., 2003, 2005). The fibroblast, being a non-glial cell type, would not be expected to produce results equivalent to those found in this study following glial cell transplantation. For this reason a comparison was made of the axonal growth promoting properties and the neuroprotective properties observed of OECs and Schwann cells to sciatic nerve derived purified populations of fibroblasts. Six rats were injected immediately after the wire knife dorsal column injury with sciatic nerve derived fibroblasts (Figure 4-9). All animals received two conditioning lesions performed 3 days before and seven days after the dorsal column injury. Four weeks after the transection of the dorsal columns all animals were injected with the tract tracer and perfusion fixation took place 2 more weeks later.

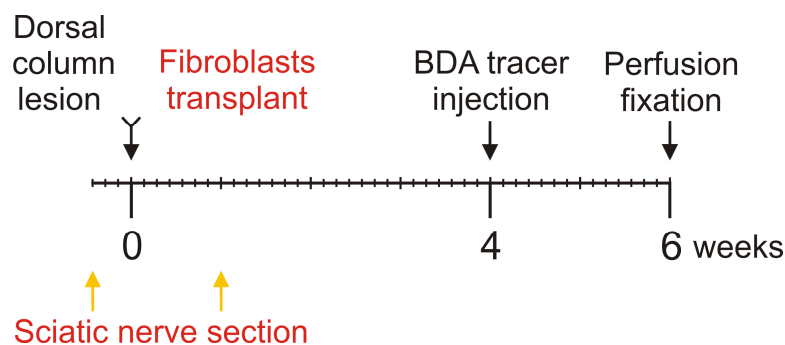


Figure 4-9. Time course of procedures performed on animals transplanted with SN fibroblasts.

Any residual growth promoting properties fibroblasts had were maximised in this study by combining transplantation with sciatic nerve transection.

4.2.3.1 Characterization of the lesion after a SN fibroblast transplant

Transplanted SN fibroblasts filled the injection site in four animals where the cavity was not at all present and partially filled the injection site of two more animals (Figure 0-12A). The lesion cavity was on average 8 times smaller than the lesion size defined by GFAP labelling ($P=0.010$). As shown in Figure 0-13, the lesion cavity size was reduced 13 fold in fibroblast transplanted animals compared to non-transplanted animals ($P=0.0007$) while it was respectively 6 and 7 times smaller than in OEC and Schwann cell transplanted animals ($P=0.045$ and $P=0.0048$ respectively). Even the lesion size was smaller in fibroblast transplanted animals than in animals of all the other treatment groups. In particular, the lesion size was reduced 1.7 times compared to animals that did not receive a cell transplant ($P=0.014$). When comparing the lesion size of rats transplanted with fibroblasts with that of rats transplanted with OECs or Schwann cells the lesion size was significantly smaller (Figure 0-13).

Although transplantation of fibroblasts was associated with a reduction of the lesion size and lesion cavity size, it was also associated with a pronounced modification of the lesion morphology under epifluorescence and light microscopy (Figure 4-10 Figure 4-11). In fact the typical GFAP borders found in the paradigms considered previously in this work were lost as the astrocytes in the nearby spinal cord tissue became oriented towards the lesion. This reactive effect might have had a detrimental effect on nearby neurons and fibres limiting regeneration.

4.2.3.2 Characterization of central canal cavitation

Central canal cavitation was observed in the majority of animals receiving a fibroblast transplant and developed mostly rostral to the lesion (Figure 0-12). No significant difference in the extent of cavitation was found between the rostral end of the lesion block, the rostral block and the thoracic block. When a comparison was made of the central canal cavitation size to that of non-transplanted animals (Figure 4-14) it was possible to detect a reduction in size at the lumbar and thoracic level which was comparable to the reduction seen after OECs or Schwann cell transplantation, however this difference was not significant.

Figure 4-10. Lesion morphology and size after a SN fibroblast transplant.

Composite of confocal image stacks depicting the deleterious effects of fibroblast transplantation on the lesion environment. Orientation of GFAP labelled astrocytes in the spinal cord surrounding the lesion was directed towards the lesion. This very unusual feature, visible even better under darkfield view in the next figure, was not observed in non-transplanted animals or in the other treatment groups. Scale bar: 200 μm .

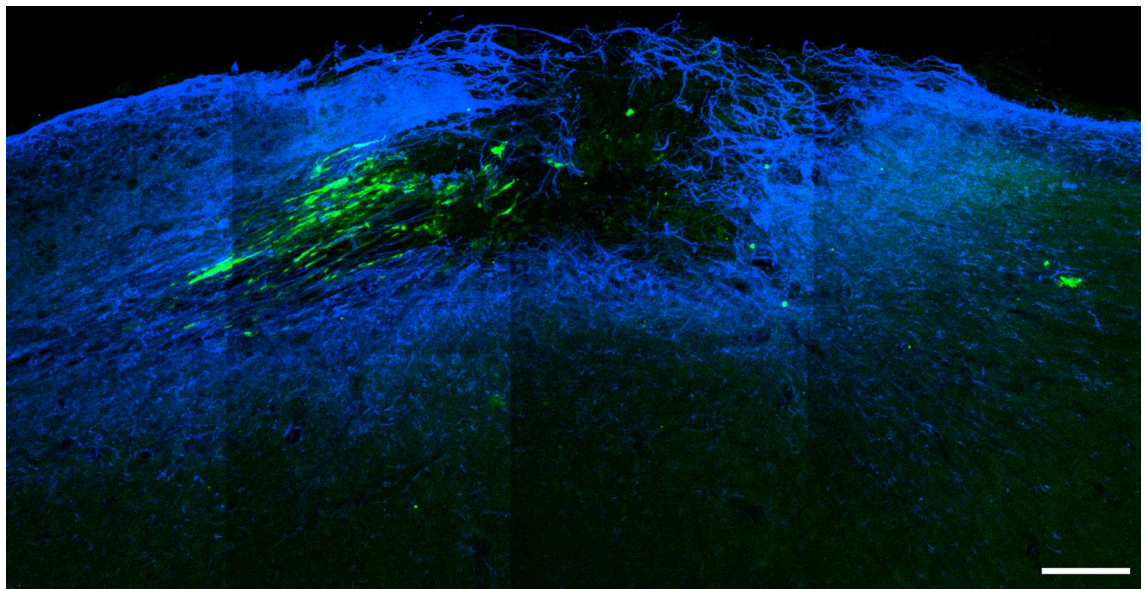
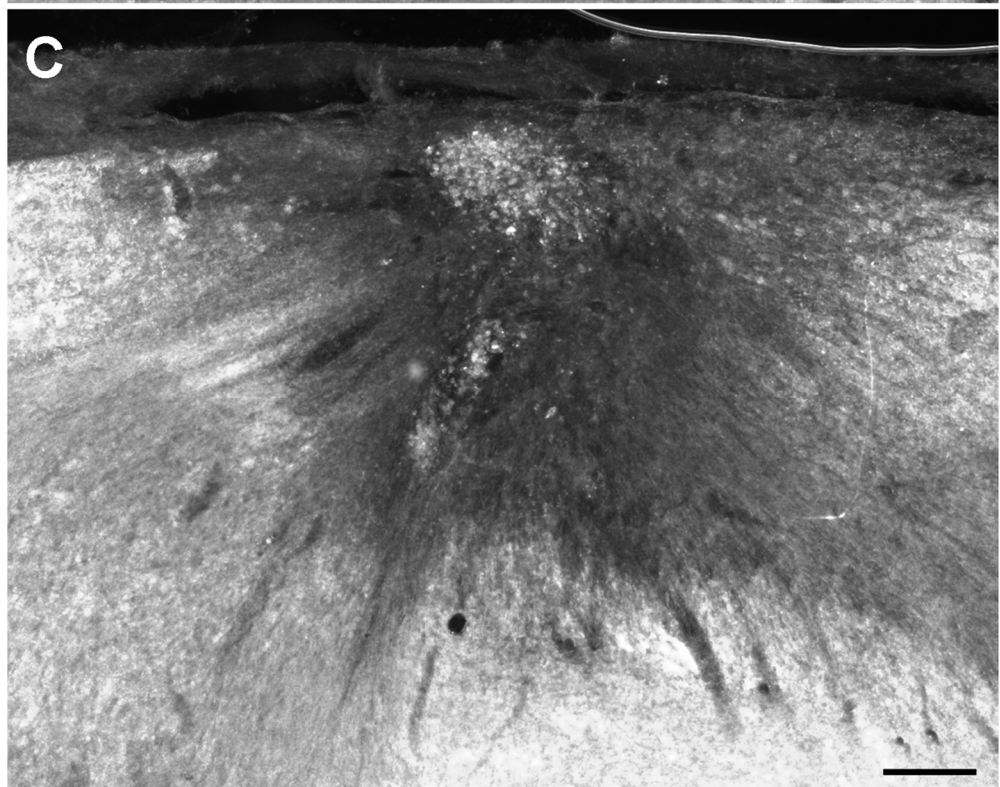
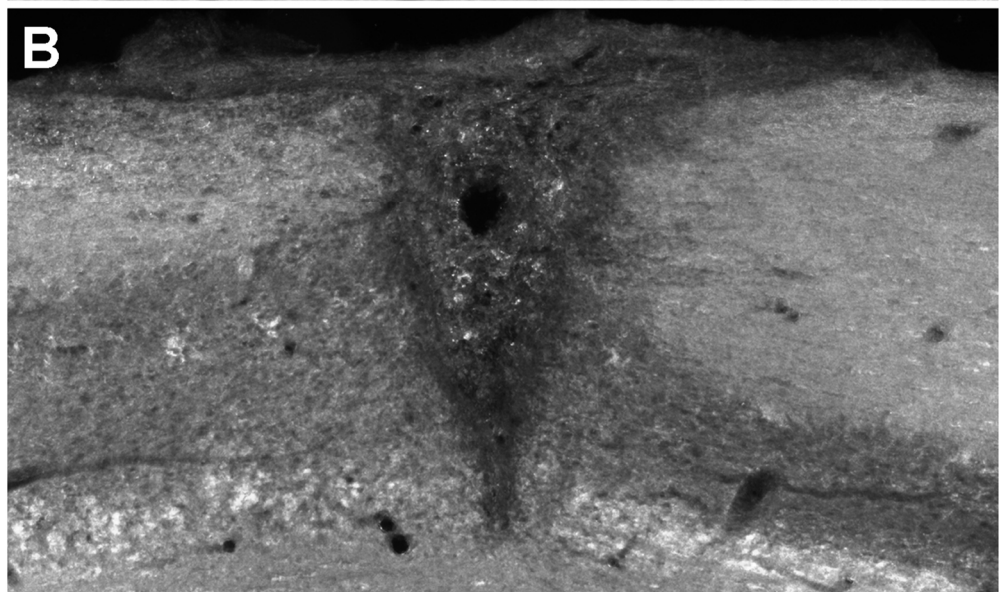
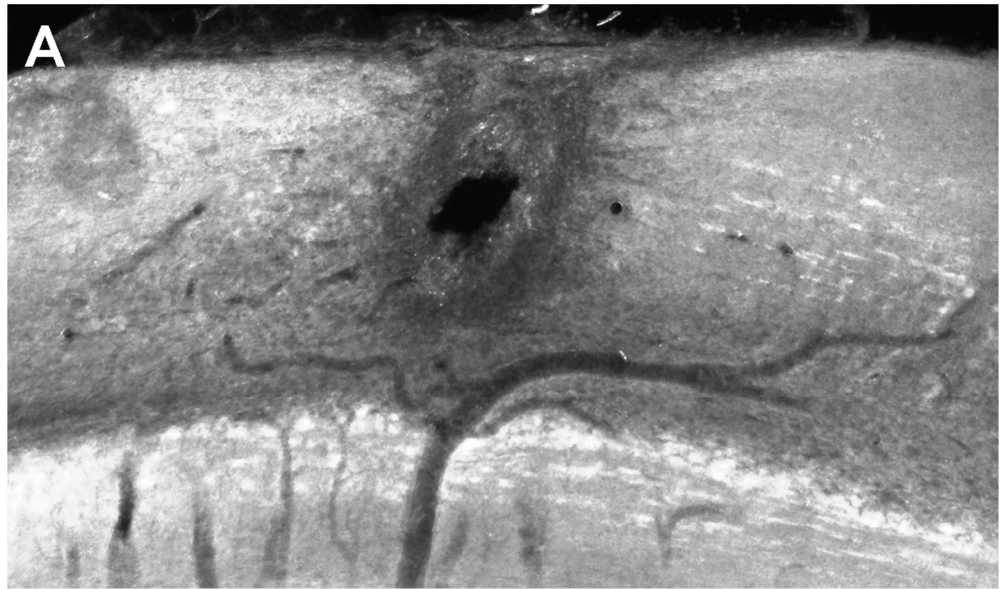


Figure 4-11. Effects of fibroblasts on morphology of the spinal cord tissue surrounding the lesion compared to that of OECs and Schwann cells 6 weeks after the dorsal column lesion/transplantation.

Images taken with a Nikon Eclipse microscope coupled with light microscopy and dark field view with a 4x objective and a Zeiss Axiocam camera. After transplantation of fibroblasts (C) the tissue surrounding the lesion appeared as traversed by lines that were directed towards the centre of the lesion. This effect was not observed after OEC (A) and Schwann cell (B) transplantation. Scale bar: 200 μm .



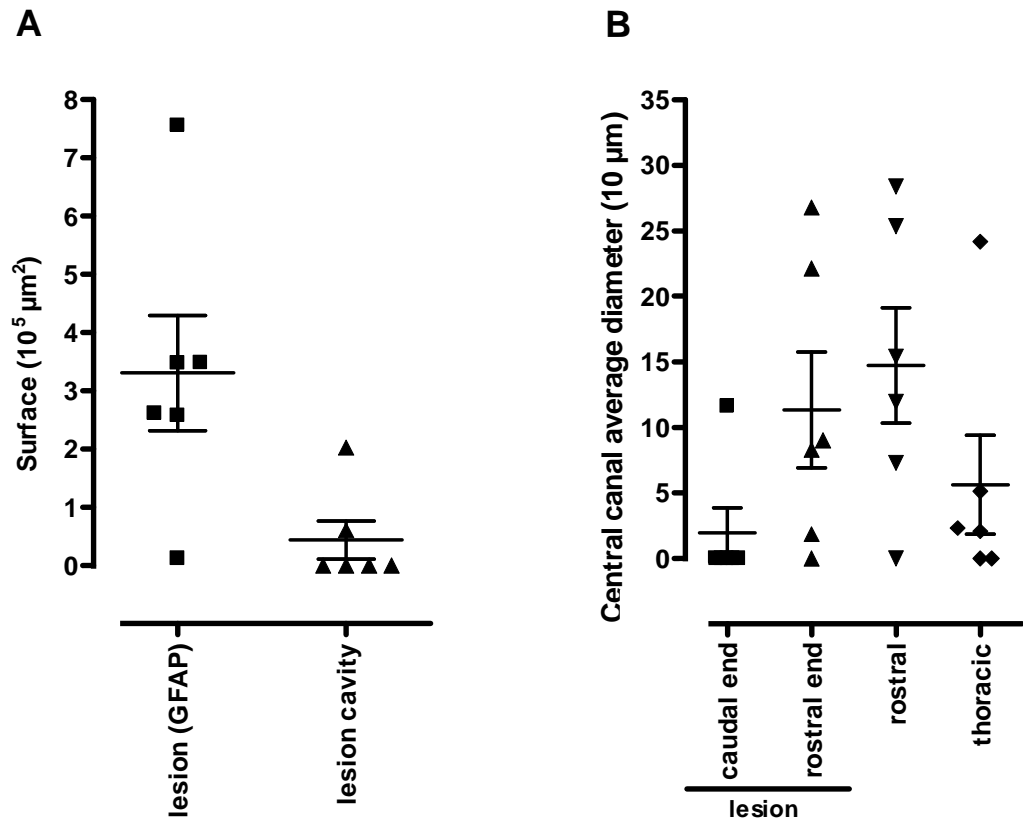


Figure 0-12. Lesion and central canal characterization 6 weeks after a dorsal column injury and fibroblast transplantation.

A) Scatter dot plot showing that the size of the lesion cavity was significantly smaller than the size of the lesion defined by the GFAP labelling ($P=0.010$). **B)** Cavitations formed in the central canal especially rostral to the injury level. No significant difference was found between the rostral end of the lesion block and the rostral block ($P=0.52$), nor between the rostral end of the lesion block and the thoracic block ($P=0.39$), nor between the rostral and thoracic blocks ($P=0.21$).

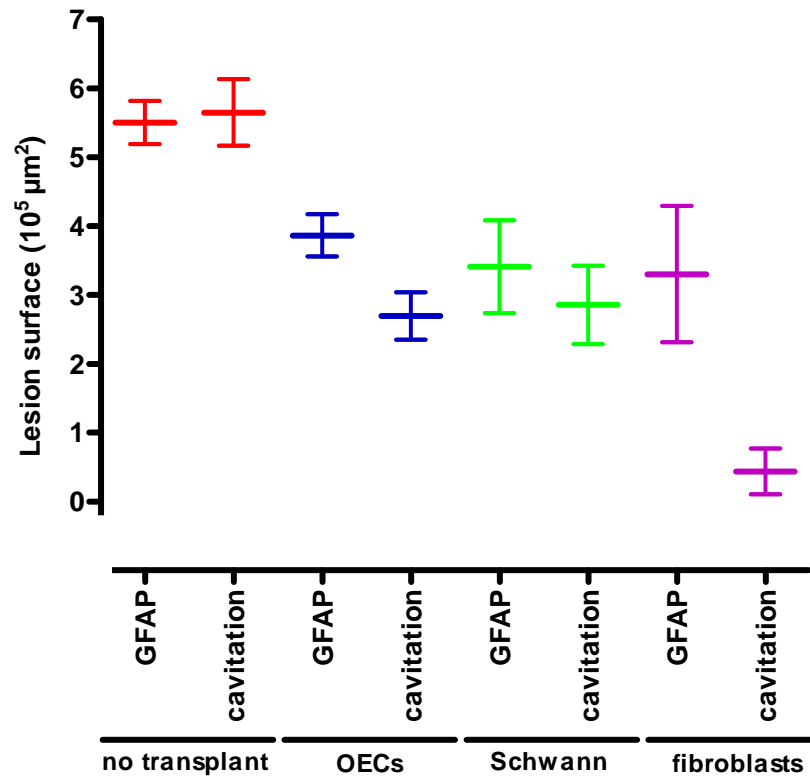


Figure 0-13. Comparison between lesion size and lesion cavity size of animals with a six week survival transplanted with Schwann cells, SN fibroblasts, OECs or of non-transplanted animals.

Schwann cell transplantation was associated with a significant reduction of the lesion size ($P=0.029$) and lesion cavity size ($P=0.0024$) when compared to non-transplanted animals; in fact, the size of the lesion and of the lesion cavity was similar to that found after OEC transplanted rats ($P=0.48$ and $P=0.82$ respectively). In addition after transplantation of SN fibroblasts a significant reduction in the lesion size ($P=0.014$) and lesion cavitation ($P=0.0007$) was found when compared to non-transplanted animals; the lesion size was not reduced when transplantation of fibroblast was compared to OEC ($P=0.55$) or Schwann cell transplantation ($P=0.94$); instead there was a significant difference between the degree of lesion cavitation in SN fibroblast transplanted rats when compared to that found when transplanted with OECs ($P=0.0048$) or Schwann cells ($P=0.045$).

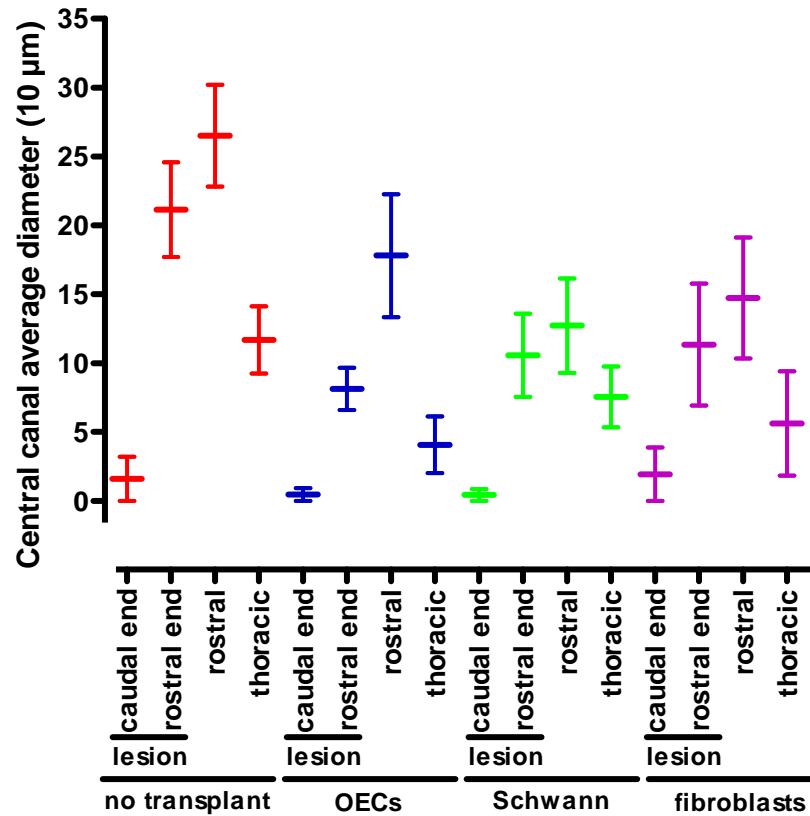


Figure 4-14. Comparison of syringomyelia formed in animals with a six week survival transplanted with Schwann cells, fibroblasts or OECs and non-transplanted animals.

Schwann cell transplantation was found to reduce significantly the degree of central canal cavitation in the rostral end of the lesion block ($P=0.015$) and in the rostral block ($P=0.014$) but not in the thoracic block ($P=0.056$) when compared to non-transplanted animals. The variation in cavitation was not significantly different between Schwann cell and OEC transplantation paradigms in the rostral end of the lesion block ($P=0.67$), the rostral blocks ($P=0.47$) and the thoracic blocks ($P=0.84$). Although transplantation of fibroblast was associated with a strong reduction of central canal size compared to non-transplanted animals, the difference was not significant for the rostral end of the lesion block ($P=0.14$), or for the rostral block ($P=0.063$), or for the thoracic block ($P=0.063$). Comparison between animals transplanted with SN fibroblasts and OECs showed no significant variation in cavitation in the rostral end of the lesion block, the rostral blocks and the thoracic blocks ($P=0.29$, $P=0.79$ and $P=0.85$ respectively). The variation was not significant also when comparing syringomyelia formation in SN fibroblast and Schwann cell transplantation paradigms in the rostral end of the lesion block, rostral blocks and thoracic blocks ($P=0.52$, $P=0.40$ and $P=0.94$ respectively).

4.2.3.3 Distribution of SN fibroblasts in the spinal cord

SN fibroblasts were distributed in the spinal cord of 67% (4/6) of animals rostral to the lesion and in all (6/6) animals caudal to the lesion. The cell distribution extended to the rostral block in half of the animals but no GFP labelled cells were detected at the thoracic level. It was not possible to define the position of fibroblasts with regards to white matter or grey matter because under the dark field view fibroblasts disrupted the typical appearance not only of the regions they reside in but also nearby regions of the spinal cord.

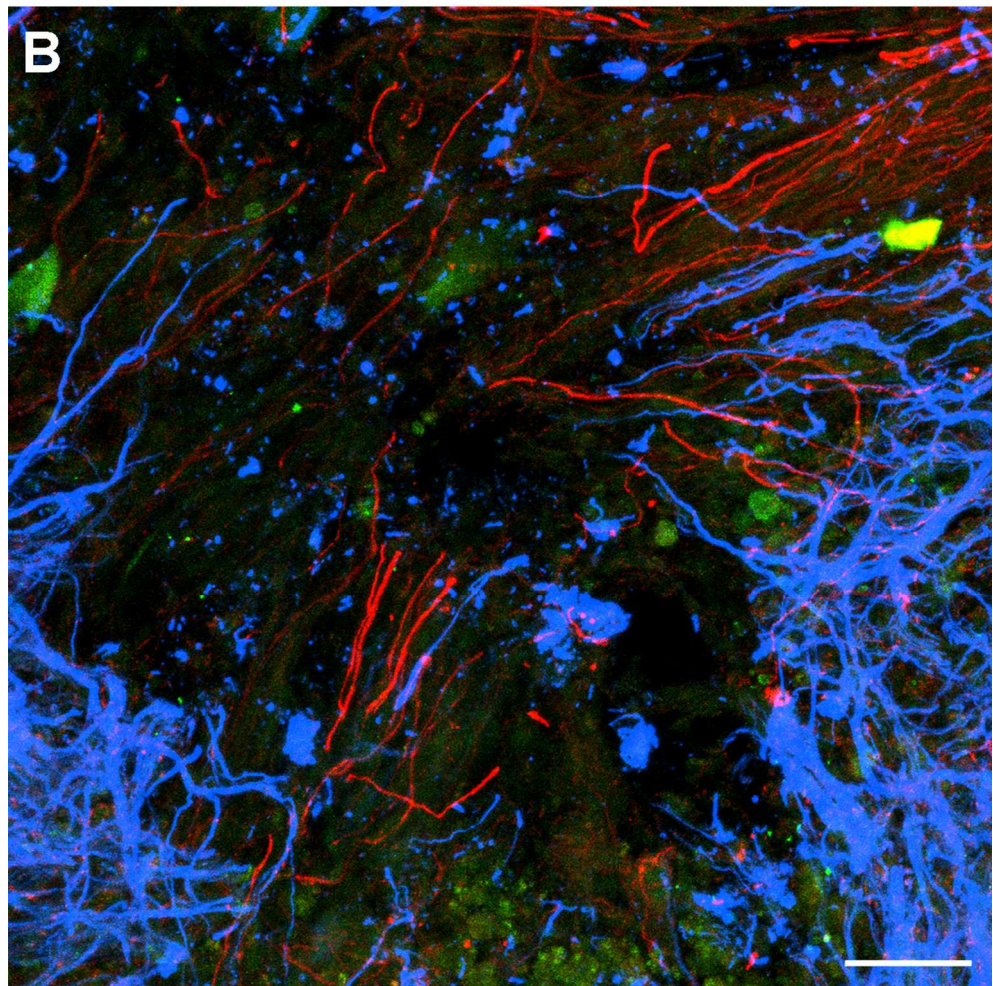
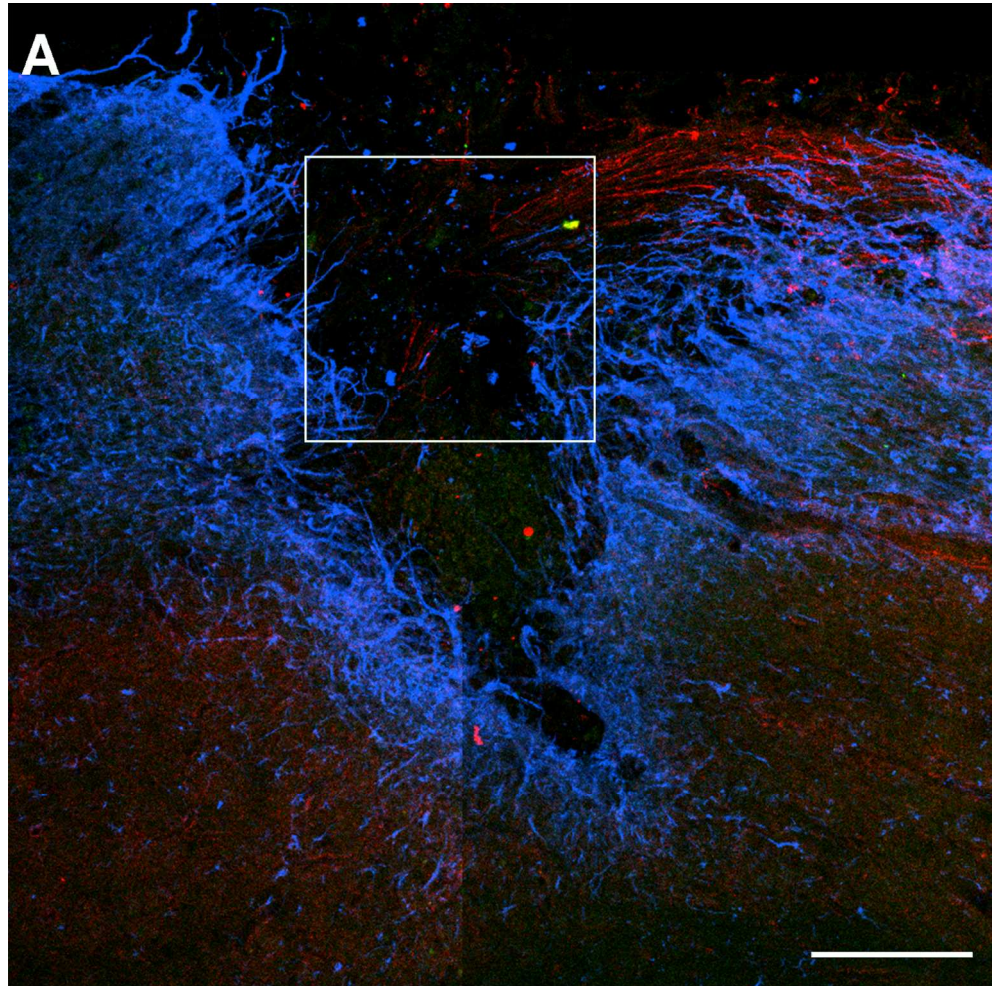
Surprisingly SN fibroblasts formed continuous tracts of GFP expressing cells extending out of the lesion. These were observed in 50% (3/3) of animals but the tracts never extended into the rostral block. The average distance the continuous tracts covered was 1270 μm from the injury. It must be noted that GFP expression did not appear to be as strong in individual fibroblasts as that observed for individual OECs or Schwann cells, possibly due to the large cytoplasm of fibroblasts which diluted the GFP protein. For this reason the distribution of SN fibroblasts could possibly be more extensive than that described in this analysis.

4.2.3.4 Regeneration of BDA labelled fibres within the transplant

Some regeneration of BDA labelled axons was detected in the transplant site of all animals injected with fibroblasts (6/6): an example is shown in Figure 4-15. As observed for OEC and Schwann cell transplants, regenerating axons were oriented randomly.

Figure 4-15. Axonal regeneration in a lesion transplanted with SN fibroblasts.

A: Composite of confocal projected images (objective 20x) that depict regeneration of BDA labelled axons (red) in the lesion site, outlined by GFAP labelling (blue), showing poor fibroblast integration (green). **B:** Higher magnification (40x) of boxed area in **A** showing axonal regeneration into the lesion. Note that very few GFP labelled fibroblasts were present in the lesion. Scale bars: 100 μm in **A** and 25 μm in **B**.



4.2.3.5 BDA labelled axons rostral to the spinal cord lesion

BDA labelled tract traced axons were located in the lateral cord rostral to the dorsal column transection in all animals. BDA labelled axons were also detected in the medial portion of the cord of 4 out of 6 animals. Following quantification of axons on parasagittal sections using epifluorescence microscopy (Table 25 and Table 26) it was possible to note that 62% of the counted axons were associated with GFP labelled fibroblasts while the remaining were located in areas devoid of GFP labelled cells, however this was mostly observed in one animal where the axons localised on the border with the lateral cord and were presumably spared. The number of BDA labelled axons rostral to the lesion was significantly lower in conditioning lesioned animals transplanted with fibroblasts compared to those of conditioning lesioned animals transplanted with OECs or Schwann cells (Figure 4-16): this decrease was on average 17 and 21 fold respectively. Nonetheless, fibroblasts combined with conditioning lesion were more effective than conditioning lesion alone at promoting regeneration/sprouting in the medial spinal cord; in fact a 3 fold average increase was found however this was non-significant (Figure 4-16).

| | Number of axons | | | | | | | | |
|--|-----------------|---------|---------|---------|---------|---------|---------|-----------|-----|
| | R 18508 | R 18608 | R 18708 | R 19108 | R 19208 | R 19408 | Average | St. Error | |
| Distance from the lesion (μm) | 200 | 0 | 5 | 0 | 0 | 10 | 0 | 2.5 | 1.7 |
| | 400 | 0 | 5 | 0 | 0 | 12 | 0 | 2.8 | 2.0 |
| | 600 | 0 | 3 | 0 | 0 | 1 | 0 | 0.7 | 0.5 |
| | 800 | 0 | 4 | 0 | 0 | 5 | 0 | 1.5 | 1.0 |
| | 1000 | 0 | 1 | 0 | 0 | 4 | 0 | 0.8 | 0.7 |
| | 1200 | 0 | 1 | 0 | 0 | 4 | 0 | 0.8 | 0.7 |
| | 1400 | 0 | 0 | 0 | 0 | 3 | 0 | 0.5 | 0.5 |
| | 1600 | 0 | 0 | 0 | 0 | 2 | 0 | 0.3 | 0.3 |
| | 3200 | 0 | 0 | 0 | 0 | 0 | 0 | 0.0 | 0.0 |
| | 3600 | 0 | 0 | 0 | 0 | 0 | 0 | 0.0 | 0.0 |
| | 4000 | 0 | 0 | 0 | 0 | 0 | 0 | 0.0 | 0.0 |
| | 4400 | 0 | 0 | 0 | 0 | 0 | 0 | 0.0 | 0.0 |
| | 4800 | 0 | 0 | 0 | 0 | 0 | 0 | 0.0 | 0.0 |
| | 10000 | 0 | 0 | 0 | 0 | 0 | 0 | 0.0 | 0.0 |
| | 10400 | 0 | 0 | 0 | 0 | 0 | 0 | 0.0 | 0.0 |
| | 10800 | 0 | 0 | 0 | 0 | 0 | 0 | 0.0 | 0.0 |
| | 11200 | 0 | 0 | 0 | 0 | 0 | 0 | 0.0 | 0.0 |
| | 11600 | 0 | 0 | 0 | 0 | 0 | 0 | 0.0 | 0.0 |

Table 25. Number of tract traced fibres associated with fibroblasts rostral to the lesion in the medial spinal cord.

Quantification of axon number rostral to the lesion performed with an epifluorescence microscope and 63x lens on parasagittal sections of the lesion block, rostral block and thoracic block.

| | Number of axons | | | | | | | | |
|--|-----------------|---------|---------|---------|---------|---------|---------|-----------|--|
| | R 18508 | R 18608 | R 18708 | R 19108 | R 19208 | R 19408 | Average | St. Error | |
| Distance from the lesion (μm) | 200 | 5 | 0 | 0 | 0 | 0 | 0.8 | 0.8 | |
| | 400 | 3 | 0 | 0 | 0 | 0 | 0.5 | 0.5 | |
| | 600 | 5 | 0 | 0 | 0 | 0 | 0.8 | 0.8 | |
| | 800 | 10 | 0 | 0 | 0 | 0 | 1.7 | 1.7 | |
| | 1000 | 6 | 0 | 0 | 0 | 0 | 1.0 | 1.0 | |
| | 1200 | 6 | 1 | 0 | 0 | 0 | 1.2 | 1.0 | |
| | 1400 | 0 | 0 | 0 | 0 | 0 | 0.0 | 0.0 | |
| | 1600 | 0 | 0 | 0 | 0 | 0 | 0.0 | 0.0 | |
| | 3200 | 0 | 0 | 0 | 0 | 0 | 0.0 | 0.0 | |
| | 3600 | 0 | 0 | 0 | 1 | 0 | 0.2 | 0.2 | |
| | 4000 | 0 | 0 | 0 | 0 | 0 | 0.0 | 0.0 | |
| | 4400 | 0 | 0 | 0 | 0 | 0 | 0.0 | 0.0 | |
| | 4800 | 0 | 0 | 0 | 0 | 0 | 0.0 | 0.0 | |
| | 10000 | 0 | 0 | 0 | 0 | 0 | 0.0 | 0.0 | |
| | 10400 | 0 | 0 | 0 | 0 | 0 | 0.0 | 0.0 | |
| | 10800 | 0 | 0 | 0 | 0 | 0 | 0.0 | 0.0 | |
| | 11200 | 0 | 0 | 0 | 0 | 0 | 0.0 | 0.0 | |
| 11600 | 0 | 0 | 0 | 0 | 0 | 0.0 | 0.0 | | |

Table 26. Number of tract traced fibres not associated with fibroblasts rostral to the lesion in the medial spinal cord.

Quantification of axon number rostral to the lesion performed with an epifluorescence microscope and 63x lens on parasagittal sections of the lesion block, rostral block and thoracic block.

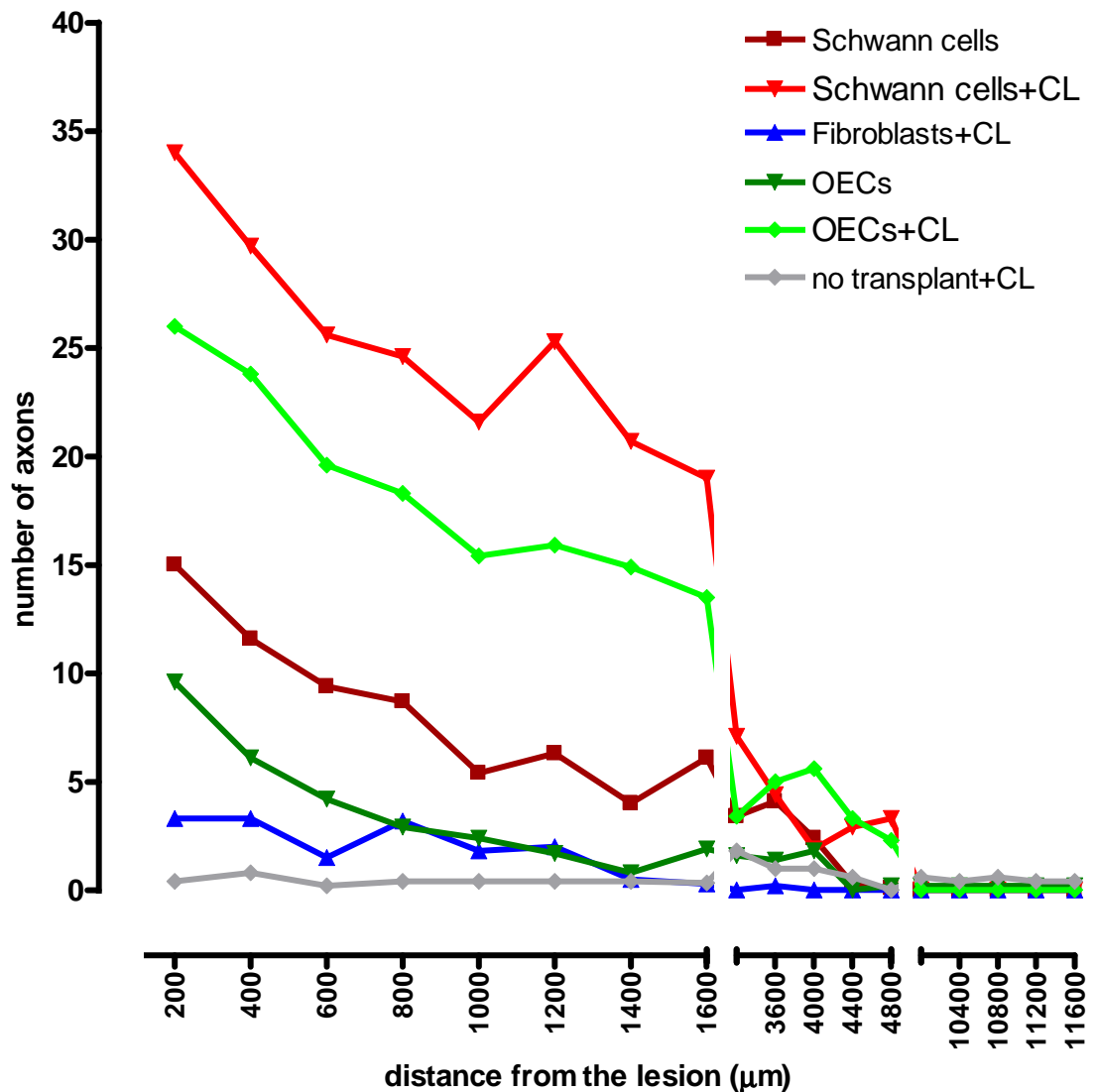


Figure 4-16. Comparison of the number of BDA labelled axons in medial cord rostral to the lesion in Schwann cell, OEC, SN fibroblast transplanted and non-transplanted animals.

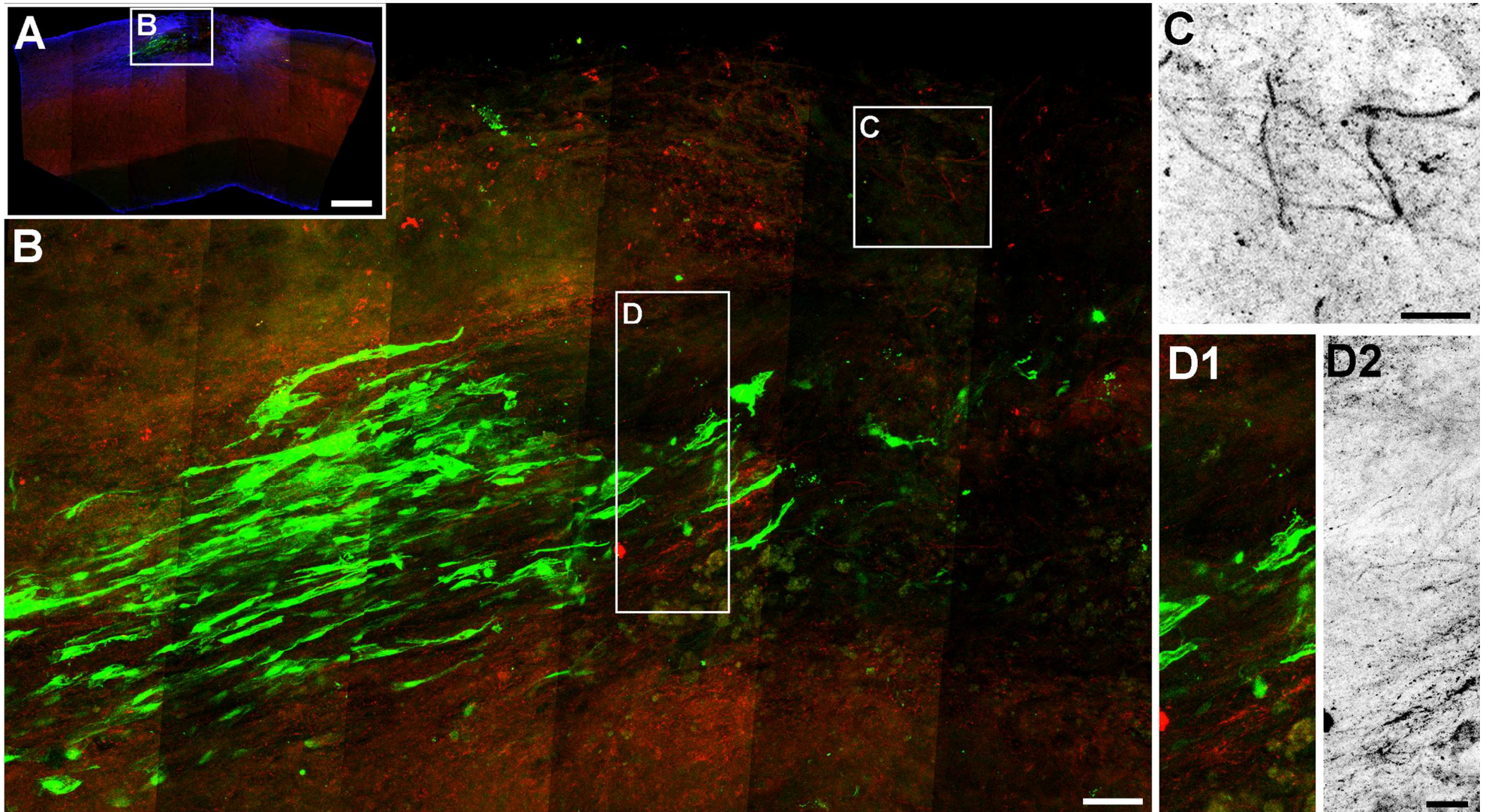
A significant difference was found in the number of BDA labelled fibres, between the Schwann cell transplantation paradigm and combined Schwann cell transplantation and conditioning lesion paradigm at a distance of 1200 µm from the lesion ($P < 0.05$). Conditioning lesioned-Schwann cell transplanted animals were associated with a significantly higher number of BDA labelled axons compared to conditioning lesioned non-transplanted animals at 1400 and 3200 µm ($P < 0.05$) and at 200, 400, 600, 800, 1000 and 1200 µm ($P < 0.005$) from the lesion. The curves were not significantly different at any distance examined between Schwann cell and OEC transplantation paradigms. Transplantation of fibroblasts combined with sciatic nerve transections was associated with a significantly lower number of fibres compared to conditioning lesioned Schwann cell transplanted animals at 200, 400 and 3600 µm ($P < 0.05$) and 600, 800, 1000, 1200 and 1400 µm ($P < 0.005$) distances from the lesion. Similarly, the difference exerted by fibroblasts and OEC injection coupled with conditioning lesions was significant at 1400 µm ($P < 0.05$), while no significant difference was found between conditioning lesioned non-transplanted animals with those transplanted with fibroblast.

4.2.3.6 Genuine long distance regeneration in SN fibroblast transplanted animals

Convincing regeneration across the graft (Table 27) was detected in 2 of the 3 animals where BDA labelling was originally found in the medial cord rostral to the injury (example in Figure 4-17). Regeneration correlated with the presence of continuous fibroblast tracts in these animals. Long distance regeneration when conditioning lesions were combined with transplantation of fibroblasts was 17 and 16 times less vigorous than that detected following respectively OECs and Schwann cell transplantation combined with sciatic nerve transection (Figure 4-18). In particular the difference in regeneration compared to the conditioning lesioned Schwann cell transplanted paradigm was significant at multiple distances from the lesion ($P < 0.05$).

Figure 4-17. Regenerating axons in a tract of fibroblasts rostral to the lesion following conditioning lesions.

A) Confocal image taken with a low power objective (10x) of a parasagittal section of the lesion block in a rat transplanted with SN fibroblasts; boxed area is depicted at higher magnification (40x) in **B**. **B)** Bridging long distance axonal regeneration was detected after fibroblast transplantation. **C)** Enlarged image of the boxed area shown in **B** that shows axons regenerating in the lesion in greyscale. **D1-D2)** Enlarged images of the boxed area shown in **B**; BDA labelled regenerating axons are depicted in greyscale in **D2**. **A-D)** composite of confocal projected image stacks. Colour codes: red (axons), green (fibroblasts), blue (astrocytes). Scale bars: 500 μm in **A**, 50 μm in **B** and 25 μm in **C-D**.



| | | Number of axons | | | | | | Average | St. Error |
|--|-------|-----------------|--------|--------|--------|--------|--------|---------|-----------|
| | | R18508 | R18608 | R18708 | R19108 | R19208 | R19408 | | |
| Distance from the lesion (μm) | 200 | - | 5 | - | 0 | 10 | - | 0.8 | 0.8 |
| | 400 | - | 5 | - | 0 | 12 | - | 0.5 | 0.5 |
| | 600 | - | 3 | - | 0 | 1 | - | 0.8 | 0.8 |
| | 800 | - | 4 | - | 0 | 5 | - | 1.7 | 1.7 |
| | 1000 | - | 1 | - | 0 | 4 | - | 1.0 | 1.0 |
| | 1200 | - | 1 | - | 0 | 4 | - | 1.2 | 1.0 |
| | 1400 | - | 0 | - | 0 | 3 | - | 0.0 | 0.0 |
| | 1600 | - | 0 | - | 0 | 2 | - | 0.0 | 0.0 |
| | 3200 | - | - | - | - | - | - | 0.0 | 0.0 |
| | 3600 | - | - | - | - | - | - | 0.2 | 0.2 |
| | 4000 | - | - | - | - | - | - | 0.0 | 0.0 |
| | 4400 | - | - | - | - | - | - | 0.0 | 0.0 |
| | 4800 | - | - | - | - | - | - | 0.0 | 0.0 |
| | 10000 | - | - | - | - | - | - | 0.0 | 0.0 |
| | 10400 | - | - | - | - | - | - | 0.0 | 0.0 |
| | 10800 | - | - | - | - | - | - | 0.0 | 0.0 |
| | 11200 | - | - | - | - | - | - | 0.0 | 0.0 |
| 11600 | - | - | - | - | - | - | 0.0 | 0.0 | |

Table 27. Number of genuine regenerating fibres rostral to the lesion in the medial spinal cord associated with fibroblasts.

Quantification of axon number rostral to the lesion performed with an epifluorescence microscope and 63x lens on parasagittal sections of the lesion block, rostral block and thoracic block. Blank cells are used to indicate that data did not meet the inclusion criteria or the stringency applied.

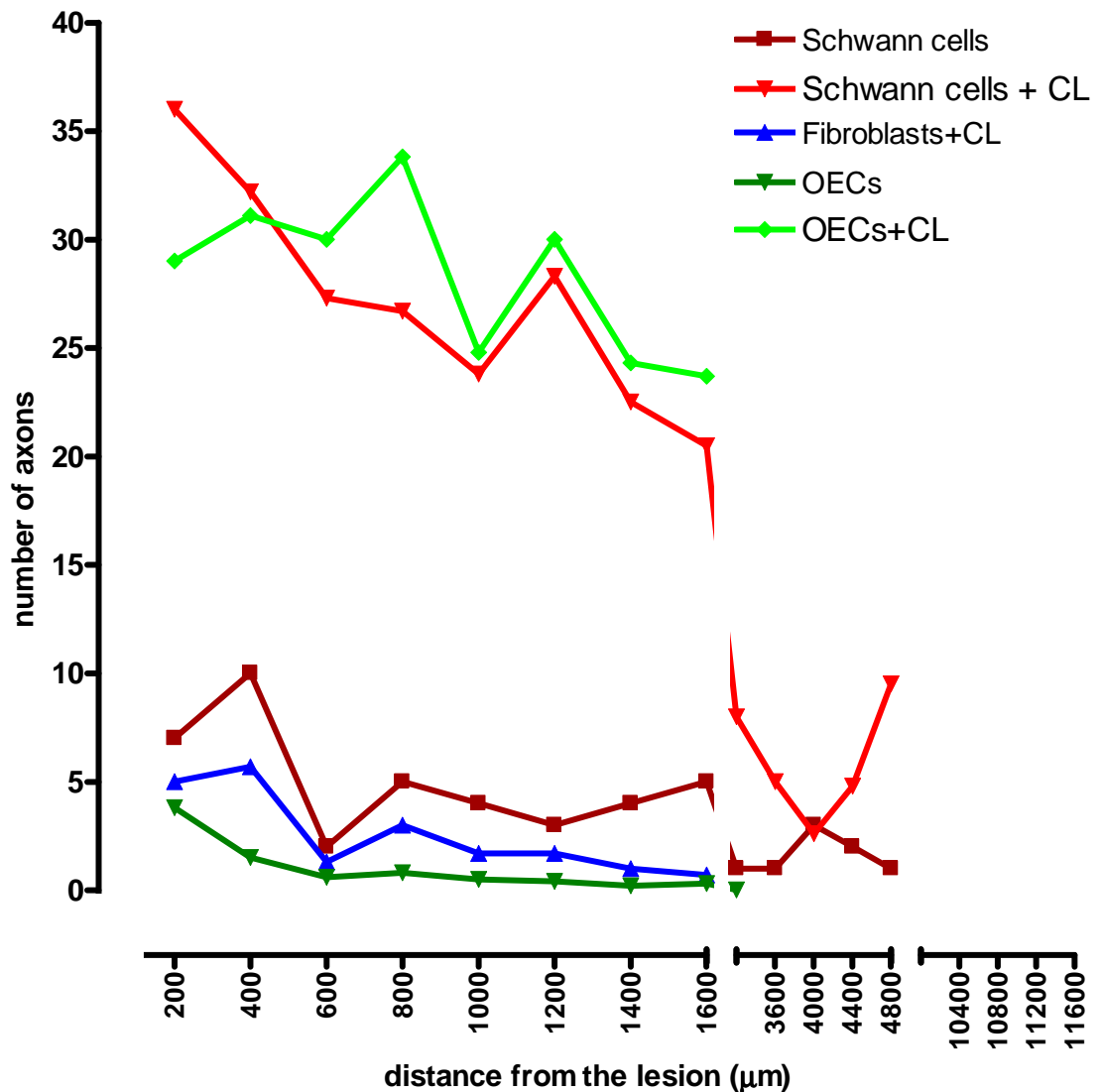


Figure 4-18. Comparison of the number of regenerating axons labelled with BDA in the medial spinal cord rostral to lesion in Schwann cell, OEC, SN fibroblast transplanted and non-transplanted animals.

Schwann cell transplantation promoted long distance axonal regeneration to a level similar to that detected after OEC transplantation; however it must be noted that regeneration was corroborated only in two animals in the Schwann cell transplantation group. Conditioning lesions potentiated the regenerative properties of Schwann cells and OECs to a comparable level. Fibroblast transplantation combined with conditioning lesions was sufficient to equal transplantation of Schwann cells and OECs in the absence of combined treatment. Regeneration following fibroblast transplantation combined with sciatic nerve transection was significantly lower than in the Schwann cell combined paradigm ($P < 0.05$ at 600, 800, 1000, 1200 and 1400 μm from the lesion); furthermore it was almost 20 times lower than OECs and Schwann cells transplantation paradigms combined with conditioning lesions.

4.3 Discussion

4.3.1 Integration of Schwann cells in the transplant site and protective effects on the lesion

Schwann cells labelled with GFP were detected in a fresh wire knife dorsal column lesion of all animals six weeks after transplantation, which is in accordance with previous studies using other lesion models (Li et al., 1994; Imaizumi et al., 2000; Dunning et al., 2004; Someya et al., 2008). Schwann cell transplantation was associated with a reduction of the lesion cavitation confirming previous reports by Takami et al. (2002) and Someya et al. (2008). Interestingly, in our present study, the integration of Schwann cells in the lesion resembled that seen in the previous chapter in which OECs were transplanted in the same lesion paradigm. In particular, as seen for OECs in the previous chapter, some animals had lesions in which Schwann cells had not integrated well in its centre and resided in the lesion walls. In these animals the lesion cavity and the lesion size were large and resembled those of non-transplanted animals. In contrast, in animals where there was good integration of GFP labelled Schwann cells detected through the lesion, a reduction in the lesion cavity size and importantly a reduction in the size of the lesion *per se* was detected, presumably by promoting the GFAP borders of the lesion to stay close together and possibly by reducing tissue loss. Conversely in non-transplanted animals the distance between the GFAP borders was higher. This finding for Schwann cells, and also described for OECs in the previous chapter, indicates that OECs and Schwann are quite similar in their capacity to prevent cavitation of the lesion and to prevent enlargement of the space between the lesion GFAP borders.

It is not clear why following both Schwann cell transplantation and OEC transplantation there was a large intra-group diversity in the integration of injected cells into the lesion. In fact for both Schwann cells and for OECs, this diversity did not appear to correlate with the population of transplanted cells, since cells from the same purification procedure which were transplanted the

same day integrated very well in the lesion of some animals but not others. It did not seem that this diversity was due to the order in which the animals were transplanted in during the same transplantation session (2-4 animals per session) as no correlation was found between the duration the cells were maintained on ice before transplantation and the success in which cells integrated into the lesion. Genetic variability between animals should not account for the variation either, as Fisher rats are an inbred rat colony and donor tissue is syngeneic with the receivers and should not raise an immune response, and also because poor cell integration in the lesion was often associated with good distribution in the spinal cord rostral and caudal to the lesion. It is possible that variability in the survival of transplanted cells in the lesion was due to surgical variability in performing the lesion and that the movement of the rat after the transplantation could have resulted in displacement of cells from the transplant site. Other reports in the literature use gel foams placed over the transplant and this may be a modification to the method in the future that might reduce such variability.

4.3.2 Labelling of primary sensory afferents in and beyond the lesion following Schwann cell transplantation

We found that after a Schwann cell transplantation tract traced axons grew into the lesion. This is in agreement with others that have reported regeneration of corticospinal axons, of GAP43 and CGRP positive axons and of adrenergic and serotonergic axons into the lesion transplanted with Schwann cells (Takami et al., 2002; Andrews et al., 2007; Kamada et al., 2005; Someya et al., 2008).

Importantly, we found that Schwann cells distributed rostral to the lesion site and created the optimal conditions for promoting axonal growth. This distribution of cells rostral to the lesion resembled closely that found after OEC transplantation as described in the first chapter of results, and was spatially associated with tract traced primary sensory afferents sprouting or regenerating beyond the lesion. Sprouting and not only regeneration had likely occurred in those animals where we observed spared fibres in the vicinity to the Schwann

cell tracts. In fact, Li et al. (1994) reported a similar axon to Schwann cell arrangement, where spared axons ran parallel to the Schwann cell tracts, and suggested that corticospinal and ascending sensory fibres sprouted on the other side of the lesion into tracts of Schwann cells located nearby. We found that the number of sprouting/regenerating axons associated with Schwann cells rostral to the lesion was higher than that detected with OECs, however the difference was not significant. This finding is in agreement with Imiazumi et al. (2000) who studied growth of primary sensory afferents after lesion and Takami et al. (2002) who studied growth of propriospinal fibres after lesion. In the present study we have shown and furthermore quantified that the majority of tract traced axons located beyond the lesion were mostly associated with Schwann cells that had distributed rostral to the lesion. This finding is in agreement with that of Menei et al. (1998) who reported, using a more invasive approach, that injecting Schwann cells into a 5 mm long lesion directed along the main axis of the spinal cord permitted a preferential growth of axons through the long trail of Schwann cells located in the 5mm long lesion. These findings and the finding in the previous chapter on OEC tract-axon association indicate that axons preferentially sprouted/regenerated close to the transplanted Schwann cells or OECs rather than into the normal host tissue.

After applying the criteria for examining only regenerating fibres, it was possible to have a quantification of genuine regeneration. In two animals we found regeneration that was restricted to the Schwann cell transplant tract in continuity with the lesion.

4.3.3 Conditioning lesions potentiated the Schwann cell growth promoting effect on axons rostral to the lesion

We have reported in the previous chapter that conditioning lesions potentiated axonal outgrowth rostral to the lesion after OEC transplantation. In the present chapter we have addressed whether conditioning lesions combined with Schwann cells promoted a similar potentiation. Importantly, we report for the first time that combination of conditioning lesions and Schwann cell transplantation

produced an increase in the number of axons counted rostral to the lesion compared to non-conditioning lesioned animals transplanted with Schwann cells. This increase was five fold and was significant. This novel finding also demonstrates that conditioning lesions enhanced sprouting/regeneration to a similar level after Schwann cell or OEC transplantation. Importantly, almost all of the axons detected rostral to the lesion were associated with the transplanted cells.

Furthermore, subtracting from the quantification potentially sprouting axons, we could detect convincing regeneration rostral to the lesion in all combined Schwann cell transplanted and conditioning lesioned animals but one. The axons were mostly associated with GFP expressing Schwann cells that formed continuous tracts exiting the lesion/transplant site. The number of axons regenerating through the Schwann cell tracts following conditioning lesions was not significantly different to that described in the previous chapter for the similar experimental procedures carried out with OECs. This is therefore the first report to indicate that Schwann cells and OECs promote similar levels of regeneration when combined with conditioning lesions of the sciatic nerve, and is probably also the only report comparing convincing long distance regeneration *per se* between Schwann cell and OEC transplanted animals.

Based on previous studies (Takami et al., 2002; Lakatos et al., 2003) that reported an increase in astrocytosis after astrocyte-Schwann cell contact compared to astrocyte-OECs contact, we would have expected to detect stronger regeneration after OEC rather than Schwann cell transplantation. In fact it has been reported that astrocytosis following Schwann cell transplantation was accompanied by an increase in the secretion of chondroitin sulphate proteoglycans which is inhibitory to axonal growth (Lakatos et al., 2003). However, we found that the number of regenerating axons rostral to the lesion following Schwann cell transplantation was similar to that found following OEC transplantation. Furthermore, we did not observe an obvious difference in the astrocyte reaction following transplantation of the two different glial cell types and this could explain the unexpected regeneration outcome; however it would be necessary to quantify the level of GFAP immunoreactivity to confirm this. If we could establish in future studies that the astrocyte response was actually different between the two transplantation paradigms, then the most

convincing hypothesis would be that Schwann cells can overcome the inhibitory effects of the glial scar allowing regeneration to occur through the scar to a similar extent as seen with OECs.

4.3.4 Contamination of Schwann cells in OEC cultures

In the present study it was not possible to find evident dissimilarities between Schwann cells and OECs in their integration into the lesion, in the protective effects exerted on the lesion, in their distribution in the host spinal cord and in the promotion they exerted on fibre growth into the lesion and beyond. These results could lead to the hypothesis that either the two cell types shared similar properties upon cell transplantation, or that OECs were outnumbered during cell culture by Schwann cells and that we transplanted Schwann cells in both cell transplantation paradigms. There is in fact no reliable method to distinguish OECs from Schwann cells (Tome et al., 2007). A recent proteomic analysis of foetal cultured OECs and adult cultured Schwann cells identified calponin, an actin-binding protein, as a marker that could specifically recognise OECs and distinguish them from Schwann cells (Boyd et al., 2006). This study led others to suggest that the OEC cultures prepared from the olfactory mucosa and bulbs by means of FACS purification were contaminated by Schwann cells as they did not express calponin (Rizek et al., 2006). In a subsequent publication by our group and others it has been shown that calponin was not expressed by rat OECs at any developmental stage (Tome et al., 2007; Ibanez et al., 2007). Furthermore, OECs did not express calponin *in vitro*; instead calponin was expressed by fibroblast like cells purified from both the olfactory system and the sciatic nerve and by astrocytes in confrontation assays (Tome et al., 2007). These findings indicate that there is no evidence to support contamination of Schwann cells in OEC cultures from the olfactory bulb. Furthermore, in our present study the olfactory bulb sort was performed with the FACS machine to select O4 positive cells. Schwann cells residing along blood vessels in the olfactory bulbs do not express O4 and it is extremely unlikely that they would be collected by the FACS machine with its stringent settings. Furthermore, in this study it was found that the highly pure (as defined by p75 labelling) cultured olfactory bulb OECs and

sciatic nerve Schwann cells transplanted in the present study, appeared to have extremely different features. In particular, Schwann cells at confluency were seeded in the tissue flasks at a significantly higher density (twofold) than OECs. Secondly, following dissociation and centrifugation in order to prepare cells for transplantation, the density of Schwann cells was significantly higher (twofold) than that of OECs. Lastly, during cell culture Schwann cells had always a spindle-like shape, while OECs appeared to switch between a spindle-like shape to an astrocyte-like flattened shape in accordance with previous reports (Barnett et al., 2004). A third hypothesis we must consider to explain why Schwann cells and OECs exerted similar effects on the lesion environment is the possibility that endogenous Schwann cells invaded the OEC transplant. In fact there is enough evidence to indicate that endogenous Schwann cells invade the lesion and possibly even the spinal cord rostral and caudal to the lesion (Bunge, 1994; Beattie et al., 1997; Keyvan-Fouladi et al., 2003; Black et al., 2006). Furthermore our group has shown that Schwann cell conditioned medium induced reactive astrogliosis and boundary formation between FACS purified OECs and astrocytes *in vitro* (Santos-Silva et al., 2007) compared to co-cultures in the absence of Schwann cell conditioned medium indicating that endogenous Schwann cells could possibly reduce the regenerative properties of transplanted OECs.

4.3.5 Transplantation of fibroblasts

SN fibroblasts were transplanted into the dorsal column lesion to determine whether the growth promoting properties and regeneration promoting properties of Schwann cells and OECs observed in the present study were a non-specific feature common to all cell types or if these were limited to particular glial cell populations. In order to maximise any growth promoting properties of fibroblasts these were transplanted in combination with conditioning lesions of the sciatic nerve. Furthermore, in the past, growth promoting properties of fibroblasts have been studied mainly through combinatorial treatments with NT3, BDNF and other growth factors or scar inhibitors especially in Mark Tuszynski's group involving skin derived fibroblasts and in one paper by Raisman's group involving SN-

fibroblasts, but little work has been performed to directly compare fibroblasts with OECs or Schwann cells (Keyvan-Fouladi et al., 2005).

SN fibroblasts prevented a cavity from forming in most animals and reduced significantly the lesion cavity size compared to non-transplanted animals in accordance with previous observations on skin derived fibroblasts (Tuszynski et al., 1994; Jones et al., 2003) and SN-fibroblasts (Keyvan-Fouladi et al., 2005). Furthermore, we found that SN-fibroblasts significantly reduced cavity formation when compared to OEC transplanted and Schwann cell transplanted animals. Interestingly, we also found that the lesion size, defined by the area delimited by the GFAP internal perimeter was reduced compared to non-transplanted, OEC transplanted and Schwann cell transplanted animals. Therefore, SN-fibroblasts were unexpectedly more effective than OECs and Schwann cells at bridging the lesion. On the other hand, we found that the spinal cord tissue around the lesion was strongly modified and disrupted, which possibly affected nearby neurons and their processes in a negative way. This effect was especially evident when a comparison was made between the lesions transplanted with fibroblasts and lesions transplant with Schwann cells or OECs or even with non-transplanted lesions. The purified populations of Schwann cells transplanted in this study contained approximately 5% of fibroblasts; interestingly, such a small proportion of fibroblasts was not high enough to exert the same effects observed with a purified population of fibroblasts.

The central canal cavitation was not diminished following fibroblast transplantation when compared to the other transplantation paradigms. In addition, syringomyelia was reduced when compared to non-transplanted animals, but this effect was not significant.

Axons grew into the lesion transplanted with SN-fibroblasts in accordance with previous findings involving transplantation of skin derived fibroblasts (McTigue et al., 1998; Willerth and Sakiyama-Elbert, 2008), but in contrast to findings in Raisman's group who could not detect any neurofilament positive axons nor P0 staining in the lesion transplanted with SN-fibroblasts (Keyvan-Fouladi et al., 2005). Furthermore we found that there were clearly fewer axons than those detected after OEC and Schwann cell transplantation. In our present study, axons were also detected in association with SN-fibroblasts distributed rostral to

the lesion. Furthermore, the numbers of axons were almost 20 times lower compared to animals transplanted with OECs or Schwann cells combined with conditioning lesions. For this reason, we suppose that in the absence of sciatic nerve transection, fibroblasts would not promote growth of axons beyond the lesion in our dorsal column lesion paradigm even if optimally distributed. This may also be true because previous reports have shown that fibroblast secreting growth factors were associated with significantly more regeneration compared to control fibroblasts (Blesch et al., 2003; Tobias et al., 2003).

Taken together, when comparing the same lesion paradigm transplanted with fibroblasts, OECs or Schwann cells, we show that although fibroblasts were more effective at bridging the lesion, fibroblasts also had a deleterious effect on the tissue surrounding the lesion and possibly induced more of a host response. Furthermore, it was found that sprouting/regeneration were significantly diminished, suggesting that fibroblast as a pure population are not an ideal cell type to restore connectivity in spinal cord injury. It is possible, however, that mixed populations of fibroblasts and OECs or Schwann cells are more suitable for transplantation. In fact fibroblasts form in the olfactory system an arrangement similar to that formed with Schwann cells in the other peripheral nerves (Li et al., 1998; Dreesmann et al., 2009) where fibroblasts and glial cells interact closely. It was in fact reported by Raisman's group that mixed populations of SN-fibroblasts and SN-Schwann cells or mixed populations of olfactory bulb derived fibroblasts and olfactory bulb derived OECs generated an environment where axons could grow in (Li et al., 1998; Keyvan-Fouladi et al., 2005).

5 Delayed OECs transplants and conditioning lesions

5.1 Introduction

In recent years an increasing number of researchers have examined the repair potential of OECs when transplanted at the time of the spinal cord injury, but extremely few studies have considered delayed transplantation paradigms. Nevertheless, a number of human clinical trials involving delayed transplantation of OECs have been carried out (e.g. Huang et al., 2003; Lima et al., 2006; Mackay-Sim et al., 2008) but the outcomes are unclear. It is therefore imperative that researches in this field define in more detail the outcome of OECs injected in delayed transplantation paradigms.

In the first chapter we reported the effects on regeneration of an OEC transplant when performed immediately after the spinal cord injury. In the present chapter we ask whether similar beneficial effects are still exerted by OECs after transplantation using a delayed cell injection paradigm. Secondly, we ask whether the combination with a delayed conditioning lesion of the sciatic nerve may enhance such a response. Thirdly, we try to understand the spatial relationship between tract traced axons on the distal side of the spinal cord and the transplanted cells.

5.1.1 Delayed transplantation

5.1.1.1 Timing of transplantation

To select the appropriate time frame for delayed transplantation we should consider spinal cord injuries in the human situation. The first point to take into account is the timing of transplantation in man relative to the earliest time point harvested OECs would be available for transplantation. Autologous

transplantation would be required to prevent rejection of the graft and the immune suppression of the injured individual (Barnett and Riddell, 2004); consequently, after the spinal cord injury a small yet sufficiently large piece of tissue from the olfactory system should be explanted and cultured to yield a sufficient number of OECs for autotransplantation. A reasonable time required for culture of OECs from patient olfactory mucosa biopsies was shown to be from 4 to 8 weeks (Mackay-Sim et al., 2008).

Secondly, we should consider the appropriate timing for intervention with respect to allowing sufficient time for the injury to stabilize. Long lasting recovery and reflex changes take place in individuals with incomplete spinal cord injuries, weeks or even months after the initial traumatic event underlying reorganization of spared pathways or remyelination of non-myelinated descending pathways (Little et al., 1999). Along with this, the presence of spared tissue bridges in the injured human cord and the finding that similar septations in the rat injured cord contain axons (Beattie et al., 1997; Radojicic et al., 2005) suggests that extreme caution should be taken by surgeons before invasive intervention. If care was not taken then treatments such as OEC transplantation could damage these spared structures and preclude spontaneous recovery. OEC transplants, for this reason, should be performed only after a long enough time window to allow and not preclude spontaneous recovery in those individuals with incomplete lesions. When looking at recovery time in rats, the development of the injury after a contusion continued up to 14 weeks and remained stable thereafter in a contusion injury model (Hill, et al., 2001), while in a crush injury model degeneration reached its peak at 4 weeks (Ramer et al., 2004a). Interestingly, with regards to behaviour recovery, moderate and mild rat contusion injury models showed behavioural open field testing improvements that reached plateau after 4 weeks (Basso et al., 1995).

Based on the two points outlined above, it therefore seems reasonable to perform OEC transplantation into a chronic rat spinal cord injury with a delay of four weeks or more (Houle and Tessler, 2003). For this reason we transplanted OECs 4 weeks after the dorsal column lesion.

5.1.1.2 Delayed transplantation of OECs

The few reports available in the literature on delayed OEC transplantation show contradictory outcomes with regard to bridging axonal regeneration in the spinal cord.

A report by Lu et al. (2002) described long distance axonal regeneration in rats following OEC transplantation into a complete transection at the thoracic level. It was reported that serotonergic axons were labelled at the caudal end of the cord and that retrograde fluorogold labelling in the brainstem raphe neurons was detected in OEC transplanted animals only (Lu et al., 2002). Interestingly, these findings, which mirror closely those of the same group on acute OEC transplantation by Lu et al. (2001) were not repeated in a replication study by Steward et al. (2006) who reported no regeneration enhancement in the OEC transplanted animals. Furthermore the study by Lu et al. (2002) lacks descriptive and photographic evidence of the relationship between fibres and transplanted cells. A second report, from the laboratory of Mary Bunge, involving contusion of the thoracic cord, indicated that OEC injection in the lesion promoted axonal sparing/regeneration in the caudal cord as retrograde tracing of fluorogold was found in the red nuclei, and in the brainstem reticular formation, vestibular complex and raphe nuclei (Plant et al., 2003). However, fluorogold labelling is not considered a reliable tracing method as fluorogold travels also in the cerebrospinal fluid. Furthermore, as for the former study no description of the relationship between distally distributed OECs and fibres was considered (Plant et al., 2003). Raisman in the same year published a paper describing regeneration of corticospinal axons beyond an electrolytic lesion 16 weeks after transplantation of OECs into 8 week old injuries (Keyvan-Fouladi et al., 2003). In this study the regenerating BDA labelled tract traced axons consisted of straight fibres localised in the white matter that sent collaterals to the grey matter where these fibres branched off (Keyvan-Fouladi et al., 2003). Based on this evidence, the morphology of these fibres was not suggestive of regeneration and raises the issue on whether they were actually truly regenerating. Especially considering that a proportion of animals in the study were found to have many spared fibres and considering that the method used to select the animals that were to be transplanted was based on behavioural testing, which can underlie a process of fibre sparing. OEC distribution in relation to the regenerating fibres

was not considered in this paper, except that mention was made of an unknown proportion of fibres which were ensheathed by periperal type myelin (Keyvan-Fouladi et al., 2003). In the following years Lopez-Vales and colleagues described in two separate papers the promoting effects of transplanted OECs on regeneration of descending axons bridging a complete thoracic transection 1 week (Lopez-Vales et al., 2006) or 45 days after the spinal cord injury (Lopez-Vales et al., 2007). In both papers BDA tract traced corticospinal fibres and serotonergic and noradrenergic fibres were found many millimetres below the lesion level in the lumbar cord only in those animals receiving a delayed OEC transplants. Unfortunately, the localization of OECs beyond the lesion was not detected as for this purpose p75 labelling was used, and it is known that OECs can lose p75 expression after transplantation.

On the other hand it has also been reported that delayed transplants of OECs did not promote lengthy axonal regeneration or sparing (Takami et al., 2002). In this study they reported that OECs injected into the cord 1 week after a moderate thoracic contusion lesion did not promote a significant increase compared to controls in regeneration/sparing of propriospinal axons or supraspinal neurons as shown by retrograde fluorogold tract tracing into the thoracic and cervical segments and into the brainstem and the cerebral cortex. In addition, anterograde BDA labelling revealed no significant increase in regeneration/sparing of corticospinal tract axons beneath the injury level (Takami et al., 2002).

Taken together, all studies that reported long distance axonal regeneration in the spinal cord following delayed OEC transplants lacked a detailed analysis of the relationship between the distribution of transplanted cells in the distal cord and the regenerating fibres. Furthermore, Steward et al. (2003) urged researches in the field to produce transparent and extensive descriptive and photographic information when defining an axon as a *bona fide* regenerating fibre rather than a spared or sprouting one. If this approach was undertaken by everyone it would be easier for the further research to ensue with faith on reports from previous findings. Oswald Steward (at the UCI-USA SCI research course I attended in 2007) and in (Steward et al. 2006) extended his comments even to lesion paradigms that apparently ablate completely the spinal cord (i.e. Lu et al., 2002; Lopez-Vales et al., 2006, 2007) as extremely ventral and lateral

located axons can demonstrate resilience even upon complete transection. Furthermore, artifactual labelling of axons occurred following BDA injection into the cortex because the tracer leaked into the ventricle and travelled through the central canal to the lesion where it was taken up by fibres on the other side (Steward et al., 2008).

5.1.1.3 Delayed conditioning lesions

As described in the general introduction, a peripheral conditioning lesion performed prior to or at the time of the central injury enhances the growth capacity of the central axons. Yet, a conditioning lesion in such paradigms would offer very little development for clinical investigation. A criterion to make any conditioning lesion treatment or any treatment aimed to reproduce a conditioning lesion practicable at the clinical level is the necessity for such a treatment to be effective when performed subsequent to the spinal cord lesion. Recently, a promising report describing the effects of delayed conditioning lesions has come from a study in Allan Basbaum's group in UCSF (Neumann et al., 2005). Adult rats received a double conditioning lesion: first a priming peripheral lesion at the time of the spinal cord injury and then a post-priming peripheral lesion 1 week later, with a 6-8 week survival period. The re-priming of the peripheral end was necessary to boost axonal growth into and beyond the central lesion in areas of white matter and at the border between white and grey matter, seemingly at a comparable level as described in the work by Neumann and colleagues (1999) that we considered in the general introduction. Importantly, this year new and extremely interesting findings were demonstrated by Ylera et al (2009) and further developed in a review by Jerry Silver (2009). In this report a post priming of the sciatic nerve 2, 4 or 8 weeks after a spinal cord lesion increased the transcription and translation levels of a number of growth associated genes including GAP43 to the same levels seen in pre priming 2, 4 and 8 weeks before the central injury. In accordance with this, DRG neurite outgrowth in culture was increased to the same level after a peripheral injury that followed or preceded the central injury of 2, 4 or 8 weeks after a peripheral injury alone but not after a central injury alone (Ylera et al., 2009). The same effect on neurite outgrowth was not reproduced *in vivo*,

probably due to the fact that the lesion scar precluded any growth response (Ylera et al., 2009). But if the delayed conditioning lesion was followed by a second central spinal cord injury then axons regenerated in and beyond the lesion site in all animals to a similar level seen in preconditioned animals (Ylera et al., 2009). Time lapse imaging produced extraordinary images showing the actual process of lesion and growth of individual injured axons *in vivo* (Ylera et al., 2009). The above findings indicate that conditioning lesions are effective at promoting axonal growth even when performed after the spinal cord lesion.

5.2 Results

5.2.1 Dorsal column wire knife lesion, 10 week survival

Of the twenty eight animals that received a delayed OEC transplant, four rats were found to be completely devoid of GFP expressing cells, the most likely explanation being that the lesion and spinal cord were missed at the time of the cell injection due to the high technical difficulty in reopening the lesion site and finding the original lesion site to inject the cells in (see methods, section 2.2.5). We decided to consider these four animals as if they had not been transplanted with cells and treat them as a control group to be able to define the wire knife dorsal column lesion appearance at a 10 week time point in the absence of successful cell transplantation (Figure 5-1).

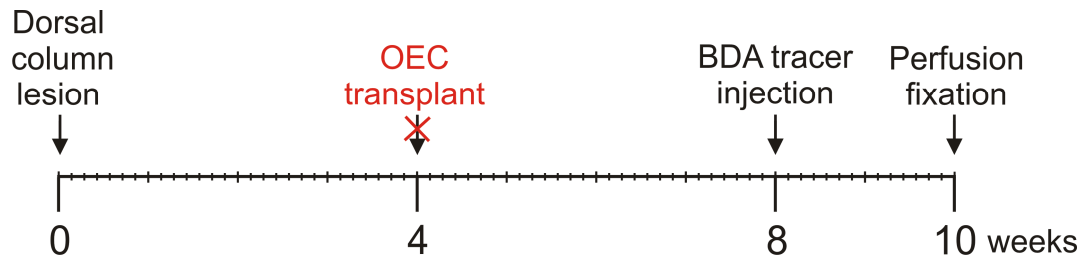
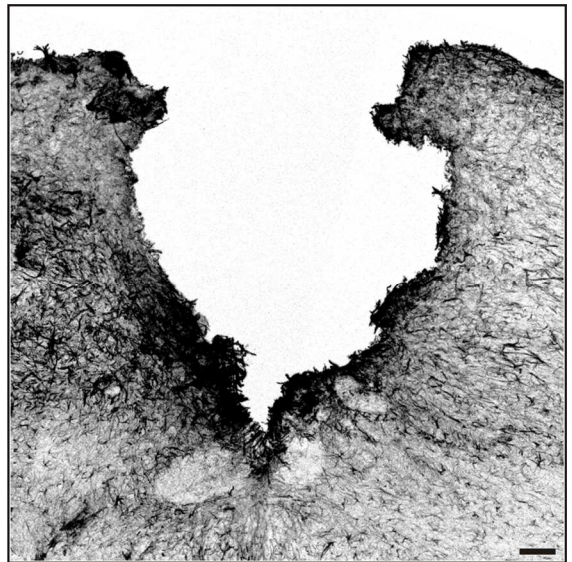
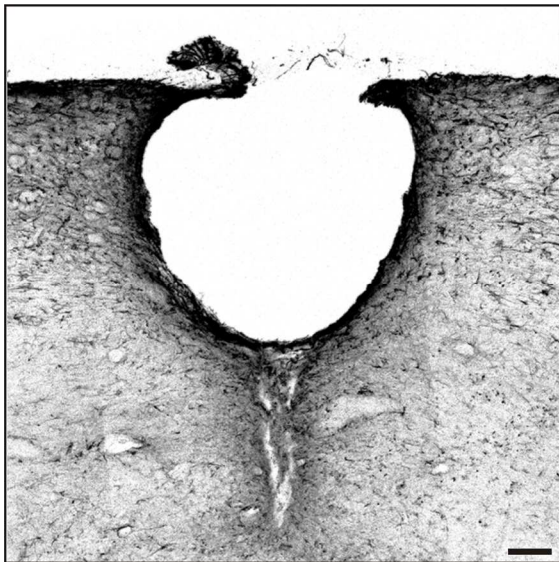


Figure 5-1. Time course of procedures performed on non-transplanted animals 10 weeks after the spinal cord lesion.

This experimental group was made up of animals that received a transplant of OECs which was likely misplaced as no GFP labelling was detected after tissue processing.

Ten weeks after the lesion a cavity was present in place of the original dorsal column injury in each of these four animals. The cavity morphology and size was not dissimilar from that observed in non-transplanted rats with a 6 week survival time (Figure 5-2) with the exception of 1 animal which developed an extremely large lesion cyst which took over almost the entire length of the lesion block, being more than ten times larger than the lesion cavity present in the other rats of the same group. This animal was not included in the quantification of lesion and central canal size. In the selected four animals GFAP labelled astrocytes formed a glial scar which surrounded the cavity and no tissue bridges were present to connect opposite sides of the lesion or directed towards the lesion core. The spinal cord tissue around the lesion area appeared normal under dark field view light microscopy, except the central canal was seen to develop cysts recapitulating what had been observed for the 6 week non-transplanted survival animals. The average lesion size, lesion cavity size and central canal size were measured and are shown in Figure 5-3.

Figure 5-2. Lesion morphology in non-transplanted animals with a 10 week survival. Confocal images of GFAP immunoreactivity of parasagittal sections spanning the lesion site from two animals. The lesion developed as a round acellular structure surrounded by a GFAP positive glial scar. No GFAP processes nor other structures were found to extend within the lesion or connect opposite sides of the lesion. Objective: 10x. Scale bars: 100 μm .



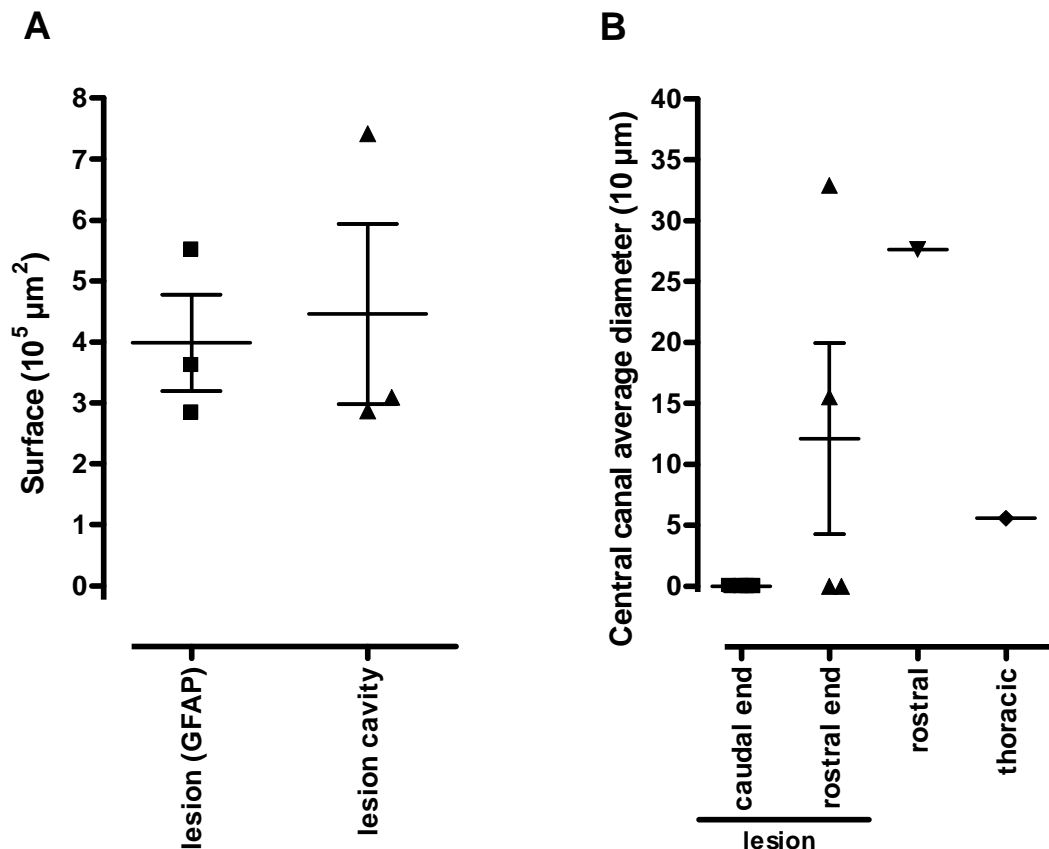


Figure 5-3. Lesion and central canal size 10 weeks after a dorsal column injury in non-transplanted animals.

A) Scatter plot comparing the size of the lesion defined by the internal perimeter of the GFAP positive glial scar surrounding the site of injury with the size of the lesion cavity. Because of the acellular composition of the lesion, the cavity size corresponded with the lesion size: mean cross sectional area defined by GFAP borders in the section with largest lesion in each rat as expected was not significantly different from mean lesion cavity cross sectional area from the section with the largest cavity in each rat ($P=0.61$). **B)** Cavitations formed in the central canal rostral to but not caudal to the injury level. The cavitation was measured as the average cavity diameter in the section with the largest extent of cavitation of each block in each animal. Central canal cavitation was measured on 3 rats in the rostral end of the lesion block, however only in one rat in segments rostral to the lesion because tissue was not collected for the other animals.

5.2.2 Delayed transplantation of OECs

OECs were detected in the lesion of all delayed transplanted animals, with the exception of those considered in the previous section. As described in section 3.2.4.1, no obvious difference was observed between animals with acutely transplanted OECs, with or without a conditioning lesion. For this reason and also because no apparent difference was present between the delayed transplantation groups with or without the conditioning lesion, data from these was pooled together to describe the lesion and central canal morphology and size in a larger number of rats. For all the remaining analysis the rats that received a conditioning lesion are considered in section 5.2.3. Twenty four rats were transplanted with OECs four weeks after the spinal cord injury and perfused six weeks later; amongst these, thirteen received only a delayed transplant (Figure 5-4) while eleven were transplanted and conditioning lesioned.

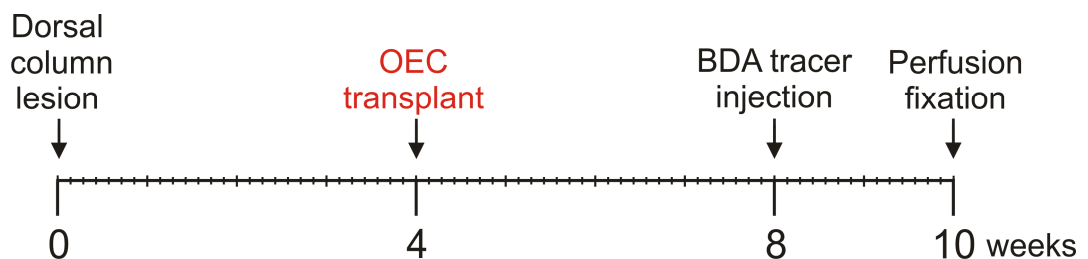


Figure 5-4. Time course of procedures performed on delayed OECs transplanted animals.

Thirteen animals were transplanted with OECs four weeks after the dorsal column lesion. Amongst these seven were also tract traced with BDA to study the regeneration of L4-5 DRG neuron sensory axons.

5.2.2.1 Characterization of the lesion after a delayed OECs transplant

As shown in Figure 5-6A, in delayed transplanted animals the lesion cavity size was significantly smaller than the lesion size defined by GFAP staining ($P=0.015$).

In particular, the cavity was not present in 58% (14/24) of lesions (an example is shown in Figure 5-5). In the subset of animals with no lesion cavity, GFP and GFAP labelled cells largely filled the cavity, that was presumably present at the time of injection 4 weeks after the lesion. In the remaining animals the lesion cavity was similar to that observed in the absence of a transplant: a single round large cyst free from any tissue bridges. GFP expressing OECs in these rats were located in the GFAP rim forming the walls of the lesion.

Notwithstanding the small number of non-transplanted animals analysed at 10 weeks, the lesion and lesion cavity sizes in these rats were significantly larger than in delayed OEC transplanted animals ($P=0.045$ and $P=0.019$ respectively) indicating that the transplant provided neuroprotection to the injured area even if the treatment started four weeks after the lesion (Figure 5-7A).

Interestingly, OECs integrated better when transplanted into a 4 week old lesion rather than into a fresh lesion. In fact the lesion cavity size 6 weeks after a delayed transplant was on average 3.1 times smaller than the lesion cavity 6 weeks after an acute OEC graft ($P<0.0001$) (Figure 5-8A).

The delayed transplant had a drastic effect on the lesion size too: firstly, the average lesion size was 2.8 times smaller when the transplant was performed chronically rather than acutely ($P<0.0001$) (Figure 5-8A); and secondly the average lesion size was 3.8 times smaller than that of non-transplanted animals analysed in section 3.2.5.1 six weeks after injury ($P=0.0020$). Both these findings indicate that delayed transplantation reduced the size of an already large lesion once this was filled with OECs.

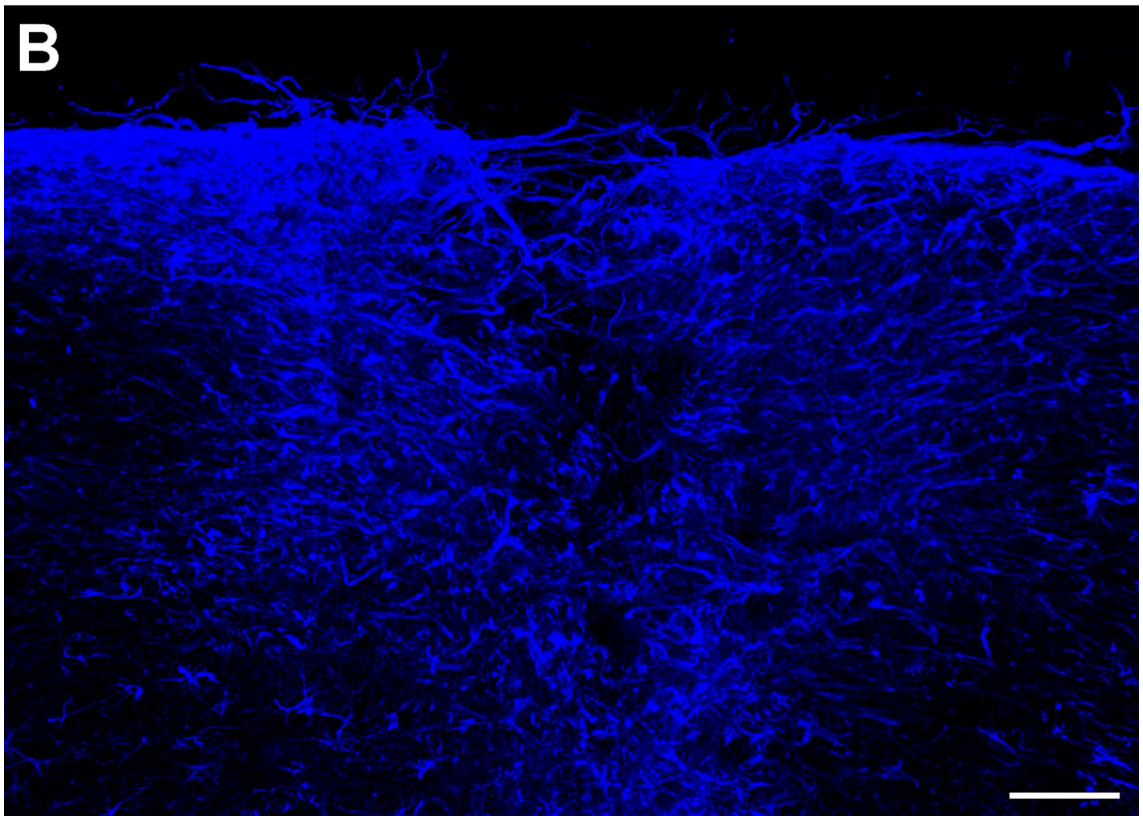
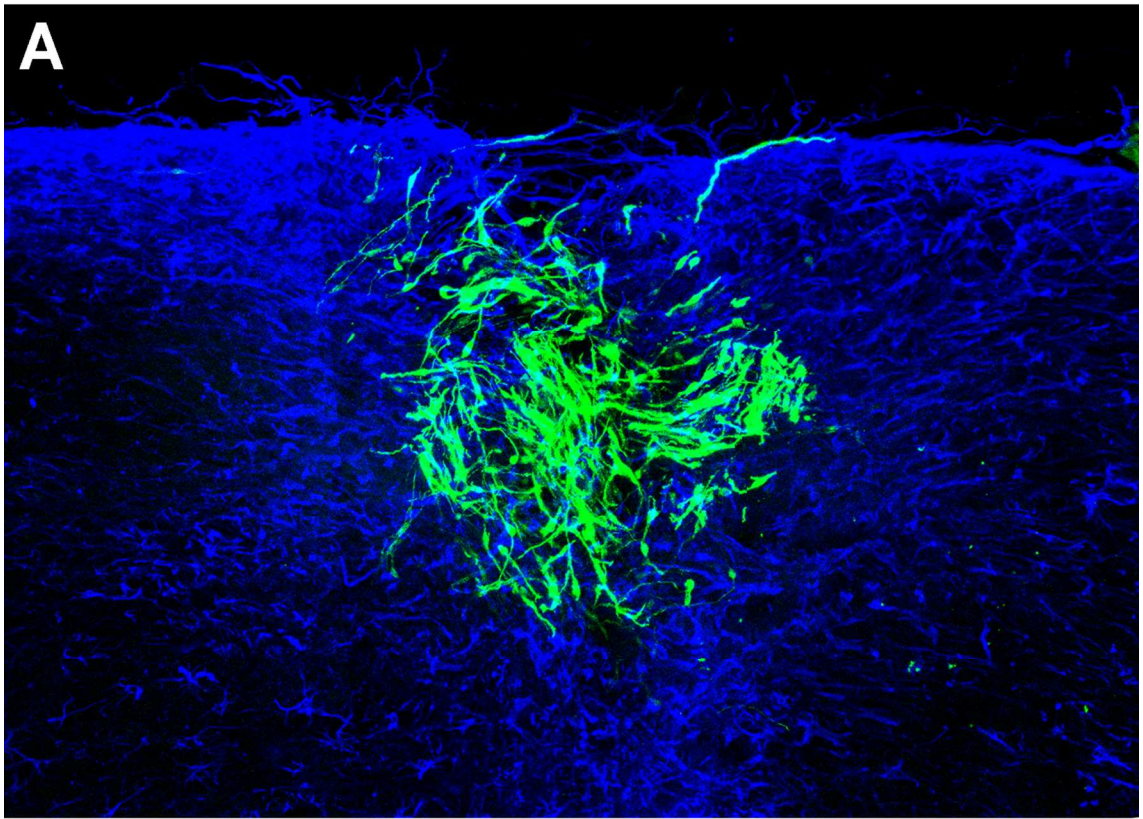
5.2.2.2 Characterization of central canal cavitation

Unlike the lesion development process, the central canal cavitation process was not reversed by a delayed transplantation (Figure 5-6B and Figure 5-7B). On the contrary the central canal cavity at the rostral end of the lesion block and in the rostral and thoracic blocks was respectively 2.1, 1.4 and 3.6 times larger than in

acutely transplanted animals from chapter 3 (as shown Figure 5-8); but none of these differences were significant.

Figure 5-5. The lesion was filled by OECs and astrocytes after delayed OEC transplantation.

A) Composite of confocal projected images of a parasagittal section. The lesion, 6 weeks after the delayed transplantation was completely filled by OECs. **B)** The same image in **A** is here depicted without the green channel to show that the lesion was also completely filled with astrocytic processes. Colour codes: green (OECs), blue (astrocytes). Objective: 10x. Scale bar: 200 μm .



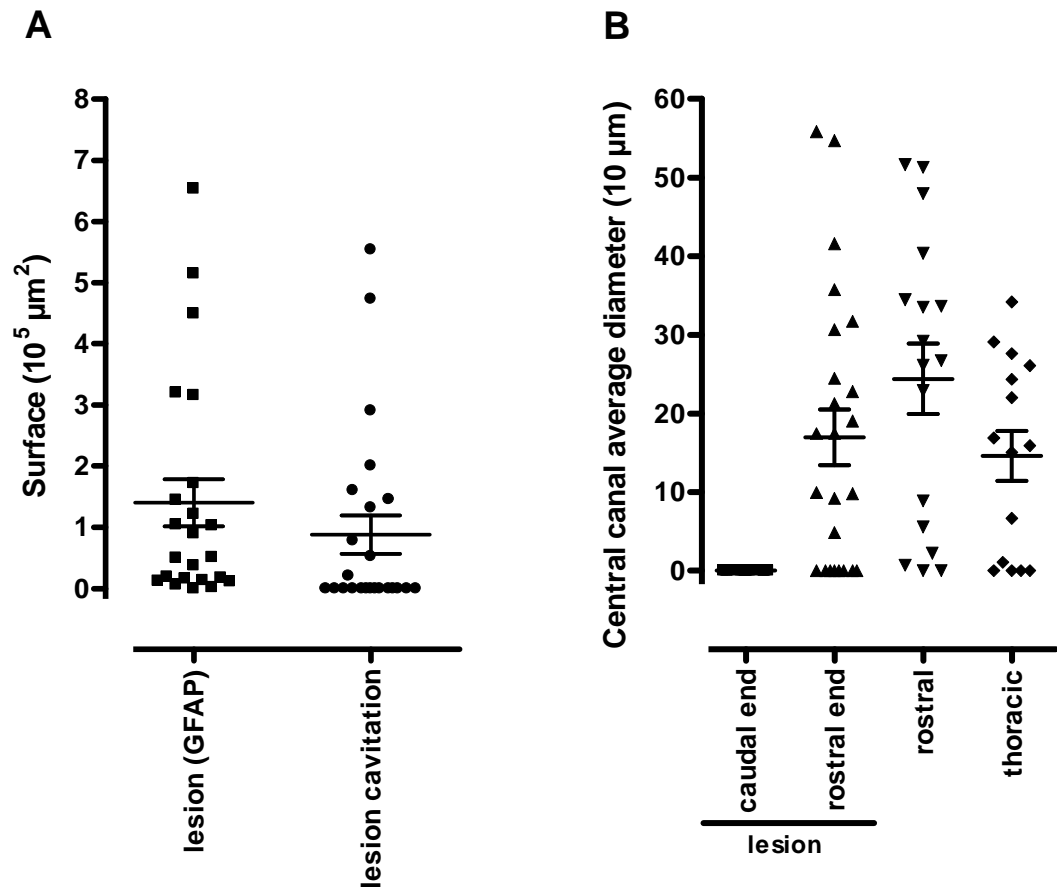


Figure 5-6. Lesion size, lesion cavity size and central canal diameter in all delayed transplanted and delayed conditioning lesioned rats pooled together.

A) Scatter dot plot showing that the size of the lesion defined by the GFAP positive glial scar surrounding the site of injury was significantly larger compared to the size of the lesion cavitation ($P=0.015$). **B)** Cavitations formed in the central canal above but not below the injury level. No significant difference was found between the rostral end of the lesion block and the rostral block ($P=0.17$), nor between the rostral end of the lesion block and the thoracic block ($P=0.15$), while a significant difference was found between the rostral and thoracic blocks ($P=0.0046$).

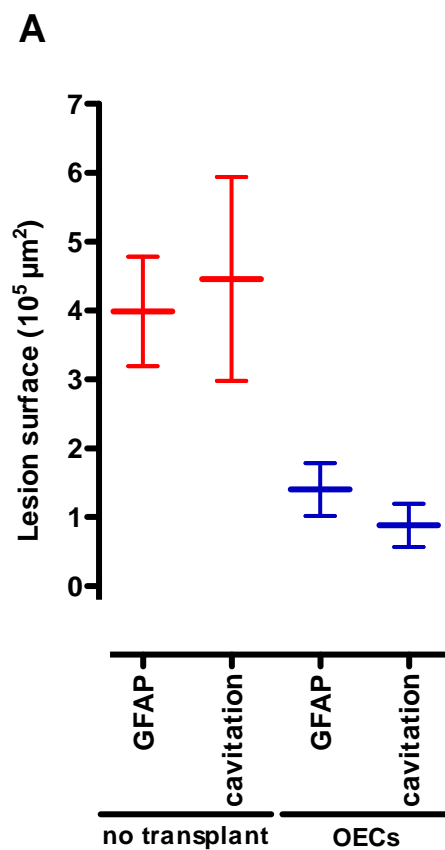


Figure 5-7. Lesion size and lesion cavity size in delayed OEC transplanted animals compared with non-transplanted animals.

The lesion size was reduced 2.9 times ($P=0.045$) 6 weeks after OEC transplantation into a four week old dorsal column lesion compared to non-transplanted animals with a 10 week survival time. The lesion cavity was reduced 5.1 times following a delayed OEC transplantation ($P=0.019$).

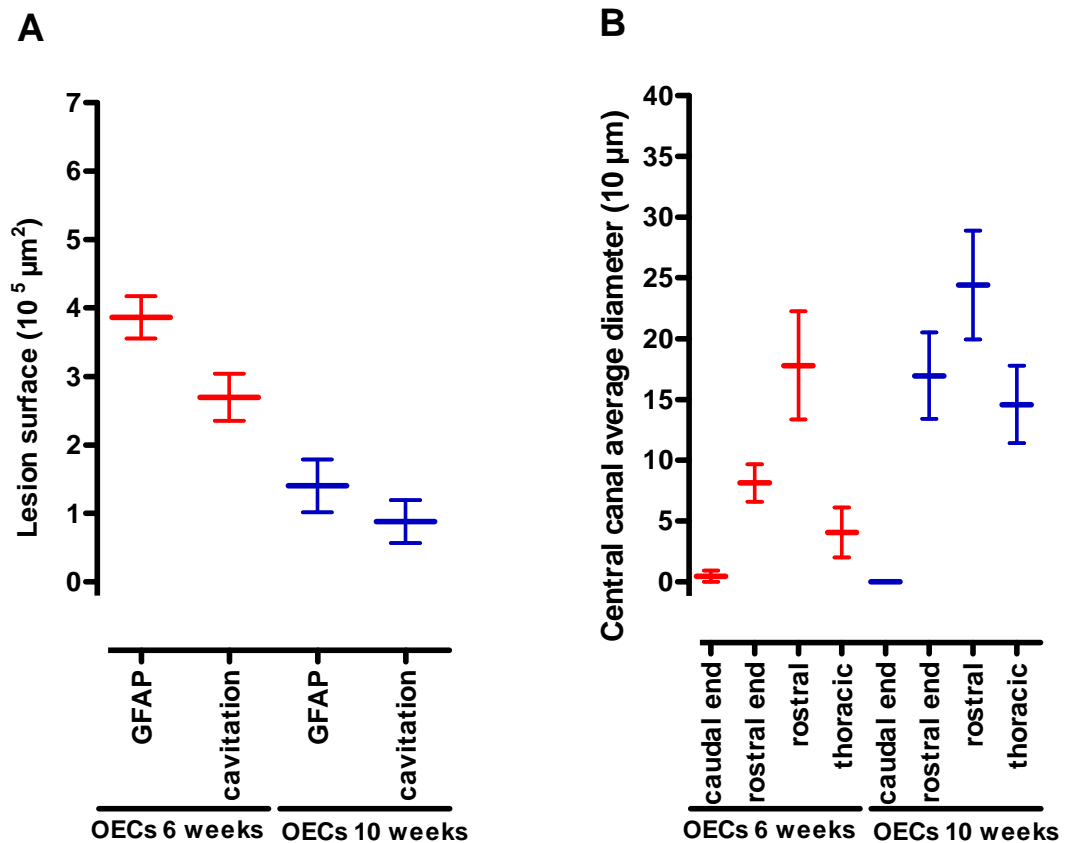


Figure 5-8. Comparison between the lesion size, lesion cavity size and central canal size following OEC transplantation into a fresh or a chronic lesion.

A) Delayed OEC transplantation reduced the lesion size 2.8 times compared to acute OEC transplantation ($P < 0.0001$), while the lesion cavitation reduction was 3.1 fold ($P < 0.0001$). **B)** Delayed OECs transplantation was associated with an increase however not significant of the central canal cavitation compared to acutely transplanted OECs: 2.1 times in the rostral end of the lesion block, 1.4 times in the rostral block and 3.6 times in the thoracic block ($P = 0.053$, $P = 0.24$ and $P = 0.086$ respectively).

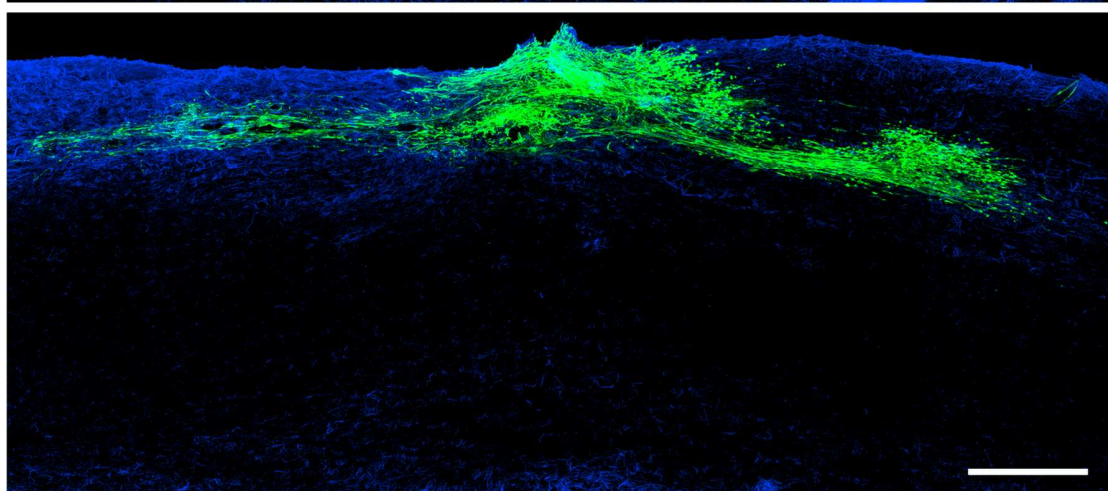
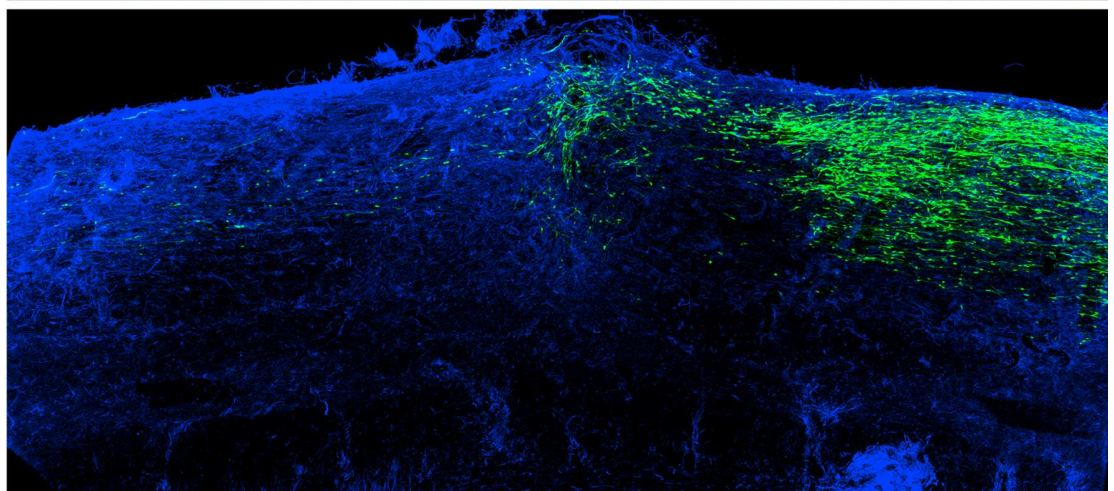
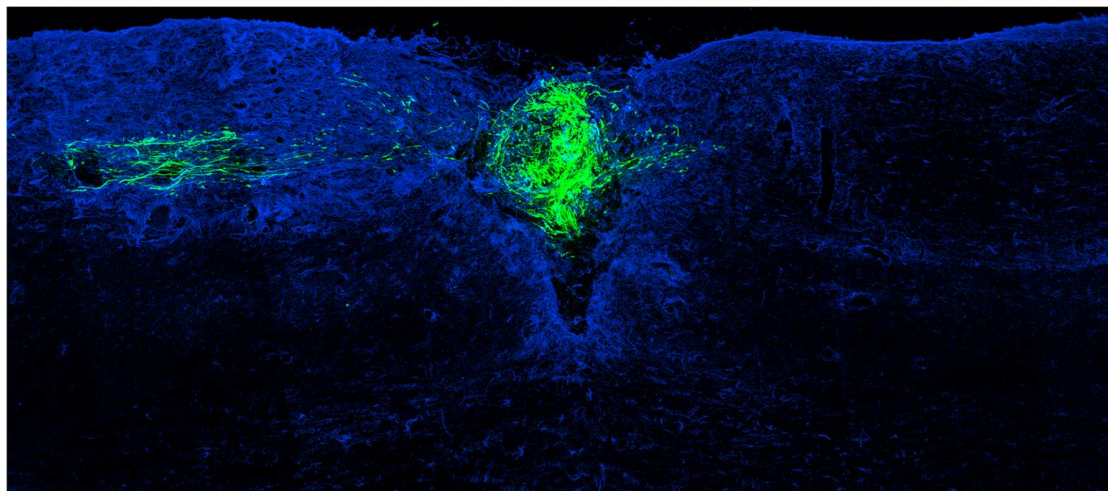
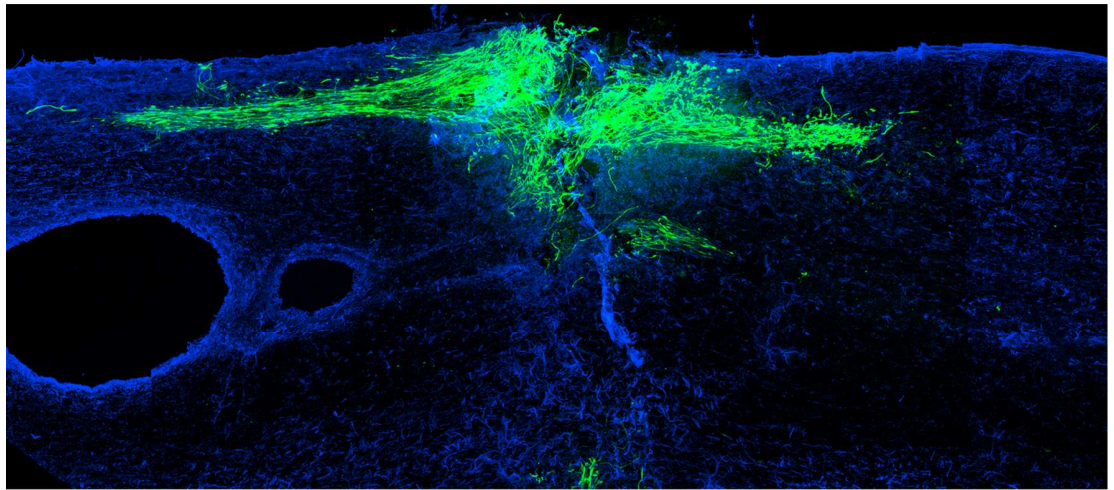
5.2.2.3 OEC distribution in the spinal cord

In the thirteen animals that received a single treatment consisting of delayed transplantation of OECs we found to our surprise that OECs had distributed out of the injection site in undamaged spinal cord tissue (see Figure 5-9 for examples). In 69% and 77% of the rats OECs had distributed respectively rostral and caudal to the lesion. In a proportion of animals the transplanted cells were detected at long distances rostral to the transplant site into the rostral and even thoracic blocks. Rostral to the injury, in most animals OECs distributed in white matter regions (63%), less frequently on the border between white matter and grey matter (29%) and even more rarely in the grey matter (13%). The cell density distinctly diminished when the distance above the injury increased. OECs were found in some cases inside the central canal even at the thoracic level.

Importantly, in 62% of the animals with a delayed transplant OECs formed continuous tracts that exited the lesion and extended for varying distances away from it; these ended on average 2900 μm rostral to the lesion in those animals where also the rostral and thoracic blocks were taken.

Figure 5-9. Images of OEC distribution in the spinal cord after delayed transplantation.

Composite confocal projected image stacks of parasagittal sections of the lesion block of four animals that show the widespread distribution of OECs (green) after a delayed transplantation in the spinal cord rostral to and caudal to the injection site. It is possible to see that OECs formed continuous cell tracts leading out of the lesion rostral to the injection point. Objective: 10x. Scale bar: 500 μm .



5.2.2.4 Regeneration of neurofilament positive fibres into the lesion

Spinal cord sections of six of the thirteen animals with a delayed transplant were processed with the neurofilament antibody to detect any regeneration that had occurred in the transplant site defined by GFAP labelling. Indeed, regeneration of neurofilament positive fibres had taken place indicating that the glial scar of lesions transplanted with OECs four weeks after the dorsal column transection was permeable to the regeneration of axons. The direction of the fibres followed closely that of the GFP labelled cells which were randomly orientated (Figure 5-10).

5.2.2.5 Regeneration of BDA labelled fibres in the lesion

In light of the fact neurofilament was found within the transplant site, the presence of ingrowth of L4-5 primary sensory afferents was also investigated. For this purpose BDA tract tracer was injected into the spinal nerves of 7 rats. Most of the BDA labelled ascending sensory axons 10 weeks after injury ended abruptly caudal to the lesion. Surprisingly though, some BDA labelled fibres were found in association with OECs in the lesion of 71% (5/7) of the animals indicating that some sensory afferent fibres even 4 weeks after the injury were able to regenerate after a delayed transplant (Figure 5-11).

Figure 5-10. Regeneration of neurofilament labelled axons in a lesion 6 weeks after a delayed transplant of OECs.

A) Confocal projected image taken with a 10x objective on a parasagittal section of the lesion site. Profuse labelling of neurofilament axons (red) was found in the lesion transplant indicating regeneration of interneurons and/or large type A dorsal root ganglia neurons. OECs are shown in green and GFAP in blue. **B)** Confocal projected image at higher magnification (40x oil) showing only the neurofilament axons of the boxed area in **A**. Profuse regenerating neurofilament positive axons were detected in the lesion transplant. Scale bars: 50 μm in **A** and 25 μm in **B**.

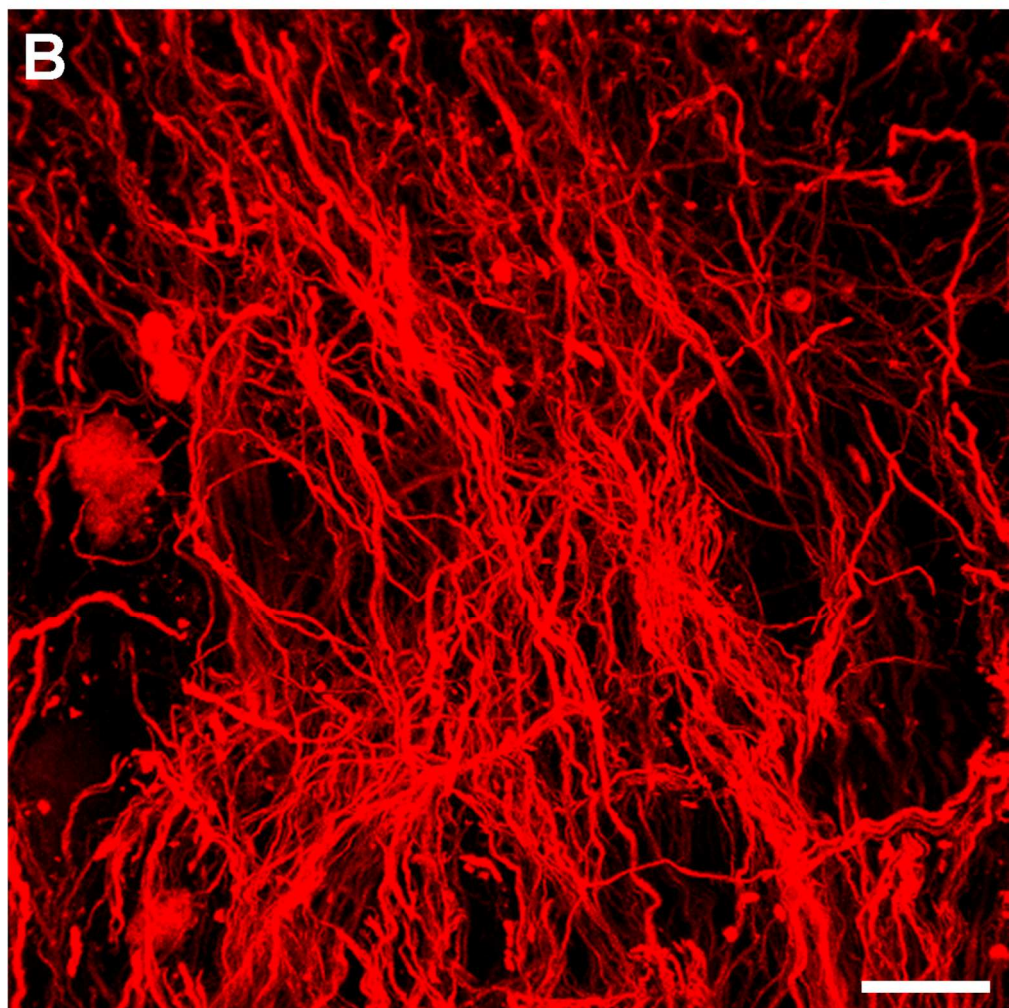
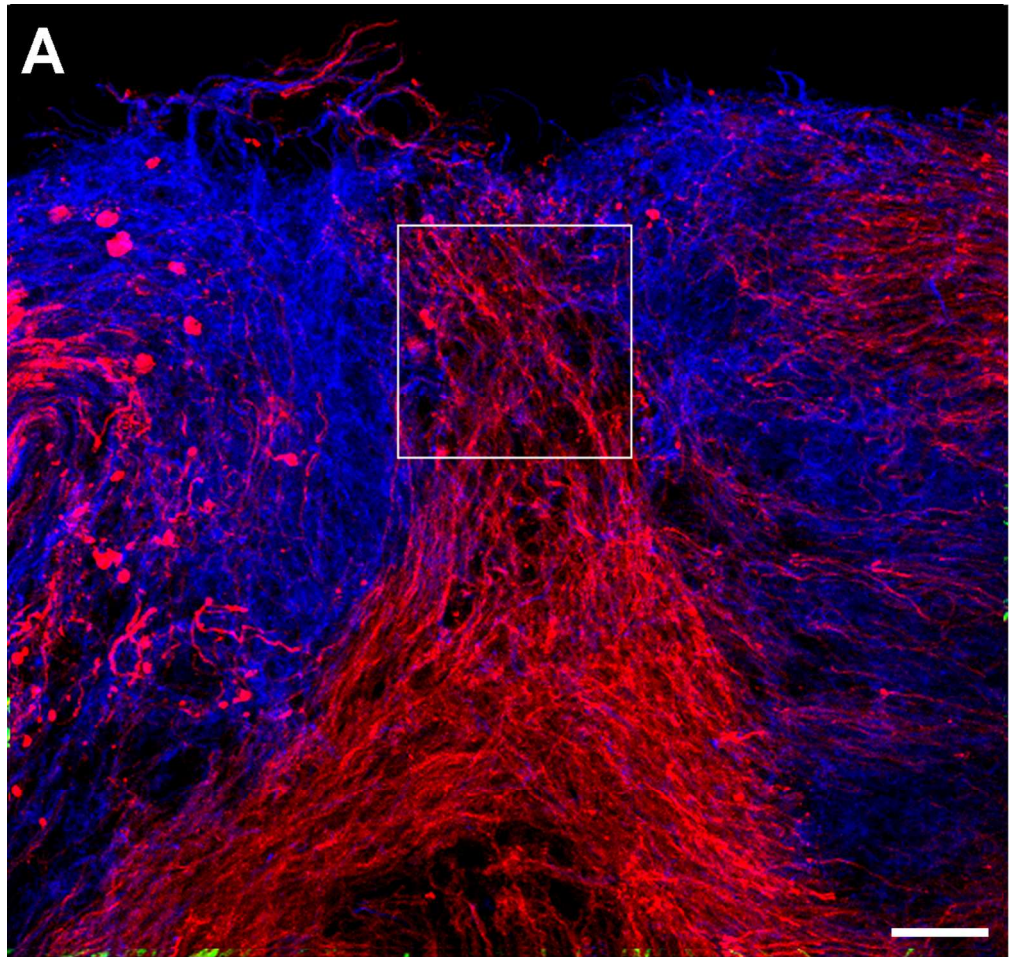
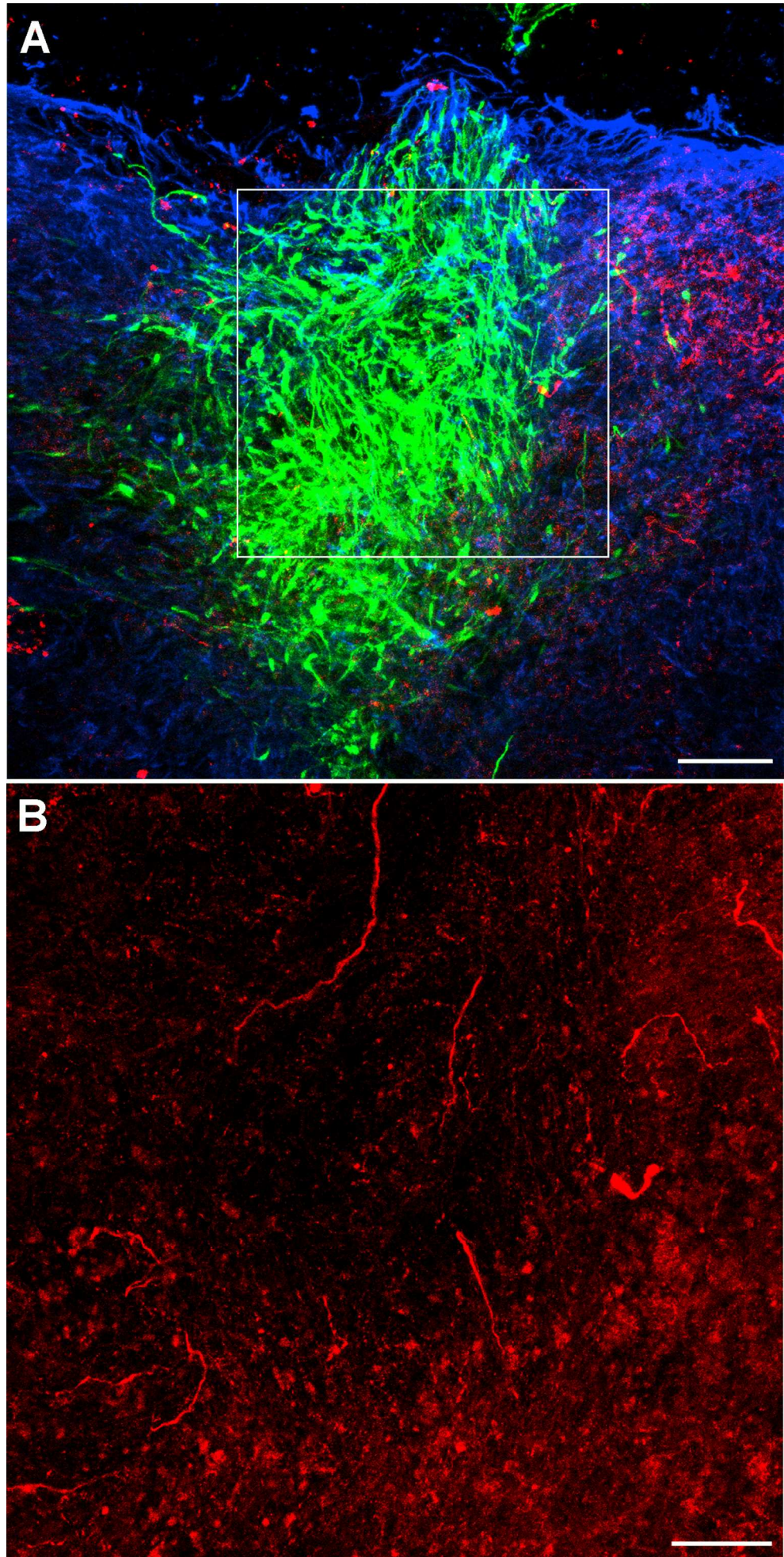


Figure 5-11. Regeneration of tract traced sensory axons in the lesion of a delayed transplanted animal.

Confocal projected image stacks of the dorsal column lesion in a parasagittal section spanning the lesion. **A)** OECs (green) integrated very well in the injection site. Objective: 10x. **B)** High magnification (40x oil) of the boxed area in **A** showing the presence of BDA labelled axons in the lesion; these axons were randomly orientated. Scale bars: 50 μm in **A** and 25 μm in **B**.



5.2.2.6 BDA labelled fibres in distal spinal cord

Once it was determined that regeneration into the injury could occur following a delayed transplantation, the question that arose was whether an optimal distribution of OECs rostral to the injury could allow for regenerating fibres to bridge the lesion and grow for long distances.

A large number of fibres were detected in the lateral cord indicating that fibre sparing was still occurring 10 weeks after injury. Similarly to the fibres described in the section 3.2.2.4.1 these fibres passed the lesion site on lateral undamaged parasagittal sections; the fibres sent collaterals to the grey matter and the trajectory and size of these axons appeared similar to that of undamaged fibres.

Importantly, some BDA labelled axons were found also in the medial spinal cord. Here the majority of fibres, 76%, were found in association with OECs; while 24% of fibres were not associated with the transplanted cells (Table 28, Table 29). The BDA labelled axons that were not associated with OECs were in most cases present on sections close to the dorsal column border and they most likely derived from spared fibres approaching the dorsal columns from the lateral cord.

| | | Number of axons | | | | | | | | |
|--|--------------|-----------------|--------|--------|-------|-------|-------|------------|------------|------------|
| | | R6007 | R21607 | R21707 | R3208 | R3308 | R5308 | R5408 | Average | St. Error |
| Distance from the lesion (μm) | 200 | 0 | 2 | 11 | 0 | 0 | 6 | 9 | 4.0 | 1.8 |
| | 400 | 0 | 2 | 2 | 0 | 0 | 4 | 4 | 1.7 | 0.7 |
| | 600 | 0 | 1 | 2 | 0 | 1 | 2 | 1 | 1.0 | 0.3 |
| | 800 | 0 | 0 | 2 | 0 | 1 | 1 | 0 | 0.6 | 0.3 |
| | 1000 | 0 | 0 | 0 | 0 | 2 | 2 | 0 | 0.6 | 0.4 |
| | 1200 | 0 | 0 | 0 | 0 | 5 | 4 | 0 | 1.3 | 0.8 |
| | 1400 | 0 | 0 | 2 | 0 | 3 | 5 | 0 | 1.4 | 0.8 |
| | 1600 | 0 | 0 | 1 | 0 | 1 | 0 | 0 | 0.3 | 0.2 |
| | 3200 | - | 0 | 0 | 0 | 0 | 0 | 0 | 0.0 | 0.0 |
| | 3600 | - | 0 | 0 | 0 | 0 | 0 | 0 | 0.0 | 0.0 |
| | 4000 | - | 0 | 0 | 0 | 0 | 0 | 0 | 0.0 | 0.0 |
| | 4400 | - | 0 | 0 | 0 | 0 | 0 | 0 | 0.0 | 0.0 |
| | 4800 | - | 0 | 0 | 0 | 0 | 0 | 0 | 0.0 | 0.0 |
| | 10000 | - | 0 | 0 | 0 | 0 | 0 | 0 | 0.0 | 0.0 |
| | 10400 | - | 0 | 0 | 0 | 0 | 0 | 0 | 0.0 | 0.0 |
| | 10800 | - | 0 | 0 | 0 | 0 | 0 | 0 | 0.0 | 0.0 |
| | 11200 | - | 0 | 0 | 0 | 0 | 0 | 0 | 0.0 | 0.0 |
| 11600 | - | 0 | 0 | 0 | 0 | 0 | 0 | 0.0 | 0.0 | |

Table 28. Number of BDA labelled fibres associated with OECs at increasing distance from the lesion in the medial spinal cord following delayed OEC transplantation.

Quantification of axon number rostral to the lesion performed with an epifluorescence microscope and 63x lens on parasagittal sections of the lesion block, rostral block and thoracic block. Blank cells are used to indicate that data did not meet the inclusion criteria.

| | | Number of axons | | | | | | | Average | St. Error |
|--|-------|-----------------|--------|--------|-------|-------|-------|-------|---------|-----------|
| | | R6007 | R21607 | R21707 | R3208 | R3308 | R5308 | R5408 | | |
| Distance from the lesion (μm) | 200 | 0 | 0 | 0 | 0 | 6 | 0 | 0 | 0.9 | 0.9 |
| | 400 | 0 | 0 | 0 | 0 | 3 | 0 | 0 | 0.4 | 0.4 |
| | 600 | 0 | 0 | 0 | 0 | 1 | 0 | 0 | 0.1 | 0.1 |
| | 800 | 0 | 0 | 0 | 2 | 0 | 0 | 0 | 0.3 | 0.3 |
| | 1000 | 0 | 0 | 0 | 2 | 0 | 0 | 0 | 0.3 | 0.3 |
| | 1200 | 0 | 0 | 0 | 0 | 0 | 0 | 0 | 0.0 | 0.0 |
| | 1400 | 0 | 0 | 0 | 0 | 0 | 0 | 0 | 0.0 | 0.0 |
| | 1600 | 0 | 0 | 0 | 0 | 0 | 0 | 0 | 0.0 | 0.0 |
| | 3200 | - | 0 | 0 | 0 | 0 | 0 | 1 | 0.2 | 0.2 |
| | 3600 | - | 0 | 0 | 0 | 0 | 0 | 6 | 1.0 | 1.0 |
| | 4000 | - | 0 | 0 | 0 | 0 | 0 | 1 | 0.2 | 0.2 |
| | 4400 | - | 0 | 0 | 0 | 0 | 0 | 0 | 0.0 | 0.0 |
| | 4800 | - | 0 | 0 | 0 | 0 | 0 | 0 | 0.0 | 0.0 |
| | 10000 | - | 0 | 0 | 0 | 1 | 0 | 0 | 0.2 | 0.2 |
| | 10400 | - | 0 | 0 | 0 | 1 | 0 | 0 | 0.2 | 0.2 |
| | 10800 | - | 0 | 0 | 0 | 1 | 0 | 0 | 0.2 | 0.2 |
| | 11200 | - | 0 | 0 | 0 | 1 | 0 | 0 | 0.2 | 0.2 |
| 11600 | - | 0 | 0 | 0 | 1 | 0 | 0 | 0.2 | 0.2 | |

Table 29. Number of BDA labelled fibres not associated with OECs at increasing distance from the dorsal column lesion in the medial spinal cord following delayed OEC transplantation.

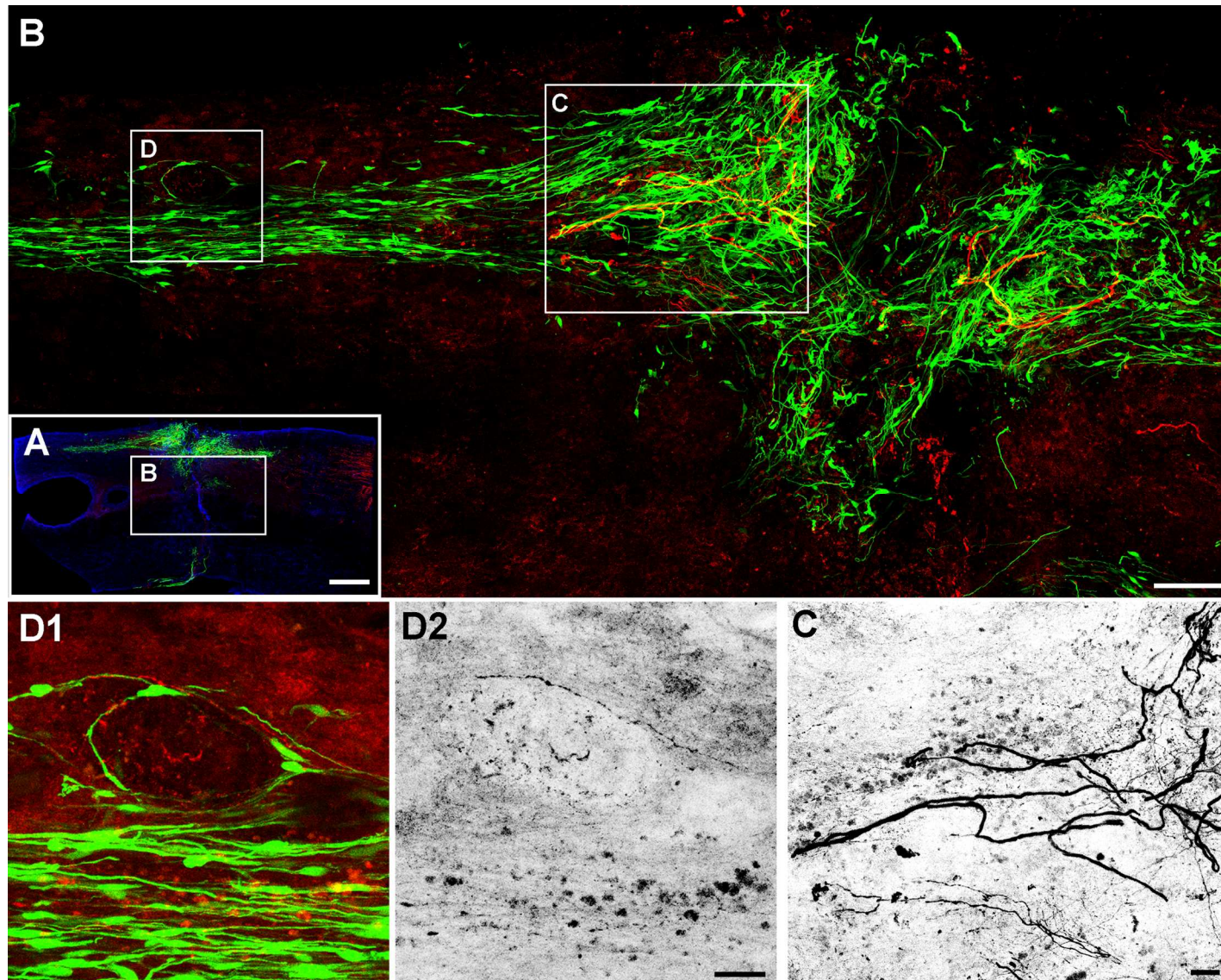
Quantification of axon number rostral to the lesion performed with an epifluorescence microscope and 63x lens on parasagittal sections of the lesion block, rostral block and thoracic block. Blank cells are used to indicate that data did not meet the inclusion criteria.

5.2.2.7 Genuine regenerating BDA labelled fibres above the lesion level

The same stringent selection criteria used in section 3.2.3.9 was applied to the data to include in the quantification only fibres that had convincingly regenerated. After this process, long distance bridging axonal regeneration was detected rostral to the lesion in three animals. All regenerating axons were located in close vicinity to OECs. An example of regeneration is shown in Figure 5-12. The fibre number quantification is shown in Table 30. This data indicates that DRG neurons can regenerate their central axons across a spinal cord lesion even after a delayed transplantation of OECs in the absence of any other treatment.

Figure 5-12. Long distance axonal regeneration following a delayed OEC transplant.

A) Confocal image taken with a low power objective (10x) of a parasagittal section of the lesion block in a rat transplanted with OECs into a 4 weeks old dorsal column lesion; boxed area is depicted at higher magnification (40x) in **B**. **B)** Continuous tract of OECs exiting the lesion paved the way for regenerating axons to grow through. **C)** Enlarged image of the boxed area in **B** that shows axons regenerating in the lesion in greyscale. **D1-D2)** Enlarged images of the boxed area in **B** with a regenerating axon located within the OEC tract. **D2)** BDA labelled regenerating axons in greyscale. **A-D)** Composite of confocal projected image stacks. Colour codes: red (axons), green (OECs), blue (astrocytes). Scale bars: 500 μm in **A**, 100 μm in **B** and 25 μm in **C-D**.



| | | Number of axons | | | | | | | Average | St. Error |
|--|-------|-----------------|--------|--------|-------|-------|-------|-------|---------|-----------|
| | | R6007 | R21607 | R21707 | R3208 | R3308 | R5308 | R5408 | | |
| Distance from the lesion (μm) | 200 | - | 2 | 11 | - | - | 6 | - | 6.3 | 2.6 |
| | 400 | - | 2 | 2 | - | - | 4 | - | 2.7 | 0.7 |
| | 600 | - | 1 | 2 | - | - | 2 | - | 1.7 | 0.3 |
| | 800 | - | 0 | 2 | - | - | 1 | 0 | 0.8 | 0.5 |
| | 1000 | - | 0 | 0 | - | - | 2 | 0 | 0.5 | 0.5 |
| | 1200 | - | 0 | 0 | - | - | 4 | 0 | 1.0 | 1.0 |
| | 1400 | - | 0 | 2 | - | - | 5 | 0 | 1.8 | 1.2 |
| | 1600 | - | 0 | 1 | - | - | 0 | 0 | 0.3 | 0.3 |
| | 3200 | - | - | - | - | - | - | - | - | - |
| | 3600 | - | - | - | - | - | - | - | - | - |
| | 4000 | - | - | - | - | - | - | - | - | - |
| | 4400 | - | - | - | - | - | - | - | - | - |
| | 4800 | - | - | - | - | - | - | - | - | - |
| | 10000 | - | - | - | - | - | - | - | - | - |
| | 10400 | - | - | - | - | - | - | - | - | - |
| | 10800 | - | - | - | - | - | - | - | - | - |
| | 11200 | - | - | - | - | - | - | - | - | - |
| 11600 | - | - | - | - | - | - | - | - | - | |

Table 30. Number of BDA labelled regenerating axons at increasing distance from the lesion in the medial spinal cord following delayed OEC transplantation.

Quantification of axon number rostral to the lesion performed with an epifluorescence microscope and 63x lens on parasagittal sections of the lesion block, rostral block and thoracic block. Blank cells are used to indicate that data did not meet the inclusion criteria or the stringency applied.

5.2.3 Combined delayed transplant and delayed conditioning lesion paradigm

To understand whether the number of axons labelled with BDA above the spinal cord lesion could be increased by combining delayed OEC transplantation with a delayed conditioning lesion, eleven animals were treated using this combination (Figure 5-13).

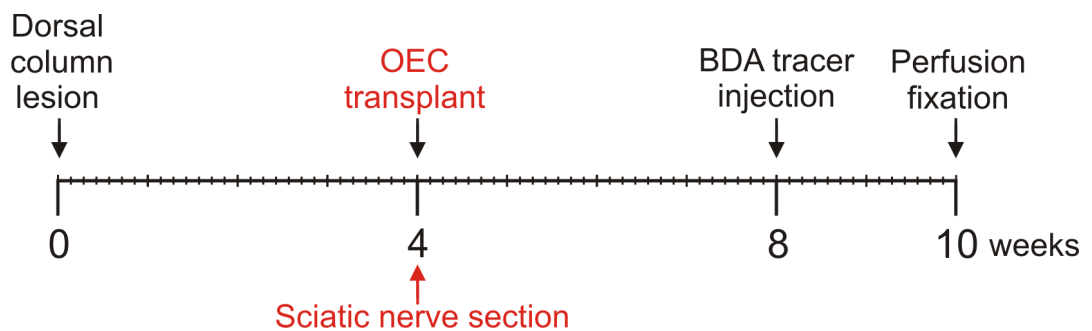


Figure 5-13. Time course of procedures performed on animals receiving delayed OEC transplant and conditioning lesion.

5.2.3.1 OEC distribution in the spinal cord

In 64% and 45% of the rats OECs had distributed respectively rostral and caudal to the lesion. In 45% of the animals OECs formed continuous tracts that exited the lesion and extended for varying distances above it. These ended on average 2640 μm above the lesion.

5.2.3.2 BDA labelled fibres within and rostral to the lesion

A variable number of BDA labelled fibres was found in association with OECs in the lesion of 73% (8/11) of the animals.

Tract traced axons were detected rostral to the lesion in the lateral cord. BDA labelled fibres were also found in the medial cord and the average increase

compared to delayed transplanted animals was 9 fold, a difference that was not however significant, probably due to the high variability. The increase was comparable with the 7 fold increase we described in section 3.2.4.4 after combining conditioning lesion with OEC transplant into a fresh lesion (Figure 5-14). The majority of fibres (92%) were associated with OECs (Table 31, Table 32). BDA labelled axons that were not associated with OECs were in most cases present on sections close to the lateral border of the dorsal columns and were presumably spared fibres or sprouting fibres in continuity with spared fibres approaching the dorsal columns.

| | | Number of axons | | | | | | | | | | | Average | St. Error | |
|--|-------------|-----------------|--------|--------|--------|--------|--------|--------|--------|--------|--------|------------|------------|------------|--|
| | | R10408 | R11208 | R11608 | R11708 | R12008 | R16208 | R16308 | R23408 | R23508 | R23708 | R23808 | | | |
| Distance from the lesion (μm) | 200 | 3 | 3 | 0 | 0 | 0 | 39 | 45 | 0 | 0 | 0 | 0 | 8.2 | 5.1 | |
| | 400 | 7 | 5 | 0 | 0 | 0 | 34 | 52 | 0 | 0 | 0 | 0 | 8.9 | 5.3 | |
| | 600 | 3 | 9 | 0 | 0 | 0 | 23 | 52 | 0 | 0 | 0 | 0 | 7.9 | 4.9 | |
| | 800 | 8 | 7 | 0 | 0 | 0 | 29 | 51 | 0 | 0 | 0 | 0 | 8.6 | 5.0 | |
| | 1000 | 5 | 6 | 0 | 0 | 0 | 33 | 45 | 0 | 0 | 0 | 0 | 8.1 | 4.7 | |
| | 1200 | 3 | 3 | 0 | 0 | 0 | 29 | 47 | 0 | 0 | 0 | 0 | 7.5 | 4.7 | |
| | 1400 | 1 | 0 | 0 | 0 | 0 | 27 | 27 | 0 | 0 | 0 | 0 | 5.0 | 3.3 | |
| | 1600 | 4 | 0 | 0 | 0 | 0 | 28 | 36 | 0 | 0 | 0 | 0 | 6.2 | 3.9 | |
| | | | | | | | | | | | | | | | |
| | 3200 | 0 | 0 | 0 | 0 | 0 | 4 | 3 | 0 | 3 | 0 | 0 | 0.9 | 0.5 | |
| | 3600 | 0 | 0 | 0 | 0 | 0 | 0 | 2 | 0 | 1 | 0 | 0 | 0.3 | 0.2 | |
| | 4000 | 0 | 0 | 0 | 0 | 0 | 0 | 0 | 0 | 1 | 0 | 0 | 0.1 | 0.1 | |
| | 4400 | 0 | 0 | 0 | 0 | 0 | 0 | 0 | 0 | 0 | 0 | 0 | 0.0 | 0.0 | |
| | 4800 | 0 | 0 | 0 | 0 | 0 | 0 | 0 | 0 | 1 | 0 | 0 | 0.1 | 0.1 | |
| | | | | | | | | | | | | | | | |
| | 1000 | 0 | 0 | - | 0 | 0 | 0 | 0 | 0 | 0 | 0 | 0 | 0.0 | 0.0 | |
| | 1000 | 0 | 0 | - | 0 | 0 | 0 | 0 | 0 | 0 | 0 | 0 | 0.0 | 0.0 | |
| 10800 | 0 | 0 | - | 0 | 0 | 0 | 0 | 0 | 0 | 0 | 0 | 0.0 | 0.0 | | |
| 11200 | 0 | 0 | - | 0 | 0 | 0 | 0 | 0 | 0 | 0 | 0 | 0.0 | 0.0 | | |
| 11600 | 0 | 0 | - | 0 | 0 | 0 | 0 | 0 | 0 | 0 | 0 | 0.0 | 0.0 | | |

Table 31. Number of BDA labelled fibres associated with OECs at increasing distance from the dorsal column lesion in the medial spinal cord following combined delayed OEC transplantation and conditioning lesions.

Quantification of axon number rostral to the lesion performed with an epifluorescence microscope and 63x lens on parasagittal sections of the lesion block, rostral block and thoracic block. Blank cells are used to indicate that data did not meet the inclusion criteria.

| | | Number of axons | | | | | | | | | | | Average | St. Error | |
|--|------|-----------------|--------|--------|--------|--------|--------|--------|--------|--------|--------|--------|---------|-----------|--|
| | | R10408 | R11208 | R11608 | R11708 | R12008 | R16208 | R16308 | R23408 | R23508 | R23708 | R23808 | | | |
| Distance from the lesion (μm) | 200 | 0 | 0 | 0 | 0 | 0 | 0 | 0 | 0 | 1 | 0 | 0 | 0.1 | 0.1 | |
| | 400 | 0 | 0 | 0 | 0 | 0 | 0 | 0 | 0 | 3 | 0 | 0 | 0.3 | 0.3 | |
| | 600 | 0 | 0 | 0 | 0 | 0 | 0 | 0 | 0 | 2 | 0 | 0 | 0.2 | 0.2 | |
| | 800 | 0 | 0 | 0 | 0 | 0 | 0 | 2 | 0 | 4 | 0 | 0 | 0.5 | 0.4 | |
| | 1000 | 0 | 0 | 0 | 0 | 0 | 0 | 3 | 0 | 3 | 0 | 0 | 0.5 | 0.4 | |
| | 1200 | 0 | 0 | 0 | 0 | 0 | 1 | 2 | 0 | 2 | 0 | 0 | 0.5 | 0.2 | |
| | 1400 | 0 | 0 | 0 | 0 | 0 | 1 | 3 | 0 | 2 | 0 | 0 | 0.5 | 0.3 | |
| | 1600 | 0 | 0 | 0 | 0 | 0 | 2 | 7 | 0 | 2 | 0 | 0 | 1.0 | 0.6 | |
| | | | | | | | | | | | | | | | |
| | 3200 | 0 | 0 | 0 | 0 | 0 | 0 | 0 | 0 | 3 | 0 | 0 | 0.3 | 0.3 | |
| | 3600 | 0 | 0 | 0 | 0 | 0 | 0 | 0 | 0 | 1 | 0 | 0 | 0.1 | 0.1 | |
| | 4000 | 0 | 0 | 0 | 0 | 0 | 0 | 0 | 0 | 1 | 0 | 0 | 0.1 | 0.1 | |
| | 4400 | 0 | 0 | 0 | 0 | 0 | 0 | 0 | 0 | 0 | 0 | 0 | 0.0 | 0.0 | |
| | 4800 | 0 | 0 | 0 | 0 | 0 | 0 | 0 | 0 | 1 | 0 | 0 | 0.1 | 0.1 | |
| | | | | | | | | | | | | | | | |
| | 1000 | 0 | 0 | - | 0 | 0 | 0 | 0 | 0 | 3 | 0 | 0 | 0.3 | 0.3 | |
| | 1000 | 0 | 0 | - | 0 | 0 | 0 | 0 | 0 | 3 | 0 | 0 | 0.3 | 0.3 | |
| 10800 | 0 | 0 | - | 0 | 0 | 0 | 0 | 0 | 3 | 0 | 0 | 0.3 | 0.3 | | |
| 11200 | 0 | 0 | - | 0 | 0 | 0 | 0 | 0 | 3 | 0 | 0 | 0.3 | 0.3 | | |
| 11600 | 0 | 0 | - | 0 | 0 | 0 | 0 | 0 | 2 | 0 | 0 | 0.2 | 0.2 | | |

Table 32. Number of BDA labelled fibres not associated with OECs at increasing distance from the dorsal column lesion in the medial spinal cord following combined delayed OEC transplantation and conditioning lesions.

Quantification of axon number rostral to the lesion performed with an epifluorescence microscope and 63x lens on parasagittal sections of the lesion block, rostral block and thoracic block. Blank cells are used to indicate that data did not meet the inclusion criteria.

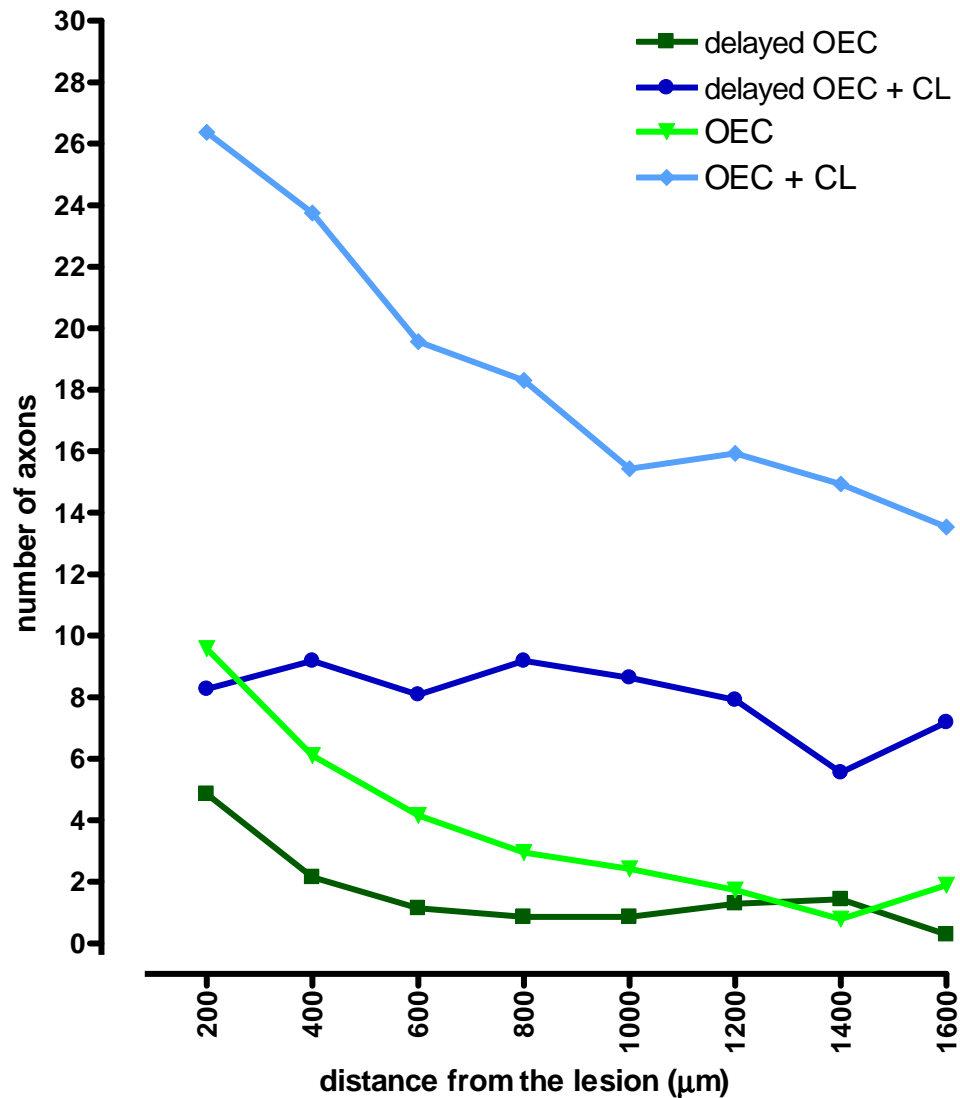


Figure 5-14. Summary of results for sprouting/regeneration of fibres rostral to the lesion in the medial cord.

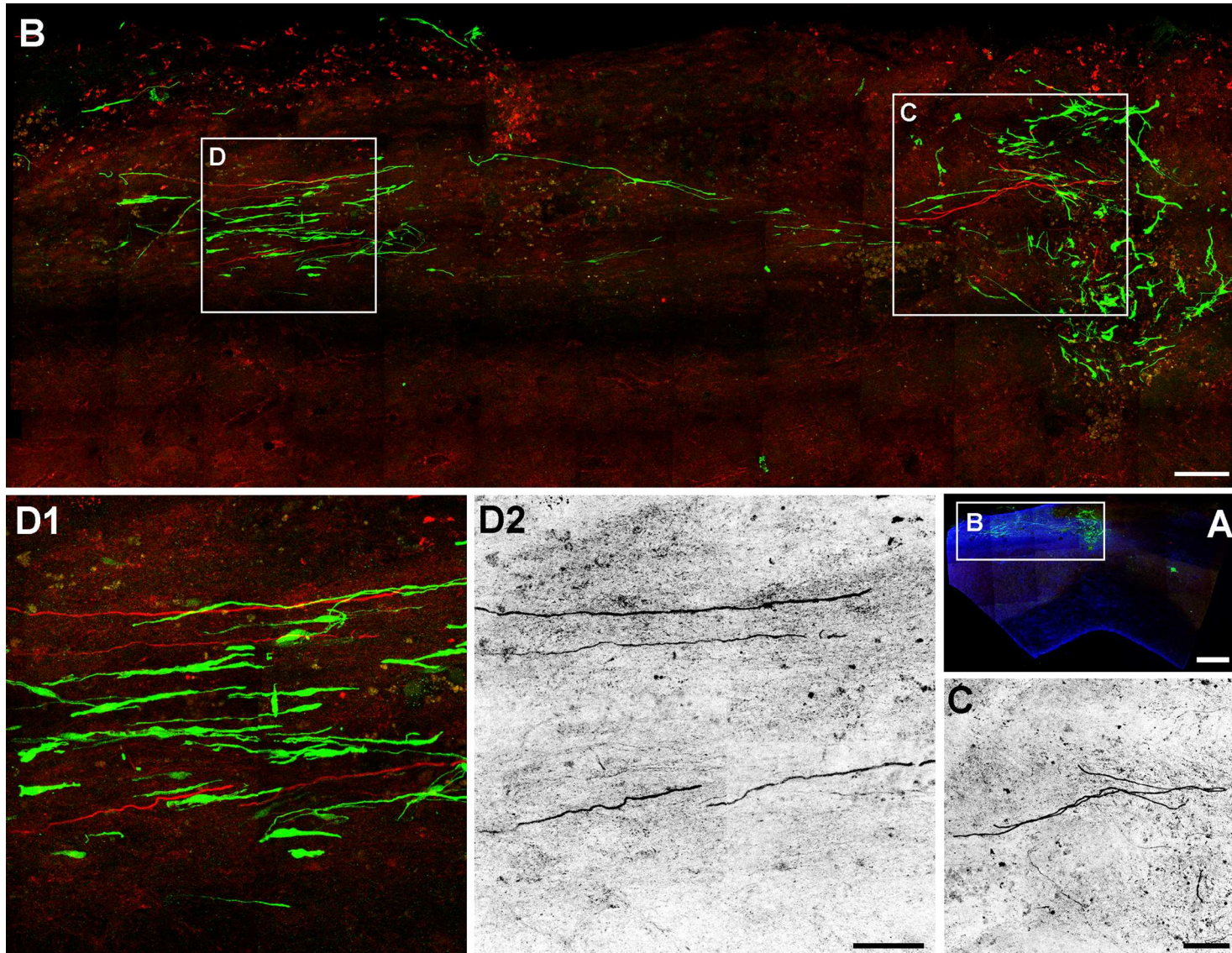
The number of BDA labelled axons following a delayed OEC transplant were half those present following an acute OEC transplantation, however the difference was not significant. Delayed conditioning lesion combined with delayed OEC transplant was associated with a 9 fold increase in the number of axons compared to delayed OEC transplant alone, however the difference was not significant. This increase was similar to the 7 fold potentiation that conditioning lesions had on fibre number following acute OEC transplantation.

5.2.3.3 Genuine regenerating BDA labelled fibres above the lesion level

Following the application of the stringent criteria to exclude spared or sprouted fibres, only two animals displayed regeneration rostral to the lesion (see example in Figure 5-15). Two more animals, although possessing continuous tracts of OECs exiting the lesion did not develop any bridging regeneration. Fibre number is shown in Table 33 and comparison with non-conditioning lesioned animals and with acute transplanted animals is shown in Figure 5-16. The difference between conditioned and non conditioned delayed transplanted animals was not significant, although this is not surprising given the limited number of animals with genuine regeneration.

Figure 5-15. Long distance axonal regeneration following delayed OEC transplantation combined with a delayed conditioning lesion.

A) Confocal image taken with a low power objective (10x) of a parasagittal section of the lesion block in a rat transplanted with OECs 4 weeks after a dorsal column lesion; boxed area is depicted at higher magnification (40x) in **B**. **B)** Tract of OECs exiting the lesion and associated with regenerating axons. The continuity of the OEC tract and of the axons in the tract with the lesion site was found on the next parasagittal section that is not shown here. **C)** Enlarged image of the boxed area in **B** that shows axons regenerating in the lesion in greyscale. **D1-D2)** enlarged images of the boxed area shown in **B** with regenerating axons. **D2)** BDA labelled regenerating axons in greyscale. **A-D)** Composite of confocal projected image stacks. Colour codes: red (axons), green (OECs), blue (astrocytes). Scale bar: 500 μm in **A**, 100 μm in **B**, 50 μm in **C-D**.



| | | Number of axons | | | | | | | | | | | Average | St. Error | |
|--|-------|-----------------|--------|--------|--------|--------|--------|--------|--------|--------|--------|--------|---------|-----------|---|
| | | R10408 | R11208 | R11608 | R11708 | R12008 | R16208 | R16308 | R23408 | R23508 | R23708 | R23808 | | | |
| Distance from the lesion (μm) | 200 | 3 | 3 | - | - | - | - | - | - | - | 0 | 0 | 1.5 | 0.9 | |
| | 400 | 7 | 5 | - | - | - | - | - | - | - | 0 | 0 | 3.0 | 1.8 | |
| | 600 | 3 | 9 | - | - | - | - | - | - | - | 0 | 0 | 3.0 | 2.1 | |
| | 800 | 8 | 7 | - | - | - | - | - | - | - | 0 | 0 | 3.8 | 2.2 | |
| | 1000 | 5 | 6 | - | - | - | - | - | - | - | 0 | 0 | 2.8 | 1.6 | |
| | 1200 | 3 | 3 | - | - | - | - | - | - | - | 0 | 0 | 1.5 | 0.9 | |
| | 1400 | 1 | - | - | - | - | - | - | - | - | 0 | 0 | 0.3 | 0.3 | |
| | 1600 | 4 | - | - | - | - | - | - | - | - | 0 | - | 2.0 | 2.0 | |
| | 3200 | - | - | - | - | - | - | - | - | - | - | - | - | - | - |
| | 3600 | - | - | - | - | - | - | - | - | - | - | - | - | - | - |
| | 4000 | - | - | - | - | - | - | - | - | - | - | - | - | - | - |
| | 4400 | - | - | - | - | - | - | - | - | - | - | - | - | - | - |
| | 4800 | - | - | - | - | - | - | - | - | - | - | - | - | - | - |
| | 1000 | - | - | - | - | - | - | - | - | - | - | - | - | - | - |
| | 1000 | - | - | - | - | - | - | - | - | - | - | - | - | - | - |
| | 10800 | - | - | - | - | - | - | - | - | - | - | - | - | - | - |
| 11200 | - | - | - | - | - | - | - | - | - | - | - | - | - | - | |
| 11600 | - | - | - | - | - | - | - | - | - | - | - | - | - | - | |

Table 33. Number of BDA labelled regenerating axons at increasing distance from the lesion in the medial spinal cord following combined delayed OEC transplantation and conditioning lesions.

Quantification of axon number rostral to the lesion performed with an epifluorescence microscope and 63x lens on parasagittal sections of the lesion block, rostral block and thoracic block. Blank cells are used to indicate that data did not meet the inclusion criteria or the stringency applied.

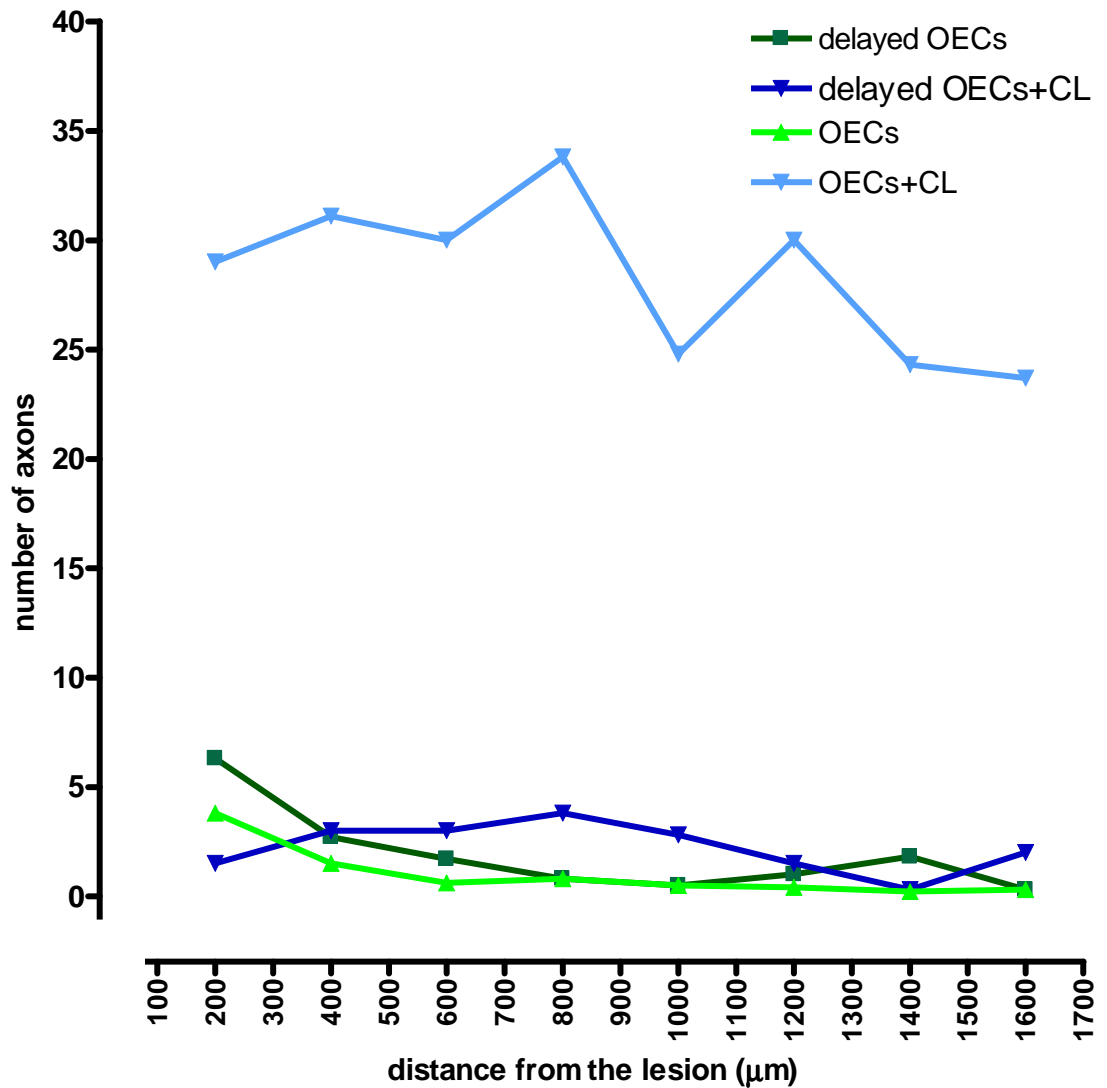


Figure 5-16. Summary of regeneration of fibres rostral to the lesion in the medial cord after applying criteria to exclude non regenerating fibres.

The number of regenerating BDA labelled axons following a delayed OEC transplant were not significantly different between acute and delayed transplanted animals. The combination of delayed OEC transplantation and delayed conditioning lesion did not promote a greater degree of regeneration rostral to the injury compared to delayed OEC transplantation alone.

5.3 Discussion

5.3.1 OEC protective effect on the lesion

In the third chapter we discussed the protective effect OEC transplantation had on the lesion 6 weeks after transplantation into a fresh wire knife dorsal column transection. In the present chapter we looked at the lesion morphology and size six weeks after a delayed transplantation paradigm. By means of GFP expression, we noted that OECs integrated in the lesion of the majority of delayed injected animals. Successful OEC integration was associated with the complete disappearance of the lesion cavity in these animals. This finding is extremely interesting as such good integration and cavity reduction was not found in animals transplanted acutely with OECs. It must be highlighted that transplantation into a fresh dorsal column lesion was performed only minutes after the lesion procedure took place that is before the lesion had degenerated and had formed a cavity. In contrast, delayed transplantation of OECs was performed 4 weeks after the dorsal column lesion procedure when supposedly a large cavity had already developed. In support of the fact that a cavity had already developed in the lesion by the time the delayed transplantation was performed, we found a large lesion cavity in animals 6 weeks after the injury and in a previous publication we reported the presence of a large cavity that formed already 2 weeks after the same lumbar wire knife dorsal column lesion paradigm (Toft et al., 2007). Furthermore, others have reported that the cavity formed by 2 days from a crush injury (Ramer et al., 2004a) or 8 days from contusion injury (Hill et al., 2001). Consequently, in our present study, delayed transplantation of OECs rather than preventing the formation of a cavity as we observed in the acute transplantation paradigm in the third chapter, largely filled an existing cavity. A similar result was reported by Plant et al. (2003) who transplanted OECs into a contusion injury concurrently or 1 week after the lesion. Plant and colleagues, in this study, in agreement with us reported a more efficacious reduction of the cavity size when the cell transplantation was

performed chronically rather than acutely. To explain these findings, we might hypothesise that the lesion environment 4 weeks after the dorsal column lesion was less hostile to OEC integration compared to a fresh dorsal column lesion. Possibly, in a chronic lesion OECs are not exposed to the same level of cytotoxicity as they are in a fresh lesion (Plant et al., 2003). Furthermore the inflammatory response which is known to contribute to the secondary destructive effects on the lesion reaches its peak during the first week after injury and decreases thereafter (Popovich et al., 1999).

Importantly, in our present study we also show that the lesion size, as defined by the astrocytic GFAP labelling, was significantly diminished 6 weeks after an OEC delayed transplantation compared to the lesion size in animals 6 weeks following acute transplantation of OECs. This could be explained either by a migration of astrocytes into the cavity thus reducing the lesion size, or because the OEC transplant acted like a glue drawing opposite lesion borders back together.

Conversely, this decrease in lesion size healing was not observed in the 10 week survival animals that were not transplanted with OECs; instead the size of the lesion and lesion cavity of these animals, with the exception of a rat that developed an extremely large lesion, was similar to those of 6 week survival non-transplanted animals. These findings in our present study are an indication that the lesion degeneration reached plateau by 6 weeks and in the following weeks it remained stable in accordance with a previous finding by Ramer et al. (2004a) who found that the lesion cavity stopped becoming larger after the fourth week.

5.3.2 *Syringomyelia*

We reported in the third chapter cavitation of the central canal 6 weeks after a dorsal column lesion following acute OEC transplantation and to a greater extent also in non-transplanted animals. In the present chapter we have shown that in delayed OEC transplanted animals at 10 weeks survival the central canal was approximately double that present in animals transplanted acutely with OECs

with a 6 week survival, however this difference was not significant. This finding indicates that whilst OEC transplantation into a fresh dorsal column lesion significantly reduced the size of the lesion, the size of the lesion cavity and the size of the central canal cavity compared to non-transplanted animals. Instead a delayed transplantation paradigm reduced significantly the lesion size and lesion cavity size but not the degree of central canal cavitation which was increased. This finding indicates that the mechanisms that underlie the development of the lesion and of the central canal are different.

5.3.3 Regeneration in the lesion

The lesion in non-transplanted animals sacrificed 10 weeks after the dorsal column transection was not a hospitable environment for regenerating axons. Instead, we found that neurofilament labelled axons had grown profusely into the delayed transplant. We then questioned the possibility that also ascending sensory dorsal root ganglia neurons could cross the glial scar and grow into the lesion transplant. BDA tract traced axons effectively regenerated into the lesion. These findings are in accordance with other studies that reported growth of corticospinal axons into the lesion (Keyvan-Fouladi et al., 2003) and CGRP positive small peptidergic axons (Andrews and Stelzner, 2007). Furthermore, we also show that primary sensory afferents can cross the glial scar and regenerate in a delayed transplant.

5.3.4 OEC distribution beyond the lesion site

The glial scar forms a barrier that seals off the lesion environment from the spinal cord tissue. Four weeks after a wire knife lesion of the dorsal columns it has been shown that the glial scar has already developed (Toft et al., 2007). Nonetheless, in the present study transplantation of OECs into the lesion cavity at this stage resulted not only in integration of the OECs into the injection site, but resulted also in an extensive distribution of the OECs rostral and caudal to the lesion. This indicates that the lesion scar was permeable to the distribution

of OECs. This information complements and confirms a study by Andrews et al., (2007) who reported that delayed transplants of OECs but not those of Schwann cells transplanted into intact spinal cord tissue rostral or caudal to the lesion were able to cross the glial scar and enter the lesion. In our present study, importantly, OECs labelled with GFP formed continuous cell tracts that exited the lesion and extended rostral recapitulating what we had observed following acute transplantation. On average these OEC tracts were even longer than those that we found after acute OEC transplantation. Moreover, the presence of optimally distributed OECs rostral to the lesion led us to question whether these could pave the way for BDA labelled axons regeneration beyond the lesion.

5.3.5 BDA labelling beyond the lesion site

Labelling of spared/sprouted/regenerated axons have been previously reported following OEC transplantation into a chronic spinal cord injury (Lu et al., 2002; Plant et al., 2003; Keyvan-Fouladi et al., 2003; Lopez-Vales et al., 2006). Interestingly, these studies all focused on descending spinal pathways and did not consider ascending pathways including the dorsal root ganglia sensory neurons. For this reason we studied the labelling of tract traced ascending primary sensory afferents after a delayed OEC transplantation into a lesion four weeks after the wire knife dorsal column transection. Importantly, six weeks after the delayed transplantation axons were detected in the medial cord rostral to the lesion in OEC transplanted animals. We showed in the third chapter that no axons were present in the medial spinal cord rostral to the lesion in non-transplanted animals 6 weeks after the lesion. These present findings show that delayed OECs transplantation alone could promote regeneration/sprouting of dorsal root ganglia neurons. Furthermore, we report that tract traced axons rostral to the lesion were mostly associated with OECs that had distributed rostral to the injection site. This is an interesting finding as previous reports have not investigated thoroughly the relation between the increased numbers of tract traced axons on the other side of the lesion and the distribution of the transplanted cells. In particular Lopez-Vales and colleagues (2007) although detecting BDA labelling beyond the injury level found no labelling of p75 nine

months after transplantation. However as p75 is a marker for both non-myelinating Schwann cells and OECs, it must therefore be considered that myelinating OECs lose p75 expression and so the cells would not be detected. In contrast Keyvan-Fouladi et al. (2003) found peripheral type myelin ensheathing corticospinal axons located on the caudal side of the lesion, but did not provide photographic evidence of it nor provided any quantitative estimate.

5.3.6 Long distance axonal regeneration

The potentiation of sprouting of the ascending primary sensory afferents observed in our results following transplantation of OECs four weeks after the lesion is an extremely important finding as these mechanisms will probably be future optimal targets for treatment in patients with incomplete lesions of the spinal cord. In the case of complete injuries, instead, bridging long distance regeneration of primary sensory afferents and of other ascending and descending sensory and motor tracts and functional reconnection will be required.

Therefore, after detecting labelling of tract traced axons beyond the lesion of delayed OEC transplanted animals we sought to discriminate convincing regeneration from sparing and sprouting. For this purpose all fibres that were potentially spared or sprouted were subtracted from the quantification.

Following this process it was seen that delayed OEC transplantation promoted bridging axonal regeneration of injured dorsal root ganglia neurons. The regenerating axons were strictly associated with OEC tracts in continuity with the lesion transplant. This new finding indicates that OECs can promote regeneration in ascending sensory pathways following injury to the spinal cord. Secondly, we report that this regeneration occurred only in animals where the OECs had integrated optimally in the lesion and had formed continuous rostral tracts in continuity with the lesion.

5.3.7 Combined delayed OEC transplant and delayed conditioning lesions

Conditioning lesions of the peripheral axons of dorsal root ganglia increase the growth state of central axons in the spinal cord and this phenomenon is evident when the central axon is lesioned. We have reported in the third chapter that coupling pre-conditioning lesions with OECs potentiated the sprouting/regeneration of axons beyond the dorsal column lesion through an acute OEC transplant, confirming a previous similar finding by Andrews et al. (2004). Furthermore we showed that in the same treatment paradigm also genuine regeneration was significantly potentiated. Recent findings (Neumann et al., 2005; Ylera et al 2009) have demonstrated that conditioning lesions were effective at increasing the growth state of the central axons even when performed in a delayed lesion paradigm. These new findings led us to question whether a delayed conditioning lesion, performed four weeks after a dorsal column lesion, combined with a delayed OEC transplant could potentiate the growth of injured axons compared to the delayed OEC transplant performed alone. We found that the number of axons that were located rostral to the lesion in the medial cord was increased when comparing animals with a combined delayed treatment paradigm to animals receiving a delayed OEC transplant only. The increase was 9 fold, similar to the potentiation of 7 times that we observed in the OEC acute combined transplantation paradigm. This new finding indicates that combination of OEC transplant and conditioning lesions, both performed four weeks after the actual spinal cord injury, are effective at promoting regeneration/sprouting.

To understand whether bridging regeneration *per se* could be augmented by this combined delayed treatment paradigm, we subtracted from the quantification of axonal labelling rostral to the lesion all the counts of axons that appeared potentially spared or sprouting. The resulting data indicates that regeneration can be claimed only in two animals. Two more animals, although possessing optimally distributed OECs, did not display any degree of regeneration. We found that on average the degree of regeneration following the combined delayed treatment paradigm was not augmented compared to OEC

transplantation alone. To interpret these unexpected results we suggest two possible explanations: 1) the conditioning lesion was more effective at promoting sparing and consequently sprouting of spared fibres into the medial cord rather than regeneration of injured axons; 2) or that the conditioning lesion was so effective at promoting both regeneration and sparing and sprouting that most of the animals where regeneration had occurred were not included in the quantification of genuine regeneration, because the minimum distance of three sections devoid of BDA labelling that were required for convincing regeneration had cut out animals where regeneration had actually occurred.

6 Conclusions

In this thesis we have investigated strategies for promoting axonal regeneration across a CNS lesion and the effect of these strategies on repair at the lesion and pathology involving the central canal.

It is well known that axons have the potential to regenerate through the PNS because this is devoid of the inhibitory cues present in the CNS, as shown by placing a peripheral nerve stump in a spinal cord lesion before the glial scar is formed (David and Aguayo, 1981). However, in the CNS axons cannot regenerate after injury due to the increased inhibition exerted by extracellular molecules such as chondroitin sulfate proteoglycans and semaphorins that are upregulated in the lesion scar and molecules such as Nogo, OmGP and MAG which are released by damaged oligodendrocytes (Raineteau and Schwab, 2001; Rosenzweig and McDonald, 2004). Axonal growth is controlled at multiple levels through exogenous inhibitory or growth promoting stimuli and by endogenous mechanisms that regulate the susceptibility of the neuron to these external stimuli and determine the resulting growth state of the axon. Therefore the best strategy to promote axonal regeneration is to act on the extrinsic and/or intrinsic regulators of axonal growth and move the balance from inhibition to growth. This is illustrated by experiments in which a small non-traumatic injury was generated in the spinal cord with a two-photon laser (Ylera et al., 2009) thus preventing the formation of a scar and large scale Wallerian degeneration. This growth limitation has also been overcome in larger experimental lesion models by reducing the inhibitory effect of the glial scar by inactivating the extracellular components that cause the inhibition: for example chondroitinase delivery (Silver and Miller, 2004) to digest CSPGs (Bradbury et al., 2002). The promotion of regeneration has also been achieved by the application of exogenous growth factors such as neurotrophins to provide a trophic source and promote axons to grow (Schnell et al., 1994). Other researchers have taken the approach of neutralising inhibitor molecules (e.g. Nogo) by delivering antibodies (Freund et al., 2006). Finally, a potential treatment after injury is based on cell transplantation which not only is known to promote a series of beneficial reparatory and protective effects on the lesion but also promotes the growth of axons through the glial scar (Verma and Fawcett, 2005).

OECs are amongst the most promising candidates for this purpose as they mediate regeneration in the peripheral and central nervous systems (Barnett and Riddell, 2004). While others have shown that OECs can promote growth of axons of DRG neurons in the spinal cord lesion (Ramon-Cueto et al., 2000; Imiazumi et al., 2000; Lu et al., 2001) they have not shown that convincing axonal regeneration can also occur. In this work we show that OECs can promote genuine bridging axonal regeneration of tract traced DRG neurons which did not occur in the absence of transplantation. We were only occasionally able to trace individual axons across the lesion site, because these could not be followed through consecutive sections. However, by excluding the possibility that axons had grown around the lesion we were able to determine indirectly that axons had grown through the lesion glial scar. In support of this we also found tract traced axons crossing the caudal border of the lesion scar and tract traced axons crossing the rostral border. It is not clear how the OECs promoted bridging axonal regeneration in the present study. There is a body of evidence that indicates OECs interact closely with astrocytes and do not cause astrocytosis while Schwann cells cause boundary formation and astrocytosis (Lakatos et al., 2003). However, these differences do not fit with our present finding that OEC and Schwann cell transplantation produces similar levels of bridging axonal regeneration. This discrepancy can be solved if we consider that endogenous Schwann cells have been reported to infiltrate spinal cord lesions (Black et al., 2006) and Schwann cell conditioned media added to OECs prevents OECs from interacting closely with astrocytes and causes astrocytosis as shown by Santos-Silva et al. (2007). This could suggest that endogenous Schwann cells infiltrated the OEC graft levelling the interactions between OECs and Schwann cells with astrocytes. In the present study bridging axonal regeneration was possibly achieved because both OECs and Schwann cells secreted growth promoting molecules that masked the scar inhibition and allowed axons to regenerate through the scar. Accordingly, it has been shown that OECs secrete NGF and BDNF and express GDNF (Woodhall et al., 2001) while Schwann cells synthesise NGF, BDNF and NT3 (Lin et al., 2003) and these molecules promote growth of axons (Kamei et al., 2007; Zhang et al., 2009). OECs and Schwann cells may also overcome the glial scar inhibition by providing a favourable substrate for the axons to grow on. In fact Schwann cells synthesise a variety of cell adhesion molecules including N-CAM, L1-CAM and N-cadherin and OECs express N-CAM, L1-

CAM, laminin and fibronectin (Lin et al., 2003) which have been shown to promote axonal growth (Becker et al., 2004; Tom et al., 2004). It is thought that the inhibition of the glial scar (CSPG and semaphorins) and of the products of myelin degeneration (Nogo, MAG) all act mainly through the small GTPase Rho on downstream regulators that modify actin turnover (Fawcett et al., 2006). By secreting cell adhesion molecules and soluble growth factors, OECs and Schwann cells might have promoted in the present work axonal regeneration across the scar by modifying the signal cascade involving Rho thus allowing axons to cross the scar. In accordance with this hypothesis it is thought that cAMP elevation following neurotrophin (NGF, BDNF or GDNF) delivery can inhibit Rho activity via protein kinase A (Qiu et al., 2000). Furthermore, viral transduction of red nucleus neurons with a dominant negative of Rock, a kinase activated by Rho, allowed these neurons to regenerate through a spinal cord lesion (Wu et al., 2009).

Conditioning lesions are thought to elevate the intrinsic growth state of the DRG neuron (Neumann et al., 2005). We performed conditioning lesions in our wire knife dorsal column lesion paradigm and found that they were not sufficient to promote axonal growth through the scar; however, when conditioning lesions were coupled with OEC or Schwann cell transplantation they boosted axonal regeneration. Conditioning lesions may also involve cAMP and possibly Rho signalling. In fact, conditioning lesions, similarly to neurotrophins, have been shown to elevate cAMP levels in the DRG and have been shown to block the inhibition of MAG/myelin via PKA (Qiu et al., 2002); PKA in turn could act on the Rho signalling pathway (Lang et al., 1996). If this was the case, it would be interesting to compare the levels of cAMP in the DRG after OEC or Schwann cell transplantation, after conditioning lesions and after combined treatments. In fact, based on the results in the present work it would be expected that cAMP levels in the DRG should be higher following combined treatment than following OEC or Schwann cell transplantation and lower still after conditioning lesions. Anyway, other signalling pathways involved in axonal growth might be involved, including ERK/MAPK, PI3/AKT and c-Jun N-terminal kinase pathways (Fawcett et al., 2006). In the present study conditioning lesions were also combined with fibroblast transplantation and promoted very little axonal growth into and beyond the lesion compared to OEC and Schwann cell transplantation. However,

axonal growth was higher than that seen in animals that had a conditioning lesion only, possibly due to the fact fibroblasts were able to reduce the lesion cavity more than Schwann cells and OECs thus potentially facilitating axonal outgrowth.

While a number of reports have indicated that the presence of transplanted OECs and Schwann cells in the lesion is related to growth of axons in and beyond the lesion, there has been very little consideration so far in studying in detail the association between axons regenerating on the distal side of the lesion and the distribution of the transplanted cells. Furthermore, this has been limited to descending systems (Xu et al., 1997; Li et al., 1998). To determine this relationship in more detail, we have studied the regeneration of axons rostral to the lesion and found that regeneration occurred only in those animals where a tract of GFP labelled transplanted cells exited the lesion and was mostly limited to the areas where also transplanted OECs and Schwann cells distributed. This finding indicates that axons preferentially regenerated through OEC and Schwann cell tracts even after crossing the glial scar. The present observation, that axons did not normally regenerate beyond the end of the cell tracts even if conditioning lesions were performed, could indicate that the host inhibitory environment was not permissive to axonal growth even at a distance from the inhibitory milieu of the scar, or that axons were not able to cross the border of the transplanted cell tracts and enter the host spinal cord because of trophic change; nevertheless axonal growth was found previously not to be restricted to grafts transplanted in the spinal cord and expressing NT3 (Fawcett et al., 2006). Although in the present study axons regenerated preferentially through tracts of transplanted cells, interestingly, they were only occasionally ensheathed by OECs or Schwann cells. This could suggest that axons grew on the substrate provided by endogenous astrocytes while the transplanted cells only provided local trophic support. In fact CNS neurons can regenerate their axons in regions of white matter following very closely the orientation of resident astrocytes and possibly using them as a substrate for growth (Davies et al., 1994, 2006).

OECs have been investigated previously in delayed transplantation paradigms and have been shown to promote axonal growth in the distal spinal cord, however the studies carried out did not show clearly that genuine regeneration instead of sparing or sprouting occurred (Lu et al., 2002; Plant et al., 2003;

Keyvan-Fouladi et al., 2003). Importantly, in this study I showed for the first time that convincing long distance, axonal regeneration can occur in the spinal cord following a delayed OECs transplantation, when OECs are optimally distributed to form tracts exiting the lesion.

In the present study, conditioning lesions were also performed with a delay of 4 weeks from the central lesion. With this timing they were able to promote a non-significant 9 fold increase in the number of sprouting/regeneration of axons in the distal cord where OECs were distributed, thus strengthening the concept that DRG neurons remain responsive to manipulations performed to modify their intrinsic growth state long after the spinal cord lesion is made, as reported previously by Ylera et al. (2009) and Neumann et al., (2005). The same cannot be said for genuine regeneration as we could not perform statistical analysis to support this, because few animals fitted the stringent criteria for regeneration. More animals should be therefore studied. Conditioning lesions were investigated as a proof of principle that increasing the intrinsic growth state of the neuron promotes regeneration. However in a clinical setting they would not be applicable; instead, manipulation of those pathways which are thought to be involved in the signal cascade initiated by the conditioning lesions should be investigated. As Neumann et al. (2002) and Qiu et al. (2002) both showed that cAMP injection into the DRG promoted some degree of regeneration compared to controls, then the results we obtained in the present study combining delayed OEC transplantation and delayed conditioning lesions could be repeated by replacing the delayed sciatic nerve transection with a delayed delivery of cAMP into the DRG. Especially considering that Pearse et al. (2004) promoted sparing and growth of axons in and beyond the lesion after combined treatment of Schwann cell transplantation and delivery of an analogue of cAMP into the lesion site, rather than in the DRG, thus not allowing discrimination between the effects of cAMP elevation on the immune response in the lesion from the direct effect of cAMP elevation on the axons.

Another open question that arises from the present work is whether the OECs and the Schwann cells are necessary only in an initial phase of the repair process to promote elongation and direct the growth cone of the regenerating axon, or are also necessary in a second phase to prevent the regenerated axon from degenerating. In the present work significantly more axons and OECs were

present two weeks after lesioning compared to the six week survival time supporting the latter explanation. However a more definitive approach to investigate this could be carried out by using transplantation of OECs or Schwann cells genetically modified to express a suicide gene to induce apoptosis in all transplanted cells and determine whether the regenerating axons would remain integrated in the host spinal cord or degenerate. For example, transduction of the herpes simplex virus thymidine kinase renders transplanted cells sensitive to the drug ganciclovir at concentrations that are non-lethal for the host cell types (Shuldiner et al., 2003).

The distance that the regenerating axons grew past the lesion in our study was compatible with the distance needed for them to form synapses with appropriate target neurons. In fact, if we had lesioned the spinal cord at the thoracic or cervical level as done by others (Imaizumi et al., 2000; Taylor et al., 2006;), the axons of the L4-L5 DRG neurons would have had to reach the dorsal column nuclei in the brain stem in order to form connections with the appropriate target neurons. Instead, by performing the dorsal column lesion at the L3-L4 level, we provided regenerating axons with a very close target, consisting of the interneurons in the dorsal and ventral horn grey matter located immediately rostral to the lesion. However, while we found with BDA tract tracing that spared fibres formed synaptic boutons, it was not possible to determine with BDA tract tracing whether regenerating axons synapsed with second order neurons. Interestingly, in future studies, we could use confocal microscopy to detect double labelling for specific markers of synapse formation and BDA labelling on the same tissue sections we have already used for the present investigation.

An estimate of the number of axons regenerating in our study after acute combined OEC transplantation and conditioning lesions shows that this was approximately 0.7%-7% of those ablated with the dorsal column lesion. This proportion is close to the 10% of fibre sparing that is needed in humans to maintain antigravity strength in antigravity muscles (Little et al., 1999). It could be of interest at this stage to investigate other treatment approaches which has been reported to promote anatomical and functional plasticity and combine them with OEC or Schwann cell transplantation and compare their regenerative response to that seen after conditioning lesions. Promising candidates for this

investigation could be chondroitinase delivery (Cafferty et al., 2008, Torn et al., 2009), delivery of the Rho-Rock pathway (Kubo and Yamashita, 2007) Nogo-antibody delivery (Schweigreiter and Bandtlow, 2006) and neurotrophin delivery (Bregman et al., 2002). However, we must consider that the quality of the connections rather than the quantity of axons crossing the lesion will likely be determinant in producing positive functional outcomes. This is why I think that rather than focusing on maximizing the number of regenerating axons crossing the lesion, which is high enough when combining OEC or Schwann cell transplant with conditioning lesions, we should now focus on approaches that can direct long distance axonal regeneration to their appropriate target locations in the spinal cord in combination with OEC or Schwann cell transplantation, and in a second phase try and promote connection of these with the local circuitry. We reported in the present study that DRG neurons regenerated mainly through the dorsal column white matter and underlying grey matter and did not regenerate in the dorsal and ventral horn grey matter which contain the targets for DRG neuron axons. For example an interesting study by Tang et al. (2007) has shown that after promoting regeneration of ascending sensory fibres past a dorsal root injury with delivery of NGF along the dorsal root entry zone, it was possible to restore their normal lamina projection pattern by injecting a vector virus carrying Semaphorin3A gene in the ventral spinal cord.

Finally, the present study has also revealed interesting insights in the neuroprotective properties of cell transplantation. We found in accordance with others that OEC, Schwann cell and fibroblast transplantation were associated with a reduction of the lesion cavity development compared to non-transplanted animals (Plant et al., 2003; Someya et al. 2008; Jones et al., 2003) suggesting neural cells may not always be necessary. Even more importantly we found a reduction of the lesion size as defined by the astrocytic marker GFAP. Furthermore, while we found that in the acute transplantation paradigm the lesion was prevented from expanding and from forming a cavity, in the delayed transplantation paradigm OECs largely filled an existing cavity and reduced the lesion size most likely by promoting astrocytes to fill the cavity. Importantly, we also found that cell transplantation had a neuroprotective effect on the grey matter surrounding the central canal. In fact, OEC and Schwann cells transplantation reduced significantly the degree of central canal cavitation

compared to that in non-transplanted animals. This important effect should be studied also in other lesion models such as contusion and compression lesions as it offers a promising solution to treat patients that suffer from syringomyelia, a pathology which is very common following spinal cord injury and other pathologies.

LIST OF REFERENCES

Akesson E, Kjaeldgaard A, Seiger A (1998) Human embryonic spinal cord grafts in adult rat spinal cord cavities: survival, growth, and interactions with the host. *Exp Neurol* 149(1):262-76.

Akiyama Y, Radtke C, Honmou O, Kocsis JD (2002) Remyelination of the spinal cord following intravenous delivery of bone marrow cells. *Glia* 39(3):229-36.

Alexander JK, Popovich PG (2009) Neuroinflammation in spinal cord injury: therapeutic targets for neuroprotection and regeneration. *Prog Brain Res* 175:125-37.

Al-Jahdari WS, Suzuki Y, Yoshida Y, Noda SE, Shirai K, Saito S, Goto F, Nakano T (2008) Growth cone collapse and neurite retractions: an approach to examine X-irradiation affects on neuron cells. *J Radiat Res (Tokyo)* 49(5):481-9..

Andersen PL, Webber CA, Kimura KA, Schreyer DJ (2000) Cyclic AMP prevents an increase in GAP-43 but promotes neurite growth in cultured adult rat dorsal root ganglion neurons. *Exp Neurol* 166(1):153-65.

Anderson KD (2004) Targeting recovery: priorities of the spinal cord-injured population. *J Neurotrauma* 21(10):1371-83.

Andrews MR, Stelzner DJ (2004) Modification of the regenerative response of dorsal column axons by olfactory ensheathing cells or peripheral axotomy in adult rat. *Exp Neurol* 190(2):311-27.

Andrews MR, Stelzner DJ (2007) Evaluation of olfactory ensheathing and schwann cells after implantation into a dorsal injury of adult rat spinal cord. *J Neurotrauma* 24(11):1773-92.

Aoki M, Fujito Y, Satomi H, Kurosawa Y, Kasaba T (1986) The possible role of collateral sprouting in the functional restitution of corticospinal connections after spinal hemisection. *Neurosci Res* 3(6):617-27.

Asher RA, Morgenstern DA, Shearer MC, Adcock KH, Pesheva P, Fawcett JW (2002) Versican is upregulated in CNS injury and is a product of oligodendrocyte lineage cells. *J Neurosci* 22(6):2225-36.

Barber PC, Lindsay RM (1982) Schwann cells of the olfactory nerves contain glial fibrillary acidic protein and resemble astrocytes. *Neuroscience* 7(12):3077-90.

Barde YA (1994) Neurotrophins: a family of proteins supporting the survival of neurons. *Prog Clin Biol Res* 390:45-56. Review.

Barnett SC, Hutchins AM, Noble M (1993) Purification of olfactory nerve ensheathing cells from the olfactory bulb. *Dev Biol* 155(2):337-50.

Barnett SC, Alexander CL, Iwashita Y, Gilson JM, Crowther J, Clark L, Dunn LT, Papanastassiou V, Kennedy PG, Franklin RJ (2000) Identification of a human olfactory ensheathing cell that can effect transplant-mediated remyelination of demyelinated CNS axons. *Brain* 123 (Pt 8):1581-8.

Barnett SC, Chang L (2004) Olfactory ensheathing cells and CNS repair: going solo or in need of a friend? *Trends Neurosci* 27(1):54-60. Review.

Barnett SC, Riddell JS (2004) Olfactory ensheathing cells (OECs) and the treatment of CNS injury: advantages and possible caveats. *J Anat* 204(1):57-67. Review.

Barnett SC, Riddell JS (2007) Olfactory ensheathing cell transplantation as a strategy for spinal cord repair: what can it achieve? *Nat Clin Pract Neurol* 3(3):152-61. Review.

Barritt AW, Davies M, Marchand F, Hartley R, Grist J, Yip P, McMahon SB, Bradbury EJ (2006) Chondroitinase ABC promotes sprouting of intact and injured spinal systems after spinal cord injury. *J Neurosci* 26(42):10856-67.

Basso DM, Beattie MS, Bresnahan JC (1995) A sensitive and reliable locomotor rating scale for open field testing in rats. *J Neurotrauma* 12(1):1-21.

Beattie MS, Bresnahan JC, Komon J, Tovar CA, Van Meter M, Anderson DK, Faden AI, Hsu CY, Noble LJ, Salzman S, Young W (1997) Endogenous repair after spinal cord contusion injuries in the rat. *Exp Neurol* 148(2):453-63.

Becker CG, Lieberoth BC, Morellini F, Feldner J, Becker T, Schachner M (2004) L1.1 is involved in spinal cord regeneration in adult zebrafish. *J Neurosci*. 24(36):7837-42.

Belyantseva IA, Lewin GR (1999) Stability and plasticity of primary afferent projections following nerve regeneration and central degeneration. *Eur J Neurosci* 11(2):457-68.

Black JA, Waxman SG, Smith KJ (2006) Remyelination of dorsal column axons by endogenous Schwann cells restores the normal pattern of Nav1.6 and Kv1.2 at nodes of Ranvier. *Brain* 129(Pt 5):1319-29.

Blesch A, Tuszynski MH (2003) Cellular GDNF delivery promotes growth of motor and dorsal column sensory axons after partial and complete spinal cord transections and induces remyelination. *J Comp Neurol* 467(3):403-17.

Boyd JG, Lee J, Skihar V, Doucette R, Kawaja MD (2004) LacZ-expressing olfactory ensheathing cells do not associate with myelinated axons after implantation into the compressed spinal cord. *PNAS* 101(7):2162-6.

Boyd JG, Jahed A, McDonald TG, Krol KM, Van Eyk JE, Doucette R, Kawaja MD (2006) Proteomic evaluation reveals that olfactory ensheathing cells but not Schwann cells express calponin. *Glia* 53(4):434-40.

Bradbury EJ, Moon LD, Popat RJ, King VR, Bennett GS, Patel PN, Fawcett JW, McMahon SB (2002) Chondroitinase ABC promotes functional recovery after spinal cord injury. *Nature* 416(6881):636-40.

Bregman BS, Coumans JV, Dai HN, Kuhn PL, Lynskey J, McAtee M, Sandhu F (2002) Transplants and neurotrophic factors increase regeneration and recovery of function after spinal cord injury. *Prog Brain Res* 137:257-73. Review.

Bretzner F, Liu J, Currie E, Roskams AJ, Tetzlaff W (2008) Undesired effects of a combinatorial treatment for spinal cord injury--transplantation of olfactory ensheathing cells and BDNF infusion to the red nucleus. *Eur J Neurosci* 28(9):1795-807.

Brockes JP, Fields KL, Raff MC (1979) Studies on cultured rat Schwann cells. I. Establishment of purified populations from cultures of peripheral nerve. *Brain Res* 6;165(1):105-18.

Brown AG, Rose PK, Snow PJ (1978) Morphology and organization of axon collaterals from afferent fibres of slowly adapting type I units in cat spinal cord. *J Physiol* 277:15-27.

Bunge RP (1994) The role of the Schwann cell in trophic support and regeneration. *J Neurol* 242(1 Suppl 1):S19-21. Review.

Bulsara KR, Iskandar BJ, Villavicencio AT, Skene JH (2002) A new millenium for spinal cord regeneration: growth-associated genes. *Spine (Phila Pa 1976)*. 1;27(17):1946-9. Review.

Cafferty WB, Bradbury EJ, Lidierrth M, Jones M, Duffy PJ, Pezet S, McMahon SB (2008) Chondroitinase ABC-mediated plasticity of spinal sensory function. *J Neurosci* 28(46):11998-2009.

Cai D, Shen Y, De Bellard M, Tang S, Filbin MT (1999) Prior exposure to neurotrophins blocks inhibition of axonal regeneration by MAG and myelin via a cAMP-dependent mechanism. *Neuron* 22(1):89-101.

Cai D, Qiu J, Cao Z, McAtee M, Bregman BS, Filbin MT (2001) Neuronal cyclic AMP controls the developmental loss in ability of axons to regenerate. *J Neurosci* 1;21(13):4731-9.

Cao Q, Zhang YP, Iannotti C, DeVries WH, Xu XM, Shields CB, Whittemore SR (2005) Functional and electrophysiological changes after graded traumatic spinal cord injury in adult rat. *Exp Neurol* 191 Suppl 1:S3-S16.

Chiba Y, Kuroda S, Maruichi K, Osanai T, Hokari M, Yano S, Shichinohe H, Hida K, Iwasaki Y (2009) Transplanted bone marrow stromal cells promote axonal regeneration and improve motor function in a rat spinal cord injury model. *Neurosurgery* 64(5):991-9; discussion 999-1000.

Chuah MI, Au C (1991) Olfactory Schwann cells are derived from precursor cells in the olfactory epithelium. *J Neurosci Res* 29(2):172-80.

Chuah MI, Tennent R, Jacobs I (1995) Response of olfactory Schwann cells to intranasal zinc sulfate irrigation. *J Neurosci Res* 1;42(4):470-8.

Chuah MI, West AK (2002) Cellular and molecular biology of ensheathing cells. *Microsc Res Tech* 58(3):216-27. Review.

Clemente CD, Windle WF (1954) Regeneration of severed nerve fibers in the spinal cord of the adult cat. *J Comp Neurol* 101: 691-731.

Coggeshall RE, Lekan HA, Doubell TP, Allchorne A, Woolf CJ (1997) Central changes in primary afferent fibers following peripheral nerve lesions. *Neuroscience*. 77(4):1115-22.

Collazos-Castro JE, Muneton-Gomez VC, Nieto-Sampedro M (2005) Olfactory glia transplantation into cervical spinal cord contusion injuries. *J Neurosurg Spine* 3(4):308-17.

Crowe MJ, Bresnahan JC, Shuman SL, Masters JN, Beattie MS (1997) Apoptosis and delayed degeneration after spinal cord injury in rats and monkeys. *Nat Med*. 3(1):73-6 Erratum in: *Nat Med* 1997 3(2):240.

David S, Aguayo AJ (1981) Axonal elongation into peripheral nervous system bridges after central nervous system injury in adult rats. *Science* 214(4523):931-3.

Davies S, Field PM, Raisman G (1994) Long interfascicular axon growth from embryonic neurons transplanted into adult myelinated tracts. *J. Neurosci* 14, 1596-1612.

- Davies S, Goucher DR, Doller C, Silver J (1999) Robust regeneration of adult sensory axons in degenerating white matter of the adult rat spinal cord. *J. Neurosci* 19, 5810-5822.
- Dent LJ, McCasland JS, Stelzner DJ (1996) Attempts to facilitate dorsal column axonal regeneration in a neonatal spinal environment. *J Comp Neurol* 372(3):435-56.
- Devon R, Doucette R (1992) Olfactory ensheathing cells myelinate dorsal root ganglion neurites. *Brain Res* 589:175-179.
- Dietz V, Curt A (2006) Neurological aspects of spinal-cord repair: promises and challenges. *Lancet Neurol* 5(8):688-94. Review.
- Dobkin BH, Havton LA (2004) Basic advances and new avenues in therapy of spinal cord injury. *Annu Rev Med* 55:255-82. Review.
- Dou CL, Levine JM (1994) Inhibition of neurite growth by the NG2 chondroitin sulfate proteoglycan. *J Neurosci* 14(12):7616-28.
- Doubell TP, Mannion RJ, Woolf CJ (1997) Intact sciatic myelinated primary afferent terminals collaterally sprout in the adult rat dorsal horn following section of a neighbouring peripheral nerve. *J Comp Neurol* 380(1):95-104.
- Doucette R (1989) Development of the nerve fiber layer in the olfactory bulb of mouse embryos. *J Comp Neurol* 285(4):514-27.
- Doucette, R (1990) Glial influences on axonal growth in the primary olfactory system. *Glia* 3:433-449.
- Doucette R (1991) PNS-CNS transitional zone of the first cranial nerve. *J Comp Neurol* 15;312(3):451-66.
- Doucette R (1995) Olfactory ensheathing cells: potential for glial cell transplantation into areas of CNS injury. *Histol Histopathol* 10:503-507.

Dreesmann L, Mittnacht U, Lietz M, Schlosshauer B (2009) Nerve fibroblast impact on Schwann cell behavior. *Eur J Cell Biol* 88(5):285-300. Epub 2009 Feb 25.

Duggan CD, Ngai J (2007) Scent of a stem cell. *Nat Neurosci* 10(6):673-4.

Dunning MD, Lakatos A, Loizou L, Kettunen M, French-Constant C, Brindle KM, Franklin RJ (2004) Superparamagnetic iron oxide-labeled Schwann cells and olfactory ensheathing cells can be traced *in vivo* by magnetic resonance imaging and retain functional properties after transplantation into the CNS. *J Neurosci* 24(44):9799-810.

Fairless R, Frame MC, Barnett SC (2005) N-cadherin differentially determines Schwann cell and olfactory ensheathing cell adhesion and migration responses upon contact with astrocytes. *Mol Cell Neurosci* 28(2):253-63.

Farbman AI (1990) Olfactory neurogenesis: genetic or environmental controls? *Trends Neurosci* 13(9):362-5. Review.

Fawcett JW, Asher RA (1999) The glial scar and central nervous system repair. *Brain Res Bull* 49(6):377-91. Review.

Fawcett JW (2006) Overcoming inhibition in the damaged spinal cord. *J Neurotrauma* 23(3-4):371-83. Review.

Fitch MT, Doller C, Combs CK, Landreth GE, Silver J (1999) Cellular and molecular mechanisms of glial scarring and progressive cavitation: *in vivo* and *in vitro* analysis of inflammation-induced secondary injury after CNS trauma. *J Neurosci* 19(19):8182-98.

Fouad K, Pedersen V, Schwab ME, Brösamle C (2001) Cervical sprouting of corticospinal fibers after thoracic spinal cord injury accompanies shifts in evoked motor responses. *Curr Biol* 11(22):1766-70.

Franceschini IA, Barnett SC (1996) Low-affinity NGF-receptor and E-N-CAM expression define two types of olfactory nerve ensheathing cells that share a

common lineage. *Dev Biol* 173(1):327-43. Erratum in: *Dev Biol* 1996 25;176(1):149.

Franklin RJ, Barnett SC (2000) Olfactory ensheathing cells and CNS regeneration: the sweet smell of success? *Neuron* 28(1):15-8. Review.

Franklin RJ, Gilson JM, Franceschini IA, Barnett SC (1996) Schwann cell-like myelination following transplantation of an olfactory bulb-ensheathing cell line into areas of demyelination in the adult CNS. *Glia* 17(3):217-24.

Franssen EH, Roet KC, de Bree FM, Verhaagen J (2009) Olfactory ensheathing glia and Schwann cells exhibit a distinct interaction behavior with meningeal cells. *J Neurosci Res* 87(7):1556-64.

Frei E, Klusman I, Schnell L, Schwab ME (2000) Reactions of oligodendrocytes to spinal cord injury: cell survival and myelin repair. *Exp Neurol* 163(2):373-80.

Freund P, Schmidlin E, Wannier T, Bloch J, Mir A, Schwab ME, Rouiller EM (2006) Nogo-A-specific antibody treatment enhances sprouting and functional recovery after cervical lesion in adult primates. *Nat Med* 12(7):790-2. Epub 2006 Jul 2. Erratum in: *Nat Med*. 2006 Oct;12(10):1220.

García-Alías G, Lopez-Vales R, For, s J, Navarro X, Verdu E (2004) Acute transplantation of olfactory ensheathing cells or Schwann cells promotes recovery after spinal cord injury in the rat. *J Neurosci Res* 75(5):632-41.

Gensel JC, Nakamura S, Guan Z, van Rooijen N, Ankeny DP, Popovich PG (2009) Macrophages promote axon regeneration with concurrent neurotoxicity. *J Neurosci* 29(12):3956-68.

Gensert JM, Goldman JE (1997) Endogenous progenitors remyelinate demyelinated axons in the adult CNS. *Neuron* 19(1):197-203.

Giuffrida R, Rustioni A (1992) Dorsal root ganglion neurons projecting to the dorsal column nuclei of rats. *J Comp Neurol* 316(2):206-20.

Gómez VM, Averill S, King V, Yang Q, Doncel Pérez E, Chacón SC, Ward R, Nieto-Sampedro M, Priestley J, Taylor J (2003) Transplantation of olfactory ensheathing cells fails to promote significant axonal regeneration from dorsal roots into the rat cervical cord. *J Neurocytol* 32(1):53-70.

Graziadei PP, Monti Graziadei GA (1985) Neurogenesis and plasticity of the olfactory sensory neurons. *Ann N Y Acad Sci* 457:127-42. Review.

Grimpe B, Silver J (2004) A novel DNA enzyme reduces glycosaminoglycan chains in the glial scar and allows microtransplanted dorsal root ganglia axons to regenerate beyond lesions in the spinal cord. *J Neurosci* 11;24(6):1393-7.

Guth L (2007) A history of nerve regeneration research. Unpublished data available at the UCI Reeve-Irvine research course, California.

Gutman AB, Warrick FB, Gutman EB (1942) Phosphorylative glycogenolysis and calcification in cartilage. *Science* 95(2470):461-462.

Hagg T, Oudega M (2006) Degenerative and spontaneous regenerative processes after spinal cord injury. *J Neurotrauma* 23(3-4):264-80. Review.

Han PJ, Shukla S, Subramanian PS, Hoffman PN (2004) Cyclic AMP elevates tubulin expression without increasing intrinsic axon growth capacity. *Exp Neurol* 189(2):293-302.

Hill CE, Beattie MS, Bresnahan JC (2001) Degeneration and sprouting of identified descending supraspinal axons after contusive spinal cord injury in the rat. *Exp Neurol* 171(1):153-69.

Hoffman PN (1989) Expression of GAP-43, a rapidly transported growth-associated protein, and class II beta tubulin, a slowly transported cytoskeletal protein, are coordinated in regenerating neurons. *J Neurosci* 9(3):893-7.

Hofstetter CP, Holmström NA, Lilja JA, Schweinhardt P, Hao J, Spenger C, Wiesenfeld-Hallin Z, Kurpad SN, Frisn J, Olson L (2005) Allodynia limits the

usefulness of intraspinal neural stem cell grafts; directed differentiation improves outcome. *Nat Neurosci* 8(3):346-53.

Houle JD, Tessler A (2003) Repair of chronic spinal cord injury. *Exp Neurol* 182(2):247-60. Review.

Huang H, Chen L, Wang H, Xiu B, Li B, Wang R, Zhang J, Zhang F, Gu Z, Li Y, Song Y, Hao W, Pang S, Sun J (2003) Influence of patients' age on functional recovery after transplantation of olfactory ensheathing cells into injured spinal cord injury. *Chin Med J (Engl)* 116(10):1488-91

Huang WL, George KJ, Ibba V, Liu MC, Averill S, Quartu M, Hamlyn PJ, Priestley JV (2007) The characteristics of neuronal injury in a static compression model of spinal cord injury in adult rats. *Eur J Neurosci* 25(2):362-72.

Huang ZH, Wang Y, Cao L, Su ZD, Zhu YL, Chen YZ, Yuan XB, He C (2008) Migratory properties of cultured olfactory ensheathing cells by single-cell migration assay. *Cell Res* 18(4):479-90.

Ibanez C, Ito D, Zawadzka M, Jeffery ND, Franklin RJ (2007) Calponin is expressed by fibroblasts and meningeal cells but not olfactory ensheathing cells in the adult peripheral olfactory system. *Glia* 55(2):144-51.

Ibarra A, Correa D, Willms K, Merchant MT, Guizar-Sahagún G, Grijalva I, Madrazo I (2003) Effects of cyclosporin-A on immune response, tissue protection and motor function of rats subjected to spinal cord injury. *Brain Res* 979(1-2):165-78.

Ibarra A, Hernández E, Lomeli J, Pineda D, Buenrostro M, Martiñón S, Garcia E, Flores N, Guizar-Sahagun G, Correa D, Madrazo I (2007) Cyclosporin-A enhances non-functional axonal growing after complete spinal cord transection. *Brain Res* 1149:200-9. Epub 2007 Mar 1.

Imaizumi T, Lankford KL, Waxman SG, Greer CA, Kocsis JD (1998) Transplanted olfactory ensheathing cells remyelinate and enhance axonal conduction in the demyelinated dorsal columns of the rat spinal cord. *J Neurosci* 18(16):6176-85.

- Imaizumi T, Lankford KL, Burton WV, Fodor WL, Kocsis JD (2000a) Xenotransplantation of transgenic pig olfactory ensheathing cells promotes axonal regeneration in rat spinal cord. *Nat Biotechnol* 18(9):949-53.
- Imaizumi T, Lankford KL, Kocsis JD (2000b) Transplantation of olfactory ensheathing cells or Schwann cells restores rapid and secure conduction across the transected spinal cord. *Brain Res* 854(1-2):70-8.
- Iwashita Y, Fawcett JW, Crang AJ, Franklin RJ, Blakemore WF (2000) Schwann cells transplanted into normal and X-irradiated adult white matter do not migrate extensively and show poor long-term survival. *Exp Neurol* 164(2):292-302.
- Jakeman LB, Wei P, Guan Z, Stokes BT (1998) Brain-derived neurotrophic factor stimulates hindlimb stepping and sprouting of cholinergic fibers after spinal cord injury. *Exp Neurol* 154(1):170-84.
- Ji B, Case LC, Liu K, Shao Z, Lee X, Yang Z, Wang J, Tian T, Shulga-Morskaya S, Scott M, He Z, Relton JK, Mi S (2008) Assessment of functional recovery and axonal sprouting in oligodendrocyte-myelin glycoprotein (OMgp) null mice after spinal cord injury. *Mol Cell Neurosci* 39(2):258-67. Epub 2008 Jul 18.
- Jirsov K, Soodar P, Mandys V, B.,r PR (1998) Cold jet: a method to obtain pure Schwann cell cultures without the need for cytotoxic, apoptosis-inducing drug treatment. *J Neurosci Methods* 78(1-2):133-7. Erratum in: *J Neurosci Methods* 1;82(2):233.
- Jones LL, Sajed D, Tuszynski MH (2003) Axonal regeneration through regions of chondroitin sulfate proteoglycan deposition after spinal cord injury: a balance of permissiveness and inhibition. *J Neurosci* 23(28):9276-88.
- Kamada T, Koda M, Dezawa M, Yoshinaga K, Hashimoto M, Koshizuka S, Nishio Y, Moriya H, Yamazaki M (2005) Transplantation of bone marrow stromal cell-derived Schwann cells promotes axonal regeneration and functional recovery after complete transection of adult rat spinal cord. *J Neuropathol Exp Neurol* 64(1):37-45.

- Kamei N, Tanaka N, Oishi Y, Hamasaki T, Nakanishi K, Sakai N, Ochi M (2007) BDNF, NT-3, and NGF released from transplanted neural progenitor cells promote corticospinal axon growth in organotypic cocultures. *Spine (Phila Pa 1976)* 32(12):1272-8.
- Kaneko N, Sawamoto K (2009) Adult neurogenesis and its alteration under pathological conditions. *Neurosci Res* 63(3):155-64. Review.
- Kerschensteiner M, Schwab ME, Lichtman JW, Misgeld T (2005) In vivo imaging of axonal degeneration and regeneration in the injured spinal cord. *Nat Med* 11(5):572-7.
- Keyvan-Fouladi N, Raisman G, Li Y (2003) Functional repair of the corticospinal tract by delayed transplantation of olfactory ensheathing cells in adult rats. *J Neurosci* 23(28):9428-34.
- Keyvan-Fouladi N, Raisman G, Li Y (2005) Delayed repair of corticospinal tract lesions as an assay for the effectiveness of transplantation of Schwann cells. *Glia* 51(4):306-11.
- Klekamp J, Vlkel K, Bartels CJ, Samii M (2001) Disturbances of cerebrospinal fluid flow attributable to arachnoid scarring cause interstitial edema of the cat spinal cord. *Neurosurgery* 48(1):174-85; discussion 185-6.
- Klekamp J (2002) The pathophysiology of syringomyelia - historical overview and current concept. *Acta Neurochir (Wien)* 144(7):649-64. Review.
- Kozlowski P, Raj D, Liu J, Lam C, Yung AC, Tetzlaff W (2008) Characterizing white matter damage in rat spinal cord with quantitative MRI and histology. *J Neurotrauma* 25(6):653-76.
- Kubo T, Yamashita T (2007) Rho-ROCK inhibitors for the treatment of CNS injury. *Recent Pat CNS Drug Discov* 2(3):173-9. Review.
- Kwon BK, Oxland TR, Tetzlaff W (2002) Animal models used in spinal cord regeneration research. *Spine (Phila Pa 1976)* 27(14):1504-10. Review.

Lakatos A, Franklin RJ, Barnett SC (2000) Olfactory ensheathing cells and Schwann cells differ in their in vitro interactions with astrocytes. *Glia* 32(3):214-25.

Lakatos A, Barnett SC, Franklin RJ (2003) Olfactory ensheathing cells induce less host astrocyte response and chondroitin sulphate proteoglycan expression than Schwann cells following transplantation into adult CNS white matter. *Exp Neurol* 184(1):237-46.

Lang P, Gesbert F, Delespine-Carmagnat M, Stancou R, Pouchelet M, Bertoglio J (1996) Protein kinase A phosphorylation of RhoA mediates the morphological and functional effects of cyclic AMP in cytotoxic lymphocytes. *EMBO J* 15(3):510-9.

Lankford KL, Sasaki M, Radtke C, Kocsis JD (2008) Olfactory ensheathing cells exhibit unique migratory, phagocytic, and myelinating properties in the X-irradiated spinal cord not shared by Schwann cells. *Glia* 56(15):1664-78.

Lawson SN, Waddell PJ (1991) Soma neurofilament immunoreactivity is related to cell size and fibre conduction velocity in rat primary sensory neurons. *J Physiol* 435:41-63.

Leung CT, Coulombe PA, Reed RR (2007) Contribution of olfactory neural stem cells to tissue maintenance and regeneration. *Nat Neurosci* 10(6):720-6. Epub 2007 Apr 29.

Li Y, Raisman G (1994) Schwann cells induce sprouting in motor and sensory axons in the adult rat spinal cord. *J Neurosci* 14(7):4050-63.

Li M, Shibata A, Li C, Braun PE, McKerracher L, Roder J, Kater SB, David S (1996) Myelin-associated glycoprotein inhibits neurite/axon growth and causes growth cone collapse. *J Neurosci Res* 46(4):404-14.

Li Y, Field PM, Raisman G (1998) Regeneration of adult rat corticospinal axons induced by transplanted olfactory ensheathing cells. *J Neurosci* 15;18(24):10514-24.

Li Y, Field PM, Raisman G (2005) Olfactory ensheathing cells and olfactory nerve fibroblasts maintain continuous open channels for regrowth of olfactory nerve fibres. *Glia* 52(3):245-51.

Lima C, Pratas-Vital J, Escada P, Hasse-Ferreira A, Capucho C, Peduzzi JD (2006) Olfactory mucosa autografts in human spinal cord injury: a pilot clinical study. *J Spinal Cord Med* 29(3):191-203; discussion 204-6.

Lin V, Cardenas DD, Cutter NC, Frost FS, Hammond MC, Lindblom LB, Perlash I, Waters R (2003) *Spinal Cord Medicine. Principles and Practice*. Demos Medical Publishing: 793.

Lindsay SL, Riddell JS, Barnett SC (2009) Olfactory mucosa for transplant-mediated repair: A complex tissue for a complex injury? *Glia*. [Epub ahead of print]

Lipson AC, Widenfalk J, Lindqvist E, Ebendal T, Olson L (2003) Neurotrophic properties of olfactory ensheathing glia. *Exp Neurol* 180(2):167-71.

Little JW, Ditunno JF Jr, Stiens SA, Harris RM (1999) Incomplete spinal cord injury: neuronal mechanisms of motor recovery and hyperreflexia. *Arch Phys Med Rehabil* 80(5):587-99. Review.

Liu CN, Chambers WW (1958) Intrasprouting of dorsal root axons; development of new collaterals and preterminals following partial denervation of the spinal cord in the cat. *AMA Arch Neurol Psychiatry* 79(1):46-61.

Lloyd DPC (1943) Neuron patterns controlling transmission of ipsilateral hind limb reflexes in cat. *J Neurophysiol* 6: 293-315.

Lopez-Vales R, Fores J, Navarro X, Verdu E (2007) Chronic transplantation of olfactory ensheathing cells promotes partial recovery after complete spinal cord transection in the rat. *Glia* 55(3):303-11.

- Lopez-Vales R, Fores J, Verdu E, Navarro X (2006) Acute and delayed transplantation of olfactory ensheathing cells promote partial recovery after complete transection of the spinal cord. *Neurobiol Dis* 21(1):57-68.
- Lu J, Feron F, Ho SM, Mackay-Sim A, Waite PM (2001) Transplantation of nasal olfactory tissue promotes partial recovery in paraplegic adult rats. *Brain Res* 889(1-2):344-57.
- Lu J, Feron F, Mackay-Sim A, Waite PM (2002) Olfactory ensheathing cells promote locomotor recovery after delayed transplantation into transected spinal cord. *Brain* 125(Pt 1):14-21.
- Lu P, Yang H, Culbertson M, Graham L, Roskams AJ, Tuszynski MH (2006) Olfactory ensheathing cells do not exhibit unique migratory or axonal growth-promoting properties after spinal cord injury. *J Neurosci* 26(43):11120-30.
- Ma Z, Cao Q, Zhang L, Hu J, Howard RM, Lu P, Whittemore SR, Xu XM (2009) Oligodendrocyte precursor cells differentially expressing Nogo-A but not MAG are more permissive to neurite outgrowth than mature oligodendrocytes. *Exp Neurol* 217(1):184-96. Epub 2009 Feb 21.
- Mackay-Sim A, Feron F, Cochrane J, Basingthwaite L, Bayliss C, Davies W, Fronck P, Gray C, Kerr G, Licina P, Nowitzke A, Perry C, Silburn PA, Urquhart S, Geraghty T (2008) Autologous olfactory ensheathing cell transplantation in human paraplegia: a 3-year clinical trial. *Brain* 131(Pt 9):2376-86.
- Matsushita M (1999) Projections from the upper lumbar cord to the cerebellar nuclei in the rat, studied by anterograde axonal tracing. *J Comp Neurol* 412(4):633-48.
- McDonald JW, Howard MJ (2002) Repairing the damaged spinal cord: a summary of our early success with embryonic stem cell transplantation and remyelination. *Prog Brain Res* 137:299-309. Review.
- McQuarrie IG, Grafstein B (1973) Axon outgrowth enhanced by a previous nerve injury. *Arch Neurol* 29(1):53-5.

- McTigue DM, Horner PJ, Stokes BT, Gage FH (1998) Neurotrophin-3 and brain-derived neurotrophic factor induce oligodendrocyte proliferation and myelination of regenerating axons in the contused adult rat spinal cord. *J Neurosci* 18(14):5354-65.
- Meijering E, Jacob M, Sarria JC, Steiner P, Hirling H, Unser M (2004) Design and validation of a tool for neurite tracing and analysis in fluorescence microscopy images. *Cytometry A* 58(2):167-76.
- Miedzybrodzki R, Tabakow P, Fortuna W, Czapiga B, Jarmundowicz W (2006) The olfactory bulb and olfactory mucosa obtained from human cadaver donors as a source of olfactory ensheathing cells. *Glia* 54(6):557-65.
- Moon LD, Fawcett JW (2001) Reduction in CNS scar formation without concomitant increase in axon regeneration following treatment of adult rat brain with a combination of antibodies to TGFbeta1 and beta2. *Eur J Neurosci* 14(10):1667-77.
- Nahm I, Shin T, Watanabe H, Masuko S (1992) Neurite regeneration in the cat recurrent laryngeal nerve: an immunohistochemical study. *Eur Arch Otorhinolaryngol* 249(7):385-8.
- Navarro X, Valero A, Gudino G, Fores J, Rodriguez FJ, Verdu E, Pascual R, Cuadras J, Nieto-Sampedro M (1999) Ensheathing glia transplants promote dorsal root regeneration and spinal reflex restitution after multiple lumbar rhizotomy. *Ann Neurol* 45(2):207-15.
- Neumann S, Woolf CJ (1999) Regeneration of dorsal column fibers into and beyond the lesion site following adult spinal cord injury. *Neuron* 23(1):83-91.
- Neumann S, Bradke F, Tessier-Lavigne M, Basbaum AI (2002) Regeneration of sensory axons within the injured spinal cord induced by intraganglionic cAMP elevation. *Neuron* 34(6):885-93.
- Neumann S, Skinner K, Basbaum AI (2005) Sustaining intrinsic growth capacity of adult neurons promotes spinal cord regeneration. *PNAS* 102(46):16848-52.

Novikov LN (2001) Labeling of central projections of primary afferents in adult rats: a comparison between biotinylated dextran amine, neurobiotin and Phaseolus vulgaris-leucoagglutinin. *J Neurosci Methods* 112(2):145-54.

O'Brien D, Dockery P, McDermott K, Fraher J (2001) Early development of rat ventral root transitional zone: an immunohistochemical and morphometric study. *J Neurocytol* 30(1):11-20.

Oudega M, Varon S, Hagg T (1994) Regeneration of adult rat sensory axons into intraspinal nerve grafts: promoting effects of conditioning lesion and graft predegeneration. *Exp Neurol* 129(2):194-206.

Oudega M, Xu XM (2006) Schwann cell transplantation for repair of the adult spinal cord. *J Neurotrauma* 23(3-4):453-67. Review.

Park E, Velumian AA, Fehlings MG (2004) The role of excitotoxicity in secondary mechanisms of spinal cord injury: a review with an emphasis on the implications for white matter degeneration. *J Neurotrauma* 21(6):754-74. Review.

Pascual JI, Gudino-Cabrera G, Insausti R, Nieto-Sampedro M (2002) Spinal implants of olfactory ensheathing cells promote axon regeneration and bladder activity after bilateral lumbosacral dorsal rhizotomy in the adult rat. *J Urol* 167(3):1522-6.

Plant GW, Christensen CL, Oudega M, Bunge MB (2003) Delayed transplantation of olfactory ensheathing glia promotes sparing/regeneration of supraspinal axons in the contused adult rat spinal cord. *J Neurotrauma* 20(1):1-16.

Plunet WT, Streijger F, Lam CK, Lee JH, Liu J, Tetzlaff W (2008) Dietary restriction started after spinal cord injury improves functional recovery. *Exp Neurol* 213(1):28-35. Epub 2008 Apr 22.

Polgár E, Shehab SA, Watt C, Todd AJ (1999) GABAergic neurons that contain neuropeptide Y selectively target cells with the neurokinin 1 receptor in laminae III and IV of the rat spinal cord. *J Neurosci* 19(7):2637-46.

Popovich PG, Guan Z, Wei P, Huitinga I, van Rooijen N, Stokes BT (1999) Depletion of hematogenous macrophages promotes partial hindlimb recovery and neuroanatomical repair after experimental spinal cord injury. *Exp Neurol* 158(2):351-65.

Priestley JV (2007) Promoting anatomical plasticity and recovery of function after traumatic injury to the central or peripheral nervous system. *Brain* 130(Pt 4):895-7. Review.

Qiu J, Cai D, Filbin MT (2000) Glial inhibition of nerve regeneration in the mature mammalian CNS. *Glia* 29(2):166-74. Review.

Qiu J, Cai D, Dai H, McAtee M, Hoffman PN, Bregman BS, Filbin MT (2002) Spinal axon regeneration induced by elevation of cyclic AMP. *Neuron* 34(6):895-903.

Radojicic M, Reier PJ, Steward O, Keirstead HS (2005) Septations in chronic spinal cord injury cavities contain axons. *Exp Neurol* 196(2):339-41.

Radojicic M, Nistor G, Keirstead HS (2007) Ascending central canal dilation and progressive ependymal disruption in a contusion model of rodent chronic spinal cord injury. *BMC Neurol* 7:30.

Radtke C, Akiyama Y, Brokaw J, Lankford KL, Wewetzer K, Fodor WL, Kocsis JD (2004) Remyelination of the nonhuman primate spinal cord by transplantation of H-transferase transgenic adult pig olfactory ensheathing cells. *FASEB J* 18(2):335-7.

Raineteau O, Schwab ME (2001) Plasticity of motor systems after incomplete spinal cord injury. *Nat Rev Neurosci* 2(4):263-73. Review.

Raisman G (1985) Specialized neuroglial arrangement may explain the capacity of vomeronasal axons to reinnervate central neurons. *Neuroscience* 14(1):237-54.

Raisman G (2001) Olfactory ensheathing cells - another miracle cure for spinal cord injury? *Nat Rev Neurosci* 2(5):369-75. Review.

Ramer LM, Au E, Richter MW, Liu J, Tetzlaff W, Roskams AJ (2004a) Peripheral olfactory ensheathing cells reduce scar and cavity formation and promote regeneration after spinal cord injury. *J Comp Neurol* 473(1):1-15.

Ramer LM, Richter MW, Roskams AJ, Tetzlaff W, Ramer MS (2004b) Peripherally-derived olfactory ensheathing cells do not promote primary afferent regeneration following dorsal root injury. *Glia* 1;47(2):189-206.

Ramón y Cajal, S. (1913, 1914) *Estudios sobre la Degeneración y Regeneración del Sistema Nervioso*, Moya, Madrid, Spain. This book was published in English in 1928 as *Degeneration and Regeneration of the Nervous System* (translated and edited by R.M. May), Oxford University Press. The translation was reprinted in 1991 as *Cajal's Degeneration and Regeneration of the Nervous System* (edited, with an introduction and additional translations, by J. DeFelipe and E.G. Jones), Oxford University Press.

Ramon-Cueto A, Nieto-Sampedro M (1994) Regeneration into the spinal cord of transected dorsal root axons is promoted by ensheathing glia transplants. *Exp Neurol* 127(2):232-44.

Ramon-Cueto A, Avila J (1998) Olfactory ensheathing glia: properties and function. *Brain Res Bull* 46(3):175-87. Review.

Ramon-Cueto A, Cordero MI, Santos-Benito FF, Avila J (2000) Functional recovery of paraplegic rats and motor axon regeneration in their spinal cords by olfactory ensheathing glia. *Neuron* 25(2):425-35.

Ranscht B, Clapshaw PA, Price J, Noble M, Seifert W (1982) Development of oligodendrocytes and Schwann cells studied with a monoclonal antibody against galactocerebroside. *PNAS* 79(8):2709-13.

Richardson PM, Issa VM (1984) Peripheral injury enhances central regeneration of primary sensory neurones. *Nature* 309(5971):791-3.

Richter MW, Fletcher PA, Liu J, Tetzlaff W, Roskams AJ (2005) Lamina propria and olfactory bulb ensheathing cells exhibit differential integration and

migration and promote differential axon sprouting in the lesioned spinal cord. *J Neurosci* 25(46):10700-11.

Riddell JS, Enriquez-Denton M, Toft A, Fairless R, Barnett SC (2004) Olfactory ensheathing cell grafts have minimal influence on regeneration at the dorsal root entry zone following rhizotomy. *Glia* 47(2):150-67.

Rizek PN, Kawaja MD (2006) Cultures of rat olfactory ensheathing cells are contaminated with Schwann cells. *Neuroreport* 17(5):459-62.

Rolls A, Schwartz M (2006) Chondroitin sulfate proteoglycan and its degradation products in CNS repair. *Adv Pharmacol* 53:357-74. Review.

Rosenfeld J, Cook S, James R (1997) Expression of superoxide dismutase following axotomy. *Exp Neurol* 147(1):37-47.

Rosenzweig ES, McDonald JW (2004) Rodent models for treatment of spinal cord injury: research trends and progress toward useful repair. *Curr Opin Neurol* 17(2):121-31. Review.

Ruitenbergh MJ, Levison DB, Lee SV, Verhaagen J, Harvey AR, Plant GW (2005) NT-3 expression from engineered olfactory ensheathing glia promotes spinal sparing and regeneration. *Brain* 128(Pt 4):839-53.

Ruitenbergh MJ, Plant GW, Christensen CL, Blits B, Niclou SP, Harvey AR, Boer GJ, Verhaagen J (2002) Viral vector-mediated gene expression in olfactory ensheathing glia implants in the lesioned rat spinal cord. *Gene Ther* 9(2):135-46.

Ruitenbergh MJ, Plant GW, Hamers FP, Wortel J, Blits B, Dijkhuizen PA, Gispen WH, Boer GJ, Verhaagen J (2003) Ex vivo adenoviral vector-mediated neurotrophin gene transfer to olfactory ensheathing glia: effects on rubrospinal tract regeneration, lesion size, and functional recovery after implantation in the injured rat spinal cord. *J Neurosci* 23(18):7045-58.

- Rydel RE, Greene LA (1988) cAMP analogs promote survival and neurite outgrowth in cultures of rat sympathetic and sensory neurons independently of nerve growth factor. *PNAS* 85(4):1257-61.
- Santos-Silva A, Fairless R, Frame MC, Montague P, Smith GM, Toft A, Riddell JS, Barnett SC (2007) FGF/heparin differentially regulates Schwann cell and olfactory ensheathing cell interactions with astrocytes: a role in astrocytosis. *J Neurosci* 27(27):7154-67.
- Sasaki M, Black JA, Lankford KL, Tokuno HA, Waxman SG, Kocsis JD (2006) Molecular reconstruction of nodes of Ranvier after remyelination by transplanted olfactory ensheathing cells in the demyelinated spinal cord. *J Neurosci* 26(6):1803-12.
- Schmalbruch H (1987) The number of neurons in dorsal root ganglia L4-L6 of the rat. *Anat Rec* 219(3):315-22.
- Schweigreiter R, Bandtlow CE (2006) Nogo in the injured spinal cord. *J Neurotrauma* 23(3-4):384-96. Review.
- Seki T, Fehlings MG (2008) Mechanistic insights into posttraumatic syringomyelia based on a novel in vivo animal model. Laboratory investigation. *J Neurosurg Spine* 8(4):365-75.
- Shnell L, Schwab M (1990) Axonal regeneration in the rat spinal cord produced by an antibody against myelin-associated neurite growth inhibitors. *Nature* 343:269-272.
- Schnell L, Schneider R, Kolbeck R, Barde YA, Schwab ME (1994) Neurotrophin-3 enhances sprouting of corticospinal tract during development and after adult spinal cord lesion. *Nature* 367(6459):170-3.
- Shen YJ, DeBellard ME, Salzer JL, Roder J, Filbin MT (1998) Myelin-associated glycoprotein in myelin and expressed by Schwann cells inhibits axonal regeneration and branching. *Mol Cell Neurosci* 12(1-2):79-91.

Shortland P, Woolf CJ, Fitzgerald M (1989) Morphology and somatotopic organization of the central terminals of hindlimb hair follicle afferents in the rat lumbar spinal cord. *J Comp Neurol* 289(3):416-33.

Shortland P, Woolf CJ (1993) Morphology and somatotopy of the central arborizations of rapidly adapting glabrous skin afferents in the rat lumbar spinal cord. *J Comp Neurol* 329(4):491-511.

Schuldiner M, Itskovitz-Eldor J, Benvenisty N (2003) Selective ablation of human embryonic stem cells expressing a "suicide" gene. *Stem Cells* 21(3):257-65.

Silver J (2009) CNS regeneration: only on one condition. *Curr Biol* 19(11):R444-6.

Silver J, Miller JH (2004) Regeneration beyond the glial scar. *Nat Rev Neurosci* 5(2):146-56. Review.

Smith PM, Lakatos A, Barnett SC, Jeffery ND, Franklin RJ (2002) Cryopreserved cells isolated from the adult canine olfactory bulb are capable of extensive remyelination following transplantation into the adult rat CNS. *Exp Neurol* 176(2):402-6.

Someya Y, Koda M, Dezawa M, Kadota T, Hashimoto M, Kamada T, Nishio Y, Kadota R, Mannoji C, Miyashita T, Okawa A, Yoshinaga K, Yamazaki M (2008) Reduction of cystic cavity, promotion of axonal regeneration and sparing, and functional recovery with transplanted bone marrow stromal cell-derived Schwann cells after contusion injury to the adult rat spinal cord. *J Neurosurg Spine* 9(6):600-10.

Sommer I, Schachner M (1981) Monoclonal antibodies (O1 to O4) to oligodendrocyte cell surfaces: an immunocytological study in the central nervous system. *Dev Biol* 83(2):311-27.

Song H, Ming G, He Z, Lehmann M, McKerracher L, Tessier-Lavigne M, Poo M (1998) Conversion of neuronal growth cone responses from repulsion to attraction by cyclic nucleotides. *Science* 281(5382):1515-8.

- Stein DG, Wright DW, Kellermann AL (2008) Does progesterone have neuroprotective properties? *Ann Emerg Med* 51(2):164-72. Epub 2007 Jun 22. Review.
- Steward O, Zheng B, Tessier-Lavigne M (2003) False resurrections: distinguishing regenerated from spared axons in the injured central nervous system. *J Comp Neurol* 459(1):1-8. Review.
- Steward O, Sharp K, Selvan G, Hadden A, Hofstadter M, Au E, Roskams J (2006) A re-assessment of the consequences of delayed transplantation of olfactory lamina propria following complete spinal cord transection in rats. *Exp Neurol* 198(2):483-99. Epub 2006 Feb 21.
- Steward O, Sharp K, Yee KM, Hofstadter M (2008) A re-assessment of the effects of a Nogo-66 receptor antagonist on regenerative growth of axons and locomotor recovery after spinal cord injury in mice. *Exp Neurol* 209(2):446-68.
- Steward O, Zheng B, Tessier-Lavigne M, Hofstadter M, Sharp K, Yee KM (2008) Regenerative growth of corticospinal tract axons via the ventral column after spinal cord injury in mice. *J Neurosci* 28(27):6836-47.
- Takami T, Oudega M, Bates ML, Wood PM, Kleitman N, Bunge MB (2002) Schwann cell but not olfactory ensheathing glia transplants improve hindlimb locomotor performance in the moderately contused adult rat thoracic spinal cord. *J Neurosci* 22(15):6670-81.
- Tandrup T (2004) Unbiased estimates of number and size of rat dorsal root ganglion cells in studies of structure and cell survival. *J Neurocytol* 33(2):173-92. Review.
- Tang XQ, Heron P, Mashburn C, Smith GM (2007) Targeting sensory axon regeneration in adult spinal cord. *J Neurosci* 27(22):6068-78.
- Taylor L, Jones L, Tuszynski MH, Blesch A (2006) Neurotrophin-3 gradients established by lentiviral gene delivery promote short-distance axonal bridging beyond cellular grafts in the injured spinal cord. *J Neurosci* 26(38):9713-21.

Thallmair M, Metz GA, Z'Graggen WJ, Raineteau O, Kartje GL, Schwab ME (1998) Neurite growth inhibitors restrict plasticity and functional recovery following corticospinal tract lesions. *Nat Neurosci* 1(2):124-31. Erratum in: *Nat Neurosci* 1998 1(4):329.

Tobias CA, Shumsky JS, Shibata M, Tuszynski MH, Fischer I, Tessler A, Murray M (2003) Delayed grafting of BDNF and NT-3 producing fibroblasts into the injured spinal cord stimulates sprouting, partially rescues axotomized red nucleus neurons from loss and atrophy, and provides limited regeneration. *Exp Neurol* 184(1):97-113.

Toft A, Scott DT, Barnett SC, Riddell JS (2007) Electrophysiological evidence that olfactory cell transplants improve function after spinal cord injury. *Brain* 130(Pt 4):970-84.

Tom VJ, Doller CM, Malouf AT, Silver J (2004). Astrocyte-associated fibronectin is critical for axonal regeneration in adult white matter. *J. Neurosci.* 24, 9282-9290.

Tom, M, Siladzic E, Santos-Silva A, Barnett SC (2007) Calponin is expressed by subpopulations of connective tissue cells but not olfactory ensheathing cells in the neonatal olfactory mucosa. *BMC Neurosci* 8:74.

Tom VJ, Kadakia R, Santi L, Houle JD (2009) Administration of chondroitinase ABC rostral or caudal to a spinal cord injury site promotes anatomical but not functional plasticity. *J Neurotrauma* (Epub ahead of print)

Tuszynski MH, Peterson DA, Ray J, Baird A, Nakahara Y, Gage FH (1994) Fibroblasts genetically modified to produce nerve growth factor induce robust neuritic ingrowth after grafting to the spinal cord. *Exp Neurol* 126(1):1-14.

van den Pol AN, Santarelli JG (2003) Olfactory ensheathing cells: time lapse imaging of cellular interactions, axonal support, rapid morphologic shifts, and mitosis. *J Comp Neurol* 458(2):175-94.

- Vaquero J, Zurita M (2009) Bone marrow stromal cells for spinal cord repair: a challenge for contemporary neurobiology. *Histol Histopathol* 24(1):107-16. Review.
- Verma P, Fawcett J (2005) Spinal cord regeneration. *Adv Biochem Eng Biotechnol* 94:43-66. Review.
- Wang KC, Koprivica V, Kim JA, Sivasankaran R, Guo Y, Neve RL, He Z (2002) Oligodendrocyte-myelin glycoprotein is a Nogo receptor ligand that inhibits neurite outgrowth. *Nature* 417(6892):941-4. Epub 2002 Jun 16.
- Weidner N, Grill RJ, Tuszynski MH (1999) Elimination of basal lamina and the collagen scar after spinal cord injury fails to augment corticospinal tract regeneration. *Exp Neurol* 160(1):40-50.
- Weidner N, Ner A, Salimi N, Tuszynski MH (2001) Spontaneous corticospinal axonal plasticity and functional recovery after adult central nervous system injury. *PNAS* 98(6):3513-8.
- Weidner N, Tuszynski MH (2002) Spontaneous plasticity in the injured spinal cord-implications for repair strategies. *Mol Psychiatry* 7(1):9-11.
- Willerth SM, Sakiyama-Elbert SE (2008) Cell therapy for spinal cord regeneration. *Adv Drug Deliv Rev* 60(2):263-76. Review.
- Williams SK, Franklin RJ, Barnett SC (2004) Response of olfactory ensheathing cells to the degeneration and regeneration of the peripheral olfactory system and the involvement of the neuregulins. *J Comp Neurol* 470(1):50-62.
- Willis W.D. and Coggeshall R.E. (2004) *Sensory Mechanisms of the Spinal Cord*, 3rd edition, Kluwer Academic/Plenum Publishers.
- Windle WF, Smart JO, Beers JJ (1958) Residual function after subtotal spinal cord transection in adult cats. *Neurology* 8(7):518-21.

Wirth ED 3rd, Reier PJ, Fessler RG, Thompson FJ, Uthman B, Behrman A, Beard J, Vierck CJ, Anderson DK (2001) Feasibility and safety of neural tissue transplantation in patients with syringomyelia. *J Neurotrauma* 18(9):911-29.

Wong J, Oblinger MM (1987) Changes in neurofilament gene expression occur after axotomy of dorsal root ganglion neurons: an in situ hybridization study. *Metab Brain Dis* 2(4):291-303.

Woodhall E, West AK, Chuah MI (2001) Cultured olfactory ensheathing cells express nerve growth factor, brain-derived neurotrophic factor, glia cell line-derived neurotrophic factor and their receptors. *Brain Res Mol Brain Res* 31;88(1-2):203-13.

Wu D, Yang P, Zhang X, Luo J, Haque ME, Yeh J, Richardson PM, Zhang Y, Bo X (2009) Targeting a Dominant Negative Rho Kinase to Neurons Promotes Axonal Outgrowth and Partial Functional Recovery After Rat Rubrospinal Tract Lesion. *Mol Ther* [Epub ahead of print].

Xu XM, Chen A, Guénard V, Kleitman N, Bunge MB (1997) Bridging Schwann cell transplants promote axonal regeneration from both the rostral and caudal stumps of transected adult rat spinal cord. *J Neurocytol* 26(1):1-16.

Yan Q, Johnson EM Jr (1988) An immunohistochemical study of the nerve growth factor receptor in developing rats. *J Neurosci* 8(9):3481-98.

Ylera B, Ertürk A, Hellal F, Nadrigny F, Hurtado A, Tahirovic S, Oudega M, Kirchhoff F, Bradke F (2009) Chronically CNS-injured adult sensory neurons gain regenerative competence upon a lesion of their peripheral axon. *Curr Biol* 19(11):930-6.

Young W (2002) Spinal cord contusion models. *Prog Brain Res* 137:231-55. Review.

Zhang L, Ma Z, Smith GM, Wen X, Pressman Y, Wood PM, Xu XM (2009) GDNF-enhanced axonal regeneration and myelination following spinal cord injury is mediated by primary effects on neurons. *Glia* 57(11):1178-91.

Zeman RJ, Bauman WA, Wen X, Ouyang N, Etlinger JD, Cardozo CP (2009)
Improved functional recovery with oxandrolone after spinal cord injury in rats.
Neuroreport 17;20(9):864-8.

Zurita M, Vaquero J, Bonilla C, Santos M, De Haro J, Oya S, Aguayo C (2008)
Functional recovery of chronic paraplegic pigs after autologous transplantation
of bone marrow stromal cells. Transplantation 86(6):845-53.